



# THE UNIVERSITY *of* EDINBURGH

This thesis has been submitted in fulfilment of the requirements for a postgraduate degree (e.g. PhD, MPhil, DClinPsychol) at the University of Edinburgh. Please note the following terms and conditions of use:

This work is protected by copyright and other intellectual property rights, which are retained by the thesis author, unless otherwise stated.

A copy can be downloaded for personal non-commercial research or study, without prior permission or charge.

This thesis cannot be reproduced or quoted extensively from without first obtaining permission in writing from the author.

The content must not be changed in any way or sold commercially in any format or medium without the formal permission of the author.

When referring to this work, full bibliographic details including the author, title, awarding institution and date of the thesis must be given.

HISTORIC DYE ANALYSIS:  
METHOD DEVELOPMENT AND NEW APPLICATIONS IN  
CULTURAL HERITAGE

LORE GERTRUD TROALEN



DOCTOR OF PHILOSOPHY  
SCHOOL OF CHEMISTRY  
THE UNIVERSITY OF EDINBURGH

2013

# DECLARATION

I declare that this thesis is my own composition, that the work described herein has been carried out by me, unless otherwise stated, and that it has not been submitted in any previous application for a higher degree.

This thesis describes the results of research carried out since the 1<sup>st</sup> January 2009, the date of my admission as a research student. The work was conducted in the School of Chemistry, The University of Edinburgh, under the supervision of Dr Alison N. Hulme and Prof. Hamish McNab and in the Conservation and Analytical Research department of the National Museums of Scotland, under the supervision of Dr James Tate.

The use of data from this thesis in any publications must therefore be referenced accordingly.

Signed: 29<sup>th</sup> March 2013.....

Date: LTroalen.....

*To My Parents,  
Thank You*



# ACKNOWLEDGMENTS

This project was supported by the Science and Heritage Programme (AHRC / EPSRC Grant ref. CDA08/411), and financial assistance was also provided by Glasgow Museums and National Museums Scotland.

I would like first to warmly thank Dr Alison N. Hulme for her supervision and for her enthusiasm during the four years of this research that made the project very enjoyable and such a learning experience. It causes great sadness that Prof Hamish McNab who was co-supervising this work is not with us today and I would like to thank him for all his contribution and inspiration during the first half of the project. Many aspects of this research, especially on porcupine quill work analysis, came from exciting discussion we all had in the first year of the project, and I hope that he would have enjoyed reading the outcomes – and some of the answers - in this thesis.

I am immensely grateful to Dr Jim Tate, previously Head of Conservation and Analytical Research department at National Museums Scotland for supporting my career break and also for sharing his broad knowledge and expertise on the analysis of museum objects.

This research would have not been possible without colleagues in the museum institutions: at the Burrell Collection, I am grateful to Helen M. Hughes, Sarah Foskett and Patricia Collins for providing access to the Sheldon tapestries; at National Museums Scotland, I would like to thank Henrietta Lidchi and Chantal Knowles for authorising the sampling of the porcupine quill references and Jill Plitnikas for extra samples collected during conservation treatment; at the Bodleian Library, I would like to thank David Howell, for providing access to the Sheldon tapestry maps and Julie Travis for assisting me in the sampling.

I would also like to thank at the University of Edinburgh Dr Lorna Eades for carrying out the ICP-OES measurements, as well as Dr Perdita Barran and Ashley Phillips for Mass Spectrometric experiments. I am grateful to Dr Lorraine Gibson at Strathclyde University, for helpful discussion on UPLC method development, and Andrew Simpson,

from Waters UK, for his cheerful and generous technical support to both HPLC and UPLC systems.

Some experiments were carried out at the LC2RMF in Paris, through a research grant provided by Eu-CHARISMA project. I would like to thank the scientific team at AGLAE accelerator especially Thomas Calligaro, Lucile Beck, Laurent Pichon and Claire Pacheco; but also Stefan Röhrs and Carolina Gutiérrez for discussion on PIXE data.

Finally, I would like also to acknowledge colleagues in the C&AR department for their support and encouragement, especially Diana de Bellaigue, Victoria Hanley, Lynn McClean and Jane Clark; and at the University of Edinburgh the postgraduate students from the Hulme group, McNab group and Barran group, I enjoyed working alongside such talented young researchers and being able to exchange ideas on some of my experiments.

Last but not least, I would like to thank my friends and my wonderful family, especially my parents, for their unfailing support.

# ABSTRACT

A review of the main natural dyes (particularly yellow flavonoids and red anthraquinones) and proteinaceous substrates used in Historical Tapestries and North American porcupine quill work was undertaken, and is summarised in Chapter 1.

The analysis of natural dyes which have been used on museum artefacts other than textiles has received little systematic study, particularly those of non-European origin. In this research, the use of Ultra Performance Liquid Chromatography (UPLC) for study of natural dyes found on historical textiles and ethnographical objects decorated with porcupine quill work is explored; this required a transfer of existing analytical protocols and methodology. The advantages of using Ultra Performance Liquid Chromatography (UPLC) was evaluated through a method development based on the separation and quantification of ten flavonoid and anthraquinone dyes as described in Chapter 2. These methods were then applied to the characterisation of the dye sources found on a group of sixteenth century historical tapestries which form an important part of the Burrell Collection in Glasgow and are believed to have been manufactured in an English workshop (Chapter 3) and also to the analysis of some late nineteenth century North American porcupine quill work from a collection owned by National Museums Scotland (Chapter 5); allowing exciting conclusions to be drawn in each case about the range of dyestuffs used in their manufacture.

The second aim of this research was the development of methodology for the non-invasive quantification of metal ion residues on porcupine quill substrates. This was achieved through a comparative study of reference porcupine quills prepared in-house with dyebaths containing a range of metal ion concentrations (copper and tin). The concentration of metal ions sorbed by the porcupine quills was then quantified with Inductively Coupled Plasma (ICP) coupled to Optical Emission Spectrometry (OES) and non-invasive Particle Induced X-Ray Emission analysis (PIXE) coupled with Rutherford

Backscattering Spectrometry (RBS) as described in Chapter 4. The responses provided by the different methods were compared and they were then applied to the study of micro-samples collected from mid-nineteenth century Northern Athapaskan porcupine quill work. Unexpectedly, the use of UPLC analysis and RBS-PIXE analysis allowed the characterisation of traded European natural dyes used with metallic mordants (copper and tin) on these samples, highlighting how European contact impacted on traditional Athapaskan porcupine quill work in the late nineteenth century (Chapter 5).

The work of this thesis has been covered in the following publications and presentations:

*Publications:*

1 Troalen, L., Phillips, A., Hughes, H., Barran, P. E., Tate, J., Hulme, A. N.: Ultra Performance Liquid Chromatographic separation of natural dyestuffs: Application to early 17th century English tapestries. *In preparation* (work described in chapter 2)

*Presentations*

1 42<sup>nd</sup> IUPAC Congress, Glasgow - UK (2009), poster: Characterisation and provenance of Natural dyestuffs by PDA-HPLC analysis: the case of the Sheldon tapestry workshop at Barcheston in the mid-16<sup>th</sup> century.

2 Glasgow Museum Annual Conference, Glasgow – UK (2009), presentation: Characterisation and provenance of Natural dyestuffs by PDA-HPLC analysis: the case of the Sheldon tapestry workshop at Barcheston in the mid-16<sup>th</sup> century.

3 29<sup>th</sup> DHA meeting (Dyes in history and Archaeology), Lisbon – Portugal (2010), presentation: English tapestry workshops in the mid-16<sup>th</sup> century: characterisation and provenance through PDA-HPLC analysis.

4 31<sup>st</sup> DHA meeting (Dyes in history and Archaeology), Antwerp – Belgium (2012), poster: English tapestry workshops in the mid-16<sup>th</sup> century: characterisation and provenance through PDA-HPLC and UPLC analysis.

5 31<sup>st</sup> DHA meeting (Dyes in history and Archaeology), Antwerp – Belgium (2012), presentation: Thorny Questions About the Athapaskan Porcupine Quill work Collection at. National Museums Scotland.

# TABLE OF ABBREVIATIONS

NMS	National Museums Scotland
UoE	The University of Edinburgh
HPLC	High Performance Liquid Chromatography
UPLC	Ultra Performance Liquid Chromatography
PDA	Photo Diode Array Detector
LOD	Limit of Detection
LOQ	Limit of Quantification
R <sub>t</sub>	Retention Time
ESI-MS	Electrospray Ionisation Mass Spectrometry
QTOF2	Quadrupole Time of Flight
MeOH	Methanol
DMSO	Dimethyl sulfoxide
TFA	Trifluoroacetic acid
ICP-OES	Inductively Coupled Plasma coupled to Optical Emission Spectroscopy
NRA	Nuclear Reaction Analysis
PIXE	Particle Induced X-ray Emission
PIGE	Particle Induced Gamma ray Emission
RBS	Rutherford Backscattering Spectroscopy

# TABLE OF CONTENTS

<b>1</b>	<b>INTRODUCTION.....</b>	<b>8</b>
1.1	HISTORICAL MATERIALS.....	9
1.1.1	<i>Historical tapestries</i> .....	9
1.1.1.1	High warp loom or “haute lice” technique.....	9
1.1.1.2	Low warp loom or “basse lice” technique.....	10
1.1.1.3	Origin of tapestry weaving in England.....	10
1.1.2	<i>Porcupine quill work</i> .....	11
1.1.2.1	Athapaskans collection at National Museums Scotland.....	12
1.2	EUROPEAN AND NORTH AMERICAN DYES SOURCES.....	13
1.2.1	<i>Natural dye classification</i> .....	14
1.2.2	<i>Direct dyes</i> .....	15
1.2.2.1	Turmeric.....	16
1.2.2.2	Safflower.....	17
1.2.2.3	Berberine containing dyes.....	18
1.2.3	<i>Mordant dyes</i> .....	19
1.2.3.1	Flavonoids.....	19
1.2.3.2	Anthraquinones.....	27
1.2.3.3	Lichens.....	33
1.2.3.4	Anthocyanidins.....	34
1.2.4	<i>Vat dyes</i> .....	35
1.2.5	<i>1856: the transition to early synthetic dyes</i> .....	37
1.3	PROTEINACEOUS FIBRES.....	39
1.3.1	<i>Protein composition and structure</i> .....	40
1.3.2	<i>Fibroin containing fibres</i> .....	40
1.3.3	<i>Keratin based fibres</i> .....	42
1.4	CONTRIBUTION OF THIS WORK.....	46
1.4.1	<i>Dye analysis and method development</i> .....	46
1.4.2	<i>Metal ion mordant analysis: method development</i> .....	47
1.5	REFERENCES.....	48
<b>2.</b>	<b>ULTRA PERFORMANCE LIQUID CHROMATOGRAPHY: METHOD DEVELOPMENT FOR THE SEPARATION OF NATURAL DYESTUFFS.....</b>	<b>61</b>
2.1	HIGH PERFORMANCE LIQUID CHROMATOGRAPHY COUPLED TO PHOTO DIODE ARRAY ANALYSIS OR MASS SPECTROMETRY.....	61
2.1.1	<i>High Performance Liquid Chromatography</i> .....	61
2.1.2	<i>Photo Diode Array Analysis</i> .....	63
2.1.3	<i>Mass Spectrometry analysis (MS)</i> .....	64
2.1.3.1	Electrospray Ionisation (ESI).....	64
2.1.3.2	Negative Electrospray Ionisation for the study of flavonoid dyes.....	65
2.2	ULTRA PERFORMANCE LIQUID CHROMATOGRAPHY.....	67
2.3	METHOD DEVELOPMENT FOR THE SEPARATION OF FLAVONOID AND ANTHRAQUINONE DYES.....	69
2.3.1	<i>Method development</i> .....	70
2.3.1.1	Transfer of HPLC method to the UPLC system.....	70
2.3.1.2	Evaluation of the UPLC methods.....	73
2.3.1.3	Repeatability and resolution factors (R <sub>s</sub> ).....	75

2.3.1.4	Linearity, calibration curves and limit of detection .....	81
2.3.1.5	UPLC-ESI Mass Spectrometry .....	86
2.3.2	<i>Evaluation of sample preparation</i> .....	89
2.4	APPLICATION TO REFERENCE MATERIALS .....	91
2.4.1	<i>Identification of minor components in acid-hydrolysed extracts of weld (Reseda</i> .....	
	<i>luteola L.) and dyer's greenweed (Genista tinctoria L.)</i> .....	92
2.4.1.1	Weld ( <i>Reseda luteola L.</i> ) .....	92
2.4.1.2	Dyer's greenweed ( <i>Genista tinctoria L.</i> ) .....	93
2.4.2	<i>Characterisation of Gt compounds by UPLC-ESI-MS</i> .....	97
2.4.3	<i>Effect of over-dyeing</i> .....	103
2.5	SUMMARY .....	105
2.6	REFERENCES .....	106
<b>3</b>	<b>INVESTIGATION OF EARLY 16<sup>TH</sup> CENTURY ENGLISH TAPESTRIES</b> .....	
	<b>ASSOCIATED TO THE "SHELDON" WORKSHOP</b> .....	<b>113</b>
3.1	HISTORICAL BACKGROUND .....	113
3.1.1	<i>Tapestry works in the Middle Ages and early Renaissance</i> .....	113
3.1.2	<i>The origin of tapestry weaving in England</i> .....	114
3.1.3	<i>The Sheldon workshop myth or reality?</i> .....	115
3.1.4	<i>Sheldon tapestries today</i> .....	117
3.1.5	<i>Sir Burrell and the Sheldon Collection</i> .....	117
3.2	SAMPLING AND DOCUMENTATION.....	118
3.2.1	<i>Burrell Collection</i> .....	118
3.2.2	<i>Bodleian Library, University of Oxford</i> .....	121
3.3	DYE ANALYSIS .....	125
3.3.1	<i>Experimental conditions</i> .....	125
3.3.1.1	Extraction protocol .....	125
3.3.1.2	HPLC System .....	125
3.3.1.3	UPLC System .....	125
3.3.2	<i>Yellow, green, orange yarns</i> .....	126
3.3.2.1	Weld ( <i>Reseda luteola L.</i> ).....	126
3.3.2.2	Dyer's greenweed ( <i>Genista tinctoria L.</i> ) .....	130
3.3.2.3	Young fustic ( <i>Cotinus Coggygria L.</i> ) .....	134
3.3.3	<i>Red, purple, pink yarns</i> .....	137
3.3.3.1	Madder species .....	137
3.3.3.2	Cochineal .....	140
3.3.3.3	Orchil dyes .....	143
3.3.3.4	Safflower ( <i>Carthamus tinctorius L.</i> ).....	144
3.4	DISCUSSION .....	148
3.5	REFERENCES .....	150
<b>4</b>	<b>CHARACTERISATION OF METALLIC MORDANTS ON PORCUPINE QUILL</b> .....	
	<b>WORK: METHOD DEVELOPMENT</b> .....	<b>156</b>
4.1	PORCUPINE QUILL SUBSTRATE.....	157
4.1.1	<i>Sorption of metal ions on keratin fibres</i> .....	157
4.1.2	<i>SEM observation of Porcupine quill</i> .....	158
4.2	ICP-OES STUDY .....	160
4.2.1	<i>ICP-OES principles</i> .....	160
4.2.2	<i>Investigation of porcupine quill references</i> .....	161



4.2.2.1	Mordanting condition .....	161
4.2.2.2	Influence of dyebath time on metal ion uptake .....	161
4.2.2.3	Quantification of copper(II) and tin(II) uptake .....	167
4.2.3	<i>Summary</i> .....	172
4.3	ION BEAM ANALYSIS .....	172
4.3.1	<i>Ion Beam Analysis principles</i> .....	172
4.3.2	<i>PIXE analysis of trace elements in porcupine quills</i> .....	174
4.3.2.1	Interaction of 3 MeV proton beam with keratin.....	174
4.3.2.2	Target description .....	177
4.3.2.3	Absorption factors and transmission of Cu(K) and Sn(L <sub>A</sub> ) X-rays in keratin.....	178
4.3.2.4	Parameter files and calibration .....	181
4.3.2.5	Quantification of copper and tin by PIXE analysis.....	185
4.3.2.6	Summary .....	188
4.3.3	<i>Rutherford Backscattering Spectrometry (RBS)</i> .....	189
4.3.3.1	RBS Principles.....	189
4.3.3.2	SIMNRA simulation: calculation of depth profile.....	191
4.3.3.3	Quantification of copper and tin by RBS analysis .....	193
4.4	DISCUSSION .....	196
4.5	REFERENCES .....	197
<b>5</b>	<b>INVESTIGATION OF NORTH AMERICAN ATHAPASKAN PORCUPINE QUILL .....</b>	
	<b>WORK FROM NATIONAL MUSEUMS SCOTLAND.....</b>	<b>204</b>
5.1	HISTORICAL BACKGROUND .....	205
5.1.1	<i>Athapaskan Cultural Group</i> .....	205
5.1.2	<i>Dye sources in Athapaskan porcupine quill work</i> .....	207
5.1.3	<i>Porcupine quill work at National Museums Scotland</i> .....	209
5.1.4	<i>Dyed porcupine quill specimens (Inv. N<sup>o</sup>: A.848.15)</i> .....	211
5.1.5	<i>Binocular Observation and Sampling</i> .....	213
5.2	DYE ANALYSIS .....	216
5.2.1	<i>Preparation of reference material</i> .....	217
5.2.1.1	Scouring.....	217
5.2.1.2	Dyeing process .....	217
5.2.1.3	Effect of the mordant.....	218
5.2.2	<i>PDA-UPLC conditions</i> .....	219
5.2.2.1	Calibration, LOD and LOQ .....	220
5.2.3	<i>Turmeric</i> .....	222
5.2.3.1	Extraction efficiency and reproducibility .....	223
5.2.3.2	Historical quills (A.848.15) .....	225
5.2.4	<i>Cochineal</i> .....	228
5.2.4.1	Porcupine quill extract.....	228
5.2.4.2	Historical quills (A.848.15) .....	231
5.2.5	<i>Blue dyes</i> .....	234
5.3	MORDANT ANALYSIS BY MICRO PIXE AND RBS .....	235
5.3.1	<i>Beam dose Q and calibration</i> .....	235
5.3.2	<i>Investigation of reference quills</i> .....	238
5.3.3	<i>Historical samples</i> .....	239
5.3.3.1	Quantification of light elements .....	240
5.3.3.2	Quantification of heavy elements .....	242
5.3.3.3	RBS analysis.....	244
5.3.3.4	ICP-OES analysis .....	246
5.4	DISCUSSION .....	248
5.5	REFERENCES .....	251

<b>6</b>	<b>CONCLUSION</b> .....	<b>258</b>
6.1	ULTRA PERFORMANCE LIQUID CHROMATOGRAPHY (UPLC).....	258
6.2	DYER'S GREENWEED MINOR COMPONENTS .....	259
6.3	EARLY ENGLISH «SHELDON» TAPESTRIES.....	259
6.4	SORPTION OF METALLIC IONS ON PORCUPINE QUILLS .....	260
6.5	MID NINETEENTH CENTURY NATIVE AMERICAN QUILL WORK.....	261
6.6	CONCLUSION .....	261
<b>7</b>	<b>EXPERIMENTAL</b> .....	<b>266</b>
7.1	MATERIALS AND CHROMATOGRAPHIC METHODS.....	266
7.1.1	<i>References materials and chemicals</i> .....	266
7.1.2	<i>Sample preparation</i> .....	266
7.1.3	<i>Solutions of standards</i> .....	267
7.1.4	<i>Chromatographic Methods</i> .....	268
7.1.4.1	HPLC system.....	268
7.1.4.2	UPLC system.....	269
7.1.4.3	UPLC ESI MS system .....	271
7.1.5	<b>METHOD DEVELOPMENT</b> .....	272
7.1.5.1	Calibration curves.....	272
7.1.5.2	Limit of detection (LOD) and quantification (LOQ) .....	274
7.1.5.3	Comparison of response: H <sub>x</sub> (AU) and [x] (ng) for genistein .....	278
7.1.6	<i>Evaluation of sample preparation</i> .....	279
7.1.7	<i>Investigation of reference yarns</i> .....	281
7.1.7.1	Weld ( <i>Reseda luteola</i> L.) .....	281
7.1.7.2	Dyer's greenweed ( <i>Genista tinctoria</i> L.) .....	282
7.2	INVESTIGATION OF MID 16 <sup>TH</sup> CENTURY ENGLISH TAPESTRIES .....	284
7.2.1	<i>Extraction protocols</i> .....	284
7.2.1.1	Hydrochloric acid extraction .....	284
7.2.1.2	Dimethyl Sulfoxide extraction.....	284
7.2.2	<i>Chromatographic methods</i> .....	285
7.2.2.1	HPLC system.....	285
7.2.2.2	UPLC system.....	285
7.2.3	<i>Dye analysis</i> .....	285
7.2.3.1	Weld ( <i>Reseda luteola</i> L.).....	285
7.2.3.2	Dyer's greenweed ( <i>Genista tinctoria</i> L.) .....	290
7.2.3.3	Young fustic ( <i>Cotinus coggygria</i> S.) .....	292
7.2.3.4	Madder species .....	294
7.2.3.5	Cochineal dyes .....	296
7.2.3.6	Safflower ( <i>Carthamus tinctorius</i> L.) .....	297
7.2.3.7	Summary .....	298
7.3	CHARACTERISATION OF METALLIC MORDANT ON PORCUPINE QUILL .....	314
7.3.1	<i>Scanning Electron Microscopy (SEM)</i> .....	314
7.3.2	<i>References of Cu<sup>2+</sup> and Sn<sup>2+</sup> preparation</i> .....	314
7.3.3	<b>ICP-OES</b> .....	315
7.3.3.1	Calibration of the system.....	315
7.3.3.2	ICP-OES sample preparation.....	316
7.3.3.3	Evaluation of dyebath conditions .....	317
7.3.3.4	ICP-OES investigation of references quills .....	321
7.3.3.5	Linear regression .....	323

7.3.4	<i>PIXE Experiment</i>	324
7.3.4.1	Keratin target	324
7.3.4.2	Mass absorption coefficient $\mu$	325
7.3.4.3	PIXE measurements	326
7.3.5	<i>Rutherford Backscattering Spectrometry (RBS)</i>	334
7.3.5.1	Calibration of detector	334
7.3.5.2	SIMNRA simulation of RBS spectra	339
7.4	INVESTIGATION OF NORTH AMERICAN ATHAPASCAN PORCUPINE QUILL WORK FROM NATIONAL MUSEUMS SCOTLAND	341
7.4.1	<i>Porcupine quills</i>	341
7.4.2	<i>Scouring process</i>	341
7.4.3	<i>Dyeing experiments with natural dyestuffs</i>	343
7.4.4	<i>UPLC analysis</i>	345
7.4.4.1	Chemicals	345
7.4.4.2	Solutions of standards	346
7.4.4.3	Chromatographic method	346
7.4.4.4	Sample preparation	346
7.4.4.5	Calibration curves, limit of detection (LOD), limit of quantification (LOQ)	347
7.4.5	<i>Turmeric analysis</i>	349
7.4.5.1	Turmeric extraction	349
7.4.5.2	Historical samples	350
7.4.6	<i>Cochineal analysis</i>	350
7.4.6.1	Porcupine quill reference	350
7.4.6.2	Historical quills	351
7.4.7	<i>Mordant analysis by PIXE, PIGE and RBS</i>	352
7.4.7.1	Beam dose $Q$ and parameter files	352
7.4.7.2	PIXE Results	355
7.4.7.3	RBS Spectra	359
7.4.7.4	ICP-OES analysis	362

# CHAPTER 1

<b>1</b>	<b>INTRODUCTION.....</b>	<b>8</b>
1.1	HISTORICAL MATERIALS.....	9
1.1.1	<i>Historical tapestries</i> .....	9
1.1.1.1	High warp loom or “haute lice” technique.....	9
1.1.1.2	Low warp loom or “basse lice” technique.....	10
1.1.1.3	Origin of tapestry weaving in England.....	10
1.1.2	<i>Porcupine quill work</i> .....	11
1.1.2.1	Athapaskans collection at National Museums Scotland.....	12
1.2	EUROPEAN AND NORTH AMERICAN DYES SOURCES.....	13
1.2.1	<i>Natural dye classification</i> .....	14
1.2.2	<i>Direct dyes</i> .....	15
1.2.2.1	Turmeric.....	16
1.2.2.2	Safflower.....	17
1.2.2.3	Berberine containing dyes.....	18
1.2.3	<i>Mordant dyes</i> .....	19
1.2.3.1	Flavonoids.....	19
1.2.3.2	Anthraquinones.....	27
1.2.3.3	Lichens.....	33
1.2.3.4	Anthocyanidins.....	34
1.2.4	<i>Vat dyes</i> .....	35
1.2.5	<i>1856: the transition to early synthetic dyes</i> .....	37
1.3	PROTEINACEOUS FIBRES.....	39
1.3.1	<i>Protein composition and structure</i> .....	40
1.3.2	<i>Fibroin containing fibres</i> .....	40
1.3.3	<i>Keratin based fibres</i> .....	42
1.4	CONTRIBUTION OF THIS WORK.....	46
1.4.1	<i>Dye analysis and method development</i> .....	46
1.4.2	<i>Metal ion mordant analysis: method development</i> .....	47
1.5	REFERENCES.....	48

## 1 INTRODUCTION

The characterisation of dyestuffs in historical textiles is highly important as it provides technical art history information on the trade and use of specific dyestuffs, and it also informs about the level of degradation of the dyestuffs and assist conservators and curators in designing specific display and storage conditions for textiles highly degraded or containing light fugitive dyes. Flavonoid dyes such as weld (*Reseda luteola* L.), dyer's greenweed (*Genista tinctoria* L.) and anthraquinone dyes such as madder (*Rubia tinctoria* L.) or American cochineal (*Dactylopius coccus* Costa) are the main dye sources found in traditional European tradition and have been used for centuries.<sup>1, 2</sup> The characterisation of natural dyes has been developed at the University of Edinburgh and National Museums Scotland (NMS) using High Performance Liquid Chromatography coupled to Photo Diode Array detection (PDA-HPLC) and Mass Spectrometry analysis (ESI-MS), with a particular focus on understanding the fading of yellow flavonoid dyes.<sup>3-12</sup> These important studies allowed the characterisation of the main natural dye sources used in historical textiles by the relative quantification of several chemical components in acid hydrolysed extracts. However degradation, including photo-oxidation reactions, has the potential to alter these components and make the unequivocal determination of biological sources difficult.<sup>13-15</sup> One of the aims of this research is to develop new chromatographic methods that would allow the characterisation of dye components present at levels that would not be detectable using conventional chromatographic system and to investigated the dye sources used on important historical tapestry pieces and Native American porcupine quill work.

This chapter will first introduce the historical materials investigated during this research with an updated review of the main dyes sources reported to have been used in Europe and North America. Particular focus will be given to flavonoid containing dyes, which were extensively studied in previous work, and the degradation processes of flavone and flavonol dyes.<sup>6, 8, 14</sup> The chemistry and structure of

proteinaceous fibres will be reviewed and the contributions of this work to the field of historical dye analysis will be addressed.

## 1.1 HISTORICAL MATERIALS

### 1.1.1 *Historical tapestries*

Tapestry is a composite textile made of coloured silk fabric, coloured woven wool, and sometimes metallic threads made of gold or silver, incorporated in small areas of the tapestry.<sup>16-18</sup> Tapestry weaving refers to a specific technique, where two sets of yarns are interlaced, most often wool and silk, but the use of linen is reported for Swiss or German tapestry dated from the sixteenth century.<sup>16, 19</sup> It is made of two types of yarns, one running parallel to the length, that is called the warp, and one parallel to the width, called the weft.<sup>20</sup> Two weaving techniques were used called high or low warp loom techniques. In both cases, the weaver worked on the reverse side of the tapestry, and the warp threads were under tension on the loom, while the weft threads were passed back and forth across the warps.<sup>16</sup> When the tapestry is woven, all the warps are covered and the tapestry is called weft-facing.<sup>16, 20, 21</sup>

#### 1.1.1.1 High warp loom or “haute lice” technique

The high warp loom technique refers to a special set-up, where the warp threads are in a vertical loom, and the weaver works from the back (*e.g.* figure 1.1). Only one thread on two (odd and even) is under tension on the loom, usually it was the warps that were nearer the weaver that were stationary.<sup>16</sup> The set-up of the vertical threads is situated above the weaver’s head, which gives a possible explanation for its name. This technique was extensively used in France and is still used today in the Gobelins factory in Paris.<sup>20, 21</sup>

### 1.1.1.2 Low warp loom or “basse lice” technique

In the low warp loom technique, the threads are on a horizontal loom (e.g. figure 1.1), all the threads (odd and even) are under tension on the loom, and they will be powered by the weaver using two pedal controlled heddles.<sup>20, 21</sup> The disadvantage of this technique was that the tapestry was fixed and facing the weaver in an inverted position, therefore he could not follow the progression of his work.<sup>16</sup>

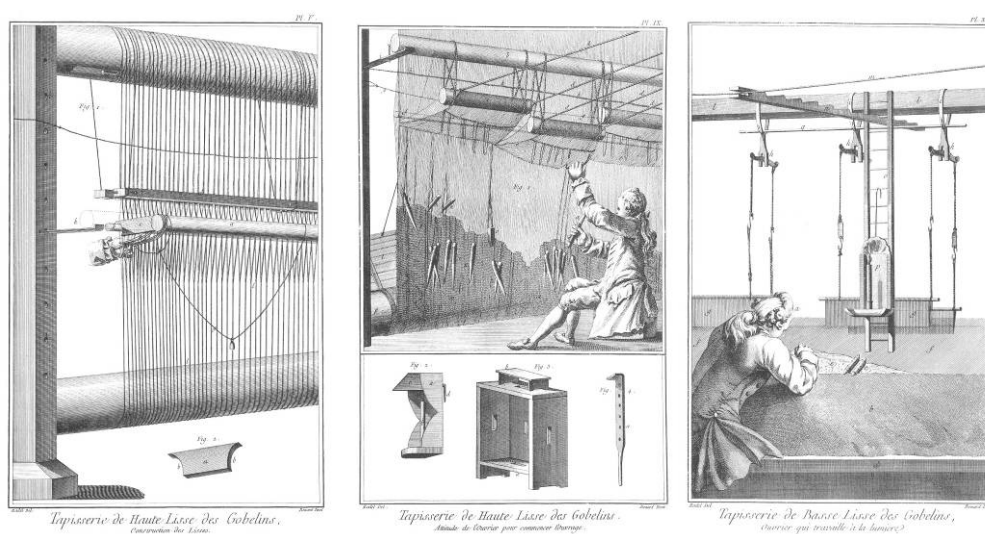


**Figure 1.1:** (left) Plate V: Gobelin High Warp Tapestry, Preparing the Looped Strings, (middle) Plate IX: Gobelin High Warp Tapestry, Position of the Workman to Start Work, (right) Plate XVIII: Gobelin Low Warp Tapestry, Workman at Work in Light. The Encyclopaedia of Diderot and d’Alembert, plates vol. 9 (1771).<sup>22 23</sup>

### 1.1.1.3 Origin of tapestry weaving in England

In contrast to the vibrant tapestry weaving industry in the Low Countries, relatively little is known on early English tapestry workshops. The early catalogue from Barnard and Wace published forty-six early English tapestries, assumed to be woven at the castle of Sir William Sheldon at Barcheston in Warwickshire.<sup>24</sup> Thus, William Sheldon could have been in charge of the first non-Royal tapestry workshop in England and since this publication the term “Sheldon” was often applied to early



English tapestries based on the assumption that this was the only workshop in England in the mid sixteenth century. However, recent art historical research from Wells-Cole and then Turner demonstrated a much complex situation in the mid sixteenth century than previously reported, with possibly other weavers' workshops in London and migration of tapestry weavers from Brussels or France to work in English workshops.<sup>25-27</sup> Today, the only pieces that are signed and clearly attributed to the Sheldon workshop are the large tapestry maps that form part of the Bodleian Library collection in Oxford, UK.<sup>28, 29</sup>

In spite of the difficulty in clearly attributing tapestries to this workshop, the first scientific study of nineteen small English tapestries which form part of the Burrell collection in Glasgow, together with the only attributed maps from the Bodleian Library, was undertaken. The identification of the dyes used in the preparation of yarns for tapestry production will provide vital information on the physical and chemical processes that the fibres have been subjected to during manufacture. It will also show if there is any consistency of dyes and materials among the Sheldon tapestries, and how these objects relate to European tapestries. This research, presented in chapter 3, will also inform future conservation and research, and influence future display strategy.

### *1.1.2 Porcupine quill work*

Indigenous communities across North America, from the North American Subarctic, Great Lakes region and the northern Plains, have long used dyed porcupine quills to decorate clothing and basketry (*e.g.* figure 1.2). Unfortunately, much more is known about the technique of porcupine quill work than the actual dyeing process and dye sources used.<sup>30-32</sup> National Museums Scotland (NMS) has the oldest and most extensive collection of nineteenth century Dene artifacts in the world today.<sup>33-36</sup> The Athapaskan and Inuit collections were collected between 1858 and 1862 and includes

around 240 Athapaskan artifacts, most of those decorated with dyed porcupine quill work.<sup>36</sup>

The analysis of dyes which have been used on museum artifacts other than textiles has received little systematic study, particularly those of non-European origin. The unique study on pre-1851 Eastern Woodlands porcupine quill work identified several dyes substances including, alkaloids, anthocyanidins, anthraquinones, indigoids species as well as several sources of tannins.<sup>37, 38</sup> Surprisingly, few flavonoid sources were identified, highlighting the need for in depth study of other cultural groups to broaden the understanding of the Native American dyeing tradition.



**Figure 1.2:** Gwich'in woman wearing headband decorated with porcupine quill work, reproduced from reference 39.<sup>39</sup>

#### 1.1.2.1 Athapaskans collection at National Museums Scotland

As part of National Museums Collection is a unique group of dyed porcupine quill samples and objects that were collected in 1862 from Sub-Arctic Athapaspan Dene people.<sup>33, 34</sup> These examples of Indigenous Art were previously described as being dyed with early synthetic dyes traded from Europe,<sup>33</sup> although the exact nature of the dyestuffs has never been scientifically investigated. As part of the development of new galleries at NMS, these objects have to be conserved for display and conditions

and regimes which will minimise damage have yet to be established. These need to be based on a better understanding of the materials and their behaviour.<sup>40</sup> Recent curatorial collaboration with the present day Northern Territories communities has revealed how significant and unique the NMS material is, especially in terms of its originality and condition.<sup>41</sup> This material will be investigated for the first time and will need the transfer of existing analytical protocols and methodology for dye analysis to porcupine quill substrates (chapter 5).

## 1.2 EUROPEAN AND NORTH AMERICAN DYES SOURCES

Natural dyes such as Madder species or shellfish purple have been used from the Antiquity, and were at that time as valuable as precious metal.<sup>1, 7</sup> The most expensive dye used in Antiquity was certainly Tyrian purple also called Imperial purple, a dye extracted from Murex shellfish (*e.g. Hexaplex trunculus*) and used to prepare Imperial silk. The extraction of the purple dye - described by Pliny the Elder - was such an expensive process that it could only be used by royalty, and it is reported that the preparation of 1 g of purple dye required the use of thousands murex shellfish.<sup>1, 7, 42</sup> Later in the Middle Ages, scarlet dyes were exclusively used for the preparation of garments for the higher members of the clergy. Several dyes have been introduced at specific times in Europe, and their presence on historical textiles can inform about trades or help to indirectly date objects. There are many examples of natural dyes traded into Europe after the discovery of the New World, these examples include: old fustic (*Chlorophora tinctoria* (L.) which was first introduced into Europe in the sixteenth century and traded from Cuba, Jamaica or Puerto Rico; American cochineal (*Dactylopius coccus Costa*) which was used in Europe from the early sixteenth century and traded from South America; American oak (*Quercus tinctoria* L.) which was used in Europe from the late eighteenth century and traded from North America.<sup>1, 2, 7</sup>

With regard to the North American quill work investigated during this research, mauve and fuchsine aniline dyes would have been already commercially available in

Europe in 1862.<sup>43, 44</sup> Trades between North America and Europe was at that time a very important business due to the fur trade and exchange of material between both continents was facilitated through the Hudson Bay's company.<sup>45, 46</sup> Furthermore, several sources mention, at least for Micmac porcupine quill work, that early synthetic dyes were quickly adopted as a replacement of natural dyes.<sup>47</sup>

### 1.2.1 Natural dye classification

Natural dyes are classified in three categories: direct dyes, mordant dyes and vat dyes.<sup>1, 2</sup> Direct dyes, *e.g.* safflower (*Carthamus tinctorius* L.) or curcuma (*Curcuma longa* L.), are applied directly to the fibre but usually are less wash- and light-fast than vat or mordant dyes (see section 1.2.2). Mordant dyes, *e.g.* weld (*Reseda luteola* L.) and madder (*Rubia tinctorum* L.), represent the vast majority of the natural dyes (see section 1.2.3). Their use requires a treatment of the textile with an aqueous solution of mordant, generally a metal salt of aluminium, copper or iron. The treatment of the fibre with a mordant can occur before the dyebath, referred to as a pre-mordanting treatment, or during the dyebath.<sup>1, 2</sup> During this treatment the mordant is absorbed by the fibre and a mordant-fibre complex or dye-mordant-fibre is created.<sup>7</sup> The use of a mordant increases the affinity of the dye components with the protein side chains of the wool or silk and assists in the formation of an insoluble coloured complex during the dyebath (figure 1.3).<sup>7</sup>

The choice of the mordant is important in the textile preparation as it will affect greatly the final colour of the textile: for example the use of copper salts will darken the colour of the dye while in contrast the use of tin salts will brighten the colour. There are many sources of mordant reported in the literature. Sources of aluminium include several biological accumulators of aluminium (*e.g.* *Diphasiastrum complanatum* L., *Diaphasiastrum alpinum* L. or *Huperzia selago* L.), potash alum [AlK(SO<sub>4</sub>)<sub>2</sub>·12H<sub>2</sub>O], or ammonium alum [Al<sub>2</sub>(NH<sub>4</sub>)<sub>2</sub>(SO<sub>4</sub>)<sub>4</sub>·12H<sub>2</sub>O].<sup>7, 48</sup> Sources of iron include green copperas, iron sulfate [Fe<sub>2</sub>(SO<sub>4</sub>)<sub>3</sub>] or iron oxide Fe<sub>2</sub>O<sub>3</sub>, while

copper mordant was obtained from copper sulfate  $[\text{CuSO}_4]$  and tin mordant was prepared from the dissolution of pewter in concentrated nitric acid (*aqua fortis*) replaced later by tin salts  $[\text{SnCl}_2]$ .<sup>2</sup> Finally, chromium mordant was not used until early in the nineteenth century and was obtained mainly from sodium or potassium bichromate  $[\text{K}_2\text{Cr}_2\text{O}_7]$ .

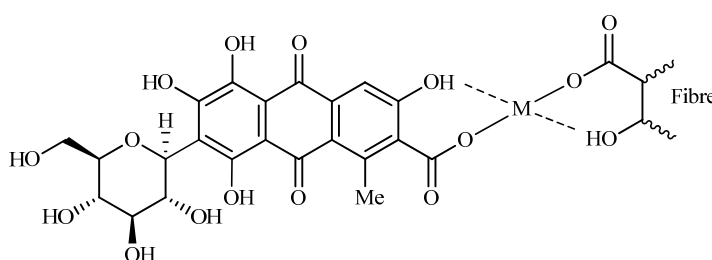


**Figure 1.3:** Example of complex formed between an anthraquinone dye molecule and a metallic mordant (M) and the side groups of a proteinaceous fibre chains, adapted from reference 6.<sup>6</sup>

Finally vat dyes, *e.g.* woad (*Isatis tinctoria L.*) and indigo (*Indigofera tinctoria L.*) are insoluble in water and require a specific treatment (see section 1.2.4). The textile is prepared under alkaline conditions in order to convert the indigo dye into a colourless and soluble leuco form. After the dyeing process, aerial oxidation reconverts the leuco dye into its insoluble form and the dye aggregates on the surface of the fibre.<sup>1, 7, 49</sup>

### 1.2.2 Direct dyes

Direct dyes, *e.g.* turmeric (*Curcuma longa L.*) and safflower (*Carthamus tinctorius L.*) are applied directly to the fibre but usually are less wash and light fast than mordant dyes.

### 1.2.2.1 Turmeric

Turmeric or curcuma, also known as Indian saffron, is obtained from the ground roots of *Curcuma domestica* Valet. (or *Curcuma longa* L.), a plant growing abundantly in the East Indies, Indonesia and China. It is a perennial herbaceous plant of the ginger family (Zingiberaceae), the colouring principle is extracted from the roots of the curcuma by washing, peeling and drying.<sup>50</sup> Turmeric is a rich source of phenolic compounds called curcuminoids and the extract of the roots of *Curcuma longa* L. contain three different diarylheptanoids: curcumin (**1**), demethoxycurcumin (**2**) and bisdemethoxycurcumin (**3**). These compounds are widely used as food additives but also in herbal medicine and several studies have shown a wide range of biological activities, including anti-arthritic effects, anti-oxidant, anti-inflammatory, anti-microbial, anti-parasitic, anti-mutagenic, and anti-cancer properties.<sup>51-53</sup>

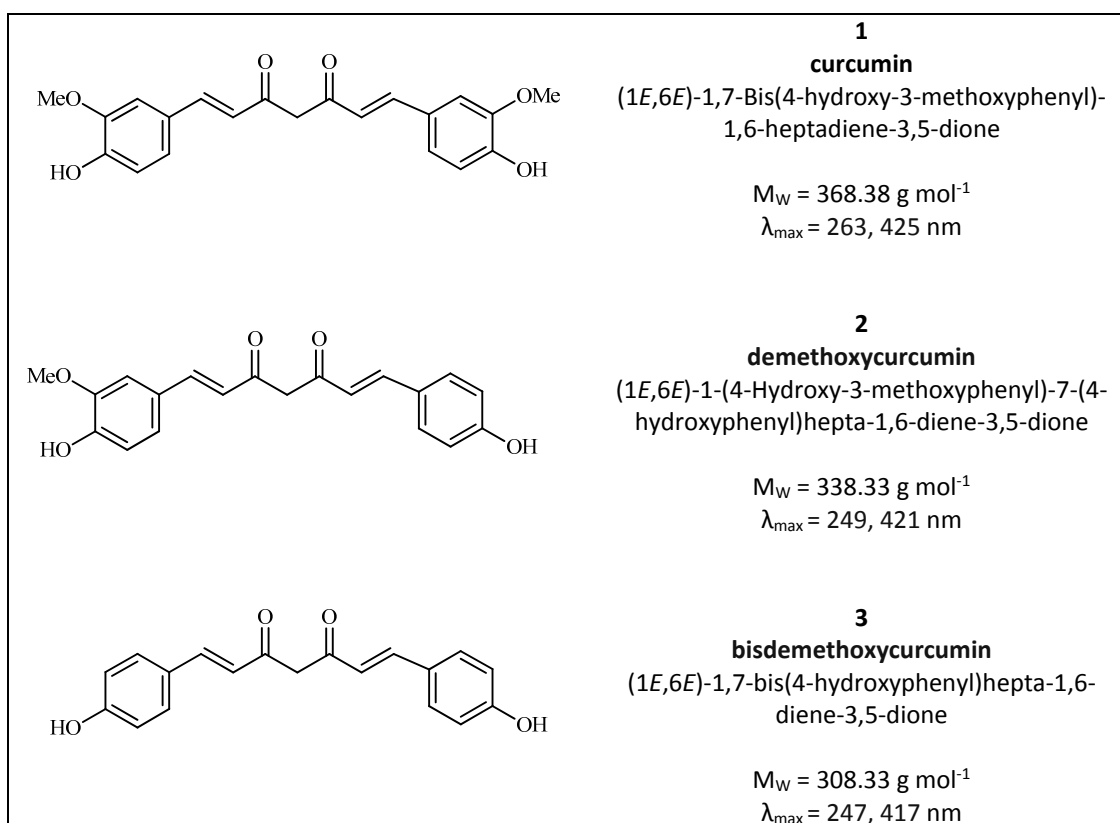


**Table 1.1:** Diarylheptanoids present in the roots of *Curcuma longa* L. species.

Turmeric can be used as a pigment or a direct dye; in its powdered form it provides a strong yellow colour. In parts of Asia turmeric water is applied as a cosmetic to lend a golden glow to the skin.<sup>50</sup> It can also be used a direct dye on cotton, wool or silk, mainly in combination with other dyes. Turmeric is frequently found in ethnographical collection and previous study has highlighted conservation problems linked to objects containing turmeric (*e.g.* poor light fastness, discoloration under acidic condition).<sup>50</sup>

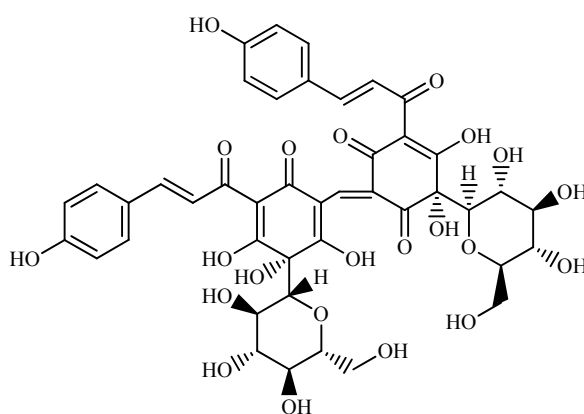
Several studies of *Curcuma longa* L. showed that the relative amounts of the curcuminoids characterised in turmeric sources is highly variable.<sup>54, 55</sup> Most of the samples collected from Sichuan areas in China, exhibited a similar composition, with curcumin (**1**) being the main component present in the turmeric extract, while samples of turmeric collected from Yunnan, Burma or India were found to contain a higher level of demethoxycurcumin (**2**).<sup>54, 55</sup>

#### 1.2.2.2 Safflower

Safflower (*Carthamus tinctorius* L.) is an annual herb of the *Asteraceae* family and has long been used as a pigment or a dye in oriental countries and is very often cited in traditional Chinese textile recipes.<sup>56</sup> Although recipes to prepare safflower sometimes appear in European dyeing textbooks,<sup>2</sup> it has been rarely characterised in European historical textiles.<sup>57</sup> Safflower contains several colouring components (yellow and red), with the red pigment carthamin (**4**) being present in powdered flower petals to the extent of 0.03 % by weight.<sup>7, 58</sup> Carthamin (**4**) is insoluble in neutral conditions but is soluble in alkaline conditions, and the re-acidification of the solution will precipitate the carthamin pigment on the fibres.<sup>7, 56</sup> Safflower produces very light fugitive pink shades when used as a direct dye on silk.<sup>56, 59</sup>

Carthamin (**4**) was first isolated in the early twentieth century and its structure has been characterised as two chalcone moieties which are fully conjugated.<sup>60</sup> The red colour of carthamin (**4**) is due to the absorption of longer wavelength of light than

those of other chalcone pigments.<sup>61, 62</sup> Recent studies have shown that it is possible to improve the content of red pigment in the flowers of safflower, by converting precarthamin into carthamin enzymatically, using a purified enzyme from the yellow petals of safflower.<sup>63</sup> The identification of safflower in historical textile is very challenging, as carthamin (**4**) pigment has a very high photo-degradation rate and is also easily destroyed during acidic extraction. However, a recent study characterised several colourless markers present in textiles extracts, but chemically these are still unidentified.<sup>56</sup> Furthermore traces of two flavonoid components, apigenin (**10**) and kaempferol (**17**), were also characterised in safflower references, with only apigenin (**10**) being present in historical samples.<sup>56</sup>

**4****carthamin**

(2Z,6S)-6-β-D-Glucopyranosyl-2-[[[(3S)-3-β-D-glucopyranosyl-2,3,4-trihydroxy-5-[(2E)-3-(4-hydroxyphenyl)-1-oxo-2-propenyl]-6-oxo-1,4-cyclohexadien-1-yl]methylene]-5,6-dihydroxy-4-[(2E)-3-(4-hydroxyphenyl)-1-oxo-2-propenyl]-4-cyclohexene-1,3-dione

$$M_w = 910.78 \text{ g mol}^{-1}$$

$$\lambda_{\max} = 245, 373, 520 \text{ nm}$$

### 1.2.2.3 Berberine containing dyes

Several alkaloid species containing berberine (**5**) can be used as direct dyes to produce yellow to orange hues, although they are not light fast.<sup>1, 64</sup> Alkaloids form a large group of N-containing components<sup>65</sup> that are more often studied for their uses



in medical preparations (*e.g.* morphine, colchicine, strychnine, caffeine) rather than for their dyeing properties.<sup>65</sup> Berberin was first isolated in the late nineteenth century,<sup>66-68</sup> and berberine containing dyes are an important yellow dye source in Asia.<sup>64</sup> The use of berberin rich dyestuffs was also recently characterised in Eastern Woodlands porcupine quill work,<sup>37, 38</sup> where three alkaloid species were identified: Tisavoyanne yellow (*Helleborus trifolis* L.), goldenseal (*Hydrastis Canadensis* L.) - both species mainly containing berberine (**5**) - and bloodroot (*Sanguinaria Canadensis* L.), an alkaloid species containing berberine (**5**) and sanguinarine (**6**).

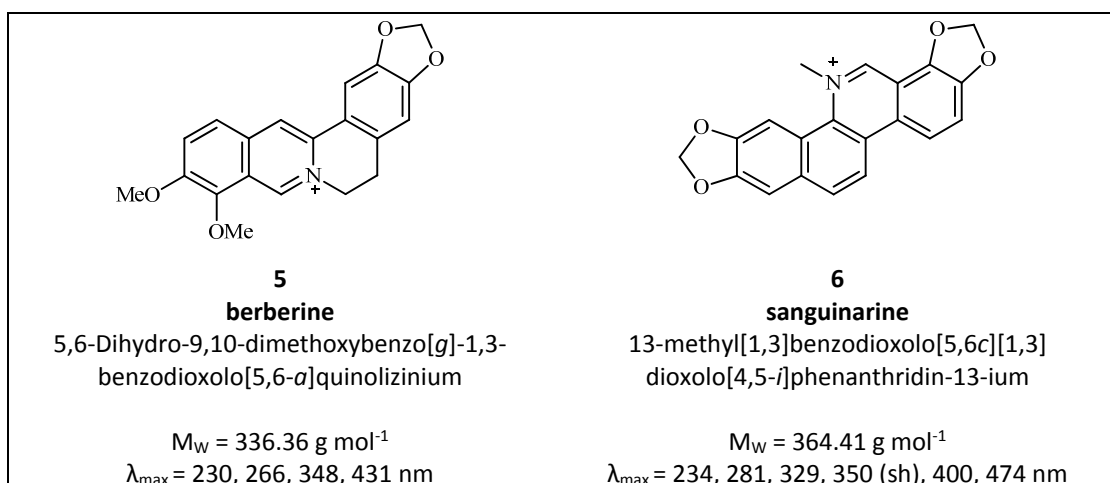


**Table 1.2:** alkaloid dyes characterised in Eastern Woodlands porcupine quill work.

### 1.2.3 Mordant dyes

Mordant dyes, *e.g.* weld (*Reseda luteola* L.) and madder (*Rubia tinctorum* L.), represent the vast majority of the natural dyes. Their use requires a treatment of the textile with an aqueous solution of mordant, generally a metal salt.

#### 1.2.3.1 Flavonoids

The majority of natural yellow dyestuff species contain flavonoid dyes. These dyes are mordant dyes and bind to the metal *via* the carbonyl group and the adjacent

phenol moiety. Flavonoid sources have been extensively studied in the past decades due to their antioxidant properties but recently there has also been a renewed interest in their use for textile dyeing as a replacement to synthetic dyes.<sup>69</sup> Flavonoid dyes occur in many plants as sugar derivatives (glycosides) and are hydrolysed in the dyebath into their parent flavonoids. There are two types of flavonoid dye sources, some species containing flavone dyes *e.g.* weld (*Reseda luteola* L.) and other containing flavonol dyes *e.g.* old fustic (*Chlorophora tinctoria* L.), quercitron bark (*Quercus velutina* Lamk) or onion skins (*Allium cepa* L.).<sup>7</sup> Flavone and flavonol dyes differ only by the presence of a hydroxyl group in the position 3 on the C-Ring in flavonol dyes (figure 1.4).

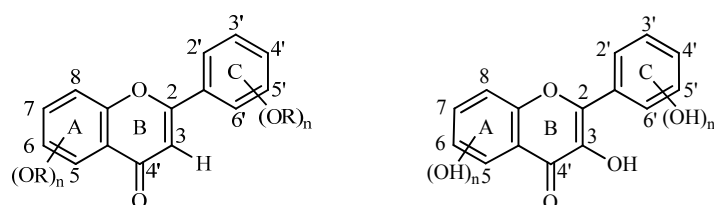
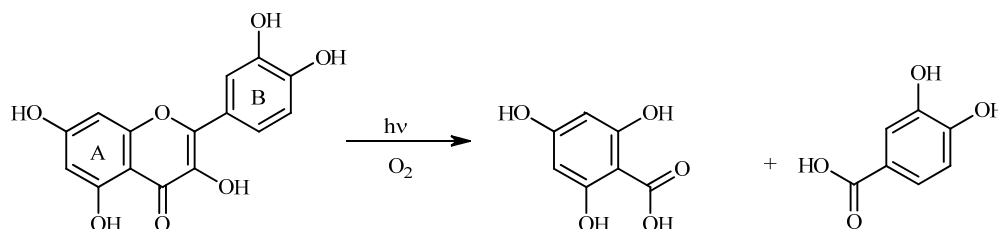


**Figure 1.4:** (left) IUPAC structure of flavone dyes; (right) IUPAC structure of flavonol dyes

Flavonol dyes are much more sensitive to photo-degradation than flavone dyes,<sup>6, 13-15</sup> and photo-oxidation studies of quercetin in solution showed that the main end products of this degradation process were 2,4,6-trihydroxy benzoic acid and 3,4-dihydroxy benzoic acid arising from both the A and the B ring of the flavonol (scheme 1.1).<sup>70</sup> As a result these plants were generally banned from the manufacture of important or expensive textiles due to their poor light fastness.<sup>1, 2, 71</sup> From previous studies, the yellow dye component most commonly detected in acid-hydrolysed extracts from historical European textiles is luteolin (**9**), a flavone which has the best light fastness of all the flavonoids found in yellow plant dyes. There are many dye sources containing luteolin, but weld (*Reseda luteola* L.) is the main source mentioned, but other dye plants containing luteolin, including sawwort

(*Serratula tinctoria* L.) and dyer's greenweed (*Genista tinctoria* L.), were acknowledged substitutes.<sup>71, 72</sup>

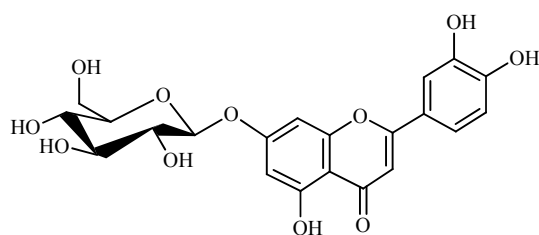


**Scheme 1.1:** Photo-oxidation mechanism of flavonol.<sup>70</sup>

### Weld

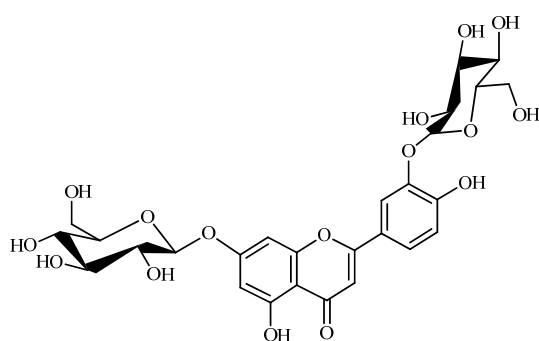
Weld (*Reseda luteola* L.) is one of the most important yellow dye source; it grows wild in most of Europe and produces a bright and fast yellow. The main constituents of weld have been well studied and include luteolin-7-*O*'-glucoside (**7**), luteolin-7,3'-di-*O*'-glucoside (**8**) and the aglycone luteolin (**9**).<sup>1, 7, 73, 74</sup> Seven other minor components including the aglycones apigenin (**10**) and chrysoeriol (**12**), together with mono and diglycosides of all three aglycones have been also identified in weld extracts.<sup>9, 75-77</sup>

The presence of weld in historical yarns is characterised by the association in the acid hydrolysed extract of the flavones luteolin (**9**) detected along with a relatively minor amount of the flavone apigenin (**10**) and the *O*-methylated flavone chrysoeriol (**12**),<sup>9, 10</sup> while the *O*-glycoside sugar derivatives present in weld extracts are usually hydrolysed to the parent flavonoid in the dye bath or during the acidic extraction.<sup>78</sup> Published accelerated light ageing studies of wool yarns dyed with weld showed that the flavones luteolin (**9**), apigenin (**10**) and *O*-methylated flavone chrysoeriol (**12**) have quite similar photo-degradation rates, although the photo-degradation rate of luteolin (**9**) and chrysoeriol (**12**) was observed to be slightly higher than the flavone apigenin (**10**).<sup>8</sup>



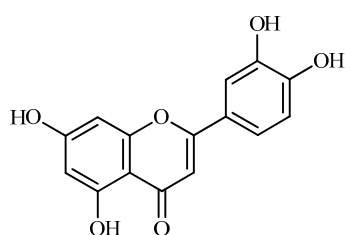
**7**  
**luteolin-7-*O'*-glucoside**  
7-*O*-beta-D-Glucosyl-5,7,3,4-  
tetrahydroxyflavone

$M_w = 448.37 \text{ g mol}^{-1}$   
 $\lambda_{\text{max}} = 255, 267 \text{ (sh)}, 350 \text{ nm}$



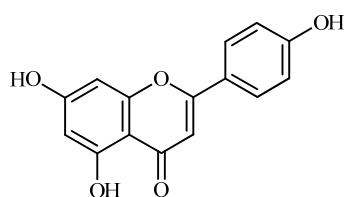
**8**  
**luteolin-7,3'-di-*O'*-glucoside**  
7,3'-*O*-beta-D-Glucosyl-5,7,3,4-  
tetrahydroxyflavone

$M_w = 610.53 \text{ g mol}^{-1}$   
 $\lambda_{\text{max}} = 269, 339 \text{ nm}$



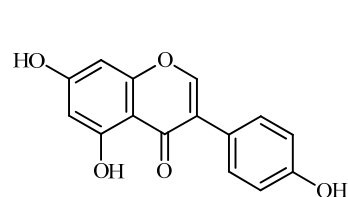
**9**  
**luteolin**  
3',4',5,7-Tetrahydroxyflavone

$M_w = 286.24 \text{ g mol}^{-1}$   
 $\lambda_{\text{max}} = 254, 266, 292 \text{ (sh)},$   
347 nm



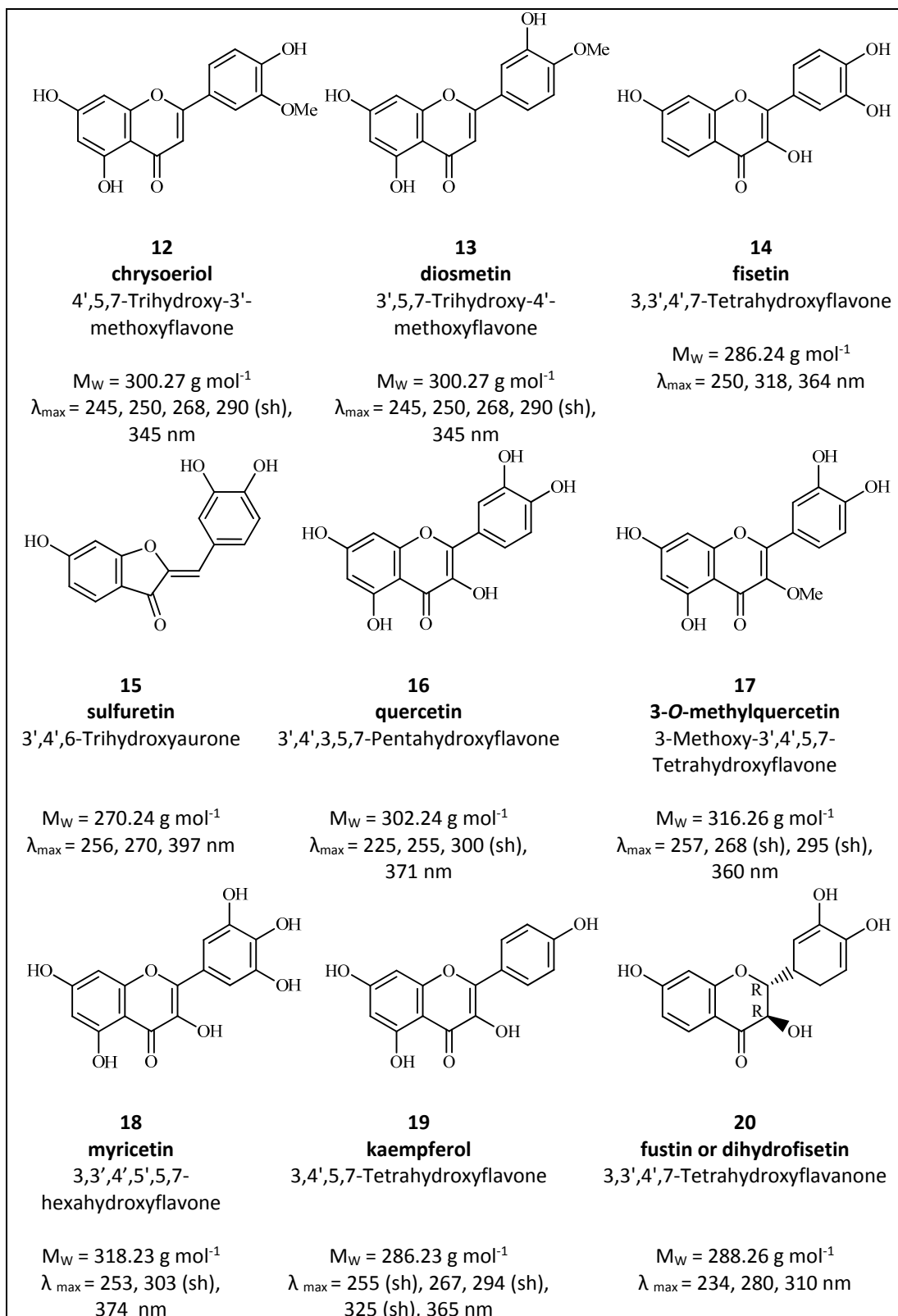
**10**  
**apigenin**  
4',5,7-Trihydroxyflavone

$M_w = 270.24 \text{ g mol}^{-1}$   
 $\lambda_{\text{max}} = 268, 300 \text{ (sh)}, 338 \text{ nm}$



**11**  
**genistein**  
4',5,7-Trihydroxyisoflavone

$M_w = 270.24 \text{ g mol}^{-1}$   
 $\lambda_{\text{max}} = 260, 334 \text{ (sh)} \text{ nm}$



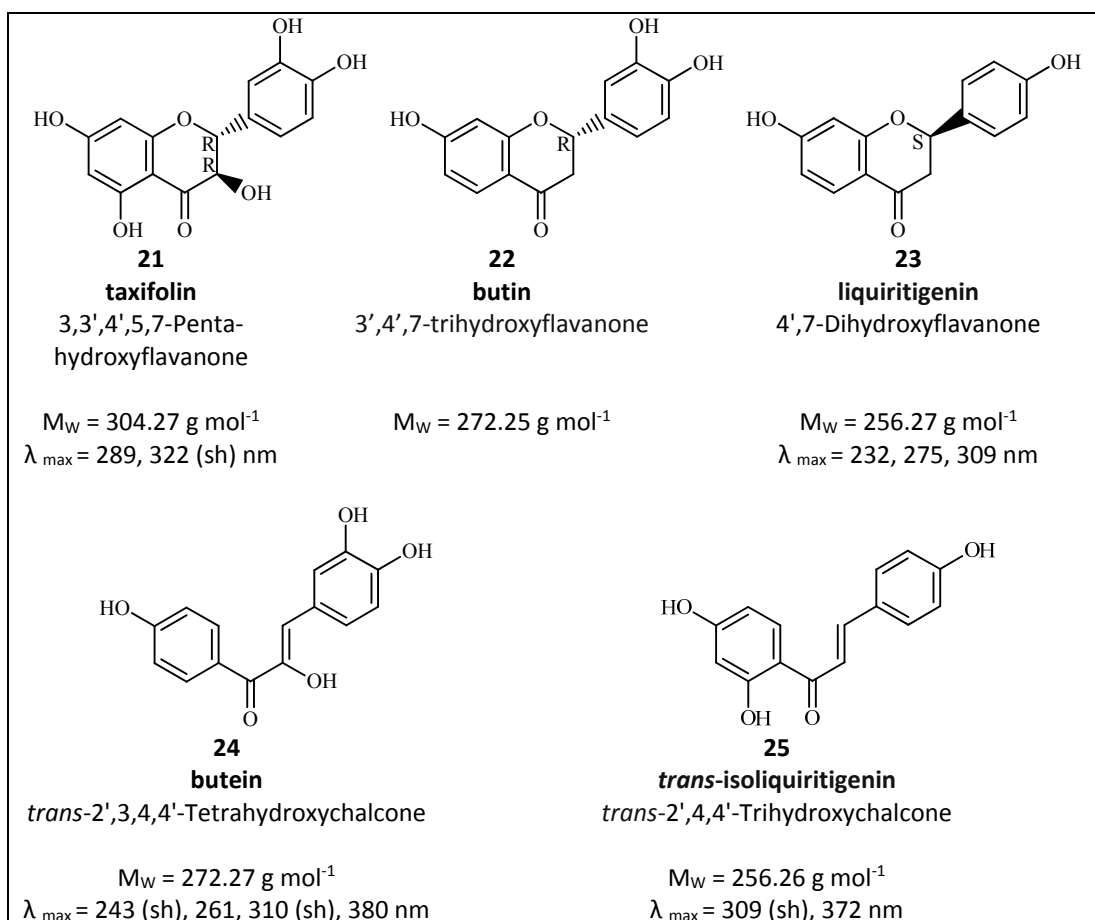


**Table 1.3:** Flavonoid dyes characterised in historical textiles.

### *Dyer's greenweed*

The second important flavonoid yellow dye source is dyer's greenweed (*Genista tinctoria* L.) that grows wild throughout Central and Southern Europe. The genus *Genista* L. (Leguminosae) consists of 87 species predominantly distributed in the mediterranean area that contain flavones, glycoflavones and a high concentration of isoflavones, particularly substituted isoflavones such as 5-methylgenistein and *O*-glucosylated isoflavones.<sup>79</sup> Different glycosides of the flavones luteolin (**9**) and apigenin (**10**) and the isoflavone genistein (**11**) are known dye components of this species.<sup>80, 81</sup>

Yarns dyed with dyer's greenweed (*Genista tinctoria* L.) are characterised by the presence in their acid hydrolysed extracts of the flavones luteolin (**9**), the isoflavone genistein (**11**) detected along with a relatively minor amount of the aglycones apigenin (**10**) and *O*-methylated flavone diosmetin (**13**).<sup>7, 8, 81</sup> Although genistein (**11**) is the main dye component found in many varieties of broom, the dye source is usually thought to be dyer's greenweed.<sup>1, 6</sup> The investigation of silk and wool yarns prepared with dyer's greenweed showed that the relative amount of the flavonoid components present in the acid hydrolysed extract was dependant on the dyeing process.<sup>8</sup> Genistein (**11**) was found to be the main dye component present on yarns subjected to a single dyebath process, while luteolin (**9**) was found to be predominant on yarns subjected to an over dyeing process.<sup>8</sup>

Accelerated light ageing studies showed that genistein (**11**) has a relatively slow photo-degradation rate compared to the other dye components luteolin (**9**) and apigenin (**10**) and although its relative amount was found to be very variable on the dyed yarns, its presence in the acid hydrolysed extract acted as a "marker" in historical samples.<sup>8</sup> Dyer's greenweed was judged to be a lower quality dye compared to weld, nevertheless it has been characterised as one of the main yellow dye source in a set of samples taken from sixteenth century Brussels' tapestries.<sup>2, 8</sup>

#### *Young fustic*

Young Fustic (*Cotinus coggygia* S.) is a yellow wood and was originally found in Italy, the Near East, Eastern Europe as well as France and Spain; it is obtained from the heartwood or inner part of the bark of the tree. This dye has been used since the Middle Ages for dyeing dark shades of yellow, but it can also produce when mordanted orange-yellow to strong red-brown colours.<sup>7</sup> Several flavonols have been reported in this dye source, including fisetin (**14**) and myricetin (**17**) and the aurone sulfuretin (**15**).<sup>1, 6, 7</sup> Recent investigation of *Cotinus coggygia* S. heartwood isolated in addition to fisetin (**14**) and sulfuretin (**15**), the flavonol quercetin (**16**), and several

flavanol components including fustin (**20**), taxifolin (**21**), butin (**22**), liquiritigenin (**23**), butein (**24**), 4',5,7-trihydroxyflavanone and *trans*- isoliquiritigenin (**25**).<sup>82</sup>

The investigation of wool yarns dyed with young fustic characterised most of the dye components mentioned above, with the exception to myricetin (**18**).<sup>8, 82</sup> It was also shown that the flavanol fustin was transformed into the flavonol fisetin during the dyeing process.<sup>82</sup> The analysis of accelerated light aged yarns showed that the relative ratio of fisetin and sulfuretin was not affected and was comparable to those observed in historical samples.<sup>82</sup> Young fustic was known to be a very light fugitive dye and was therefore often used for the production of lower value textiles, it was also used to dye the silk inside decorative metal threads decoration.<sup>8</sup>

#### *Sawwort*

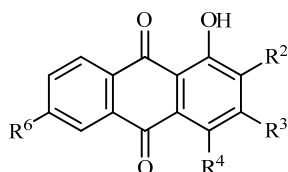
Sawwort (*Serratula tinctoria* L.) is a yellow dye source sometimes mentioned in the European dyeing text books.<sup>71, 72</sup> The main flavonoids present in sawwort (*Serratula tinctoria* L.) leaves are luteolin (**9**) and its corresponding glycoside luteolin-7-*O*-glucoside (**7**), luteolin-4'-*O*-glucoside and 3-methylquercetin,<sup>73, 83</sup> Yarns dyed with sawwort are characterised by the association in the acid hydrolysed extract of the flavones luteolin (**9**) and apigenin (**10**) as well as minor amounts of the flavonol components quercetin (**16**), 3-*O*-methylquercetin (**17**) and kaempferol (**19**).<sup>8, 15, 83</sup> The investigation of un-aged and light aged sawwort samples showed that the minor flavonol components quercetin, 3-*O*-methylquercetin (**17**) and kaempferol (**19**) were very sensitive to photo-oxidative degradation and therefore could not be used as "markers" in historical samples.<sup>8, 13, 15</sup> Accelerated light ageing studies confirmed that only the flavones luteolin (**9**) and apigenin (**10**) were found in acid hydrolysed extracts of aged sawwort samples and highlighted the importance of identifying the presence of the aglycone chrysoeriol to differentiate sawwort (*Serratula tinctoria* L.) from weld (*Reseda luteola* L.).<sup>8, 15</sup>



### 1.2.3.2 Anthraquinones

#### *Madder species*

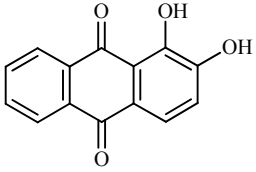
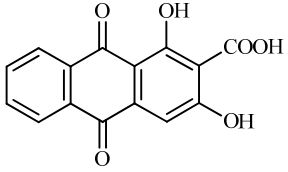
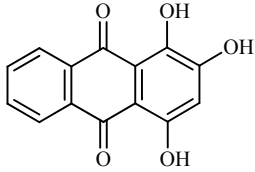
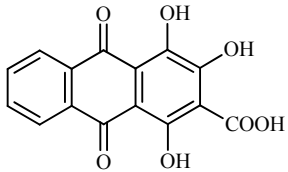
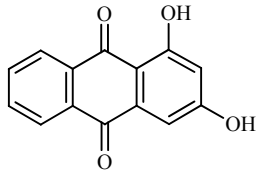
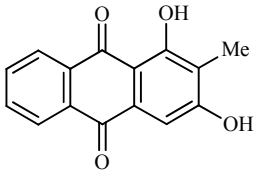
Madder is one of the most important red dye species, it is based on the anthraquinone ring system substituted in only one of the rings (figure 1.5). Madder dyes can be obtained from the roots of different species of the Rubiaceae family including madder (*Rubia tinctorum* L.), wild madder (*Rubia peregrina* L.), munjeet (*Rubia cordifolia* L.), ladies' bedstraw (*Galium verum* L.) and several species of *Relbunium* native to South America.<sup>1, 2, 7</sup> Madder was usually used to produce red colours but it could also produce pinks to purples shades depending on the mordant used.<sup>7</sup> In traditional North American porcupine quill work, the roots of stiff marsh bedstraw (*Galium tinctorium* L. Scop) are reported to have been used by Native Americans to produce red porcupine quillwork.<sup>1, 84</sup> The exact composition of the dyestuffs found in the roots of *Galium tinctorium* L. is not well studied rendering identification of the madder species on porcupine quill work difficult.<sup>37, 38</sup>



**Figure 1.5:** IUPAC structure of anthraquinones dyes.

Madder species contain a complicated mixture of anthraquinones including: alizarin (**26**), munjistin (**27**), purpurin (**28**), pseudopurpurin (**29**), xanthopurpurin (**30**) and rubiadin (**31**) and associated glycosides.<sup>64, 85</sup> The anthraquinone contents of madder roots are complex and several studies have shown that the concentration of the different anthraquinones found within the same *Rubia* species is highly variable depending on the age and the environment of the plant inducing variability in the proportion of dyestuffs extracted from the roots of the plant.<sup>86-88</sup> Furthermore, the use of a strong acidic extraction during sample preparation induces the

decarboxylation of several anthraquinones, especially pseudopurpurin (**29**) and munjistin (**27**), as well as the hydrolysis of the glycoside precursors into their aglycone forms, which further complicates the identification of specific species.<sup>64, 89.</sup>  
<sup>90</sup> The main compounds found in extracts of various species of *Rubia* or *Rubia*-dyed textiles can be found in table 1.4.<sup>91</sup>

 <p><b>26</b> <b>alizarin</b> 1,2-dihydroxyanthraquinone</p> <p><math>M_w = 240.21 \text{ g mol}^{-1}</math> <math>\lambda_{\text{max}} = 230 \text{ (sh), 248, 280, 433 nm}</math></p>	 <p><b>27</b> <b>munjistin</b> 1,4-dihydroxyanthraquinone - 2-carboxylic acid</p> <p><math>M_w = 284.22 \text{ g mol}^{-1}</math> <math>\lambda_{\text{max}} = 247, 289, 420 \text{ nm}</math></p>	 <p><b>28</b> <b>purpurin</b> 1,2,4-trihydroxyanthraquinone</p> <p><math>M_w = 256.21 \text{ g mol}^{-1}</math> <math>\lambda_{\text{max}} = 256, 296, 456, 482, 515 \text{ nm}</math></p>
 <p><b>29</b> <b>pseudopurpurin</b> 1,2,4-trihydroxyanthraquinone 3-carboxylic acid</p> <p><math>M_w = 300.24 \text{ g mol}^{-1}</math> <math>\lambda_{\text{max}} = 258, 283 \text{ (sh), 474, 494, 526 (sh) nm}</math></p>	 <p><b>30</b> <b>xanthopurpurin</b> 1,3-dihydroxyanthraquinone</p> <p><math>M_w = 240.24 \text{ g mol}^{-1}</math> <math>\lambda_{\text{max}} = 246, 284, 415 \text{ nm}</math></p>	 <p><b>31</b> <b>rubiadin</b> 1,3-Dihydroxy-2-methylanthraquinone</p> <p><math>M_w = 254.26 \text{ g mol}^{-1}</math> <math>\lambda_{\text{max}} = 241 \text{ (sh), 245, 279, 414 nm}</math></p>

**Table 1.4:** Anthraquinone dyes characterised in madder species.

*Rubia tinctorum* L. is the most common species of madder and probably also the most studied.<sup>92-95</sup> The roots of *Rubia tinctorum* L. contain an alizarin precursor, ruberythric acid and the primeveroside of lucidin (**17**), that are usually converted into

alizarin (**26**) and lucidin (table 1.5, entry 17) during dyeing process. Lucidin is usually not observed in dyed textiles<sup>91</sup> and it has been suggested that lucidin oxidises to nordamnacanthol (table 1.5, entry 18) in the presence of oxygen by endogenous enzymes<sup>96</sup> or that is converted enzymatically to a quinone groups (see table 1.5).<sup>91, 97</sup> It was assumed that the presence of munjistin (**27**) was characteristic of *Rubia munjista* L., while the presence of rubiadin (**31**) was characteristic of *Rubia peregrina* L..<sup>89</sup> However, a recent study has shown that there are no reliable markers to distinguish both species and that textiles dyed with *Rubia peregrina* L. and *Rubia munjista* L. both contain mostly purpurin (**28**), munjistin (**27**) and pseudopurpurin (**29**), but little or no alizarin (**26**) or 6-hydroxyrubiadin.<sup>91</sup> The same study has shown that it is however relatively easy to distinguish *Rubia akane* L., *Rubia tinctorum* L. and *Rubia cordifolia/Rubia peregrina* L. from each other, as they contain 6-hydroxyrubiadin, alizarin and purpurin (only), respectively, as unique markers.<sup>91</sup> Finally, rubiadin (**31**) was found to be present in varying amounts in textiles dyed with several species of madder and was dismissed as a reliable marker for *Rubia peregrina* L..<sup>91</sup> Accelerated light ageing studies of wool yarns dyed with alizarin, purpurin and *Rubia tinctorum* L. showed that purpurin (**26**) exhibited a higher photo-degradation rate than alizarin (**28**).<sup>98</sup>

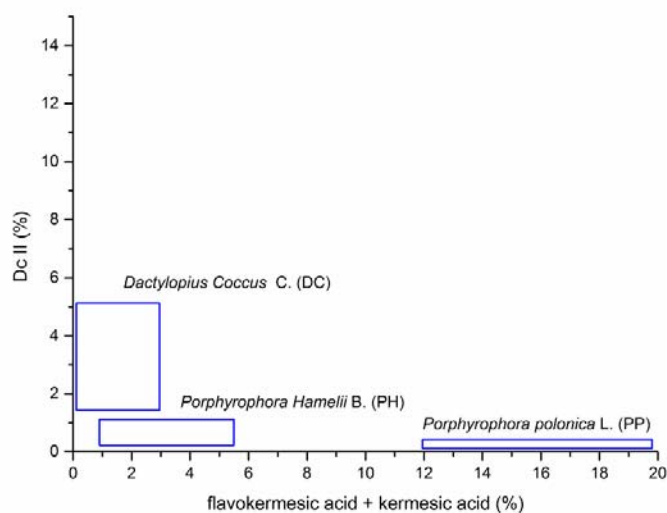
Entry	Common Name	Substituent				$M_w$ g mol <sup>-1</sup>
		R <sub>2</sub>	R <sub>3</sub>	R <sub>4</sub>	R <sub>6</sub>	
1	Alizarin ( <b>26</b> )	OH	H	H	H	240
2	Munjistin ( <b>27</b> )	COOH	OH	H	H	284
3	Munjistin+Glc	COOH	OGlc	H	H	446
4	Purpurin ( <b>28</b> )	H	OH	OH	H	256
5	Pseudopurpurin ( <b>29</b> )	COOH	OH	OH	H	300
6	Pseudopurpurin+Glc	COOH	OH	OGlc	H	462
7	Xanthopurpurin ( <b>30</b> )	H	OH	H	H	240
8	Rubiadin ( <b>31</b> )	CH <sub>3</sub>	OH	H	H	254
9		CH <sub>3</sub>	OGlc+Rha+2Ac	H	OH	662
10		CH <sub>3</sub>	OGlc+Rha+2Ac	H	OH	662
11		CH <sub>3</sub>	OGlc+Rha+Ac	H	OH	620

12		CH <sub>3</sub>	OGlc+Rha	H	OH	578
13	6-Hydroxyrubiadin	CH <sub>3</sub>	OH	OH	H	270
14	Galiosin	COOH	OH	OGlc+Xyl	H	594
15	Ruberythric acid	OGlc+Xyl	H	H	H	534
16	Lucidin primeveroside	CH <sub>2</sub> OH	OGlc+Xyl	H	H	564
17	Lucidin	CH <sub>2</sub> OH	OH	H	H	270
18	Nordamnacanthol	CHO	OH	H	H	268

**Table 1.5:** List of compounds found in extracts of various species of Rubia or Rubia-dyed textiles, abbreviations refers to anthraquinone substituents in structure above: Glc, glucose; Rha, rhamnose; Xyl, xylose; Ac, Acetyl, from reference 91.<sup>91</sup>

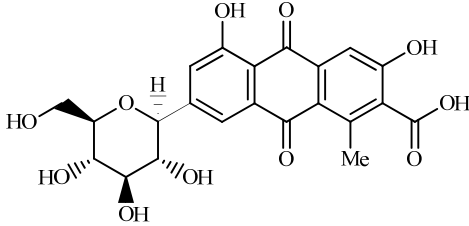
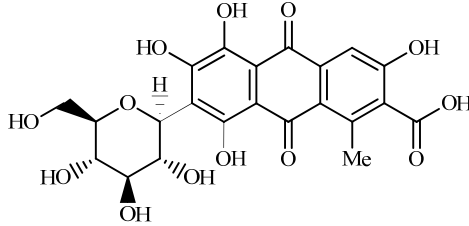
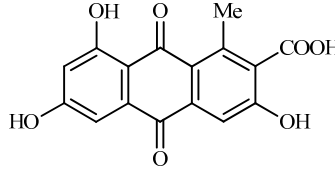
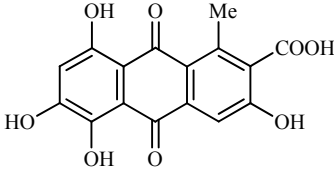
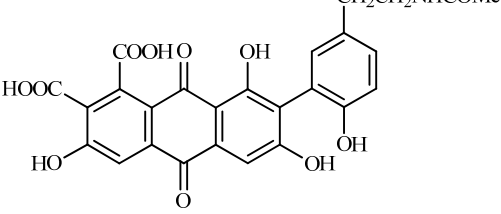
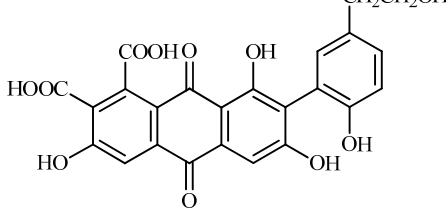
### *Insect dyes*

Red insect dyes were one of the most precious natural red dyes, due to their intense hues and colour fastness.<sup>7</sup> The chromophores present in scale insect dyes are derivatives of anthraquinone (figure 1.5) and these dyes were mainly used as mordant dyes binding to the metal *via* the carbonyl and the adjacent phenol groups.<sup>99</sup> Several plant parasitic scales insect from the Coccidea family were used for the preparation of red dyes and historical documents specifically refer to five insect species: kermes (*Kermes vermilio* Planchon), lac dye (*Kerria lacca* K.), Polish cochineal (*Porphyrophora polonica* L.), Armenian cochineal (*Porphyrophora hamelii* Brandt) and American cochineal (*Dactylopius coccus* Costa).<sup>1, 2, 100-102</sup> However, a recent taxonomic revision of the *Porphyrophora* and *Dactylopius* genus has revealed the existence of 57 different cochineal species, meaning that other species might have been also used.<sup>103-105</sup> Kermes was the main insect red dye used in Europe until the sixteenth century when it was widely replaced by American cochineal.<sup>101-103</sup> The main components of the kermes dye are kermesic acid (**34**) and flavokermesic acid (**35**), while the main component found in the acid hydrolysed extract of cochineal species is carminic acid (**33**), see figure 1.6.



**Figure 1.6:** Graphical interpretation of the composition of the acid hydrolysed extract of the three important insect dye sources found in historical textiles, using the relative amounts of the peak areas integrated at 275 nm, from reference 106.<sup>106, 107</sup>

Previous studies have shown that the identification of cochineal species in historical textiles can be based on a graphical system involving the integration of peak areas at 275 nm from several minor markers called Dc II (**32**), Dc IV, Dc VII, flavokermesic acid (**35**) and kermesic acid (**34**).<sup>89, 107</sup> However, a recent analytical study based on multivariate data analysis proved to be more conclusive in the identification of several cochineal species.<sup>105</sup> The presence in the acid hydrolysed extract of the minor component Dc II (**32**), recently characterised as 7-C-glycoside of flavokermesic acid, is particularly important, as it allows the discrimination between Armenian cochineal (*Porphyrophora hamelii* Brandt) and American cochineal (*Dactylopius coccus* Costa).<sup>9, 107, 108</sup>

	
<p><b>32</b> <b>Dc II</b> 7-α-D-Glucopyranosyl-3,6,8-Trihydroxy-1-methyl-anthraquinone 2-carboxylic acid</p>	<p><b>33</b> <b>carminic acid</b> 7-α-D-Glucopyranosyl-3,5,6,8-Tetrahydroxy-1-methyl-anthraquinone 2-carboxylic acid</p>
<p><math>M_w = 477.38 \text{ g mol}^{-1}</math> <math>\lambda_{\text{max}} = 286, 435 \text{ nm}</math></p>	<p><math>M_w = 492.38 \text{ g mol}^{-1}</math> <math>\lambda_{\text{max}} = 276, 312 \text{ (s)}, 496 \text{ nm}</math></p>
	
<p><b>34</b> <b>kermesic acid</b> 3,6,8-Trihydroxy-1-methyl-anthraquinone 2-carboxylic acid</p>	<p><b>35</b> <b>flavokermesic acid</b> 3,5,6,8-Tetrahydroxy-1-methyl-anthraquinone 2-carboxylic acid</p>
<p><math>M_w = 330.25 \text{ g mol}^{-1}</math> <math>\lambda_{\text{max}} = 276, 312 \text{ (s)}, 498 \text{ nm}</math></p>	<p><math>M_w = 346.25 \text{ g/mol}</math> <math>\lambda_{\text{max}} = 286, 433 \text{ nm}</math></p>
	
<p><b>36</b> <b>laccaic acid A</b> 7-[5-[2-(Acetylamino)ethyl]-2-hydroxyphenyl]-9,10-dihydro-3,5,6,8-tetrahydroxy-9,10-dioxo-1,2-anthracenedicarboxylic acid</p>	<p><b>37</b> <b>laccaic acid B</b> 3,6,8-Trihydroxy-1-methyl-anthraquinone 2-carboxylic acid</p>
<p><math>M_w = 537.43 \text{ g mol}^{-1}</math> <math>\lambda_{\text{max}} = 287, 225, 490 \text{ nm}</math></p>	<p><math>M_w = 496.38 \text{ g mol}^{-1}</math> <math>\lambda_{\text{max}} = 287, 225, 490 \text{ nm}</math></p>

**Table 1.6:** Anthraquinone dyes characterised in coccid insect species.

### 1.2.3.3 Lichens

Lichen dyes are often referred to in the literature under the generic name of “*orchil*” dyes and produced a less expensive, although not light fast, purple colour.<sup>7</sup> These dyes could also, depending on the dyebath conditions, produce red, purple or orange hues.<sup>1,7</sup> The purple dyes found in lichen species are based on litmus (**38**) and orcein (**39**) and were obtained by fermentation of extracts from lichens of different species in the presence of ammonia and air. The lichens contain orsellinic acid depside (**40**), which after hydrolysis are decarboxylated into the colourless orcinol (**41**), and then oxidised in the presence of ammonia and air into the dyes litmus (**38**) or orcein (**39**), see scheme 1.2.<sup>1, 109</sup> The most important sources in Europe were *Rocella tinctoria* D.C. and *Rocella fuciformis* D.C., although other lichens might have also been used such as *Pertusaria dealbescens* Erichs. and *Orchrolechia tartarea* L..<sup>1, 7, 110</sup>

The characterisation of orchil dyes is complicated because of their high photo degradation rate and the fact that these dyes are easily destroyed during the acidic extraction from the textile.<sup>2</sup> Both litmus (**38**) and orcein (**39**) dyes present a chromophore with a maximum absorption around 550 - 575 nm, and  $\beta/\gamma$ -amino orceinimine are present in fresh orcein.<sup>111</sup> The use of orchil dye was prohibited in the manufacture of tapestries, as it was known to be a very light fugitive dye, nevertheless its presence has been previously reported on Flemish tapestries.<sup>2</sup>

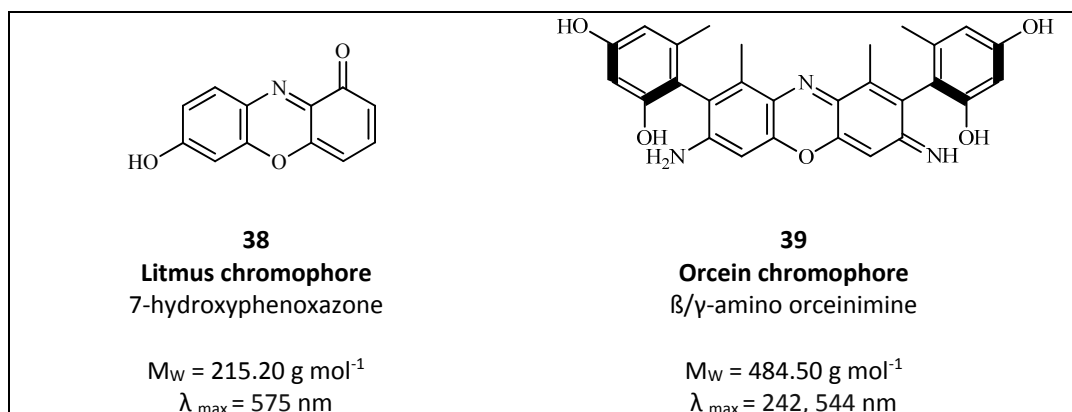


**Table 1.7:** Litmus and orcein chromophores.





<b>43</b> <b>cyanidin</b> 3,3',4',5,7- Pentahydroxyflavylium	<b>44</b> <b>delphinidin</b> 3,3',4',5,5',7- Hexahydroxyflavylium	<b>45</b> <b>malvidin</b> 3,4',5,7-Tetrahydroxy-3',5'- dimethoxyflavylium
$M_w = 287.24 \text{ g mol}^{-1}$ $\lambda_{\text{max}} = 538 \text{ nm}$	$M_w = 303.24 \text{ g mol}^{-1}$ $\lambda_{\text{max}} = 548 \text{ nm}$	$M_w = 331.30 \text{ g mol}^{-1}$ $\lambda_{\text{max}} = 546 \text{ nm}$

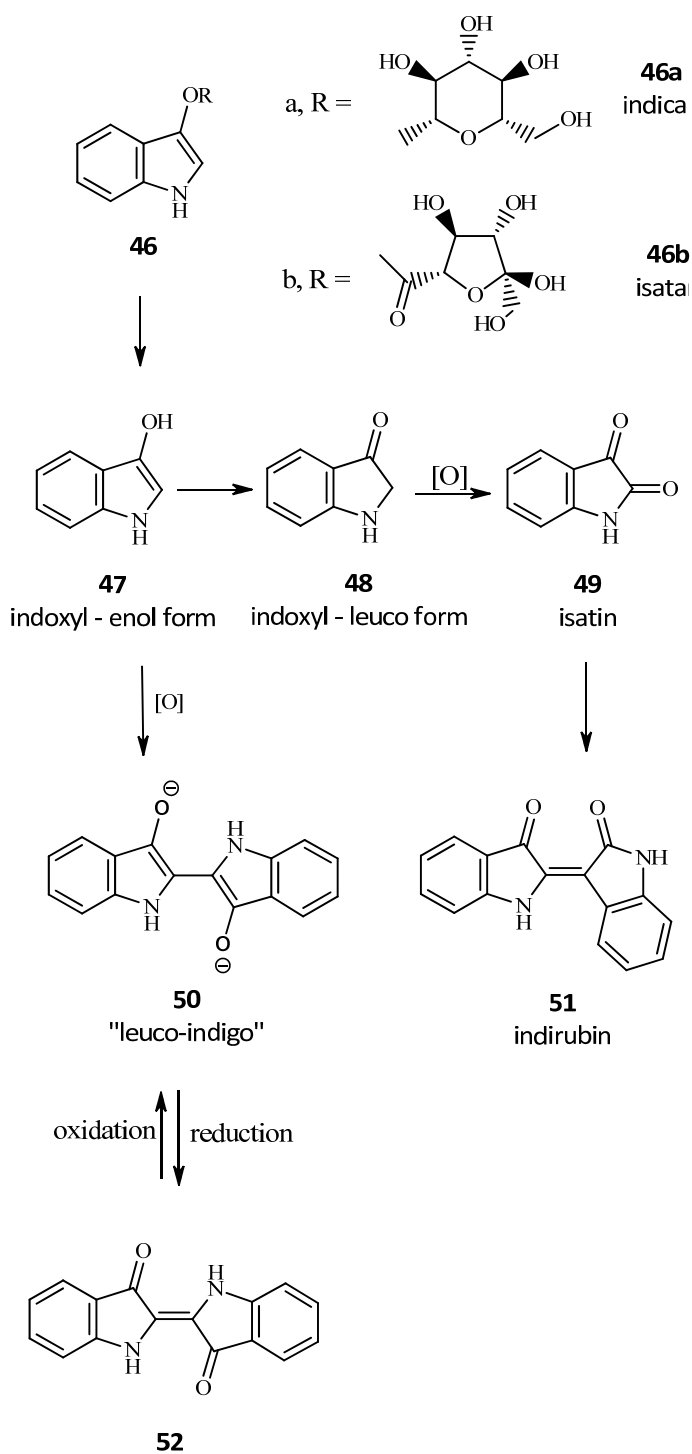
**Table 1.8:** Anthocyanidin dyes characterised in Eastern Woodlands porcupine quill work.

#### 1.2.4 Vat dyes

Vat dyes found in European textiles tradition include indigo (*e.g.* the indigo plant *Indigofera tinctoria* L.) and woad (*Isatis tinctoria* L.) species. These indigo dyes are characterised by the presence of indirubin (**51**) and indigotin (**52**) and the term indigo might refer to the plant, the colour or the indigotin pigment.

<b>51</b> <b>indirubin</b> 3-(1,3-dihydro-3-oxo-2h-indol-2-ylidene) -1,3-dihydro-2h-indol-2-on	<b>52</b> <b>indigotin</b> 2,2-(1,3-dihydro-3-oxo-2H-indol-2-ylidene) -1,2-dihydro-
$M_w = 262.27 \text{ g mol}^{-1}$ $\lambda_{\text{max}} = 241, 290, 365, 544 \text{ nm}$	$M_w = 262.27 \text{ g mol}^{-1}$ $\lambda_{\text{max}} = 242, 287, 339, 615 \text{ nm}$

**Table 1.9:** Indigoid dyes characterised in indigofera species.

Scheme 1.3: formation of indigotin pigment.<sup>7</sup>

Indigofera species originally grew in tropical and temperate Asia, as well as parts of Africa, while in temperate climates the main source of indigotin was woad (*Isatis tinctoria* L.). The cultivation of woad was a very important industry in Europe from the Middle Ages up to the sixteenth century, and indigo was not imported into Europe before the seventeenth century.<sup>7</sup> Indican (**46a**) occurs in *Indigofera* plants, while indican (**46a**) and isatan (**46b**) are occurring in woad (*Isatis tinctoria* L.). These precursors are colourless and soluble in water. The vat process requires working under alkaline and oxidising conditions (see scheme 1.3). During the first step of fermentation, the indoxyl glycosides are converted by enzymatic hydrolysis into indoxyl enol and keto tautomers (**47** and **48**). These indoxyl compounds then oxidise by exposure to air into a ‘leuco-indigo’ (**50**) that then reconverts into the insoluble blue pigment indigotin (**52**).<sup>7</sup> The dye then aggregates on the surface of the fibre.<sup>1, 7, 49</sup> Textiles dyed with these two plants contain indigotin (**52**) and minor amounts of indirubin (**51**).<sup>6</sup>

### 1.2.5 1856: the transition to early synthetic dyes

The synthesis of the first synthetic dye “mauve” in 1856 by W.H. Perkin is one of the most important discoveries in the history of science and technology.<sup>43, 112, 113</sup> The synthesis of mauve is said to be an accidental discovery by W.H. Perkin in 1856, while he was trying to synthesize quinine, the anti-malaria drug. Perkin oxidised aniline using potassium dichromate, whose toluidine impurities (*o*-toluidine and *p*-toluidine) reacted with the aniline, yielding a mauve solid (scheme 4).<sup>114-116</sup> Mauve was patented in 1856 and marks the birth of aniline dyes which were quickly produced industrially.<sup>113</sup>

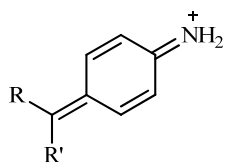
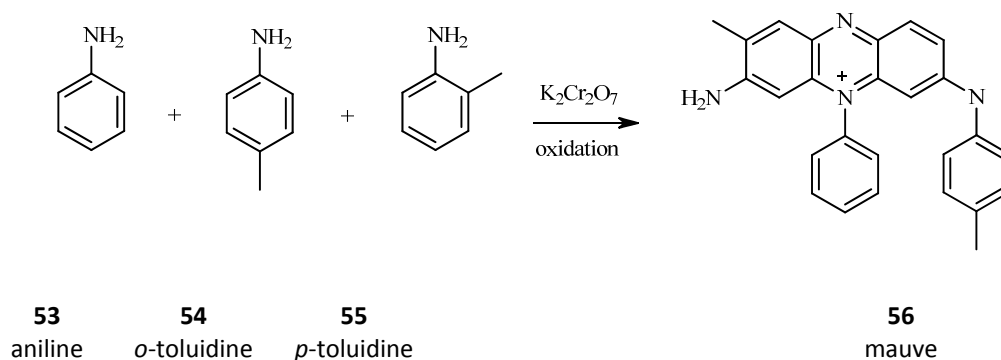


**Figure 1.7:** Aniline dye chromophore.



**Scheme 1.4:** Perkin's reaction to yield mauve.

Mauve is a complex mixture of methyl derivatives of 7-amino-5-phenyl-3-(phenylamino)phenazin-5-ium, and a recent investigation of historical mauve samples identified the presence of twelve components.<sup>117, 118</sup> Mauveine A (**57**) and mauveine B (**58**) were found to be the main components, with smaller amounts of two and three methyl derivatives of pseudo-mauveine (**60**) together with several other methylated derivatives (mauveine B2 and mauveines C25a+b).<sup>117, 118</sup> Finally pseudo-mauveine (**60**), which was described by Perkin as a second colouring matter in the mauve dye, was also recently identified for the first time in historical samples.<sup>118</sup> A few years after the discovery of mauve, a number of aniline dyes were produced on a large scale directly from aniline obtained from the coal tar industry.<sup>119</sup> The most iconic dyes included the first triphenylmethane dye fuchsine, synthesised in 1858 by Verguin and the diphenylmethane Auramine O, synthesised in 1883.<sup>44</sup> The large range of colour of aniline dye colour comes from addition or subtraction of methyl groups bound to this system via the amine group (figure 1.7). These early synthetic dyes were however renowned for their rates of high photo-degradation and they were quickly replaced by azo dyes by the end of the nineteenth century.

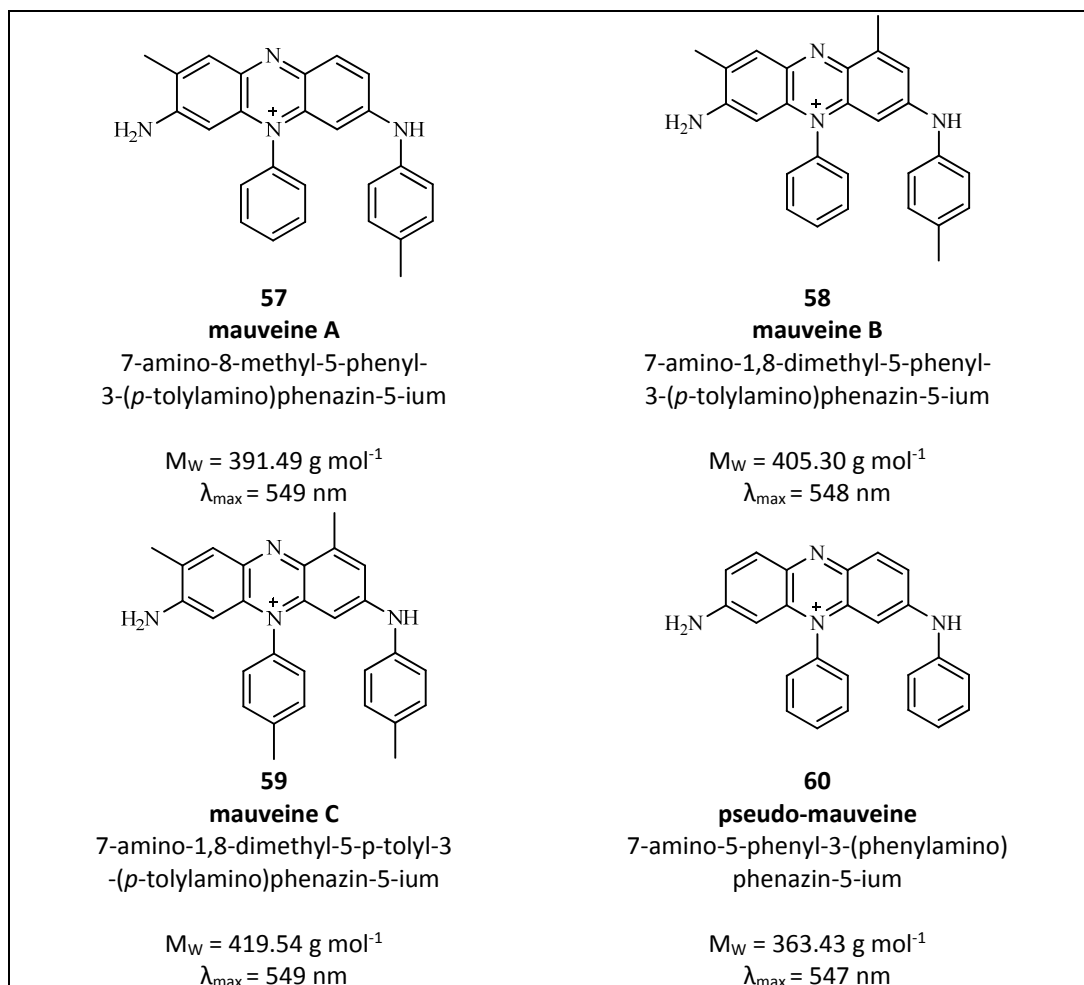


**Table 1.10:** The main chromophores present in aniline mauve dye.

### 1.3 PROTEINACEOUS FIBRES

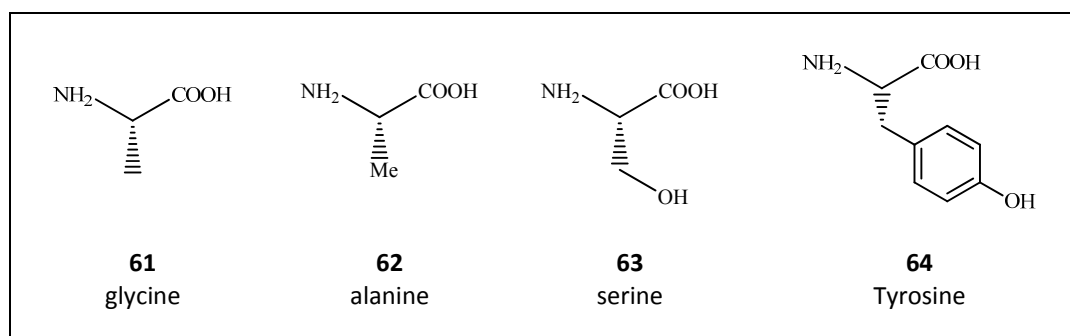
This section discusses the different type of substrates that were investigated during this research. The two types of fibres commonly used in the construction of tapestries are silk and wool, while in North American tradition leather garments and basketry objects were decorated with dyed porcupine quills. These substrates are all proteinaceous fibres and their chemical composition and macro-structure will be briefly introduced in the following sections.

### 1.3.1 Protein composition and structure

Proteins are made of several  $\alpha$  - amino acid monomeric units, which are linked in sequence *via* amino and carboxyl groups to form a polypeptide chain, which forms the primary structure of the protein. This structure is then stabilised into a secondary structure through hydrogen bonds and the two main secondary structures are  $\alpha$  - helices and  $\beta$  - sheets. Finally the tertiary structure of the protein corresponds to a spatial arrangement due to interactions between amino acids that are relatively far apart along the polypeptide chain.<sup>120</sup>

### 1.3.2 Fibroin containing fibres

Silk is the product of the secretion of larvae of a variety of insect from the Bombycidae family. The main source of silk is the insect *Bombyx mori*, which was exploited from the third millennium B.C. in China, then in the Middle East and later in Europe around the sixth century.<sup>121</sup> Fibroin is mainly composed of four amino-acids glycine (**61**), alanine (**62**), serine (**63**) and tyrosine (**64**) and a minor amount of cystine (**65**).<sup>121, 122</sup> The structure of silk is based on two filaments of fibroin, a highly crystalline protein, bonded together by a largely amorphous protein called sericin, a natural macromolecular protein.<sup>123, 124</sup> The presence of both organised crystalline and amorphous regions provides the mechanical properties of the silk. The composition and structure of fibroin is variable between species and some studies showed a correlation between the amino acid sequences present in fibroin and the physical properties of silk.<sup>125, 126</sup>



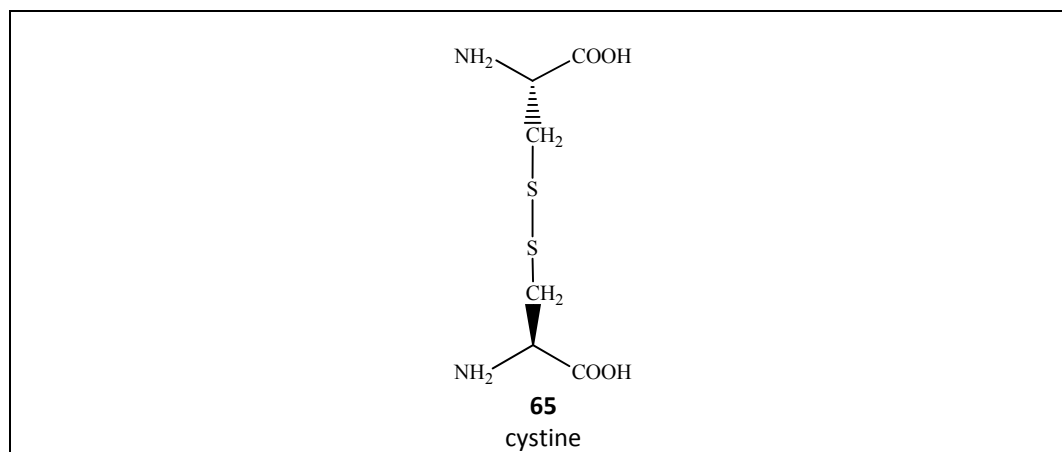


**Table 1.11:** The main amino acids present in fibroin.

Early X-ray diffraction studies revealed that the silk of caterpillars contain pleated  $\beta$  sheets<sup>127</sup> and later study showed that the crystalline material in *Bombyx mori* silk fibroin is in the form of ribbon-like filaments.<sup>128</sup> The preponderance of small amino acid residues allows the arrangement of the protein chains into the  $\beta$  - sheet configuration, held together by hydrogen bonds (figure 1.8).<sup>121</sup>

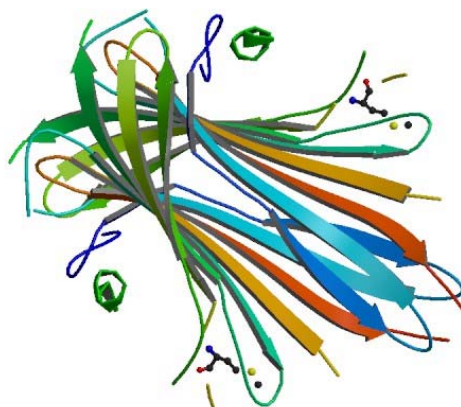
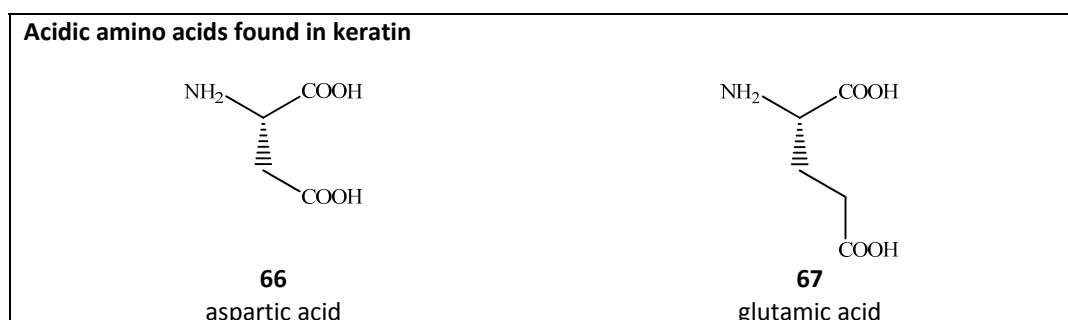


**Figure 1.8:** N-Terminal domain of *Bombyx mori* fibroin, with characteristic  $\beta$  - sheet configuration. Reproduced from Protein Data Bank.<sup>129</sup>

The preparation of raw silk for textile manufacture consists in removing sericin through a degumming process. Sericin is insoluble in cold water, it can however be hydrolysed by various processes, especially at high temperature (boiling water), in alkaline condition and with the addition of several inorganic salts or oxidising agents, such as hydrogen peroxide.<sup>121, 124, 130</sup> The use of oxidising agent can however induce breakage of the peptide bond at tyrosine residues and oxidation of tyrosine side-chains into acidic groups.<sup>130</sup> Furthermore; it can also affect the fibre structure and fibroin alignment and therefore affect the mechanical and morphological properties of the silk.<sup>121, 131</sup> Silk is also affected by photo-degradation, especially ultra violet radiation, and the photo-yellowing of silk is attributed to the oxidation of tyrosine residues.<sup>17, 121, 122, 132-134</sup> Photo-tendering of silk is induced by cleavage of hydrogen bonds, followed by oxidation of the tyrosine residues and hydrolytic fission of the polypeptide chains, resulting in a loss in fibre strength.<sup>17, 121, 132</sup> Finally, a recent study on the degradation mechanism of fibroin in enzyme solutions (protease XIV) showed that silk fibroin films with highest  $\beta$ -sheet content showed the highest degradation rate.<sup>135</sup>

### 1.3.3 Keratin based fibres

Keratin is the main component of hair, nails, scales, quills, horns and feathers, it is made of a sulphur-rich fibrous protein. The composition of keratin varies between species, but the structures of some of the important amino acids present in keratin proteins are indicated below.<sup>8, 136</sup>





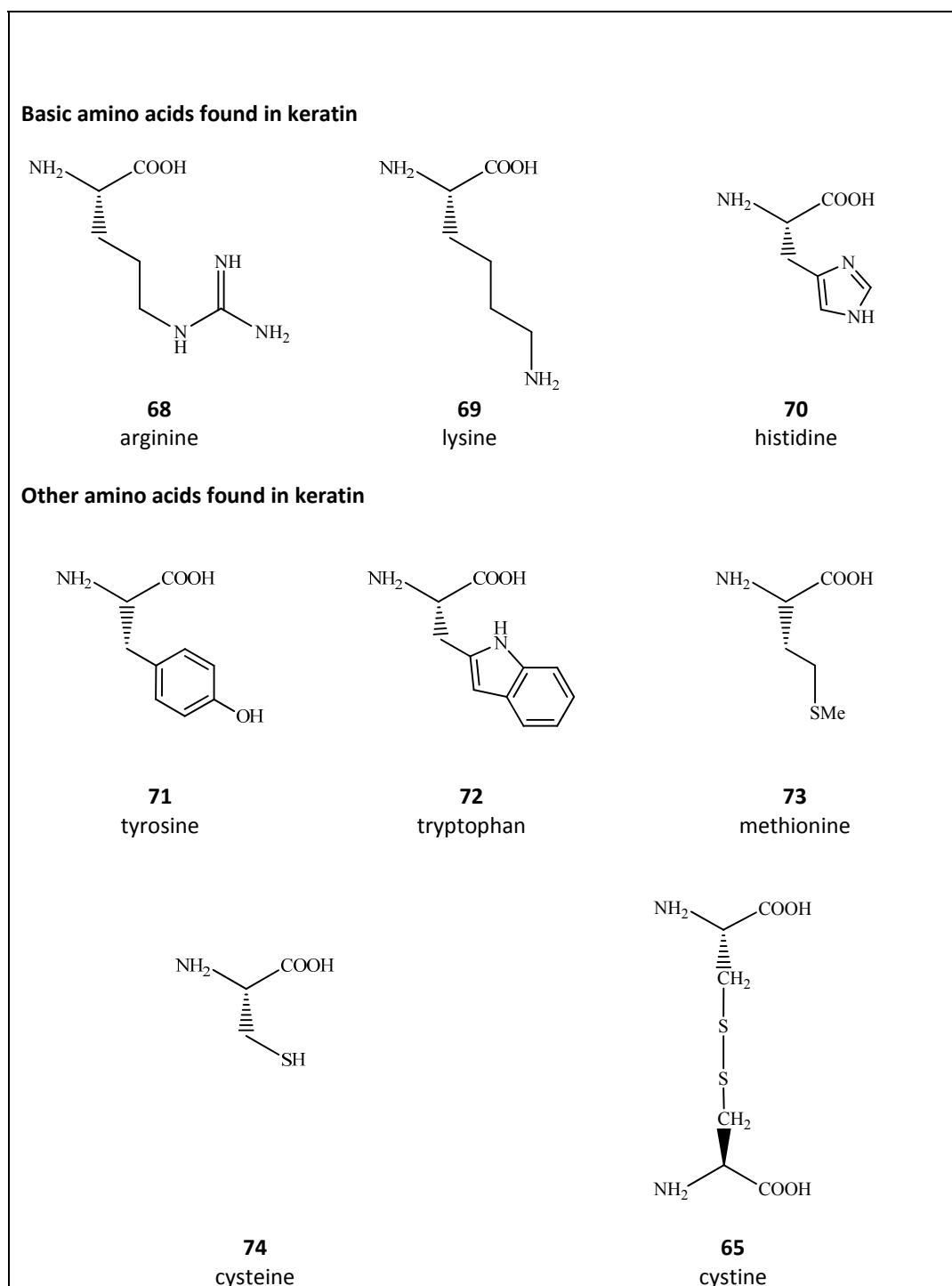


**Table 1.12:** The main amino acids present in keratin.

The structure and composition of keratin - containing tissues has been the subject of early X-ray diffraction studies.<sup>137, 138</sup> Keratins are classified in two groups, soft and hard keratins, with hard keratin containing higher level of sulphur.<sup>138-141</sup> Soft keratins are found in the epidermis of the skin, while hard keratins are the main component of hairs, nails, wool and quills. Keratins can also be classified as  $\alpha$ ,  $\beta$ , feather and amorphous, based on their X-ray scattering patterns.<sup>140, 141</sup>  $\alpha$  - Keratin is found in hard mammalian keratinous tissues, while  $\beta$  - keratin is found in stretched mammalian keratin and shows similarity in its X-ray diffraction pattern to feather.<sup>137, 140-142</sup> In the case of keratin, this classification corresponds also to the secondary polypeptide structure, with  $\alpha$ -keratin being organised into  $\alpha$  - helical coiled coils, and  $\beta$  - keratin being organised in pleated  $\beta$  - sheets.<sup>140</sup>

Hard  $\alpha$  - keratin is made of two polypeptide chains of different molecular weight (labelled I and II), characterised by an alternation of coiled coil parts and non helical segments, with the two chains parallel in the two-stranded rope segments and in axial register (figure 1.9).<sup>140, 143, 144</sup> The individual polypeptide chains are cross-linked to each other through disulphide bonds from cysteine residues, forming a microfibril structure,<sup>145</sup> and keratin molecules bundle together to form intermediate filaments, a complex assembly of heterodimers. It has been shown that there are between 23 and 32 chains bundle together to form an approximately cylindrical intermediate filament, with disulphide bonds from cysteine residues cross-linking between adjacent molecules in the surface lattice structure of the intermediate filaments (figure 1.10).<sup>146</sup>

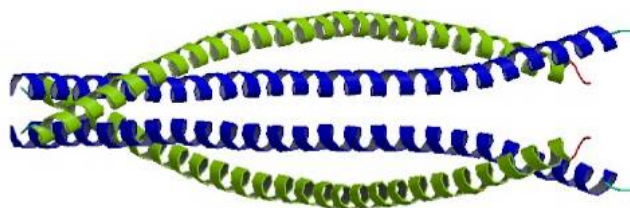


**Figure 1.9:** Hetero-complex of coil 2B domains of human intermediate filament protein, reproduced from Protein Data Bank.<sup>147</sup>

Wool is described as a very sophisticated biological composite material, with a strongly hierarchical organisation of sub-units:  $\alpha$  - keratin chains, intermediate filaments, fibre.<sup>148</sup> The chemical constituents of the wool and porcupine quill cells are predominantly hard  $\alpha$  - keratin proteins, although lipids and carbohydrates are also present in significant quantities on the fibre surface, resulting in its hydrophobic properties.<sup>17, 148</sup> The complex structure of  $\alpha$  - keratin fibre is described in figure 1.10. Wool and porcupine quills consist of a “soft” medulla, a “hard” cortex and a cuticle constituted of overlapping scales. Wool is obtained mainly from sheep but also from goats for the manufacture of cashmere, while Native North Americans used the quills from *Erethizon* species for porcupine quill work.

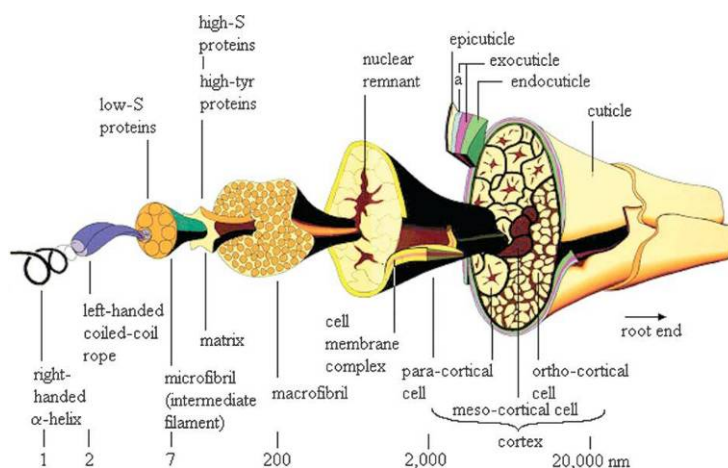
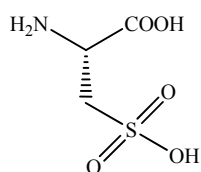


**Figure 1.10:** Structure of the  $\alpha$  - keratin fibre under various magnifications, reproduced from reference 148.<sup>148</sup>

Prior to dyeing, both wool and porcupine quills need to be cleaned from the oils that cover its surface, through a degreasing process, also called scouring. This process is important to increase the wettability and therefore the dyeability of the fibre.<sup>17, 149</sup> Several processes are used for the scouring wool, including alkaline treatments that can potentially damage the fibres, as cystine residues can easily be oxidised into cysteic acid (**75**) in mild oxidising conditions.<sup>150-153</sup> This oxidation will break

disulphide bonds and alter the mechanical properties of the keratin fibres.<sup>154</sup> Finally, wool is also sensitive to photo-degradation (ultra violet irradiation) and the photo-yellowing of wool is attributed to the oxidation of tyrosine residues, that induces the oxidation of tryptophan residues leading to the formation of kynurenine and other yellow kynurenine derivatives.<sup>17, 155, 156</sup>



**75**  
cysteic acid

## 1.4 CONTRIBUTION OF THIS WORK

This research on historical dyes analysis aims to improve existing chromatographic methods for the study of natural dyes on historical textiles and to develop the methodology so other substrates, such as porcupine quills, could also be investigated. The analysis of dyes which have been used on museum artefacts other than textiles has received little systematic study, particularly those of non-European origin, and a transfer of existing analytical protocols and methodology for dye analysis to porcupine quill substrates will be necessary prior to investigating important artefacts. The second aim of this research is to develop a methodology for the characterisation of metallic mordant residues found on porcupine quill work.

### 1.4.1 *Dye analysis and method development*

High Performance Liquid Chromatographic (HPLC) separation followed by Photo Diode Array (PDA) or Mass Spectrometry (ESI MS) analysis are long-established

techniques for the characterisation of natural dyes,<sup>11, 89</sup> as they allow the characterisation of dye sources by the relative quantification of several minor chemical components in acid hydrolysed extracts.<sup>6, 8, 9, 15</sup> However, PDA-HPLC chromatographic methods do not always provide a low enough detection limit, and the very small amounts of material available for sampling on historical textiles and the poor light fastness of yellow flavonoid dyes often makes the identification of dyestuff species in this field quite challenging and sometimes renders the characterisation of minor components impossible. For these reasons, transfer of the classical High Performance Liquid Chromatography (HPLC) method used at National Museums Scotland for the investigation of natural dyes to Ultra Performance Liquid Chromatography (UPLC) will be explored in the second chapter of this thesis. The new chromatographic method will be developed on a selection of dye standards and then evaluated against a series of reference yarns. This new method will then be applied in the third chapter of the thesis to the characterisation of the main dye sources found in wool and silk yarns sampled from a group of important mid sixteenth century English tapestries. Finally, in the fifth chapter of the thesis the UPLC method will be applied to the investigation of dye sources found on North American porcupine quill work and the results obtained from dye analysis will be related to other important porcupine quill work collections.

#### *1.4.2 Metal ion mordant analysis: method development*

The second aim of this research is the development of a methodology for the non – invasive quantification of metal ion residues on porcupine quill substrates. To this end, in the fourth chapter of the thesis a comparative study will be made of reference porcupine quills prepared in-house using dyebaths containing a range of metal ion concentrations (copper and tin). The concentration of metal ions sorbed by the porcupine quills will then be quantified with Inductively Coupled Plasma (ICP) coupled to Optical Emission Spectrometry (OES) and non-invasive Particle Induced X-Ray Emission analysis (PIXE) and Rutherford Backscattering Spectrometry

(RBS). Recent method development for the study of archaeological bones demonstrated the value of combining non-invasive PIXE and RBS analysis, as it allowed simultaneous quantification of inorganic components and organic residues.<sup>157, 158</sup> Although there have been a few studies using PIXE analysis for the quantification of heavy metal contaminants in human hair,<sup>159, 160</sup> this has never been applied to porcupine quills and will therefore need method development. Finally the use of RBS analysis to quantify heavy metal residues (such as copper or tin) in keratin will be evaluated through the investigation of reference quill samples. The different methods will be compared and then they will be applied to the study of Northern Athapaskan porcupine quill samples, and the results of this study will be presented in the fifth chapter of the thesis.

## 1.5 REFERENCES

1. Cardon, D. (2003). *Le monde des teintures naturelles*. Belin, Paris.
2. Hofenk de Graaf, J. H. (2005). *The Colourful Past*. Archetype Publications.
3. Quye, A., Wouters, J. (1992). An application of HPLC to the identification of natural dyes. *Dyes Hist. Archaeol.*, **10**, 48-54.
4. Ferreira, E. S. B., Quye, A., McNab, H., Hulme, A. N., Wouters, J., Boon, J. J. (1999). The analytical characterisation of flavonoid photodegradation products: a novel approach to identifying natural yellow dyes in ancient textiles. *Preprint of the ICOM Committee for Conservation, 12th Triennial Meeting*, **1**, 221-227.
5. Ferreira, E. S. B., Quye, A., McNab, H., Hulme, A. N., Wouters, J., Boon, J. J. (2001). Development of analytical techniques for the study of natural yellow dyes in historic textiles. *Dyes Hist. Archaeol.*, **16/17**, 179-186.
6. Ferreira, E. S. B. (2002). *New Approaches Towards the Identification of Yellow Dyes in Ancient Textiles*. The University of Edinburgh, PhD Thesis.
7. Ferreira, E. S. B., McNab, H., Hulme, A. N., Quye, A. (2004). The natural constituent of historical textile dyes. *Chem. Soc. Rev.*, **33**, 329-336.
8. Peggie, D. A. (2006). *The Development and Application of Analytical Methods for the Identification of Dyes on Historical Textiles*. The University of Edinburgh, PhD Thesis.

9. Peggie, D. A., Hulme, A. N., McNab, H., Quye, A. (2008). Towards the identification of characteristic minor components from textiles dyed with weld (*Reseda luteola* L.) and those dyed with Mexican cochineal (*Dactylopius coccus* Costa). *Microchim. Acta*, **162**, 371-380.
10. Ferreira, E. S. B., Quye, A., Hulme, A. N., McNab, H. (2003). LC-Ion Trap MS and PDA-HPLC - Complementary techniques in the analysis of Flavonoid dyes in historical textiles: The case study of an 18th-century Herald's Tabard. *Dyes Hist. Archaeol.*, **19**, 13-18.
11. Hulme, A. N., McNab, H., Peggie, D. A., Quye, A. (2005). Negative ion electrospray mass spectrometry of neoflavonoids. *Phytochem.*, **66**, 2766-2770.
12. McNab, H., Ferreira, E. S. B., Hulme, A. N., Quye, A. (2009). Negative ion ESI-MS analysis of natural yellow dye flavonoids: An isotopic labelling study. *Int. J. Mass Spectrom.*, **284**, 57-65.
13. Smith, G. J., Thomsen, S. J., Markham, K. R., Andary, C., Cardon, D. (2000). The photostabilities of naturally occurring 5-hydroxyflavones, flavonols, their glycosides and their aluminium complex. *J. Photochem. Photobiol. A: Chem.*, **136**, 87-91.
14. Ferreira, E. S. B., Quye, A., MacNab, H., Hulme, A. N. (2002). Photo-oxidation of Quercetin and Morin as Markers for the characterisation of natural flavonoid yellow dyes in Ancient textile. *Dyes Hist. Archaeol.*, **18**, 63-72.
15. Hulme, A. N., McNab, H., Peggie, D. A., Quye, A. (in press). The chemical characterisation of aged and unaged fibre samples dyed with sawwort (*Serratula tinctoria*) using PDA-HPLC and HPLC ESI MS. *Dyes Hist. Archaeol.*, **22**.
16. Campbell, T. P. (2003). The Art and Magnificence of Renaissance Tapestries: Introduction. In *Tapestry in the Renaissance: Art and Magnificence*, Campbell, T. P., Ed. The Metropolitan Museum of Art, Yale University Press: New Haven and London: 3-12.
17. Hacke, A.-M. (2006). *Investigation into the Nature and Ageing of Tapestry Materials*. The University of Manchester, PhD Thesis.
18. Hacke, A.-M., Carr, C. M., Brown, A., Howell, D. (2003). Investigation into the nature of metal threads in a Renaissance tapestry and the cleaning of tarnished silver by UV / Ozone (UVO) treatment. *J. Mater. Sci.*, **38**.
19. Campbell, T. P. (2003). Artists and Cartoonists in Northern Europe 1380 -1480. In *Tapestry in the Renaissance: Art and Magnificence*, Campbell, T. P., Ed. The Metropolitan Museum of Art, Yale University Press: New Haven and London, 73.
20. Bennett, A. G. (1976). *Five centuries of Tapestry, from the Fine Arts Museums of San Francisco*. The Fine Arts Museums of San Francisco.
21. Coffinet, J. (1971). *Arachné ou l'art de la tapisserie*. Genève: Editions de la Coulouvreniere.
22. "Tapisserie de haute-lisse des Gobelins," *Encyclopédie ou Dictionnaire raisonné des sciences, des arts et des métiers, vol. 9 (plates) (Paris, 1771)*.  
<http://hdl.handle.net/2027/spo.did2222.0001.616> (25-11-2012).
23. "Tapisserie de basse-lisse des Gobelins," *Encyclopédie ou Dictionnaire raisonné des sciences, des arts et des métiers, vol. 9 (plates) (Paris, 1771)*.  
<http://hdl.handle.net/2027/spo.did2222.0001.617> (25-11-2012).

24. Barnard, E. A. B., Wace, A. J. B. (1928 ). *The Sheldon tapestry weaver and their work*. Society of Antiquaries of London Oxford.
25. Turner, H. L. (2002). Finding the Sheldon weavers: Richard Hyckes and the Barcheston tapestry works reconsidered. *Textile Hist.*, **33**, 137-161.
26. Turner, H. L. (2008). Tapestry sections depicting the Prodigal Son: how safe is an attribution to Mr Sheldon's tapestry venture at Barcheston? *Archaeologia Aeliana*, **XXXVII**, 183-96.
27. Turner, H. L. (2008). Tapestries once at Chastleton House and Their Influence on the Image of the Tapestries Called Sheldon: A Reassessment. *The Antiquaries Journal*, **88**, 313-346.
28. Turner, H. L. (2002). The Sheldon tapestry maps belonging to the Bodleian. *Bodleian Library Record*, **17**, 293-313.
29. Turner, H. L. (2010). *No Mean Prospect: Ralph Sheldon's Tapestry Maps*. Plotwood Press.
30. Orchard, W. C. (1916). *The Technique of Porcupine-Quill Decoration Among the North American Indians*. Kessinger Publishing, Reprint 2009.
31. Thompson, J. (2001). *Fascinating Challenges: Studying Material Culture with Dorothy Burnham*. Canadian Museum of Civilization.
32. Thompson, J. (1990). *Pride of the Indian Wardrobe, Northern Athapaskan footwear*. University of Toronto Press, for the Bata Shoe Museum.
33. Idiens, D. (1974). The Athapaskan Indian collection in the Royal Scottish Museum. In *The Athapaskans: Strangers of the North. An international travelling exhibition from the collection of the National Museum of Man, Canada, and the Royal Scottish Museum*, National Museum of Man: Ottawa, 15-16.
34. Idiens, D. (1979). A catalogue of Northern Athapaskan Indian Artefacts in the collection of the Royal Scottish Museum, Edinburgh. *Royal Scottish Museum Information Series, Art and Archaeology*, **3**.
35. Andrews, T. D. (2006). *Dè T'a Hoti Ts'eeda, We live securely by the land: An exhibition of Dene material selected from the collections from the National Museums Scotland*. Prince of Wales Northern Heritage Centre.
36. Knowles, C. (2007). Objects journeys: outreach work between National Museums Scotland and the Tlicho. In *Material Histories*, Marischal Museum, University of Aberdeen.
37. Cole, C., Heald, S. (2010). The History and Analysis of Pre-Aniline Native American Quillwork Dyes. *TSA Symposium, Paper 14*.
38. Cole, C. L. (2010). *The contextual analysis of pre-1856 Eastern Woodlands quillwork dyes through identification by Liquid Chromatography - Mass Spectroscopy*. The University of Delaware, PhD Thesis.
39. Thompson, J. (1994). *From the land, two hundred years of Dene clothing*. Canadian Museum of Civilization.
40. del Hoyo-Meléndez, J. M., Mecklenburg, M. F. (2010). A survey on the light-fastness properties of organic-based Alaska Native artifacts. *J. Cult. Herit.*, **11**, 493-499.



41. Knowles, C. (2008). Objects journeys: outreach work between National Museums Scotland and the Tlicho. In *Material Histories*, Marischal Museum, University of Aberdeen.
42. Pliny the Elder *Histoire Naturelle, Livre IX*. Les Belles Lettres, Paris.
43. Garfield, S. (2000). *Mauve: how one man invented a colour that changed the world*. Faber & Faber Ltd, London, U. K.
44. Cooksey, C., Dronsfield, A. (2009). Fuchsine or magenta: the second most famous aniline dye. A short memoir on the 150th anniversary of the first commercial production of this well known dye. *Biotech. Histochem.*, **84**, 179-183.
45. Lindsay, D. (1987). The Hudson's Bay Company-Smithsonian Connection and Fur Trade Intellectual Life: Bernard Rogan Ross, A Case Study. In *Le Castor Fait Tout: Selected Papers of the Fifth North America Fur Trade Conference*, Trigger, B. G., Ed. Montreal: Lake St Louis Historical Society: 587-617.
46. Lindsay, D. (1993). *Science in the Subarctic: trappers, traders, and the Smithsonian Institution*. Smithsonian Institution Press, Washington.
47. Whitehead, R. H. (1982). *Micmac quillwork: Micmac Indian techniques of porcupine quill decoration, 1600-1950*. Nova Scotia Museum.
48. Duff, D. G., Sinclair, R.S. (1988). The Use of Aluminium in Clubmoss as a Dye Mordant. *Dyes Hist. Archaeol.*, **7**, 25-31.
49. Balfour-Paul, J. (1998). *Indigo*. London, British Museum Press.
50. Lee, D. J., Bacon, L., Daniels, V. (1985). Some Conservation Problems Encountered with Turmeric on Ethnographic Objects. *Studies in Cons.*, **30**, 184-188.
51. Funk, J. L., Frye, J. B., Oyarzo, J. N., Zhang, H., Timmermann, B. N. (2009). Anti-Arthritic Effects and Toxicity of the Essential Oils of Turmeric (*Curcuma longa* L.). *J. Agric. Food Chem.*, **58**, 842-849.
52. Jayaprakasha, G. K., Jagan Mohan Rao, L., Sakariah, K. K. (2002). Improved HPLC Method for the Determination of Curcumin, Demethoxycurcumin, and Bisdemethoxycurcumin. *J. Agric. Food Chem.*, **50**, 3668-3672.
53. Li, R., Xiang, C., Ye, M., Li, H. F., Zhang, X., Guo, D. A. (2011). Qualitative and Quantitative analysis of curcuminoids in herbal medicines derived from *Curcuma* species. *Food Chem.*, **126**, 1890-1895.
54. Cheng, J., Weijun, K., Yun, L., Jiabo, W., Haitao, W., Qingmiao, L., Xiaohu, X. (2010). Development and validation of UPLC method for quality control of *Curcuma longa* Linn.: Fast simultaneous quantitation of three curcuminoids. *J. Pharm. Biomed. Anal.*, **53**, 43-49.
55. Li, S., Yuan, W., Deng, G., Wang, P., Yang, P., Aggarwal, B. B. (2011). Chemical Composition and Product Quality Control of Turmeric (*Curcuma longa* L.). *Pharmaceutical Crops*, **2**, 28-54.

56. Wouters, J., Grzywacz, C. M., Claro, A. (2010). Markers for Identification of Faded Safflower (*Carthamus tinctorius* L.) Colorants by HPLC-PDA-MS: Ancient fibres, pigments, paints and cosmetics derived from Antique recipes. *Studies in Cons.*, **55**, 186-203.
57. Degano, I., Lucejko, J. J., Colombini, M. P. (2011). The unprecedented identification of Safflower dyestuff in a 16th century tapestry through the application of a new reliable diagnostic procedure. *J. Cult. Herit.*, **12**, 295-299.
58. Meselhy, M. R., Kadota, S., Momose, Y., Hatakeyama, N., Kusai, A., Hattori, M., Namba, T. (1993). Two New Quinochalcone Yellow Pigments from *Carthamus tinctorius* and Ca<sup>2+</sup> Antagonist Activity of Tinctormine. *Chemical & Pharmacological Bull.*, **41**, 1796-1802.
59. Sewell, W. G., Hsiung, C. D., Swei, T. D., Wei, S. H. (1939). The Natural Dyes of Szechwan, West China. *J. Soc. Dyers Colour.*, **55**, 412-415.
60. Kametaka, T.; Perkin, A. G. (1910). CXXX.-Carthamine. Part I. *J. Chem. Soc., Trans.*, **97**, 1415-1427.
61. Takahashi, Y., Miyasaka, N., Tasaka, S., Miura, I., Urano, S., Ikura, M., Hikichi, K., Matsumoto, T., Wada, M. (1982). Constitution of two coloring matters in the flower petals of *Carthamus Tinctorius* L. *Tetrahedron Lett.*, **23**, 5163-5166.
62. Takahashi, Y., Saito, K., Yanagiya, M., Ikura, M., Hikichi, K., Matsumoto, T., Wada, M. (1984). Chemical Constitution of Safflor Yellow B, A Quinochalcone From the Petals of *Carthamus tinctorius* L. *Tetrahedron Lett.*, **25**, 2471-2474.
63. Cho, M. H., Paik, Y. S., Hahn, T. R. (2000). Enzymatic Conversion of Precarthamin to Carthamin by a Purified Enzyme from the Yellow Petals of Safflower. *J. Agric. Food Chem.*, **48**, 3917-3921.
64. Schwappe, H. (1993). *Handbuch der Naturalfarbstoffe*. Nikol Verladsgesellschaft, Hamburg.
65. Azimova, S. S., Yunusov, M. S. (2012). Natural Compounds – Alkaloids. In Springer Berlin Heidelberg.
66. Perrins, J. D. (1862). XLIII - On berberine - contributions to its history and revision of its formula. *J. Chem. Soc.*, **15**, 339-356.
67. Perkin, W. H. (1889). XII - On berberine - Part I. *J. Chem. Soc., Trans.*, **55**, 63-90.
68. Perkin, W. H. (1890). LXXI - Contributions from the Laboratories of the Heriot Watt College, Edinburgh. On berberine. Part II. *J. Chem. Soc., Trans.*, **57**, 992-1106.
69. Zarkogianni, M., Mikropoulou, E., Varella, E., Tsatsaroni, E. (2011). Colour and fastness of natural dyes: revival of traditional dyeing techniques. *Color. Technol.*, **127**, 18-27.
70. Matsuura, T., Matsushima, H., Nakashima, R. (1970). Photo-induced reactions XXXVI: Photosensitized oxygenation of 3-hydroxyflavones as a model for quercetinase. *Tetrahedron Lett.*, **26**, 435-443.
71. Andary, C., Prunac, S., Cardon, D. (1995). Yellow Dyes of Historical Importance: A Multi-Disciplinary Study. II-Chemical Analysis of Weld and Sawwort. *Dyes Hist. Archaeol.*, **14**, 33-38.

72. Cardon, D. (1995). Yellow Dyes of Economic Importance: Beginnings of a Long-Term Multi-Disciplinary Study. *Dyes Hist. Archaeol.*, **13**, 59-73.
73. Kaiser, R. (1993). Quantitative Analysis of Flavonoids in Yellow Dye Plants Species Weld (*Reseda luteola* L.) and Sawwort (*Serratula tinctoria* L.). *Angew. Bot.*, **67**, 128-131.
74. Yuldashev, M. P., Batirov, E., Malikov, V. M., Yuldasheva, N. P. (1996). Flavonoids of Psoralea drupaceae and Reseda luteola. *Chem. Nat. Compd.*, **32**, 923-924.
75. Cristea, D., Bareau, I., Vilarem, G. (2003). Identification and quantitative HPLC analysis of the main flavonoids present in weld (*Reseda luteola* L.). *Dyes Pigm.*, **57**, 267-272.
76. Marques, R., Sousa, M. M., Oliveira, M. C., Melo, M. J. (2009). Characterization of weld (*Reseda luteola* L.) and spurge flax (*Daphne gnidium* L.) by high-performance liquid chromatography-diode array detection-mass spectrometry in Arraiolos historical textiles. *J. Chromatogr. A*, **1216**, 1395-1402.
77. Villela, A., van der Klift, E. J. C., Mattheussens, E. S. G. M., Derksen, G. C. H., Zuilhof, H., van Beek, T. A. (2011). Fast chromatographic separation for the quantitation of the main flavone dyes in *Reseda luteola* (weld). *J. Chromatogr. A*, **1218**, 8544-8550.
78. Zhang, X., Laursen, R. A. (2005). Development of mild extraction methods for the analysis of natural dyes in textiles of historical interest using LC-Diode Array Detector-MS. *Anal. Chem.*, **77**, 2022-2025.
79. Rigano, D., Cardile, V., Formisano, C., Maldini, M. T., Piacente, S., Bevilacqua, J., Russo, A., Senatore, F. (2009). *Genista sessilifolia* DC. and *Genista tinctoria* L. inhibit UV light and nitric oxide-induced DNA damage and human melanoma cell growth. *Chem-Biol. Interact.*, **180**, 211-219.
80. Perkin, A. G.; Horsfall, L. H. (1900). CXXV - Genistein. Part II. *J. Chem. Soc., Trans.*, **77**, 1310-1314.
81. Perkin, A. G., Newbury, F. G. (1899). LXXIX - The Colouring Matters contained in Dyer's Broom (*Genista tinctoria*) and Heather (*Calluna vulgaris*). *J. Chem. Soc., Trans.*, **75**, 830-839.
82. Valianou, L., Stathopoulou, K., Karapanagiotis, I., Magiatis, P., Pavlidou, E., Skaltsounis, A. L., Chryssoulakis, Y. (2009). Phytochemical analysis of young fustic (*Cotinus coggygia*; heartwood) and identification of isolated colourants in historical textiles. *Anal. Bioanal. Chem.*, **394**, 871-882.
83. Guinot, P., Gargadennec, A., La Fisca, P., Fruchier, A., Andary, C., Mondolot, L. (2009). *Serratula tinctoria*, a source of natural dye: Flavonoid pattern and histolocalization. *Ind. Crop. Prod.*, **29**, 320-325.
84. Forster, J. R. (1772). A Letter from Mr. John Reinhold Forster, F. R. S. to William Watson, M. D. Giving Some Account of the Roots Used by the Indians, in the Neighbourhood of Hudson's-Bay, to Dye Porcupine Quills. *Phil. Trans. R. Soc.*, **62**, 54-59.
85. Thompson, R. H. (1971). *Naturally occurring quinones*. Academic Press Inc., London.
86. Burnett, R. A., Thomson, R. H. (1968). Natural Occurring Quinones. Part XV. Biogenesis of the Anthraquinones in *Rubia tinctorum* L. (Madder). *J. Chem. Soc.*, 2437-2441.

87. Sanyova, J. (1998). Étude des pigments organiques préparés à partir des racines rubiacées européennes. In *Art et Chimie la couleur: actes du Congrès*, Goupy, J., Mohen, J. P., Ed. CNRS: 14-17.
88. Sanyova, J. (2001). *Contribution à l'étude de la structure et des propriétés des laques de garance*. Université Libre de Bruxelles, PhD Thesis.
89. Wouters, J., Verhecken, A. (1985). High-performance liquid chromatography of anthraquinones: Analysis of plant and insect extracts and dyed textiles. *Studies in Cons.*, **30**, 119-128.
90. Sanyova, J., Reisse, J. (2006). Development of a mild method for the extraction of anthraquinones from their aluminum complexes in madder lakes prior to HPLC analysis. *J. Cult. Herit.*, **7**, 229-235.
91. Mouri, C., Laursen, R. (2012). Identification of anthraquinone markers for distinguishing *Rubia* species in madder-dyed textiles by HPLC. *Microchim. Acta*, **179**, 105-113.
92. Derksen, G. C. H., van Beek, T. A., de Groot, A., Capelle, A. (1998). High-performance liquid chromatographic method for the analysis of anthraquinone glycosides and aglycones in madder root (*Rubia tinctorum* L.). *J. Chromatogr. A*, **816**, 277-281.
93. Derksen, G. C. H., Niederländer, H.A.G., van Beek, T.A. (2002). Analysis of anthraquinones in *Rubia tinctorum* L. by liquid chromatography coupled with diode-array UV and mass spectrometric detection. *J. Chromatogr. A*, **978**, 119-127.
94. Derksen, G. C. H., van Beek, T. A. (2002). *Rubia tinctorum* L. In *Studies in natural products chemistry*, Rahman, A., Ed. Elsevier, Amsterdam: 629-684.
95. Derksen, G. C. H., Lelyveld, G. P., van Beek, T. A., Capelle, A., de Groot, E. (2004). Two validated HPLC methods for the quantification of alizarin and other anthraquinones in *Rubia tinctorum* cultivars. *Phytochem Anal.*, **15**, 397-406.
96. Derksen, G. C. H., Naayer, M., van Beek, T. A., Capelle, A., Haaksman, I. K., van Doren, H. A., de Groot, A. (2003). Chemical and enzymatic hydrolysis of anthraquinone glycosides from madder roots. *Phytochem Anal.*, **14**, 137-144.
97. Ishii, Y., Okamura, T., Inoue, T., Fukuhara, K., Umemura, T., Nishikawa, A. (2010). Chemical structure determination of DNA bases modified by active metabolites of lucidin-3-O-primeveroside. *Chem Res Toxicol.*, **23**, 134-141.
98. Clementi, C., Nowik, W., Romani, A., Cibir, F., Favaro, G. (2007). A spectrometric and chromatographic approach to the study of ageing of madder (*Rubia tinctorium* L.) dyestuff on wool. *Anal. Chim. Acta* **596**, 46-54.
99. Atabey, H., Sari, H., Al-Obaidi, F. N. (2012). Protonation Equilibria of Carminic Acid and Stability Constants of Its Complexes with Some Divalent Metal Ions in Aqueous Solution. *J. Solution Chem.*, **41**, 793-803.
100. Cardon, D. (1990). Kermes, a dying dye. *J. Soc. Dyers Colour.*, **106**, 191-192.
101. Lee, R. L. (1951). American Cochineal in European Commerce, 1526-1625. *J. Mod.Hist.* , **23**, 205-224.

102. Donkin, R. A. (1977). Spanish Red: An Ethnogeographical Study of Cochineal and the Opuntia Cactus. *T. Am. Philos. Soc.*, **67**, 1-84.
103. Chávez-Moreno, C., Tecante, A., Casas, A. (2009). The Opuntia (*Cactaceae*) and Dactylopius (*Hemiptera: Dactylopiidae*) in Mexico: a historical perspective of use, interaction and distribution. *Biodivers. and Conserv.*, **18**, 3337-3355.
104. Vahedi, H. A., Hodgson, C. J. (2007). Some species of the hypogeal scale insect Porphyrophora Brandt (*Hemiptera: Sternorrhyncha: Coccoidea: Margarodidae*) from Europe, the Middle East and North Africa. *Systematics and Biodiversity*, **5**, 23-122.
105. Serrano, A., Sousa, M., Hallett, J., Lopes, J., Oliveira, M. (2011). Analysis of natural red dyes (cochineal) in textiles of historical importance using HPLC and multivariate data analysis. *Anal. Bioanal. Chem.*, **401**, 735-743.
106. Wouters, J., Verhecken, A. (1989). The Coccid Insect Dyes: HPLC and Computerized Diode-Array Analysis of Dyed Yarns. *Studies in Cons.*, **34**, 189-200.
107. Wouters, J., Verhecken, A. (1989). The scale insect dyes (*Homoptera: Coccoidea*). Species recognition by HPLC diode array analysis of the dyestuffs. *Annl. Soc. ent. Fr. (N.S.)*, **25**, 393 - 410.
108. Phipps, E., Shibayama, N. (2010). Tracing Cochineal Through the Collection of the Metropolitan Museum. *TSA Symposium, Paper 44*.
109. Beecken, H., Gottschalk, E. M., v Gizycki, U., Krämer, H., Maassen, D., Matthies, H. G., Musso, H., Rathjen, C., Zdhorszky, U. I. (2003). Orcein and Litmus. *Biotech. Histochem.*, **78**, 289-302.
110. Cardon, D., du Chatenet, G. (1990). *Guide des teintures naturelles. Plante - Lichens - Champignons - Mollusques et Insectes*. Les guides du Naturaliste, Delachaux et Niestle, Paris.
111. Hutchin, E. (2005). *Investigation into Purple Dyes made from Lichen and their analysis at the National Museums of Scotland*. The University of Edinburgh, MChem project.
112. Travis, A. S. (1990). Perkin's Mauve: Ancestor of the Organic Chemical Industry. *Tech. Cult.*, **31**, 51-82.
113. Travis, A. S. (1993). *The Rainbow Makers: The Origins of the Synthetic Dyestuffs Industry in Western Europe*. Lehigh University Press.
114. Perkin, W. H. (1862). XIX - On colouring matters derived from coal tar. *Q. J. Chem. Soc.*, **14**, 230-255.
115. Perkin, W. H. (1879). LXXIV - On mauveine and allied colouring matters. *J. Chem. Soc., Trans.*, 717-732.
116. Meth-Cohn, O., Smith, M. (1994). What did W. H. Perkin Actually Make when He Oxidised Aniline to Obtain Mauveine? *J. Chem. Soc. Perkin Trans.*, 5-7.
117. Seixas de Melo, J., Takato, S., Sousa, M., Melo, M. J., Parola, A. J. (2007). Revisiting Perkin's dye(s): the spectroscopy and photophysics of two new mauveine compounds (B2 and C). *Chem. Commun.*, 2624 - 2626.

118. Sousa, M. M., Melo, M. J., Jorge, P. A., Morris, P. J. T., Rzepa, H. S., Seixas de Melo, J. S. (2008). A Study in Mauve: Unveiling Perkin's Dye in Historic Samples. *Chem. Eur. J.*, **14**, 8507-8513.
119. Travis, A. S. (1992). Science's powerful companion: A. W. Hofmann's investigation of aniline red and its derivatives. *Brit. J. Hist. Sci.*, **25**, 27-44.
120. Berezovskaya, Y. (2012). *Investigation of Protein - on Interactions by Mass Spectrometry and Ion Mobility Mass Spectrometry*. The University of Edinburgh, PhD Thesis.
121. Robson, R. M. (1998). Silk: Composition, Structure, and Properties. In *The Handbook of Fiber Chemistry*, Lewin, M., Pearce, E.M., (eds), Ed. Marcel Dekker Inc, 2nd edition: 416-463.
122. Garside, P., Wyeth, P. (2006). Textiles. In *Conservation Science*, May, M., Jones, M., Ed. RSC publishing.
123. Gamo, T., Inokuchi, T., Laufer, H. (1977). Polypeptides of fibroin and sericin secreted from the different sections of the silk gland in *Bombyx mori*. *Insect Biochem*, **7**, 285.
124. Mondal, M., Trivedy, K., Nirmal Kumar, S. (2007). The silk proteins, sericin and fibroin in silkworm, *Bombyx mori* Linn. - a review. *Caspian J. Env. Sci.*, **5**, 63-76.
125. Zurovec, M., Sehnal, F. (2002). Unique molecular architecture of silk fibroin in the waxmoth, *Galleria mellonella*. *J. Biol Chem*, **277**, 22639-22647.
126. Fedic, R., Zurovec, M., Sehnal, F. (2003). Correlation between Fibroin Amino Acid Sequence and Physical Silk Properties. *J. Biol Chem*, **268**, 35255-35264.
127. Pauling, L., Corey, R. B. (1953). Two Rippled-Sheet Configurations of Polypeptide Chains, and a Note about the Pleated Sheets. *Proc. Natl. Acad. Sci. U.S.A.*, **39**, 253-256.
128. Dobb, M. G., Fraser, R. D. B., MacRae, T. P. (1967). The fine structure of silk fibroin. *J. Cell Biol*, **32**, 289-295.
129. He, Y. X., Zhang, N. N., Li, W. F., Jia, N., Chen, B. Y., Zhou, K., Zhang, J., Chen, Y., Zhou, C. Z. (2012). N-Terminal domain of *Bombyx mori* fibroin mediates the assembly of silk in response to pH decrease. *J. Mol. Biol.*, **418**, 197-207.
130. Masayoshi, N., Kobayashi, K. (1954). Fine structure of silk fibroin. VI. Difference in the disintegration of silk fibroin by hydrogen peroxide and by dilute alkali solution. *J. Soc Textile Cellulose Ind (Japan)*, 131-134.
131. Ho, M., Wang, H., Lau, K. (2012). Effect of degumming time on silkworm silk fibre for biodegradable polymer composites. *Appl. Surf. Sci.*, **258**, 3948-3955.
132. Tsukada, M., Hirabayashi, K. (1980). Change of silk fibroin structure by ultraviolet radiation. *J. Polym. Sci. Pol. Lett.*, 507-511.
133. Baltova, S., Vassileva, V., Valtcheva, E. (1998). Photochemical behaviour of natural silk- I. Kinetic investigation of photoyellowing. *Polymer degrad. stab.*, **60**, 53-60.
134. Baltova, S., Vassileva, V. (1998). Photochemical behaviour of natural silk II. Mechanism of fibroin photodestruction. *Polymer degrad. stab.*, **60**, 61-65.

135. Lu, Q., Zhang, B., Li, M., Zuo, B., Kaplan, D. L., Huang, Y., Zhu, H. (2011). Degradation Mechanism and Control of Silk Fibroin. *Biomacromolecules*, **12**, 1080-1086.
136. Block, R. J. (1939). The composition of keratins: the amino acid composition of hair, wool, horn, and other eukeratins. *J. Biol. Chem.*, **128**, 181-186.
137. Astbury, W. T., Street, A. (1931). X-ray studies of the structure of hair, wool, and related fibres. I. General. *Phil. Trans. R. Soc. Lond. A*, **230**, 75-101.
138. Bear, R. S. (1944). X-ray diffraction studies on protein fibers. II. Feather rachis, porcupine quill tip and clam muscle. *JACS*, **66**, 2043-2050.
139. Giroud, A., Leblond, C. P. (1951). The Keratinization of epidermis and its derivatives, especially the hair, as shown by X-Ray diffraction and histochemical studies. *Ann. N. Y. Acad. Sci.*, **53**, 613-626.
140. Fraser, R. D. B., MacRae, T. P., Rogers, G. E. (1972). *Keratins, Their Composition, Structure and Biosynthesis*. Springfield, Ill., Thomas Publishers.
141. Busson, B., Engström, P., Doucet, J. (1999). Existence of various structural zones in keratinous tissues revealed by X-ray microdiffraction. *J. Synchrotron Radiat.*, **6**, 1021-1030.
142. Astbury, W. T., Beighton, E. (1961). Structure of Feather Keratin. *Nature*, **191**, 171-173.
143. Huggins, M. L. (1957). The Structure of Alpha Keratin. *Proc. Natl. Acad. Sci. USA*, **43**, 204-209.
144. Fraser, R. D. B., MacRae, T. P., Parry, D. A. D., Suzuki, E. (1986). Intermediate Filaments in  $\alpha$ -keratins. *Proc. Natl. Acad. Sci. USA*, **83**, 1179-1183.
145. Parry, D. A. D. (1995). Hard  $\alpha$ -keratin IF: A structural model lacking a head-to-tail molecular overlap but having hybrid features characteristic of both epidermal keratin and vimentin IF. *Protein Struct. Funct. Genet.*, **22**, 267-272.
146. Parry, D. A. D. (1996). Hard  $\alpha$ -keratin intermediate filaments: an alternative interpretation of the low-angle equatorial X-ray diffraction pattern, and the axial disposition of putative disulphide bonds in the intra- and inter-protofilamentous networks. *Int. J. Biol. Macromol.*, **19**, 45-50.
147. Lee, C. H., Kim, M. S., Chung, B. M., Leahy, D. J., Coulombe, P. A. (2012). Structural basis for heteromeric assembly and perinuclear organization of keratin filaments. *Nat. Struct. Mol. Biol.*, **19**, 707-715.
148. Popescu, C., Höcker, H. (2007). Hair - the most sophisticated biological composite material. *Chem. Soc. Rev.*, **36**, 1282-1291.
149. Shao, J., Hawkyard, C. J., Carr, C. M. (1997). Investigation into the Effect of UV/Ozone Treatments on the Dyeability and Printability of Wool. *J. Soc. Dyers Colour.*, **113**, 126-131.
150. Andrews, J. C. (1932). The oxidation of cysteine in acid solution. *J. Biol. Chem.*, **97**, 657-662.
151. Andrews, J. C. (1933). The racemisation and oxidation of cysteine in acid solution. *J. Biol. Chem.*, **102**, 263-268.

- 
152. Millington, K. R., Church, J. S. (1997). The photodegradation of wool keratin II. Proposed mechanisms involving cysteine. *J. Photochem. Photobiol. B, Biol.*, **39**, 204-212.
153. White, A., Fishman, J. B. (1936). The formation of taurine by the decarboxylation of cysteic acid. *J. Biol. Chem.*, **116**, 457-461.
154. Hill, R. R., Ghadimi, M. J. (1996). Alkali-promoted yellowing of wool. Yellow degradation products from a model for protein-bound cystine. *J. Soc. Dyers Colour.*, **112**, 148-152.
155. Schäfer, K., Goddinger, D., Höcker, H. (1997). Photodegradation of Tryptophan in Wool. *J. Soc. Dyers Colour.*, **113**, 350-355.
156. Nicholls, C. H., Pailthorpe, M. T. (1976). Primary Reactions in the Photoyellowing of Wool Keratin. *J. Text. I.*, **67**, 397-403.
157. Beck, L., de Viguerie, L., Walter, Ph., Pichon, L., Gutiérrez, P. C., Salomon, J., Menu, M., Sorieul, S. (2010). New approaches for investigating paintings by ion beam techniques. *Nucl. Instr. Meth. B*, **268**, 2086-2091.
158. Beck, L., Cuif, J. P., Pichon, L., Vaubailon, S., Dambricourt Malassé, A., Abel, R. L. (2012). Checking collagen preservation in archaeological bone by non-destructive studies (Micro-CT and IBA). *Nucl. Instr. Meth. B*, **273**, 203-207.
159. Li, H. K., Akselsson, K. R. (1985). A quantitative basis for hair analysis using PIXE. *Nucl. Instr. Meth. B*, **12**, 248-256.
160. Frey, H. U., Otto, G., Vogt, J. (1988). Thick target PIXE analyses of elemental distributions across the surface and inside human fingernails. *Nucl. Instr. Meth. B*, **30**, 83-89.



## **CHAPTER 2**

---

<b>2. ULTRA PERFORMANCE LIQUID CHROMATOGRAPHY: METHOD DEVELOPMENT FOR THE SEPARATION OF NATURAL DYESTUFFS .....</b>	<b>61</b>
2.1 HIGH PERFORMANCE LIQUID CHROMATOGRAPHY COUPLED TO PHOTO DIODE ARRAY ANALYSIS OR MASS SPECTROMETRY .....	61
2.1.1 <i>High Performance Liquid Chromatography</i> .....	61
2.1.2 <i>Photo Diode Array Analysis</i> .....	63
2.1.3 <i>Mass Spectrometry analysis (MS)</i> .....	64
2.1.3.1 Electro spray Ionisation (ESI) .....	64
2.1.3.2 Negative Electro spray Ionisation for the study of flavonoid dyes .....	65
2.2 ULTRA PERFORMANCE LIQUID CHROMATOGRAPHY .....	67
2.3 METHOD DEVELOPMENT FOR THE SEPARATION OF FLAVONOID AND ANTHRAQUINONE DYES .....	69
2.3.1 <i>Method development</i> .....	70
2.3.1.1 Transfer of HPLC method to the UPLC system .....	70
2.3.1.2 Evaluation of the UPLC methods .....	73
2.3.1.3 Repeatability and resolution factors (Rs) .....	75
2.3.1.4 Linearity, calibration curves and limit of detection .....	81
2.3.1.5 UPLC-ESI Mass Spectrometry .....	86
2.3.2 <i>Evaluation of sample preparation</i> .....	89
2.4 APPLICATION TO REFERENCE MATERIALS .....	91
2.4.1 <i>Identification of minor components in acid-hydrolysed extracts of weld (Reseda luteola L.) and dyer's greenweed (Genista tinctoria L.)</i> .....	92
2.4.1.1 Weld ( <i>Reseda luteola L.</i> ) .....	92
2.4.1.2 Dyer's greenweed ( <i>Genista tinctoria L.</i> ) .....	93
2.4.2 <i>Characterisation of Gt compounds by UPLC-ESI-MS</i> .....	97
2.4.3 <i>Effect of over-dyeing</i> .....	103
2.5 SUMMARY .....	105
2.6 REFERENCES .....	106

## **2. ULTRA PERFORMANCE LIQUID CHROMATOGRAPHY: METHOD DEVELOPMENT FOR THE SEPARATION OF NATURAL DYESTUFFS**

High performance Liquid chromatography (HPLC) coupled to Diode Array detection (PDA) has been used since the 1980s for the investigation of natural dyestuffs in historical textiles,<sup>1, 2</sup> with increased use in recent years of Electro-Spray Ionisation Mass Spectrometry analysis (HPLC-ESI-MS).<sup>3-7</sup> The very small amounts of material available for sampling from historical textiles and the poor light fastness of several natural dyes often makes the identification of dyestuff species in this field quite challenging and sometimes renders the characterisation of minor components impossible. For these reasons the transfer of the classical PDA-HPLC method used at National Museums Scotland (NMS) for the investigation of natural dyes to Ultra Performance Liquid Chromatography (PDA-UPLC) was explored. In this chapter, the HPLC chromatographic method was compared with two UPLC chromatographic methods and the level of additional information provided in practice by PDA-UPLC over PDA-HPLC was assessed with the analysis of a selection of reference materials.

### **2.1 HIGH PERFORMANCE LIQUID CHROMATOGRAPHY COUPLED TO PHOTO DIODE ARRAY ANALYSIS OR MASS SPECTROMETRY**

#### *2.1.1 High Performance Liquid Chromatography*

Chromatography refers to several techniques allowing the separation of a mixture of analytes and is composed of two phases, one stationary and one mobile. The development of chromatography started first in the 1950s with the use of Thin Layer Chromatography (TLC), followed by the development of Gas Chromatography (GC) and then Liquid Chromatography (LC) in the 1960s.<sup>8</sup> In High Performance Liquid (HPLC), also sometime called High Pressure Liquid Chromatography, the mobile phase is a liquid, which can be composed of a mixture of an organic phase and an aqueous phase, circulating through a column packed with stationary phase at a

certain flow rate.<sup>8</sup> Different analytes travel through the system at different migration rates, due to their differing partition between the stationary phase and the mobile phase, and will be adsorbed onto the stationary phase.<sup>8</sup> In the case of natural dye analysis, the system is used in reverse phase, which means that the column contains a non-polar stationary phase, while the mobile phase is a polar eluent. As a result the more polar components in the analysed solution will be eluted faster than non-polar components and the relation between the volume of mobile phase and retention is expressed in equation 2.1.

$$V_R = t_R \times F \quad \text{Equation 2.1}$$

$V_R$  represents the volume of mobile phase that flowed during the time  $t_R$  required for a component to elute from the chromatographic system, at the flow rate  $F$ . This volume  $V_R$  is also the sum of  $V_M$ , the dead space or the mobile phase volume, and the stationary phase volume  $V_S$  multiplied by the partition coefficient  $K$  (equation 2.2).

$$V_R = V_M + KV_S \quad \text{Equation 2.2}$$

The partition coefficient  $K$  corresponds to the concentration of the analyte A in the stationary phase  $[A]_S$  divided by the concentration of the analyte A in the mobile phase  $[A]_M$  and can also be expressed as the phase volume ratio  $\beta$  multiplied by the partition ratio  $k$  (equations 2.3 and 2.4).

$$K = \frac{[A]_S}{[A]_M} = \beta k \quad \text{Equation 2.3}$$

$$\beta = \frac{V_M}{V_S} \quad \text{Equation 2.4}$$

Finally, the separation factor  $\alpha$  of two analytes A and B can be calculated as the ratio of their partition coefficients (equation 2.5). The resolution factor  $R_S$  is used to

calculate the degree of separation of the analytes A and B, and corresponds to twice the ratio of the distance between their peak maxima divided by the sum of the width  $W$  of each peak (equation 2.6). A  $R_s$  value of 1.5 is necessary for complete separation.

$$\alpha = \frac{K_B}{K_A} \quad \text{Equation 2.5}$$

$$R_s = 2 \times \frac{[(t_R)_B - (t_R)_A]}{W_A + W_B} \quad \text{Equation 2.6}$$

### 2.1.2 Photo Diode Array Analysis

For the analysis of natural product dyestuffs, the HPLC system is usually coupled to a Photo Diode Array (PDA) detector, made of a large number of photodiodes, each of them being sensitive over a specific wavelength range. PDA analysis is used for the characterisation of dyestuff chromophores, as they have very characteristic UV-Vis spectra. The photodiodes provide spectral analysis of the light which is absorbed ( $A$ ), following the Beer Lambert law (equation 2.7). The relationship between absorbance versus concentration is only valid if the solutions are well-equilibrated and diluted, as it assumes that the refractive index of the sample remains constant, that the light is monochromatic, and that no stray light reaches the detector element. In the case of concentrated solutions, the Beer Lambert law is not validated and the linearity relationship between absorbance and concentration is not observed.

$$A = \log \frac{I_0}{I} = \epsilon lc \quad \text{Equation 2.7}$$

In equation 2.7,  $A$  is a dimensionless quantity measured in absorbance units (AU),  $I_0$  is the incident intensity of radiation and  $I$  the transmitted intensity of radiation,  $\epsilon$  corresponds to the molar extinction coefficient of the analyte ( $\text{L mol}^{-1}\text{cm}^{-1}$ ),  $l$  is the

path length of detector flow cell (1 cm) and  $c$  the concentration of analyte in the mobile phase passing through the detector ( $\text{mol L}^{-1}$ ). After transformation by the software, the combined measurements acquired using the photodiode array will produce a UV-Vis spectrum which is characteristic for each eluted component. Each unique combination of retention time and UV-Vis spectra allows the characterisation of the molecules present in the solution.

### 2.1.3 Mass Spectrometry analysis (MS)

Mass spectrometry (MS) is an analytical technique used for measuring the molecular weight of an ionised chemical and is often coupled to chromatographic systems, such as High Performance Liquid Chromatography (HPLC) or Gas Chromatography (GC).<sup>9</sup> A mass spectrometer consists of an ionisation source, a mass analyser where ions are separated based on their mass to charge ratio ( $m/z$ ) and a detector to register the resulting ion current which is displayed in the format of a  $m/z$  spectrum.<sup>10</sup> The ionisation of the analyte is a critical step in mass spectrometric measurements and with regard to dye analysis, Electrospray Ionisation (ESI), is the most widely ionisation technique used,<sup>11-13</sup> but other ionisation methods can be used depending on the nature of the analyte.<sup>10</sup> Other ionisation methods include Atmospheric Pressure Chemical Ionisation (APCI), Chemical Ionisation (CI), Electron Impact (EI), Fast Atom Bombardment (FAB), Field Desorption / Field Ionisation (FD/FI), Matrix Assisted Laser Desorption Ionisation (MALDI), Thermospray Ionisation (TSP).<sup>10</sup> Finally, there is also a variety of analysers such as magnetic sector, quadrupole, and time-of-flight (TOF).<sup>10</sup>

#### 2.1.3.1 Electrospray Ionisation (ESI)

In Electrospray Mass Spectrometry (ESI-MS) the analytes are ionised by a combined process of desolvation and protonation or de-protonation.<sup>14</sup> The sample is introduced through a high voltage (3 - 4 kV) stainless steel capillary at a flow rate between  $1 \mu\text{L min}^{-1}$  and  $1 \text{ mL min}^{-1}$ , and the resulting spray (aerosol) will contain highly charged

micron-sized droplets of solvated analyte ions, which will become even smaller as they evaporate further.<sup>10</sup> Either positive or negative voltage can be applied to generate positive or negative ions. As the solvent evaporates, the droplet forms a ‘Taylor cone’ which emits smaller droplets from its tip (figure 2.1). During this process, the charge density of the droplets increases, which will lead to the destabilisation and disintegration of the droplet due to increasing electrostatic repulsion (Coulombic fission).<sup>3</sup> This charge balancing process involves electrochemical oxidation/reduction of the components of the metal capillary and/or the species in solution.<sup>3, 15</sup>

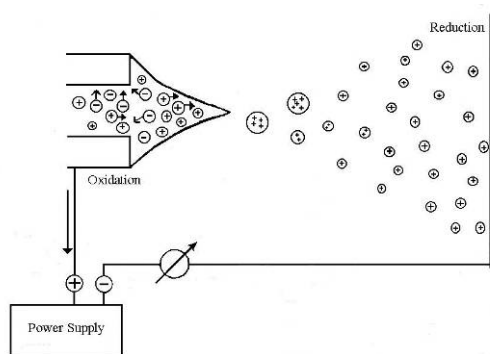
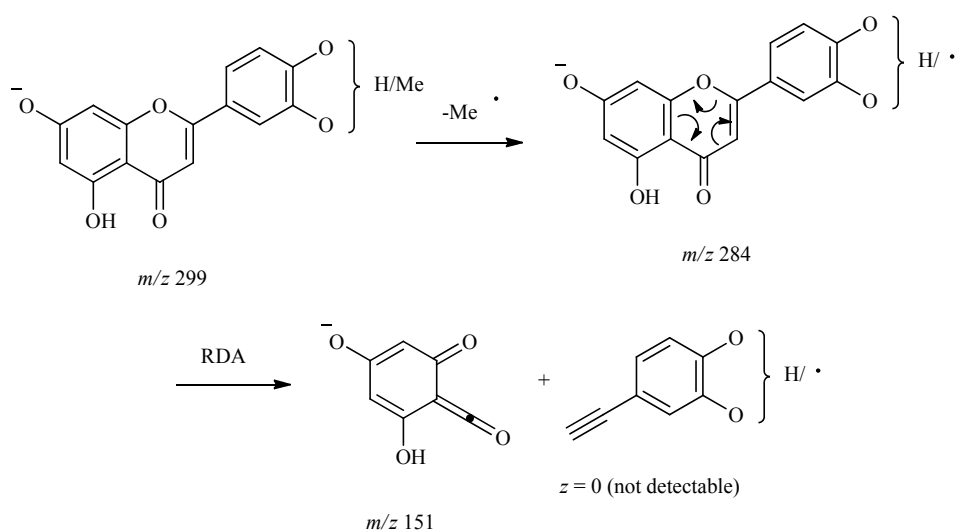


**Figure 2.1:** Electro spray ionisation (based on a published diagram).<sup>16</sup>

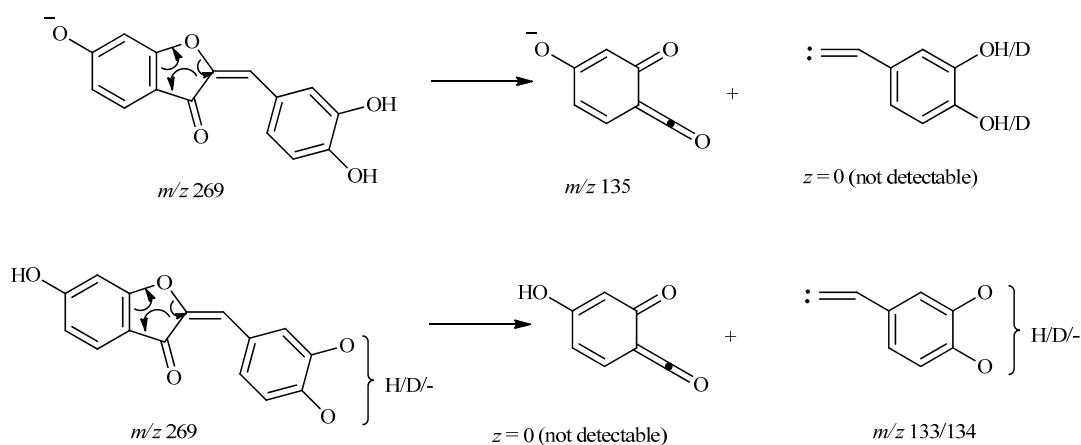
### 2.1.3.2 Negative Electro spray Ionisation for the study of flavonoid dyes

Previous studies have shown that Mass Spectrometry analysis of flavonoid and isoflavonoid dyes may be achieved effectively using negative ionisation electro spray mass spectrometry,<sup>3, 11, 13, 17</sup> and allowed the characterisation of several fragmentation mechanisms using secondary and tertiary Mass Spectrometry ion fragmentation ( $MS^2$  and  $MS^3$ , corresponding to secondary fragmentation after ion isolation).<sup>3, 13</sup> These included for flavonoid dyes a retro-Diels-Alder fragmentation observed for flavones and flavonols (scheme 2.1) and an M-122 fragmentation characteristic of 3',4'-dihydroxyflavonols. It was also found that the presence of a  $m/z$  125 fragment ion

was characteristic of 2'-hydroxyflavonols, while the presence of an ion at  $m/z$  149 was characteristic of 4'-hydroxyflavones.<sup>3, 13</sup> Finally, the investigation of the MS<sup>2</sup> spectra of the aurone sulfuretin (**15**), showed two major low-mass fragment ions at  $m/z$  135 and  $m/z$  133 in the non-deuteriated species, corresponding to a retro-cheletropic mechanism (Scheme 2.2).<sup>6</sup>



**Scheme 2.1:** The retro-Diels-Alder (RDA) negative ion ESI-MS fragmentation of *O*-methylated luteolin isomers.<sup>13</sup>



**Scheme 2.2:** Major negative ion ESI breakdown path of sulfuretin (**15**).<sup>6</sup>



## 2.2 ULTRA PERFORMANCE LIQUID CHROMATOGRAPHY

The main limitation of High Performance Liquid Chromatography (HPLC) is its low efficiency, due to the small diffusion coefficients of the analytes in the liquid phase compared to the higher diffusion coefficient observed in gaseous phase for Gas Chromatography (GC).<sup>18</sup> These small diffusion coefficients results in slow diffusion speeds in the stationary phase.<sup>18</sup> In recent years, HPLC techniques have been improved by the development of sub-2  $\mu\text{m}$  packing materials for the stationary phase use in chromatography column, with the development of Ultra High Performance Liquid Chromatography (UHPLC) and with Ultra Performance Liquid Chromatography (UPLC<sup>®</sup>) techniques.<sup>19</sup> The use of a smaller particle size improves the diffusion coefficients by shortening the analytes' diffusion path. This is explained by the simplified van Deemter equation (equation 2.8), which describes the relation between efficiency (expressed as the height equivalent to a theoretical plate,  $H$ ), linear velocity ( $u$ ) and particle size ( $d_p$ ), and where  $\lambda$  is the particle shape (with regard to the packing),  $D_m$  is the diffusion coefficient of the mobile phase,  $\gamma$ ,  $\omega$  are constants. This equation states that the smaller the particle size, the better the mass transfer rate ( $c$  term) and smaller the Eddy diffusion effect ( $a$  term).<sup>20, 21</sup>

$$H = 2\lambda d_p + \frac{2\gamma D_m}{u} + f(k) \frac{d_p^2}{D_m} u = a + \frac{b}{u} + cu \quad \text{Equation 2.8}$$

This means that shorter columns packed with smaller particles should provide the same efficiency of separation as would be obtained by longer columns packed with larger particles. This can be explained by the fact that the number of theoretical plates remains constant, as the Resolution  $R_s$  of the column is proportional to the square root of the number of plates  $N$  (equation 2.9), with  $N$  inversely proportional to the particle size  $d_p$  (equation 2.10).

$$R_s = \frac{\sqrt{N}}{4} \times \frac{(\alpha - 1)}{\alpha} \times \frac{k}{(k + 1)} \quad \text{Equation 2.9}$$

$$N \propto \frac{1}{d_p}$$

Equation 2.10

A recent published study presented a practical evaluation of Ultra Performance Liquid Chromatography (UPLC) by means of van Deemter and Knox plots for acetophenone.<sup>20</sup> Figure 2.2 shows the optimal velocities ( $u_{\text{opt}}$ ) at minimum plate heights ( $H_{\text{min}}$ ) and compared these values for two XBridge HPLC columns: C18, 3.5  $\mu\text{m}$ , 150  $\times$  4.6 mm and C18, 5  $\mu\text{m}$ , 250  $\times$  4.6 mm (length  $\times$  i.d.) and an Acquity UPLC column: BEH C18, 1.7  $\mu\text{m}$ , 100  $\times$  2.1 mm (length  $\times$  i.d.). This graphic shows that the highest optimal velocity is observed for the 1.7  $\mu\text{m}$  particle column and that the curve appears ‘flat’ at higher velocities, meaning that increasing the velocity above the optimal value leads to a relatively small decrease in efficiency.<sup>20</sup>

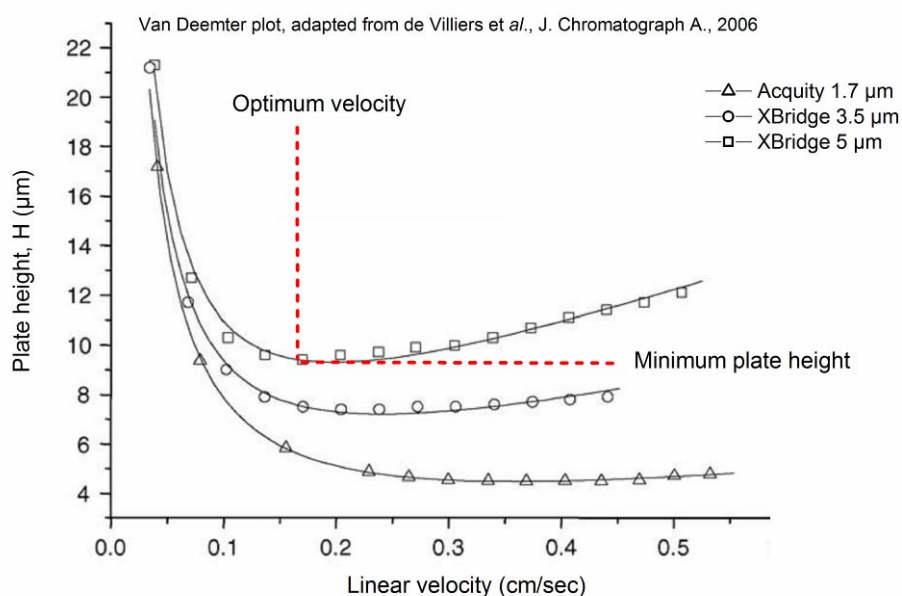


**Figure 2.2:**  $H$ – $u$  plots obtained for acetophenone on Acquity and XBridge columns. Columns: XBridge C18, 3.5  $\mu\text{m}$ , 150  $\times$  4.6mm (length  $\times$  i.d.); XBridge C18, 5  $\mu\text{m}$ , 250  $\times$  4.6mm (length  $\times$  i.d.), Acquity BEH C18, 1.7  $\mu\text{m}$ , 100  $\times$  2.1mm (length  $\times$  i.d.). Adapted from reference 20.<sup>20</sup>

The negative effect of a decrease in particle size is a corresponding increase in back-pressure of the mobile phase by about nine times (versus 5  $\mu\text{m}$ ) or three times (versus 3  $\mu\text{m}$ ).<sup>22</sup> Conventional HPLC instruments only provide maximum pressures between 4,000 and 6,000 psi and are unable to cope with such increased back-pressure. UHPLC and UPLC<sup>®</sup> instruments are therefore developed to have a much higher pressure limit, above 15,000 psi.<sup>23</sup> However, several other issues also arise from the reduction in particle size, including extra-column band-broadening, frictional heating<sup>24</sup> and a requirement for higher data acquisition rates.<sup>25</sup> But these can be reduced by minimising tubing volumes and the use of specialised fittings to control band-broadening and the use of detectors capable of very fast data acquisition rates.<sup>22, 25</sup>

### 2.3 METHOD DEVELOPMENT FOR THE SEPARATION OF FLAVONOID AND ANTHRAQUINONE DYES

As part of a survey of the natural dyestuffs used in the manufacture early English tapestries from the Burrell Collection (Glasgow, UK) and Bodleian Library (Oxford, UK), several yarns of wool and silk were investigated by High Performance Liquid Chromatography coupled to Photo Diode Array analysis (PDA-HPLC). One of the principle concerns of the study was the identification of the yellow flavonoid dyes used, including sawwort (*Serratula tinctoria* L.) and weld (*Reseda luteola* L.). However, it was found that the PDA-HPLC chromatographic method routinely employed at National Museums Scotland (NMS),<sup>1, 6, 26</sup> did not provide a low enough detection limit at 254 nm, the wavelength typically used in the detection of yellow dyestuffs (figure 2.3). The method also only allowed partial baseline resolution of the flavone luteolin (**9**) and isoflavone genistein (**11**), and did not provide baseline separation of the isomeric luteolin methyl ethers chrysoeriol (**12**) and diosmetin (**13**).<sup>6</sup> Whilst there have been recent reports of the application of UPLC and UHPLC to flavonoids and anthraquinones,<sup>27-31</sup> none of these studies have been limited by the re-extraction requirements of dyed historical textiles, or by the critical constraints of

sample size which can be taken from important historical objects. In the following sections, the NMS HPLC chromatographic method is compared with two UPLC chromatographic methods and the level of additional information provided in practice by PDA-UPLC over PDA-HPLC will be assessed through the application of both methods to the analysis of reference materials and historical samples (chapter 3).

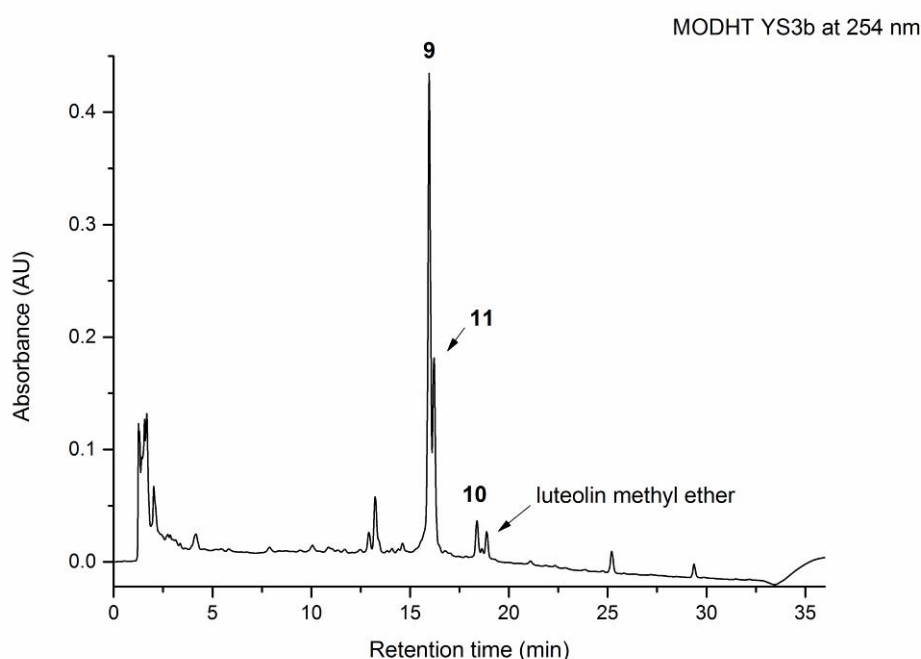


**Figure 2.4:** HPLC Chromatogram of the acid hydrolysed extract of reference MODHT YS3a, dyed with dyer's greenweed (*Genista tinctoria* L.), showing partial baseline resolution of luteolin (9) and genistein (11). Chromatogram extracted at 254 nm.

### 2.3.1 Method development

#### 2.3.1.1 Transfer of HPLC method to the UPLC system

The chromatographic methods were developed on an Acquity Ultra Performance Liquid Chromatography system (UPLC<sup>®</sup>) from Waters Ltd (figure 2.5). The system consisted of the ACQUITY UPLC<sup>®</sup> sample organiser, a column manager, a binary solvent manager, a sample manager and a tuneable UV (TUV) Photodiode Array

(PDA) detector covering the range 200 - 500 nm. The Acquity system is designed to work at very high pressure, up to 15,000 psi, which is much higher compared to the HPLC system, where the maximum back pressure is equivalent to 3,500 - 4,000 psi.

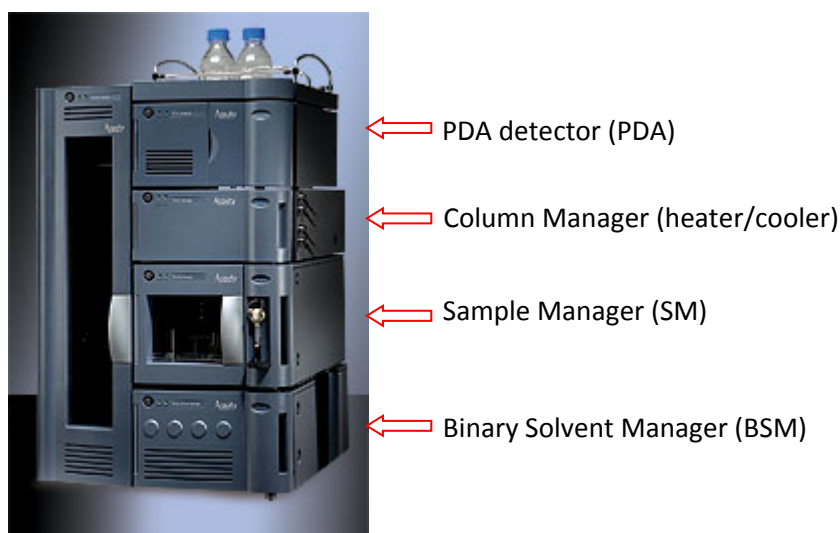


**Figure 2.5:** ACQUITY UPLC® system.



**Figure 2.6:** left: BEH C18 50 × 2.1 mm (1.7 μm) UPLC column, right: in line filter

Two Ultra Performance Liquid Chromatography columns were evaluated for the separation of natural dyes: a UPLC column BEH C18 reverse phase column, 1.7 μm particle size, 50 × 2.1 mm (length × i.d.), and a PST BEH C18 reverse phase column, 1.7 μm particle size, 150 × 2.1 mm (length × i.d.), both set-up with an in-line filter in

order to protect the columns from particles contamination (figure 2.7). These columns are packed with Ethylene-Bridged Hybrid Particles (BEH), and were recently developed by Waters for UPLC system. The BEH particles are highly spherical, with a specific surface area of  $185 \text{ m}^2 \text{ g}^{-1}$  and an average pore diameter of  $130 \text{ \AA}$ , and allow work over the range of pH 1 - 12 and at very high pressure.<sup>32</sup>

It is possible to transfer the gradient used on the HPLC system to the Acquity UPLC by calculating the equivalent volume columns, flow rates and gradient profiles.<sup>33, 34</sup> The equivalent volume columns are calculated from equation 2.11, where  $L$  corresponds to the length of the column in cm and  $r$  is the diameter of the column in cm. The equivalent UPLC flow rate  $F_2$  can be calculated from equation 2.12, using the initial HPLC flow rate  $F_1$ , both column's internal diameter  $d_c$  (mm) and the particle diameters  $d_p$  ( $\mu\text{m}$ ) of both columns.<sup>33, 34</sup> Finally the UPLC equivalent gradient profile  $t_{g2}$  is obtained from equation 2.13, where  $t_{g1}$  is the HPLC original gradient (min),  $V_{02}$  is the new UPLC column void and  $V_{01}$  the original HPLC column void, while  $F_2$  and  $F_1$  are the UPLC and HPLC columns flow rates calculated previously.

$$V = L \times \pi \times r^2 \quad \text{Equation 2.11}$$

$$F_2 = F_1 \times \left( \frac{d_{c2}^2}{d_{c1}^2} \right) \times \left( \frac{d_{p1}}{d_{p2}} \right) \quad \text{Equation 2.12}$$

$$t_{g2} = t_{g1} \times \left( \frac{V_{02}}{V_{01}} \right) \times \left( \frac{F_2}{F_1} \right) \quad \text{Equation 2.13}$$

The equivalent gradient profiles were calculated for UPLC columns BEH C18  $50 \times 2.1$  mm,  $1.7 \mu\text{m}$  and PST BEH C18  $150 \times 2.1$  mm,  $1.7 \mu\text{m}$ , using the Acquity column calculator transfer and are presented in table 2.1. For both UPLC columns, the equivalent flow rate taking into account the particle size would be  $740 \mu\text{L min}^{-1}$ , however these theoretical calculations did not consider the mobile phase viscosity,

which is known to be higher for methanol than for acetonitrile. It was therefore necessary to reduce considerably the flow rate and increase the temperature of the column in order to limit the viscosity of the mobile phase and reduce as much as possible the back-pressure in the system. Method B working with BEH C18  $50 \times 2.1$  mm,  $1.7 \mu\text{m}$ , used a flow rate of  $500 \mu\text{L min}^{-1}$  and a temperature of  $55 \text{ }^\circ\text{C}$ , while method C working with PST BEH C18  $150 \times 2.1$  mm,  $1.7 \mu\text{m}$ , used a flow rate of  $250 \mu\text{L min}^{-1}$  and a temperature of  $55 \text{ }^\circ\text{C}$ . Both methods allowed a back pressure of 8500 - 9000 psi to be employed, and the gradient and equivalent volume columns were then re-adjusted accordingly. Details on the columns specificities and chromatographic methods can be found in section 6.1.

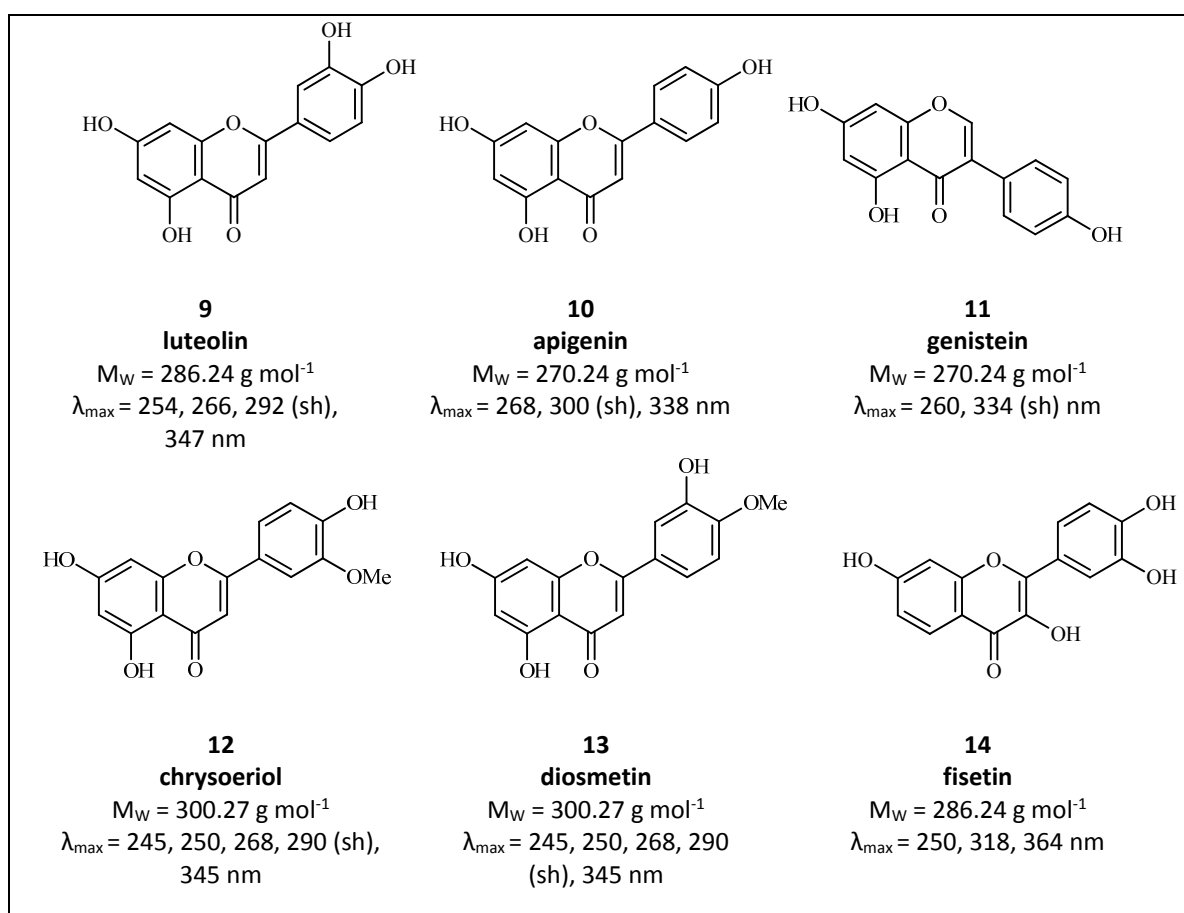
	Time (min)	% A aqueous	% B organic	Column Volume $\text{cm}^3$	Flow rate ( $\mu\text{L min}^{-1}$ )
UPLC column $50 \times 2.1$ mm ( $1.7 \mu\text{m}$ )	0	77	23	0	740
	0.34	77	23	2.19	740
	3.29	10	90	18.96	740
	3.4	77	23	0.73	740
	4.08	77	23	4.38	740
UPLC column $150 \times 2.1$ mm ( $1.7 \mu\text{m}$ )	0	77	23	0	740
	1.13	77	23	2.19	740
	9.97	10	90	18.96	740
	10.31	77	23	0.73	740
	12.35	77	23	4.38	740

**Table 2.1:** Calculation of the equivalent volume columns and flow rates to two UPLC columns; corresponding to the HPLC method A using the Acquity column calculator software.

### 2.3.1.2 Evaluation of the UPLC methods

The chromatographic methods were evaluated based on several performance characteristics defined by Hartmann *et al.*, for the validation of chromatographic methods.<sup>35</sup> These performance characteristics were the repeatability (random error of the method), the specificity (ability to determine the analyte in the presence of other compounds), the limit of detection (lowest sample concentration that can be

detected), the limit of quantification (lowest sample concentration that can be quantified) and the linearity (ability of the method to obtain test results which are proportional to the concentration in the sample).<sup>35</sup> The methods were based on the separation and quantification of ten flavonoid and anthraquinone standards, allowing the characterisation of the main species usually found in historical tapestries. Seven flavonoid dyes were selected and included the flavones luteolin (**9**) and apigenin (**10**), the isoflavone genistein (**11**), the two *O*-methylated flavones chrysoeriol (**12**) and diosmetin (**13**), the flavonol fisetin (**14**) and the aurone sulfuretin (**15**), with in addition the three anthraquinone dyes alizarin (**26**), purpurin (**28**) and carminic acid (**32**) (table 2.2).





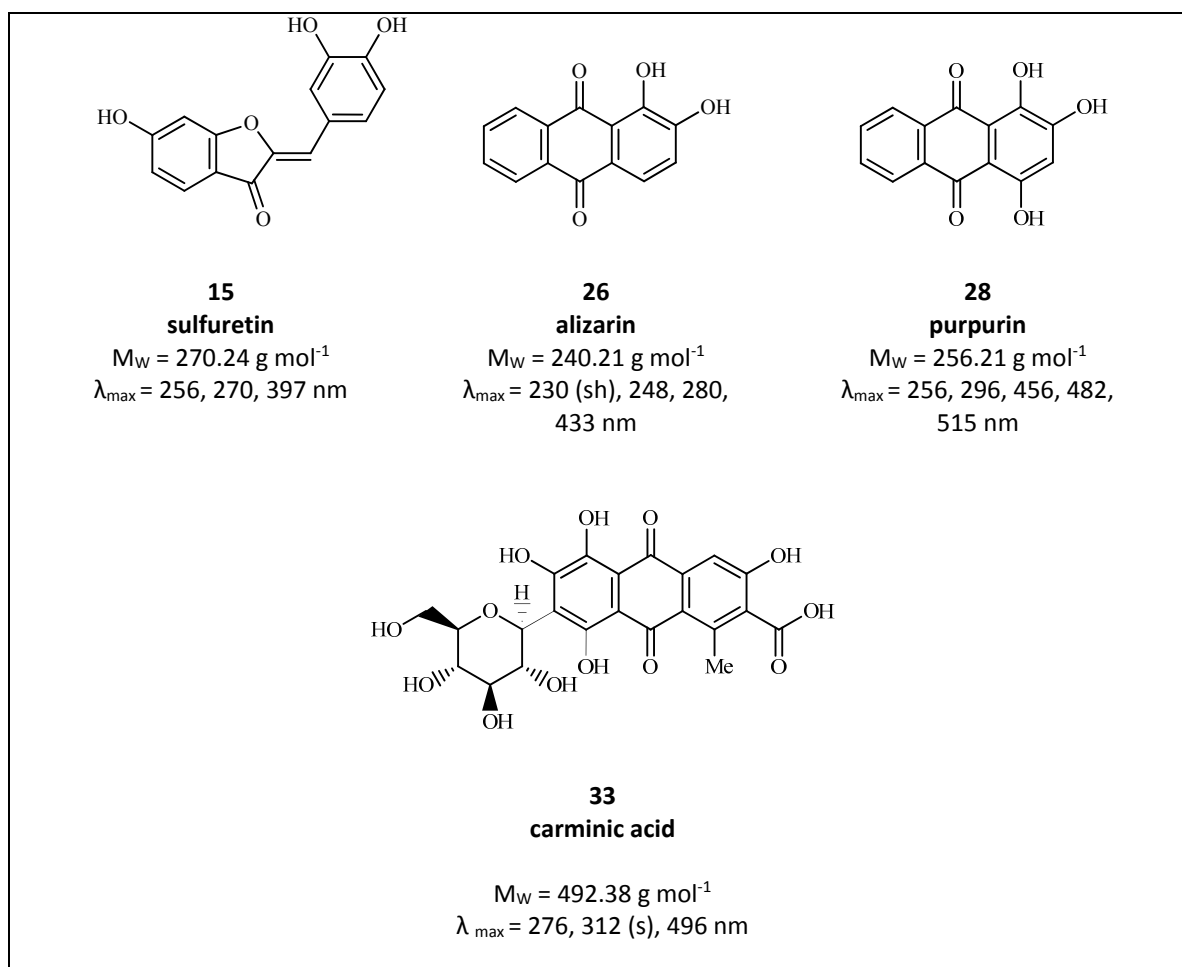


**Table 2.2:** Flavonoid and anthraquinone dyes selected for UPLC method development ( $\lambda_{\text{max}}$  correspond to theoretical values in ethanol).

### 2.3.1.3 Repeatability and resolution factors ( $R_s$ )

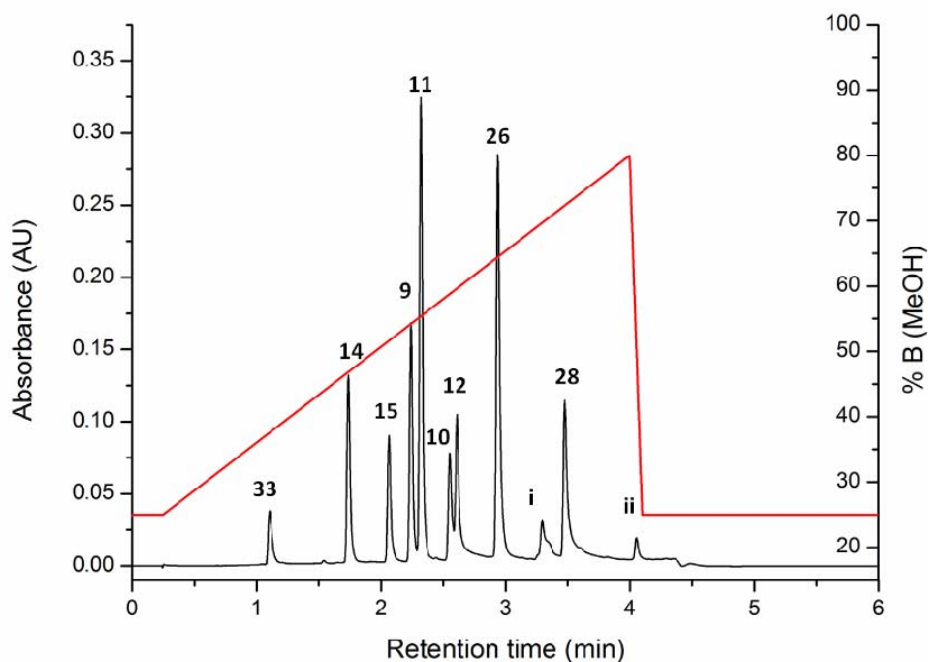
The repeatability of the methods was evaluated over several measurements of a reference solution containing several dye standards. It was found that both UPLC methods presented a much higher repeatability compared to the HPLC method, which exhibited higher variations in retention time. For all the dye standards the average variation on 7 measurements ranged between 0.05 - 0.9 % for the  $50 \times 2.1$  mm UPLC column and on 14 measurements between 0.04 - 0.06 % for the  $150 \times 2.1$

mm UPLC column, with the exception of carminic acid and purpurin which showed slightly higher variation (see table 2.2).

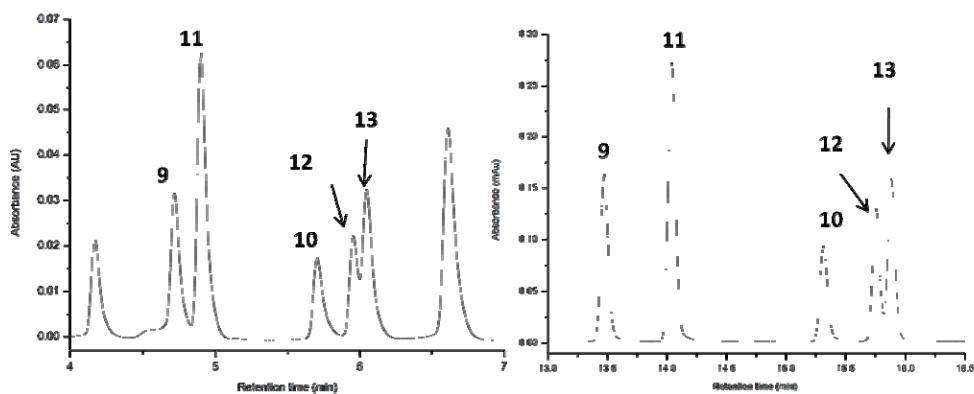
	Method A	Method B	Method C
	ODS2, 150 × 4.6 mm, 5 μm	BEH C18, 50 × 2.1 mm, 1.7 μm	PST BEH C18, 150 × 2.1 mm, 1.7 μm
Compound (x)	R <sub>t</sub> ± s (min) [n=7]	R <sub>t</sub> ± s (min) [n=7]	R <sub>t</sub> ± s (min) [n=12]
carminic acid ( <b>33</b> )	5.8 ± 0.3	1.10 ± 0.01	5.79 ± 0.12
fisetin ( <b>14</b> )		1.740 ± 0.003	10.561 ± 0.004
sulfuretin ( <b>15</b> )		2.067 ± 0.003	12.49 ± 0.01
luteolin ( <b>9</b> )	15.0 ± 0.3	2.244 ± 0.003	13.47 ± 0.01
genistein ( <b>11</b> )	15.3 ± 0.2	2.323 ± 0.003	14.03 ± 0.01
apigenin ( <b>10</b> )	17.4 ± 0.3	2.556 ± 0.003	15.26 ± 0.01
chrysoeriol ( <b>12</b> )		2.614 ± 0.002	15.69 ± 0.01
diosmetin ( <b>13</b> )			15.87 ± 0.01
alizarin ( <b>26</b> )	19.8 ± 0.4	2.942 ± 0.002	17.72 ± 0.01
purpurin ( <b>28</b> )	24.0 ± 0.7	3.481 ± 0.002	20.77 ± 0.05

**Table 2.2:** Comparing retention time variability for the separation of flavonoid dyes.

The UPLC chromatographic method B used the shorter column and employed a 6 minutes run time (including an equilibration period). This method allowed the separation of 9 out of 10 standards (figure 2.5). Although the retention times were much shorter compared to HPLC Method A, the R<sub>s</sub> value for the separation of luteolin (**9**) / genistein (**11**) was 0.83 compared to the value of 0.78 obtained by HPLC. However, the separation of the *O*-methylated regioisomers chrysoeriol (**12**) and diosmetin (**13**) was not achieved. In order to achieve a better separation, a longer gradient was tested. This method B' allowed a slightly better separation of luteolin (**9**) / genistein (**11**) and apigenin (**10**) /chrysoeriol (**12**) to be achieved with R<sub>s</sub> values of 1.10 and 1.80, respectively (see figure 2.6 left and section 6.1 for gradient information). However it only provided a R<sub>s</sub> value of 0.68 for the separation of the regioisomers chrysoeriol (**12**) and diosmetin (**13**), which was not suitable for quantification of both isomers while in solution together.

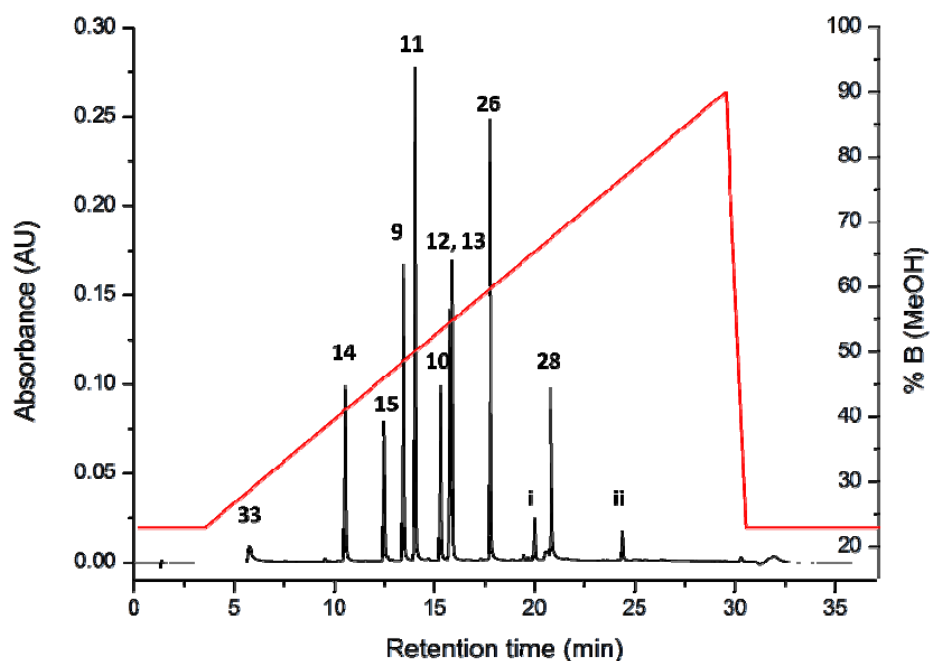


**Figure 2.5:** UPLC Method B: using BEH C18, 1.7  $\mu\text{m}$ , 2.1 x 50 mm column, showing the separation of carminic acid (**33**), fisetin (**14**), sulfuretin (**15**), luteolin (**9**), genistein (**11**), apigenin (**10**), chrysoeriol (**12**), alizarin (**26**) and purpurin (**28**). Standard solution at 20  $\mu\text{g mL}^{-1}$  recorded at 254 nm (2.5  $\mu\text{L}$  injection volume). Peaks i and ii are impurities.



**Figure 2.6 (left):** UPLC Method B': using BEH C18, 1.7  $\mu\text{m}$ , 2.1 x 50 mm column and with a lower slope for the gradient, allowing partial separation of regioisomers chrysoeriol (**12**) and diosmetin (**13**) [ $R_s = 0.68$ ]; **(right):** UPLC Method C: using PST BEH C18, 1.7  $\mu\text{m}$ , 2.1 x 150 mm column allowing separation of regioisomers chrysoeriol (**12**) and diosmetin (**13**) [ $R_s = 1.32$ ]

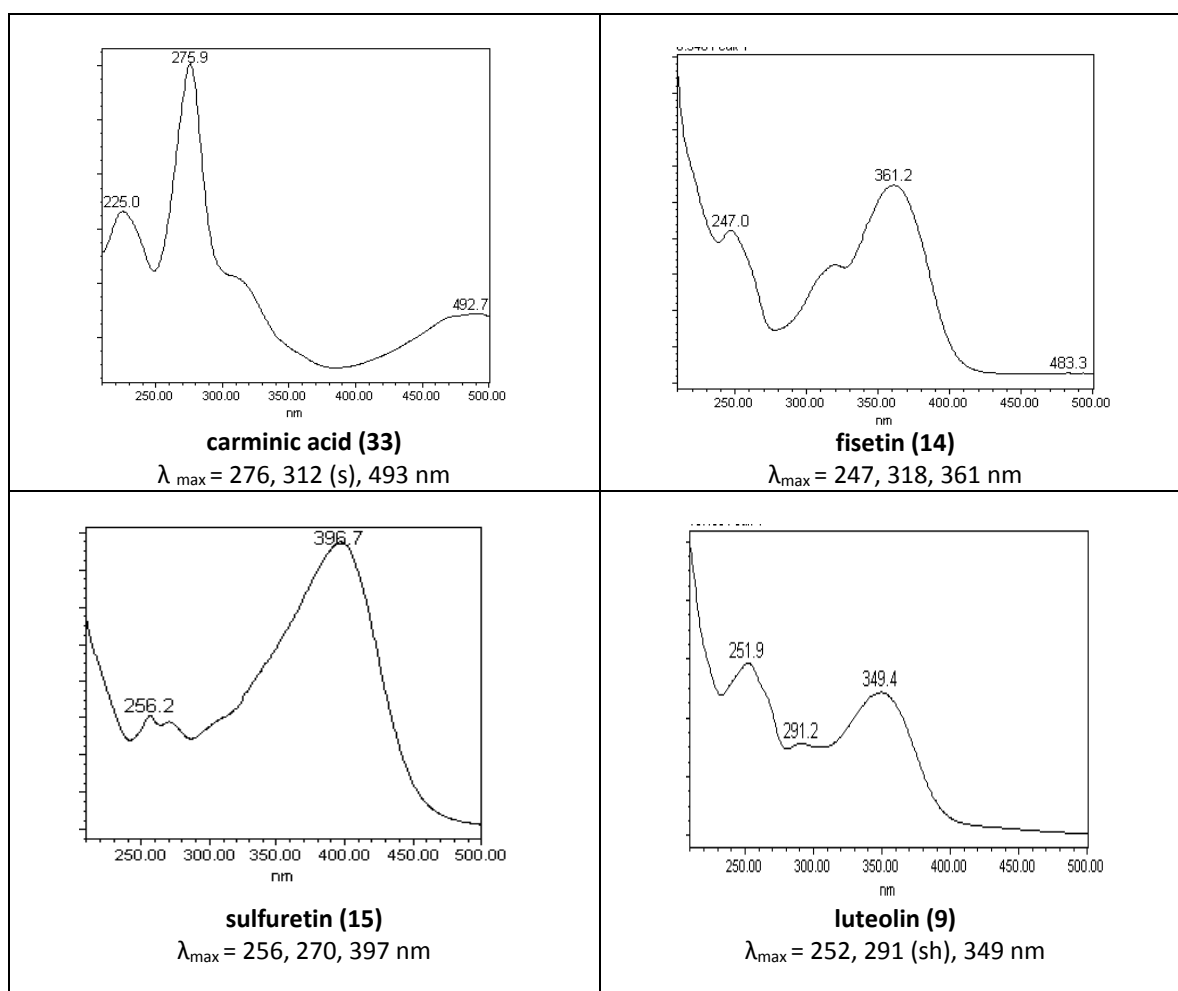
Finally; the UPLC chromatographic Method C, developed on the longer column, employed a 37 minutes run time (including an equilibration period) and allowed a much better separation of all the standards including the regioisomers chrysoeriol (**12**) and diosmetin (**13**) (figures 2.7). The  $R_s$  factors were greatly improved to 3.13 for luteolin (**9**) / genistein (**11**) and 2.88 and 1.32 for respectively apigenin (**9**) / chrysoeriol (**12**) and chrysoeriol (**12**) /diosmetin (**13**) (figure 2.6 right and table 2.3).



**Figure 2.7:** UPLC Method C: using PST BEH C18, 1.7  $\mu\text{m}$ , 2.1 x 150 mm column, showing the separation of carminic acid (**33**), fisetin (**14**), sulfuretin (**15**), luteolin (**9**), genistein (**11**), apigenin (**10**), chrysoeriol (**12**), diosmetin (**13**), alizarin (**26**) and purpurin (**28**). Standard solution at  $10 \mu\text{g mL}^{-1}$  recorded at 254 nm (5  $\mu\text{L}$  injection volume). Peaks i and ii are impurities present in the standard solutions of alizarin and purpurin respectively.

Compound (x)	Method A	Method B	Method C
	ODS2, 150 × 4.6 mm, 5 μm	BEH C18, 50 × 2.1 mm, 1.7 μm	PST BEH C18, 150 × 2.1 mm, 1.7 μm
	R <sub>s</sub> value	R <sub>s</sub> value	R <sub>s</sub> value
Luteolin (9)			
genistein (11)	lu/gen: 0.78	lu/gen: 0.83	lu/gen: 3.13
apigenin (10)		ap/chrys: 1.41	ap/chrys: 2.88
chrysoeriol (12)			chrys/diosm : 1.32
diosmetin (13)			

**Table 2.3:** Comparing resolution factors ( $R_s$  values calculated as  $R_s = 2 (t_{R-B} - t_{R-A}) / w_{b-A} + w_{b-B}$ ) for the separation of flavonoid dyes.



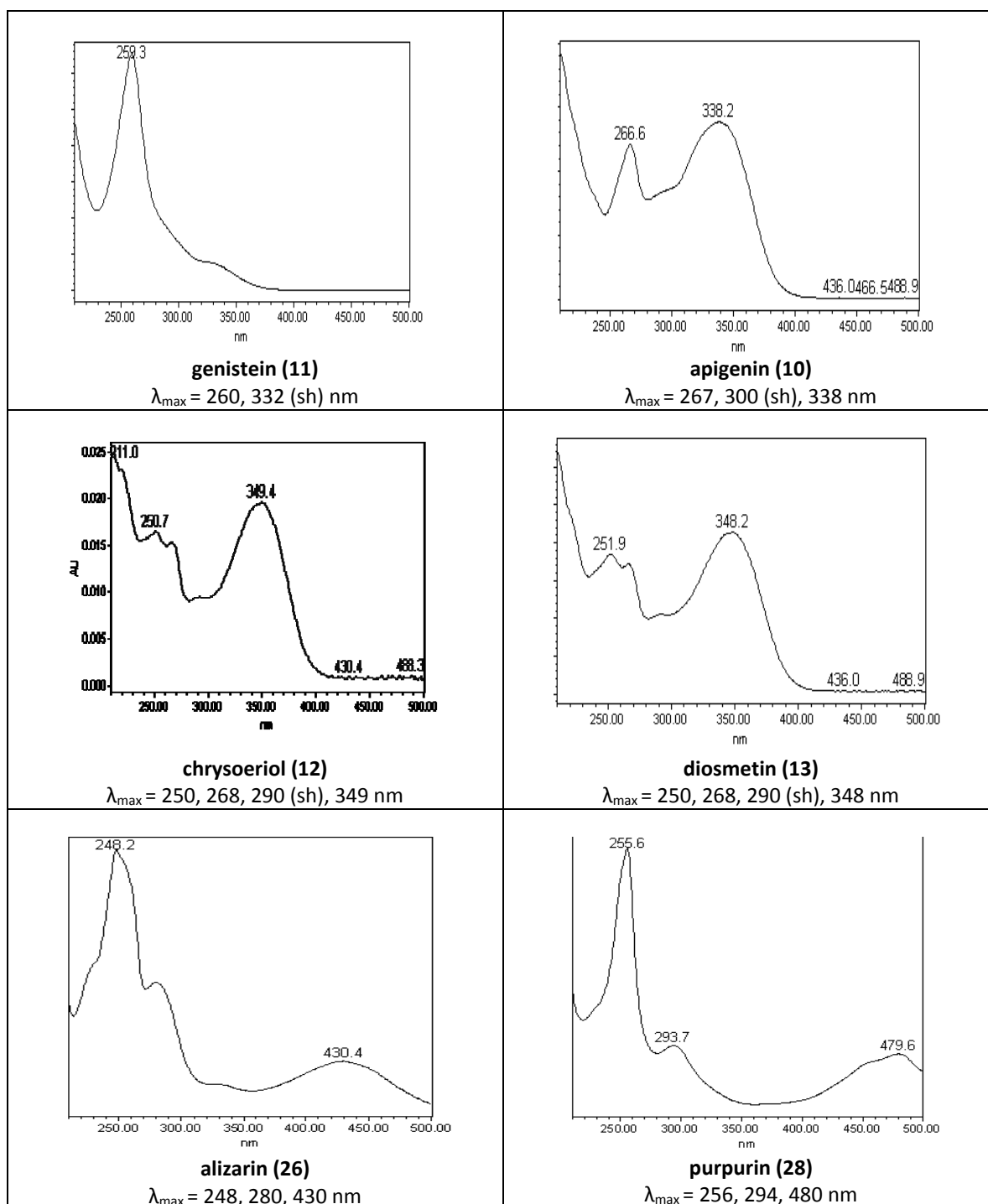


**Table 2.4:** PDA spectra of flavonoid and anthraquinone standards by order of elution, obtained during UPLC method development.

### 2.3.1.4 Linearity, calibration curves and limit of detection

The areas of the peaks were observed to correlate linearly with the concentrations of the solutions over the range of concentrations studied ( $[x]$  ( $\mu\text{g mL}^{-1}$ ) vs.  $A_x$  ( $R^2$ )). These concentrations corresponded to those expected from historical textile samples and typically ranged between 0.2 and 40  $\mu\text{g mL}^{-1}$ . On the UPLC system seven or eight solutions were used to calculate the calibration curves and each solution was investigated in triplicate, while on the HPLC system six solutions of standard were manually injected once over a similar range of concentrations. Table 2.4 presents the linearity range and calibration curve obtained for the isoflavone genistein (**11**) based on measurements done on the HPLC system using method A and UPLC system using methods B and C. The calibration curves of the nine other dye standards can be found in section 7.1, calculated at 254 nm and 350 nm for flavonoid dyes and 254 nm and 430 nm for anthraquinone dyes.

<b>Method A : HPLC ODS(2), 150 × 4.6 mm, 5 <math>\mu\text{m}</math> : each solution analysed once</b>				
<b>Compound [x]</b>	<b>[x] (<math>\mu\text{g mL}^{-1}</math>) vs. <math>A_x</math> (<math>R^2</math>)</b>	<b>n [<math>\mu\text{g mL}^{-1}</math>]</b>	<b>[x] (<math>\mu\text{g mL}^{-1}</math>) vs. <math>A_x</math> (<math>R^2</math>)</b>	<b>n [<math>\mu\text{g mL}^{-1}</math>]</b>
	<b>254 nm</b>		<b>350 nm</b>	
<b>Genistein (11)</b>	$y = 116528x - 130158$ (0.9905)	n = 6 [2 - 40]	$y = 9003.8x - 14107$ (0.9864)	n = 6 [2 - 40]
<b>Method B : UPLC, 50 × 2.1 mm, 1.7 <math>\mu\text{m}</math> : each solution analysed in triplicate</b>				
	<b>254 nm</b>		<b>350 nm</b>	
<b>Genistein (11)</b>	$y = 30627x + 4886$ (0.994)	n = 7 [0.5 - 80]	$y = 2574.5x - 158.27$ (0.9983)	n = 7 [0.5 - 80]
<b>Method C : UPLC, 150 × 2.1 mm, 1.7 <math>\mu\text{m}</math> : each solution analysed in triplicate</b>				
	<b>254 nm</b>		<b>350 nm</b>	
<b>Genistein (11)</b>	$y = 123813x + 7069.6$ (0.9998)	n = 8 [0.2 - 40]	$y = 8742.4x + 1178.2$ (0.9996)	n = 7 [0.1 - 40]

**Table 2.4:** Calibration curves and linearity range obtained for genistein (**11**) with HPLC Method A, and UPLC Method B and Methods C, at 254 nm and 350 nm.

The limit of detection (LOD) and limit of quantification (LOQ) are usually estimated from a defined ratio of the analyte response, measured in peak height, to the maximum fluctuation of the background noise measured around the elution time of the analyte.<sup>35</sup> Several blanks have been defined for chromatographic method validation:<sup>36</sup> a solvent blank, which can be defined as a solution containing the reagents in the same quantity used to prepare the calibration solution; an analytical blank, containing all the reagents and has been analysed in the same way as the samples; and a matrix blank, which has exactly the same composition as the sample except for the analyte to be analysed.<sup>36</sup> This study used the average value of the baseline noise  $H_{\text{noise}}$  of several solvent blanks, considering all data points, and the LOD and LOQ values were calculated following the calculation presented in a recent method development for the quantification of several flavones present in weld extracts.<sup>30</sup>

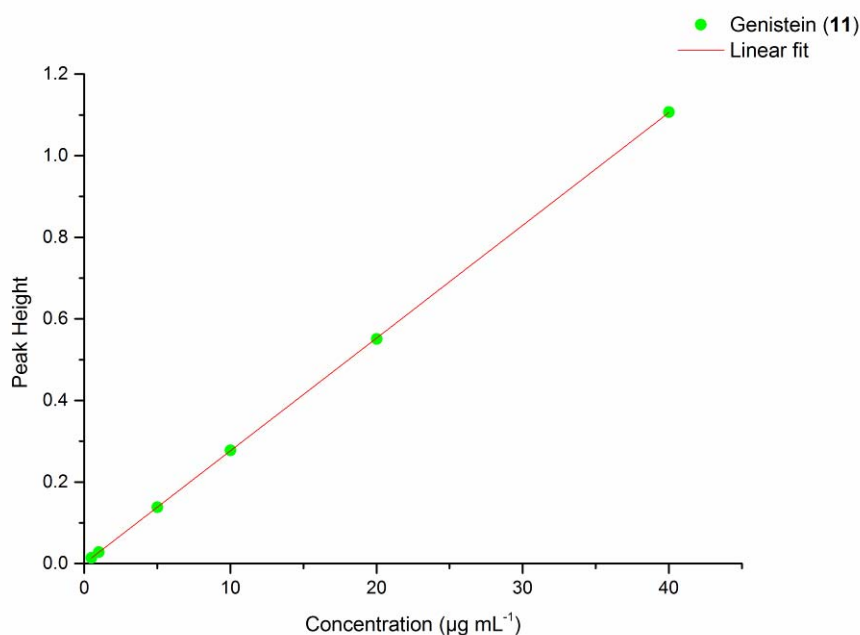


**Figure 2.8:** Linearity of peak Height with the concentrations of the solutions over the range of concentrations studied ( $[x]$  ( $\mu\text{g mL}^{-1}$ ) vs.  $H_x$  ( $R^2$ )), obtained for genistein, at 254 nm with Method C. Range was  $0.02 - 40 \mu\text{g mL}^{-1}$  and linearity:  $[y = 0.02764x + 8.75 \times 10^{-5}; R^2 = 0.999]$ .



For the UPLC system (Method B and C), the limits of detection (LOD) and limit of quantification (LOQ) were calculated based on the slopes (S) of the calibration curves (concentration [x] ( $\mu\text{g mL}^{-1}$ ) vs. height  $H_x$  (AU)) and the baseline noise  $H_{\text{noise}}$  of 6 solvent blanks analysed (s). For a few samples the noise drifted slightly below zero (e.g.  $[-(5 \pm 1) \times 10^{-4}]$ ) and as a result the  $|H_{\text{noise}}|$  was used for the calculation of the LOD and LOQ. The Concentration vs. Peak Height relationship was calculated using the raw data of each standard and the intercepts of the equations were set to zero and used to calculate the LOD and LOQ values. The LOD were calculated as  $(3.3 \times s)/S$  and the LOQ as  $(10 \times s)/S$ , and these are reported in  $\text{ng mL}^{-1}$  as is conventional in the field (table 2.5).

On HPLC system (Method A), some issues arose during these experiments, possibly due to a recent replacement of the flow cell, and it was found at 254 nm that the baseline drifted below zero while the organic phase was increasing in the gradient. For this reason, because of the negative value of the noise, the best estimation of the LOD and LOQ at 254 nm was obtained as  $(2.3 \times s)/S$  and the LOQ as  $(9 \times s)/S$ , using the  $|H_{\text{noise}}|$  of 4 solvent blanks analysed. At 350 and 430 nm the LOD and LOQ were calculated based on the slopes (S) of the calibration curves (concentration [x] ( $\mu\text{g mL}^{-1}$ ) vs. height  $H_x$  (AU)) and the baseline noise  $H_{\text{noise}}$  of 4 solvent blanks analysed (s). The Concentration vs. Peak Height relationship was calculated using the raw data of each standard and the intercepts of the equations were set to zero and used to calculate the LOD and LOQ values (table 2.5). The LOD and LOQ values obtained for each standard using the three developed chromatographic methods were also estimated based on the signal-to-noise ratio and provided similar figures.

The HPLC system at NMS did not achieve in these experiments very low LOD and LOQ values at 254 nm due to the drift of the baseline, however at 350 nm the LOD of both luteolin and apigenin for a 20  $\mu\text{L}$  injection volume were 3 ng. These values compare well to those found in earlier studies,<sup>37</sup> but are 12 times higher than recent work carried out on the quantification of the main flavone dyes in *Reseda luteola* L.<sup>30</sup> With regards to anthraquinone dyes, the LOD of alizarin and purpurin at 254 nm are

13 to 30 times higher than those found in previous HPLC studies, but at 430 nm for a 20  $\mu$ L injection volume these lower to 19 and 82 ng, respectively.<sup>38</sup>

In contrast, on the UPLC system, the baselines of the UV detector at 254 nm were very low and stable and the baseline averaged  $(5 \pm 1) \times 10^{-4}$  AU (UPLC column  $50 \times 2.1$  mm) and  $(9 \pm 1) \times 10^{-4}$  AU (UPLC column  $150 \times 2.1$  mm), see section 6.1. As a result all the standards showed a very low detection limit with the LOD and LOQ values at 254 nm being around 100 times lower than on the HPLC system. For an injection volume of 2.5  $\mu$ L, the LOD ranged between 1 ng for genistein and 6 ng for purpurin for Method B, and for an injection volume of 5  $\mu$ L 0.5 ng for genistein and 5 ng for purpurin for Method C. Furthermore, the detection limit of chrysoeriol and diosmetin at 350 nm could be lowered to 0.2 ng and 0.3 ng respectively by using Method C (table 2.5). Finally, when the response ( $H_x$ , AU) vs. the mass of analyte injected ( $[x] \times \text{vol}$ , ng) is compared across Methods A-C, we observe for all the standards that UPLC Method C has the greatest response, with a correlation coefficient ten times higher than that measured for HPLC Method A (figure 2.9). These results confirm that chromatographic Method C is best adapted for the study of historical samples as it allows the highest signal to noise response for all the analytes and offers a much better separation of all the natural dyes.

<b>Method A:</b> HPLC, ODS(2) Spheroclone Column, 150 × 4.6 mm, 5 μm (injection volume 20 μL)						
	254 nm		350 nm		430 nm	
Compound [x]	LOD ± s (ng)	LOQ ± s (ng)	LOD ± s (ng)	LOQ ± s (ng)	LOD ± s (ng)	LOQ ± s (ng)
carminic acid (33)	5 ± 2	15 ± 6			36 ± 5	108 ± 17
luteolin (9)	111 ± 12	434 ± 48	3 ± 1	9 ± 3		
genistein (11)	57 ± 6	224 ± 25	25 ± 9	77 ± 29		
apigenin (10)	175 ± 6	684 ± 22	3 ± 1	8 ± 3		
alizarin (26)					19 ± 1	58 ± 3
purpurin (28)					82 ± 6	248 ± 19
<b>Method B:</b> UPLC, BEH C18 Column, 50 × 2.1 mm, 1.7 μm (injection volume 2.5 μL)						
	254 nm		350 nm		430 nm	
Compound [x]	LOD ± s (ng)	LOQ ± s (ng)	LOD ± s (ng)	LOQ ± s (ng)	LOD ± s (ng)	LOQ ± s (ng)
carminic acid (33)	1.2 ± 0.3	3.7 ± 0.8			3.7 ± 1.9	11.1 ± 5.6
fisetin (14)	2.8 ± 0.6	8.6 ± 1.9	1.4 ± 0.2	4.2 ± 0.6		
sulfuretin (15)	3.6 ± 0.8	11.0 ± 2.4	1.2 ± 0.2	3.6 ± 0.6		
luteolin (9)	1.8 ± 0.4	5.4 ± 1.2	1.2 ± 0.2	3.6 ± 0.6		
genistein (11)	1.1 ± 0.2	3.2 ± 0.7	8.2 ± 1.3	24.9 ± 3.9		
apigenin (10)	5.0 ± 0.3	15.2 ± 0.9	1.7 ± 0.3	5.2 ± 0.8		
chrysoeriol (12)	6.1 ± 0.3	18.4 ± 1.0	2.5 ± 0.4	7.5 ± 1.2		
diosmetin (13)	4.5 ± 0.3	13.5 ± 0.8	1.6 ± 0.2	5.0 ± 0.8		
alizarin (26)	2.0 ± 0.1	5.9 ± 0.3			0.7 ± 0.3	2.02 ± 1.02
purpurin (28)	6.1 ± 0.3	18.4 ± 1.0			3.7 ± 1.8	11.1 ± 5.6
<b>Method C:</b> UPLC, PST BEH C18 Column, 150 × 2.1 mm, 1.7 μm (injection volume 5 μL)						
	254 nm		350 nm		430 nm	
Compound [x]	LOD ± s (ng)	LOQ ± s (ng)	LOD ± s (ng)	LOQ ± s (ng)	LOD ± s (ng)	LOQ ± s (ng)
carminic acid (33)	1.9 ± 1.1	5.9 ± 3.2			7.0 ± 1.4	21.3 ± 4.2
fisetin (14)	1.4 ± 0.2	4.2 ± 0.7	0.4 ± 0.1	1.2 ± 0.2		
sulfuretin (15)	1.8 ± 0.3	5.6 ± 0.9	0.4 ± 0.1	1.2 ± 0.2		
luteolin (9)	0.9 ± 0.1	2.6 ± 0.4	0.33 ± 0.04	1.0 ± 0.1		
genistein (11)	0.5 ± 0.1	1.6 ± 0.3	2.9 ± 0.4	8.7 ± 1.1		
apigenin (10)	1.9 ± 0.1	5.7 ± 0.3	0.33 ± 0.04	1.0 ± 0.1		
chrysoeriol (12)	1.2 ± 0.1	3.4 ± 0.2	0.24 ± 0.03	0.7 ± 0.1		
diosmetin (13)	1.2 ± 0.1	3.7 ± 0.2	0.27 ± 0.03	0.8 ± 0.1		
alizarin (26)	0.77 ± 0.03	2.3 ± 0.1			0.6 ± 0.1	1.7 ± 0.3
purpurin (28)	5.1 ± 2.7	15.3 ± 8.1			2.6 ± 0.5	7.7 ± 1.5

**Table 2.5:** LOD and LOQ values calculated for Methods A-C, based on the slopes (S) of the calibration curves (concentration [x] (μg mL<sup>-1</sup>) vs. height (H<sub>x</sub>, AU) and the baseline noise H<sub>noise</sub> of solvent blanks analysed (s) - at 254, 350 and 430 nm. [Data compiled from Chapter 7, section 7.1.5.2, tables 7.4, 6.5 and 7.6].

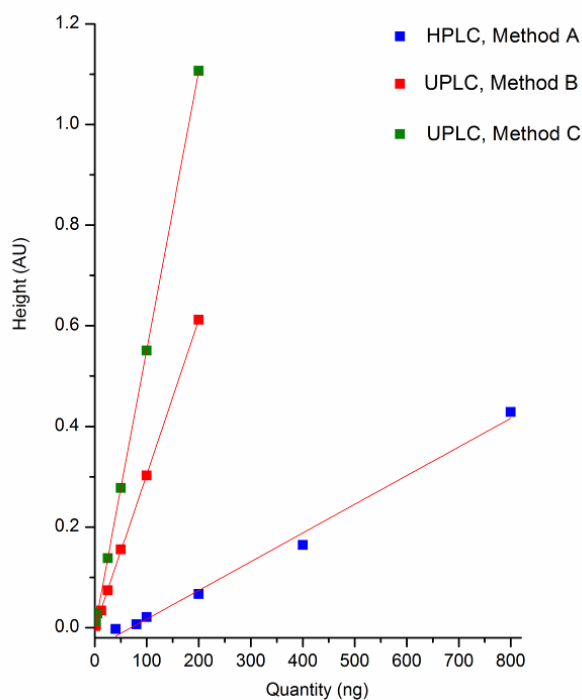


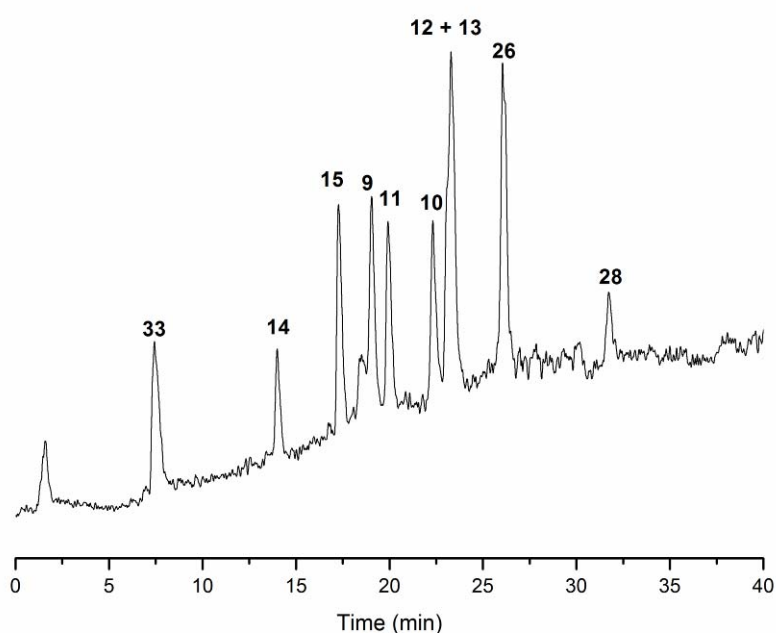
**Figure 2.9:** Comparing the relation between  $H_x$  (AU) and  $[x]$  (ng) for genistein at 254 nm; Method A:  $y = 0.0006x - 0.0398$  [ $R^2 = 0.9928$ ]; Method B:  $y = 0.0031x - 0.0018$  [ $R^2 = 0.9999$ ]; Method C:  $y = 0.0055x + 9E-05$  [ $R^2 = 1$ ]

### 2.3.1.5 UPLC-ESI Mass Spectrometry

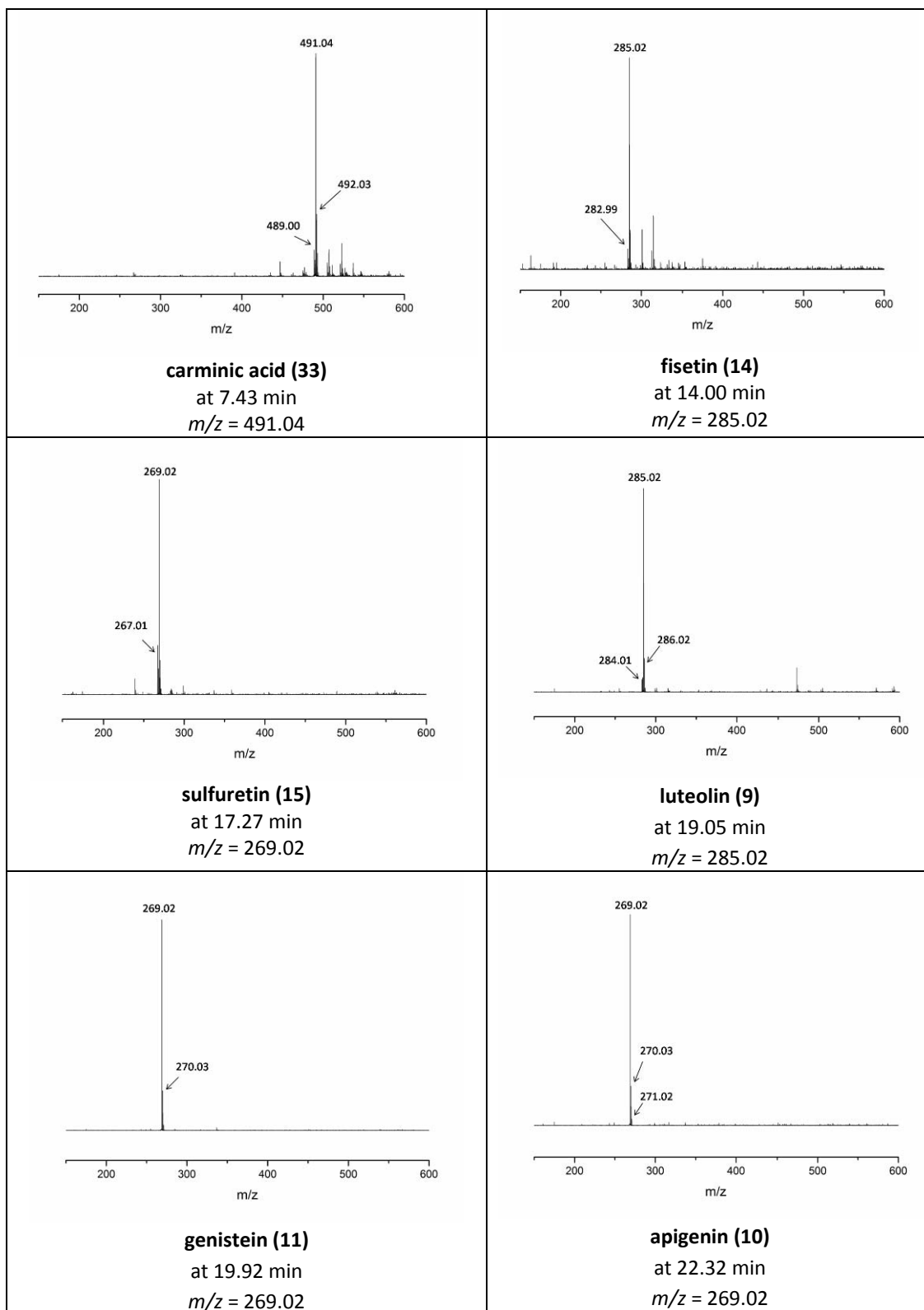
A limited number of measurements were also conducted connecting the UPLC system to a QTOF2 Mass Spectrometer (MS), in order to check the potential for UPLC-ESI-MS analysis. The separation of the standards was achieved using a PST BEH C18 reverse phase column, 1.7  $\mu\text{m}$  particle size, 150  $\times$  2.1 mm (length  $\times$  i.d.). The gradient developed in section 2.3.1.2 was adjusted in order to achieve a better separation of the regio-isomers chrysoeriol (**12**) and diosmetin (**13**) and MS analysis was conducted in negative ionisation mode (see section 7.1 for experimental details).

The method was tested on a solution of dye standard and the Total Ion Count (TIC) collected in negative ionisation mode is presented in figure 2.10. This first attempt in coupling the UPLC system to ESI-MS analysis was quite satisfactory, as the separation

of the dye components was achieved and the MS ESI<sup>-</sup> spectra of the reference dyes were collected (table 2.6). It was however not possible with MS ESI<sup>-</sup> to achieve good separation of the regio-isomers chrysoeriol (**12**) and diosmetin (**13**) and it was found that the PDA detector provided better separation of the two dye components. Nevertheless, the method will be applied in the following sections to the analysis of reference yarns.



**Figure 2.10:** Total Ion Count (TIC) collected in negative ionization mode with UPLC Method C': PST BEH C18, 1.7  $\mu\text{m}$ , 2.1 x 150 mm column. Identified in the chromatograms are the  $[\text{M-H}]^-$  and significant cluster ions of: carminic acid (**33**), fisetin (**14**), sulfuretin (**15**), luteolin (**9**), genistein (**11**), apigenin (**10**), chrysoeriol (**12**), diosmetin (**13**), alizarin (**26**) and purpurin (**28**). Standard solution with all components at  $10 \mu\text{g mL}^{-1}$  except for carminic acid which was at  $70 \mu\text{g mL}^{-1}$  (5  $\mu\text{L}$  injection volume).



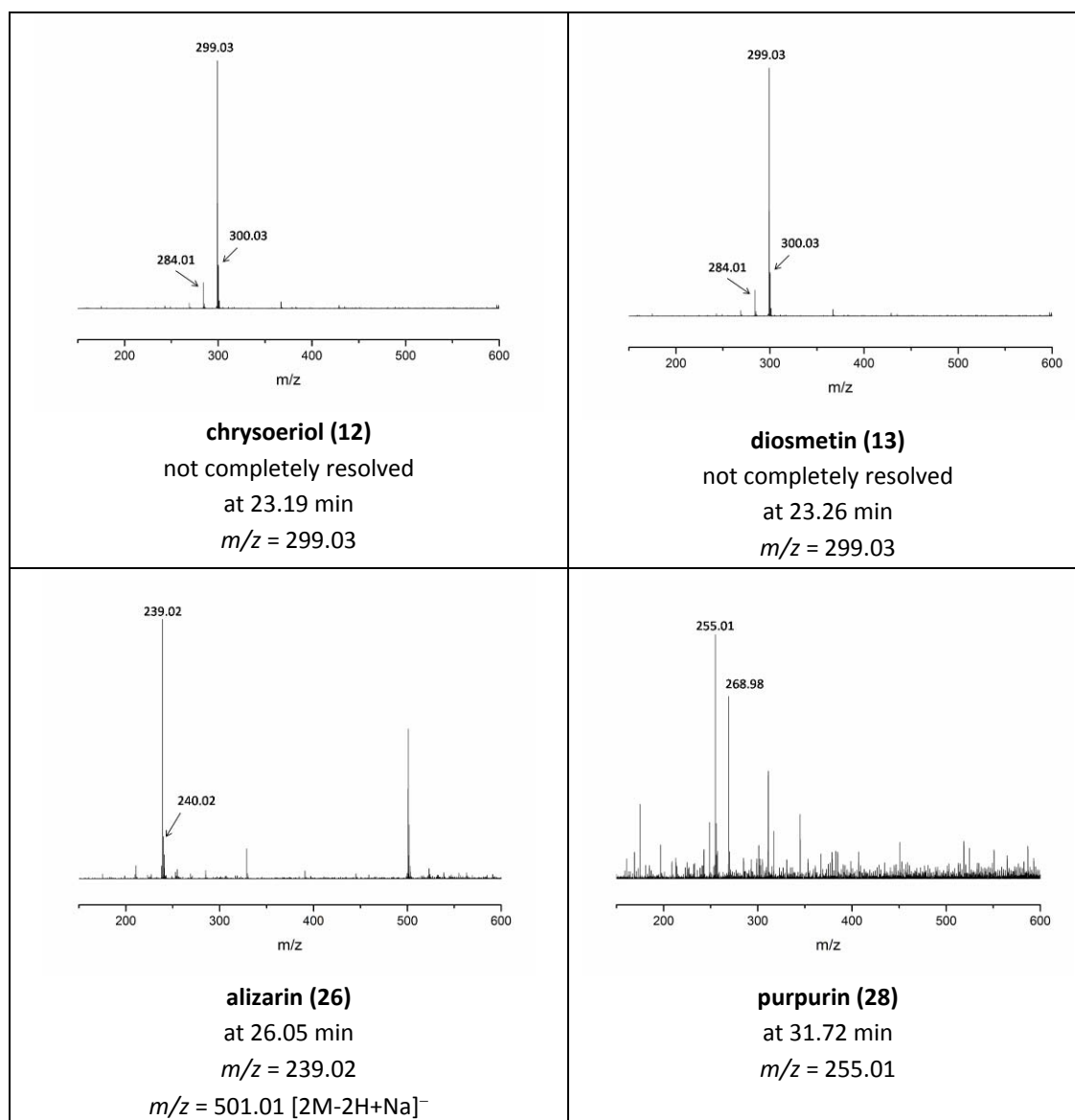


**Table 2.6:** TOF MS ESI<sup>-</sup> spectra of flavonoid and anthraquinone standards

### 2.3.2 Evaluation of sample preparation

Previous studies using a hydrochloric acid extraction protocol allowed the characterisation of the main natural dyes used in European historical textiles by the relative quantification of chemical components in the acid hydrolysed extracts and successfully identified several flavonoid based species including weld (*Reseda*

*luteola* L.), dyer's greenweed (*Genista tinctoria* L.), sawwort (*Serratula tinctoria* L.), young fustic (*Cotinus coggygria* L.), old fustic (*Chlorophora tinctoria* L.) and quercitron bark (*Quercus velutina* Lamk).<sup>39-42</sup> Despite a number of drawbacks associated with this method which have been reported in the literature (including the esterification or decarboxylation of the carboxyphenols present in flavonoids and anthraquinones<sup>1, 39, 43, 44</sup> and conversion of any flavonoid-*O*-glycosides into their aglycones,<sup>44, 45</sup>), given its widespread use and the wealth of examples in the literature which could be used for comparison of the results, it was decided for the extraction element of the sample preparation to focus on a hydrochloric acid extraction protocol.

Filtration of the extract prior to analysis is an important step in sample preparation (especially when dealing with historical textile samples that may well be compromised by solid contaminants), despite the inevitable accompanying loss of analyte. Thus analyte recovery and reproducibility associated with the sample preparation protocol used for UPLC analysis was compared with that of the sample preparation protocol routinely used for HPLC analysis at NMS using mock extraction protocols (section 7.1.6). These experiments showed that the two sample preparation methods provided equivalent recovery of all the natural dyes; but that the UPLC filtration method using 0.2  $\mu\text{m}$  PTFE syringe filters, provided greater reproducibility (table 2.7).

The relative recovery after hydrochloric acid hydrolysis, syringe-filtration, solvent evaporation and reconstitution ranged from 84 and 103 %, with *s* values from 0.1 and 3.9 %, with the exception of purpurin (**28**) which showed a higher standard deviation possibly due to the difficulty in re-solubilising it completely after extraction. The most notable exception was provided by the chrysoeriol (**12**) standard which systematically gave a higher peak area post extraction than that found in the starting solution, most probably due to the hydrolysis of insoluble glycosides in the reference sample under the acidic extraction conditions. Finally, the carminic acid (**33**) and



fisetin (**14**) standards seemed to be more sensitive to hydrochloric acid hydrolysis and were recovered at a much lower percentage.

Compound (x)	Concentration $\pm$ s ( $\mu\text{g.mL}^{-1}$ )	Recovery $\pm$ s [n = 3]	
		Polyethylene Filters, 55 $\mu\text{m}$ (%)	PTFE syringe Filters, 0.2 $\mu\text{m}$ (%)
carminic acid ( <b>33</b> )	77.1 $\pm$ 3.0	63.9 $\pm$ 13.4	51.9 $\pm$ 6.6
fisetin ( <b>14</b> )	15.6 $\pm$ 0.1	66.8 $\pm$ 22.1	65.6 $\pm$ 8.5
sulfuretin ( <b>15</b> )	15.9 $\pm$ 0.1	91.9 $\pm$ 2.1	93.6 $\pm$ 2.1
luteolin ( <b>9</b> )	16.9 $\pm$ 0.1	86.0 $\pm$ 8.3	80.0 $\pm$ 3.6
genistein ( <b>11</b> )	16.6 $\pm$ 0.1	91.5 $\pm$ 1.5	89.0 $\pm$ 2.5
apigenin ( <b>10</b> )	12.5 $\pm$ 0.1	111.1 $\pm$ 4.6	103.1 $\pm$ 5.0
chrysoeriol ( <b>12</b> )	7.8 $\pm$ 0.1	147.2 $\pm$ 8.9	139.5 $\pm$ 7.5
diosmetin ( <b>13</b> )	16.5 $\pm$ 0.1	88.9 $\pm$ 5.7	81.3 $\pm$ 3.9
alizarin ( <b>26</b> )	13.0 $\pm$ 0.1	92.3 $\pm$ 2.5	92.2 $\pm$ 0.3
purpurin ( <b>28</b> )	12.2 $\pm$ 0.2	84.0 $\pm$ 36.3	88.0 $\pm$ 9.9

**Table 2.7:** Comparing relative recovery after hydrochloric acid hydrolysis followed by filtration using Polyethylene 55  $\mu\text{m}$  and PTFE 0.2  $\mu\text{m}$  filters. [Data compiled from Chapter 7, section 7.1.6].

## 2.4 APPLICATION TO REFERENCE MATERIALS

In the following sections, yellow reference yarns prepared during the Monitoring of Damage to Historical Tapestries project (MODHT) will be investigated by UPLC analysis and the level of additional information provided in practice over HPLC will be assessed.<sup>6, 46</sup>

## 2.4.1 Identification of minor components in acid-hydrolysed extracts of weld (*Reseda luteola* L.) and dyer's greenweed (*Genista tinctoria* L.)

### 2.4.1.1 Weld (*Reseda luteola* L.)

Weld (*Reseda luteola* L.) is one of the most widely found yellow dye in European historical tapestries. The acid hydrolysed extracts of yarns dyed with weld are characterised by the association of luteolin (**9**,  $R_t = 13.47$  min, [ $\lambda_{\max} = 252, 291$  (sh), 349 nm]) with a relatively minor amount of the aglycone apigenin (**10**,  $R_t = 15.26$ , [ $\lambda_{\max} = 267, 300$  (sh), 338 nm]) and traces of a luteolin methyl-ether component. A previous study has shown that the minor component present in the acid hydrolysed extract of weld is chrysoeriol (**12**).<sup>40</sup> The UPLC investigation reported here of weld dyed yarn references confirmed that the minor component present in the acid hydrolysed extract was chrysoeriol (**12**,  $R_t = 15.69$ , [ $\lambda_{\max} = 251, 268, 290$  (sh), 349 nm]), which was found for wool and silk threads to average 2.9 and 3.0 % of the total relative amount of the flavonoids present in the extract, respectively (table 2.9).

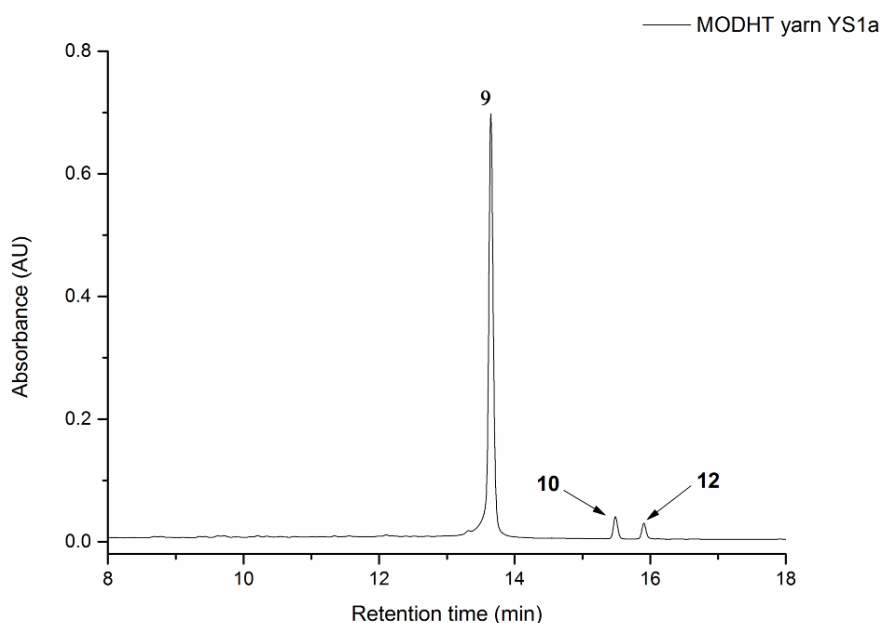


**Figure 2.11:** UPLC chromatogram of the acid hydrolysed reference MODHT YS1a (weld) monitored at 254 nm. Identified in the chromatogram are the flavones luteolin (**9**), apigenin (**10**) and the luteolin methyl-ether chrysoeriol (**12**).

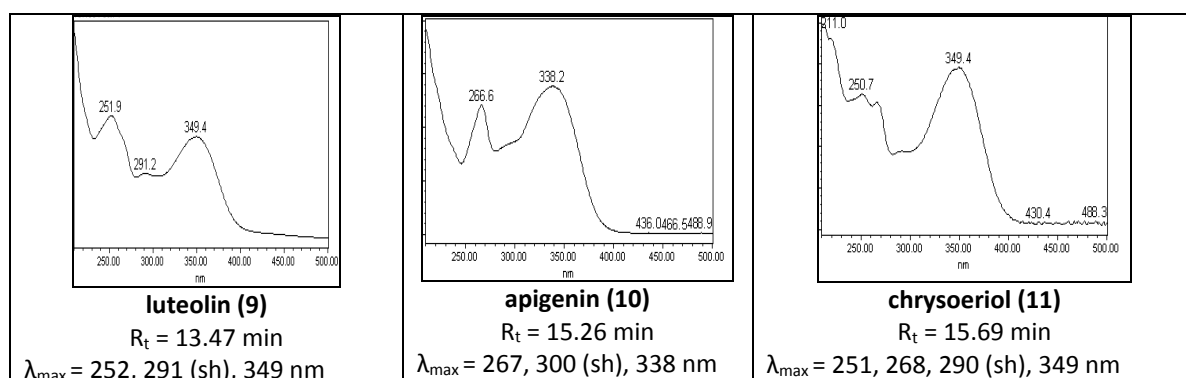


**Table 2.10:** PDA spectra of flavonoid dyes characterised in reference sample MODHT YS1a of weld.

	Relative Amount: average $\pm$ s (%), n=3		
	luteolin (9)	apigenin (10)	chrysoeriol (12)
MODHT YW1	93.0 $\pm$ 0.4	4.3 $\pm$ 0.3	2.8 $\pm$ 0.2
MODHT YS1a	92.8 $\pm$ 0.2	4.0 $\pm$ 0.1	3.1 $\pm$ 0.1

**Table 2.9:** Relative amount of the flavonoid dyes identified in the acid hydrolysed extract of weld reference samples (wool and silk). [Data compiled from Chapter 7, section 7.1.7.1, table 7.9].

#### 2.4.1.2 Dyer's greenweed (*Genista tinctoria* L.)

Dyer's greenweed (*Genista tinctoria* L.) is another important yellow dye source in Europe, and previous work has characterised it as the main yellow source on a group of important sixteenth century Brussels tapestries.<sup>6</sup> The acid hydrolysed extracts of yarns dyed with dyer's greenweed are characterised by the association of the flavone luteolin (**9**) with the isoflavone genistein (**11**), a relatively minor amount of the aglycone apigenin (**10**) and traces of a luteolin methyl-ether component.<sup>3, 6</sup> A previous Mass Spectrometry study identified the presence of an *O*-methylated

flavone presenting a retro-Diels-Alder fragmentation indicating a methoxy group substituent in the B-ring, which was identified as diosmetin (**12**).<sup>3</sup>

UPLC investigation of the MODHT yellow wool (YW2) and silk (YS3a) reference samples dyed with dyer's greenweed showed that both fibres present a very similar dye component profile, with the main dye component luteolin (**9**,  $R_t = 13.47$  min,  $[\lambda_{\max} = 252, 291$  (sh), 349 nm]), genistein (**11**,  $R_t = 14.03$  min,  $[\lambda_{\max} = 260, 332$  (sh) nm]), and apigenin (**10**,  $R_t = 15.26$  min,  $[\lambda_{\max} = 267, 300$  (sh), 338 nm]) exhibiting similar relative amounts at 254 nm. In addition, UPLC analysis showed for the first time that both luteolin methyl-ethers chrysoeriol (**12**,  $R_t = 15.69$  min,  $[\lambda_{\max} = 251, 268, 290$  (sh), 349 nm]) and diosmetin (**13**,  $R_t = 15.87$  min,  $[\lambda_{\max} = 252, 268, 290$  (sh), 348 nm]) are present in low levels in the acid hydrolysed extracts (figure 2.12). Chrysoeriol (**12**) was found to average 1.3 and 1.2 % (wool and silk, respectively), while diosmetin (**13**) was found to average 2.4 and 2.3 % (wool and silk, respectively) of the total relative amount of the flavonoids present in the extracts (table 2.11). The presence of chrysoeriol (**12**) and diosmetin (**13**) in the acid hydrolysed extracts yarn dyed with *Genista tinctoria* L. might not be surprising given the fact that they are related compounds and that chrysoeriol has been reported to occur in some *Genista* species.<sup>47</sup>

Four unknown components were also characterised in the acid hydrolysed extract of both silk and wool yarns and named respectively after *Genista tinctoria* L., Gt1 ( $R_t = 10.06$  min), Gt2 ( $R_t = 11.67$  min), Gt3 ( $R_t = 12.17$  min) and Gt4 ( $R_t = 14.61$  min), all exhibiting a maximum absorption between 255 and 261 nm, which indicates an isoflavonoid structure. Of these, Gt3 often is present at levels which are detectable using the new UPLC method in historical textile samples hence we have further investigated the structure of this component and the minor component Gt2, and the effect of the dyeing process on their uptake onto wool and silk fibres.

	Relative Amount: average $\pm$ s (%), n=4				
	MODHT YW2	MODHT YS3a	MODHT YS3b	MODHT YS3c	MODHT YS3d
Gt1	ND	2.0 $\pm$ 0.9	0.7 $\pm$ 1.2	ND	1.5 $\pm$ 1.2
Gt2	4.6 $\pm$ 0.5	3.6 $\pm$ 1.3	1.1 $\pm$ 1.6	3.5 $\pm$ 1.0	4.9 $\pm$ 1.1
Gt3	20.8 $\pm$ 1.8	19.2 $\pm$ 2.8	14.0 $\pm$ 1.5	11.4 $\pm$ 1.8	7.0 $\pm$ 2.1
luteolin ( <b>9</b> )	25.5 $\pm$ 2.6	30.2 $\pm$ 2.7	39.8 $\pm$ 1.4	42.9 $\pm$ 2.3	58.2 $\pm$ 3.7
genistein ( <b>11</b> )	34.8 $\pm$ 1.0	34.3 $\pm$ 1.6	33.2 $\pm$ 2.7	28.5 $\pm$ 2.3	19.5 $\pm$ 1.2
Gt4	3.9 $\pm$ 2.2	2.1 $\pm$ 0.2	2.0 $\pm$ 0.6	3.1 $\pm$ 0.2	1.9 $\pm$ 0.3
apigenin ( <b>10</b> )	6.7 $\pm$ 0.3	5.2 $\pm$ 0.4	4.6 $\pm$ 0.4	5.0 $\pm$ 0.7	2.9 $\pm$ 0.3
chrysoeriol ( <b>12</b> )	1.3 $\pm$ 0.6	1.2 $\pm$ 0.2	1.4 $\pm$ 0.1	1.6 $\pm$ 0.4	1.3 $\pm$ 0.1
diosmetin ( <b>13</b> )	2.4 $\pm$ 0.7	2.3 $\pm$ 0.3	3.2 $\pm$ 0.3	4.0 $\pm$ 0.8	2.8 $\pm$ 0.4

**Table 2.11:** The relative amount of the flavonoid and isoflavonoid dyes characterised in the acid hydrolysed extract of reference yarns dyed with dyer's greenweed, YW2 and YS3a and others subjected to over dyeing (YS3b to d), monitored at 254 nm. [Data compiled from Chapter 7, section 7.1.7.2, table 7.10].

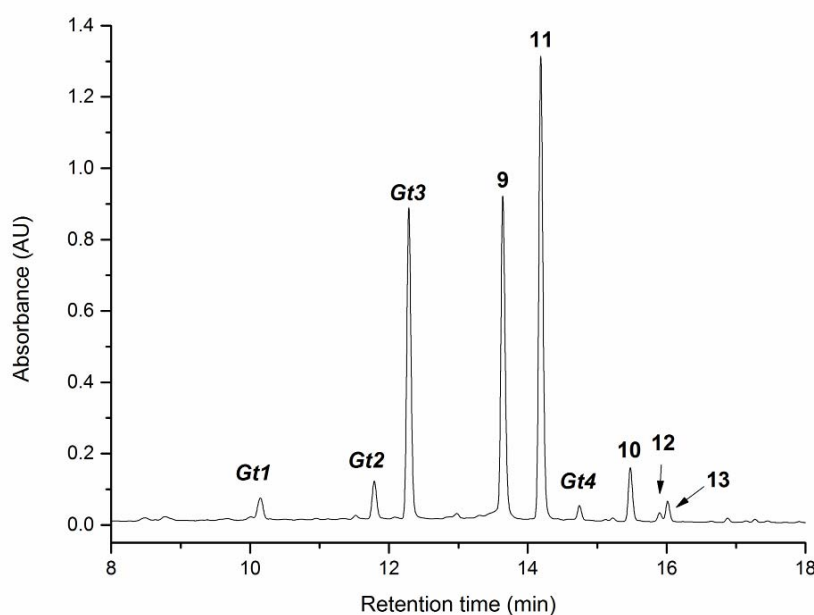


**Figure 2.12:** UPLC chromatogram of the acid hydrolysed reference MODHT YS3a (dyer's greenweed) monitored at 254 nm. Identified in the chromatogram are the flavones luteolin (**9**), apigenin (**10**) and the isoflavone genistein (**11**), associated to smaller amount of four unidentified components **Gt1**, **Gt2**, **Gt3** and **Gt4** and the two luteolin methyl-ether chrysoeriol (**12**) and diosmetin (**13**).

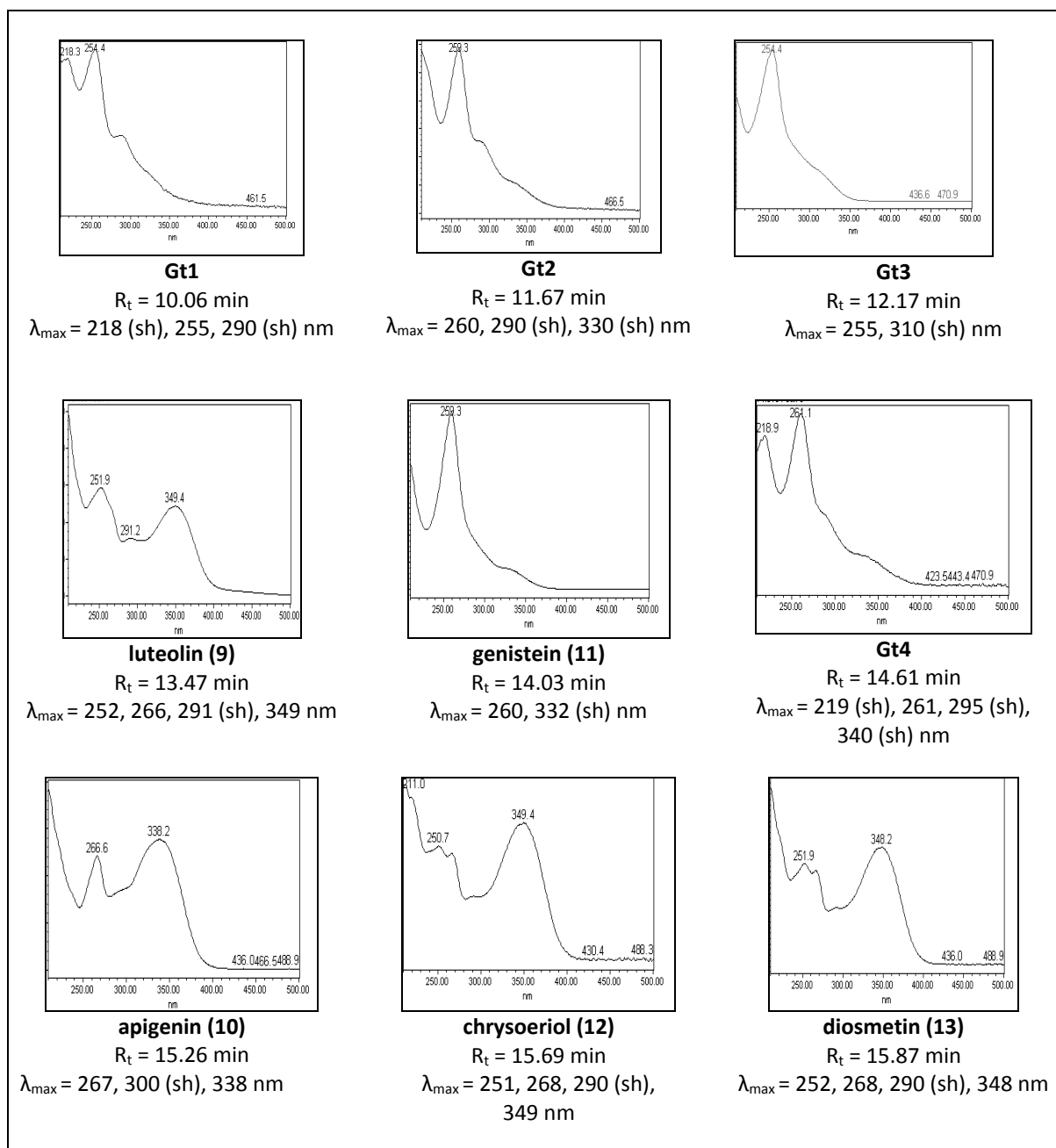
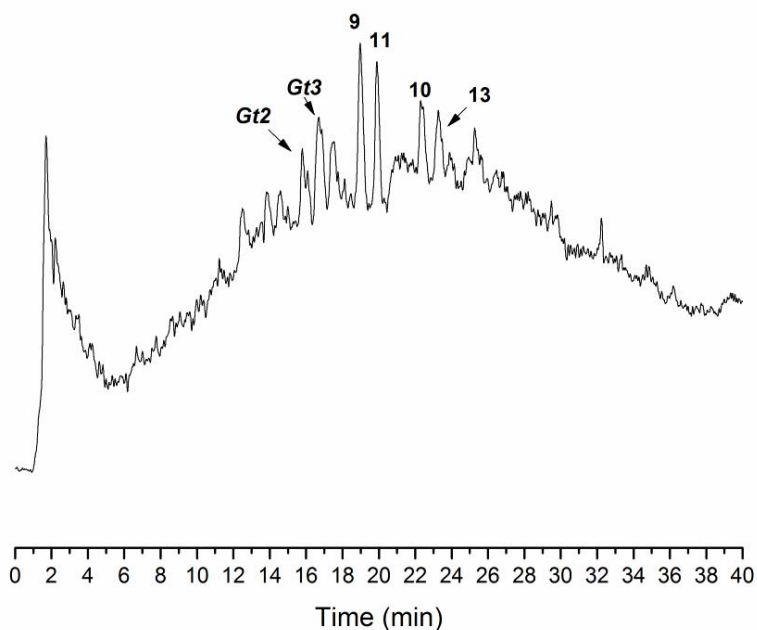


**Table 2.12:** PDA spectra of flavonoid dyes characterised in reference sample MODHT YS3a of dyer's greenweed.

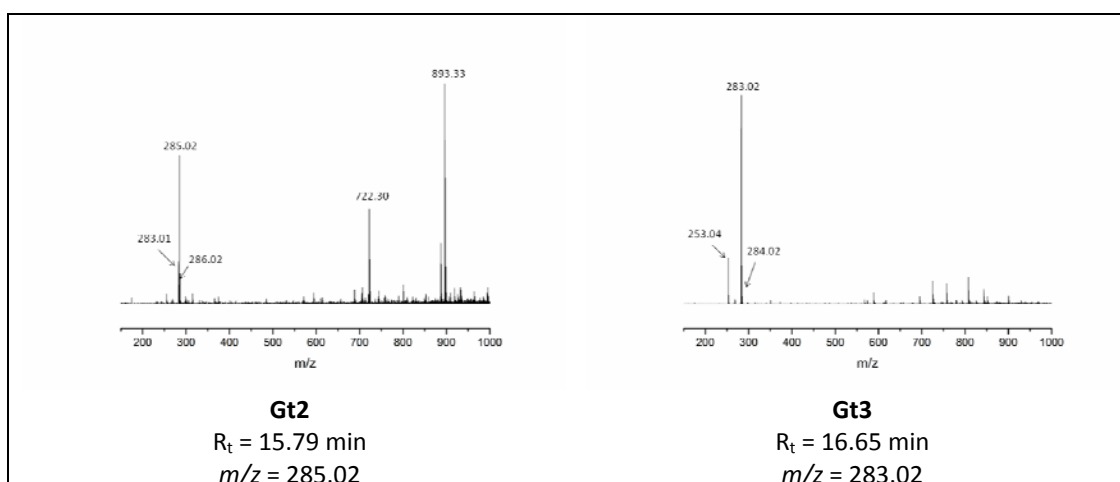
### 2.4.2 Characterisation of Gt compounds by UPLC-ESI-MS

In order to characterise these unknown Gt components, the reference yarn YS3a was analysed using the UPLC-ESI-MS method developed in section 2.3.1.5. The combined information gained by UV-Vis spectra, retention time and ESI<sup>-</sup> spectra should hopefully allow some structure attribution. The Total Ion Count (TIC) of the reference sample was found to be relatively noisy (figure 2.13), showing that although the PDA-UPLC chromatogram appear relatively free of contaminants, this is not the case with ESI-MS and it would be necessary to improve the sample preparation in order to allow a better signal-to-noise ratio. Nevertheless it was possible to identify on the TIC spectra significant cluster ions of unknown components Gt2, Gt3, the flavones luteolin (**9**,  $R_t = 18.96$  min and  $m/z$  285) and apigenin (**10**,  $R_t = 22.45$  min and  $m/z$  269), the isoflavone genistein (**11**,  $R_t = 19.91$  min and  $m/z$  269), and a luteolin methyl-ether [identified by retention time in the UPLC chromatogram as diosmetin (**13**,  $R_t = 23.26$  min and  $m/z$  299)].

The extracted [M-H]<sup>-</sup> spectra characterised the unknown component Gt2 ( $R_t = 15.79$  min) with an  $m/z$  of 285.03 (ESI<sup>-</sup>), while the [M-H]<sup>-</sup> spectra of unknown component Gt3 ( $R_t = 16.65$  min) showed an  $m/z$  of 283.03 (ESI<sup>-</sup>). The ion traces extracted for  $m/z$  284.63-285.44 and  $m/z$  282.56-283.41 is shown in figure 2.14 and the TOF MS ESI<sup>-</sup> spectra of Gt2 and Gt3 are found in table 2.13.

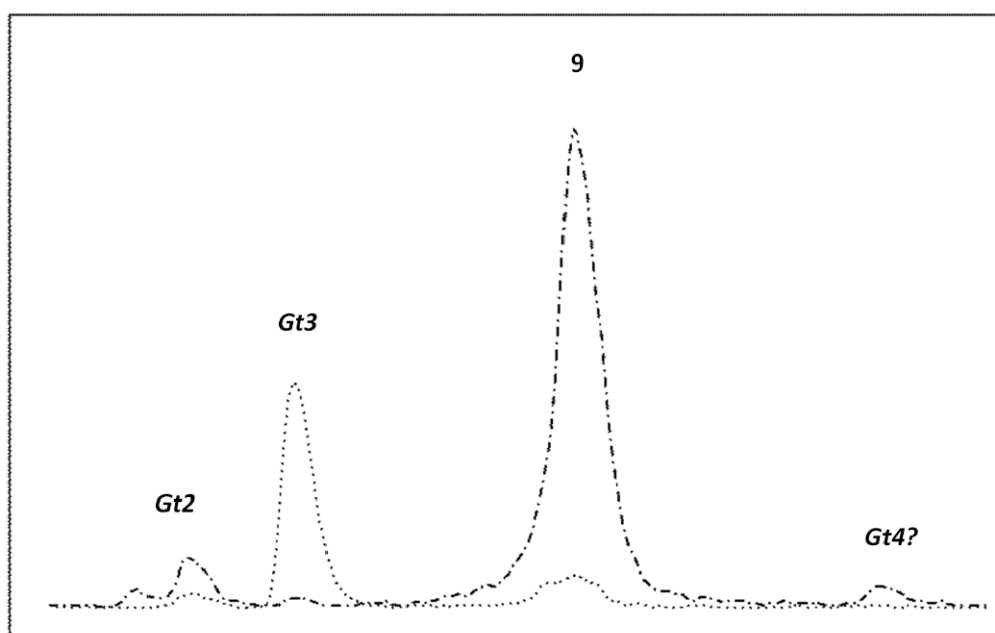


**Figure 2.13:** Total Ion Count (TIC) collected in negative ionization mode with UPLC Method C' of the acid hydrolysed reference MODHT YS3a (dyer's greenweed). Identified in the chromatogram are the  $[M-H]^-$  and significant cluster ions of unknown components Gt2, Gt3, the flavones luteolin (**9**) and apigenin (**10**), the isoflavone genistein (**11**), and a luteolin methyl-ether [identified by retention time in the UPLC chromatogram as diosmetin (**13**)].



**Table 2.13:** TOF MS ESI- spectra of the minor component Gt2 and Gt3.



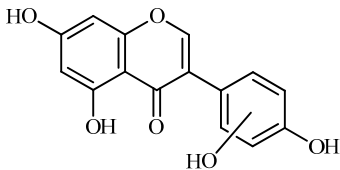
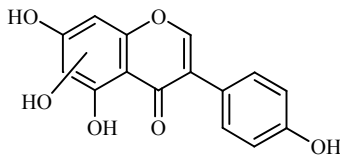
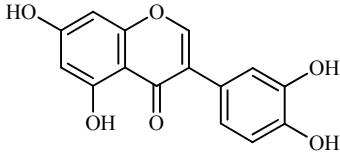
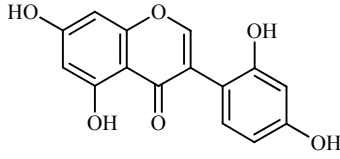
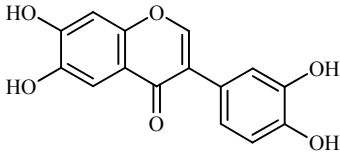
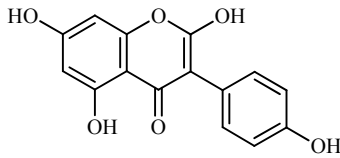
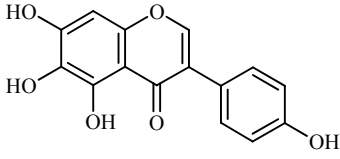
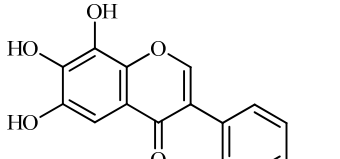


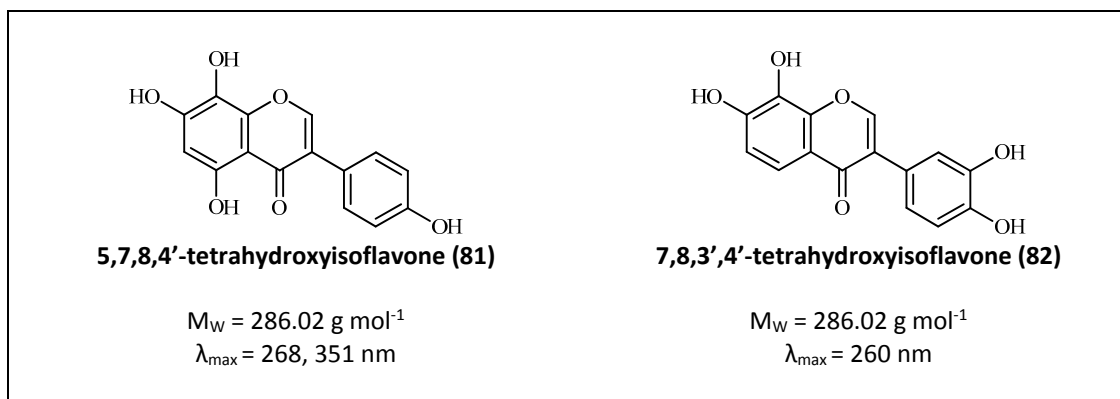
**Figure 2.14:** UPLC-ESI-MS (-ve mode) selected ion traces for  $m/z$  284.63-285.44 (••) and 282.56-283.41 (- -).

### Gt2

The minor component Gt2 exhibits a maximum absorption at 260 nm, which indicates an isoflavonoid structure with an  $m/z$  of 285.02 (ESI<sup>-</sup>) that corresponds to the isoflavone genistein with an additional OH. Several isomeric isoflavone structures corresponding to this level of hydroxyl substitution have been reported in the literature with 5,7,3',4'-tetrahydroxyisoflavone (orobol, **76**); 6,7,3',4'-tetrahydroxyisoflavone (**78**); 2,5,7,4'-tetrahydroxy-isoflavone (**79**) and 7,8,3',4'-tetrahydroxyisoflavone (**82**) exhibiting a maximum absorption between 258 and 262 nm. However only 5,7,3',4'-tetrahydroxyisoflavone (orobol, **76**) and 6,7,3',4'-tetrahydroxyisoflavone (**78**) have shoulder peaks reported at 287 nm and 288, 325 nm respectively, that could correspond to the UV-vis spectra of Gt2. In the absence of detailed MS-MS studies or reference samples for comparison it is not possible to

offer a definitive structure for this component, however from these orobol (**76**) is the most likely attribution, as it has been identified in several *Genista* species growing in Italy and also in *Genista tinctoria* L..<sup>48, 49</sup>

	
<p><b>Gt2</b>  <math>M_w = 286.02 \text{ g mol}^{-1}</math>  <math>R_t = 11.67 \text{ min (UPLC) or } 15.79 \text{ min (UPLC-ESI-MS)}</math>  <math>\lambda_{\text{max}} = 260, 290 \text{ (sh), } 330 \text{ (sh) nm}</math></p>	
 <p><b>orobol (76)</b>  <b>5,7,3',4'-tetrahydroxyisoflavone</b></p> <p><math>M_w = 286.02 \text{ g mol}^{-1}</math>  <math>\lambda_{\text{max}} = 262, 287 \text{ (sh) nm}</math></p>	 <p><b>2'-Hydroxygenistein (77)</b>  <b>7,8,2',4'-tetrahydroxyisoflavone</b></p> <p><math>M_w = 286.02 \text{ g mol}^{-1}</math>  <math>\lambda_{\text{max}} = 230, 255, 265, 350 \text{ nm}</math></p>
 <p><b>6,7,3',4'-tetrahydroxyisoflavone (78)</b></p> <p><math>M_w = 286.02 \text{ g mol}^{-1}</math>  <math>\lambda_{\text{max}} = 258, 288, 325 \text{ nm}</math></p>	 <p><b>2,5,7,4'-tetrahydroxyisoflavone (79)</b></p> <p><math>M_w = 286.02 \text{ g mol}^{-1}</math>  <math>\lambda_{\text{max}} = 258 \text{ nm}</math></p>
 <p><b>5,6,7,4'-tetrahydroxyisoflavone (80)</b></p> <p><math>M_w = 286.02 \text{ g mol}^{-1}</math>  <math>\lambda_{\text{max}} = 270 \text{ nm}</math></p>	 <p><b>6,7,8,4'-tetrahydroxyisoflavone (81)</b></p> <p><math>M_w = 286.02 \text{ g mol}^{-1}</math>  <math>\lambda_{\text{max}} = 264, 322 \text{ nm}</math></p>

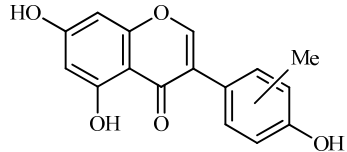
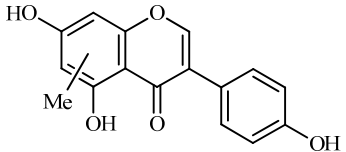
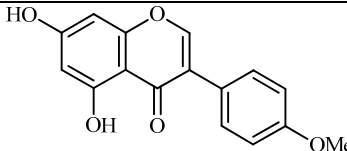
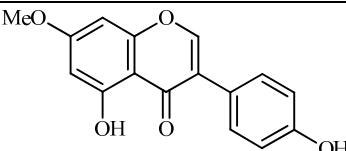
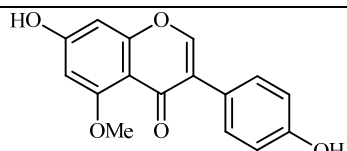
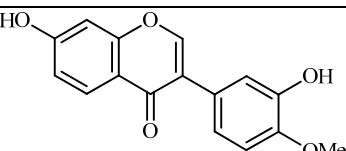


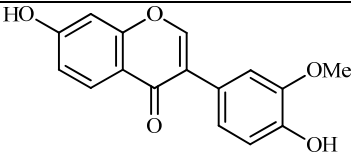
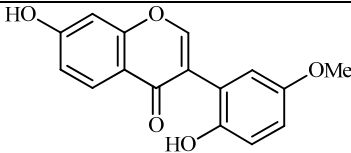
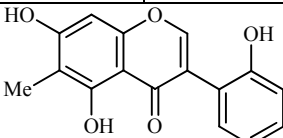
**Table 2.14:** Proposed structures for the minor component Gt2 and possible hydroxy isoflavone components, UV-Vis values (EtOH) obtained from published references 50 and 51.<sup>50, 51</sup>

### Gt3

The minor component Gt3 exhibits an  $m/z$  of 283.03 (ESI<sup>-</sup>) that corresponds to an *O*- or *C*-methylated isoflavonoid related to genistein. This component presents a maximum absorption at 254 nm. Several *O*-methylated isoflavones have been reported in the literature including biochanin A (**83**), prunetin (**84**), 5-*O*-methyl genistein (**85**), calycosin (**86**), glycitein (**87**) and 7,6'-dihydroxy-3'-methoxyisoflavone (**88**), and the *C*-methylated isoflavone abronisoflavone (**89**) has also been reported, although not in *Genista* species. From these structures, it is possible to exclude biochanin A (**83**) and prunetin (**84**), both of which exhibit a maximum absorption at 262 nm, and calycosin (**86**) and glycitein (**87**), both of which exhibit a maximum absorption at 248 nm and 260 nm. In the absence of detailed MS-MS studies or reference samples for comparison it is not possible to confirm the structure of Gt3, but 5-*O*-methyl genistein (**85**) has been reported to occur in *Genista tinctoria* L. and present a maximum absorption at 256 nm.<sup>48, 49, 52</sup> It would be a related compound to genistein (**11**) and the methyl substitution in the A ring could explain the different maximum absorption observed on the UV-vis spectra.

Finally, the minor component Gt4 eluted on UPLC spectra closely to genistein (**11**) at 14.61 min and exhibited a maximum absorption at 261 nm. Although it was not possible to extract the  $[M-H]^-$  spectra of this component, it does clearly appear in the select ion trace spectra for the mass range  $m/z$  282.56-283.41 (figure 2.14). This would suggest that this compound exhibits a similar mass to Gt3, and the maxima observed on the UV-vis spectra at 261 nm, associated to an elution time after genistein (**11**) would suggest the presence of biochanin A (**83**), a methylgenistein compound that has been characterised in several *Genista* species including *Genista tinctoria* L.<sup>52, 53</sup>

	
<b>Gt3</b> $M_W = 284.02 \text{ g mol}^{-1}$ $R_t = 12.17 \text{ min (UPLC) or } R_t = 16.65 \text{ min (UPLC-ESI-MS)}$ $\lambda_{\text{max}} = 255, 310 \text{ (sh) nm}$	
	
<b>biochanin A (83)</b> $M_W = 284.26 \text{ g mol}^{-1}$ $\lambda_{\text{max}} = 262, 326 \text{ (sh) nm}$	<b>prunetin (84)</b> $M_W = 284.26 \text{ g mol}^{-1}$ $\lambda_{\text{max}} = 262, 327 \text{ (sh) nm}$
	
<b>5-O-methyl genistein (85) or isoprunetin</b> $M_W = 284.26 \text{ g mol}^{-1}$ $\lambda_{\text{max}} = 256 \text{ nm}$	<b>calycosin (86)</b> $M_W = 284.26 \text{ g mol}^{-1}$ $m_{\text{ix}} = 248, 290 \text{ (sh) nm}$

 <p><b>glycitein (87)</b>  <math>M_w = 284.26 \text{ g mol}^{-1}</math>  <math>\lambda_{\text{max}} = 260, 320 \text{ nm}</math></p>	 <p><b>7,6'-dihydroxy-3'-methoxy-isoflavone (88)</b>  <math>M_w = 284.26 \text{ g mol}^{-1}</math>  <math>\lambda_{\text{max}} = 227, 255, 290, 308 \text{ nm}</math></p>
 <p><b>abronisoflavone (89)</b>  <math>M_w = 284.26 \text{ g mol}^{-1}</math>  <math>\lambda_{\text{max}} = 269, 295 \text{ (sh) nm}</math></p>	

**Table 2.15:** Proposed structure for the minor component Gt3 and possible *O*- and *C*-methylated isoflavone components with similar  $M_w$ , UV-Vis values (EtOH) obtained from published references 50, 54-56.<sup>50, 54-56</sup>

### 2.4.3 Effect of over-dyeing

The composition of dyestuffs extracted from historical textile samples is known to vary due to the effects of ageing, but it is also thought to be dependent on workshop practices such as over-dyeing (where a yarn is treated with successive dyebaths in order to achieve the desired colour or hue).<sup>6</sup> Silk reference samples prepared by over-dyeing with successive dyer's greenweed dye baths (YS3a-d, one to four baths respectively) were examined by UPLC (figure 2.15). While the silk reference YS3a showed the highest level of Gt3 and genistein (**11**) compared to luteolin (**9**), this is reversed when the textile has been over-dyed. It has been suggested that luteolin (**9**) binds with the mordant more efficiently than the isoflavone genistein (**11**),<sup>6</sup> so the latter is displaced with each additional dyeing, or alternatively that genistein (**11**), degrades preferentially under the dyebath conditions.<sup>6</sup> This suggestion is supported by the fact that several studies of soy products showed that isoflavonoid compounds, especially genistein (**11**), degrade easily at elevated temperature.<sup>57, 58</sup>

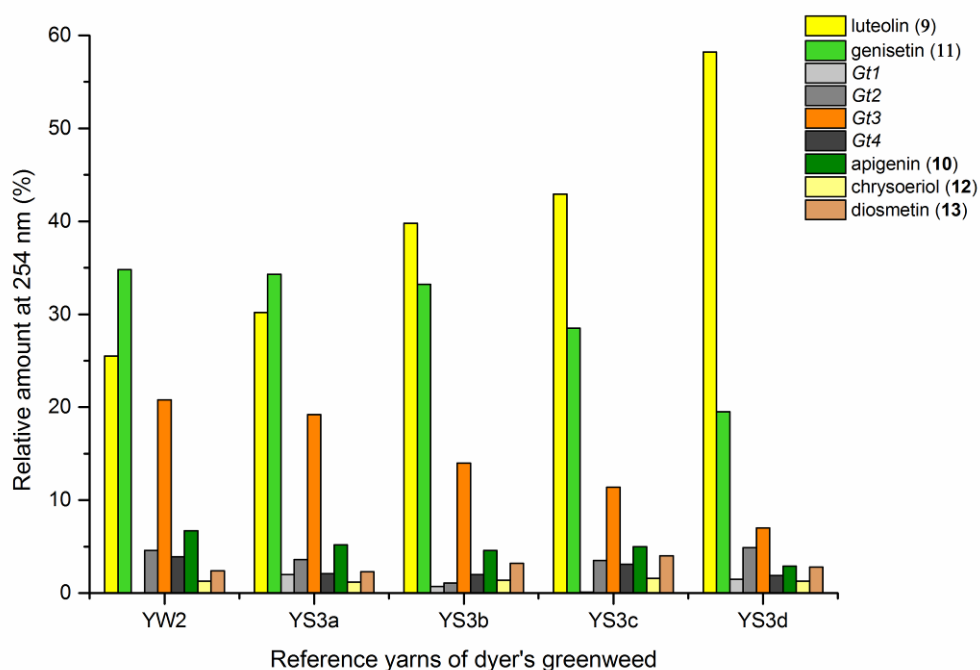


**Figure 2.15:** Relative amounts of the flavonoid dyes present in the acid-hydrolysed extracts of wool (YW2) and silk (YS3a) MODHT reference samples and a series of over-dyed (YS3b-d) samples; monitored at 254 nm. [Data compiled from Chapter 7, section 7.1.7.2, table 7.10].

It is therefore not surprising, given the fact that Gt3 and genistein (**11**) are likely to be related compounds, that the level of Gt3 fixed onto the yarn decreases similarly to genistein (**11**) after over dyeing. The presence in high quantities of both colourless components genistein (**11**) and Gt3 on wool and silk yarns after a single dye bath would clearly affect the achieved colour and might explain why dyer's greenweed was judged to be of lower quality than that of weld due to the need for multiple dyeing to obtain a proper yellow colour.<sup>59</sup> Finally, from these new observations, the minor components chrysoeriol (**12**), diosmetin (**13**), Gt1, Gt2 and Gt4 are not greatly affected by the textile preparation and are equally present in very low concentrations (figure 2.15).

## 2.5 SUMMARY

UPLC separation has been shown to provide a robust method for the identification of a range of natural product dyestuffs. The LOD for all the standards examined was lowered by around hundred times compared with HPLC methods which are routinely used in the analysis of historic dyestuffs and the observed response for each analyte injected was ten times higher. This opens up exciting possibilities for heritage applications, as objects from which sampling was previously not possible may now be examined due to the greatly reduced requirements for sample size (typically below 500  $\mu\text{g}$ ). The UPLC method developed using a shorter run time gives excellent separation for a wide range of dyestuffs and will enable the rapid analysis of multiple samples from objects. This level of data acquisition will allow techniques such as principal component analysis to be applied for the first time to historic dyestuff analysis, the results of which will provide new information for curators regarding the provenance of objects and inform decisions regarding their conservation and display. The second method developed, using a longer run time, enabled the identification of very minor components and closely-eluting regio-isomers and was combined effectively with ESI-MS analysis.

Finally, four previously un-reported *Genista* related components, named Gt1, Gt2, Gt3 and Gt4 were characterised in yarns dyed with dyers' greenweed (*Genista tinctoria* L.) and TOF-ESI-MS analysis combined to PDA-UPLC allowed some possible structure attributions. The minor component Gt2 was found to exhibit a maximum absorption at 260 nm, which indicated an isoflavonoid structure with an  $m/z$  of 285.02 (ESI<sup>-</sup>) that corresponded to the isoflavone genistein with an additional OH. While the minor component Gt3 exhibited a maximum absorption at 254 nm with an  $m/z$  of 283.03 (ESI<sup>-</sup>) that corresponded to an *O*-methylated isoflavonoid related to genistein. Further analysis using MS-MS fragmentations will be carried out in order to offer a definitive structure of these components.

The advantages of UPLC analysis have been demonstrated on reference materials and its application to real historical materials is reported in the following chapters of the thesis, through the analysis of historical samples from early English tapestries (chapter 3) and mid nineteenth century North American porcupine quill work (chapter 5).

## 2.6 REFERENCES

1. Wouters, J., Verheeken, A. (1985). High-performance liquid chromatography of anthraquinones: Analysis of plant and insect extracts and dyed textiles. *Studies in Cons.*, **30**, 119-128.
2. Nowik, W. (1996). Application de la chromatographie en phase liquide à l'identification des colorants naturels des textiles anciens. *Analysis Magazine* **24**, 37-40.
3. Ferreira, E. S. B. (2002). *New Approaches Towards the Identification of Yellow Dyes in Ancient Textiles*. The University of Edinburgh, PhD Thesis.
4. Ferreira, E. S. B., Hulme, A. N., McNab, H., Quye, A. (2003). LC-MS Trap MS and PDA-HPLC complementary techniques in the analysis of different components of flavonoids dyes: the example of Persian berries (*Rhamnus sp.*). *Dyes Hist. Archaeol.*, **19**, 19-23.
5. Ferreira, E. S. B., Quye, A., Hulme, A. N., McNab, H. (2003). LC-Ion Trap MS and PDA-HPLC - Complementary techniques in the analysis of Flavonoid dyes in historical textiles: The case study of an 18th-century Herald's Tabard. *Dyes Hist. Archaeol.*, **19**, 13-18.
6. Peggie, D. A. (2006). *The Development and Application of Analytical Methods for the Identification of Dyes on Historical Textiles*. The University of Edinburgh, PhD Thesis.
7. Rosenberg, E. (2008). Characterisation of historical organic dyestuffs by liquid chromatography – mass spectrometry. *Anal. Bioanal. Chem.*, **391**, 33-57.
8. Miller, J. M. (1988). *Chromatography: concepts and contrasts*. John Wiley & Sons.
9. Davis, R., Frearson, M. (1987). *Mass Spectrometry*. John Wiley & Sons.
10. Ashcroft, A. E. (1997). *Ionization Methods in Organic Mass Spectrometry*. Barnett, N. W., The Royal Society of Chemistry.
11. Hulme, A. N., McNab, H., Peggie, D. A., Quye, A. (2005). Negative ion electrospray mass spectrometry of neoflavonoids. *Phytochem.*, **66**, 2766-2770.
12. Rafaelly, L., Heron, S., Nowik, W., Tchaplá, A. (2008). Optimisation of ESI-MS detection for the HPLC of anthraquinones. *Dyes Pigm.*, **77**, 191-203.
13. McNab, H., Ferreira, E. S. B., Hulme, A. N., Quye, A. (2009). Negative ion ESI-MS analysis of natural yellow dye flavonoids: An isotopic labelling study. *Int. J. Mass Spectrom.*, **284**, 57-65.



14. Heck, A. J. R. (2008). Native mass spectrometry: a bridge between interatomics and structural biology. *Nature Methods*, **5**, 927-933.
15. Van Berkel, G. J. (1997). The Electrolytic Nature of Electrospray. In *Electrospray Ionisation Mass Spectrometry: Fundamentals, Instrumentation & Applications*, John Wiley & Son, Inc, New York: 65-105.
16. Ikonomou, M. G., Blades, A. T., Kebarle, P. (1991). Electrospray-Ion spray: A comparison of mechanisms and performance. *Anal. Chem.*, **63**, 1989-1998.
17. Ablajan, K. (2011). A study of characteristic fragmentation of isoflavonoids by using negative ion ESI-MS. *J. Mass. Spectrom.*, **46**, 77-84.
18. Welsch, T., Michalke, D. (2003). (Micellar) electrokinetic chromatography: an interesting solution for the liquid phase separation dilemma. *J. Chromatogr. A* **1000**, 935-951.
19. Cabooter, D., Desmet, G. (2012). Chapter 1: General Overview of Fast and High-resolution Approaches in Liquid Chromatography. In *UHPLC in Life Sciences*, Guillaume, D., Veuthey, J.-L., Ed. RSC Chromatography Monographs No. 16: 1-28.
20. de Villiers, A., Lestremau, F., Szucs, R., Gélébart, S., David, F., Sandra, P. (2006). Evaluation of ultra performance liquid chromatography: Part I. Possibilities and limitations. *J. Chromatogr. A*, **1127**, 60-69.
21. Fekete, S., Olah, E., Fekete, J. (2011). Fast liquid chromatography: The domination of core-shell and very fine particles. *J. Chromatogr. A*, **1228**, 57-71.
22. Nováková, L., Matysová, L., Solich, P. (2006). Advantages of application of UPLC in pharmaceutical analysis. *Talanta*, **68**, 908-918.
23. Pieters, S., Dejaegher, B., Vander Heyden, Y. (2010). Emerging analytical separation techniques with high throughput potential for pharmaceutical analysis, part I: Stationary phase and instrumental developments in LC. *Comb. Chem. High Throughput Screen.*, **13**, 510-529.
24. Gritti, F., Guiochon, G. (2010). On the extra-column band-broadening contributions of modern, very high pressure liquid chromatographs using 2.1 mm I.D. columns packed with sub-2  $\mu\text{m}$  particles. *J. Chromatogr. A*, **1217**, 7677-7689.
25. Stroh, J. G., Petucci, C. J., Brecker, S. J., Nogle, L. M., (2008). Sub-2  $\mu\text{m}$  HPLC coupled with sub-ppm mass accuracy for analysis of pharmaceutical compound libraries. *J. Sep. Sci.*, **31**, 3698-3703.
26. Quye, A., Wouters, J. (1992). An application of HPLC to the identification of natural dyes. *Dyes Hist. Archaeol.*, **10**, 48-54.
27. Wang, J., Li, H., Jin, C., Qu, Y., Xiao, X. (2008). Development and validation of a UPLC method for quality control of rhubarb-based medicine: Fast simultaneous determination of five anthraquinone derivatives. *J. Pharm. Biomed. Anal.*, **47**, 765-770.
28. Chen, X. J., Ji, H., Zhang, Q. W., Tu, P. F., Wang, Y. T., Guo, B. L., Li, S. P. (2008). A rapid method for simultaneous determination of 15 flavonoids in Epimedium using pressurized liquid extraction and ultra-performance liquid chromatography. *J. Pharm. Biomed. Anal.*, **46**, 226-235.

29. Baranowska, I., Magiera, S. (2011). Analysis of isoflavones and flavonoids in human urine by UHPLC. *Anal. Bioanal. Chem.*, **399**, 3211-3219.
30. Villela, A., van der Klift, E. J. C., Mattheussens, E. S. G. M., Derksen, G. C. H., Zuilhof, H., van Beek, T. A. (2011). Fast chromatographic separation for the quantitation of the main flavone dyes in *Reseda luteola* (weld). *J. Chromatogr. A*, **1218**, 8544-8550.
31. Deng, X., Gao, G., Zheng, S., Li, F. (2008). Qualitative and quantitative analysis of flavonoids in the leaves of *Isatis indigatica* Fort. by ultra-performance liquid chromatography with PDA and electrospray ionization tandem mass spectrometry detection. *J. Pharm. Biomed. Anal.*, **48**, 562-567.
32. Wyndham, K. D., O'Gara, J. E., Walter, T. H., Glose, K. H., Lawrence, N. L., Alden, B. A., Izzo, G. S., Hudalla, C. J., Iraneta, P. C. (2003). Characterization and Evaluation of C18 HPLC Stationary Phases Based on Ethyl-Bridged Hybrid Organic/Inorganic Particles. *Anal. Chem.*, **75**, 6781-6788.
33. Guillarme, D., Nguyen, D. T. T., Rudaz, S., Veuthey, J. L. (2008). Method transfer for fast liquid chromatography in pharmaceutical analysis: Application to short columns packed with small particle. Part II: Gradient experiments. *Eur. J. Pharm. Biopharm.*, **68**, 430-440.
34. Debrus, B., Rozet, E., Hubert, P., Veuthey, J.-L., Rudaz, S., Guillarme, D. (2012). Chapter 3: Method Transfer Between Conventional HPLC and UHPLC. In *UHPLC in Life Sciences*, Guillarme, D., Veuthey, J.-L., Ed. RSC Chromatography Monographs No. 16: 67-101.
35. Hartmann, C., Smeyers-Verbeke, J., Massart, D. L., McDowall, R. D. (1998). Validation of bioanalytical chromatographic methods. *Journal of Pharmaceutical and Biomedical Analysis*, **17**, 193-218.
36. Massart, L. M., Vandeginste, B. G. M., Buydens, L. M. C., De Jong, S., Lewi, P. J., Smeyers-Verbeke, J. (1997). In *Handbook of Chemometrics and Qualimetrics*, 427.
37. Gaspar, H., Moiteiro, C., Turkman, A., Coutinho, J., Carnide, V. (2009). Influence of soil fertility on dye flavonoids production in weld (*Reseda luteola* L.) accessions from Portugal. *J. Sep. Sci.*, **32**, 4234-4240.
38. Derksen, G. C. H., van Beek, T. A., de Groot, A., Capelle, A. (1998). High-performance liquid chromatographic method for the analysis of anthraquinone glycosides and aglycones in madder root (*Rubia tinctorum* L.). *J. Chromatogr. A*, **816**, 277-281.
39. Ferreira, E. S. B., Quye, A., MacNab, H., Hulme, A. N. (2002). Photo-oxidation of Quercetin and Morin as Markers for the characterisation of natural flavonoid yellow dyes in Ancient textile. *Dyes Hist. Archaeol.*, **18**, 63-72.
40. Peggie, D. A., Hulme, A. N., McNab, H., Quye, A. (2008). Towards the identification of characteristic minor components from textiles dyed with weld (*Reseda luteola* L.) and those dyed with Mexican cochineal (*Dactylopius coccus* Costa). *Microchim. Acta*, **162**, 371-380.
41. Ferreira, E. S. B., McNab, H., Hulme, A. N., Quye, A. (2004). The natural constituent of historical textile dyes. *Chem. Soc. Rev.*, **33**, 329-336.
42. Hulme, A. N., McNab, H., Peggie, D., Quye, A. (accepted). The chemical characterisation of aged and unaged fibre samples dyed with sawwort (*Serratula tinctoria*) using PDA-HPLC and HPLC ESI MS. *Dyes in History and Archaeology*, **22** (in Press).

43. Schweppe, H. (1993). *Handbuch der Naturfarbstoffe*. Nikol Verlagsgesellschaft, Hamburg.
44. Wouters, J., Grzywacz, C. M., Claro, A. (2011). A Comparative Investigation of Hydrolysis Methods to Analyze Natural Organic Dyes by HPLC-PDA: Nine Methods, Twelve Biological Sources, Ten Dye Classes, Dyed Yarns, Pigments and Paints. *Studies in Cons.*, **56**, 231-249.
45. Zhang, X., Laursen, R. A. (2005). Development of mild extraction methods for the analysis of natural dyes in textiles of historical interest using LC-Diode Array Detector-MS. *Anal. Chem.*, **77**, 2022-2025.
46. Hacke, A.-M. (2006). *Investigation into the Nature and Ageing of Tapestry Materials*. The University of Manchester, PhD Thesis.
47. Tosun, F., Akyuz Kizilay, C., Tosun, A. U. (2009). Flavonoids and isoflavonoids from *Genista sessilifolia* DC. growing in Turkey. *Chem. Nat. Compd.*, **45**, 83-84.
48. Noccioli, C., Luciardi, L., Barsellini, S., Favro, C., Bertoli, A., Bader, A., Loi, M. C., Pistelli, L. (2012). Flavonoids from two Italian *Genista* species: *Genista cilentina* and *Genista sulcitana*. *Chem. Nat. Compd.*, **48**, 672-673.
49. Rigano, D., Cardile, V., Formisano, C., Maldini, M. T., Piacente, S., Bevilacqua, J., Russo, A., Senatore, F. (2009). *Genista sessilifolia* DC. and *Genista tinctoria* L. inhibit UV light and nitric oxide-induced DNA damage and human melanoma cell growth. *Chem-Biol. Interact.*, **180**, 211-219.
50. Kulling, S. E., Honig, D. M., Simat, T. J., Metzler, M. (2000). Oxidative in Vitro Metabolism of the Soy Phytoestrogens Daidzein and Genistein. *J. Agric. Food Chem.*, **48**, 4963-4972.
51. Ducret Awouafack, M., Spiteller, P., Lamshoeft, M., Kusari, S., Ivanova, B., Tane, P., Spiteller, M. (2011). Antimicrobial Isopropenyl-dihydrofuranisoflavones from *Crotalaria lachnophora*. *J. Nat. Prod.*, **74**, 272-278.
52. Łuczkiwicz, M., Głód, D., Baczek, T., Bucinski, A. (2004). LC-DAD UV and LC-MS for the Analysis of Isoflavones and Flavones from In Vitro and In Vivo Biomass of *Genista tinctoria* L. *Chromatographia*, **60**, 179-185.
53. Tůmova, L., Tůma, J. (2011). The effect of UV light on isoflavonoid production in *Genista tinctoria* culture in vitro. *Acta Physiol Plant*, **33**, 635-640.
54. Wollenweber, E., Papendieck, S., Schilling, G. (1993). A Novel C-Methyl Isoflavone from *Abronia latifolia*. *Nat. Prod. Lett.*, **3**, 119-122.
55. Yi, Y., Cao, Z., Yang, D., Cao, Y., Wua, Y., Zhao, S. (1998). A New Isoflavone from *Smilax glabra*. *Molecules*, **3**, 145-147.
56. Xiao, H. B., Krucker, M., Albert, K., Liang, X. M. (2004). Determination and identification of isoflavonoids in *Radix astragali* by matrix solid-phase dispersion extraction and high-performance liquid chromatography with photodiode array and mass spectrometric detection. *J. Chromatogr. A.*, **1032** 117-124.
57. Ungar, Y., Osundahunsi, O. F., Shimoni, E. (2003). Thermal Stability of Genistein and Daidzein and Its Effect on Their Antioxidant Activity. *J. Agric. Food Chem.*, **51**, 4394-4399.

58. Eisen, B., Ungar, Y., Shimoni, E. (2003). Stability of Isoflavones in Soy Milk Stored at Elevated and Ambient Temperatures. *J. Agric. Food Chem.*, **51**, 2212-2215.
59. Hofenk de Graaf, J. H. (2005). *The Colourful Past*. Archetype Publications.

## **CHAPTER 3**

<b>3</b>	<b>INVESTIGATION OF EARLY 16<sup>TH</sup> CENTURY ENGLISH TAPESTRIES ASSOCIATED TO THE “SHELDON” WORKSHOP .....</b>	<b>113</b>
3.1	HISTORICAL BACKGROUND.....	113
3.1.1	<i>Tapestry works in the Middle Ages and early Renaissance.....</i>	<i>113</i>
3.1.2	<i>The origin of tapestry weaving in England .....</i>	<i>114</i>
3.1.3	<i>The Sheldon workshop myth or reality?.....</i>	<i>115</i>
3.1.4	<i>Sheldon tapestries today.....</i>	<i>117</i>
3.1.5	<i>Sir Burrell and the Sheldon Collection.....</i>	<i>117</i>
3.2	SAMPLING AND DOCUMENTATION.....	118
3.2.1	<i>Burrell Collection.....</i>	<i>118</i>
3.2.2	<i>Bodleian Library, University of Oxford .....</i>	<i>121</i>
3.3	DYE ANALYSIS .....	125
3.3.1	<i>Experimental conditions.....</i>	<i>125</i>
3.3.1.1	Extraction protocol .....	125
3.3.1.2	HPLC System .....	125
3.3.1.3	UPLC System .....	125
3.3.2	<i>Yellow, green, orange yarns.....</i>	<i>126</i>
3.3.2.1	Weld ( <i>Reseda luteola</i> L.).....	126
3.3.2.2	Dyer’s greenweed ( <i>Genista tinctoria</i> L.).....	130
3.3.2.3	Young fustic ( <i>Cotinus Coggygria</i> L.).....	134
3.3.3	<i>Red, purple, pink yarns.....</i>	<i>137</i>
3.3.3.1	Madder species .....	137
3.3.3.2	Cochineal .....	140
3.3.3.3	Orchil dyes.....	143
3.3.3.4	Safflower ( <i>Carthamus tinctorius</i> L.).....	144
3.4	DISCUSSION.....	148
3.5	REFERENCES .....	150

### 3 INVESTIGATION OF EARLY 16<sup>TH</sup> CENTURY ENGLISH TAPESTRIES ASSOCIATED TO THE “SHELDON” WORKSHOP

Historical tapestries were very expensive pieces of work that were only available to the Royal Families or the very wealthy. Their manufacture was a controlled process and great attention was paid to the choice of the dye species used for their creation. The art of tapestry weaving reached its apogee at the end of the Middle Ages, especially in France and Flanders, a French province until 1526,<sup>1</sup> with the manufacture of exquisite pieces of work, produced by renowned artists and their workshops. Their iconography can be complex, as they often included symbolic emblems, mottoes, or coats of arms, associated with religious or mythological themes.<sup>2,3</sup> Today surviving tapestries are still exhibited in European Royals palaces, historic houses or castles and provide invaluable graphical information on important historical periods.<sup>3</sup>

#### 3.1 HISTORICAL BACKGROUND

##### 3.1.1 Tapestry works in the Middle Ages and early Renaissance

Tapestry weaving developed in France from the thirteenth century and there was a strict control of the weaver's apprenticeship and qualification. It is reported that weavers were not organised into a guild before the fourteenth century,<sup>1</sup> but nevertheless historical records report already in 1277 on existing weavers' apprenticeships in Paris:

*“nul ne peut devenir tisserand s'il n'a accompli tous les services imposés pour être tisserand; ... nul tisserand ne peut travailler à une tapisserie sans avoir effectué les étapes exigées”.*<sup>4</sup>

Prior to the fourteenth century and the development of the low warp technique, mainly embroidery cloths were manufactured. An example of large scale

embroidery is the famous and often misnamed Bayeux tapestry, possibly manufactured in England around 1066 - 1082.<sup>1,5</sup> Iconic Medieval tapestries include the Apocalypse tapestry, manufactured in Paris between 1377 and 1379,<sup>6</sup> today conserved in the castle at Angers in France and the famous The Lady and the Unicorn, manufactured in Flanders around 1500,<sup>6</sup> today part of the collection of the museum of the Middle Ages in Cluny cloister in Paris.<sup>2</sup>

Parisian weaving workshops declined in the fifteenth century, due to political instability with the Hundred Year's War between the Kingdom of England and the Kingdom of France for control of the French throne. At this time Paris was occupied by English political forces and weakened by civil war, famine and then the plague in 1418. This situation induced significant population migration, including the migration of weavers, to the South of France and then to Italy.<sup>6</sup> In the meantime other important tapestry workshops at Arras, Tournai, Aubusson, Beauvais and Bruges were developed, and later in the sixteenth century Brussels, that became important centres of tapestry weaving in Europe.<sup>6</sup> During the sixteenth century, the religious wars between Catholics and Protestants, induced other population migrations, and they especially affected Flemish weavers who escaped from the Low Countries to England, where they settled down and introduced the art of tapestry weaving.<sup>6</sup>

### 3.1.2 The origin of tapestry weaving in England

In contrast to the vibrant tapestry weaving industry in the Low Countries, there is relatively little art historical research on early English tapestries.<sup>7-9</sup> Although it is often believed that foreign weavers started to settle in England during the reign of Edward III (1216 - 1272), prior to 1619 with the development of the Mortlake workshop next to London, it has been unclear if other workshops were weaving tapestries in England, or if English nobles would have commissioned tapestries from Flanders or French workshops.<sup>1</sup> The early work from Barnard and Wace on the



Sheldon workshop in 1928 presented forty-six early English tapestries, assumed to be woven at the castle of Sir William Sheldon at Barcheston in Warwickshire.<sup>8</sup> Thus, William Sheldon could have been in charge of the first non-Royal tapestry workshop in England and since this publication the term “Sheldon” was often applied to early English tapestries based on the assumption that this was the only workshop in England in the mid sixteenth century. However, recent art historical publications from Wells-Cole and then Turner demonstrated a much complex situation, and the main finds of their research will be discussed in the following sections.<sup>10-13</sup>

### 3.1.3 The Sheldon workshop myth or reality?

Recent art historical research from Turner on the “Sheldon” workshop provided more understanding of the development of tapestry weaving in England and the pieces that were woven at Barcheston.<sup>10-12, 14, 15</sup> William Sheldon acquired the manor of Weston, near Warwickshire in 1534, and then in 1561 the manor of Barcheston, where he set-up the first non-Royal English tapestry workshop in 1570. In preparation for this, it is said that his son Ralph Sheldon (1537 - 1613) spent time abroad around the year 1555 with a Flemish weaver named Richard Hyckes (1524 - 1621), in order to learn the art of weaving in the Low Countries.<sup>12</sup> Richard Hyckes was later to become the director of the Sheldon factory.<sup>11, 12</sup> It still remains unclear whether Richard Hyckes was a Flemish emigrant or an Englishman of Flemish origin, and if he signed all the pieces made at Barcheston. However, the quality of the pieces signed by Richard Hyckes (figure 3.1), clearly demonstrate that he was an expert in tapestry weaving, an art described by Turner as unknown in England at that time, and gives some indication that he was most certainly a Flemish weaver.<sup>12, 15</sup> Turner also showed that Richard Hyckes was working as the Queen’s Arrasmaker at the Great Wardrobe department in London from 1569 until 1609,<sup>12, 13</sup> and she explained that this position was a royal appointment where the holder was employed

to repair tapestries and to supply the materials for which he would then be reimbursed.<sup>16</sup>

It has been suggested that the manor of Barcheston could have been not only a production workshop but also a training place, where Richard Hyckes was teaching the art of weaving,<sup>12, 14</sup> and Turner could trace the names of twelve weavers who worked at Barcheston and then left, possibly after completing their apprenticeship, to join the Great Wardrobe in London.<sup>12, 14</sup> Today it is quite accepted that the workshop produced large tapestry maps,<sup>15, 17, 18</sup> but also possibly smaller sized works, especially cushions covers often depicting biblical scenes, although these have been so far attributed to the Sheldon workshop only on stylistic criteria.<sup>7, 19</sup> However, recent curatorial research especially on the Chastleton House tapestries, proved that it is not possible reliably to attribute these tapestries to the Sheldon workshop,<sup>13, 14</sup> and suggested that several other small tapestry workshops could have been set-up next to London.<sup>14, 19</sup>



**Figure 3.1:** Detail of tapestry map of Worcestershire, © Trustees of Victoria and Albert Museum, London – courtesy of the Bodleian Library, University of Oxford. Reproduced from reference 15.<sup>15</sup>

### 3.1.4 Sheldon tapestries today

Tapestries attributed to the Sheldon workshop can be found today mainly in the collection of the Victoria and Albert Museum in London, the Bodleian Library in the University of Oxford and the Burrell Collection in Glasgow.<sup>7-9, 17, 18</sup> Most of these tapestries are large maps, illustrating the Midlands countryside of England (figure 3.1), but the Burrell collection holds nineteen small size tapestries, that have being much less studied in comparison to the large tapestry maps from the Bodleian Library.<sup>10, 11</sup> A reassessment of the collection of early English tapestries is currently being undertaken at the Burrell Collection, which aims to publish an updated catalogue of these pieces.

### 3.1.5 Sir Burrell and the Sheldon Collection

Sir William Burrell (1861 - 1958) was a wealthy Glasgow ship owner and a fine collector of works of art. He is considered as one of the most important collectors in Scotland and donated his entire collection to the city of Glasgow in 1944.<sup>20</sup> In the late nineteenth and early twentieth century he amassed a vast collection, which included around two hundred Medieval and Renaissance tapestries. This tapestry collection is one of the twenty largest collections in Europe and one of the most important in the United Kingdom. It includes pieces of extreme importance, including medieval and early sixteenth century Burgundian and Flemish tapestries, and also a large group of slightly lower quality European tapestries, dating from the fifteenth and sixteenth centuries.<sup>20-22</sup> But the singularity of the collection is certainly this unique group of nineteen English tapestries, dating from the mid sixteenth century and attributed to the Sheldon workshop.

These early English tapestries were collected by Burrell through various sources between 1916 and 1951, but unfortunately for some of them, it is not possible to trace their acquisition.<sup>23, 24</sup> This probably means that some of the tapestries were acquired by Burrell before 1911, as after this date he recorded his purchases in Purchase Books. The last date recorded for the acquisition of a 'Sheldon' piece was

1952, a few years after he donated his collection to the city of Glasgow. Among these tapestries is a complete set of six cushion covers depicting the story of *Susanna and the Elders*, which was purchased by Sir Burrell in 1936 from J. M. Botibel, an art dealer (Inv. N°: 47.9 to 47.14, figure 3.2). This is the only complete set, although the numbering of the scenes does not follow the narrative sequence (47.6: *Susanna on her way to the bath*; 47.10: *Susanna at her bath*; 47.12: *Susanna before the Judge*; 47.11: *Susanna led to Execution*; 47.13: *The Elders before Daniel*; 47.14: *The Stoning of the Elders*).<sup>24</sup>

## 3.2 SAMPLING AND DOCUMENTATION

In order to shed more light on these pieces, and as part of a curatorial reassessment of the Burrell collection, condition reports on the nineteen small tapestries were prepared by the textile conservators. This gave the opportunity to look at the complete group of tapestries in great detail and to decide on a sampling strategy with regard to dyes analysis.

### 3.2.1 Burrell Collection

Two sampling campaigns were conducted at the Burrell Collection in order to select yarns for dye analysis and around 250 samples were collected from thirteen tapestries. The first sampling campaign took place in March 2009 with the textile conservators at the Burrell collection. Due to the large number of items to investigate, it was decided at first to focus on the complete set of tapestries depicting the story of *Susanna and the Elders* (figure 3.2, Inv. N° 47.9 to 47.14) and three other tapestries depicting similar biblical scenes, but purchased before 1911 (figure 3.3, Inv. N°: 47.6 to 47.8). These two groups of tapestries were particularly interesting, as they showed slight differences in their graphics and presented different levels of degradation of the yellow hues. Of these, tapestries 47.6 and 47.9 - that are

duplicates of the same biblical scene (*Susanna on her way to the bath*) - were sampled with a particular interest in the characterisation of flavonoid and anthraquinone dyes. Due to the small size of the pieces, silk was found to be present in higher quantities than is usually found in larger woven pieces, and as a result the samples collected included a large number of silk yarns (yellow, green, pink) but also wool yarns (green, red, orange, purple). Each sample location was recorded by means of coordinates (x; y). The samples were then weighed and photographed using a stereo-microscope (Olympus SZX12,  $\times 7 - 90$ ) equipped with an optical camera (Olympus DP70) in order to confirm the fibre identification. Finally, a sample code was attributed to each sample starting with the accession number of the tapestry followed by two letters referring to the colour and the yarn, followed by the sample number (e.g. sample 47.6 GW1 refers to a green wool yarn).



**Figure 3.2:** Early English tapestries representing the story of *Susanna and the Elders*, complete set of six (A to F, Inv. N°: 47.9 to 47.14), circa 1600, © Glasgow City Museums.





**Figure 3.3:** Early English tapestries representing scenes from the story of *Susanna and the Elders* (A to C Inv. N°: 47.6 to 47.8), circa 1600, © Glasgow City Museums.

A second sampling campaign was then undertaken in June 2010, in order to complete the sampling of the *Susanna* series. In addition to the nine *Susanna* tapestries, four tapestries were included to this study: a long Cushion Cover representing “*Faith, Charity and Hope*” (Inv. N° 47.19) and a small panel representing “*Judith and the Head of Holofernes*” with the Motto: *Si Deus nobiscum / Quis contra nos* (Inv. N° 47.23), both of unknown provenance (figure 3.4 A-B),<sup>24</sup> and two armorial tapestries one with the coat of arms of Sacheverell (Inv. N° 47.17) and the other one with the arms of Walter Jones and Eleanor Pope (Inv. N° 47.21). Tapestry 47.17 is dated to 1578 -1580 and is related to a similar tapestry part of the Victoria and Albert Museum Collection (V&A T.195-1914),<sup>9, 24</sup> while tapestry 47.21 was found at Chastleton House in 1919, and acquired after several transactions by Sir Burrell in 1934 from F. Partridge & Sons (figure 3.4 C-D).<sup>14, 24</sup>





**Figure 3.4:** Early English tapestries A: “*Faith, Charity and Hope*” (Inv. N° 47.19); B: “*Judith and the Head of Holofernes*” (Inv. N° 47.23), C: coat of arms of Sacheverell; D: coat of arms of Walter Jones and Eleanor Pope, circa 1600, © Glasgow City Museums.

### 3.2.2 Bodleian Library, University of Oxford

Finally, an exciting possibility arose to sample three tapestry maps of secure Sheldon provenance from the Bodleian Library, while these were being conserved at the Shephard Travis Textile Conservation Studio Ltd. This was a unique opportunity to investigate dated and signed pieces that would allow us to compare and contrast the dye sources characterised with those found on the tapestries from the Burrell Collection.<sup>15, 17, 18</sup> These tapestries must have been extraordinary expensive items and their vibrant original colours can still be observed while looking at their reverse sides, where the flavonoid dyes were protected from photo-degradation (figure 3.5).



**Figure 3.5:** Observation of the photo-degradation of yellow flavonoid dyes, © L. Troalen.



In contrast to the small *Susanna* pieces, the tapestry maps are very large woven pieces and only small number of silk yarns could be sampled for dye analysis. Around 50 samples were collected and these included several yellow and green wool yarns expected to contain flavonoid dyes, but also black, brown, red and purple wool yarns and a few purple silk yarns. The first tapestry investigated represents a map of Worcestershire and is signed by Richard Hyckes and dated to after 1579 (Map 1, figure 3.6); while the second tapestry represents a map of Oxfordshire and is signed with the date 1588 (Map 2, figure 3.7); finally a fragment part of a tapestry map representing Warwickshire and dated to 1590 was also included in the study (Map 3, figure 3.8).<sup>15, 17, 18</sup>



**Figure 3.6:** Tapestry map of Worcestershire (5 × 5 metres), signed Richard Hyckes, with scale and divider “borrowed” from the map of Anglia included in Saxton’s Atlas of 1579,<sup>15</sup> © Trustees of Victoria and Albert Museum, London - courtesy of the Bodleian Library, University of Oxford. Reproduced from reference 15.<sup>15</sup>





**Figure 3.7:** Tapestry map of Oxfordshire, fragment excised in the eighteenth century (approx. 5 × 5 metres), signed with the date 1588,<sup>15</sup> © Trustees of Victoria and Albert Museum, London – courtesy of the Bodleian Library, University of Oxford. Reproduced from reference 15.<sup>15</sup>



**Figure 3.8:** Fragment of tapestry map of Warwickshire, with the Camden's Britannia Paraphrase dated to 1590,<sup>15</sup> © Trustees of Victoria and Albert Museum, London – courtesy of the Bodleian Library, University of Oxford. Reproduced from reference 15.<sup>15</sup>

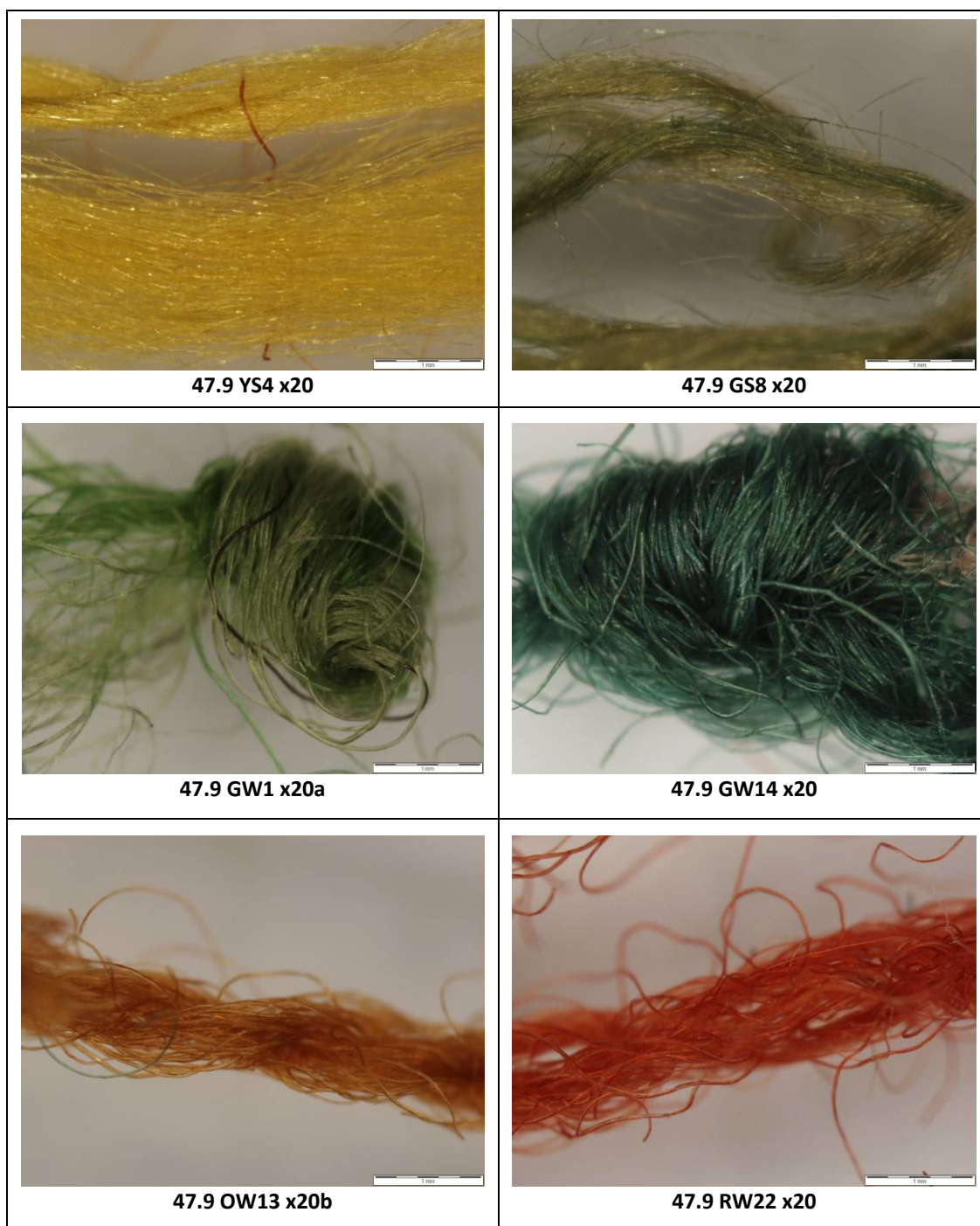


**Table 3.1:** Binocular observation of the main colours and type of yarns investigated during this study, for all images scale bar is 1 mm.

### 3.3 DYE ANALYSIS

#### 3.3.1 Experimental conditions

##### 3.3.1.1 Extraction protocol

The extraction of the historical samples was carried out using a strong hydrochloric acid extraction (chapter 2). The drawbacks associated with this method will be taken into account for the interpretation of several samples, especially those containing anthraquinone dyes which are particularly sensitive to esterification or decarboxylation of the carboxyphenols present.<sup>25-28</sup> Furthermore, it was understood that this would also hydrolyse any glycoside precursors into their aglycone forms, limiting somewhat species identification.<sup>27, 29</sup> Nevertheless, the use of hydrochloric acid extraction will allow comparison of the results with previous important studies on historical tapestries.<sup>30, 31</sup> A few samples suggested to be sensitive to hydrochloric acid extraction protocol were also extracted with dimethyl sulfoxide (DMSO).<sup>32</sup> The details of the extraction protocols can be found in section 7.2.

##### 3.3.1.2 HPLC System

The great majority of the samples were investigated using the HPLC system at National Museums Scotland, following Method A (chapter 2) using a Phenomenex Spherclone ODS(2) reverse phase column, with 5  $\mu\text{m}$  particle size, 150  $\times$  4.6 mm (length  $\times$  i.d.), and a guard column containing the same stationary phase. Details on HPLC system and chromatographic method can be found in section 7.1.

##### 3.3.1.3 UPLC System

Several samples were found to be difficult to characterise by HPLC and were further investigated using the UPLC system at the University of Edinburgh (chapter 2) following Method C using a BEH C18 reverse phase column, with 1.7  $\mu\text{m}$  particle

size, 150 × 2.1 mm (length × i.d.), and in-line filter. Details of the UPLC system and chromatographic method can be found in section 7.1.

### 3.3.2 Yellow, green, orange yarns

#### 3.3.2.1 Weld (*Reseda luteola* L.)

The main dye source characterised in this study was weld (*Reseda luteola* L.), which was found in one hundred and twelve samples across the Burrell Collection and the tapestry maps from the Bodleian Library. HPLC analysis of the acid hydrolysed extracts of weld characterised the association of the flavones luteolin (**9**,  $R_t = 15.1$  min, [ $\lambda_{\max} = 252, 292$  (sh), 349 nm]) and apigenin (**10**,  $R_t = 17.3$  min, [ $\lambda_{\max} = 267, 300$  (sh), 338 nm]) and traces of the *O*-methylated flavone chrysoeriol (**12**,  $R_t = 17.8$  min, [ $\lambda_{\max} = 251, 268, 290$  (sh), 349 nm]). Additionally the green yarns contained indigotin (**52**,  $R_t = 22.5$  min [ $\lambda_{\max} = 242, 287, 339, 615$  nm]), indicating the use of an indigo-type species, most likely woad (*Isatis tinctoria* L.), while alizarin (**26**,  $R_t = 20.3$  min, [ $\lambda_{\max} = 230$  (sh), 248, 280, 430 nm]) and purpurin (**28**,  $R_t = 24.7$  min, [ $\lambda_{\max} = 256, 296, 456, 482, 515$  nm]) were characterised in the orange yarns, indicating the use of a madder-type species.

A previously published study showed that the relative amounts of the flavonoid components characterised in the acid hydrolysed extract of weld (*Reseda luteola* L.) were altered by photo-degradation.<sup>31</sup> It was found that the photo-degradation of luteolin (**9**) and chrysoeriol (**12**) components occurred in reference wool yarns dyed with weld (*Reseda luteola* L.) at a faster rate than apigenin.<sup>31</sup> This resulted in the amount of apigenin in the acid hydrolysed extracts increasing relative to luteolin (**9**) and chrysoeriol (**12**) in artificially aged samples.<sup>31</sup> In the historical samples investigated in this study, it was found for both silk and wool yarns that the level of apigenin (**10**) and chrysoeriol (**12**) were greatly increased compared to what was observed in reference yarns (table 3.1).<sup>31</sup> The yellow silk yarns were found to average 8.7 % apigenin and 5.1 % chrysoeriol, while the wool yarns contained

systematically slightly lower level of apigenin that ranged between 5.9 % and 8.3 % and chrysoeriol that ranged between 3.6 and 4.0 % (table 3.1).

Yarn	$\lambda$ nm	<i>Relative Amount (Area, %)</i>		
		Luteolin (9)	Apigenin (10)	Chrysoeriol (12)
MODHT YS1a	254	92.8 $\pm$ 0.2	4.0 $\pm$ 0.1	3.1 $\pm$ 0.1
Historical Yellow Silk [48 samples]	254	86.2 $\pm$ 3.6	8.7 $\pm$ 3.1	5.1 $\pm$ 1.2
Historical Green Silk [11 samples]	254	87.0 $\pm$ 1.9	7.9 $\pm$ 1.2	5.1 $\pm$ 0.8
MODHT YW1	254	93.0 $\pm$ 0.4	4.3 $\pm$ 0.3	2.8 $\pm$ 0.2
Historical Yellow Wool [12 samples]	350	89.1 $\pm$ 3.2	8.3 $\pm$ 1.7	3.7 $\pm$ 0.9
Historical Wool [23 samples]	350	90.4 $\pm$ 3.1	5.9 $\pm$ 2.2	3.6 $\pm$ 0.8
Historical Red Wool [14 samples]	350	89.8 $\pm$ 5.7	7.2 $\pm$ 4.8	4.0 $\pm$ 2.0

**Table 3.1:** Relative amounts of the dyestuff in the acid hydrolysed extract of reference yarns and historical yarns, extracted at 254 nm. [For individual yarn see chapter 7, tables 7.11 and 7.12]

Perhaps the higher level of apigenin found in the silk samples analysed would suggest that the silk yarns have suffered a higher level of photo-degradation, compared to the wool yarns (figure 3.4). It was found also that these silk yarns systematically contained a much higher level of flavonoid dyes for the same weight of sample, suggesting a higher starting dye content, as would be expected from the structure of silk fibres (chapter 1, section 1.3.2). It has been previously suggested that the higher susceptibility of the luteolin derivatives to photo-degradation might be due to the additional hydroxyl functionality in the B-ring, as the chemical reactivity of flavonoids is known to largely be controlled by the structure of ring C, with less influence being attributed to the number and position of OH substituents on rings A and B.<sup>31, 33</sup> But in spite of our observations on historical silk yarns, it seems that the reactivity of the luteolin derivatives to photo-degradation might also be dependant on

the type of substrate, although artificial ageing experiment of silk yarns dyed with weld would be necessary to confirm this hypothesis.

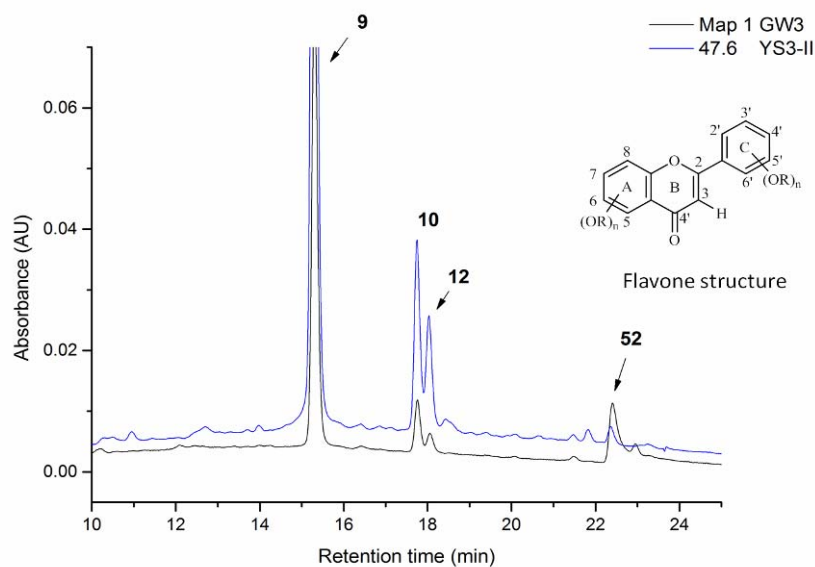


**Figure 3.4:** HPLC chromatogram of the acid hydrolysed of historical samples Bodleian MAP 1 GW3 and Burrell 47.6 YS3-II dyed with weld (*Reseda luteola* L.) monitored at 254 nm. The components luteolin (9), apigenin (10) and chrysoeriol (12) were identified in both extracts, but exhibited different relative amounts.

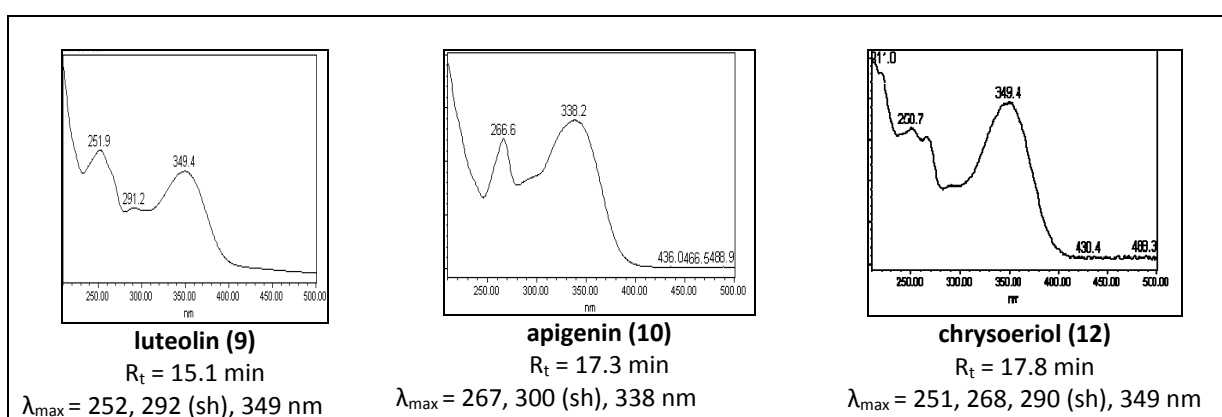


**Table 3.2:** PDA spectra of flavonoid dyes characterised in the acid hydrolysed extracts of historical samples.



The dyestuff composition was compared against the compositions determined by HPLC in previous artificial ageing experiments,<sup>31</sup> it was found in general that both silk and wool historical yarns exhibited a much higher level of photo-degradation and a wider distribution of dyestuff composition was observed (figure 3.5 and 3.6). Some samples exhibited a much higher level of apigenin around 15 to 20 % that did not seem to be explained only by photo-degradation. It is therefore possible to consider the use for another dye source containing a higher level of apigenin that could have been mixed with weld or alternatively that specific preparation of the yarn, such as over-dyeing, could have affected the uptake of apigenin onto the yarns, paralleling what was observed on silk yarns that were over-dyed with dyer's greenweed (chapter 2). These anomalous compositions were also observed in a few historical samples analysed from sixteenth century Brussels tapestries.<sup>31</sup>

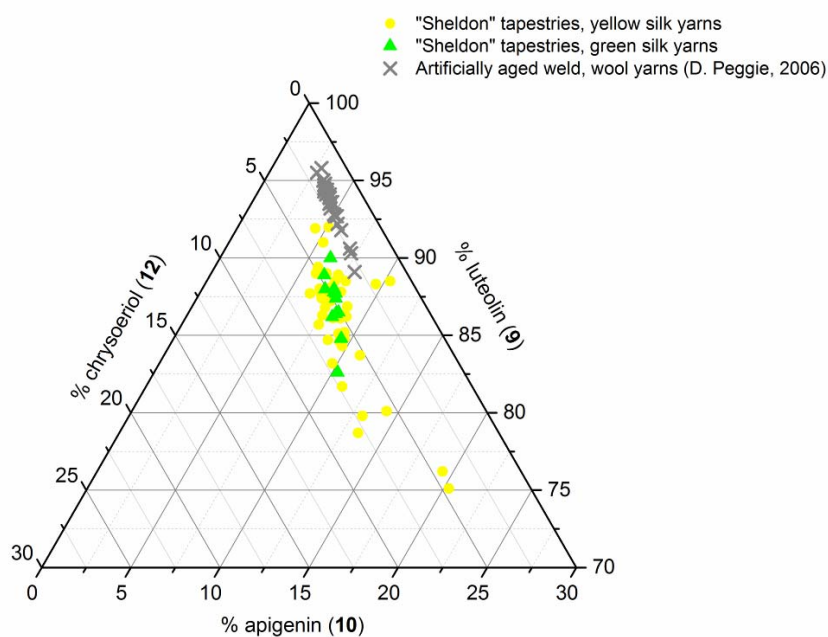


**Figure 3.5:** Ternary representation of the relative amounts of apigenin (10), luteolin (9) and chrysoeriol (12) characterised in the acid hydrolysed extracts of historical silk yarns monitored at 254 nm and artificially aged wool yarns. [Data compiled from chapter 7, table 7.11 and D. Peggie thesis].<sup>31</sup>

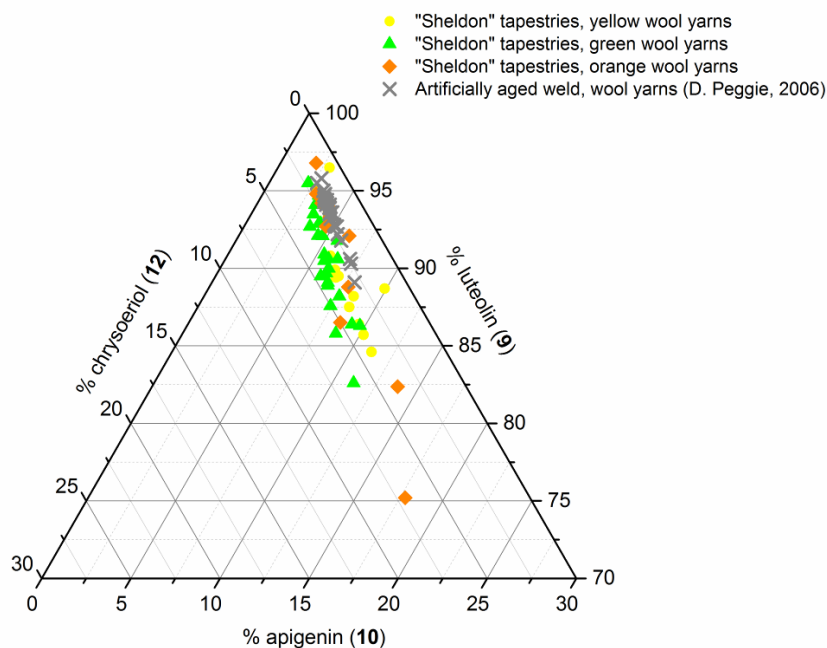


**Figure 3.6:** Ternary representation of the relative amounts of apigenin (**10**), luteolin (**9**) and chrysoeriol (**12**) characterised in the acid hydrolysed extracts of historical wool yarns monitored at 350 nm and artificially aged wool yarns. [Data compiled from chapter 7, table 7.12 and D. Peggie thesis].<sup>31</sup>

### 3.3.2.2 Dyer's greenweed (*Genista tinctoria* L.)

The second important dye source characterised in this study was dyer's greenweed (*Genista tinctoria* L.), which was found in around twenty samples. HPLC investigation of the acid hydrolysed extract of dyer's greenweed characterised the association of the flavones luteolin (**9**,  $R_t = 15.1$  min,  $[\lambda_{\max} = 252, 292$  (sh), 349 nm]) and apigenin (**10**,  $R_t = 17.6$  min,  $[\lambda_{\max} = 267, 300$  (sh), 338 nm]), the isoflavone genistein (**11**,  $R_t = 15.4$  min,  $[\lambda_{\max} = 260, 335$  (sh)nm]) and the methylated isoflavonoid compound Gt3 ( $R_t = 12.4$  min,  $[\lambda_{\max} = 255, 310$  (sh) nm]), along with indigotin (**52**,  $R_t = 22.5$  min,  $[\lambda_{\max} = 242, 287, 339, 615$  nm]) in the green yarns.

It was found difficult on the HPLC system to clearly identify and integrate the minor *O*-methylated flavone components, so in order to characterise the minor components



present in historical samples, several yarns were investigated using the UPLC system. In all the samples investigated only one *O*-methylated flavone was characterised, which corresponded well, by the comparison of retention times to chrysoeriol (**12**,  $R_t = 15.69$  min). In order to confirm the structure of the *O*-methylated flavone four historical samples were re-analysed by reconstituting an acid hydrolysed extract of the sample with a solution of diosmetin (**13**;  $2 \mu\text{g mL}^{-1}$ ) in methanol:water (1/1 v/v). Comparison of the diosmetin peak area for these spiked extracts with that of the starting solution of diosmetin showed a very close correlation; this combined with the obvious appearance of a new peak in the chromatogram strongly suggests that for all the samples chrysoeriol was the only *O*-methylated flavone present in the acid hydrolysed extract (figure 3.7 and table 3.4). As yet there is no explanation of why diosmetin was not found in the aged samples; this highlights that further investigation of the light fastness of both *O*-methylated flavone isomers is needed.

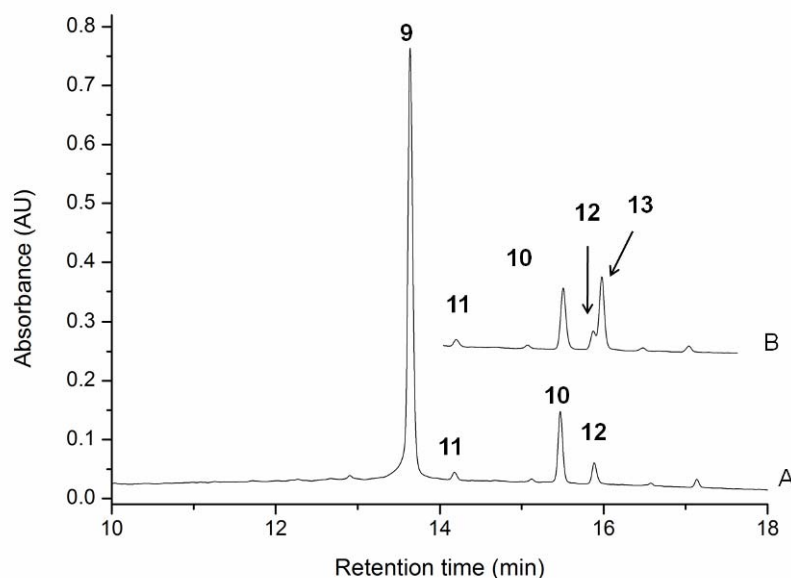


**Figure 3.7:** UPLC chromatogram showing the characterisation of flavonoid dyes present in the acid-hydrolysed extract of the Burrell historical sample 47.14 GW3 (A) and then spiked with diosmetin (B), both monitored at 350 nm.

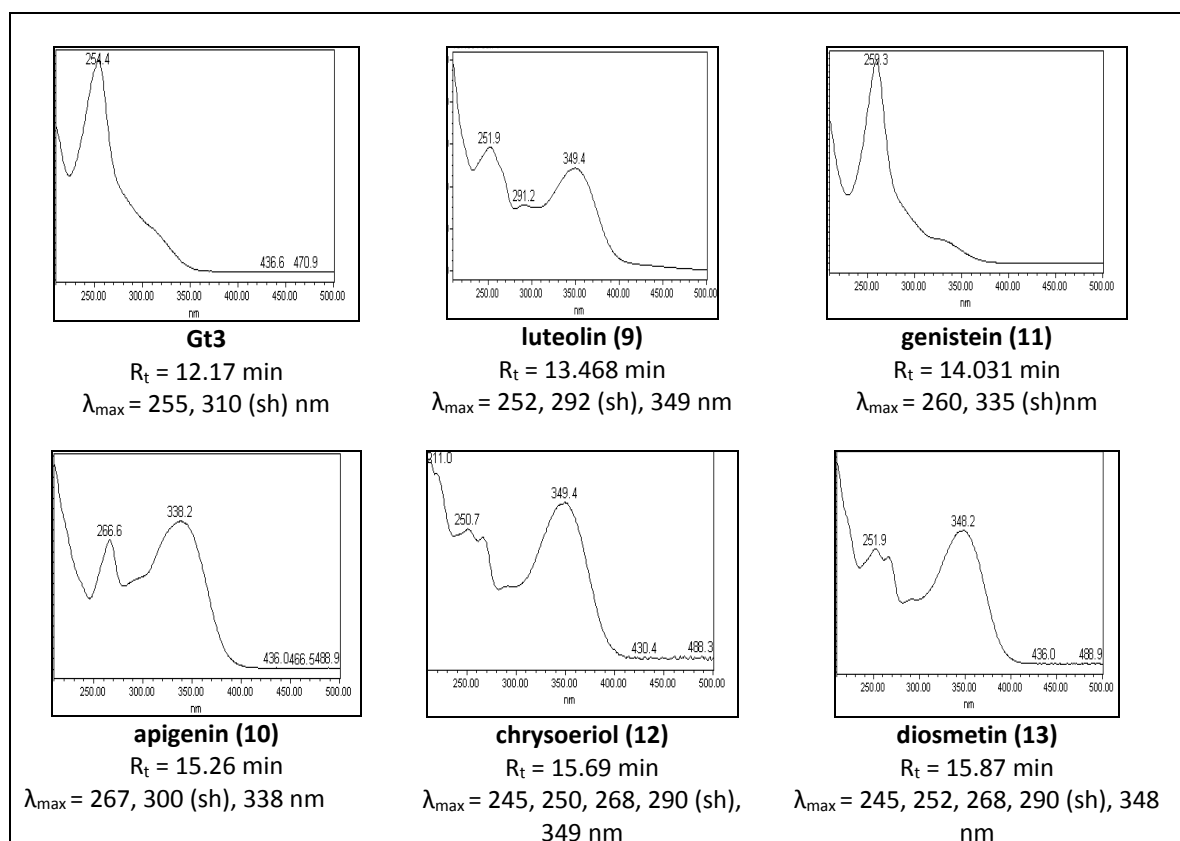


**Table 3.3:** PDA spectra of flavonoid dyes characterised in historical sample 47.14 GW3 (UPLC system).

UPLC system	Identified compound [x] Area ( $\mu\text{V} \times \text{sec}$ ) and % recovery, (n=1) at 350 nm					
Sample ID	luteolin (9)	genistein (11)	Apigenin (10)	chrysoeriol (12)	diosmetin (13)	Recovery %
47.14 GW3	1672111	32243	238364	67571	263523	89
47.21 YS21	736521	143314	542363	22984	293018	99
47.21 YSIII-1	2787069	107970	605737	29573	303657	103
47.11 GW-II-1	960518	178938	103816	34828	269887	91
	Spiking solution, diosmetin [ $2 \mu\text{g mL}^{-1}$ ] Area ( $\mu\text{V} \times \text{sec}$ ); (n=3) at 350 nm					
	diosmetin (13)					
Spiking solution	296127 $\pm$ 4648					

**Table 3.4:** Peak areas ( $\mu\text{V} \times \text{sec}$ ) of chromophores identified at 350 nm in the acid hydrolysed extract of four historical samples spiked with diosmetin ( $2 \mu\text{g mL}^{-1}$ ). [For details see chapter 7, table 7.14].

Accelerated ageing studies showed that genistein (**11**) has a relatively slow photo-degradation rate compared to the other dye components luteolin (**9**) and apigenin (**10**).<sup>31</sup> The presence in most of the historical yarns investigated of both the isoflavone genistein (**11**) and the methylated isoflavonoid compound Gt3, would suggest that they exhibit similar photo-degradation rates.

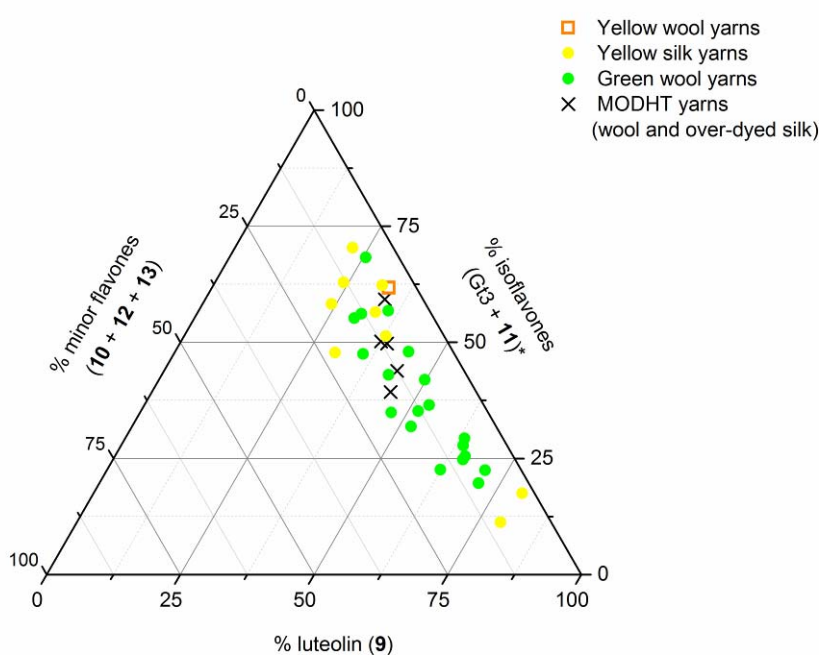


**Figure 3.8:** Ternary representation of the relative amounts of luteolin (**9**), isoflavonoids [Gt3 and genistein (**11**) and \* Gt1, Gt2 and Gt4 for reference samples] and minor flavones components [apigenin (**10**), chrysoeriol (**12**), diosmetin (**13**)] characterised in the acid hydrolysed extracts of historical wool yarns monitored at 254 nm and from over-dyed silk reference yarns. [Data compiled from chapter 7, table 7.10 and table 7.13].

It was observed that the relative amounts of isoflavonoid dyes were very variable in historical yarns, which would suggest that these variations could be related to the textile preparation, as it was found that the level of isoflavonoid components, Gt3 and genistein (**11**) decreased in silk yarn references subjected to over-dyeing processes, while the quantity of luteolin (**9**) was found to increase (chapter 2). These

differences in yarn preparation are highlighted in the ternary representation of the relative amounts of luteolin (**9**), isoflavonoid dyes [Gt3 and genistein (**11**)] and minor flavones components [apigenin (**10**), chrysoeriol (**12**) and diosmetin (**13**)]. It is possible then to graphically compare the dye profile of the historical samples to those of over-dyed silk references. From these observations, it does seem that most of the yellow yarns were not over-dyed, from the exception of two yarns, while in contrast most of the green yarns were over-dyed. The scattering of the composition might also reflect variation in the levels of photo-degradation of the samples (figure 3.8)

### 3.3.2.3 Young fustic (*Cotinus Coggygia* L.)

Surprisingly, several wool samples found only in the Burrell tapestries, exhibited a pale yellow to orange colour but were found difficult to characterise using the HPLC system, due to their high levels of degradation. These samples were further investigated using the UPLC system which allowed the characterisation of the aurone sulfuretin (**15**,  $R_t = 12.72$  min, [ $\lambda_{max} = 256, 270, 397$  nm]), associated with the flavone luteolin (**9**,  $R_t = 13.72$  min, [ $\lambda_{max} = 252, 266, 292$  (sh), 349 nm]). In addition small amounts of flavonol components including fisetin (**14**,  $R_t = 10.79$  min, [ $\lambda_{max} = 248, 318, 361$  nm]) and two un-identified components named yf1 ( $R_t = 11.02$  min, [ $\lambda_{max} = 250$  (sh), 318, 344 nm]) and yf2 ( $R_t = 11.73$  min, [ $\lambda_{max} = 244, 318, 347$  nm]) were identified with the flavone apigenin (**10**,  $R_t = 15.55$  min, [ $\lambda_{max} = 267, 300$  (sh), 338 nm]) and the *O*-methylated flavone chrysoeriol (**12**,  $R_t = 15.85$  min, [ $\lambda_{max} = 251, 268, 290$  (sh), 349 nm]). For several samples, the isoflavone genistein (**11**,  $R_t = 14.26$  min, [ $\lambda_{max} = 260, 332$  (sh) nm]) associated with the methylated isoflavonoid compound Gt3 ( $R_t = 12.35$  min, [ $\lambda_{max} = 255, 310$  (sh) nm]), were additionally characterised (see figure 3.9, table 3.5 and data compiled in chapter 6, table 6.15).

The presence of both fisetin (**14**) and sulfuretin (**15**) dye components identify young fustic species (*Cotinus coggygia* S.), although no myricetin (**17**, [ $\lambda_{max} = 253, 303$  (sh), 374 nm]) or dihydrofisetin (**20**, [ $\lambda_{max} = 234, 280, 310$  nm]) reported in other studies were characterised in these extracts.<sup>31, 34, 35</sup> Because the flavones luteolin (**9**),

apigenin (**10**) and the isoflavone genistein (**11**) are not reported to occur in young fustic species, their presence is more likely to correspond to the presence of weld (*Reseda luteola* L.) or dyer's greenweed (*Genista tinctoria* L.).<sup>31, 35</sup> The use of Young fustic (*Cotinus coggygria* S.) is surprising, as this yellow dye was known to be very light fugitive and was therefore often prohibited in the manufacture of tapestries. Nevertheless, it is often found on the core of decorative metal threads,<sup>31</sup> and its presence has been previously reported, although rarely, on contemporaneous Flemish tapestries.<sup>36</sup> The presence of residual flavonoid dyestuffs found in all the samples could either reflect cross-contamination with the dye weld or dyer's greenweed during dyebath preparation, or other general workshop practices. It is worth noting that the use of young fustic mixed with weld has been characterised in several pieces of Italian velvet clothes dated from the mid fifteenth century.<sup>37</sup>

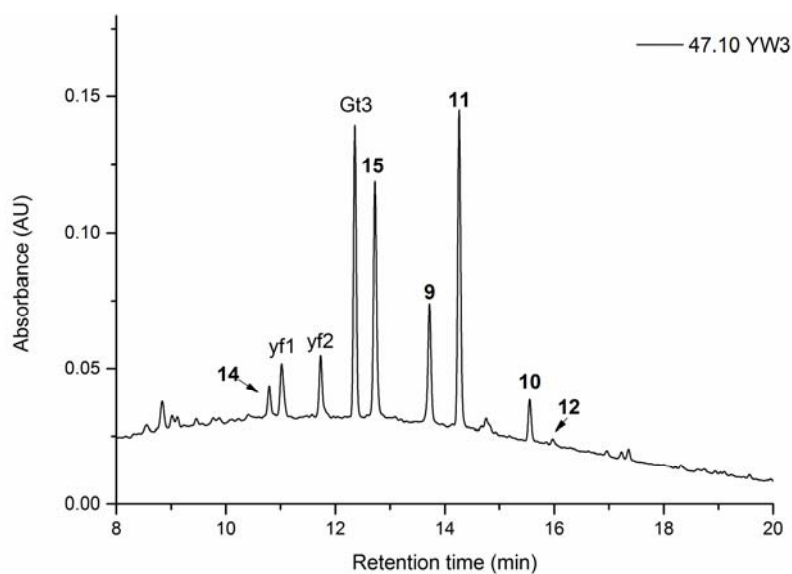


**Figure 3.9:** UPLC chromatogram showing the flavonoid dyes present in the acid-hydrolysed extract of the Burrell historical sample 47.10 YW3 monitored at 254 nm [yf1 and yf2 correspond to unknown young fustic components].

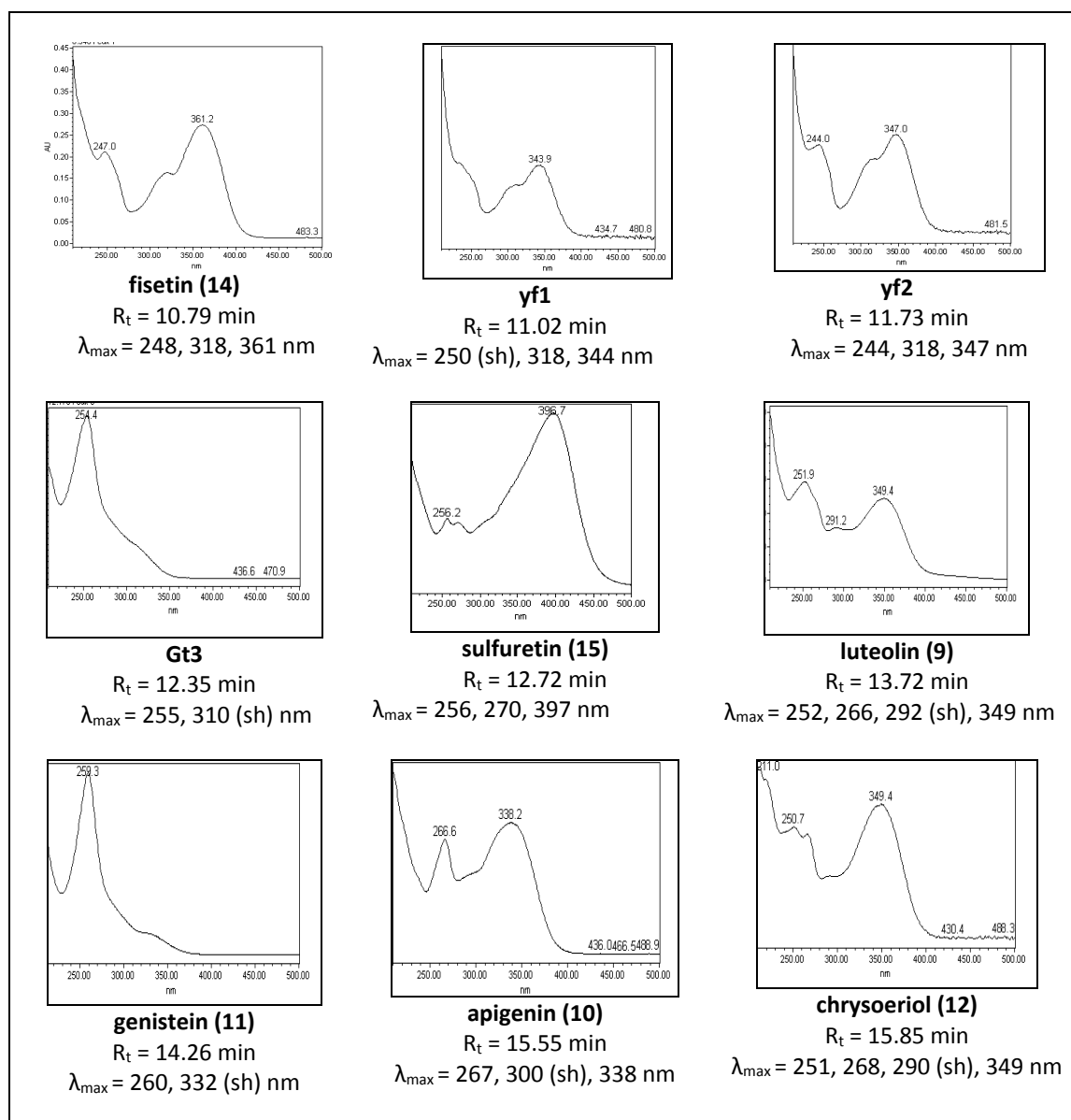


**Table 3.5:** PDA spectra of flavonoid dyes characterised in the acid-hydrolysed extract of the Burrell historical sample 47.10 YW3 monitored at 254 nm.

### 3.3.3 Red, purple, pink yarns

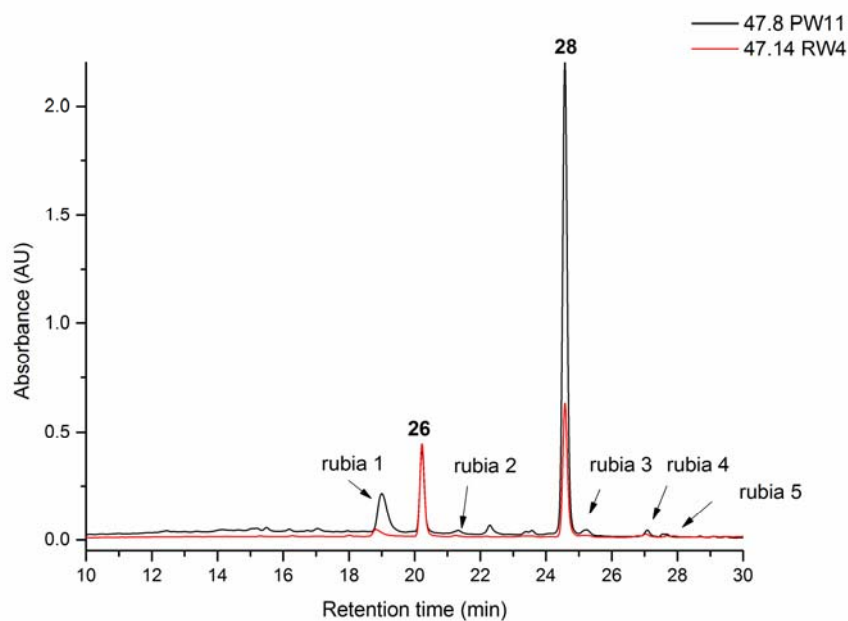
#### 3.3.3.1 Madder species

It was unsurprising that madder was found to be present in the majority of the orange, red and purple yarns investigated. Madder was characterised in 30 samples and was found to be mixed with weld (*Reseda luteola* L.) in orange yarns and sometimes associated to indigotin (**52**,  $R_t = 22.5$  min, [ $\lambda_{\max} = 242, 287, 339, 615$  nm]), suggesting the use of woad (*Isatis tinctoria* L.) for the deeper shades of purple. In many samples the unknown component Nowik C ( $R_t = 8.37$  min, [ $\lambda_{\max} = 259, 306, 339$  nm]) characteristic of degraded brazilwood species was also detected.<sup>31</sup>

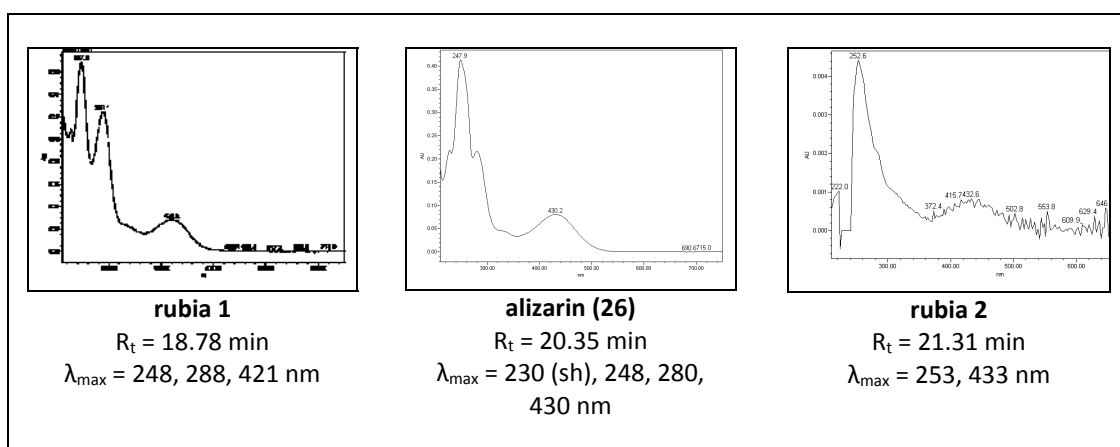
The identification of madder species in historical textiles is known to be extremely difficult, as the relative amounts of the anthraquinone dyestuffs present in the roots of madder species are complex and highly variable depending on the age and the environment of the plant inducing variability in the proportion of dyestuffs extracted from the roots of the plant.<sup>38-40</sup> Furthermore, the use of a strongly acidic extraction induces the decarboxylation of several anthraquinones, especially pseudopurpurin (**29**) and munjistin (**27**), as well as the hydrolysis of the glycoside precursors into their aglycone forms, which further complicates the identification of specific species.<sup>25, 26, 41</sup>

The two anthraquinone dyes characterised in the acid hydrolysed extracts of historical wools, were alizarin (**26**,  $R_t = 20.35$  min, [ $\lambda_{\max} = 248, 280, 430$  nm]) and purpurin (**28**,  $R_t = 24.67$  min, [ $\lambda_{\max} = 256, 296, 482, 515$  (s) nm]) and several unidentified anthraquinone compounds named rubia 1 ( $R_t = 18.78$  min, [ $\lambda_{\max} = 248, 288, 421$  nm]), Rubia 2 ( $R_t = 21.31$  min, [ $\lambda_{\max} = 253, 433$  nm]), rubia 3 ( $R_t = 25.23$  min, [ $\lambda_{\max} = 257, 295, 476$  nm]), rubia 4 ( $R_t = 27.15$  min, [ $\lambda_{\max} = 248, 283, 411$  nm]) and rubia 5 ( $R_t = 30.92$  min, [ $\lambda_{\max} = 257, 295, 420$  nm]), see table 3.6. The absorption maxima of these rubia components were compared to published values of anthraquinone dyes reported to occur in madder species.<sup>40</sup> However, due to the similarities in absorption maxima of several anthraquinone dyes and in the absence

of the analysis of reference standards, these minor components remained unidentified.



**Figure 3.10:** HPLC chromatogram highlighting the differences in the madder dye profiles, observed in two acid hydrolysed extracts of Burrell historical samples 47.8 PW11 and 47.14 RW4, both monitored at 254 nm.





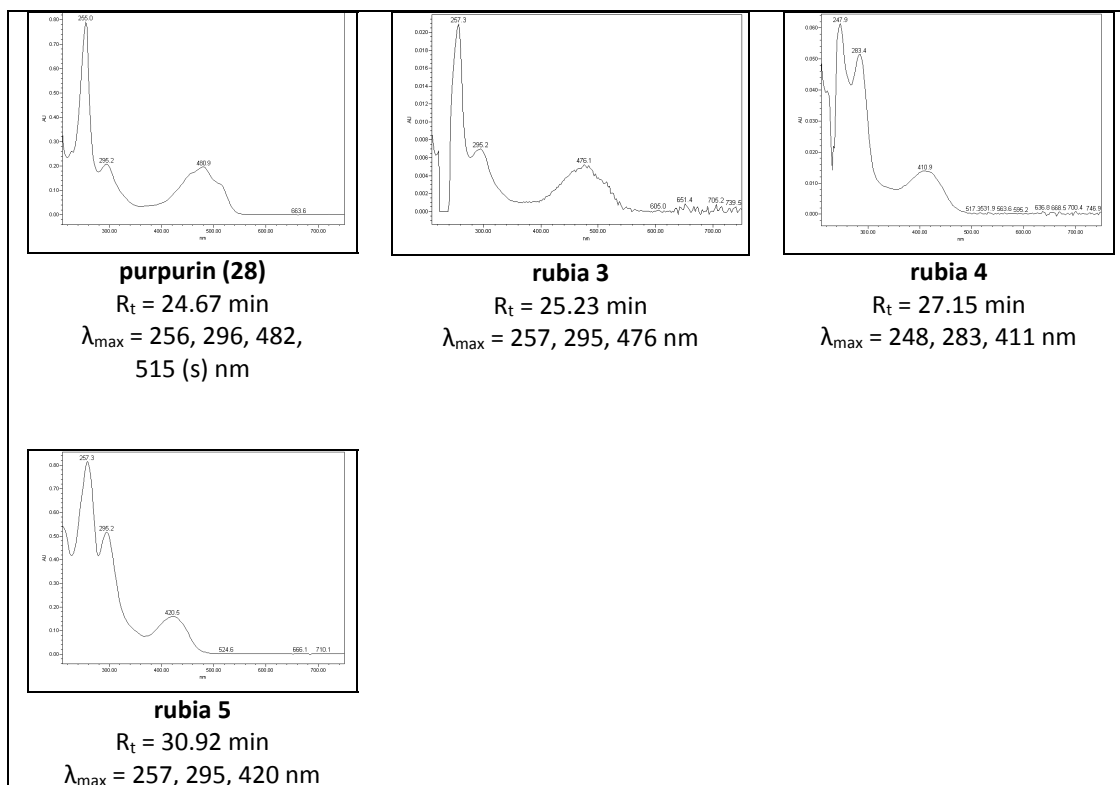


**Table 3.6:** PDA spectra of anthraquinone dyes characterised in the acid-hydrolysed extract of historical sample dyed with madder-type species, monitored at 254 nm.

A high variability in the purpurin content was observed between samples; and several purple or brown yarns exhibited a very high level of purpurin accounting for 80 % of the total anthraquinone dye composition (figure 3.10 and data compiled in chapter 7, table 7.16). These purpurin-rich yarns were only characterised on the Burrell tapestries, while the tapestry maps from the Bodleian Library exhibited the levels of alizarin (25 - 30 %) and purpurin (42 - 54 %) typically found in *Rubia tinctorum* L. extracts. It is indeed most likely that the principal dye source available at that time would have been *Rubia tinctorum* L., which was highly cultivated in Europe.<sup>34</sup> Nevertheless, *Galium* species (e.g. *Galium verum* or Lady's Bedstraw) are often reported to be used in Northern countries, and an unidentified *Galium* species was characterised on the prestigious early sixteenth century Fetternear banner part of

National Museums Scotland collection.<sup>42</sup> It is therefore not unlikely, that several dyes sources could have been used for the manufacture of the small tapestries, but this would need further chromatographic investigation, with the use of an extraction protocol that would conserves the original composition of the dye extract more closely.

### 3.3.3.2 Cochineal

Cochineal dyes were characterised in 18 samples and was found on all the tapestries, which was surprising given their very early dates. Red insect dyes were extremely expensive and probably some of the most precious natural red dyes, due to their intense hues and colour fastness. Cochineal was characterised in wool yarns, where it was sometime mixed with indigotin (**52**,  $R_t = 22.5$  min, [ $\lambda_{\max} = 242, 287, 339, 615$  nm]), and silk yarns of which several were found to contain ellagic acid ( $R_t = 8.97$  min, [ $\lambda_{\max} = 254, 310$  (s), 366 nm]), a source of tannins. The main dye component characterised in all the acid hydrolysed extracts was carminic acid (**33**,  $R_t = 5.73$  min, [ $\lambda_{\max} = 276, 312$  (s), 496 nm]) that averaged 90.2 % of the relative amounts at 275 nm. The dye component DcII (**32**,  $R_t = 5.16$  min, [ $\lambda_{\max} = 282, 438$  nm]) was found to average 4 % of the relative amounts and was associated to the minor amounts (< 2 %) of the dye components Dc IV ( $R_t = 12.15$  min, [ $\lambda_{\max} = 276, 312$  (s), 496 nm]), Dc VII ( $R_t = 13.80$  min, [ $\lambda_{\max} = 277, 312$  (s), 492 nm ]), flavokermesic acid (**35**,  $R_t = 17.51$  min, [ $\lambda_{\max} = 283, 439$  nm]) and kermesic acid (**34**,  $R_t = 18.34$  min, [ $\lambda_{\max} = 273, 312$  (s), 482 nm]), figure 3.11.

Cochineal species can be differentiated using a graphical system involving the integration at 275 nm of the peak areas of the minor markers Dc II (**32**), Dc IV, Dc VII, flavokermesic acid (**35**) and kermesic acid (**34**).<sup>25, 43</sup> Although this system has been recently disputed in a study using multivariate data analysis, it still provides some identification of several cochineal species, and more particularly, the level of the minor component Dc II (**32**) in the acid hydrolysed extract allows discrimination between Armenian cochineal (*Porphyrophora hamelii* Brandt) and American

cochineal (*Dactylopius coccus* Costa).<sup>43-46</sup> Comparison of the relative amounts of the dye components characterised in the acid hydrolysed extracts of the historical samples showed a good correlation to those of wool and silk reference yarns dyed with Mexican cochineal (*Dactylopius coccus* Costa). However, three samples of wool sampled from tapestries at the Burrell Collection exhibited a higher level of Dc II (6 to 12 %) than the expected range for Mexican cochineal extracts (1.5 to 5 %). An explanation for this could be an over estimation of the level of Dc II due a close elution with carminic acid ( $R_t = 5.16$  min vs.  $R_t = 5.73$  min).

Four samples from the Bodleian tapestry maps exhibited a low Dc II level (< 1 %), and a slightly higher level in flavokermesic acid and kermesic acid (2 to 3 %) and fall therefore closer to the compositional range expected for Armenian cochineal (*Porphyrophora hamelii* Brandt).<sup>43, 47</sup> Three of these samples (two silk and one wool yarns) were sampled from the fragment of the tapestry map of Warwickshire (Map 3), supposedly dated to 1590; while the fourth sample corresponded to a wool yarn collected on the tapestry map representing Worcestershire and dated to 1579 (Map 1). It has been reported that the uptake of cochineal dye slightly varies depending on the type of yarns and that the relative amount of Dc II characterised in the acid hydrolysed extract of silk is often lower than the one of wool. This is indeed observed from the analysis of the MODHT reference yarns, where the relative amount in Dc II average only 2 % for the silk yarn, while 4 % were characterised in the wool yarn. However, due to their early date of production (1579 - 1590), it is possible that another red dye source could have been used for the manufacture of the tapestry maps, as cochineal dye imported by the Spaniards into Europe would have not been available in London before 1560s.<sup>48, 49</sup> For these reasons, the low Dc II cochineal species characterised in these four samples remained un-identified.

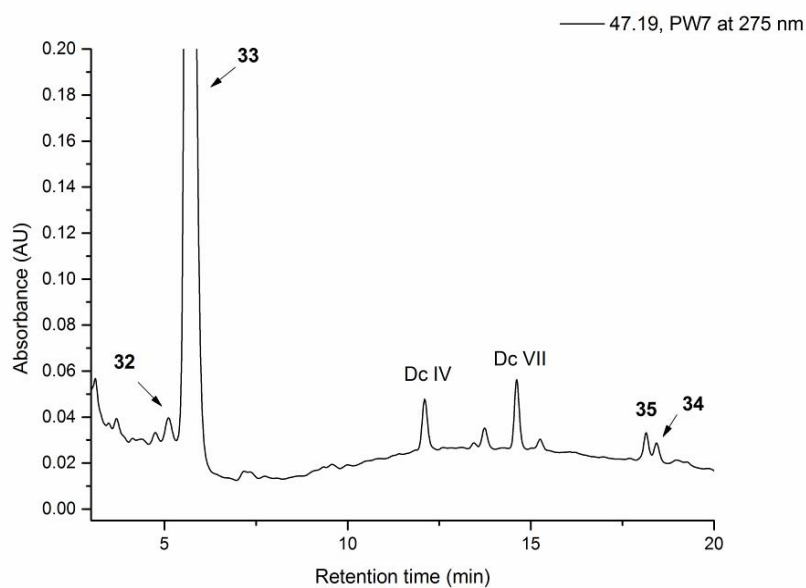


**Figure 3.11:** HPLC chromatogram of the acid hydrolysed extract of Burrell historical sample 47.19 PW7, monitored at 275 nm.

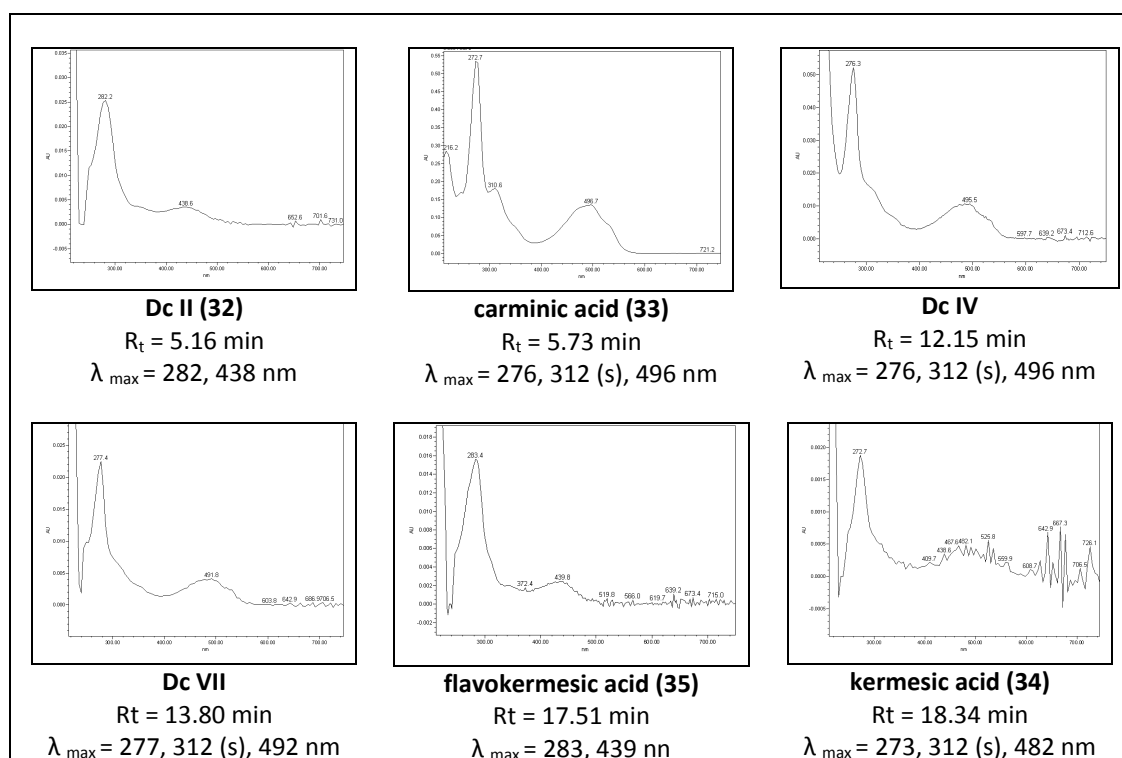


**Table 3.7:** PDA spectra of cochineal dyes characterised in the acid-hydrolysed extract of Burrell historical sample 47.19 PW7, monitored at 275 nm.

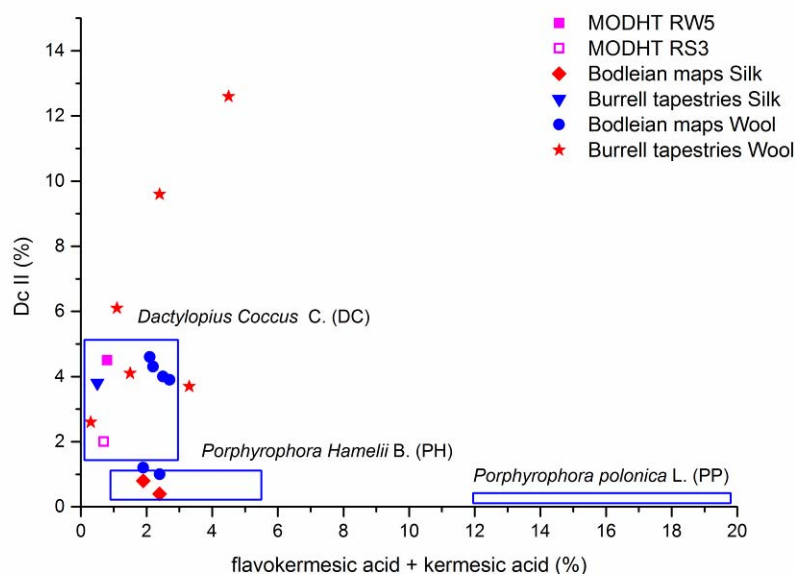


**Figure 3.12:** Graphical interpretation of the composition of the acid hydrolysed extract of the historical samples investigated. Integration of peak areas was carried out at 275 nm.<sup>43, 47</sup> [Data compiled from chapter 7 table 7.17].

### 3.3.3.3 Orchil dyes

Several wool yarns from the Burrell tapestries only, exhibited traces of a dye component presenting a maximum absorption around 530 nm that might be related to an orchil dye ( $R_t = 20.7$  min,  $[\lambda_{\max} = 267, \sim 530$  nm]). This unknown dye was sometimes found associated with traces of indigotin (**52**,  $R_t = 22.5$  min,  $[\lambda_{\max} = 242, 287, 339, 615$  nm]) and in other cases traces of carminic acid (**32**,  $R_t = 5.73$  min,  $[\lambda_{\max} = 276, 312$  (s), 496 nm]).

The characterisation of orchil dyes in historical textiles is difficult, due their high photo-degradation rate and also the fact that their structure is easily destroyed during the acidic extraction from the textile.<sup>36</sup> Closer observation of all the small tapestries revealed the characteristic faded colour of orchil dyes on the light-exposed face,

while a strong purple colour could still be observed at the of the tapestry (figure 3.12). The use of orchil dye, similarly to young fustic, was prohibited in the manufacture of tapestries, as it was known to be a very light fugitive dye, nevertheless its presence has been previously reported on Flemish tapestries.<sup>36</sup>



**Figure 3.12:** Observation of purple hues possibly realised with an orchil dye on the Burrell tapestry 47.9, front and back.

#### 3.3.3.4 Safflower (*Carthamus tinctorius* L.)

The last dye source characterised in all the Burrell historical tapestries is safflower (*Carthamus tinctorius* L.). This was found in a group of seven pink silk yarns that were analysed using the UPLC system (figure 3.13 and 3.14). Several flavonoid dyes were found to be present in trace quantities in the acid hydrolysed extracts of these yarns including the flavones luteolin (**9**,  $R_t = 13.47$  min, [ $\lambda_{\max} = 253, 266, 292$  (sh), 352 nm]) and apigenin (**10**,  $R_t = 15.26$  min, [ $\lambda_{\max} = 267, 300$  (sh), 338 nm]) and the *O*-methylated flavone chrysoeriol (**12**,  $R_t = 15.69$  min, [ $\lambda_{\max} = 251, 268, 290$  (sh), 349 nm]). In addition, the components Ct1 ( $R_t = 13.34$  min, [ $\lambda_{\max} = 269$  nm]), Ct2 ( $R_t = 14.02$  min, [ $\lambda_{\max} = 283$  nm]), Ct3 ( $R_t = 14.68$  min, [ $\lambda_{\max} = 221, 291$  nm]) and Ct4 ( $R_t = 15.32$  min, [ $\lambda_{\max} = 294$  nm]), recently characterised as the minor components present in aged safflower extracts were identified in all the samples.<sup>50</sup> The main component of safflower is carthamin (**4**,  $R_t = 17.57$  min, [ $\lambda_{\max} = 245, 373, 520$  nm]), a

dye which is very sensitive to hydrochloric extraction, although it may be eluted from the thread using DMSO. The presence of carthamin was further confirmed in two of the silk yarns after DMSO extraction (chapter 7, table 7.18).<sup>32</sup>



**Figure 3.13:** Detail of the back of Burrell tapestry 47.9 showing the pink silk dyed with safflower.

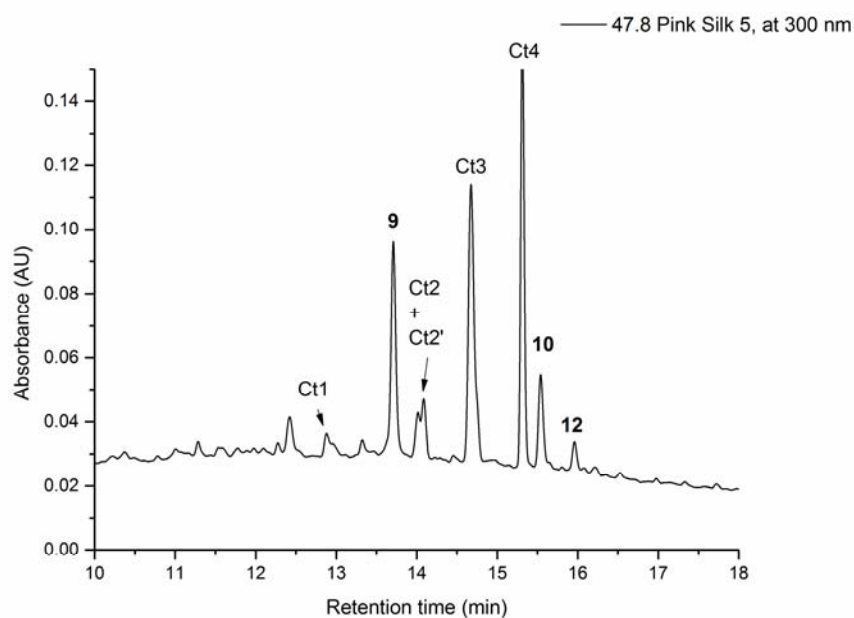


**Figure 3.14:** UPLC chromatogram showing the flavonoid dyes present in the acid hydrolysed extract of Burrell historical sample 47.8 Pink S5, monitored at 300 nm. [Ct2' corresponds to an unknown component, possibly an isomer of Ct2].

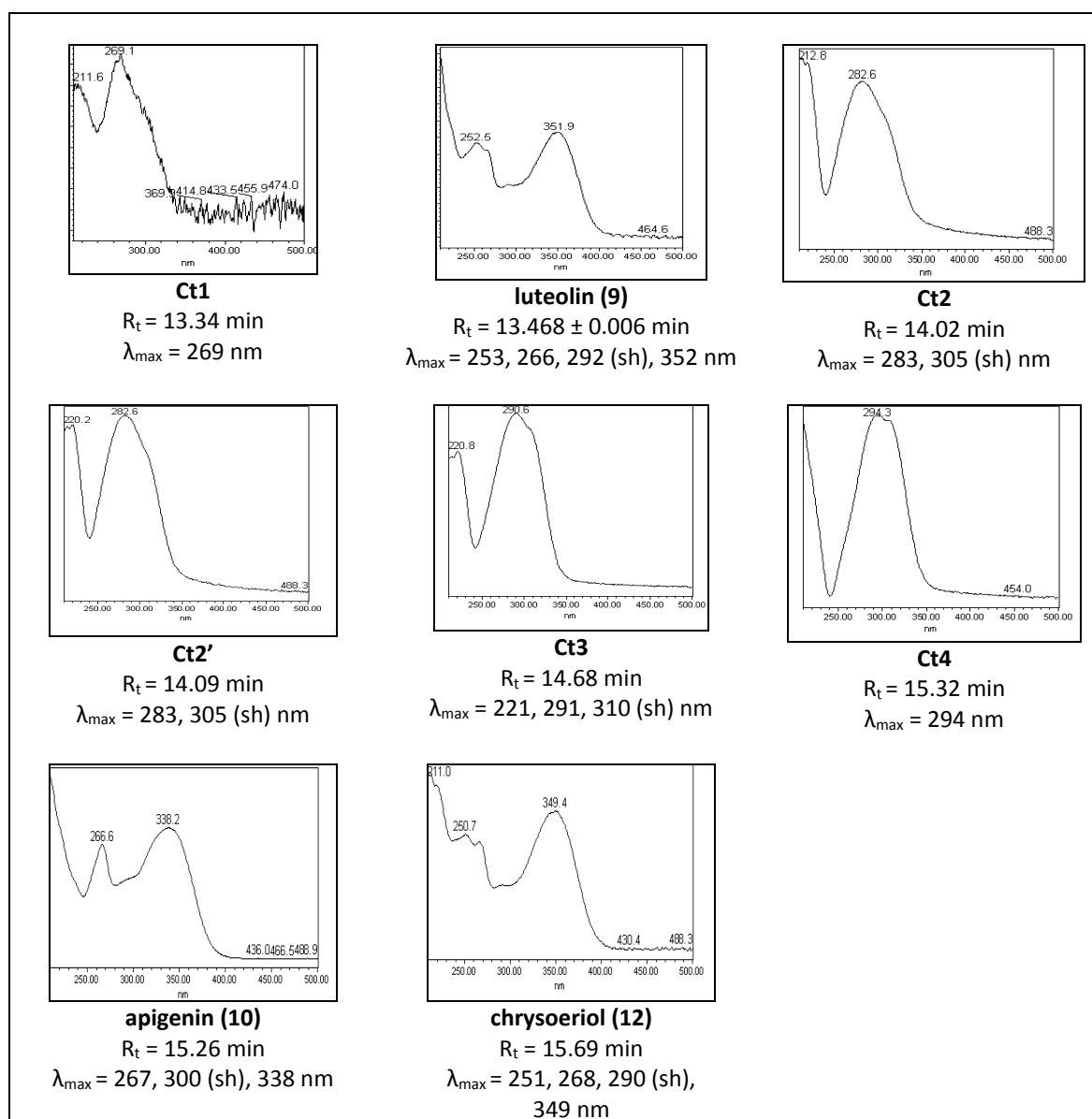


**Table 3.8:** PDA of the flavonoid dyes present in the acid hydrolysed historical sample 47.8 Pink S5, monitored at 300 nm. The minor Ct components characteristic of safflower dye were identified using the UV-Vis maxima and shoulders (nm) reported in the recent work of Wouters *et al.* (2010).<sup>50</sup>

All the extracts exhibited similar relative compositions at 300 nm, with the unknown components Ct3 being present in higher quantity (25 - 30 %) than Ct1, Ct2 and Ct4



(figure 3.15). Furthermore, UPLC allowed the separation of a new component that eluted closely to Ct2 and exhibited a similar UV-visible spectrum. This unknown component named Ct2' ( $R_t = 14.09$  min,  $[\lambda_{\max} = 283$  nm]) was characterised in all the sample extracts and could possibly correspond to an isomer of Ct2, although this would require further mass spectrometric analysis.

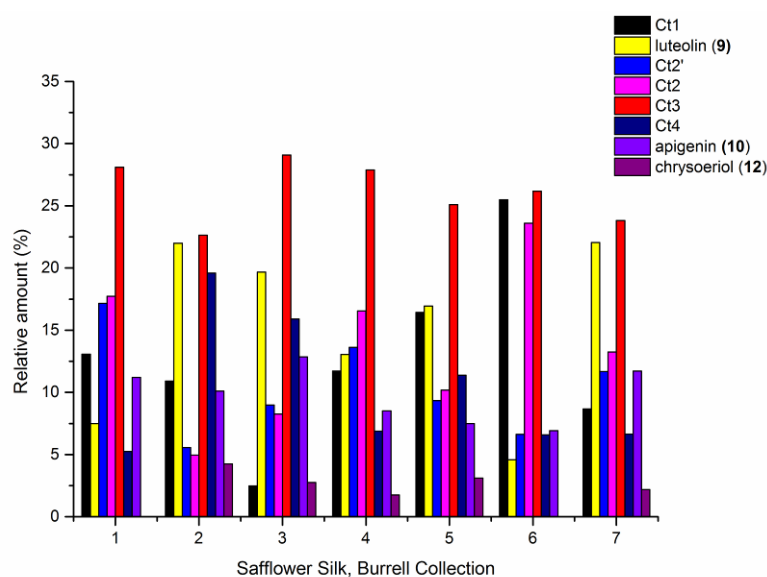


**Figure 3.15:** Relative amounts of the dye components characterised in the acid hydrolysed Burrell silk yarns dyed with safflower, monitored at 300 nm. [Data compiled from chapter 7, table 7.18].

It has been reported that apigenin (**10**) and kaempferol (**19**,  $[\lambda_{\max} = 255$  (sh), 267, 294 (sh), 325 (sh), 365 nm]) are usually found in small amounts in safflower extracts, but that only apigenin is usually characterised in aged yarns dyed with safflower.<sup>50</sup> Therefore the association of luteolin (**9**), apigenin (**10**) and chrysoeriol (**12**) in the extracts is more likely to be due to the presence of weld (*Reseda luteola* L.), suggesting similar workshop practices as found for the yellow samples. Given their fugitive nature, it is quite remarkable that UPLC analysis of the acid hydrolysed extract has allowed the characterisation of minor flavonoid Ct components, and hence identification of the dye source. Safflower dye has only been characterised

once on a mid-sixteenth century European tapestry, prior to this study.<sup>32</sup> Thus its presence on several Burrell English tapestries is particularly notable in an historic context as safflower would have been traded into Europe.

### 3.4 DISCUSSION

This study has demonstrated the benefits to the study of historical textiles of combining HPLC and UPLC systems. While a large number of historical samples could be easily characterised using a conventional HPLC system, it was found crucial to investigate several yarns using the UPLC system. This allowed the detection and integration of very minor components, providing a more secure identification of several dye sources such as young fustic (*Cotinus coggygria* Scop.) or safflower (*Carthamus tinctorius* L.). New information was also gained on the characterisation of the *O*-methylated flavones present in the acid hydrolysed extract of historical yarns dyed with dyer's greenweed (*Genista tinctoria* L.).

The range of dye sources characterised on the Sheldon tapestry maps included weld (*Reseda luteola* L.), madder (*Rubia tinctorum* L.), woad (*Isatis tinctoria* L.) or Mexican cochineal (*Dactylopius coccus* Costa). The unique yellow dye source was found to be weld, which differed from what was characterised on a study of important sixteenth century Brussels tapestries, where both dyer's greenweed (*Genista tinctoria* L.) and weld (*Reseda luteola* L.) were found, although weld was also the predominant dye source characterised in wool yarns.<sup>31</sup> The use of weld is not surprising as this would have been a much better quality dye, with a higher content of luteolin, but it might indicate different workshop practices in England compared to the Low Countries. The presence of American cochineal (*Dactylopius coccus* C.), characterised on all the Sheldon tapestry maps is certainly noticeable, as cochineal would have been a very expensive dye traded from South America and only available in London from the 1560s.<sup>48, 49</sup> Furthermore, the fact that this dye was used in large woven areas surely demonstrate the very high value of the tapestry maps.

The small tapestries from the Burrell collection are somewhat surprising, as they exhibit a much larger range of dye sources, including several high quality dye sources, such as weld (*Reseda luteola* L.), dyer's greenweed (*Genista tinctoria* L.), madder (*Rubia tinctorum* L.), woad (*Isatis tinctoria* L.) or Mexican cochineal (*Dactylopius coccus* Costa), but also several low quality dye sources, such as young fustic (*Cotinus coggygria* Scop.) or lichen dyes, usually prohibited from the manufacture of historical tapestries because of their poor light fading qualities. This might indicate that although these tapestries would have been in their time very expensive pieces of work, they might not have been produced in the same workshop that produced the tapestry maps. Thus, dye analysis supports recent art historical research from Turner on a group of nine early English tapestries representing *Judith with the Head of Holofernes* (including Burrell tapestry 47.23), where it was suggested that these tapestries were of lower quality and corresponded more likely to the possessions of less wealthy members of society.<sup>19</sup> The range of dyes characterised on both *Susanna* series of Burrell collection is extremely consistent, and from dyestuff analysis alone it seems that they are related and were most likely to have been produced in the same workshop. Similarly to what was observed in the tapestry maps, weld was the predominant yellow dye source found in silk and wool yarns, with only a few green wool yarns exhibiting the presence of dyer's greenweed (*Genista tinctoria* L.). This differed from what was characterised on a study of important sixteenth century Brussels tapestries, where dyer's greenweed was found to be the predominant dye source found in silk yarns.<sup>31</sup>

The more noticeable find is certainly the presence of safflower dye (*Carthamus tinctorius* L.), which was characterised on all the small tapestries and would have been imported into Europe. The presence of safflower dye is extremely rare but not without precedent in Europe at that time,<sup>32</sup> although safflower is more often mentioned in seventeenth and eighteenth century dye recipes.<sup>34</sup> This would need more art historical research, especially on the Port Books to find information on the type of dyestuffs that London merchants were importing.<sup>51</sup> Other interesting

information could be found in the accounts records from the Great Wardrobe, that would have recorded any materials bought for tapestry repairs, although a recent research from Turner for the period 1559 – 1607 showed that it was often not recorded whether the yarns purchased were dyed or un-dyed (with exception to red colour) and reported that occasionally some yarns were described as being of *diversibus coloribus* (i.e. various colours) but without information on the type of dyestuffs used.<sup>16</sup> Finally, it would be particularly interesting to investigate contemporary English embroidered clothes,<sup>22</sup> known to exhibit similar pink hues, and to have in spite of these new results a closer examination of the tapestry maps from the Bodleian Library, to see whether safflower dye was more often used than what would be expected from the historical written sources.

### 3.5 REFERENCES

1. Guiffrey, J. (1886). *Histoire de la Tapisserie depuis le Moyen Age jusqu'à nos jours*. Alfred Mame & Fils, Tours.
2. Souchal, G. (1973). *Masterpieces of tapestry: From the Fourteenth to the Sixteenth Century (translation of: Chefs-d'oeuvre de la tapisserie du XIVE au XVIe siècle)*. The Metropolitan Museum of Art, Yale University Press.
3. Campbell, T. P. (2003). The Art and Magnificence of Renaissance Tapestries: Introduction. In *Tapestry in the Renaissance: Art and Magnificence*, Campbell, T. P., Ed. The Metropolitan Museum of Art, Yale University Press: New Haven and London: 3-12.
4. Coffinet, J. (1971). *Arachné ou l'art de la tapisserie*. Genève: Editions de la Coulouvreniere.
5. Demarcel, G. (1977). *Tapisseries, 1. Moyen Age et première Renaissance*. Musées Royaux d'art et d'histoire, Bruxelles.
6. Jarry, M. (1968). *La tapisserie des origines à nos jours*. Librairie Hachette Paris.
7. Kendrick, A. F. (1924). *Catalogue of Tapestries, Victoria and Albert Museum, Department of Textile*. Board of Education London.
8. Barnard, E. A. B., Wace, A. J. B. (1928 ). *The Sheldon tapestry weaver and their work*. Society of Antiquaries of London Oxford.
9. Wingfield - Digby, G. F. (1980). *The Victoria and Albert Museum - Catalogue of Tapestries Medieval and Renaissance*. HMSO, London.

10. Wells-Cole, A. (1990). The Elizabethan Sheldon tapestry maps. *Burlington Magazine*, **132**, 392-401.
11. Wells-Cole, A. (1997). Art and Decoration in Elizabethan Jacobean England 221 - 235.
12. Turner, H. L. (2002). Finding the Sheldon weavers: Richard Hyckes and the Barcheston tapestry works reconsidered. *Textile Hist.*, **33**, 137-161.
13. Turner, H. L. (2008). Tapestry sections depicting the Prodigal Son: how safe is an attribution to Mr Sheldon's tapestry venture at Barcheston? *Archaeologia Aeliana*, **XXXVII**, 183-96.
14. Turner, H. L. (2008). Tapestries once at Chastleton House and Their Influence on the Image of the Tapestries Called Sheldon: A Reassessment. *The Antiquaries Journal*, **88**, 313-346.
15. Turner, H. L. (2010). *No Mean Prospect: Ralph Sheldon's Tapestry Maps*. Plotwood Press.
16. Turner, H. L. (2012). Working Arras and Arras Workers: Conservation in the Great Wardrobe under Elizabeth I. *Textile Hist.*, **43**, 43-60.
17. Turner, H. L. (2002). "A wittie devise": the Sheldon tapestry maps belonging to the Bodleian Library, Oxford. *Bodleian Library Record*, **17**, 293-313.
18. Turner, H. L. (2003). The Sheldon tapestry maps: Their content and context. *Cartogr. J.*, **40**, 39-49.
19. Turner, H. L. (2010). Some Small Tapestries of Judith with the Head of Holofernes: Should They Be Called Sheldon? *Text. Hist.*, **41**, 161-181.
20. Marks, R. (1983). *The Burrell Collection*. Harper Collins Publishers, Glasgow City Council (Museums).
21. (1979 ). *Late Gothic Art from the Burrell Collection. A selection of Tapestries and Sculpture* The Scottish Art Council.
22. Arthur, L. (1995). *Embroidery 1600 - 1700 at the Burrell Collection*. Glasgow Museums.
23. Collins, P., personal communication reporting on Burrell Purchase Books. In 2010.
24. Turner, H. L. *Annotated List of 'Sheldon' tapestries now known with bibliography*. (<http://www.tapestriescalledsheldon.info/index.html> - accessed February 2013).
25. Wouters, J., Verhecken, A. (1985). High-performance liquid chromatography of anthraquinones: Analysis of plant and insect extracts and dyed textiles. *Studies in Cons.*, **30**, 119-128.
26. Schweppe, H. (1993). *Handbuch der Naturalfarbstoffe*. Nikol Verlagsgesellschaft, Hamburg.
27. Wouters, J., Grzywacz, C. M., Claro, A. (2011). A Comparative Investigation of Hydrolysis Methods to Analyze Natural Organic Dyes by HPLC-PDA: Nine Methods, Twelve Biological Sources, Ten Dye Classes, Dyed Yarns, Pigments and Paints. *Studies in Cons.*, **56**, 231-249.
28. Ferreira, E. S. B., Quye, A., MacNab, H., Hulme, A. N. (2002). Photo-oxidation of Quercetin and Morin as Markers for the characterisation of natural flavonoid yellow dyes in Ancient textile. *Dyes Hist. Archaeol.*, **18**, 63-72.

29. Zhang, X., Laursen, R. A. (2005). Development of mild extraction methods for the analysis of natural dyes in textiles of historical interest using LC-Diode Array Detector-MS. *Anal. Chem.*, **77**, 2022-2025.
30. Ferreira, E. S. B. (2002). *New Approaches Towards the Identification of Yellow Dyes in Ancient Textiles*. The University of Edinburgh, PhD Thesis.
31. Peggie, D. A. (2006). *The Development and Application of Analytical Methods for the Identification of Dyes on Historical Textiles*. The University of Edinburgh, PhD Thesis.
32. Degano, I., Łucejko, J. J., Colombini, M. P. (2011). The unprecedented identification of Safflower dyestuff in a 16th century tapestry through the application of a new reliable diagnostic procedure. *J. Cult. Herit.*, **12**, 295-299.
33. Tournaire, C., Croux, S., Maurette, M-T., Beck, I., Hocquaux, M., Braun, A. (1993). Antioxidant activity of flavonoids: efficiency of singlet oxygen quenching. *J Photoch Photobio B*, **19**, 195-215.
34. Cardon, D. (2003). *Le monde des teintures naturelles*. Belin, Paris.
35. Valianou, L., Stathopoulou, K., Karapanagiotis, I., Magiatis, P., Pavlidou, E., Skaltsounis, A. L., Chrysoulakis, Y. (2009). Phytochemical analysis of young fustic (*Cotinus coggygia*; heartwood) and identification of isolated colourants in historical textiles. *Anal. Bioanal. Chem.*, **394**, 871-882.
36. Hofenk de Graaf, J. H. (2005). *The Colourful Past*. Archetype Publications.
37. van Bommel, M., Joosten, I. (2009). What Colours Tell You: the Identification of Dyes in Historical Objects. In *Silk, Gold and Crimson: Secrets and Technology at the Visconti and Sforza Courts*, Buss, C., Ed. Silvana Editoriale: 167-174.
38. Burnett, R. A., Thomson, R. H. (1968). Natural Occurring Quinones. Part XV. Biogenesis of the Anthraquinones in *Rubia tinctorum* L. (Madder). *J. Chem. Soc.*, 2437-2441.
39. Sanyova, J. (1998). Étude des pigments organiques préparés à partir des racines rubiacées européennes. In *Art et Chimie la couleur: actes du Congrès*, Goupy, J., Mohen, J. P., Ed. CNRS: 14-17.
40. Sanyova, J. (2001). *Contribution à l'étude de la structure et des propriétés des laques de garance*. Université Libre de Bruxelles, PhD Thesis.
41. Sanyova, J., Reisse, J. (2006). Development of a mild method for the extraction of anthraquinones from their aluminum complexes in madder lakes prior to HPLC analysis. *J. Cult. Herit.*, **7**, 229-235.
42. Quye, A. (1996). Dyes analysis of the Fetternear Banner (C&AR 9248), AR Report 96/27. *NMS, unpublished data*.
43. Wouters, J., Verhecken, A. (1989). The scale insect dyes (*Homoptera: Coccoidea*). Species recognition by HPLC diode array analysis of the dyestuffs. *Annl. Soc. ent. Fr. (N.S.)*, **25**, 393 - 410.
44. Serrano, A., Sousa, M., Hallett, J., Lopes, J., Oliveira, M. (2011). Analysis of natural red dyes (cochineal) in textiles of historical importance using HPLC and multivariate data analysis. *Anal. Bioanal. Chem.*, **401**, 735-743.

45. Peggie, D. A., Hulme, A. N., McNab, H., Quye, A. (2008). Towards the identification of characteristic minor components from textiles dyed with weld (*Reseda luteola* L.) and those dyed with Mexican cochineal (*Dactylopius coccus* Costa). *Microchim. Acta*, **162**, 371-380.
46. Phipps, E., Shibayama, N. (2010). Tracing Cochineal Through the Collection of the Metropolitan Museum. *TSA Symposium, Paper 44*.
47. Wouters, J., Verheeken, A. (1989). The Coccid Insect Dyes: HPLC and Computerized Diode-Array Analysis of Dyed Yarns. *Studies in Cons.*, **34**, 189-200.
48. Lee, R. L. (1951). American Cochineal in European Commerce, 1526-1625. *J. Mod.Hist.* , **23**, 205-224.
49. Kirby, J., Spring, M., Higgitt, C. (2005). The technology of eighteenth and nineteenth-century red lake pigments. *National Gallery Technical Bulletin*, **28**, 69-95.
50. Wouters, J., Grzywacz, C. M., Claro, A. (2010). Markers for Identification of Faded Safflower (*Carthamus tinctorius* L.) Colorants by HPLC-PDA-MS: Ancient fibres, pigments, paints and cosmetics derived from Antique recipes. *Studies in Cons.*, **55**, 186-203.
51. Turner, H. L. (2013). The Tapestry Trade in Elizabethan London: Products, Purchasers, and Purveyors. *London Journal*, **38**, 18-33.

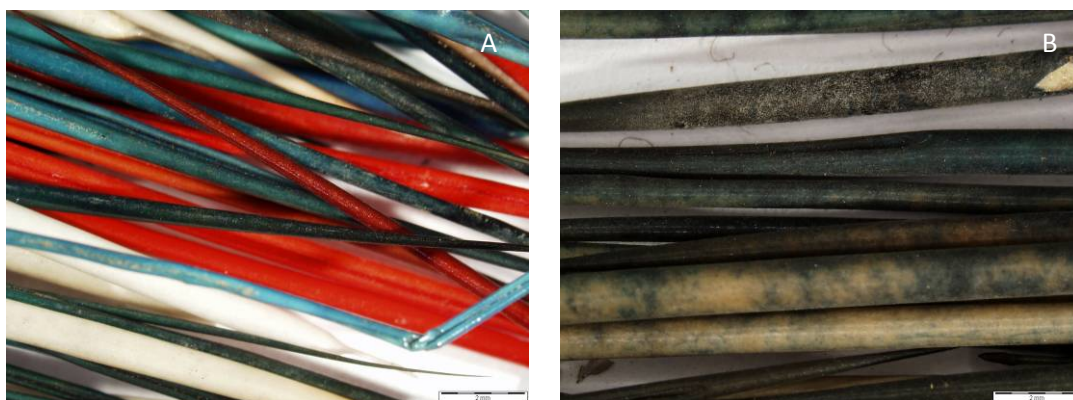
# CHAPTER 4



<b>4</b>	<b>CHARACTERISATION OF METALLIC MORDANTS ON PORCUPINE QUILL</b>	
	<b>WORK: METHOD DEVELOPMENT .....</b>	<b>156</b>
4.1	PORCUPINE QUILL SUBSTRATE .....	157
4.1.1	<i>Sorption of metal ions on keratin fibres</i> .....	157
4.1.2	<i>SEM observation of Porcupine quill</i> .....	158
4.2	ICP-OES STUDY .....	160
4.2.1	<i>ICP-OES principles</i> .....	160
4.2.2	<i>Investigation of porcupine quill references</i> .....	161
4.2.2.1	Mordanting condition .....	161
4.2.2.2	Influence of dyebath time on metal ion uptake .....	161
4.2.2.3	Quantification of copper(II) and tin(II) uptake .....	167
4.2.3	<i>Summary</i> .....	172
4.3	ION BEAM ANALYSIS .....	172
4.3.1	<i>Ion Beam Analysis principles</i> .....	172
4.3.2	<i>PIXE analysis of trace elements in porcupine quills</i> .....	174
4.3.2.1	Interaction of 3 MeV proton beam with keratin .....	174
4.3.2.2	Target description .....	177
4.3.2.3	Absorption factors and transmission of Cu(K) and Sn(L <sub>A</sub> ) X-rays in keratin .....	178
4.3.2.4	Parameter files and calibration .....	181
4.3.2.5	Quantification of copper and tin by PIXE analysis .....	185
4.3.2.6	Summary .....	188
4.3.3	<i>Rutherford Backscattering Spectrometry (RBS)</i> .....	189
4.3.3.1	RBS Principles .....	189
4.3.3.2	SIMNRA simulation: calculation of depth profile .....	191
4.3.3.3	Quantification of copper and tin by RBS analysis .....	193
4.4	DISCUSSION .....	196
4.5	REFERENCES .....	197

## 4 CHARACTERISATION OF METALLIC MORDANTS ON PORCUPINE QUILL WORK: METHOD DEVELOPMENT

This chapter presents a method development for the characterisation of metallic mordants on aboriginal dyed porcupine quills. Indigenous communities across North America from the North American Subarctic, Great Lakes region and the Northern Plains, have long used dyed porcupine quills to decorate clothing and basketry. Unfortunately, much more is known about the technique of porcupine quill work<sup>1-3</sup> than the actual dyeing process and dye sources used. As part of this research, a unique set of dyed raw quill samples and objects collected in 1862 from Sub-Arctic Athakaspan Dene people was investigated.<sup>4, 5</sup> Microscopic observation of the specimens showed some very bright lightfast colours of red, orange, yellow, green and blue, while others especially blue quills exhibit very faded colours, suggesting different dyeing processes and the use of different metallic mordants (figures 4.1-A and B).



**Figures 4.1:** Optical Microscopic observations of some of the specimens collected in 1862, (A) A.1862.15 Box 2 and (B) A.1862.15 Box 9a, both at magnification x 7

Preliminary investigation of the quill materials at National Museums Scotland using non-invasive X-Ray Fluorescence analysis (XRF) identified traces of copper and tin on several quills, but offered limited application, as the system cannot detect elements below 0.1% abundance and does not have a micro-focus to allow the

investigation of very small samples. Indeed, due to the very low concentration of mordant usually found in historical textiles, Inductively Coupled Plasma (ICP) coupled to Optical Emission Spectrometry (OES) or Mass Spectrometry (MS) is usually used, allowing a limit of detection as low as parts per million (ppm) or parts per billion (ppb).<sup>6,7</sup> In many cases however, the interpretation of the results from the analysis of historical sample extracts remains problematic, due to the observation of large amounts of contaminants such as aluminium or iron.<sup>6, 8</sup> Furthermore, this requires multiple sampling of the same object in order to perform both dye analysis and mordant investigation, which in the case of the porcupine quill work collection was not possible.

In this chapter we explore the possibility of using a non-invasive approach for the study of metal ion mordants by Ion Beam Analysis. The method was developed based on the study of porcupine quills standards prepared in house with a range of concentration of copper(II) and tin(II) ions. These “standards” were investigated using ICP-OES, non-invasive Particle Induced X-Ray Emission analysis (micro-PIXE) and Rutherford Backscattering Spectrometry (RBS). The results obtained with the different techniques will be compared and discussed.

## 4.1 PORCUPINE QUILL SUBSTRATE

### 4.1.1 Sorption of metal ions on keratin fibres

Keratin fibres, especially hair, wool and chicken feathers, have long been studied for their capacity to adsorb metal ions.<sup>9-12</sup> This may be applied to water purification or to the accumulation of precious metals (gold, platinum) from aqueous solution.<sup>10, 11</sup> The interaction of keratin with metal ions is very complex and has been the subject of several studies, which show that the uptake of metal ions depends on many variables including the type of fibre, the metal ion, and the experimental conditions (concentration of metal ions, temperature, time).<sup>9, 10, 12-14</sup> The model usually used to describe the adsorption of metal ions on keratin in solution is the d’Arcy - Watt

model, that contains three components representing two types of primary adsorption processes (Langmuir-type and Henry-type adsorption) and a third one, describing multilayer formation of water molecules.<sup>14</sup> The Langmuir's isotherm is valid for monolayer adsorption on a homogeneous surface with equally available adsorption sites and without interactions (equation 4.1).

$$\frac{C_e}{q_e} = \frac{1}{q_{max}} \times C_e + \frac{1}{K_L \times q_{max}} \quad \text{Equation 4.1}$$

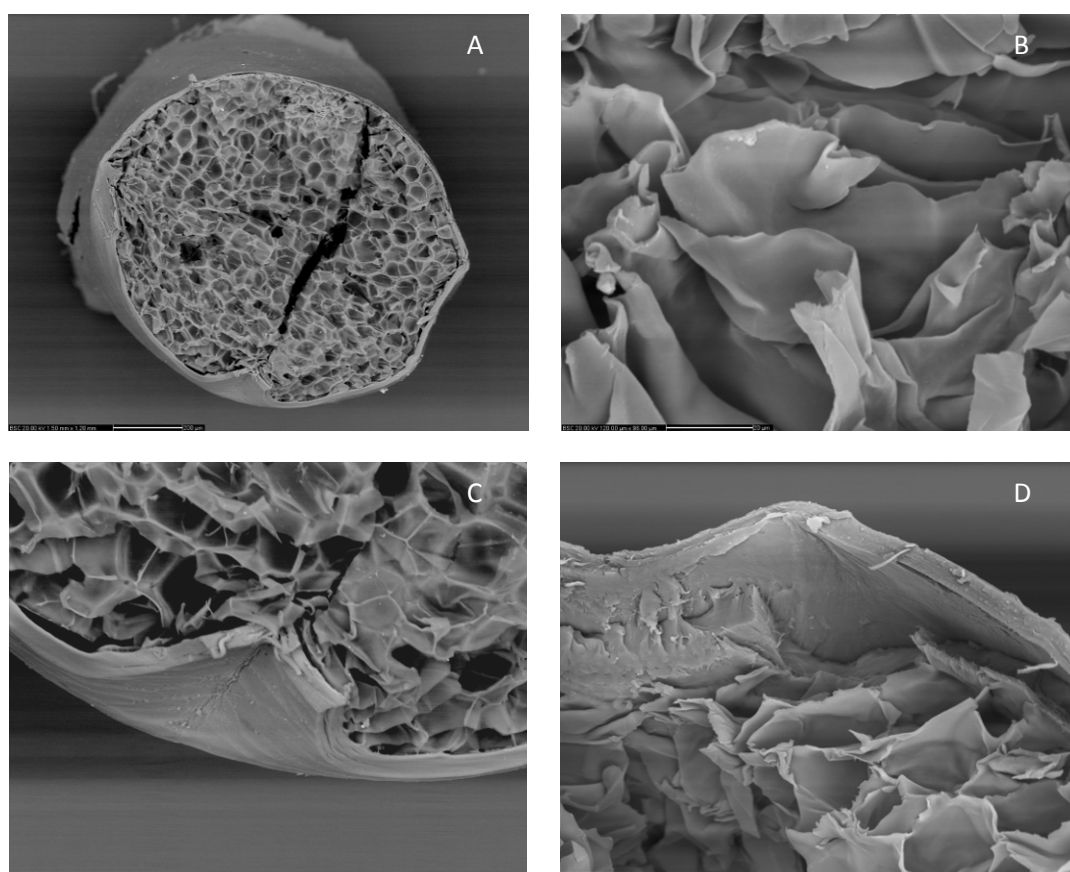
In this equation  $C_e$  ( $\text{mg L}^{-1}$ ) is the equilibrium concentration of the metal ions in solution and  $q_e$  ( $\text{mg g}^{-1}$ ) is the adsorption capacity at equilibrium. The constant  $q_{max}$  ( $\text{mg g}^{-1}$ ) is the maximum adsorption capacity and relates to the binding energy of the metal ions, while the constant  $K_L$  ( $\text{L mg}^{-1}$ ) is the effective dissociation constant for the metal ions studied. A plot of  $C_e/q_e$  against  $C_e$  should be a straight line, where  $K_L$  corresponds to the (gradient)<sup>-1</sup> and  $q_{max}$  to  $(K_L \times \text{intercept})^{-1}$ .<sup>9, 12</sup>

The exact binding site of the metal ions on the keratin is not well known, especially the involvement of nitrogen sites, but studies using Electron Spin Resonance (ESR) showed a carboxylate binding mechanism for chromium(II-VI) and copper(II), and a possible N-donor site interaction for copper(II).<sup>15, 16</sup>

#### 4.1.2 SEM observation of Porcupine quill

The quills used by Native American peoples are from *Erethizon* species. These quills consist of a “soft” medulla and a “hard” cortex and a cuticle, with the cuticle forming a strong cylindrical outer shell (figures 4.2-A-D).<sup>17</sup> Porcupine quills are predominantly made of hard  $\alpha$ -keratin proteins, although lipids and carbohydrates are also present in significant quantities (chapter 1).<sup>18-21</sup> These quills can be variable in size but typically range between 1.5 mm and 2.5 mm in diameter. Cuticle measurements were undertaken using a Scanning Electron Microscope working with a Backscattered Electron Detector in controlled pressure mode (SEM-BSC).

Measurements were taken on the section of several porcupine quills in order to assess homogeneity within the same quill and also possible variation between quills. From these observations, the cuticle thickness is 58  $\mu\text{m}$  on average, ranging from 35  $\mu\text{m}$  to 100  $\mu\text{m}$  for the larger quills. There is however a fairly low variation within the same quill cross-section ( $< 5 \mu\text{m}$ ), see table 4.1.



**Figures 4.2:** Backscattered Electron Micrographs (SEM-BSC): (A) cross-section of a porcupine quill, scale bar is 200  $\mu\text{m}$ ; (B) detail of cortex, scale bar is 20  $\mu\text{m}$ ; (C) detail of cuticle, scale bar is 50  $\mu\text{m}$ ; (D) detail of cuticle and cortex, scale bar is 20  $\mu\text{m}$ .

	Quill 1	Quill 2	Quill 3	Quill 4	Quill 5	Quill 6	Quill 7
Cuticle ( $\mu\text{m}$ )	$65.1 \pm 5.0$	$43.0 \pm 3.4$	$64.1 \pm 3.4$	$50.2 \pm 3.5$	$100.9 \pm 4.2$	$50.3 \pm 4.9$	$35.6 \pm 2.4$

**Table 4.1:** SEM measurements of *Erethizon* porcupine quill cuticles. [Data compiled from Chapter 7, section 7.3.1, table 7.20].

## 4.2 ICP-OES STUDY

### 4.2.1 ICP-OES principles

Inductively Coupled Plasma (ICP) coupled to Optical Emission Spectrometry (OES) is an atomic spectroscopy technique that allows the concentration of metals to be determined at concentrations as low as ~10 parts per trillion, and up to 1000 parts per million.<sup>22, 23</sup> Atomic spectroscopy techniques include flame atomic absorption spectroscopy (FAAS), atomic or optical emission spectroscopy (AES or ICP-OES) and atomic fluorescence spectroscopy (AFS). FAAS is based on the analysis of the absorption of optical radiation by the atoms constituting the sample, while AES or OES are based on the measurement of the intensity of the light emitted by the atoms constituting the sample, and AFS is based on the analysis of the fluorescence of the atoms constituting the sample.

$$N_i = \frac{N_0 g_i}{g_0} \exp\left(\frac{-E_i}{kT}\right) \quad \text{Equation 4.2}$$

ICP-OES analysis is based on the Boltzman Distribution Law (equation 4.2) that states that in a system in thermodynamic equilibrium, the number of atoms  $N_i$  in the excited state, is proportional the number of atoms in the ground state ( $N_0$ ), with an energy  $E_0 = 0$ , and  $g_i$  and  $g_0$  are the statistical weights of the  $j$ th and ground states, respectively and  $k$  is a constant.<sup>23</sup> This means that the intensity of atomic emission is critically dependent on temperature and that the plot of emission intensity against sample concentration should be a straight line. Optical emission spectrometers (OES) contain a device responsible for bringing the sample to a high enough temperature; the optics including a mono- or polychromater and a microcomputer that controls the instrument. The inductively coupled plasma (ICP) torch consists of a quartz tube (15 to 30 mm diameter) through which an inert gas, usually argon, flows.

For these experiments the system was calibrated using two standard solutions, one of copper and the other one tin, both at  $1000 \mu\text{g mL}^{-1}$ . The calibration curves were obtained by preparing a range of concentrations with calibrated micro-pipettes, allowing the analysis of concentration ranging between 200 and  $0.02 \mu\text{g mL}^{-1}$  (see section 7.3.3.1). Two wavelengths were selected: 327.393 nm for the analysis of copper(II) and 283.994 nm for the analysis of tin(II).

## 4.2.2 Investigation of porcupine quill references

### 4.2.2.1 Mordanting condition

The cleaning and dyeing processes of porcupine quills are discussed in more details in chapter 5. For this experiment, a set of standards of porcupine quills were prepared by dyeing several quills (200 mg) in a 50 mL dyebath containing cochineal dye (2.00 g) and variable amounts of copper(II) sulphate and tin(II) chloride, in order to obtain the following concentrations: 100; 500; 1000; 2500; 5000; 10,000 and  $15,000 \mu\text{g mL}^{-1}$  [for dyebaths details see Chapter 7, section 7.3.2 and table 7.21].

### 4.2.2.2 Influence of dyebath time on metal ion uptake

Of tin(II) and copper(II), the sorption of copper onto keratin fibres is probably the most studied. It has been observed that the uptake of metal ions on keratin fibres depends on the treatment time and temperature, with longer heating times and higher temperatures showing a great increase in the total uptake of the fibres.<sup>10, 13</sup> From these results, the maximum uptake of copper on wool and human hair is generally observed after one hour in the metal ion solution, while optimal uptake was observed by working below  $85 \text{ }^\circ\text{C}$ .<sup>9, 13</sup> The uptake of metal ions was found to be proportional to their concentration in the dyebath but to be variable between ions, with copper(II) exhibiting the higher total sorption compared to other metal ions such as manganese(II), zinc(II) and arsenic(III). At an equilibrium concentration of  $0.3 \mu\text{g}$

$\text{mL}^{-1}$  the sorption of copper(II) on human hair was found to be  $0.035 \mu\text{g mg}^{-1}$  of dry fibre at  $25 \text{ }^\circ\text{C}$ , three fold greater than the sorption of zinc(II) and thirty time fold greater than the sorption of manganese(II).<sup>9</sup>

In order to relate these observations to porcupine quills, several quills (200 mg) were heated at  $85 \text{ }^\circ\text{C}$  in a cochineal dye bath containing copper(II) or tin(II) at  $1000 \mu\text{g mL}^{-1}$  for several hours. Quills were collected, as well as dye bath fractions, after one hour, two hours and five hours and subjected to ICP-OES analysis. The quantities of copper(II) or tin(II) consumed from the dye bath and sorbed onto the porcupine quills are presented in the figures 4.4 and 4.5.

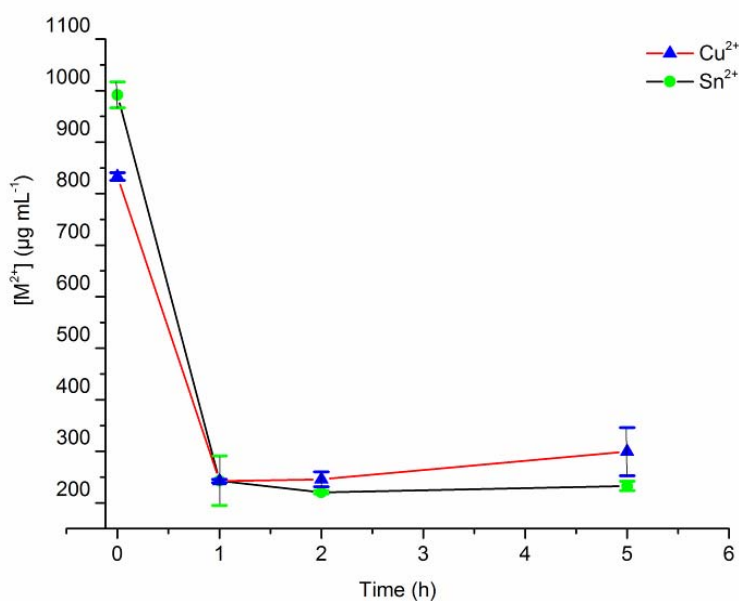


**Figure 4.4:** Plot showing the concentration of copper(II) and tin(II) ( $\mu\text{g mL}^{-1}$ ) in the dye bath, after heating at  $85 \text{ }^\circ\text{C}$  for 1h, 2h and 5 h, determined by ICP-OES. Mean values and standard deviation obtained from triplicate measurements. [Data compiled from Chapter 7, section 7.3.3, tables 7.24 and 7.25].



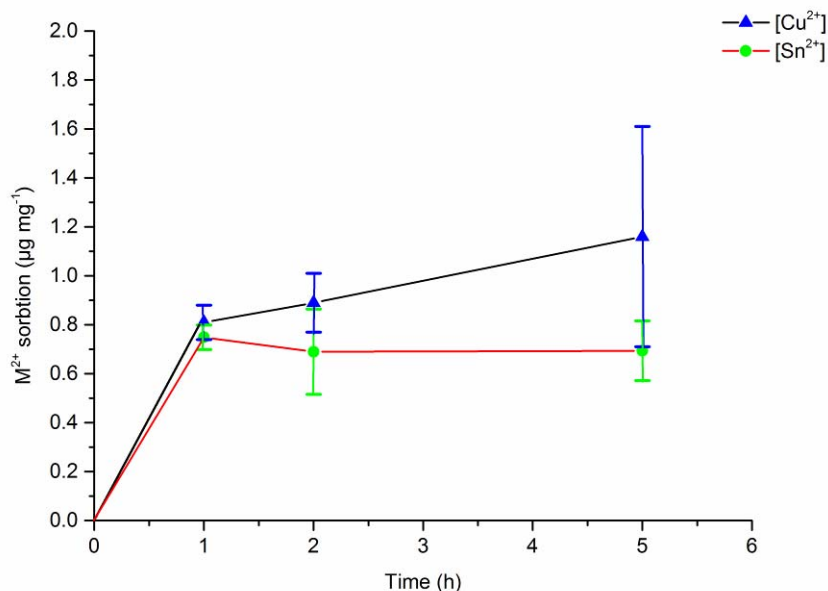


**Figure 4.5:** Plot showing the quantity of copper(II) and tin(II) sorbed onto the porcupine quill substrate ( $\mu\text{g mg}^{-1}$ ) after heating the dye bath at  $85\text{ }^{\circ}\text{C}$  for 1 h, 2 h and 5 h determined by ICP-OES. Mean values and standard deviation obtained from triplicate measurements. [Data compiled from Chapter 7, section 7.3.3, tables 7.26 and 7.27].

For both dye baths ICP-OES analysis showed that the concentration of free copper(II) and tin(II) metal ions fall very rapidly during the first hour of the experiment, with the amount of copper decreasing from  $833\ \mu\text{g mL}^{-1}$  to  $242\ \mu\text{g mL}^{-1}$ , while the concentration of tin(II) was found to decrease from  $992\ \mu\text{g mL}^{-1}$  to  $243\ \mu\text{g mL}^{-1}$ . After this the metal ion content of both dye baths plateaus with only minor variation of the copper(II) and tin(II) content observed (figure 4.6). The most likely explanation of this rapid change in concentration is the formation of an insoluble lake with the carminic acid. It is however surprising that ICP-OES only detected the quantity of free metal ion present in the dye bath, but this could be explained by the

fact that the insoluble lake would have been discarded during filtration of the extract prior ICP-OES analysis.

Carminic acid is a bi-dentate ligand which coordinates with the metal ions with the carboxyl and the hydroxy group *ortho* to this in positions 2 and 3 (figure 4.7).<sup>24</sup> Five deprotonation sites are known as follow: the first deprotonation occurs with the carboxylic group in position 2 at a  $pK_{a1}$  value of 3.39, followed by the hydroxy group in position 5 with a  $pK_{a2}$  of 5.78, and then the hydroxy group in position 6 with a  $pK_{a3}$  of 8.35. The last two dissociations correspond to the hydroxyl groups in position 8 with a  $pK_{a4}$  value of 10.27 and in position 3 will dissociate last and showed a  $pK_{a5}$  value of 11.51.<sup>24</sup>

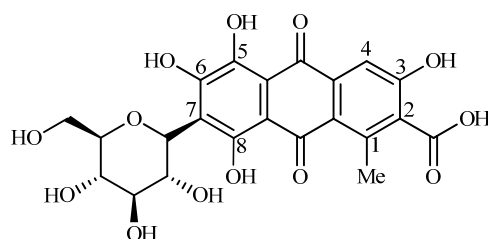


**Figure 4.6:** Carminic acid with its five deprotonation sites: carboxyl group in position 2 and hydroxyl groups in positions 3, 5, 6 and 8.<sup>24</sup>

The dyebaths were not buffered but the measurement of the pH at the start of the experiment showed pH values of 2.60 and 4.41; meaning that carminic acid was in its first deprotonated form and able to bind to the metal ions to form either a dye-metal-fibre complex<sup>25</sup> or a dye-metal-dye complex (figure 4.7-A and B), but three dimensional structure involving several metal ions and dye molecules could also form, as observed by Soubayrol and co-workers in their study of alizarin lake with aluminium(III).<sup>26</sup> Furthermore, in the case of tin(II), there is a distinct possibility that some reaction could occur between the catechol unit of carminic acid and tin(II) leading to the formation of a tin(IV)-catechol ligand, as was observed in early studies

from Wakley and Varga, Budesinsky and later Hernández-Méndez and co-workers (figure 4.8-A-B).<sup>27-29</sup>

The stability of the some carminic acid complexes has been studied and were found to be as follow: copper(II) > zinc(II) > nickel(II) > cobalt(II) > mercury(II).<sup>24</sup> Although we do not have similar information for tin(II) or tin(IV), we can note that after one hour 29.1 % of copper and 24.5 % of tin remain free in solution. This would suggest that both copper(II) and tin(II)/tin(IV) strongly complex with carminic acid and exhibit a similar stability (table 4.2).

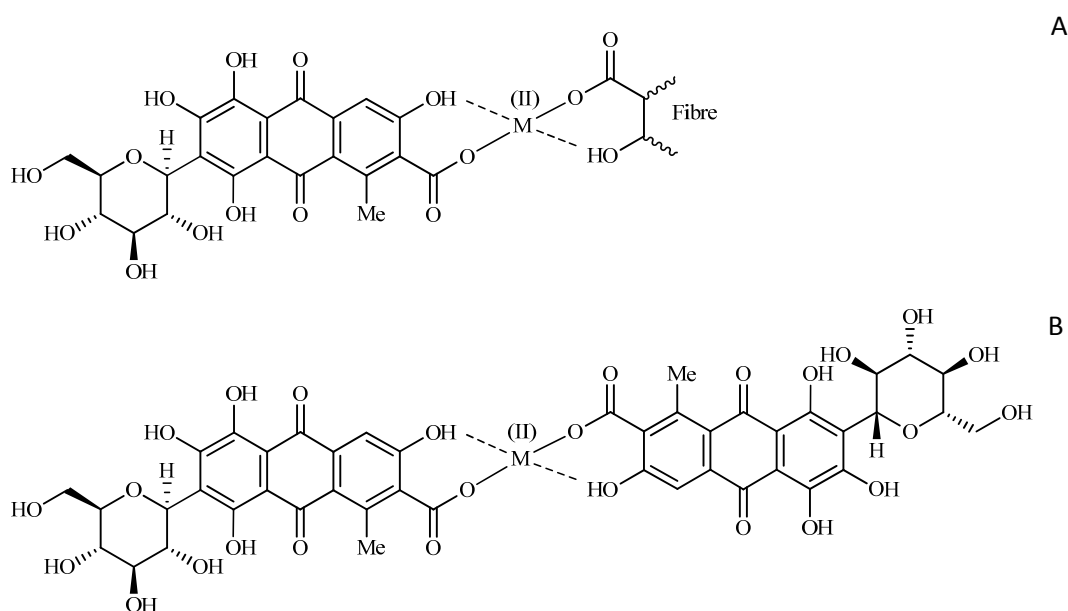


**Figure 4.7:** Possible structure of the dye-metal-fibre (A); dye-metal-dye (B) complexes formed during the dyebath experiments.

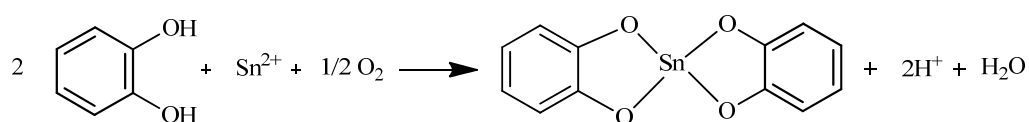


**Figure 4.8:** Reaction between catechol unit and tin(II) under oxidative condition, as reported in early study from Hernández-Méndez and co-workers.<sup>29</sup>

pH	carminic acid (mol)	Cu <sup>2+</sup> t = 0 (mol)	Cu <sup>2+</sup> t = 1h (mol)	% free Cu <sup>2+</sup> t= 1h
4.41	$4.062 \times 10^{-3}$	$6.549 \times 10^{-4}$	$1.903 \times 10^{-4}$	29.1 %
pH	carminic acid (mol)	Sn <sup>2+</sup> t = 0 (mol)	Sn <sup>2+</sup> t = 1h (mol)	% free Sn <sup>2+</sup> t= 1h
2.60	$4.062 \times 10^{-3}$	$4.196 \times 10^{-4}$	$1.028 \times 10^{-4}$	24.5 %

**Table 4.2:** Mol of free metal ion [copper(II) or tin(II)] present in the dyebath containing 2 g cochineal (equivalent to 2 g carminic acid) and 200 mg porcupine quills after one hour at 85 °C, Values were obtained by ICP-OES analysis from triplicate measurements. [Data compiled from Chapter 7, section 7.3.3, tables 7.26 and 7.27].

These results are disappointing with regard to the sorption of copper(II) and tin(II) onto porcupine quills, as only a minor amount of metal ions has been able to interact with the substrate (table 4.3). After one hour in the dyebath ICP-OES analysis showed quite similar amounts of metal ions were adsorbed by the porcupine quills. The sorption averaged 0.81 µg of copper(II) per mg of substrate and 0.75 µg of tin(II) per mg of substrate, which corresponds to an average of 0.3 - 0.4 % of the total of metal ions introduced (or 1.2 - 1.3 % of the free metal ions after one hour in the dyebath). After one hour, we observe a stabilisation of the uptake of tin(II), while the uptake of copper(II) slightly increases to reach 1.16 µg of copper per mg of substrate after five hours.<sup>9, 13</sup> These observations correspond well to what has been reported in other studies, where the uptake of metal ions on wool or hair usually showed a plateau after one hour in the metal ion solution. The slight increase in the sorption of copper has been reported to happen after heating wool for an extended period at 85 °C and is attributed to keratin hydrolysis and subsequent *in situ* precipitation of CuS.<sup>13</sup>

It is not possible to directly relate these sorptions to other studies, because the behaviour of porcupine quills is unknown, but these values seem much smaller. Similar experiments working at a concentration of copper of 1200 µg mL<sup>-1</sup> found an

uptake of 9.4  $\mu\text{g}$  of copper(II) per mg of wool, or 39 % of the quantity of copper introduced after one hour in the dyebath at 85°C.<sup>13</sup> The low uptake of metal ions by the quills might be related to the difference in thicknesses of the cuticles of the two substrates, which was found to average 58  $\mu\text{m}$  for porcupine quills compared to a reported value of 1 to 4  $\mu\text{m}$  for wool,<sup>30</sup> and must greatly affect exchange with the dyebath.

Dyebath at t = 0 h		Quills at t = 1 h		Sorption %
[Cu <sup>2+</sup> ] ( $\mu\text{g mL}^{-1}$ )	Cu <sup>2+</sup> ( $\mu\text{g}$ )	[Cu <sup>2+</sup> ] ( $\mu\text{g mg}^{-1}$ )	Cu <sup>2+</sup> ( $\mu\text{g}$ )	Cu <sup>2+</sup>
833 $\pm$ 8	(4.2 $\pm$ 1.2) $\times 10^4$	0.81 $\pm$ 0.07	162 $\pm$ 14	0.39
[Sn <sup>2+</sup> ] ( $\mu\text{g mL}^{-1}$ )	Sn <sup>2+</sup> ( $\mu\text{g}$ )	[Sn <sup>2+</sup> ] ( $\mu\text{g mg}^{-1}$ )	Sn <sup>2+</sup> ( $\mu\text{g}$ )	Sn <sup>2+</sup>
992 $\pm$ 25	(5.0 $\pm$ 1.2) $\times 10^4$	0.75 $\pm$ 0.05	148 $\pm$ 10	0.30

**Table 4.3:** Mass ( $\mu\text{g}$ ) of metal ion [copper(II) or tin(II)] at t = 0h and sorbed at t = 1 h onto 200 mg of porcupine quills, in 50 mL dyebath containing 2.00 g cochineal at 85 °C. Mean values obtained by ICP-OES from triplicate measurements. [Data compiled from Chapter 7, section 7.3.3, tables 7.26 and 7.27].

#### 4.2.2.3 Quantification of copper(II) and tin(II) uptake

In order to understand better the uptake of metal ions on porcupine quills, several dyeing experiments were conducted using the same dyebath conditions, but with increased concentrations of copper(II) and tin(II). The quills were removed after one hour and observed under Scanning Electron Microscopy (SEM-BSC) and investigated by ICP-OES. These microscopic observations showed that the porcupine quills are less affected than wool by high concentrations of mordants, and changes were observed such as a shrinking of the cuticle scales from a tin(II) concentration of 5000  $\mu\text{g mL}^{-1}$  (figures 4.9-A and B). Above this concentration, the structure of the quills started to collapse and the quills were very brittle. In comparison, Scanning Electron Microscopic observation of wool fibres dyed with a

tin(II) concentration of  $2500 \mu\text{g mL}^{-1}$  showed extensive damage, with shrinking of the structure and significant lifting of the scales (figures 4.9-C and D). These observations correspond well to what is reported for the tin-weighting of silk, where silk loaded with excess of tin(IV) chloride was found to be more brittle and yellowish brown in color, with the fibers burst open.<sup>31</sup>

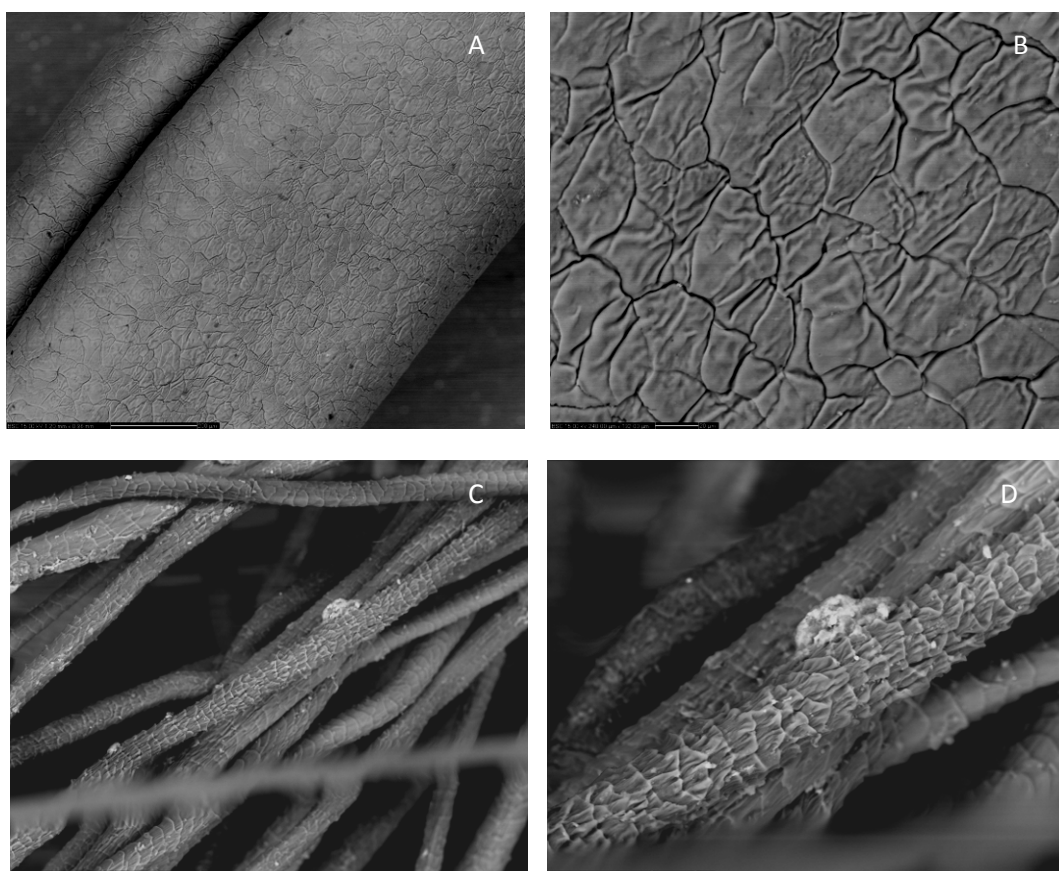


**Figure 4.9:** Scanning Electron Micrographs (SEM-BSC), (A) porcupine quills after treatment in a dyebath containing  $5000 \mu\text{g mL}^{-1}$  of tin(II), scale bar is  $200 \mu\text{m}$ ; (B) detail showing shrinking of the scales, scale bar is  $20 \mu\text{m}$ ; (C) wool fibre after treatment in a dyebath containing  $2500 \mu\text{g mL}^{-1}$  of tin(II) showing extensive damages of the fibres, scale bar is  $100 \mu\text{m}$ ; (D) detail of a wool fibre, scale bar is  $20 \mu\text{m}$ . [for SEM observation of un-scoured porcupine quill, see section 7.4.2].

For each dyebath of copper(II) and tin(II), three porcupine quill samples were investigated by ICP-OES analysis. Previous studies on hair behaviour showed that, depending on the experimental conditions, there is not necessarily an equilibrium between the concentration in solution and the uptake in metal ions onto the fibre.<sup>9</sup> As a result, it is difficult to make any predictions on the behaviour of porcupine quills during the dyebath experiments, although from previous observations (section 4.1.3.2) it appears that after one hour, an equilibrium is reached between carminic acid, metal ions and the porcupine quill substrate. For this reason, it was not possible to produce a Langmuir isotherm, especially as no measurement of the equilibrium concentration was systematically recorded. One possible representation of the sorption of copper(II) and tin(II) on porcupine quills would then be a plot linear/linear, where the sorbed quantity of metals ions in  $\mu\text{g mg}^{-1}$  of fibre is expressed as a function of the dyebath concentration at  $t = 0$  h. Figures 4.10 and 4.11 show that ICP-OES measurements provided a reasonable linear correlation between the concentration of metal ions in the dyebath and the uptake on porcupine quills expressed in  $\mu\text{g}$  per  $\text{mg}$  of substrate, although the series of tin standards exhibited less homogeneity than copper. The uptake of copper(II) and tin(II) at  $1000 \mu\text{g mL}^{-1}$  were slightly different from what was observed in the previous experiment (section 4.1.3.2). This could possibly be due to some heterogeneity between porcupine quills. The total uptake of copper ranged between 0.2 and 0.4 % for the different dyebaths, while the uptake of tin was systematically higher and ranged between 0.5 and 4.4 % (table 4.4).

These differences could be explained by different affinity of the metal ions with the porcupine substrate, with tin(II) exhibiting a higher affinity than copper(II). Different affinity of metals ions for human hair have been reported, where copper(II) exhibited a much higher sorption than manganese(II), zinc(II) or arsenic(III).<sup>9</sup> In this published study, the differences in sorption were explained by the fact that copper(II) had the greatest ligand field stabilisation value and the smaller radius size compared to manganese(II) and zinc(II).<sup>9</sup> Furthermore, the greater sorption of copper(II) was

also explained by its greater binding capacity to the sulfur of keratin and the stability of the copper - sulfur interaction.<sup>9</sup> Similar high affinity of copper was also observed in a study focused on madder dyeing process, where copper(II) was found to present a higher affinity with wool fibres than iron(II) and aluminium(III).<sup>32</sup> Although we do not have similar study for tin(II), the use of tin is reported for weighting silk and a study on cumulative tin-weighting of silk using tin(IV) chloride showed that the weight of the silk increased directly with the number of times the process was repeated. This study also showed that the uptake of tin on wool was much higher than on any other substrates, showing a very strong affinity of tin(IV) for keratin based fibres.<sup>31</sup> It is therefore likely, despite the different oxidation state, that tin(II) would also have a high affinity for porcupine quills substrates, especially as under the dyebath conditions, tin(II) could easily be oxidised in tin(IV) (see section 4.2.2.1).

Dyebath t = 0 h	Quills at t = 1 h	Sorption %	Dyebath t = 0 h	Quills at t = 1 h	Sorption %
Cu <sup>2+</sup> (µg)	Cu <sup>2+</sup> (µg)	Cu <sup>2+</sup>	Sn <sup>2+</sup> (µg)	Sn <sup>2+</sup> (µg)	Sn <sup>2+</sup>
0.5 × 10 <sup>4</sup>	18 ± 4	0.37	0.5 × 10 <sup>4</sup>	220 ± 24	4.40
2.5 × 10 <sup>4</sup>	51 ± 17	0.20	2.5 × 10 <sup>4</sup>	390 ± 314	1.56
5.0 × 10 <sup>4</sup>	86 ± 18	0.17	5.0 × 10 <sup>4</sup>	248 ± 6	0.50
12.5 × 10 <sup>4</sup>	454 ± 80	0.36	12.5 × 10 <sup>4</sup>	3973 ± 1064	3.18
50.0 × 10 <sup>4</sup>	1449 ± 100	0.29	25.0 × 10 <sup>4</sup>	4312 ± 580	1.72
75.0 × 10 <sup>4</sup>	2372 ± 492	0.32	50.0 × 10 <sup>4</sup>	13675 ± 1244	2.74
			75.0 × 10 <sup>4</sup>	19145 ± 108	2.55

**Table 4.4:** mass (µg) of metal ion [copper(II) or tin(II)] at t = 0h and sorbed at t = 1 h onto 200 mg of porcupine quills, in a 50 mL dyebath at 85 °C, containing 2.00 g cochineal. Mean values obtained by ICP-OES from triplicate measurements. [Data compiled from Chapter 7, section 7.3.3, tables 7.29 and 7.30].



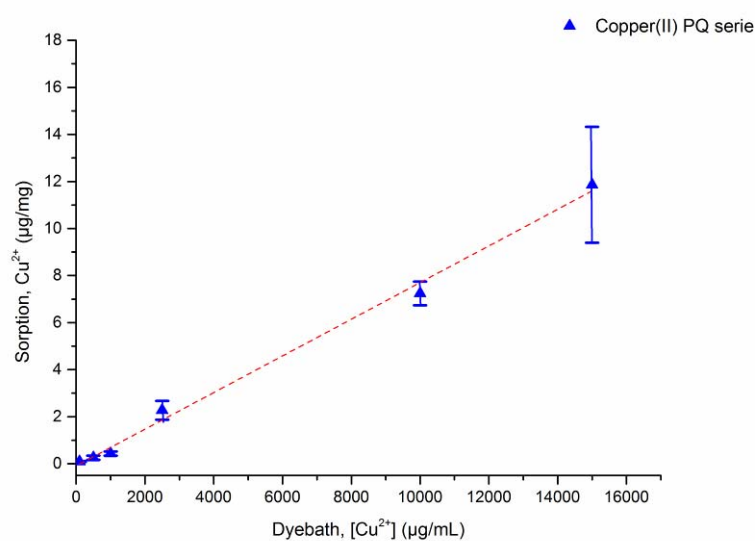


**Figure 4.10:** Linear plot of the dye bath concentration ( $x$ , [Cu<sup>2+</sup>] in  $\mu\text{g mL}^{-1}$ ) at  $t = 0$  h vs. the sorption of copper(II) in  $\mu\text{g}$  per mg of quill substrate, measured by ICP-OES. Mean values and standard deviation obtained from triplicate measurements [ $y = 7.79 \times 10^{-04}x - 0.08801$  ( $R^2 = 0.99438$ )]. [Data compiled from Chapter 7, section 7.3.3, table 7.30].

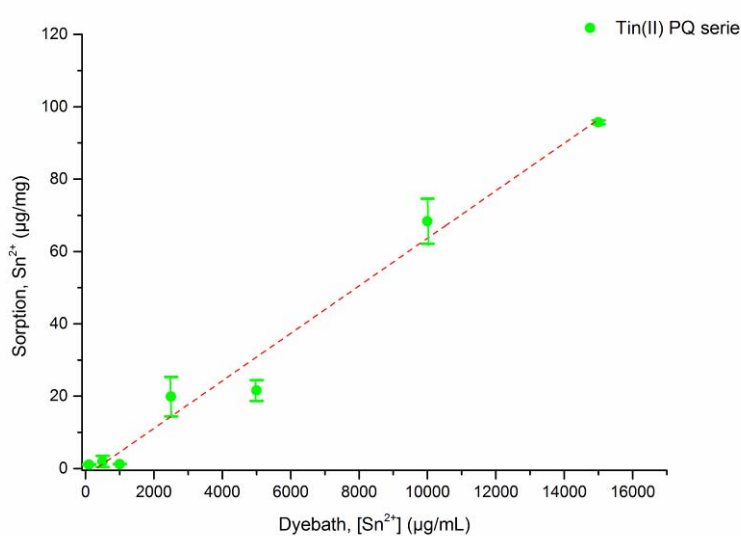


**Figure 4.11:** Linear plot of the dye bath concentration ( $x$ , [Sn<sup>2+</sup>] in  $\mu\text{g mL}^{-1}$ ) at  $t = 0$  h vs. the sorption of tin(II) in  $\mu\text{g}$  per mg of quill substrate, measured by ICP-OES. Mean values and standard deviation obtained from triplicate measurements [ $y = 0.00657x - 2.02765$  ( $R^2 = 0.97776$ )]. [Data compiled from Chapter 7, section 7.3.3, table 7.29].

### 4.2.3 Summary

ICP-OES investigation showed that the set of porcupine quills exhibited a range of concentrations in tin(II) and copper(II) and that the sorption of metal ions showed a reasonably linear correlation with the initial dyebath metal ion concentration. The total uptake of copper ranged between 0.2 and 0.4 % for the different dyebaths, while the uptake of tin was systematically higher and ranged between 0.5 and 4.4 %. It was also observed that the maximum sorption was reached after one hour of the dyeing process at 85°C, which compared well with observations in other studies on wool and human hair. Finally, the adsorbed quantities of metal ions by the porcupine quills in  $\mu\text{g mg}^{-1}$  were much smaller than previous studies on wool. This observation suggested that the thickness of the cuticle adversely affected metal ions exchange with the dyebath.

## 4.3 ION BEAM ANALYSIS

### 4.3.1 Ion Beam Analysis principles

Ion Beam Analysis (IBA) refers to several analytical techniques developed in the late 1950s and includes Rutherford Backscattering Spectrometry (RBS), Nuclear Reactions Analysis (NRA) and Elastic Recoil Detection Analysis (ERDA). In the late 70s a technique using accelerated particles was developed, referred under the term of PIXE - for Particle Induced X-Ray Emission analysis - this technique is today widely used for cultural heritage study, as it allows a non-invasive investigation of many materials, is multi-elemental, and provides a limit of detection as low as parts per million (ppm).<sup>33-35</sup>

The principles of the main IBA techniques are described in figure 4.12.<sup>34</sup> Rutherford Backscattering Spectrometry (RBS) is based on an elastic interaction between a positively charged ions and the atomic nuclei present in the sample,<sup>34, 36</sup> while Nuclear Reactions Analysis (NRA) is based on the interaction of the projectile with the nuclei of the material under investigation resulting in a nuclear reaction, followed

by the emission of gamma rays for example in the case of Particle Induced Gamma-ray Emission (PIGE).<sup>34</sup> Finally Particle Induced X-ray Emission (PIXE) is based on the interaction of a particle, usually a proton, expelling an electron from the inner shell of the target nuclei, followed by an electronic re-arrangement and the emission of characteristic X-rays, following the rules of the Moseley's Law (figure 4.13).<sup>33, 34, 37</sup> The great advantages of these techniques is that they can be used simultaneously for the study museum objects and offer complementary information.<sup>34</sup> Particle Induced X-Ray Emission (PIXE) and Particle Induced Gamma-ray Emission analysis (PIGE) are used for bulk analysis and are very sensitive, while Rutherford Backscattering Spectrometry (RBS) and Elastic Recoil Detection Analysis (ERDA) are used for the determination of layer thicknesses and find application in the study of depth profiles.<sup>38-40</sup>

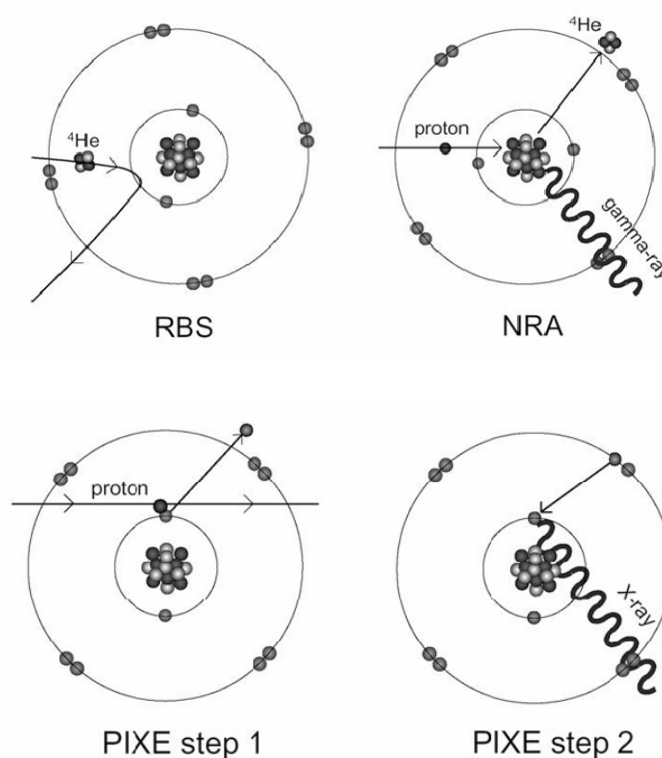


**Figure 4.12:** Physical principles of Rutherford Backscattering Spectrometry (RBS), Nuclear Reactions Analysis (NRA) and Particles Induced X-Ray Emission (PIXE) analysis, reproduced from Calligaro *et al.*, 2004.<sup>34</sup>

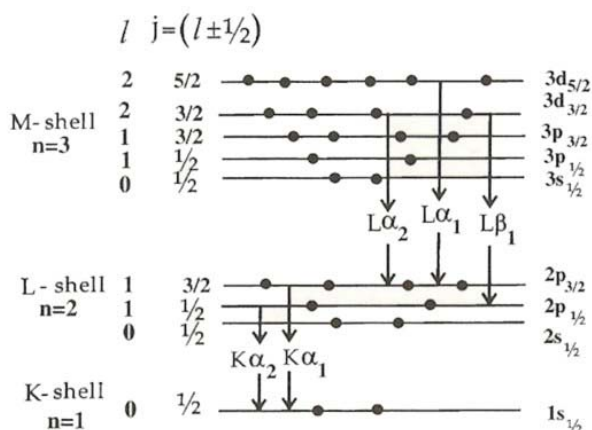


**Figure 4.13:** Notation of characteristic X-ray transitions including related energy levels, quantum numbers and electron occupation.<sup>37</sup>

### 4.3.2 PIXE analysis of trace elements in porcupine quills

#### 4.3.2.1 Interaction of 3 MeV proton beam with keratin

PIXE measurements are typically conducted using a 3 MeV accelerated proton beam, the X-rays emitted by the target is collected by a Si(Li) detector, and the limit of detection typically lies in the range of 1 to 10 ppm.<sup>34</sup> PIXE is not often used for the study of organic materials, because these are sensitive to heat and can be damaged by the irradiation. Nevertheless, PIXE combined with RBS analysis has been successfully applied to the study of metal point drawings, easel paintings and bones, all containing a combination of organic and inorganic components.<sup>41-44</sup> With regard to keratin analysis, early studies using PIXE investigation of human hair and human finger nails have been reported but highlighted the difficulty in quantifying traces of inorganic elements in an organic matrix.<sup>45, 46</sup> A later study used a standard-free method for the quantitative analysis of human hair, using zinc levels as an internal standard and reported that the concentration of sulfur could not be used as an internal standard due to its volatilisation during irradiation. It was observed that the level of sulfur decreased by up 23% for an integrated dose of 80  $\mu\text{C}$ .<sup>47</sup>

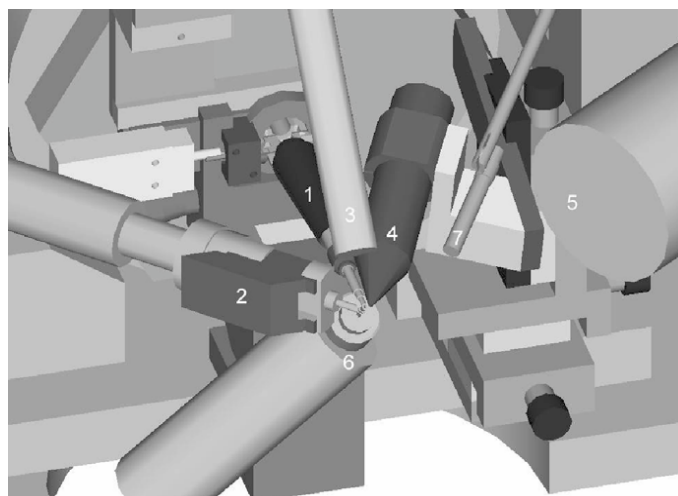


**Figure 4.14:** AGLAE external microprobe layout, reproduced from Calligaro *et al.*, 2004.<sup>34</sup> (1) focusing coil, (2) exit nozzle, (3) Si(Li) detector for 1 - 15 keV range, (4) Si(Li) detector for 5 - 40 keV range, (6) Peltier cooled X-ray detector for monitoring the beam dose using the PIXE signal emitted by the  $\text{Si}_3\text{N}_4$  exit foil.

In this study, all the measurements were undertaken at the AGLAE external micro-beam (Accelerator Grand Louvre d'Analyse Elementaire, LC2RMF-Paris); the set-up of the detectors is described in figure 4.14.<sup>34, 48</sup> In order to understand the interaction of the 3 MeV proton beam and helium ions with the porcupine quill; it is possible to model the energy loss using the range  $R$  which ions travel through the keratin.<sup>34</sup> The range  $R$  corresponds to the maximum distance the ion beam can penetrate in the material and is related to the rate of energy loss per unit length ( $dE/dx$ ) expressed in  $\text{keV } \mu\text{m}^{-1}$  (equation 4.3).<sup>34</sup> This rate of energy loss is proportional to the atomic number of the incident ion and the target,<sup>34</sup> here a porcupine quill, described by the average atomic composition of keratin (table 4.5).<sup>49</sup>

$$R = \int_0^{E_0} \left(\frac{dE}{dx}\right)^{-1} \times dE$$

**Equation 4.3**

Density $\rho$ (g/cm <sup>3</sup> )	Keratin layer, composition by atoms				
	C (12.011)	H (1.008)	O (15.999)	N (14.007)	S (32.066)
1.3	0.33	0.462	0.102	0.094	0.012

**Table 4.5:** density (g cm<sup>-3</sup>) of keratin and composition by atoms based on an average composition by weight (Wt %) of 51 % carbon, 21 % oxygen, 17 % nitrogen 6 % hydrogen and 5 % sulfur.<sup>49, 50</sup>

The range to which the beam will travel into the keratin can then be simulated using the density of keratin<sup>50</sup> (1.3 g cm<sup>-3</sup>) and TRIM software (SRIM 2003 version).<sup>51</sup> From this simulation it is predicted that the 3 MeV proton beam and helium ions will travel to a maximum depth of 136  $\mu\text{m}$  into the keratin, so through the average 58  $\mu\text{m}$  cuticle of the porcupine quill (section 4.1.2). Furthermore, due to the thickness of the quill (> 1 mm) the beam energy will decrease inside the quill, inducing some irradiation damage (figure 4.15).

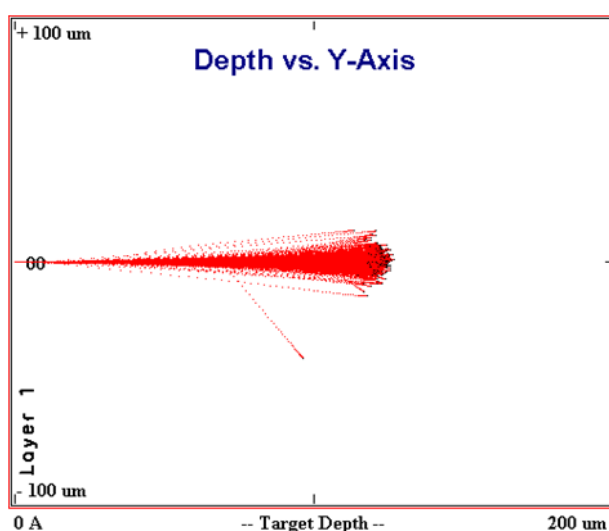


**Figure 4.15:** Penetration depth and angular distribution due to scattering processes of protons in keratin. Simulation of the trajectory of a 3 MeV protons beam inside obtained from TRIM software.<sup>51</sup>

### 4.3.2.2 Target description

It is important to define properly the porcupine quill target in order to accurately model the PIXE experiment. From the range calculated above, it is possible to rule out a thin layer target, where the beam would have gone through the porcupine quill.<sup>34</sup> It is not clear however if the model used for the study of human fingernails could be applied to porcupine quills.<sup>46</sup> In this study fingernails were defined as a thick homogenous target (equations 4.4 and 4.5), where  $A_i$  corresponds to atomic mass and  $c_i$  to the mass content of element  $i$ . The terms  $\omega_i$ ,  $k_i$  and  $\sigma_i(E)$  correspond to the fluorescence yield, branching ratio and cross-section of the considered shell element  $i$ .  $N_A$  corresponds to the Avogadro number and  $\varepsilon(E_x)$  corresponds to the X-ray detection efficiency,  $N$  is the number of ions with the energy  $E_0$  falling on the target, and  $\theta_a$  and  $\theta_0$  the ion-impact and X-ray take off angles. Finally,  $S_j(E)$ ,  $\mu_j(E)$  are the stopping power and attenuation cross section of the matrix  $j$ .<sup>46</sup>

$$Y_i(E_x) = \frac{N_A}{A_i} \varepsilon(E_x) \omega_i k_i N c_i I_i(E_0) \quad \text{Equation 4.4}$$

$$I_i(E_0) = \int_{E_0}^0 \sum_j^{c_j(E)} c_j S_j(E_x) \times \exp \left\{ - \sum_j c_j \mu_j(E_x) \frac{\cos \theta_a}{\cos \theta_0} \int_{E_0}^E \sum_j c_j S_j(E') \right\} dE \quad \text{Equation 4.5}$$

In order to confirm that the cuticle of the porcupine quill can be described as a thick homogeneous target, microscopic observation were undertaken using Scanning Electron Microscopy (SEM-BSC). Due to the limit of detection of the X-ray Dispersive Energy system (EDX), it was only possible to investigate the references containing the higher level of tin. This showed that the majority of tin(II) was absorbed by the cuticle layer, where the concentration in sulfur is also the highest, while minor amounts of tin were absorbed inside the quill (figures 4.16 and 4.17). On the SEM-BSC micrograph, the first microns of the cuticle layer appear brighter suggesting a small gradient in composition, although EDX analysis through the cuticle only showed small variation of the chlorine and tin contents (section 7.3).

This would suggest that it would be reasonable to consider a thick homogenous target for the quantification of the PIXE measurements, although clearly porcupine quills do not fall into standard model for PIXE analysis. Furthermore, the quantification of tin and copper in the cuticle layer might differ from the values obtained by ICP-OES analysis where a section of the porcupine quill was used.

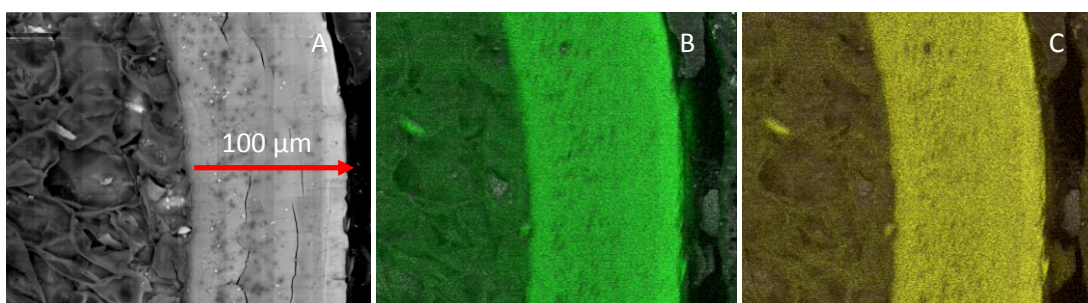


**Figure 4.16:** (A) Scanning Electron Micrograph (SEM-BSC) of a polished cross-section of porcupine quill prepared in a dye bath containing tin(II) chloride at  $10,000 \mu\text{g mL}^{-1}$ ; (B) Elemental mapping of tin (Sn,  $L_{\alpha}$  line); (C) Elemental mapping of sulfur (S, K line), at 20 kV at  $\times 500$  magnification.

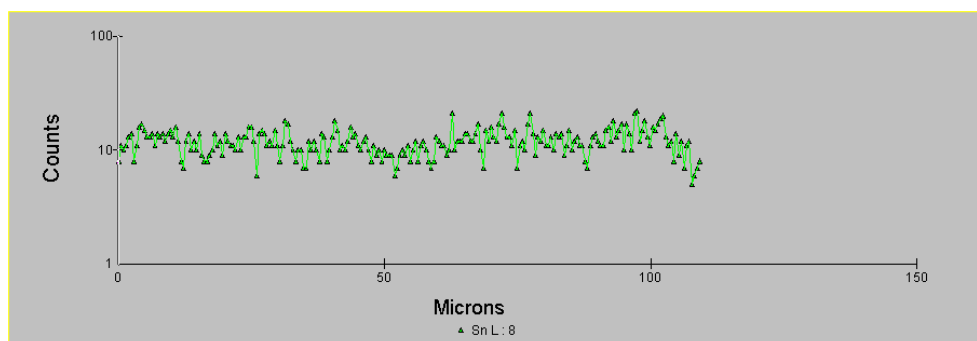


**Figure 4.17:** Line scan through the cuticle, at 20 kV, showing the variation in tin content.

#### 4.3.2.3 Absorption factors and transmission of Cu(K) and Sn( $L_{\alpha}$ ) X-rays in keratin

It is possible, using the GUPIX software,<sup>52, 53</sup> to calculate the effective analysed depth of the characteristic X-ray line of copper and tin in keratin. This showed that



both copper and tin exhibit similar depth profiles, as the software provided the values of 69.5  $\mu\text{m}$  for the  $L_A$  X-ray line (3.44 keV) and 72.10  $\mu\text{m}$  for the K X-ray line (25.271 keV) for tin and for copper a depth penetration of 78.5  $\mu\text{m}$  for the K X-ray line (8.047 keV).

The second important factor to take into consideration is the mass absorption coefficient  $\mu$  expressed in  $\text{cm}^2 \text{g}^{-1}$ , that is calculated considering the total atomic absorption cross-section  $\sigma_a$  of the atoms constituting the material using the equation 4.6, where  $N_A$  corresponds to Avogadro number and  $A$  is the atomic weight.<sup>54</sup> In the case of keratin, it is possible to calculate the  $\mu$  coefficients of tin and copper taking into account the atomic composition of keratin, and the total atomic absorption cross-section  $\sigma_a$  of the atoms constituting keratin (table 4.6). From these calculations, the mass attenuation coefficients  $\mu$  are very different for tin depending on the X-ray lines selected, Sn  $L_A$  gives a  $\mu$  value of 124.48  $\text{cm}^2 \text{g}^{-1}$ , Sn K gives a  $\mu$  value 0.53  $\text{cm}^2 \text{g}^{-1}$  and Cu K a  $\mu$  value of 10.63  $\text{cm}^2 \text{g}^{-1}$  (table 4.6). It might be therefore surprising, given the differences in the mass absorption coefficients  $\mu$ , that the effective analysed depth for K X-ray line (25.271 keV) of tin is only 72.1  $\mu\text{m}$ . This can be explained by the fact that in light target, such as keratin, the depth analysed is more affected by the depth penetration of the beam (here 136  $\mu\text{m}$ ) than the attenuation of the X-Ray.

	Sn $L_A$ , 3.44 keV	Sn K, 25.271 keV	Cu K, 8.047 keV
Penetration depths ( $\mu\text{m}$ ) [95 %]	69.5 $\pm$ 0.7	72.1 $\pm$ 1.0	78.5 $\pm$ 0.9
Mass attenuation coefficient $\mu$ ( $\text{cm}^2 \text{g}^{-1}$ )	124.48	0.53	10.63
Transmission in 80 $\mu\text{m}$ of keratin, $T = e^{-\mu\rho d}$	27.40%	99.45%	89.50%

**Table 4.6:** Depth profiles ( $\mu\text{m}$ ), mass attenuation coefficient  $\mu$  and transmission  $T$ , calculated for Sn( $L_A$ ) and Cu(K) using GUPIX and GUCSA software, with the average atomic composition of keratin.<sup>52, 53</sup> [Data compiled from Chapter 7, section 7.3.4, table 7.35].

$$\mu = \frac{N_A}{A} \times \sigma_A = \frac{N_A}{M_w} \sum_i x_i \sigma_{ai} \quad \text{Equation 4.6}$$

$$I = I_0 e^{-\mu \rho d} \quad \text{Equation 4.7}$$

The mass absorption coefficient  $\mu$  will also affect the transmitted intensity  $I$  through the keratin; as this is expressed as a function of the mass absorption coefficient  $\mu$ , the density  $\rho$  ( $\text{g cm}^{-3}$ ) and the thickness of the material  $d$  (cm) (equation 4.7).<sup>54</sup> When calculating the percentage of transmitted intensity  $I$  for a layer of  $80 \mu\text{m}$  of keratin, which corresponds to the maximum depth for the analysis of tin and copper, the transmitted intensity will be only 27.4% for tin  $L_A$  compared to 99.4 % for tin K and 89.5 % for copper K (table 4.6). This means that in the case of tin, geometrical effects such as the circular shape of the porcupine quill might affect the analysis of tin when considering the  $L_A$  line (figure 4.18), while the quantification of tin and copper using their K lines should not be much affected although using the  $L_A$  line might provide a lower limit of detection for the analysis of tin.

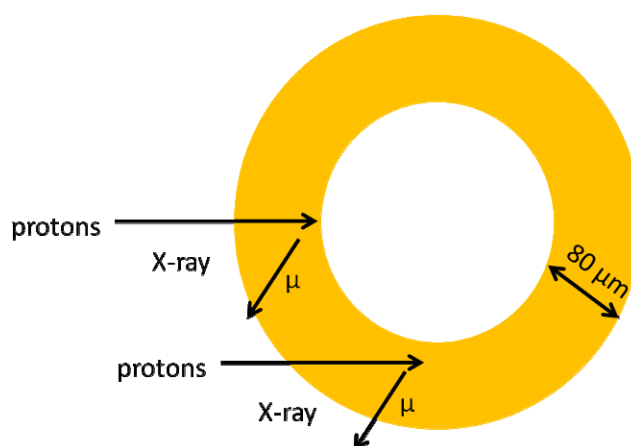


**Figure 4.18:** Analysis of porcupine quill by PIXE measurements.

#### 4.3.2.4 Parameter files and calibration

PIXE measurements were carried out using a 3 MeV proton external set-up with two Si(Li) X-ray detectors: a Low Energy detector (LE), for the 1 - 15 keV range and a High Energy detector (HE), for the 1 - 40 keV range. These detectors recorded simultaneously the composition low-Z matrix elements and the high-Z trace elements present in the matrix<sup>34</sup> and quantification was performed using the GUPIXWIN software package.<sup>53</sup> GUPIXWIN is a non-linear-least-square fitting programme designed for PIXE spectra that allows the calculation of the element concentrations from their X-ray peak areas in the spectrum, taking into account, in the case of a thick homogeneous target, self-absorption effects and the energy dependent production rates of X-rays.<sup>53</sup> Usually an element present in the matrix and visible at both low and high energy, such as iron (Fe,  $Z = 26$ ), will be used by the software to link the concentrations of the elements present in the matrix and at trace levels.<sup>53</sup> The challenge in analysing porcupine quill samples arises from the fact that keratin is made of elements that are invisible to the detectors. Only sulfur (S,  $Z = 16$ ) will be visible at both low and high energy but it is present in such a small amount that it will not allow the low and high energy detectors to be linked. As a result the quantification of the elements characterised by low and high energy detectors was undertaken using separate parameter files.

As a first attempt to investigate porcupine quills, the experiment was undertaken with an average current of 2 to 4 nA for an analysis time between 240 and 300 sec, corresponding to an integrated dose  $Q$  of 1  $\mu\text{C}$ . In order to reduce the damage to the quills, analysis was undertaken by scanning an area of  $100 \times 500 \mu\text{m}$  (chapter 6). During this set of measurements, the beam showed some instability, especially at the start of experiment, and this is indirectly expressed through the variation of dose per second recorded and shown below as a graphical interpretation (figure 4.19). This variability in the beam charge ( $Q$ ) will affect the calculation of the concentration, as it is not possible to control the exact irradiation received by the material analysed using an external micro-beam (in opposite to internal micro-beam). To reduce such

variation, the system is equipped with a Peltier cooled X-ray detector that monitors the beam dose, meaning that the integrated dose should in theory be kept constant during the experiment as it is expressed as a function of current multiplied by irradiation time (equation 4.8).

$$Q(C) \propto I(A) \times t(\text{sec})$$

Equation 4.8

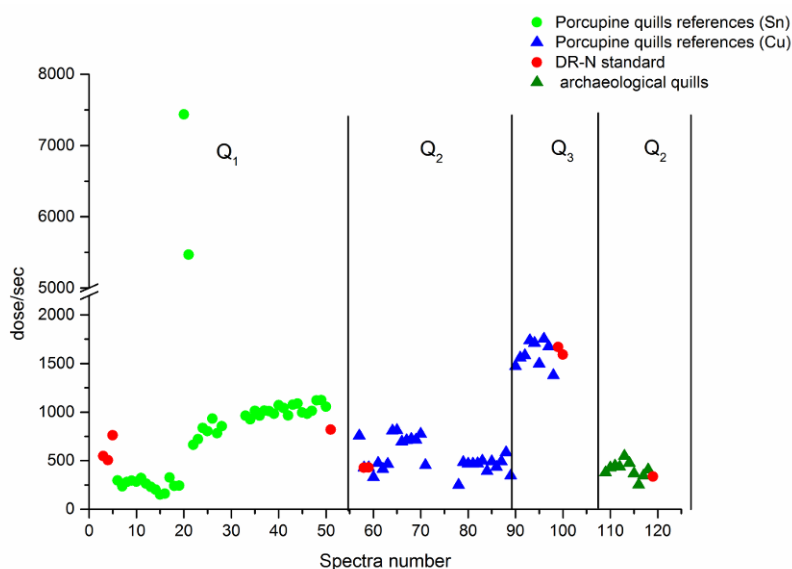


**Figure 4.19:** Evolution of the dose / sec recorded during the analysis of porcupine quills references containing tin and copper; and a small selection of historical quills. A DR-N standard was analysed regularly in order to calculate the accurate value the beam charge  $Q$ . [Data compiled from Chapter 7, section 7.3.4, table 7.40].

Previous observation showed that porcupine quill will be considered as equivalent to a thick target (section 4.2.1.3) and therefore that the concentration  $C_Z$  of element  $Z$  in the sample will be expressed by the yield  $Y_Z$ , expressed in counts per unit concentration (equation 4.9):<sup>34</sup> In order to have an accurate calculation of the trace

elements present in the keratin matrix, it is important to know the exact value of the beam dose  $Q$  and the value of the quantity  $H$ , which translates the element peak area for the given charge collected into an element concentration.<sup>52</sup> This would be ideally done by analysing porcupine quill standard of exactly known composition,<sup>34</sup> but in the absence of such standard, this was achieved by analysing a DR-N standard containing several elements as oxides (figures 4.20 and 4.21).

These measurements allowed the exact beam charge ( $Q$ ) and the quantity ( $H$ ) values to be calculated for the set of experiments, and provided an accurate quantification of the DR-N standard when summed up by GUPIXWIN to 100 percent (equation 4.10). The values obtained for the different elements present in the DR-N standard were quantified for both low and high energy detectors and compared to their theoretical values (figures 4.20 and 4.21). The values of  $Q$  and  $H$  calculated for the different experiment segments were then used to create the parameter file for the quantification of the porcupine quills, working in matrix mode with the matrix defined as keratin using its relative weight percentage composition (table 4.7).<sup>34</sup>

$$C_Z = \frac{N_Z}{Y_Z} \quad \text{Equation 4.9}$$

$$C_Z = \frac{\left(\frac{N_Z}{Y_Z}\right)}{\sum_{Z'} \left(\frac{N_{Z'}}{Y_{Z'}}\right)} \quad \text{implying} \quad \sum_Z C_Z = 100\% \quad \text{Equation 4.10}$$

	Entry 1 to 57	Entry 60 to 89	Entry 90 to 107	Entry 108 to 118
Low Energy	Q <sub>1</sub> : 0.0065 μC H: 1	Q <sub>2</sub> : 0.0075 μC H: 1	Q <sub>3</sub> : 0.0105 μC H: 1	Q <sub>2</sub> : 0.0075 μC H: 1
High Energy (Be, 125 μm and 28.5 mm air)	Q <sub>1</sub> : 0.0065 μC H: 1	Q <sub>2</sub> : 0.0075 μC H: 1	Q <sub>3</sub> : 0.0120 μC H: 1	Q <sub>2</sub> : 0.0075 μC H: 1

**Table 4.7:** Values of the beam dose ( $Q$ ) and the quantity ( $H$ ) for the different segments of the experiments, as shown in figure 4.17.

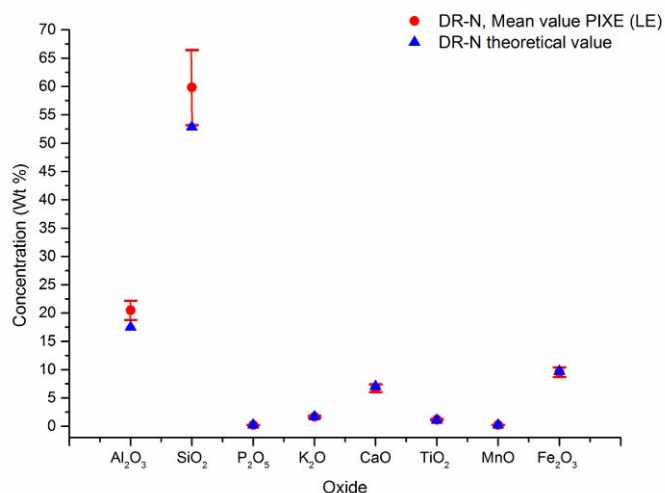


**Figure 4.20:** Quantification of the DR-N standards using low energy detector during the experiment, obtained values obtained are compared to theoretical values. Note that it was not possible to accurately quantify the elements aluminium (Al, Z = 13) and silicon (Si, Z = 14). [Data compiled from Chapter 7, section 7.3.4, table 7.38].

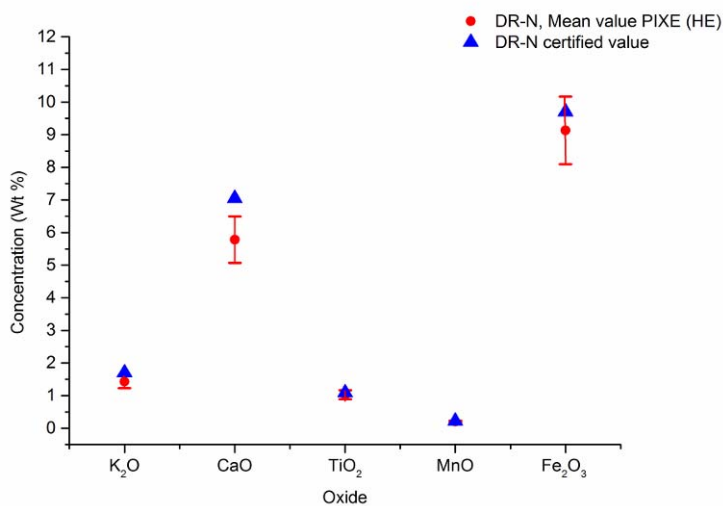


**Figure 4.21:** Quantification of the DR-N standards using high energy detector during the experiment, obtained values obtained are compared to theoretical values. [Data compiled from Chapter 7, section 7.3.4, table 7.39].

#### 4.3.2.5 Quantification of copper and tin by PIXE analysis

Due to accelerator maintenance at the time of these experiments, it was not possible to quantify accurately the K line of tin for this set of measurements. As a result, the quantification values discussed below were obtained from the High Energy detector; using the  $L_A$  line of tin and K lines of sulfur, chlorine and copper for GUPIX calculations.

##### 4.3.2.5.1 Copper reference porcupine quills

Similarly to what was observed by ICP-OES analysis, the copper references were found to be quite homogeneous by PIXE analysis. The stability of the beam dose during the measurements allowed inter-comparison of the references. The level of sulfur was found to range from 2.20 Wt % for the lower concentration in copper to 5.00 Wt % for the more concentrated samples. This can be explained by the fact that the copper was introduced with the sulfate anion, which was also slightly absorbed by the keratin. Similarly to what was observed by ICP-OES, the levels of copper present in the cuticle layer of the porcupine quill were much lower than those observed for the tin references, and copper was found to range between 0.01 Wt % and only 2.26 Wt % for the highest concentration. A linear plot of the dye bath concentration (x,  $[Cu^{2+}]$  in  $\mu g mL^{-1}$ ) vs. Wt % of copper characterised by PIXE analysis showed a linear correlation (figure 4.22), with a comparable standard deviation to that found by ICP-OES (around 20 %), although some measurements were more dispersed.

##### 4.3.2.5.2 Tin reference porcupine quills

The porcupine quill references prepared in tin(II) chloride dye baths were analysed at the start of the experiment when the beam showed more variation of the dose, which affected the quantification. This impacted on the quantification of sulfur which

should be in theory the same for all the samples. Sulfur content ranged between 1.31 Wt % and 2.45 Wt % due to the variation of the beam dose  $Q$  (table 4.7). In order to evaluate the concentration of tin and inter-compare the measurements it was therefore decided to normalise the sulfur content to 2.00 Wt % and apply this corrective factor to the concentration of tin and chlorine. These results can be found in table 4.8 and showed after normalisation, that the level of tin ranged between 0.01 Wt % for the lower concentration to 15.00 Wt % for the higher concentration. The level of chlorine was found to range between 0.002 Wt % and 4.45 Wt % for the more concentrated dye baths. The heterogeneity of the tin references observed by ICP-OES analysis was similarly observed by PIXE analysis and the linear plot of the dye bath concentration ( $x$ ,  $[\text{Sn}^{2+}]$  in  $\mu\text{g mL}^{-1}$ ) vs. the percentage of tin characterised in Wt % showed a reasonable linear correlation with almost a saturation level for the two highest concentrations (figure 4.23). This could be explained by the difficulty of quantifying tin when its concentration is present in higher quantity than the matrix, which alters the representation of the target.



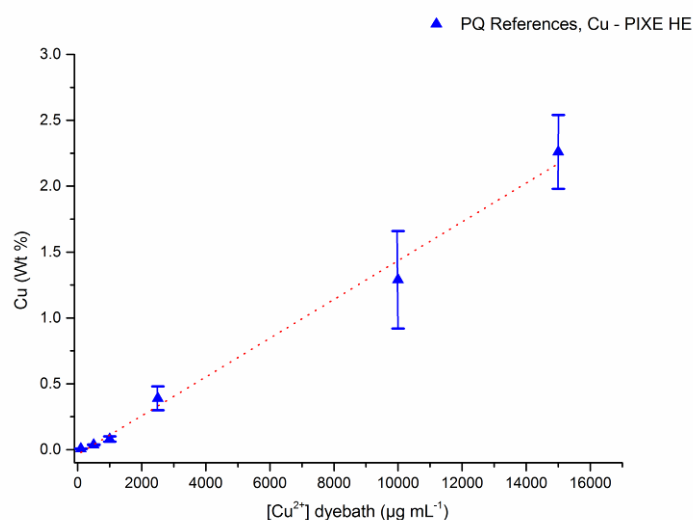


**Figure 4.22:** Linear plot of the dyebath concentration of  $[\text{Cu}^{2+}]$  ( $\mu\text{g mL}^{-1}$ ) vs sorbed copper determined by PIXE analysis (Wt %). Mean values and standard deviation obtained from six measurements on three different porcupine quills.  $[y = 1.47 \times 10^{-04}x - 0.03642$  ( $R^2 = 0.98977$ )]. [Data compiled from Chapter 7, section 7.3.4, table 7.42].

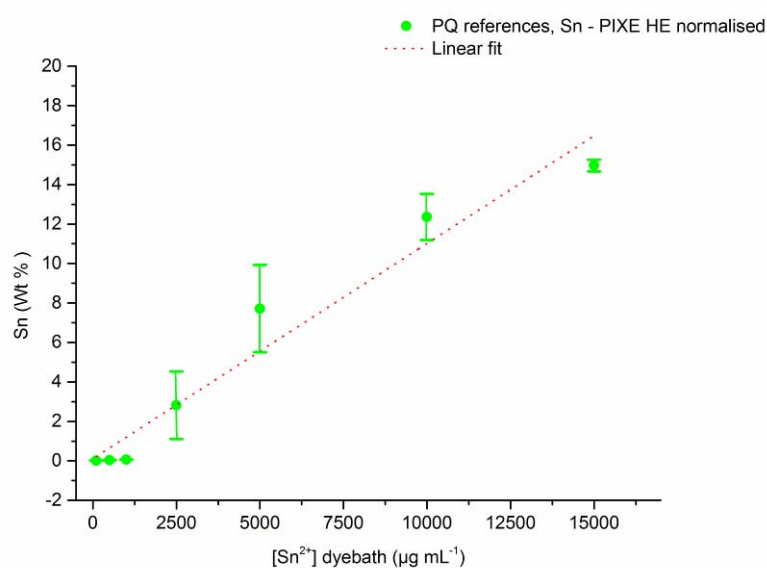


**Figure 4.23:** Linear plot of the dyebath concentration of  $[\text{Sn}^{2+}]$  ( $\mu\text{g mL}^{-1}$ ) vs. sorbed tin determined by PIXE after normalisation to 2 Wt % sulfur (Wt %). Mean values and standard deviation obtained from six measurements on three different porcupine quills.  $[y = 0.00109x + 0.10849$  ( $R^2 = 0.94753$ )]. [Data compiled from Chapter 7, section 7.3.4, table 7.41].

[Sn <sup>2+</sup> ] µg/mL	PIXE (Wt %)			PIXE (Wt %), normalised		
	16 S (K)	50 Sn (L <sub>A</sub> )	17 Cl (K)	16 S (K)	50 Sn (L <sub>A</sub> )	17 Cl (K)
100	2.30 ± 0.45	0.011 ± 0.004	0.019 ± 0.007	2.00	0.009 ± 0.003	0.017 ± 0.005
500	1.97 ± 0.18	0.04 ± 0.01	0.14 ± 0.01	2.00	0.04 ± 0.01	0.14 ± 0.01
1000	2.45 ± 0.48	0.07 ± 0.01	0.41 ± 0.04	2.00	0.06 ± 0.01	0.34 ± 0.05
2500	1.34 ± 0.34	1.83 ± 1.15	1.01 ± 0.29	2.00	2.82 ± 1.71	1.55 ± 0.39
5000	1.32 ± 0.44	4.74 ± 1.23	1.41 ± 0.45	2.00	6.81 ± 1.95	2.00 ± 0.31
10000	1.68 ± 0.74	10.20 ± 4.60	2.56 ± 1.16	2.00	12.35 ± 1.17	3.09 ± 0.43
15000	1.85 ± 0.65	13.82 ± 4.64	4.20 ± 1.77	2.00	14.96 ± 0.29	4.45 ± 0.33
[Cu <sup>2+</sup> ] µg/mL	16 S K	29 Cu (K)				
100	2.22 ± 0.29	0.007 ± 0.002				
500	2.31 ± 0.19	0.037 ± 0.003				
1000	3.38 ± 0.64	0.08 ± 0.02				
2500	4.43 ± 0.78	0.39 ± 0.09				
10000	4.96 ± 0.22	1.29 ± 0.37				
15000	5.01 ± 0.45	2.26 ± 0.28				

**Table 4.8:** PIXE Wt % concentration of tin, copper, chlorine and sulfur characterised in reference quills. Mean values obtained from six measurements on three different porcupine quills. [Data compiled from Chapter 7, section 7.3.4, tables 7.41 and 7.42].

#### 4.3.2.6 Summary

PIXE measurements were carried out successfully on the reference materials prepared with variable levels of copper(II) and tin(II). It was found that the 3 MeV proton and helium ion beams were penetrating to a maximum depth of 136 µm, causing damage to the sample due to irradiation and transfer of beam energy into the target. The quantification of the trace elements present in the porcupine quills was achieved with the GUPIXWIN software package treating the cuticle of the quill as a homogeneous thick target. It was found crucial to have access to the exact value of the beam charge  $Q$  during the experiment, as any variation impacted directly on the quantification. This was achieved through the analysis of a known standard DR-N during the experiments, which was used as an external standard to control the value

of the beam dose  $Q$ . The levels of copper in porcupine quills were found to range between 0.01 and 2.26 Wt % for the highest dye bath concentrations, while the levels of tin ranged from 0.01 to 15.00 Wt %. For both set of references a reasonably linear correlation was observed between the dye bath concentrations of metal ions vs. the percentage of metal ions characterised by PIXE in Wt %, suggesting a good correlation with the results obtained by ICP-OES analysis. As well to copper and tin, it was also possible to quantify simultaneously the level of sulfur and chlorine. However other elements such as calcium, potassium and iron could also be quantified, which would particularly be interesting for the analysis of historical materials.

### 4.3.3 Rutherford Backscattering Spectrometry (RBS)

#### 4.3.3.1 RBS Principles

Rutherford Backscattering Spectrometry (RBS) consists of an elastic collision, meaning that there is no energy lost or gained during the collision,<sup>40</sup> between a projectile with high kinetic energy, here 3 MeV protons and helium nuclei from the incident beam, and the stationary particles located in the target (figure 4.24). For a given angle, typically in the range 150 - 170°, the ion recoil energy is characteristic of the mass of the target nucleus. RBS allows the quantitative determination of the composition of a material and depth profiling of individual elements. The method is quantitative without the need for reference samples and non-destructive, it is also very sensitive for heavy elements (ppm).<sup>40</sup> The RBS technique is often used for the analysis of intermediate or heavy elements in a light material and a recent study demonstrated its application for the characterisation of organic fractions present in archaeological and recent bones.<sup>44</sup>

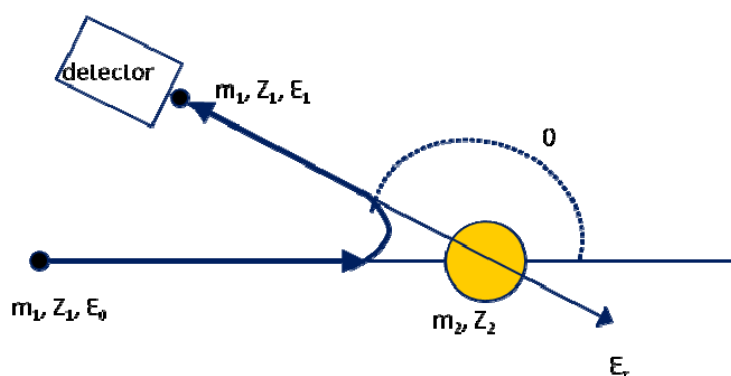


**Figure 4.24:** Elastic collision between the incident particles ( $m_1, Z_1$ ) and the target ( $m_2, Z_2$ ).  $E_0$  corresponds to the energy of the incident particles,  $E_1$  the energy of the scattered particles and  $E_r$  the recoiled energy.<sup>55</sup>

The backscattered projectile has an energy  $E_1$  reduced from the initial energy of the projectile  $E_0$  (equation 4.11), where  $k$  is the kinematical factor (equation 4.12) and is expressed as a function of the projectile ( $m_1$ ) and the target nucleus ( $m_2$ ), with  $\theta_1$  scattering angle of the projectile in the laboratory.

$$E_1 = k \times E_0$$

**Equation 4.11**

The probability of observing a backscattered event is expressed by the differential cross-section (equation 4.13), where  $Z_1$  and  $Z_2$  are the atomic numbers of the incident particle and the nucleus target.<sup>40</sup> This probability will be higher for a heavy nucleus, because it is expressed as the square of the electric charge  $Z$  (equation 4.13) and a heavy nucleus will have a higher recoil energy (equation 4.11).<sup>40</sup> Rutherford scattering cross-sections have been measured since 1950 for many elements and are available in the simulation software SIMNRA developed by the Max-Planck-Institute for Plasma Physics, in Germany.<sup>56</sup>

As well as Rutherford cross-sections, several non-Rutherford cross-sections can be used to simulate RBS spectra. These nuclear reactions correspond to scattering with non-Rutherford cross-sections and are also called RBS, but use inelastic scattering nuclear reactions (NRA) and ERDA. Non-Rutherford reactions are very important for the quantification of light- $Z$  elements, as their cross sections are multiplied by a factor of 10 approximately in comparison with Rutherford cross-sections.<sup>40, 44, 57</sup> Several non-Rutherford cross-sections specific to the set-up used in AGLAE accelerator at  $150^\circ$  were used for the quantification of carbon, oxygen and nitrogen [see Chapter 7, section 7.3.5].

$$k = \frac{E_1}{E_0} = \left[ \frac{m_1 \cos \theta - \sqrt{(m_2^2 - m_1^2 \sin^2 \theta)}}{(m_1 + m_2)} \right]^2 \text{ with : } m_1 < m_2 \quad \text{Equation 4.12}$$

$$\frac{d\sigma}{d\Omega} = \left( \frac{Z_1 Z_2 e^2}{4E_{inc}} \right)^2 \times \frac{4}{\sin^4 \theta} \times \frac{\left[ \sqrt{1 - \left[ \frac{m_1}{m_2} \sin \theta \right]^2} + \cos \theta \right]^2}{\sqrt{1 - \left[ \frac{m_1}{m_2} \sin \theta \right]^2}} \quad \text{Equation 4.13}$$

#### 4.3.3.2 SIMNRA simulation: calculation of depth profile

The RBS measurements were recorded simultaneously to the PIXE experiments and RBS spectra were simulated using the SIMNRA software by virtually overlapping the contribution of the different atoms present in the cuticle layer. It was found to be more reproducible to model the target as a single layer of keratin doped with different amount of metal ions. The depth of keratin analysed by RBS can be calculated using a reference containing a high quantity of tin that should be very visible on the spectra (figure 4.25). It was then possible to evaluate accurately the thickness of the keratin layer as  $140000 \times 10^{15}$  atoms  $\text{cm}^{-2}$ . The average molecular weight of keratin can easily be converted using the Avogadro number to  $1.29 \times 10^{-7}$

$\text{g cm}^{-2}$  for  $10^{15}$  atoms  $\text{cm}^{-2}$  and the depth of keratin analysed can then be calculated using the thickness of this layer ( $140000 \times 10^{15}$  atoms  $\text{cm}^{-2}$ ) and the density of keratin ( $1.3 \text{ g cm}^{-3}$ ) and corresponds to  $13.6 \mu\text{m}$ . This means that only the first few microns of the cuticle will be analysed by RBS (table 4.9).

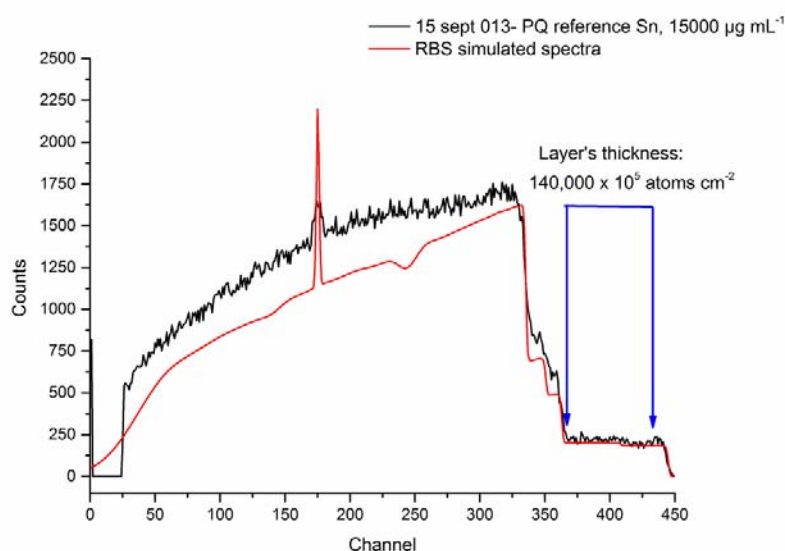


**Figure 4.25:** RBS spectra 15sept 013. The spectra simulated with SIMNRA software (red) using both Rutherford and non-Rutherford cross-sections (in red), allowed the evaluation of the thickness investigated.

<i>Layers</i>	<i>1</i>	<i>2</i>
<b>Thickness (<math>10^{15}</math> at <math>\text{cm}^{-2}</math>)</b>	1000	140000
<b>Composition</b>	He : 1	C : 0.33 H : 0.458 O : 0.1000 S : 0.01 N : 0.090 Sn : 0.0012

**Table 4.9:** Atomic composition and thicknesses of virtual layers of spectra 15sept 013 doped with excess of tin simulated with SIMNRA software.

#### 4.3.3.3 Quantification of copper and tin by RBS analysis

The RBS spectra obtained from several references were simulated by SIMNRA and the atomic composition of the metal ion-containing layer converted into weight composition (Wt %) to allow direct comparison with PIXE analysis. The variation of the beam dose  $Q$  is indirectly assessed on the RBS spectra through the number of incident particles ( $*sr$ ) that can be adjusted by the software. For the copper reference samples the number of incident particles was little variable, which confirmed the PIXE observations, and lying between  $2.80 \times 10^{10}$  and  $3.41 \times 10^{10} *sr$ . Figure 4.26 shows the simulated RBS spectra of a porcupine quill prepared in  $15,000 \mu\text{g mL}^{-1}$  copper(II) dyebath. The simulated spectra was found to fit closely to the RBS spectra, although the fronts of carbon and oxygen were found to be slightly offset, which could be explained by the fact that RBS is very sensitive to carbon contamination; traces of organic residues such as oils left from scouring process could be picked up by the RBS detector. Sulfur was fitted using Rutherford cross-sections only, as the value of the non-Rutherford cross-sections was not available for the AGLAE system; this might need to be improved for future measurements. The RBS simulated spectrum provided a very close correlation for the concentration of copper and sulfur compared to the values obtained by PIXE analysis (table 4.10). Small differences were found in the sulfur content that was slightly under estimated by RBS simulation, but the copper content was found to be very close to PIXE measurements and ranged between 0.25 and 2.00 Wt %. It was found that below 0.25 Wt % copper could be detected by RBS but it could not be quantified.

Entry	$[Cu^{2+}]$ ( $\mu\text{g mL}^{-1}$ )	Dose $Q$ ( $\mu\text{C}$ )	Particles $*sr$	RBS (Wt %)		PIXE (Wt %)	
				S	Cu	S	Cu
15sep092	500	0.0120	$2.80 \times 10^{10}$	3.38	0.25	2.28	0.04
15sep087	1000	0.0075	$3.41 \times 10^{10}$	3.59	0.25	3.67	0.08
15sep080	2500	0.0075	$3.06 \times 10^{10}$	3.38	0.42	4.10	0.43
15sep067	10000	0.0075	$3.37 \times 10^{10}$	3.76	1.08	5.05	1.20
15sep062	15000	0.0075	$3.01 \times 10^{10}$	4.12	2.05	5.14	2.00

**Table 4.10:** Dose  $Q$  ( $\mu\text{C}$ ) used for GUPIX calculation compared to particles number ( $*sr$ ) fitted by SIMNRA for several measurements containing copper. The atomic composition of virtual layers was converted into weight percentage (Wt %) to allow direct comparison with PIXE analysis. [Data compiled from Chapter 7, section 7.3.5, table 7.47].

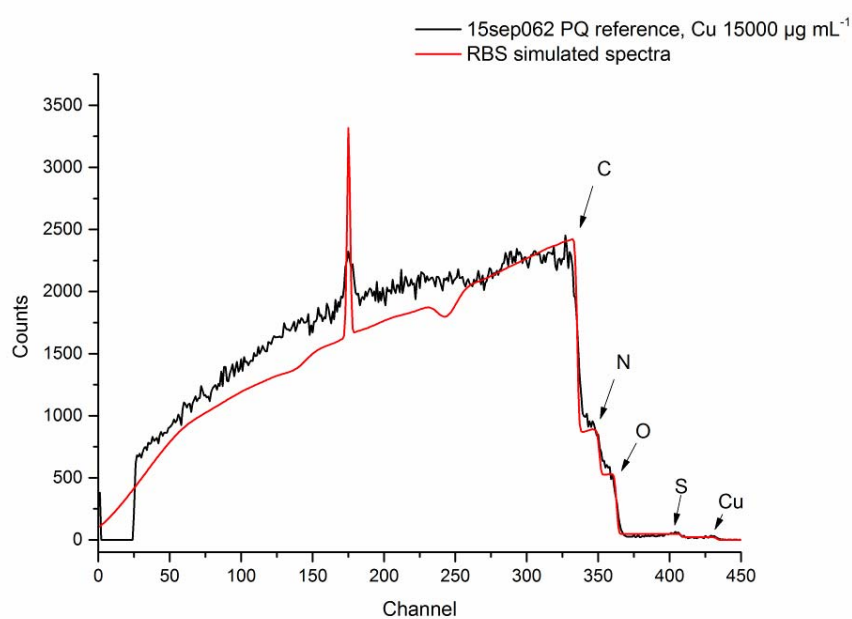


**Figure 4.26:** RBS spectra 15sept 062, porcupine quill prepared in 15000  $\mu\text{g mL}^{-1}$  copper(II) dye bath, and simulated RBS spectra with SIMNRA software using both Rutherford and non-Rutherford cross-sections (in red). [Data compiled from Chapter 7, section 7.3.5, table 7.47].



RBS simulation was also done on several samples containing tin and chlorine. As can be observed on figure 4.27, tin is very visible on the RBS spectra and can be easily quantified in the keratin matrix. The numbers of incident particles was much more variable for the selected simulated spectra and ranged between  $1.62 \times 10^{10}$  and  $2.44 \times 10^{10}$   $^*sr$ , confirming the variation of beam dose  $Q$  observed during PIXE analysis. It was found difficult to quantify both sulfur and chlorine using Rutherford cross-sections only, because their kinematic factors are very close. As a result the quantification of sulfur by RBS analysis was not as accurate as that for the copper containing samples. The concentrations of tin characterised in the RBS simulated spectra were very close to the values obtained by PIXE analysis after normalisation of the sulfur content to 2.00 Wt %. This showed that the control of the beam dose  $Q$  is crucial for accurate PIXE quantification. Interestingly, due to the possibility of adjusting the number of incidents particles with SIMNRA software; the quantification of tin was found to be unaffected by RBS analysis but was systematically slightly over-estimated compared to PIXE (table 4.11). This could mean that the first microns of the keratin are slightly more concentrated in tin than the rest of the cuticle, and correlates what was observed previously by SEM-BSC imaging [Figure 4.16, section 4.3.3.2]:

Entry	$[Sn^{2+}]$ ( $\mu g mL^{-1}$ )	Dose ( $\mu C$ )	Particles $^*sr$	RBS (Wt %)			PIXE corrected (Wt %)		
				S	Sn	Cl	S	Sn	Cl
15 sept 030	2500	0.0065	$1.62 \times 10^{10}$	2.5	2.32	0.14	2.0	1.94	2.04
15 sept 025	5000	0.0065	$1.76 \times 10^{10}$	3.11	7.93	0.43	2.0	5.96	2.28
15 sept 010	10000	0.0065	$2.44 \times 10^{10}$	1.85	12.35	1.64	2.0	10.21	2.93
15 sept 015	15000	0.0065	$2.22 \times 10^{10}$	2.77	15.42	3.06	2.0	14.96	4.45

**Table 4.11:** Dose  $Q$  ( $\mu C$ ) used for GUPIX calculation compared to particles number ( $^*sr$ ) fitted by SIMNRA for several measurements containing tin. The atomic composition of virtual layers was converted into weight percentage (Wt %) to allow direct comparison with PIXE analysis, after normalisation to 2.0 Wt % of sulfur. [Data compiled from Chapter 7, section 7.3.5, table 7.46].

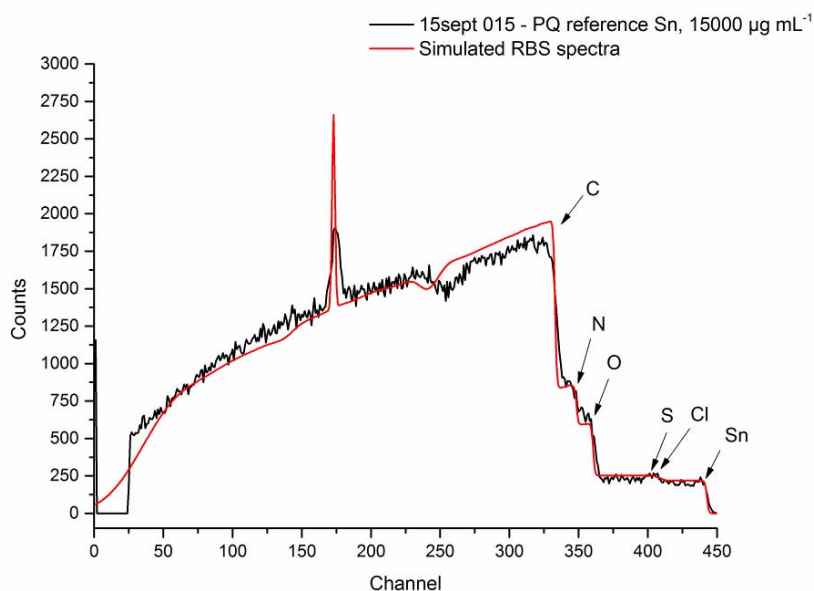


**Figure 4.27:** RBS spectra 15sept 015, porcupine quill prepared in  $15000 \mu\text{g mL}^{-1}$  tin(II) dye bath, and simulated RBS spectra produced by SIMNRA software using both Rutherford and non-Rutherford cross-sections. [Data compiled from Chapter 7, section 7.3.5, table 7.46].

#### 4.4 DISCUSSION

The sorption of copper(II) and tin(II) onto porcupine quills were studied by ICP-OES, which showed a reasonably linear correlation with the initial dye bath metal ion concentration. The adsorbed quantities of metal ions by the porcupine quills in  $\mu\text{g mg}^{-1}$  were however much smaller than previous studies on wool, with the total uptake of tin being systematically higher than copper. This reference set of porcupine quills was then non-invasively investigated by RBS-PIXE analysis and the weight concentrations (Wt %) measured on the surface of the porcupine quills, i.e. adsorbed in the cuticle layer, were evaluated with both techniques. The quantification of the trace elements present in the porcupine quills by PIXE was however found to be altered by some variation in the beam charge  $Q$  during the experiment. It would be necessary for future experiments to control this parameter

better in order to obtain a more accurate quantification of the trace elements. Nevertheless, for both set of references (copper and tin) a reasonably linear correlation was also observed between the dyebath concentrations of metal ions vs. the weight concentration (Wt %) characterised by PIXE, and suggested a good correlation with the results obtained by ICP-OES analysis. These surface measurements could however not be directly compared due to the fact that in the case of ICP-OES a complete cross-section of porcupine quill was subjected to analysis. Finally RBS analysis allowed complementary information on the lights elements present in the cuticle layer, such as carbon, oxygen, nitrogen and sulfur. The simulated RBS spectra generated with SIMNRA software allowed a good quantification of traces copper or tin present in the keratin layer, even for the lowest concentrations. This non-invasive approach using combined RBS-PIXE analysis will be applied to the study of nineteenth century porcupine quill work from National Museums Scotland collection and the results obtained from this study will be discussed in chapter 5.

## 4.5 REFERENCES

1. Orchard, W. C. (1916). *The Technique of Porcupine-Quill Decoration Among the North American Indians*. Kessinger Publishing, Reprint 2009.
2. Thompson, J. (2001). *Fascinating Challenges: Studying Material Culture with Dorothy Burnham*. Canadian Museum of Civilization.
3. Thompson, J. (1990). *Pride of the Indian Wardrobe, Northern Athapaskan footwear*. University of Toronto Press, for the Bata Shoe Museum.
4. Idiens, D. (1974). The Athapaskan Indian collection in the Royal Scottish Museum. In *The Athapaskans: Strangers of the North. An international travelling exhibition from the collection of the National Museum of Man, Canada, and the Royal Scottish Museum*, National Museum of Man: Ottawa, 15-16.
5. Idiens, D. (1979). A catalogue of Northern Athapaskan Indian Artefacts in the collection of the Royal Scottish Museum, Edinburgh. *Royal Scottish Museum Information Series, Art and Archaeology*, 3.

6. Dussubieux, L., Ballard, M. W. (2005). Using ICP-MS to detect Inorganic elements in Organic materials: a new tool to identify mordants or dyes on Ancient Textiles *MRS Proceedings, Material Issues in Art and Archaeology* **852**, 291-296.
7. Rezić, I., Steffan, S. (2007). ICP-OES determination of metals present in textile materials. *Microchem. J.*, **85**, 46-51.
8. Peggie, D. A. (2006). *The Development and Application of Analytical Methods for the Identification of Dyes on Historical Textiles*. The University of Edinburgh, PhD Thesis.
9. Fergusson, J. E., Holzbecher, J., Ryan, D. E. (1983). The sorption of copper(II), manganese(II), zinc(II) and arsenic(II) onto human hair and their desorption. *Sci. Total Environ.*, **26**, 121--135.
10. Suyama, K., Fukazawa, Y., Suzumara, H. (1996). Biosorption of Precious Metal Ions by Chicken Feather. *Appl. Biochem. Biotech.*, **57-58**, 67-74.
11. Kar, P., Misra, M. (2004). Use of keratin fiber for separation of heavy metals from water. *J. Chem. Technol. Biotechnol.*, **79**, 1313-1319.
12. Aluigi, A., Corbellini, A., Rombaldoni, F., Mazzuchetti, G. (2012). Wool-derived keratin nanofiber membranes for dynamic adsorption of heavy-metal ions from aqueous solutions. *Textile Res. J.*
13. Sheffield, A., Doyle, M. J. (2005). Uptake of Copper(II) by Wool. *Textile Res. J.*, **75**, 203-207.
14. Wortmann, F. J., Augustin, P., Popescu, C. (2001). Temperature dependence of the water-sorption isotherms of wool. *J Appl Polym Sci.*, **79**, 1054-1061.
15. Carr, C. M., Evans, J. C., Roberts, W. (1987). An X-Ray Photoelectron and Electron Spin Resonance Study of Wool Treated with Aqueous Solutions of Chromium and Copper Ions. *Textile Res. J.*, **57**, 109-113.
16. Kobot, S. (1993). Sites for Cu(II) Stabilization in Wool Keratin. *Textile Res. J.*, **63**, 159.
17. Chou, S. F., Overfelt, R. A. (2011). Tensile deformation and failure of North American porcupine quills. *Materials Science and Engineering: C*, **31**, 1729-1736.
18. Bear, R. S. (1944). X-ray diffraction studies on protein fibers. II. Feather rachis, porcupine quill tip and clam muscle. *JACS*, **66**, 2043-2050.
19. Giroud, A., Leblond, C. P. (1951). The Keratinization of epidermis and its derivatives, especially the hair, as shown by X-Ray diffraction and histochemical studies. *Ann. N. Y. Acad. Sci.*, **53**, 613-626.
20. Fraser, R. D. B., MacRae, T. P., Rogers, G. E. (1972). *Keratins, Their Composition, Structure and Biosynthesis*. Springfield, Ill., Thomas Publishers.
21. Busson, B., Engström, P., Doucet, J. (1999). Existence of various structural zones in keratinous tissues revealed by X-ray microdiffraction. *J. Synchrotron Radiat.*, **6**, 1021-1030.
22. Lauri, H. J., Lajunen, P., Perämäki (1992). *Spectrochemical Analysis By Atomic Absorption And Emission*. RSC Publishing.

23. Ebdon, L., Evans, E. H., Fisher, A., Hill, S. J. (1998). *An introduction to analytical atomic spectrometry*. Willey & Sons.
24. Atabey, H., Sari, H., Al-Obaidi, F. N. (2012). Protonation Equilibria of Carminic Acid and Stability Constants of Its Complexes with Some Divalent Metal Ions in Aqueous Solution. *J. Solution Chem.*, **41**, 793-803.
25. Ferreira, E. S. B., McNab, H., Hulme, A. N., Quye, A. (2004). The natural constituent of historical textile dyes. *Chem. Soc. Rev.*, **33**, 329-336.
26. Soubayrol, P., Dana, G., Man, P. P. (1996). Aluminium-27 Solid-State NMR Study of Aluminium Coordination Complexes of Alizarin. *Magn. Reson. Chem.*, **34**, 638-645.
27. Wakley, W. D., Varga, L. P. (1972). Stability constants of tin-pyrocatechol violet complexes from computer analysis of absorption spectra. *Anal. Chem.*, **44**, 169-178.
28. Budesinsky, B. W. (1972). The Complexation of Tin(IV) with Catechol Violet. *Analyst*, **97**, 909-910.
29. Hernández Méndez, J., Moreno Cordero, B., Carabias Martínez, R., Gutiérrez Dávila, L. (1987). Spectrophotometric determination of tin(IV) with catechol violet sensitized with polyvinylpyrrolidone. *Microchem. J.*, **35**, 288-292.
30. Wolfram, L. J., Lindemann, M. K. O. (1971). Some Observations on the Hair Cuticle. *J. Soc. Cosmet. Chem.*, **22**, 839-850.
31. Sakaguchi, I. (1969). Cumulative Tin-Weighting of Silk with Stannic Chloride. *Textile Res. J.*, **39**, 1053-1055.
32. Manhita, A., Ferreira, V., Vargas, H., Ribeiro, I., Candeias, A., Teixeira, D., Ferreira, T., Dias, C. B. (2011). Enlightening the influence of mordant, dyeing technique and photodegradation on the colour hue of textiles dyed with madder - A chromatographic and spectrometric approach. *Microchem. J.*, **98**, 82-90.
33. Moretto, P., Beck, L. (2004). Émission X induite par particules chargées (PIXE): théorie. *Techniques de l'Ingénieur, analyse et caractérisation*, **P2558**, P 2 558 1-17.
34. Calligaro, T., Dran, J. C., Salomon, J. (2004). Ion beam microanalysis. In *Non-destructive Microanalysis of Cultural Heritage Materials*, Janssens, K., Van Grieken, R., Ed. Wilson and Wilson's, Elsevier: 227-276.
35. Beck, L., Pichon, L., Moignard, B., Guillou, T., Walter, P. (2011). IBA techniques: Examples of useful combinations for the characterisation of cultural heritage materials. *Nucl. Instr. Meth. B*, **269**, 2999-3005.
36. Trouslard, P., Trocellier, P. (2002). Spectrométrie de collisions élastiques et de réactions nucléaires. Théorie. *Techniques de l'Ingénieur, analyse et caractérisation*, **P2560**, P 2 560 1-31.
37. Verma, H. R. (2007). *Atomic and Nuclear Analytical Methods*. Springer-Verlag Berlin-Heidelberg.
38. Moretto, P., Beck, L. (2003). Émission X induite par particules chargées (PIXE): applications. *Techniques de l'Ingénieur, analyse et caractérisation*, **P3**, 2557.1-2557.8.

39. Beck, L., Barrandon, J. N. (1991). Non destructive depth profiling using the PIGE technique. *Nucl. Instr. Meth. B*, **61**, 100-105.
40. Mayer, M. (2003). *Rutherford Backscattering Spectrometry (RBS)*. Workshop on Nuclear Data for Science and Technology: Materials Analysis, Max-Planck-Institut für Plasmaphysik - EURATOM Association, Garching, Germany.
41. Reiche, I., Radtke, M., Berger, A., Gärner, W., Merchel, S., Riesemeier, H., Bevers, H. (2006). Spatially resolved synchrotron radiation induced X-ray fluorescence analyses of rare Rembrandt silverpoint drawings. *Appl. Phys. A-Mater*, **83**, 169-173.
42. Beck, L., Jeynes, C., Barradas, N. P. (2008). Characterization of paint layers by simultaneous self-consistent fitting of RBS/PIXE spectra using simulated annealing. *Nucl. Instr. Meth. B*, **266**, 1871-1874.
43. Beck, L., de Viguierie, L., Walter, Ph., Pichon, L., Gutiérrez, P. C., Salomon, J., Menu, M., Sorieul, S. (2010). New approaches for investigating paintings by ion beam techniques. *Nucl. Instr. Meth. B*, **268**, 2086-2091.
44. Beck, L., Cuif, J. P., Pichon, L., Vaubaillon, S., Dambricourt Malassé, A., Abel, R. L. (2012). Checking collagen preservation in archaeological bone by non-destructive studies (Micro-CT and IBA). *Nucl. Instr. Meth. B*, **273**, 203-207.
45. Li, H. K., Akselsson, K. R. (1985). A quantitative basis for hair analysis using PIXE. *Nucl. Instr. Meth. B*, **12**, 248-256.
46. Frey, H. U., Otto, G., Vogt, J. (1988). Thick target PIXE analyses of elemental distributions across the surface and inside human fingernails. *Nucl. Instr. Meth. B*, **30**, 83-89.
47. Sera, K., Futatsugawa, S., Matsuda, K. (1999). Quantitative analysis of untreated bio-samples. *Nucl. Instr. Meth. B*, **150**, 226-233.
48. Calligaro, T., Dran, J.-C., Ioannidou, E., Moignard, B., Pichon, L., Salomon, J. (2000). Development of an external beam nuclear microprobe on the Aglae facility of the Louvre museum. *Nucl Instrum and Meth B*, **161-163**, 328-333.
49. Zahn, H., Wortmann, F. J., Wortmann, G., Schäfer, K., Hoffmann, R., Finch, R. (2000). Wool. In *Ullmann's Encyclopedia of Industrial Chemistry*, Wiley-VCH: 395-421.
50. Masson, P. (1963). Density and Structure of Alpha-Keratin. *Nature*, **197**, 179 - 180.
51. Biersack, J. P., Haggmark, L. G. (1980). A Monte Carlo computer program for the transport of energetic ions in amorphous targets *Nucl. Instr. Meth. B*, **174**, 257-269.
52. Maxwell, J. A., Campbell, J. L., Teesdale, W. J. (1989). The Guelph PIXE software. *Nucl. Instr. Meth. B*, **43**, 218 - 230.
53. Maxwell, J., Weatherstone, A., Campbell, I. (2005). GUPIXWIN Manual. University of Guelph.
54. Gullikson, E. M. (2001). X-Ray Data Booklet, Section 1.6 Mass absorption coefficients. In Thompson, A. C., Vaughan, D., Ed. University of California Press, Berkeley, CA.

55. Pacheco, C. (2007). *Etude de films d'or sur matière vitreuse: Application à la céramique glaçurée Islamique médiévale; Asie Centrale XIV<sup>e</sup>-XV<sup>e</sup> s., Iran XII<sup>e</sup>-XIII<sup>e</sup> s.* Université Michel de Montaigne, Bordeaux III, PhD Thesis.
56. Mayer, M. *SIMNRA: Simulation of RBS, ERD and NRA spectra* (<http://home.rzg.mpg.de/~mam/>), 1996.
57. Pichon, L., Beck, L., Walter, Ph., Moignard, B., Guillou, T. (2010). A new mapping acquisition and processing system for simultaneous PIXE-RBS analysis with external beam. *Nucl. Instr. Meth. B*, **268**, 2028-2033.

# CHAPTER 5



<b>5</b>	<b>INVESTIGATION OF NORTH AMERICAN ATHAPASKAN PORCUPINE QUILL WORK FROM NATIONAL MUSEUMS SCOTLAND.....</b>	<b>204</b>
5.1	HISTORICAL BACKGROUND.....	205
5.1.1	<i>Athapaskan Cultural Group</i> .....	205
5.1.2	<i>Dye sources in Athapaskan porcupine quill work</i> .....	207
5.1.3	<i>Porcupine quill work at National Museums Scotland</i> .....	209
5.1.4	<i>Dyed porcupine quill specimens (Inv. N°: A.848.15)</i> .....	211
5.1.5	<i>Binocular Observation and Sampling</i> .....	213
5.2	DYE ANALYSIS.....	216
5.2.1	<i>Preparation of reference material</i> .....	217
5.2.1.1	Scouring.....	217
5.2.1.2	Dyeing process.....	217
5.2.1.3	Effect of the mordant.....	218
5.2.2	<i>PDA-UPLC conditions</i> .....	219
5.2.2.1	Calibration, LOD and LOQ.....	220
5.2.3	<i>Turmeric</i> .....	222
5.2.3.1	Extraction efficiency and reproducibility.....	223
5.2.3.2	Historical quills (A.848.15).....	225
5.2.4	<i>Cochineal</i> .....	228
5.2.4.1	Porcupine quill extract.....	228
5.2.4.2	Historical quills (A.848.15).....	231
5.2.5	<i>Blue dyes</i> .....	234
5.3	MORDANT ANALYSIS BY MICRO PIXE AND RBS.....	235
5.3.1	<i>Beam dose Q and calibration</i> .....	235
5.3.2	<i>Investigation of reference quills</i> .....	238
5.3.3	<i>Historical samples</i> .....	239
5.3.3.1	Quantification of light elements.....	240
5.3.3.2	Quantification of heavy elements.....	242
5.3.3.3	RBS analysis.....	244
5.3.3.4	Confirmation by ICP-OES.....	246
5.4	DISCUSSION.....	248
5.5	REFERENCES.....	251

## **5 INVESTIGATION OF NORTH AMERICAN ATHAPASKAN PORCUPINE QUILL WORK FROM NATIONAL MUSEUMS SCOTLAND**

Indigenous communities across North America, from the North American Subarctic, Great Lakes region and the Northern Plains, have long used dyed porcupine quills to decorate clothing and basketry. Porcupine quill work was replaced in the nineteenth century by bead work and although quill work continued into the twentieth century it is relatively rare today. There were a multitude of styles and techniques used to decorate garments with quill work,<sup>1, 2</sup> and special care was given to the colour of the porcupine quills to realise the patterns. Today the knowledge on dyeing techniques of porcupine quills is very limited and little is known about the actual dyeing processes and dyes sources used by Native Americans,<sup>3</sup> with only one comprehensive study on the characterisation of the dye sources found in pre-1856 Eastern Woodlands porcupine quill work.<sup>4, 5</sup> This chapter presents the scientific investigation of a group of dyed porcupine quills specimens collected in 1862 from Northern Athapaskans and today found in the collection at National Museums Scotland collection.<sup>6, 7</sup> To the addition of these specimens, a few samples removed during conservation work from contemporaneous Athapaskan objects were added to broaden the study.

In the first part of the chapter, the material investigated will be contextualised, using existing important curatorial research on the Athapaskan cultural group.<sup>2, 8-10</sup> The challenges arising from the investigation of dyed porcupine quill work will be presented with regard to sampling, extraction and dyes analysis. Several natural dyes were characterised by Ultra Performance Liquid Chromatography (PDA-UPLC). These results will be discussed and compared to published data on contemporary Eastern Woodlands quill work. Finally, the concentration of several metallic mordants was characterised by non-invasive Proton Induced X-Ray Emission analysis (PIXE) coupled to Rutherford Backscattering Spectrometry (RBS). The

application of these non-invasive techniques to the study of porcupine quill work is innovative and provided new information on the use of mordant chemicals traded from Europe into North America after contact. This study highlights how European contact impacted on traditional Athapaskan's porcupine quill work and reflects on the important cultural changes that took place in the late nineteenth century.

## 5.1 HISTORICAL BACKGROUND

### 5.1.1 Athapaskan Cultural Group

The term Athapaskan (also written Athabaskan, Athabaskan and Athapascan), refers to both a cultural group and a language family, which includes twenty three native languages.<sup>11</sup> Athapaskans, also called “Dene”, are Native American Indians and can be subdivided into three groups, Northern Athapaskan, Pacific Coast Athapaskan and Southern Athapaskan.<sup>6</sup> Northern Athapaskans represent the majority of Athapaskan people and include the Tlicho, the Gwich'in, the Slavey, and the Chypewyan, all living in the interior of Alaska and Northern Canada (figure 5.1).



**Figure 5.1:** “Denendeh, The Land of the People”, by David Laverie. Reproduced from Thompson, 1994.<sup>10</sup>

Traditionally, before European contact, the Dene harvested the land's resources.<sup>9</sup> They were hunters and fishermen and used animal hides, sinews, bones, porcupine quills, and the bark and roots of the trees, to make clothings, containers, tools, snowshoes and canoes. Northern Athapaskan artefacts are very rare and significant collections include the Canadian Museum of Civilization and National Museums Scotland.<sup>6</sup> Clothing was a very important aspect of Athapaskan culture,<sup>9, 10</sup> clothes and footwear were manufactured from tanned caribou hides and were adapted to the climate of the Sub-arctic. Nevertheless, these clothes were also decorated with sophisticated embroidery using dyed porcupine quills - but also moose hair or goose quills - and fringing (figures 5.2 A-B).<sup>9, 10, 12</sup> There are only a few known pre-contact examples of porcupine quill work, but this was an important form of work, and the earliest garment decorated with porcupine quill work among the Athapaskans is in the Canadian Museum of Civilization and can be dated to circa 1800.<sup>8, 13</sup>



**Figure 5.2:** A: Athapaskan Shirt or tunic of moose leather ornamented with porcupine quills (Inv. N°: A.848.10); B: Athapaskan Moccasins, summer shoes plain, Slave Indians (Inv. N°: A.848.6 and A), © Trustees of National Museums Scotland.

In the late eighteenth century, Dene people started to interact with Europeans and were involved in the fur trade. These contacts initiated a period of rapid cultural changes, which is reflected in the traditional crafts.<sup>8, 10</sup> Soon Athapaskans started to incorporate in their embroidery work glass beads, that they had exchanged against fur with Europeans.<sup>8</sup> Beads were very extremely sought after because they were easier to use and prepare and the European influence can also be observed through the introduction of floral patterns that were mixed with the traditional geometric one.<sup>8, 14</sup> The interest of Athapaskans for traded beads is reported in the testimony from Frederic Wentze, working for the North West Company in the Mackenzie territories in 1814:

*“For two successive years, a pressing demand had been made for beads, it being well understood that the Loucheux tribe would scarcely trade anything else, and for the want of this, their favourite article, they preferred taking back to their tents the peltries they had brought to trade; this neglect must necessarily diminish the amount of returns”.*<sup>15</sup>

### 5.1.2 Dye sources in Athapaskan porcupine quill work

Each area used local vegetable dyes for dyeing porcupine quills, but because Native American Indians did not have a written language, the only information available today on the preparation of porcupine quills is from European observers. A recent review of Native Indians dyeing techniques strengthens that these transcriptions were often inaccurate or fragmentary.<sup>3</sup> This was explained by the fact that Native people would have kept secret some part of the dyeing process or by a lack of understanding of Europeans, trying to find similarities with European dyeing techniques.<sup>3</sup> One of the most often quoted recipes<sup>1, 3</sup> is part of the ethnographic observation of Daniel Harmon reporting on Sub-arctic people for the years 1810 - 1819.<sup>16</sup> In his journal, Harmon described the preparation of dyed porcupine quills as a process where the quills and dyestuff(s) were boiled together in a “vessel” until the desired colour was reached:

*“The women manifest much ingenuity and taste, in the work which they execute with porcupine quill. The colour of the quills is various, beautiful and durable; and the art of dyeing them is practiced only by females. To colour black, they make use of a chocolate coloured stone, which they burn, and pound fine, and put into a vessel, with the bark of the hazel-nut tree. The vessel is then filled with water, and into it the quills are put, and the vessel is placed over a small fire, where the liquor in it is permitted to simmer, for two or three hours. The quills are then taken out; and put on a board to dry, and rubbed over with bear’s oil, they become of a beautiful shining black, and are fit for use. To dye red or yellow, they make use of certain roots, and the moss which they find, on a species of the fir tree. These are put, together with the quills, into a vessel, filled with water, made acid by boiling currants or gooseberries in it”.<sup>16</sup>*

Several ethnographical observations on Athapaskans mention natural dyes, tannins or pigments that were used for the preparation of porcupine quill work.<sup>1, 3, 10</sup> These include: hazel-nut bark with a chocolate stone<sup>16</sup> or charcoal<sup>17</sup> for black hues; currants,<sup>16</sup> cranberries,<sup>18</sup> tisavoyanne red<sup>19</sup> (or savoyan<sup>18</sup>) sometime mixed with ochre pigment for red hues;<sup>17</sup> various species of blueberries were used for blue hues,<sup>17</sup> while alder bark<sup>17</sup> and tisavoyanne yellow<sup>19</sup> were used for yellow hues. Frederic Wentze reports on the dyeing and colours of Athapaskan quill work in 1807:

*“The dyes made use of by the Indians to stain porcupine quills and feathers, which are the only thing they stain, are the roots of plant which the Canadians call Savoyan; its colour is of an orange cast. This root, boiled with cranberry, dyes a beautiful light red; the dyes for yellow are another small root which they gather in marshy plains.”<sup>18</sup>*

Red and yellow seemed to be particularly important colours and the first European description of Athapaskan porcupine quill dyeing techniques referred specifically to these two native dye plants “tisavoyanne yellow” and “tisavoyanne red”.<sup>3</sup> These plants correspond respectively to the species *Helleborus trifolius* L. - an alkaloid rich dye plant<sup>20</sup> - and *Galium tinctorium* L. Scop - a type of bedstraw growing in North America<sup>20</sup> - and were characterised as the main dye sources in Eastern Woodlands quill work.<sup>4, 5</sup> Mid-nineteenth century Athapaskan porcupine quill work is

characterised by the use of bands of blue, red and natural colour, produced with natural dye sources (figure 5.3),<sup>8</sup> while later these dyes were replaced by aniline dyes to realise red, purple, pink, orange, yellow and green hues.<sup>8</sup> The replacement of natural dyes by aniline dyes is also reported for the Micmac cultural group living in Nova Scotia, where quill work was prepared with aniline dyes as soon as they became available to Native Indians in the late nineteenth century.<sup>21</sup> Colours in Athapaskan motifs are usually used equally with each colour layer being three stitches wide. A standard Athapaskan motif such as the diamond is repeated in rows and the colours, including pinks, purples, and bright yellows, distinguish this work from that of the Algonkian.<sup>8</sup>



**Figure 5.3:** Athapaskan fringe for a woman's dress of tanned caribou skin cut into thongs which are wrapped in alternate pairs with red, blue and white porcupine quills to give a netted effect and strung with white beads (Inv. N°: A.848.13), © Trustees of National Museums Scotland.

### 5.1.3 Porcupine quill work at National Museums Scotland

National Museums Scotland (NMS) has the oldest and most extensive collection of nineteenth century Dene artifacts in the world today.<sup>6, 7, 22, 23</sup> The Athapaskan

collection was collected between 1858 and 1862 and strongly reflects on the history of National Museums Scotland and how ethnographical and scientific collections were build-up in the mid-nineteenth century, but it is also a testimony to the interaction of Scotland with the rest of the world.

The Royal Museum, a precursor of NMS, was founded in 1854 under the title of the Industrial Museum of Scotland, and its first director was Professor George Wilson (1818-1859).<sup>6</sup> George Wilson was an enthusiastic chemist, who also held the chair in Technology at the University of Edinburgh, and was passionate about public education.<sup>24, 25</sup> Iconic scientific items collected by George Wilson include the Lyon Playfair and Joseph Black glassware collection, that testify today of the teaching of chemistry at the University of Edinburgh in the early nineteenth century.<sup>26</sup> During an inaugural lecture, delivered at the University of Edinburgh in 1855, George Wilson described his vision for the Industrial Museum of Scotland:

“An Industrial Museum is intended to be a repository for all the objects of useful art, including the raw materials with which each art deals, the finished products into which it converts them, drawings and diagrams explanatory of the processes through which it puts those materials, models or examples of the machinery with which it prepares and fashions them, and the tools which specially belong to it, as a particular craft.”<sup>24</sup>

In 1854, George Wilson sent out a call to Scots overseas to involve them in collecting and sending back to Scotland ethnographical collections. The museum started to collect objects from all over the world including West and South Africa, North and South America, West Indies, China, and the Pacific.<sup>6</sup> The story of how the Athapaskan collection was built up with the support of George Wilson’s brother has been the subject of many publications.<sup>6, 7, 23</sup> Daniel Wilson, a Professor at the University of Toronto was able to get the support of Sir George Simpson, Overseas Governor of the Hudson’s Bay Company, who forwarded Wilson’s call to employees working in remote trading posts in Canada.<sup>6</sup> Scots working for the Hudson’s Bay Company were involved in the fur trade and collecting Natural Sciences specimens,



contributing to the development of the renowned collection of the Smithsonian Institution.<sup>27, 28</sup> On behalf of National Museums Scotland they also collected, hundreds of objects (mainly Athapskan but also Inuit), and the NMS collection today includes around 240 Athapaskan artifacts.<sup>23</sup>

The main contributor to National Museums Scotland collection was Bernard Rogan Ross,<sup>6, 23</sup> who was a chief trader at Fort Simpson from 1858 to 1862 and in charge of the Mackenzie River District.<sup>23</sup> Ross had a particular interest in porcupine quill work and as a result, collected both final artifacts but also the raw materials that were used to produce them, making the NMS collection particularly significant today. Ross also collected porcupine quill work that is today part of the National Museum of the American Indian collection (Smithsonian Institution), these materials offer an interesting parallel to the collection of National Museums Scotland.<sup>23</sup>

#### 5.1.4 Dyed porcupine quill specimens (Inv. N°: A.848.15)

As part of the development of new galleries at NMS, several Athapaskan artifacts were conserved and this gave the opportunity for an in-depth study of these materials. The characterisation of the dyestuffs used for the production of the objects is crucial in order to understand their behaviour to display conditions and to determine the regimes which will minimise damage, especially with regard to the fading of the porcupine quill work. Due to the limited knowledge of dye extraction from porcupine quill substrates,<sup>5</sup> it was decided to develop an analytical approach focusing on the raw materials collected in 1862 by Bernard Ross.<sup>7, 29</sup> These materials will be investigated for the first time; questions raised in the past regarding the nature of the dyestuffs used to produce the vivid shades of red and blue will be addressed. For example in the 1974 catalogue on the Athapaskan collection, McFadyen Clark described the quills samples as:

“Natural, and some coloured in red and blue with European aniline dyes”.<sup>29</sup>

On the black and white photography shown in the 1974 Athapaskan catalogue, the porcupine quill samples, appear bundled in little groups and associated with other raw materials described as goose quills and moose hair, also said to be dyed with European aniline dyes.<sup>29</sup> The use of aniline dyes already in 1862 in North America would be quite peculiar, even taking into account the existing trade between Europe and Canada with the Hudson Bay Company. Indeed, at that time in Europe, mauvein (1856) and fuchsine (1858) would have been just discovered and synthesised from the coal tar industry (chapter 1, section 1.2.4).<sup>30</sup> In order to shed more light on the nature of the samples it was necessary to refer back to their original description from the museum registry book, when they were given an accession number in 1862:

848, October 24<sup>th</sup> 1862 - North American Indian Specimens

Entry 15: porcupine quills from *Erithezon epi(s)canthus*, yellow species, European dyes, Slave Indians

- a) White
- b) Dark Blue dyed with indigo
- c) Light Blue dyed with Indigo
- d) Dark green from Indigo and Turmeric
- e) Light Green from Indigo and Turmeric
- f) Yellow with Turmeric
- g) Orange
- h) Scarlet dyed with Cochineal

Entry 17: dyed goosed quills for embroidery shoes, Slave Indians

Entry 18: Moose Deer Hair, plain and dyed for embroidering fringes belts, Slave Indians

The NMS registry book (1858-1861) provided some interesting information and showed that not only dyed porcupine quills but also specimens of goose quills and moose hair were collected from Athapaskans in 1862. The porcupine quill samples

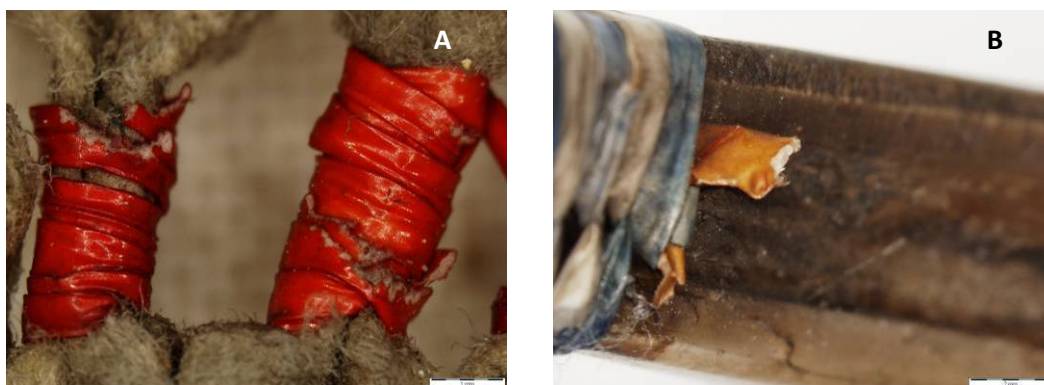
were registered under the entry 15 (A.848.15) and were described by colour with some information on their dyeing processes. Several natural dyes were specifically named: turmeric, indigo and cochineal. There was however, no mention of the colours or the dyes used to prepare the samples of goose quills and moose hair (Inv. N°: A.848.17 and A.848.18). From this description it does seem clear that these dyes originally described as “European” dyes were all natural dyes but traded from Europe into North America - probably through the Hudson Bay Company - which was later wrongly transcribed as European aniline dyes.

#### 5.1.5 Binocular Observation and Sampling

Due to some relocation of the ethnographical collection from National Museums Scotland to a new storage area at the National Museums Collection Centre, it was not possible to access the samples of goose quills and moose hair, so these are not included in this study. As a result, and also due to time constraints, a sub-set of porcupine quills was selected for both dye and mordant analysis, together with around ten micro-samples removed during conservation work from a small group of Athapaskan artifacts. The investigation of these samples allowed a direct comparison of the raw porcupine quill specimens with some of the artifacts manufactured and collected at the same time and will be discussed in the following sections.

The porcupine quill specimens were not found in their original state, but they were grouped by colour in small little transparent boxes, although some boxes contained mixed colours. It was not recorded when this packaging happened, and whether the moose hair samples were now mixed with the porcupine quills samples. Some quills were indeed very thin and could be moose hair, but this would need to be confirmed by a specialist. In order not to disturb the specimens, a label was given to each little box (1 to 19) and a selection of porcupine quills was collected from each box for binocular observation and then analysis.

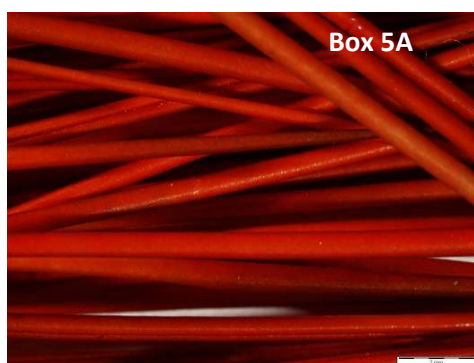
Microscopic observation showed that the colours were very well preserved and that the specimens still exhibited very bright hues. The range of colours is extraordinary, as can be observed in the micrographs below, with various shades of blues, green, orange, yellow, and red; together with very pale quills that could be either un-dyed or more faded than the rest of the materials. In general the porcupine quills appeared very dry and brittle, with several quills being already broken. The dyestuffs were found to be only present on the cuticle layer of the porcupine quills, while the inside of the quills remained un-dyed, this was also observed on several objects (figure 5.4- A and B).



**Figure 5.4:** Binocular micrographs left (A) detail of red porcupine quill work (Inv. N° A.845.13), scale is 1 mm; right (B) detail of orange porcupine quill work (Inv. N° A.480.6), scale is 2 mm.

The main colours in the sample box are red and blue, with a third of the sample box being made of red or orange porcupine quills (figure 5.5, e.g. boxes 5A, 6, 7, 8). The red hues were very bright and intense, and would suggest the use of a specific dyeing process to achieve such a bright effect. Other bright colours included shades of green, blue and yellow. Interestingly, for each bright shade an equivalent colour was found but with a much faded aspect (figure 5.5, e.g. boxes 3 and 18). This would suggest that some of the quills might have been manufactured with the same dyestuffs but using a different metallic mordant. This is particularly noticeable for

the blue quills, with some of the quills exhibiting a very intense homogeneous and bright blue colour, while others exhibited a much darker shade, with a spotty surface aspect that would be expected from indigo dye (figure 5.5, e.g. box 1 and 2). Finally, the sporadic appearance of a small layer of a white salt was also observed on the surface of several quills; but it did not seem to be colour related, as these salt residues were observed on red, orange and blue quills (see figure 5.5, e.g. boxes 2, 6 and 8).



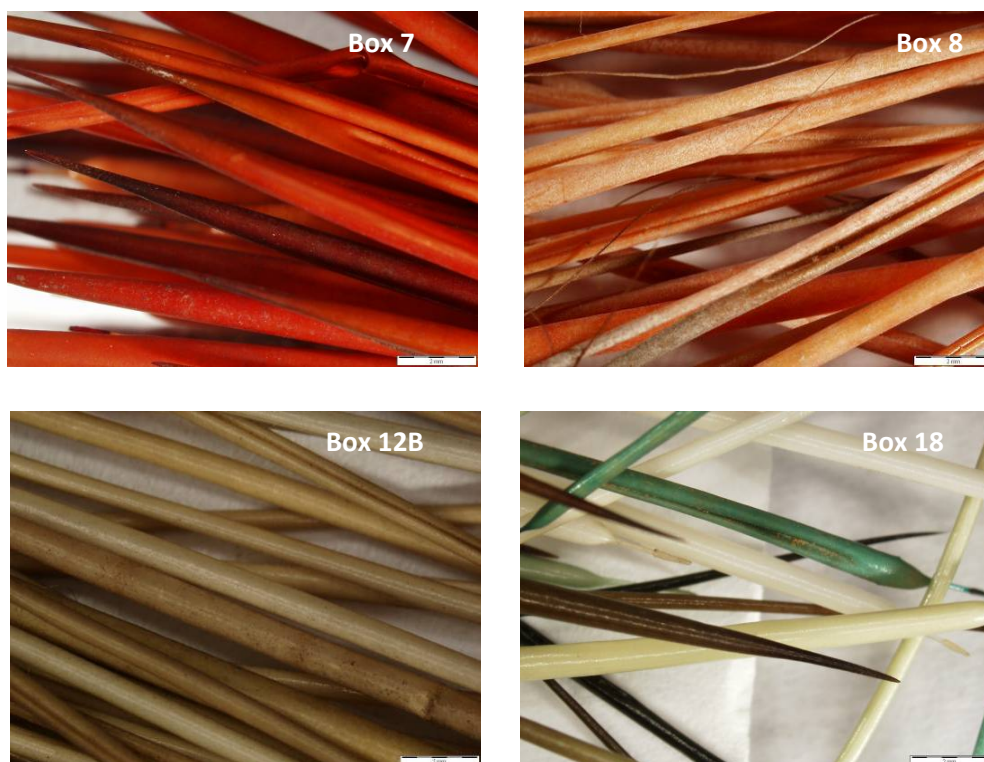


**Figure 5.5:** Examples of dyed porcupine quill specimens collected in 1862 (Inv. N°: A.845.15), for all scale bar is 2 mm.

## 5.2 DYE ANALYSIS

Prior to investigating the historical materials it was necessary to prepare a set of reference materials that could be destroyed during the method development and be used to build-up a reference library for National Museums Scotland. Due to the rarity of information available in the literature on dyeing procedure for porcupine quills, several experiments were undertaken in order to first clean the surface of the porcupine quills and then proceed to their dyeing using a range of natural dyes. The scouring and dyeing processes of porcupine quills will be discussed in the following sections.

## 5.2.1 Preparation of reference material

### 5.2.1.1 Scouring

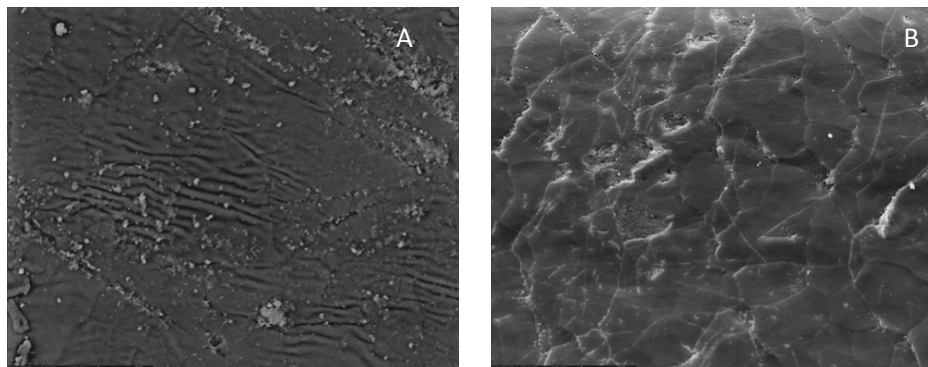
Prior to dyeing, porcupine quills need to be cleaned from the oils that cover their surface, through a degreasing process called scouring. Although there are several recipes available in the literature for scouring wool, no such information is available for porcupine quills. A recent review on Native American dyeing techniques used ashes and calcium for the scouring of porcupine quills, but the effectiveness of the cleaning process was not determined.<sup>3</sup> It was therefore decided to test several cleaning agents including potassium hydroxide soap, potassium bicarbonate and calcium oxide, working at various concentrations and pH (section 7.4). The effect of the cleaning processes was then observed using Scanning Electron Microscopy (SEM-BSC) and treatments showing damage of the surface of the quills were discarded (figure 5.6-A). After scouring, the porcupine quills showed a clean surface with slight lifting of the scales (figure 5.6-B). The best cleaning was achieved under slightly alkaline conditions with a succession of cleaning processes, incorporating the use of calcium oxide and potassium bicarbonate [see Chapter 7, section 7.4.2].

### 5.2.1.2 Dyeing process

The reference materials were prepared with a range of natural dyes including turmeric (*Curcuma longa* L.), Mexican cochineal (*Dactylopius coccus* Costa), weld (*Reseda luteola* L.), dyer's greenweed (*Genista tinctoria* L.) and madder (*Rubia tinctorum* L.), working with various metallic mordants (alum, cream of tartar, copper sulfate and tin(II) chloride). Because vat dyeing is a complicated process, it was decided not to undertake experiments with indigo dye. The best results were provided with quills that had been previously properly cleaned, working with an excess of dyestuff (typically 3:1 w/w of dry fibre) and at a temperature of 85 – 90 °C. In order to reproduce closely the process of porcupine quills dyeing described in



European transcriptions,<sup>3</sup> it was decided to proceed with a single dyebath, mixing the metallic mordant and the dyestuffs together [see Chapter 7, section 7.4.3].



**Figures 5.6:** Backscattered Electron Micrographs (SEM-BSC): (A) damaged surface of a porcupine quill cuticle after treatment with excess of calcium oxide; (B) cleaned surface of a porcupine quill showing slight lifting of the scales, both scales are 20  $\mu\text{m}$ .

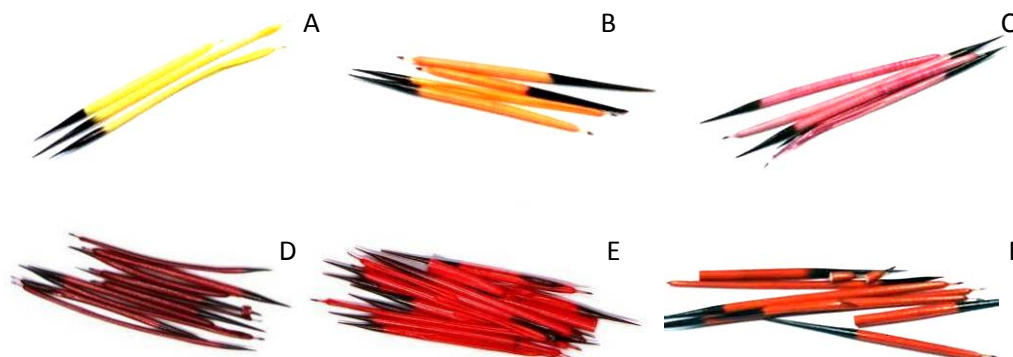


**Figure 5.7:** References porcupine quills: (A) turmeric, (B) mixture of turmeric and cochineal, (C, D, E) cochineal at various concentration and mordant and (F) madder.

### 5.2.1.3 Effect of the mordant

The effect on the final colour of cochineal prepared with various mordants is shown in the microscopic observations below (figure 5.8). At lower concentration cochineal provided with alum a pale pink colour (A, PQ7, section 7.4.3), while using a more



concentrated dyebath it provided a stronger pink hue (B, PQ8a, section 7.4.3), which was shifted to a red hue with the addition of cream of tartar (C, PQ8b, section 7.4.3). Finally, the use of a combination of alum, cream of tartar and tin (II) chloride provided a bright scarlet hue similar to what was observed in the sample box (D, PQ8c, section 7.4.3).

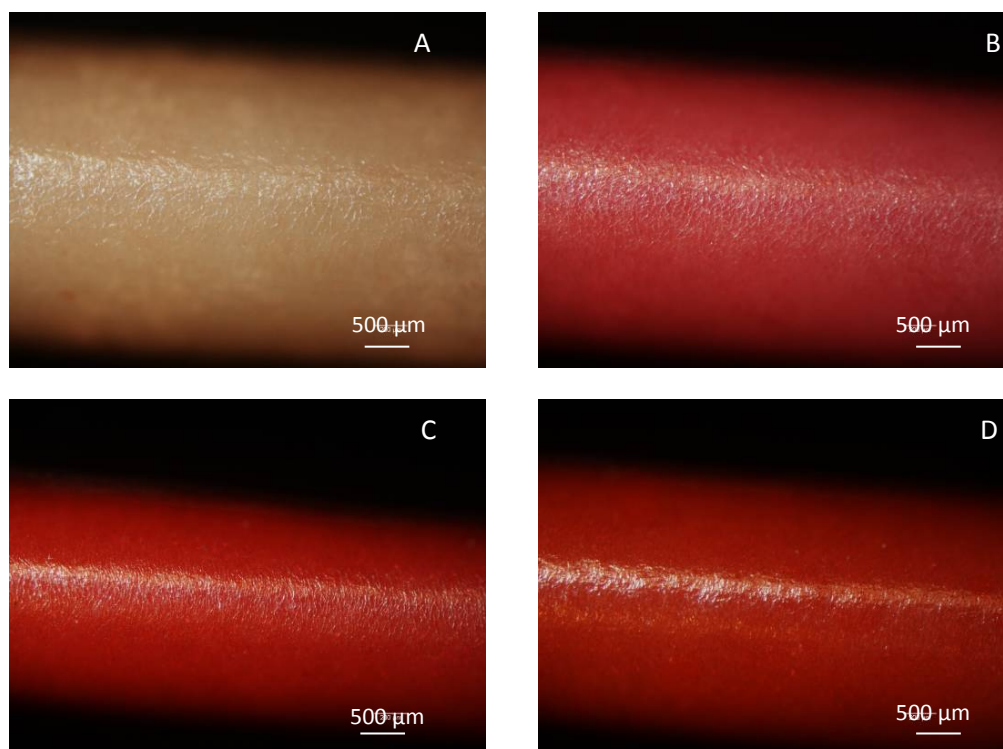


**Figure 5.8:** Microscopic observation of reference porcupine quills: dyed with cochineal and different mordants. (A) cochineal PQ7 ; (B) cochineal PQ8a; (C) cochineal PQ8b; (D) cochineal PQ8c. For all scale is 500  $\mu\text{m}$ .

### 5.2.2 PDA-UPLC conditions

From previous microscopic observations, it was clear that the investigation of porcupine quill work would be challenging, as only the thin outer cuticle layer contains dyestuffs for extraction and analysis. Furthermore, sampling porcupine quill work is far more complicated than historical textiles, where the back of an

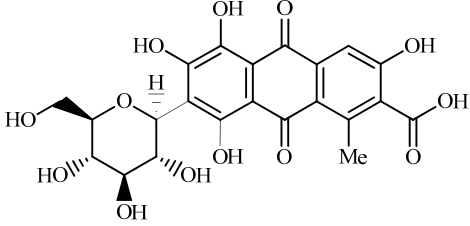
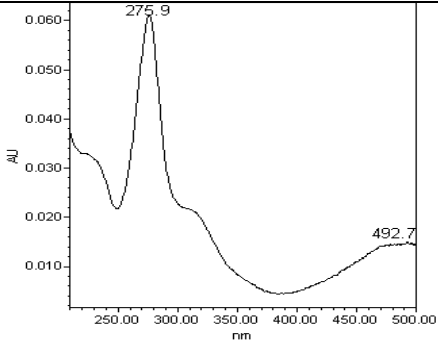
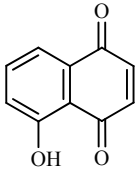
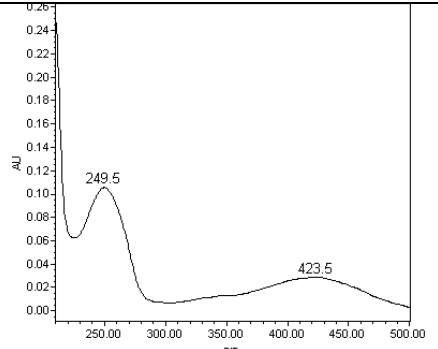
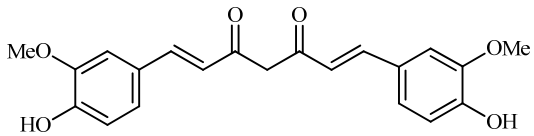
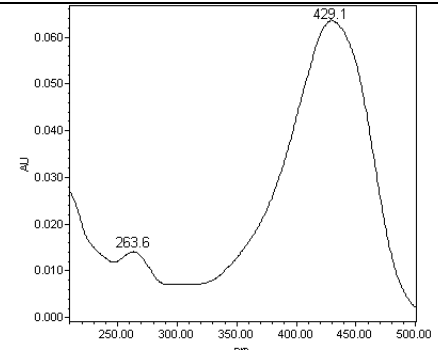
object often offers the possibility to easily sample a small thread of wool or silk. Several micro-samples (< 1 mg) could be removed during conservation work, but characterising such small samples would be very challenging using conventional chromatographic techniques (figure 5.9). For these reasons, Ultra High Performance Chromatography (PDA-UPLC) was the best suited technique, as the method developed for the investigation of historical tapestries proved to be robust for the separation of the natural dyes and offered a limit of detection as low as 1.5 to 0.3 ng (chapter 2).



**Figure 5.9:** Small fragment of red porcupine quill removed during conservation work (inv N° A.845.13), scale is 1 mm

#### 5.2.2.1 Calibration, LOD and LOQ

In addition to carminic acid (**33**), which was calibrated previously, two extra dyestuffs were used to calibrate the UPLC system: curcumin (**1**) and juglone (**90**), the latter being a source of tannin, that was predominantly characterised in Eastern Woodlands porcupine quill works.<sup>5</sup> Due to the range of the PDA detector on the UPLC system (200 – 500 nm), limited investigation could be undertaken of the blue dyes, this would need to be further investigated using a conventional HPLC system at National Museums Scotland, but could not be performed during this research.

 <p style="text-align: center;"><b>33</b> <b>carminic acid</b></p> <p style="text-align: center;"><math>M_W = 492.38 \text{ g mol}^{-1}</math> <math>R_t = 5.788 \pm 0.116 \text{ min}</math> <math>\lambda_{\text{max}} = 276, 312 \text{ (s)}, 493 \text{ nm}</math></p>	
 <p style="text-align: center;"><b>90</b> <b>Juglone</b></p> <p style="text-align: center;"><math>M_W = 174.16 \text{ g mol}^{-1}</math> <math>R_t = 12.098 \pm 0.010 \text{ min}</math> <math>\lambda_{\text{max}} = 249, 330 \text{ (s)}, 408 \text{ (s)}, 424 \text{ nm}</math></p>	
 <p style="text-align: center;"><b>1</b> <b>curcumin</b></p> <p style="text-align: center;"><math>M_W = 368.38 \text{ g mol}^{-1}</math> <math>R_t = 20.407 \pm 0.009 \text{ min}</math> <math>\lambda_{\text{max}} = 264, 429 \text{ nm}</math></p>	

**Table 5.1:** Standards of carminic acid, juglone and curcumin used for the calibration of UPLC system.

The system used Method C developed in chapter 2, working with a BEH C18 reverse phase column, 1.7  $\mu\text{m}$  particle size, 150  $\times$  2.1 mm (length  $\times$  i.d.), set-up with in-line filter (see section 7.4 for chromatographic conditions). The retention times, limit of

detection (LOD) and limit of quantification (LOQ) obtained for these standards are presented in the table 5.2.

Compound (x)	Retention time	LOD $\pm$ s (ng)	LOQ $\pm$ s (ng)
	R <sub>t</sub> $\pm$ s (min)		
	[n=12]		
carminic acid <b>33</b> (430 nm)	5.788 $\pm$ 0.116	7.02 $\pm$ 1.40	21.27 $\pm$ 4.23
juglone <b>90</b> (254 nm)	12.098 $\pm$ 0.010	2.20 $\pm$ 0.09	6.65 $\pm$ 0.26
curcumin <b>1</b> (450 nm)	20.407 $\pm$ 0.009	3.99 $\pm$ 0.19	12.08 $\pm$ 0.56

**Table 5.2:** Retention time variability, LOD and LOQ values using UPLC Method C, based on the slopes (S) of the calibration curves (concentration [x] ( $\mu\text{g mL}^{-1}$ ) vs. height (H<sub>x</sub>, AU) and the baseline noise H<sub>noise</sub> of sample blanks analysed (s) - at 254 nm (juglone), 430 nm (carminic acid) and 450 nm (curcumin). [Data compiled from chapter 7, section 7.4.4, tables 7.49 and 7.50].

### 5.2.3 Turmeric

Turmeric is a mixture of three diarylheptanoids: curcumin (**1**), demethoxycurcumin (**2**) and bisdemethoxycurcumin (**3**), chapter 1. It is well known that these dyes are easily degraded during a strong acidic extraction with concentrated hydrochloric acid.<sup>31</sup> As a result, two alternative extractions protocols were tested for the analysis of turmeric extracts. The first extraction used a published “mild” acidic solution of trifluoroacetic acid (TFA), while the second extraction used dimethyl sulfoxide (DMSO), following a published protocol originally developed for the investigation of safflower dye.<sup>32, 33</sup> The reproducibility and efficiency of both extractions were tested using porcupine quill reference PQ6 dyed with turmeric [see Chapter 7, section 7.4.5, table 7.51].

### 5.2.3.1 Extraction efficiency and reproducibility

The extraction method using trifluoroacetic acid was found to be less effective than dimethyl sulfoxide (DMSO), which extracted more of the dyestuffs and was also found to be more reproducible (figure 5.10).

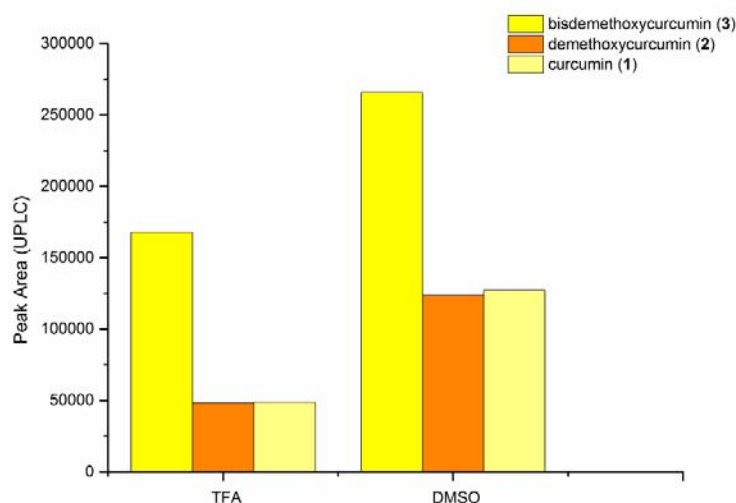


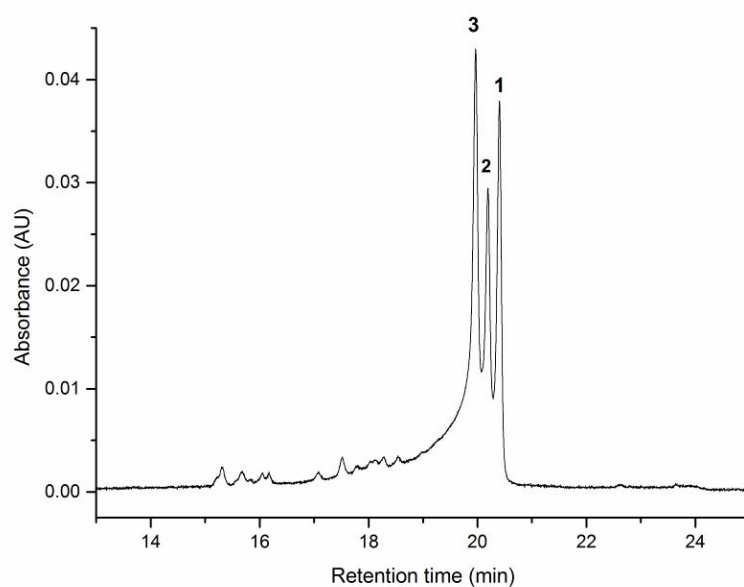
**Figure 5.10:** Comparing the peak areas of diarylheptanoids extracted from reference PQ6 (1 mg) using TFA and DMSO methods, monitored at 450 nm. [Data compiled from chapter 7, section 7.4.5, table 7.51].

	Relative Amount: average $\pm$ s (%), n=5, at 450 nm		
	bisdemethoxycurcumin (3)	demethoxycurcumin (2)	curcumin (1)
Porcupine quill (PQ6)	59.0 $\pm$ 9.1	20.7 $\pm$ 3.2	20.2 $\pm$ 5.9

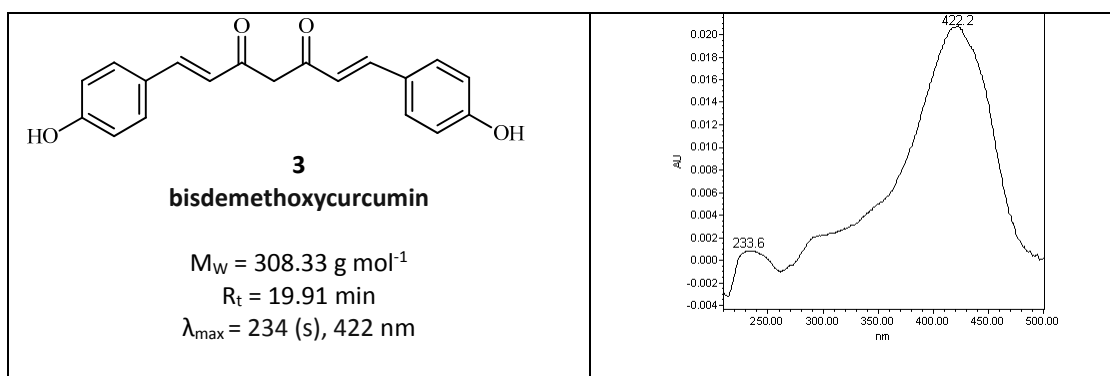
**Table 5.3:** Average relative amount of the diarylheptanoids extracted from 1 mg of porcupine quill PQ6 dyed with turmeric, using a DMSO extraction method, monitored at 450 nm. [Data compiled from chapter 7, section 7.4.5, table 7.52].

The main component extracted from the porcupine quill reference PQ6 was found to be systematically bisdemethoxycurcumin (**3**,  $R_t = 19.91$  min, [ $\lambda_{\max} = 234$  (s), 422 nm]), which averaged 59 % of the total amount of the diarylheptanoid dye extract, while demethoxycurcumin (**2**,  $R_t = 20.15$  min, [ $\lambda_{\max} = 226$  (s), 426 nm]) and

curcumin (**1**,  $R_t = 20.36$  min, [ $\lambda_{\max} = 233$  (s), 428 nm]) averaged respectively 20.7 % and 20.2 % (table 5.3). The extraction with DMSO was however found to be less reproducible than the concentrated hydrochloric acid method, and the extracts exhibited a higher standard deviation that could be due to the poor baseline separation. This lower reproducibility was however also reported using the mild trifluoroacetic acid procedure for a study of historical textiles dyed with turmeric.<sup>32</sup>



**Figure 5.11:** Chromatogram of the DMSO extract of the diarylheptanoids from reference porcupine quill PQ6 dyed with turmeric, monitored at 450 nm [by order of elution: bisdemethoxycurcumin (**3**), demethoxycurcumin (**2**) and curcumin (**1**)].



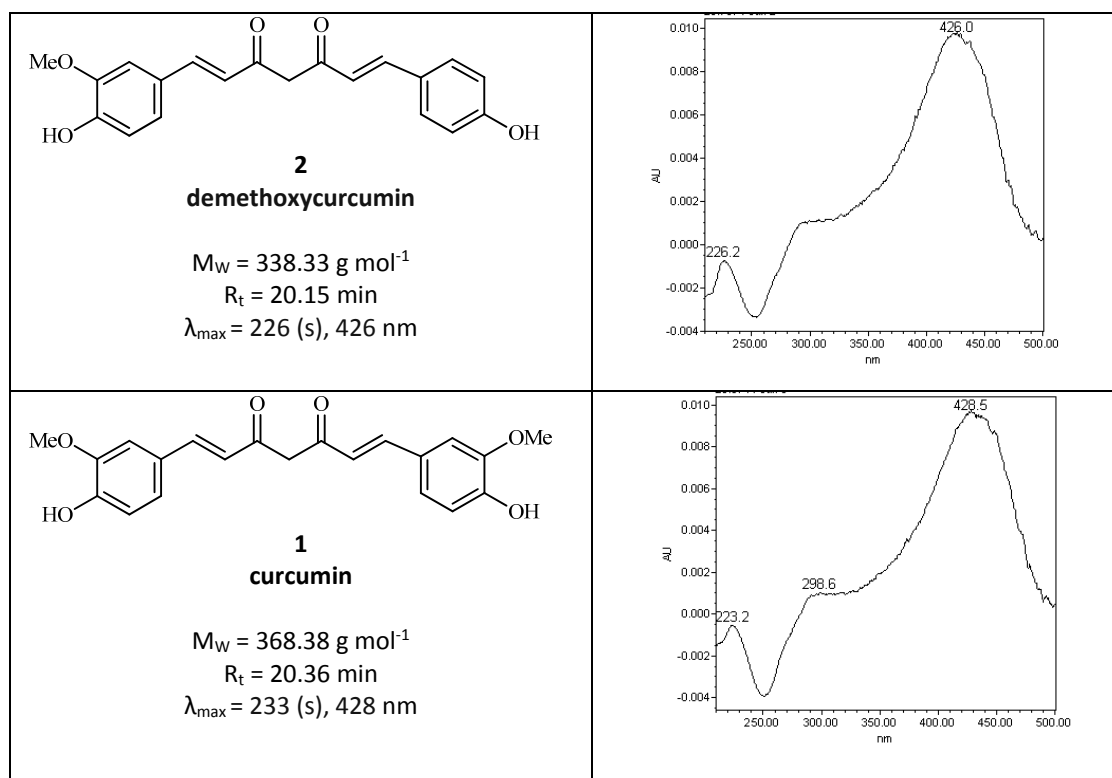


**Table 5.4:** Diarylheptanoids extracted from 1 mg of porcupine quill PQ6, using DMSO, monitored at 450 nm.

### 5.2.3.2 Historical quills (A.848.15)

Thirteen porcupine quills were selected for analysis and extracted using dimethyl sulfoxide. These quills exhibited a range of colour: yellow (pale and bright hues), orange, green (light and dark green) and dark blue. Curcumin (**1**,  $R_t = 20.36 \text{ min}$ , [ $\lambda_{\max} = 233 \text{ (s)}, 428 \text{ nm}$ ]), demethoxycurcumin (**2**,  $R_t = 20.15 \text{ min}$ , [ $\lambda_{\max} = 226 \text{ (s)}, 426 \text{ nm}$ ]) and bisdemethoxycurcumin (**3**,  $R_t = 19.91 \text{ min}$ , [ $\lambda_{\max} = 234 \text{ (s)}, 422 \text{ nm}$ ]) were characterised in all the extracts, with the exception of a dark blue quill which exhibited a high level of tannins (ellagic acid). Turmeric was found to be associated with cochineal (carminic acid, **33**) in the orange samples, while it was mixed with an unidentified blue dye for the shades of green. Four samples exhibited an unknown component, eluting at 7.4 min and named unknown 1 (figure 5.12). This component exhibited three absorption maxima  $\lambda_{\max}$  at 234, 300 and 438 nm and was observed in

light green and yellow porcupine quills. It could possibly correspond to an alkaloid component, although the UV/Visible spectra did not match close enough to those of berberine (**5**,  $\lambda_{\text{max}} = 230, 266, 348, 431 \text{ nm}$ ) or sanguinarine (**6**,  $\lambda_{\text{max}} = 234, 281, 329, 350 \text{ (sh)}, 400, 474 \text{ nm}$ ), that were characterised in a study on Eastern Woodland quill work,<sup>5</sup> to allow a positive identification as either of those.

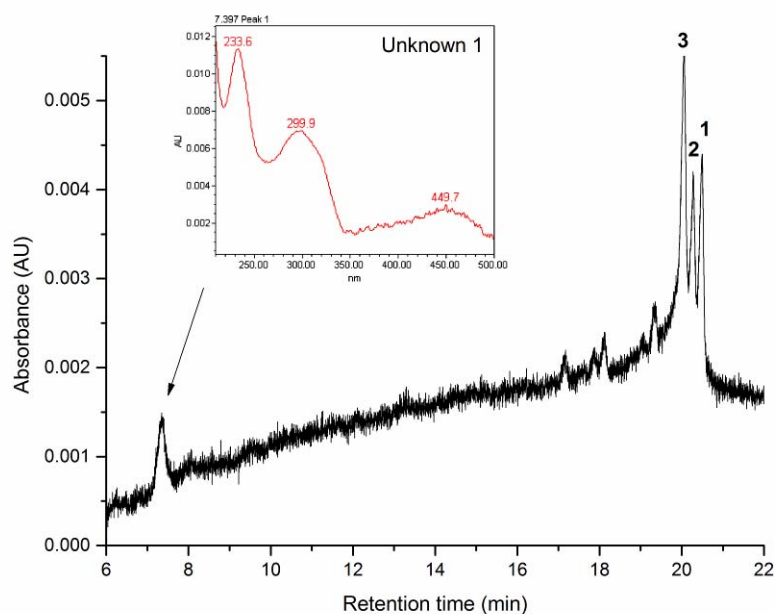


**Figure 5.12:** UPLC chromatogram of the DMSO extract of a yellow porcupine quill (A.845.15 Box 4), monitored at 450 nm [by order of elution: unknown 1, bisdemethoxycurcumin (**3**), demethoxycurcumin (**2**) and curcumin (**1**)].

Most of the historical quills exhibited a close composition to the extract from porcupine quill reference PQ6, prepared with commercial turmeric. The amount of bisdemethoxycurcumin ranged between 43 and 60 %, but a few samples exhibited a lower level of bisdemethoxycurcumin (figure 5.12). It is not possible to relate these compositions to a source of turmeric, although the historical quills were found to be closer to Indian turmeric, because published studies on turmeric rhizomes showed that the diarylheptanoid contents are very variable.<sup>34, 35</sup> Furthermore, the affinity of the three diarylheptanoids with the porcupine quill substrate is unknown and will



greatly affect the dye profile after extraction. As a general observation, curcumin (**1**) is the main component present in most of the turmeric species, while bisdemethoxycurcumin (**3**) is always characterised as the main component in the porcupine quill extract, which could be explained by a higher affinity for the quill substrate.

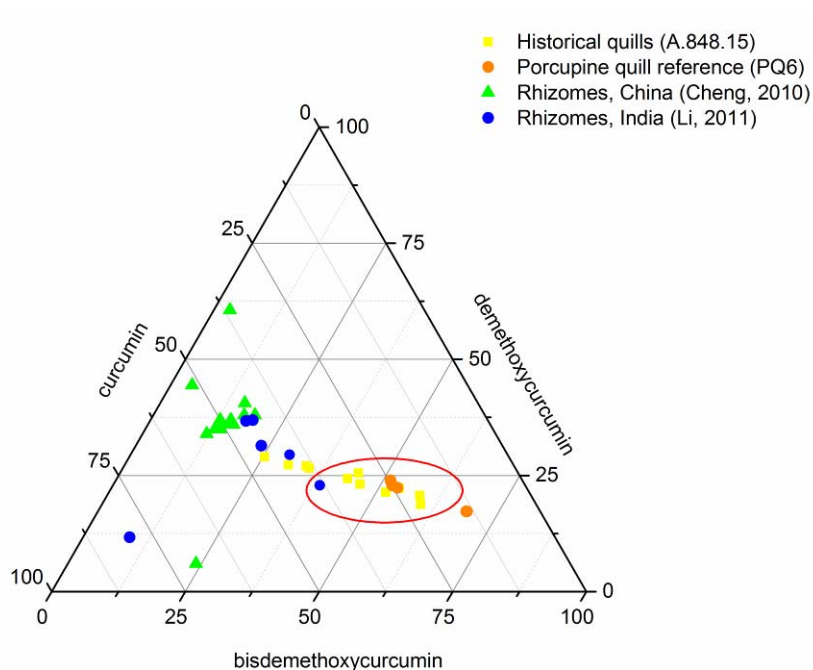


**Figure 5.12:** Ternary diagram of the relative amounts of bisdemethoxycurcumin (**3**), demethoxycurcumin (**2**) and curcumin (**1**) characterised in DMSO extracts of reference porcupine quill PQ6 and historical quills A.848.15. The composition of the extract is compared to the rhizome composition of *Curcuma Longa* L. from China and India (Cheng et al., 2010 and Li et al., 2011).<sup>34, 35</sup> [Data compiled from Chapter 7, section 7.4.5, tables 7.52 and 7.53].

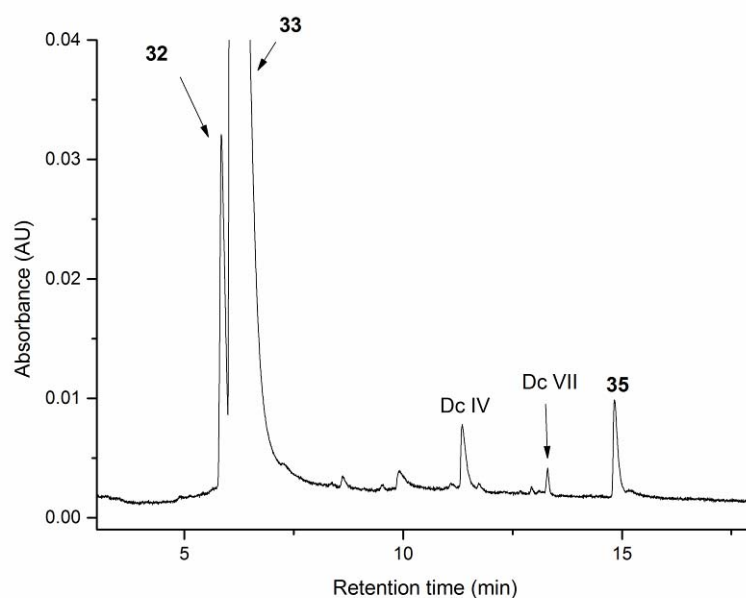
## 5.2.4 Cochineal

### 5.2.4.1 Porcupine quill extract

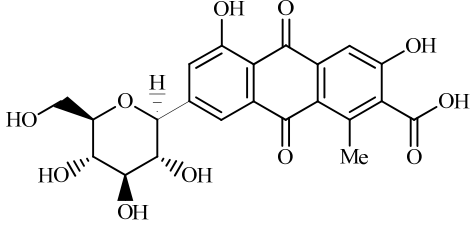
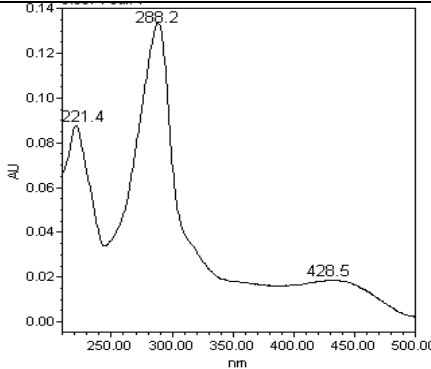
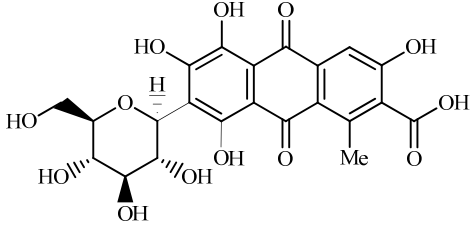
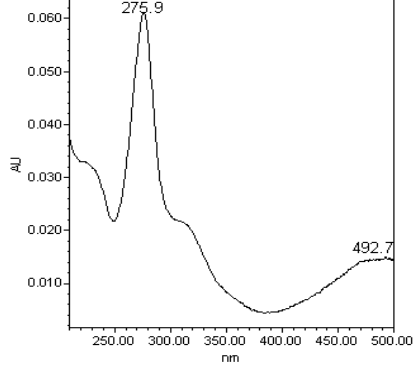
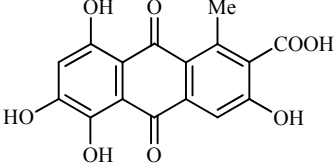
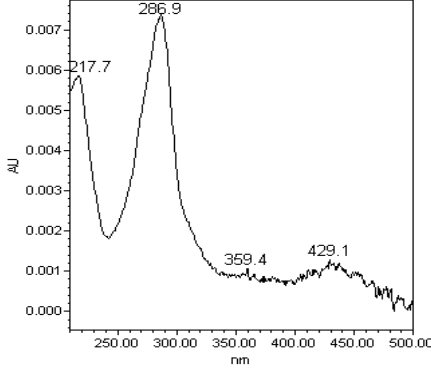
Although the major colouring component characterised in the acid hydrolysed extract of yarns dyed with red insect dyes is often carminic acid (**33**), minor constituents can be characteristic of a particular species. These specific “marker components” can then be compared with those from freshly dyed reference materials, and indicate the use of particular biological sources. It is well established that the identification of cochineal species in historical textiles can be based on a graphical system involving the integration of peak areas from three minor markers DcII (**32**), flavokermesic acid (**35**) and kermesic acid (**34**),<sup>36, 37</sup> with the minor component Dc II (**32**) usually found in an amount of 2 to 4 % in wool yarns and 1 to 2 % in silk yarns dyed with *Dactylopius Coccus* Costa.<sup>38</sup>

Prior to investigating historical porcupine quills, a reference quill dyed with American cochineal (*Dactylopius Coccus* Costa) was extracted using a strong hydrochloric acid solution in order to characterise its dye profile (see section 7.4). The main component characterised in the acid hydrolysed extracts of porcupine quill was carminic acid (**33**,  $R_t = 6.12$  min, [ $\lambda_{\max} = 276, 312$  (s), 493 nm]) associated with a small amount of the components Dc II (**32**,  $R_t = 5.86$  min, [ $\lambda_{\max} = 289, 429$  nm]), Dc IV ( $R_t = 11.43$  min, [ $\lambda_{\max} = 276, 312$  (s), 496 nm]), and flavokermesic acid (**35**,  $R_t = 14.98$  min, [ $\lambda_{\max} = 287, 430$  nm]). The other minor components, Dc VII and kermesic acid (**34**), reported to occur in *Dactylopius Coccus* Costa extracts were found to be below the limit of detection at 275 nm but traces of Dc IV (< 0.4 %;  $R_t = 13.30$  min) was detected at 430 nm (figure 5.14). Notably, the acid hydrolysed extracts of the reference porcupine quill exhibited some slight differences in composition to that of wool or silk, with the minor component Dc II being present in an amount ranging between 5 to 9 %, while flavokermesic acid was found to be present in an amount of 1.9 % (table 5.6). These compositions are clearly out of the range offered by Wouters and Verhecken for *Dactylopius Coccus* Costa extracts (figure 5.15).<sup>36, 39</sup> These differences could be explained by the nature of the

porcupine quill substrate, inducing a different uptake of the cochineal dye during the dyebath process. In support to this, it is worth noting that Dc II (**32**) and flavokermesic acid (**35**) are related compounds; as a recent study showed that the minor component Dc II is likely to be a 7-C-glycoside of flavokermesic acid.<sup>40</sup> Finally, it was also found, that the composition of the acid hydrolysed extract of the reference porcupine quill material was more variable, which could be due to the porcupine quill substrate being less homogeneous than wool.



**Figure 5.14:** UPLC chromatogram of the acid hydrolysed extract of porcupine quill reference (PQ Sn  $100 \mu\text{g mL}^{-1}$ ) dyed with American cochineal, monitored at 430 nm [by order of elution: Dc II (**32**), carminic acid (**33**), minor component Dc IV, Dc VII and flavokermesic acid (**35**)].

 <p><b>32</b> <b>Dc II</b></p> <p><math>M_w = 477.38 \text{ g mol}^{-1}</math> <math>R_t = 5.86 \text{ min}</math> <math>\lambda_{\text{max}} = 289, 429 \text{ nm}</math></p>	
 <p><b>33</b> <b>carminic acid</b></p> <p><math>M_w = 492.38 \text{ g mol}^{-1}</math> <math>R_t = 6.11 \text{ min}</math> <math>\lambda_{\text{max}} = 276, 312 \text{ (s)}, 493 \text{ nm}</math></p>	
 <p><b>35</b> <b>flavokermesic acid</b></p> <p><math>M_w = 346.25 \text{ g/mol}</math> <math>R_t = 14.98 \text{ min}</math> <math>\lambda_{\text{max}} = 287, 430 \text{ nm}</math></p>	

**Table 5.5:** Anthraquinone dyes extracted from 1 mg of porcupine quill reference (PQ Sn  $100 \mu\text{g mL}^{-1}$ ) dyed with American cochineal, monitored at 275 nm and 430 nm.

	Relative Amount: average $\pm$ s (%), n=3					
	Dc II (32)	carminic acid (33)	Dc IV	Dc VII	flavokermesic. acid (35)	kermesic acid (34)
275 nm	7.0 $\pm$ 1.9	88.5 $\pm$ 2.2	2.6 $\pm$ 1.0	nd	1.9 $\pm$ 0.1	nd
430 nm	7.02 $\pm$ 0.7	89.3 $\pm$ 0.8	1.5 $\pm$ 0.1	0.4 $\pm$ 0.1	1.7 $\pm$ 0.1	nd

**Table 5.6:** Averaged relative amounts of the dyestuff compounds in an acid hydrolysed extract of porcupine quill reference (PQ Sn 100  $\mu\text{g mL}^{-1}$ ) dyed with American cochineal, monitored at 275 nm and 430 nm. [Data compiled from Chapter 7, section 7.4.6, table 7.54].

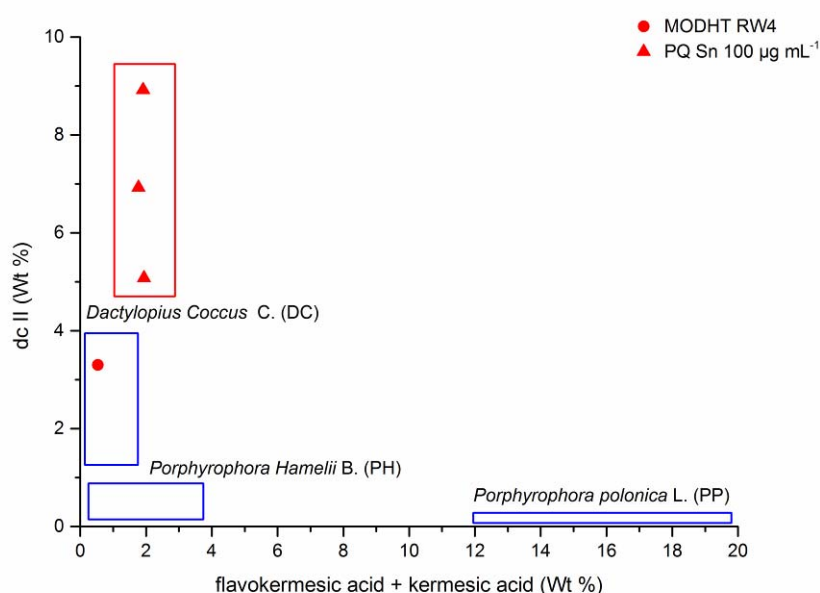


**Figure 5.15:** Graphical representation of the different cochineal dyes species adapted from Wouters and Verhecken 1989, showing the composition of a reference wool extract (MODHT RW5) and the reference porcupine quill extracts, monitored at 275 nm. [Data compiled from Chapter 7, section 7.4.6, table 7.54].

#### 5.2.4.2 Historical quills (A.848.15)

Twenty three porcupine quills were selected for analyses, as well as five micro-samples removed from four objects during conservation (Inv. N°: A.848.12;

A.848.13; A.848.45 and A.848.49), and these were extracted using a strong hydrochloric acid solution. The quills exhibited a range of bright orange and red hues. Carminic acid (**33**,  $R_t = 6.59$  min, [ $\lambda_{\max} = 276, 312$  (s), 493 nm]) associated with the minor component Dc II (**32**,  $R_t = 6.14$  min, [ $\lambda_{\max} = 289, 429$  nm]), was detected in all twenty three samples. In eleven samples the carminic acid (**33**,  $R_t = 6.59$  min, [ $\lambda_{\max} = 276, 312$  (s), 493 nm]) was also associated with a minor amount of flavokermesic acid (**35**,  $R_t = 15.12$  min, [ $\lambda_{\max} = 287, 430$  nm]). The samples were found to contain only small quantities of dyestuff and it was therefore decided to work at 430 nm where the signal to noise was found to be better. This was supported by the fact that the relative amounts of the dye components extracted from the reference quill were found to be very close at 430 nm and 275 nm (table 5.6). The acid hydrolysed extracts were found to be very heterogeneous in composition with the relative amount of Dc II ranging between 5 % and 65 %, while the level of carminic acid ranged between 10 % and 97 %. Only a few samples exhibited similar relative amounts to the acid hydrolysed extract of the porcupine quill reference, but it does seem likely that the historical porcupine quills were dyed with *Dactylopius Coccus* Costa (figure 5.16).

An unknown component eluting at 8.39 min was characterised in sixteen historical quill samples ranging between 1 and 30 % of the total relative amount. This component named unknown 2, exhibited absorption maxima at  $\lambda_{\max} = 228, 281$  and 470 nm and seems clearly related to cochineal dyes. The presence of a maximum absorption peak at 281 nm would suggest that it is related to flavokermesic acid, but this would need to be confirmed further with mass spectrometric studies (figure 5.17). It was also observed that in the porcupine quill extracts, carminic acid eluted systematically later and showed a higher variability in retention time ( $R_t = 5.79 \pm 0.12$  min vs  $R_t = 6.14 \pm 0.60$  min). This was also observed for all the other minor red components (table 5.7). It is possible that the variability in retention time could be due to the presence of a metallic mordant, which would affect the chromatographic

analysis, as it has been reported in a study on carminic lakes that the extracts exhibited longer and more variable retention times.<sup>41</sup>

Retention time $\pm$ s <sub>r</sub> (min), n = 25					
Dc II (32)	carminic acid (33)	unknown 2	Dc IV	Dc VII	flavokermesic acid (35)
6.14 $\pm$ 0.60	6.59 $\pm$ 0.61	8.39 $\pm$ 0.55	11.72 $\pm$ 0.65	13.13 $\pm$ 0.60	15.12 $\pm$ 0.61

**Table 5.7:** Variation in the retention time observed for the analysis of twenty five historical porcupine quills.

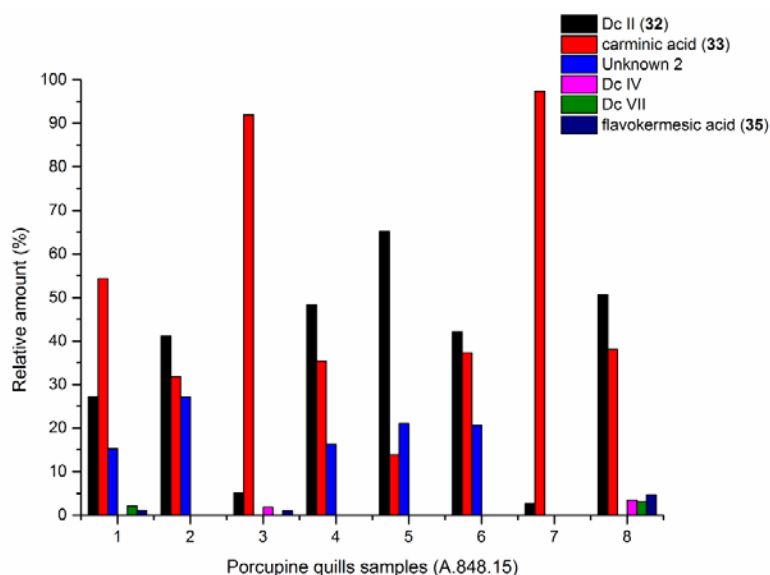


**Figure 5.16:** Relative amount of the dyestuffs characterised in the acid hydrolysed extract of eight red historical porcupine quills, highlighting the high variability in the relative amount of the individual components, monitored at 430 nm. [Data compiled from Chapter 7, section 7.4.6, table 7.55].

Finally; the micro-samples investigated from the objects A.845.13 and A.845.12 showed the presence of carminic acid and Dc II, characterising *Dactylopius Coccus* Costa, while the micro-samples removed from objects A.848.45 and A.848.49

contained minor amounts of alizarin and purpurin, characteristic of a madder species. It is not possible to conclude whether these samples were dyed with a local *Galium* species or imported madder, but in both cases alizarin was found to be the main component present in the acid hydrolysed extracts.

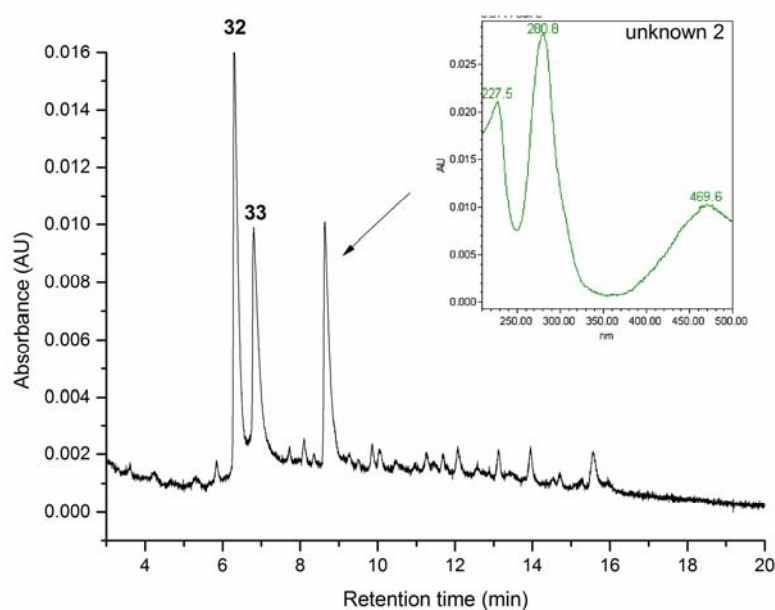


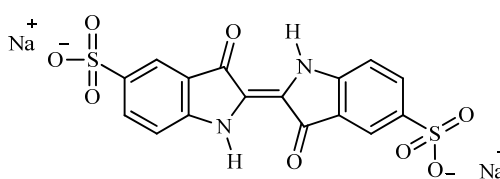
**Figure 5.17:** Chromatogram of the acid hydrolysed extract of porcupine quill A.848.15 Box 2 monitored at 430 nm [by order of elution: Dc II (**32**), carminic acid (**33**), and unknown 2)].

### 5.2.5 Blue dyes

It was not possible to characterise the blue dyes in this study, as the PDA detector of the UPLC system does not allow analysing wavelengths above 500 nm. However, some extraction tests were carried out and showed that the blue dyestuff used to produce the darker shades “spotted” blue hues were insoluble in hydrochloric acid solution but easily extracted with DMSO, suggesting the presence of indigo dyes. However, for the brighter shades of blue, it was found that the blue dye was easily extracted and solubilised in the hydrochloric acid solution, and did not seem to be



affected by the pH change. This would suggest that indigo carmine (**91**), a sulfonated indigo could have been used for the stronger blue hues, but this conclusion would need further chromatographic investigation. Indigo carmine is a blue dye and water-soluble ( $pK_a = 11.4$  and  $13$ ), that was synthesised first in 1743 by Johann Christian Barth and used in Europe from 1770 until the beginning of the twentieth century.<sup>42</sup>



**91**

Indigo carmine

23,3'-dioxo-2,2'-bis-indolyden-5,5'-disulfonic acid disodium salt

$M_w = 466.36 \text{ g mol}^{-1}$

$\lambda_{\text{max}} = 250, 290, 420 \text{ (s)}, 610 \text{ nm}$

### 5.3 MORDANT ANALYSIS BY MICRO PIXE AND RBS

#### 5.3.1 Beam dose $Q$ and calibration

The system was calibrated following the same process as described in chapter 4, with the values of the beam charge  $Q$  and the quantity  $H$  calculated over the set of experiments using a DR-N standard. It was found in the experiments discussed in chapter 4, that although the beam dose  $Q$  was kept to a very low level, some damage due to the irradiation was visible with naked eye on some of the porcupine quills and appeared as a brown spot. It was therefore decided to work at a much lower beam dose  $Q$  for the investigation of historical materials in order to limit, as much as possible, beam damage during irradiation. The beam was found to be much more stable for this set of experiments (figure 5.18) and only minor re-adjustments of the dose  $Q$  were necessary. The beam dose ranged between  $0.00200$  and  $0.00238 \mu\text{C}$  and these values were used to create the parameter file for the quantification of the

porcupine quills; working matrix mode with the matrix defined as keratin using percentage composition by relative weight (Wt %) (table 5.8).

The values obtained for the different elements present in the DR-N standard were quantified for both low and high energy detectors (LE and HE) and compared to their theoretical values (figures 5.18 and 5.19). The parameter files used for the low energy detector (LE) did not allow a good quantification of several light elements including magnesium, aluminium and silicon that were systematically over-estimated, but provided similar quantification of the elements potassium, calcium, phosphorus, titanium, manganese and iron to that which was obtained with the high energy detector (HE).

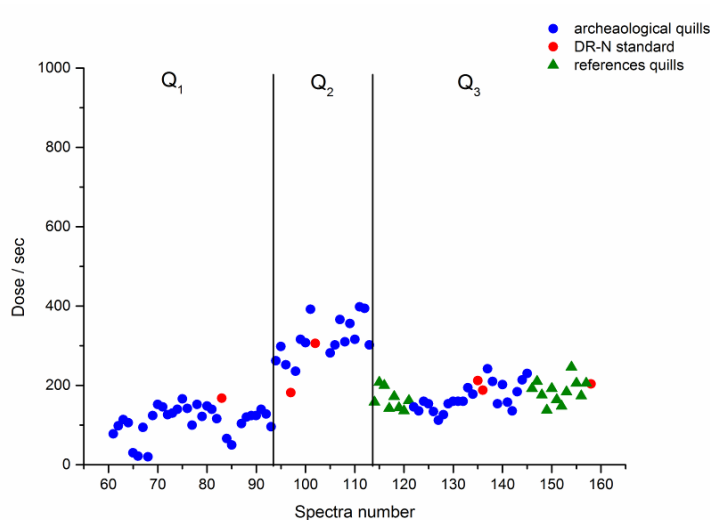


**Figure 5.17:** Evolution of the dose / sec during the analysis. A DR-N standard was analysed regularly in order to calculate the beam charge  $Q$ . [Data compiled from Chapter 7, section 7.4.7, table 7.56].

	Entry 61 to 93	Entry 94 to 113	Entry 114 to 157
Low Energy (Be, 125 $\mu\text{m}$ )	Q1: 0.00238 $\mu\text{C}$ H: 0.063	Q2: 0.00270 $\mu\text{C}$ H: 0.063	Q3: 0.00230 $\mu\text{C}$ H: 0.063
High Energy (28.5 mm air)	Q1: 0.00238 $\mu\text{C}$ H: 1	Q2: 0.00200 $\mu\text{C}$ H: 1	Q3: 0.00215 $\mu\text{C}$ H: 1

**Table 5.8:** Values of the beam dose  $Q$  and the quantity  $H$  for the different segments of the experiments, as shown in figure 5.17.

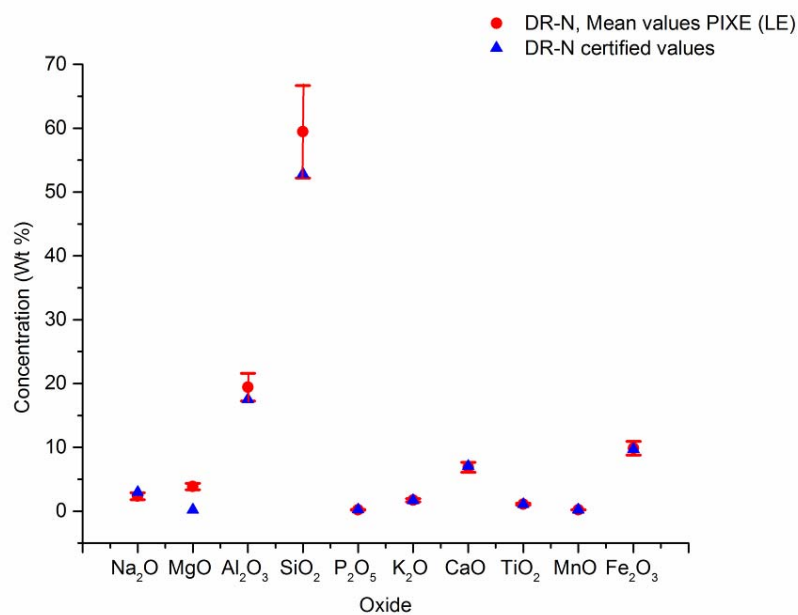


**Figure 5.18:** Quantification of the DR-N standards using the low energy detector. [Data compiled from Chapter 7, section 7.4.7, table 7.57].

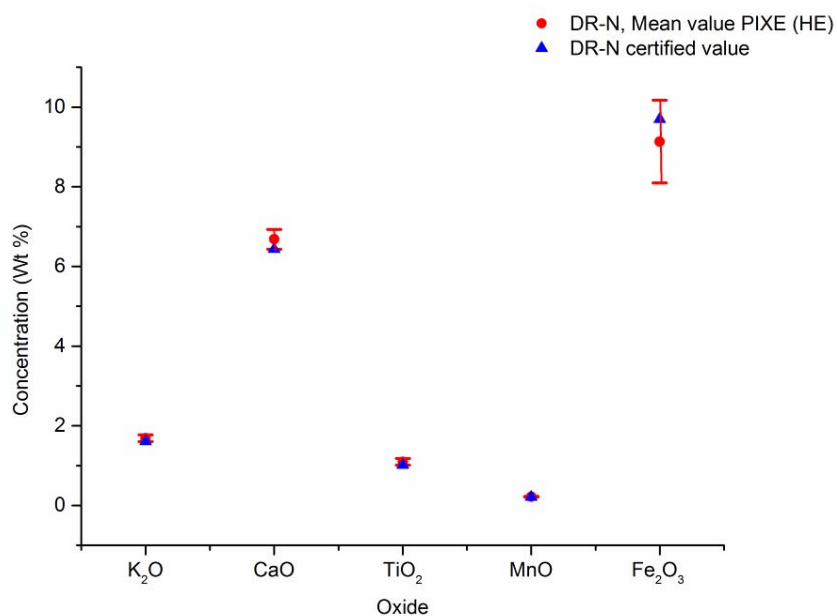


**Figure 5.19:** Quantification of the DR-N standards using the high energy detector. [Data compiled from Chapter 7, section 7.4.7, table 7.58].

### 5.3.2 Investigation of reference quills

Several of the reference quills prepared for the dyeing experiments were also analysed by PIXE in order to compare the information obtained using low and high energy detectors and also to see if it would be possible to differentiate between dyeing processes. The results obtained for two scoured quills (entries 1 and 2), several quills prepared with combinations of alum and cream of tartar (entries 6, 7 and 8), as well as traces of tin (entries 4, 5 and 9) and chromium (entry 3) can be found in table 5.9.

Due to their poor correlation with the DR-N standard at low energy, it was decided that the quantification of aluminium and silicon was not reliable, and their quantification is not presented in this study. It was found that the sulfur concentration was more homogeneous with the high energy detector (HE) and evaluated to 2 %, while the values obtained from the low energy detector (LE) were more variable and slightly over estimated with a level of sulfur evaluated to 3 %. Potassium and calcium were detected with both detectors at trace levels and for a few samples prepared with cream of tartar (entries 3, 4 and 8) it was found that the level of potassium was slightly higher around 0.7 - 1 %, and as would be expected, this was found to be more visible using the low energy detector. Finally, using the high energy detector, traces of zinc were detected in the blank porcupine quills and also in all the quills dyed at a concentration of 50 ppm (all entries). Heavy elements such as chromium (entry 3) or tin (entries 4, 5 and 9) were easily detected in the reference quills, meaning that it is possible to differentiate between dyebath recipes and it was found that the quantification of tin using the  $L_A$  line offered a lower limit of detection, at approximately 100 ppm.

These results were very encouraging for future studies of historical specimens and suggest that it should be possible to gain information not only on the presence of trace heavy metals but also several light elements, such potassium or calcium that could indicate specific dyeing processes.

Entry	Low Energy (LE)	Matrix, Wt %			Traces, ppm					
		16 S K	19 K K	20 Ca K	24 Cr K	26 Fe K	29 Cu K	30 Zn K	50 *Sn K	50 Sn LA
1	Blank 1	3.16	0.01	0.02	0	10	0	32	0	0
2	Blank 2	4.26	0.13	0.04	13	5	12	25	0	0
3	PQ4b (Al, K, Cr)	4.02	<b>0.72</b>	0.07	<b>1229</b>	0	13	92	0	0
4	PQ5a (Al, K, Sn, Cl)	3.61	<b>1.02</b>	0.05	0	0	50	24	0	<b>102</b>
5	PQ5b (Al, K, Sn, Cl)	3.88	0.53	0.09	0	0	24	119	0	0
6	PQ6 (Al)	2.98	0.58	0.10	0	0	0	23	0	0
7	PQ8a (Al)	0.00	0.01	0.00	6	0	11	0	0	0
8	PQ8b (Al, K)	3.78	<b>0.68</b>	0.12	10	8	15	35	0	13
9	PQ8c (Al, K, Sn)	3.95	0.27	0.07	9	0	0	0	0	<b>282</b>
	<b>Mean</b>	<b>3.17</b>	<b>0.54</b>	<b>0.07</b>						
	<b>stdv</b>	<b>1.44</b>	<b>0.33</b>	<b>0.04</b>						
	High Energy (HE)	16 S K	19 K K	20 Ca K	24 Cr K	26 Fe K	29 Cu K	30 Zn K	50 *Sn K	50 Sn LA
1	Blank quill 1	2.06	0.01	0.04	0	4	3	54	0	0
2	Blank quill 2	2.77	0.01	0.04	2	11	6	73	0	28
3	PQ4b (Al, K, Cr)	1.64	<b>0.39</b>	0.04	<b>1282</b>	8	5	87	0	0
4	PQ5a (Al, K, Sn, Cl)	2.15	<b>0.70</b>	0.04	4	0	14	52	0	<b>112</b>
5	PQ5b (Al, K, Sn, Cl)	2.25	0.42	0.07	2	8	7	55	<b>274</b>	<b>482</b>
6	PQ6 (Al)	1.99	0.48	0.08	0	1	6	43	0	<b>229</b>
7	PQ8a (Al)	2.09	0.21	0.03	0	2	9	48	0	0
8	PQ8b (Al, K)	2.12	<b>0.53</b>	0.10	0	0	4	44	0	48
9	PQ8c (Al, K, Sn)	1.96	0.19	0.05	0	4	2	42	<b>200</b>	<b>293</b>
	<b>Mean</b>	<b>2.03</b>	<b>0.42</b>	<b>0.06</b>						
	<b>stdv</b>	<b>0.20</b>	<b>0.18</b>	<b>0.03</b>						

**Table 5.9:** Comparing information collected at low and high energy on a set of porcupine quill references, prepared with various dyebath conditions. [Data compiled from Chapter 7, section 7.4.7.2, tables 7.60 and 7.61].

### 5.3.3 Historical samples

Around 85 historical porcupine quills were investigated from the specimen box A.848.15, selecting a large range of colours: bright and dark blue; bright and dark green, orange, red, yellow and several of the un-dyed (?) or faded quills. Despite

lowering the beam dose, some slight damage of the surface of the porcupine quills was still observed after irradiation, but this remained very minor considering that the area analysed was only  $100 \times 500 \mu\text{m}$ . This damage was visible under binocular observation and appeared as a light brown spot sometime with some discoloration of the dyestuff (figure 5.19). The results obtained for the quantification of light and heavy elements will be discussed in the following sections.

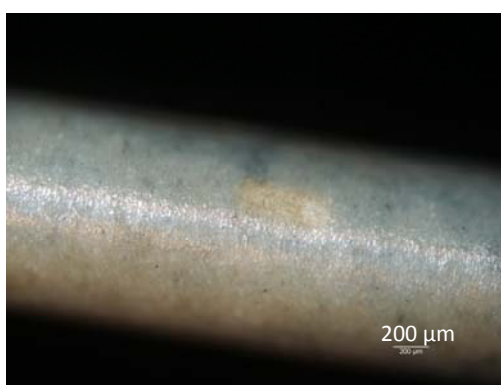


**Figure 5.19:** Discoloration of the surface of one of the porcupine quill specimen in A.848.15 observed after irradiation, irradiated area is  $100 \times 500 \mu\text{m}$  (scale bar is  $200 \mu\text{m}$ ).

### 5.3.3.1 Quantification of light elements

Most of the porcupine quills investigated exhibited trace levels of calcium and potassium, evaluated to 0.02 - 0.04 Wt % for calcium and below 0.2 Wt % for potassium. However, a few blue and green porcupine quills exhibited however a higher level of potassium ranging between 0.4 and 0.8 Wt %, which was found to be associated to slightly higher level of calcium ranging between 0.11 and 0.14 Wt% (figure 5.20). Because these levels are very low it appears difficult to attribute the presence of potassium and calcium to specific dyebath procedures as their presence could also be the result of contamination. Finally, several quills exhibited a high level of sodium (1 to 3 Wt %), and although the quantification of sodium might not

be reliable due to its easy volatilisation under irradiation, this is clearly visible in figure 5.21. These higher levels of sodium were observed in blue, green, orange and several “colourless” quills and did not seem therefore to be colour related. In general chlorine was found to be present in very minor quantities and ranged between 0.02 and 0.27 Wt % and did not particularly increase with the sodium content, excluding the presence of sodium chlorine salt. It is worth noting that the use of ashes - a source of sodium or potassium - is reported in Micmac quill dyeing recipes for blue hues:

*“Blue. The bark of the beech is boiled about an hour; a table spoon of hardwood ashes, which have been put into a half-gallon of boiled water are added.”<sup>21</sup>*

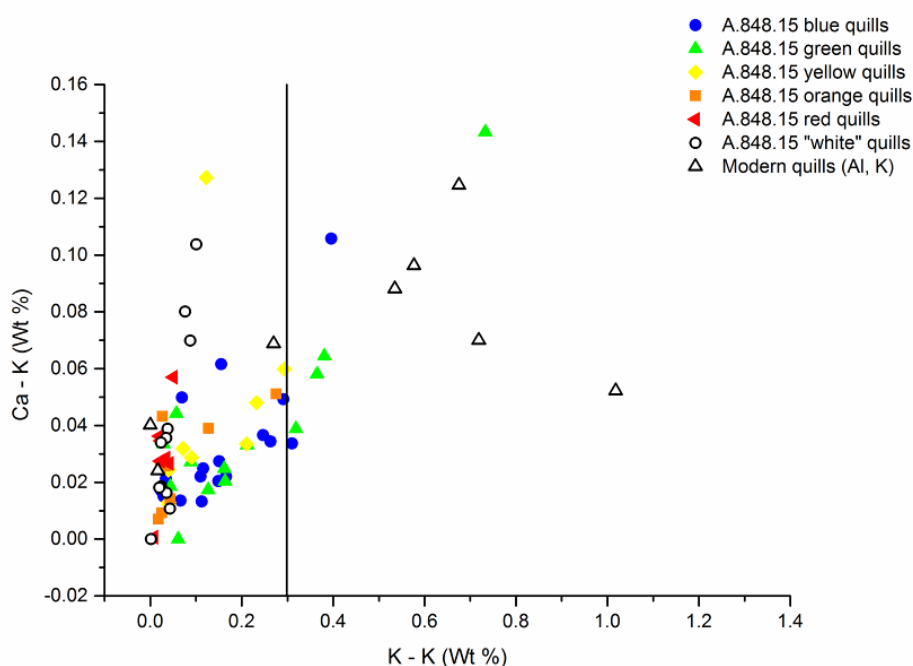


**Figure 5.20:** Concentration of potassium (K) versus calcium (Ca) expressed as weight percentage (Wt %), quantified from samples in the specimen box A.848.15 using the low energy detector (LE). [Data compiled from Chapter 7, section 7.4.7.2, tables 7.59 and 7.60].

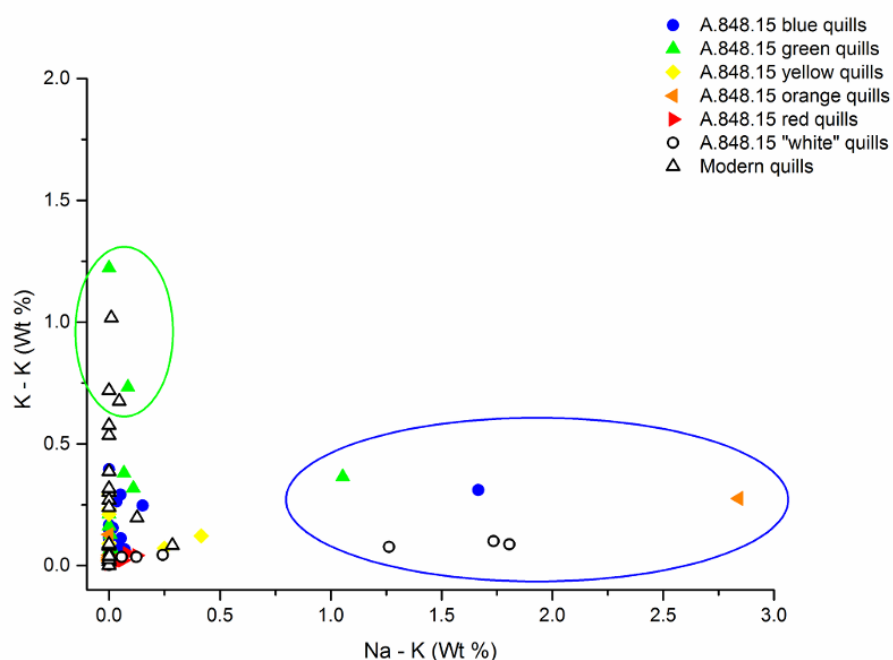


**Figure 5.21:** Concentration of sodium (Na) versus potassium (K) expressed as weight percentage (Wt %), quantified from samples in the specimen box A.848.15 using the low energy detector (LE). [Data compiled from Chapter 7, section 7.4.7.2, tables 7.59 and 7.60].

### 5.3.3.2 Quantification of heavy elements

The investigation of the heavy elements present in the specimens A.845.15 showed some exciting results, with both tin and copper characterised in various amount in all the porcupine quills investigated. Tin was found to be present in higher quantities in the red and oranges hues, reaching a level of 0.4 to 1.5 Wt %, while copper was found predominantly in the darker shades of blue and green and reached 0.3 Wt % for the most concentrated one (figure 5.22). Tin was also detected in the brighter shades of blue, where the level of tin was around 0.2 - 0.4 Wt %. While the “colourless” porcupine quills exhibited also minor amounts of tin and copper suggesting that either these quills were pre-mordanted or that these were previously dyed and now extremely faded. Chlorine was characterised in very minor amount suggesting that tin was not used as a tin(II) or tin(IV) chloride, but more likely as a



tin oxide, obtained by dissolving tin in nitric acid.<sup>43</sup> The level of sulphur was found to be higher in the blue and green specimens, ranging between 2.5 and 4.5 Wt %, and the higher level of sulfur seemed also to correspond for a few quills to higher levels of copper, but the correlation was not systematic, and is not possible to conclude that copper was used as a copper sulfate (figure 5.23). Finally arsenic and mercury were characterised below 25 ppm in all the historical specimens, indicating that these were unlikely to have been treated in the past with inorganic pesticides containing mercury and arsenic, such as arsenic trioxide  $\text{As}_2\text{O}_3$ ,  $\text{Pb}_3[\text{AsO}_4]_2$  or  $\text{HgCl}_2$ .<sup>44, 45</sup>

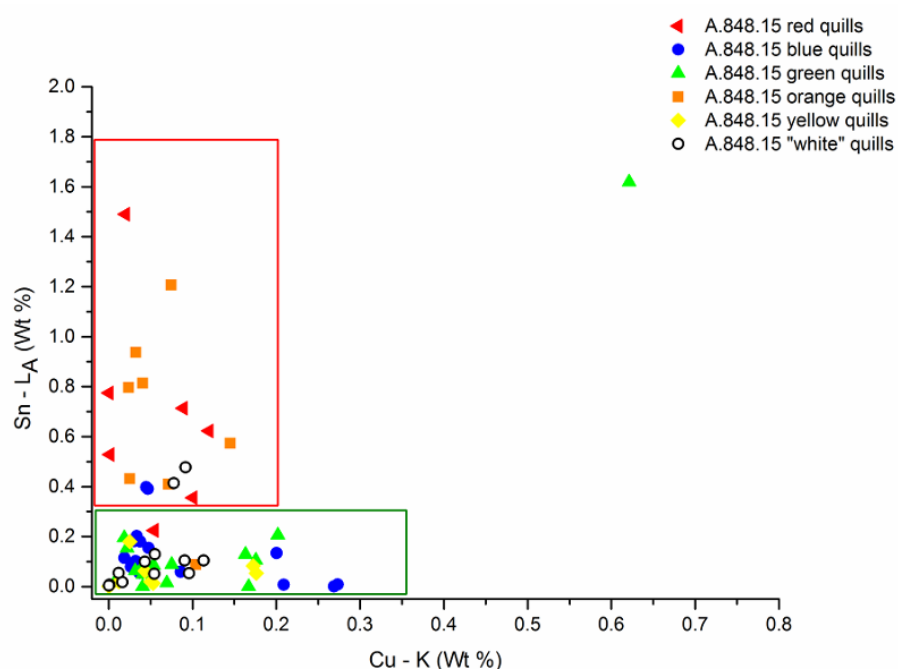


**Figure 5.22:** Concentration of copper (Cu) versus tin (Sn) expressed in weight percentage (Wt %), quantified from samples in the specimen box A.848.15 using the high energy detector (HE). [Data compiled from Chapter 7, section 7.4.7.2, tables 7.59 and 7.61].

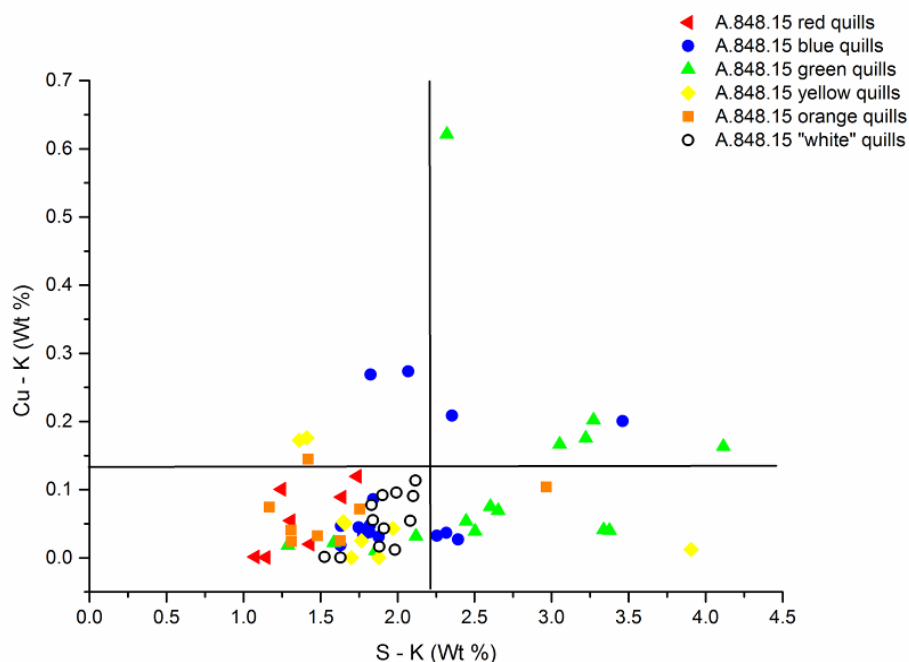


**Figure 5.23:** Concentration of sulfur (S) versus copper (Cu) expressed in weight percentage (Wt %), quantified from samples in the specimens box A.848.15 using the high energy detector (HE). [Data compiled from Chapter 7, section 7.4.7.2, tables 7.59 and 7.61].

### 5.3.3.3 RBS analysis

The RBS spectra obtained from several historical specimens were simulated by SIMNRA and the atomic composition of keratin layer containing tin and / or copper was then converted into its weight percentage composition (Wt %) to allow direct comparison with PIXE analysis. Figure 5.24 shows the simulated RBS spectra of a green porcupine quill containing small amount of tin and copper. The simulated spectra was found to fit closely to the RBS spectra and the concentration carbon and oxygen were better estimated than could be achieved with modern porcupine quill samples, suggesting that the surface contained less carbon rich contaminants.

It was however found difficult to quantify the level of copper by RBS, as most of the quills also exhibited minor amounts of tin. The probability of having a Rutherford reaction is higher for tin than copper and as a result, the tin signal masks the signal of

copper, meaning that low concentrations of copper cannot be estimated. The results obtained for a few porcupine quills are presented in table 5.20. For both sulphur and tin, the quantification by RBS gave a slight over estimation compared to the values obtained by PIXE, which could indicate that surface and bulk composition are different, with the first microns of the cuticle exhibiting a higher level of sulphur and tin. This could possibly correspond to a deposition of the mordant on the surface of the cuticle.

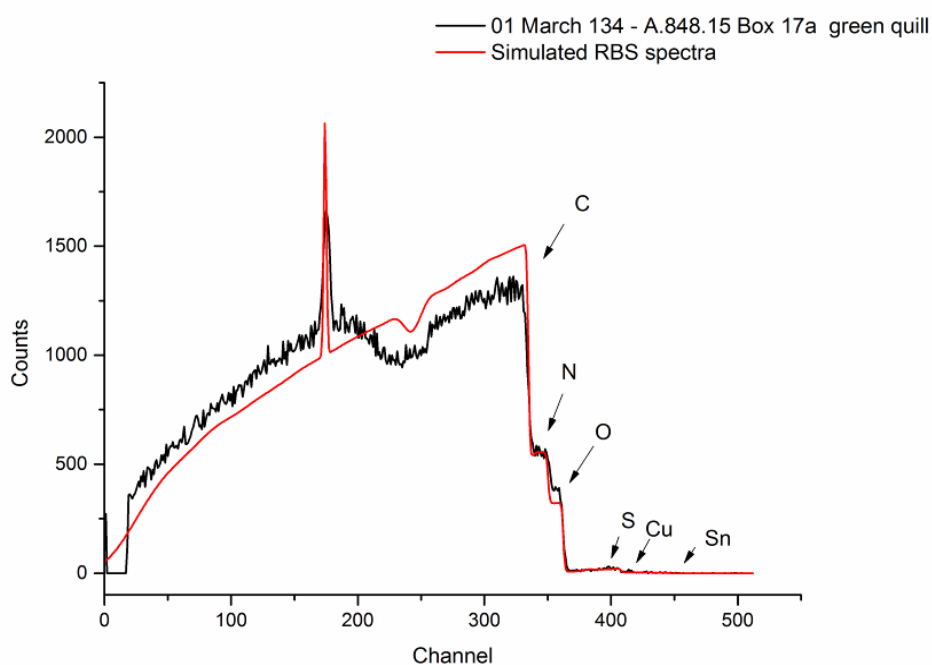


**Figure 4.24:** RBS spectra 01March 134, green porcupine quill (A.848.15 Box 1(a) and simulated RBS spectra with SIMNRA software using both Rutherford and non-Rutherford cross-sections (in red). [see Chapter 7, section 7.4.7.3, table 7.63].

<i>Entry</i>	<i>Particles *sr</i>	<i>RBS (Wt %)</i>			<i>PIXE (Wt %) HE</i>		
		<i>S</i>	<i>Cu</i>	<i>Sn</i>	<i>S</i>	<i>Cu</i>	<i>Sn</i>
01 March 099	$2.00 \times 10^{10}$	3.00	0.17	0.80	1.90	0.09	0.48
01 March 107	$2.00 \times 10^{10}$	3.48	ND	0.81	1.83	0.08	0.41
01 March 122	$1.78 \times 10^{10}$	3.32	ND	2.15	1.17	0.07	1.21
01 March 134	$1.92 \times 10^{10}$	3.50	0.26	0.16	3.01	0.17	0.06

**Table 5.20:** Number of beam particles (\*sr) fitted by SIMNRA for several measurements of historic porcupine quills investigated by RBS. The atomic composition of virtual layers was converted into weight percentage to allow direct comparison with PIXE analysis. [see Chapter 7, section 7.4.7.3, table 7.63].

#### 5.3.3.4 ICP-OES analysis

In order to confirm those analyses a small set of porcupine quills were also re-investigated by ICP-OES and the results obtained were compared to the results of PIXE analysis. In addition, six micro-samples, removed during conservation treatment from objects A.848.13 and A.849.7 (figure 5.25) were also investigated. ICP-OES confirmed that both copper and tin were present in substantial concentrations in all the porcupine quills, with the level of tin reaching 20 to 30  $\mu\text{g}$  per mg of quill in the more concentrated samples. Considering the low sorption level of porcupine quill for tin and copper (chapter 4), it would be reasonable to believe that the specimens were prepared in dyebaths containing a rather high concentration of mordants, although of course the exact dyebath conditions remain unknown. Double mordanting is not a common practice in the preparation of historical textiles and it is rather surprising that both copper and tin are present in all the specimens. It is not however possible to directly correlate ICP-OES and PIXE measurements, using the quantification curves obtained from reference porcupine quills (chapter 4), because the aged porcupine quills specimens appeared less dense than fresh one. perhaps due to desiccation over time. Thus the masses from which the metal ions were extracted for ICP-OES cannot be directly correlated. Interestingly similar levels of tin and copper were found in the samples removed from objects (blue,

green, red and white), confirming that these objects were very likely to have been manufactured from the raw specimens collected in 1862 (table 5.21).



**Figure 5.25:** A.849.7, bracelet made with porcupine quills dyed with native dyes: Canadian Indians, Slavey, © Trustees of National Museums Scotland

	ICP-OES ( $\mu\text{g per mg quill}$ )		PIXE (Wt %)	
	<i>Sn</i>	<i>Cu</i>	<i>Sn</i>	<i>Cu</i>
<b>A.848.15</b>				
Box 2, red	29	2	1.71	< 0.01
Box 2, red	17	3	0.82	0.01
Box 4, orange	20	2	0.65	0.02
Box 4, yellow	14	3	0.10	0.02
Box 5A, red	18	1	0.88	nd
Box 5B, red	20	2	0.41	0.01
Box 5B, bright red	12	1	0.26	0.01
Box 6 Q1, bright red	10	1	0.63	nd
Box 6 Q2, red	9	2	0.18	< 0.01
Box 7, bright blue	9	2	0.49	0.03
Box 8, orange	14	1	0.83	< 0.01
Box 8, orange (salt)	11	2	0.56	< 0.01
Box 14A, red	12	2	0.06	< 0.01
Box 16B, orange	9	1	0.02	0.01
Box 9A, bright blue	2	0.4	0.31	< 0.01

Box 9A, spotted blue	9	2	0.21	0.01
Box 17A, dark green	5	1	0.21	0.02
Box 17B, dark green	13	5	< 0.01	0.06
Box 18, yellow	3	0.4	0.10	nd
<b>Objects</b>				
A.848.13, pink	31	5		
A.849.13, green	58	15		
A.848.13, blue	29	4		
A.848.13, white	11	2		
A.849.7, green	19	5		
A.849.7, blue	13	5		

**Table 5.21:** Comparison of the levels of tin and copper obtained by ICP-OES and PIXE analysis on a small set of porcupine quills specimen (A.848.15) and several samples removed from objects A.848.13 and A.849.7. [Data compiled from Chapter 7, section 7.4.7.4, table 7.64].

## 5.4 DISCUSSION

The investigation of the raw specimens and porcupine quill work collected in 1862 from Northern Athapaskan showed unexpected results, with the exclusive use of American cochineal (*Dactylopius Coccus* Costa), turmeric (*Curcuma longa* L.) and unidentified blue dyes (indigo and possibly indigo carmine).

These results strongly differ from the study of Eastern Woodlands porcupine quill recently undertaken at the National Museum of the American Indian (Smithsonian Institute).<sup>4, 5</sup> In this study, thirty four objects dated pre-1856 from different cultural groups in the Eastern Woodlands were investigated (Mik'maq, *Ojibwe*, Delaware, Seneca, Huron, *Iroquois*, Mohegan, Great Lakes). Sixty six samples of black, blue, yellow, red and brown were analysed and showed exclusive use of local natural dyes, including the use of madder (possibly *Galium* species), tannins (gallic acid and juglone), several alkaloid dye sources (berberine), indigo and anthocyanidin dyes. Only two samples in this study exhibited the presence of carminic acid, and the dye

source was reported to be American cochineal, that would have been made available through European contact. Indeed, there is no evidence of trade routes extending from Mexico into North America, while trades routes of cochineal from South America into Europe however have a long history, and it is well known that cochineal was traded into Europe as early as the sixteenth century.<sup>43, 46</sup>

The exclusive use from 1862 of imported European dyes by Athapaskans in 1862 highlights how European contact impacted on traditional porcupine quill work in the late nineteenth century. It is unknown if these dyes were already traded into North America and quickly adopted by Athapaskan people for the preparation of porcupine quills, as they would have much easier to use than local natural dyes. But these technical changes correspond well to what is reported with the use of glass beads for embroidery.<sup>8</sup> It is also possible that Bernard Ross provided some raw materials for the manufacture of the objects he commissioned. More art historical research would be needed, looking specifically at the account books from the Hudson Bay Company on the trade of dyestuffs. Although records seemed to give accounts mainly of what was traded from the Indians (furs primarily), as opposed to what was given to them.<sup>47</sup> Nevertheless, beads are mentioned in some records and were traded at 2 beavers per pound of beads.<sup>47</sup>

Cochineal appeared in the museum's registry under the term of scarlet, which a European terminology, referring to the use cochineal prepared with tin mordant. Unsurprisingly, considering the red hues observed in the specimens, tin was found to be present associated with a smaller amount of copper in all the specimens and objects investigated. By changing the concentrations of these two mordants, bright and darker hues using the same dyestuff were obtained. It would be legitimate to question if these metallic salts were a voluntary addition or the result of dyeing the quills using copper or tin vessels that would have depleted the metal ions during the dyebaths. Native copper was available in the Lake Superior region and there are examples of personal ornaments made of copper such as earrings or bracelets, but also copper knives in the Southern Alaska.<sup>48, 49</sup> Nevertheless, metal artifacts before

European contact are rare in the Dene culture, but the use of European copper or brass kettles is reported to occur after contact, these being exchanged for fur with Europeans. Copper kettles are mentioned in several ethnographic studies, but none specifically related to the dyeing of porcupine quills, but there is no mention of the use of pewter vessels that would explain the level of tin characterised in the specimens.<sup>50-52</sup> It is however reported that European dyes and mordant were already traded to Nova Scotia in the 1830s, suggesting that by 1862 these materials would have been also available in the Northern territories.<sup>21</sup>

“The majority (of the dyes) were imported, and included indigo, logwood and ground redwood, with various mordants ... Newspapers in Nova Scotia during the early 1800s advertised, *“dyestuffs just received from London”*, and *“finest quality Spanish indigo”*. One 1830 advertisement list *“indigo, logwood, redwood, alum, copperas, vitriol ....”*<sup>21</sup>

The use of mordants reflects a change in dyeing technologies and it is possible that the high contents and variations of tin and copper reflect of some experimentation with these new materials. It is not clear why the analysis of cochineal seemed to be particularly affected by the level of mordant and whether the concentrations of mordant in the dye bath affected the uptake of the cochineal dye onto the porcupine quills. Alternatively, it is also possible that residual amounts of tin and copper in the acid hydrolysed extract affected the chromatographic analysis. This would need to be further investigated by studying more reference materials and possibly improving the sample preparation prior to UPLC analysis.

Finally, the thesis will also help in the design of appropriate conditions and regimes for display,<sup>53, 54</sup> which will minimise further light damage, as published research into the light fastness of natural dyes has shown that cochineal and indigo are moderately stable, while turmeric and indigo carmine have higher rates of photodegradation.<sup>42, 55</sup> It would be also interesting, given the nature of the porcupine quills to see if the excess of mordant affects the fading properties of the natural dyes, and further dye testing on the quill specimens from the Athapaskan collection is intended using micro-fading system.<sup>54, 55</sup> It is also intended to extend dye analysis to a larger



number of artifacts from National Museums Scotland collection in order to document better the use of new dyestuffs, especially in the period immediately after these objects were collected (1860 - 1870), when early synthetic dyes would have been traded from Europe into North America.

## 5.5 REFERENCES

1. Orchard, W. C. (1916). *The Technique of Porcupine-Quill Decoration Among the North American Indians*. Kessinger Publishing, Reprint 2009.
2. Thompson, J. (2001). *Fascinating Challenges: Studying Material Culture with Dorothy Burnham*. Canadian Museum of Civilization.
3. Bohr, R., Lindsay, A. (2009). Dyeing commodities whether in Roote or floure: Reconstructing Aboriginal dye techniques from Documentary and Museum sources. *Material Culture Review*, **69**, 21 - 35.
4. Cole, C., Heald, S. (2010). The History and Analysis of Pre-Aniline Native American Quillwork Dyes. *TSA Symposium, Paper 14*.
5. Cole, C. L. (2010). *The contextual analysis of pre-1856 Eastern Woodlands quillwork dyes through identification by Liquid Chromatography - Mass Spectroscopy*. The University of Delaware, PhD Thesis.
6. Idiens, D. (1974). The Athapaskan Indian collection in the Royal Scottish Museum. In *The Athapaskans: Strangers of the North. An international travelling exhibition from the collection of the National Museum of Man, Canada, and the Royal Scottish Museum*, National Museum of Man: Ottawa, 15-16.
7. Idiens, D. (1979). A catalogue of Northern Athapaskan Indian Artefacts in the collection of the Royal Scottish Museum, Edinburgh. *Royal Scottish Museum Information Series, Art and Archaeology*, **3**.
8. Duncan, K. C. (1989). *Northern Athapaskan Art: A Beadwork Tradition*. University of Washington Press, Seattle.
9. Thompson, J. (1990). *Pride of the Indian Wardrobe, Northern Athapaskan footwear*. University of Toronto Press, for the Bata Shoe Museum.
10. Thompson, J. (1994). *From the land, two hundred years of Dene clothing*. Canadian Museum of Civilization.
11. Krauss, M. E., Golla, V. K. (1981). Northern Athapaskan Languages. In *Handbook of North American Indians, Vol. 6, Subarctic*, Sturtevant, W. C., Ed. Smithsonian Institution: Washington DC, 67-85.

12. Thompson, J. (2001). Traditional Summer clothing of the Dena'ina and the Gwich'in: Variation on a theme. In *Fascinating Challenges. Studying Material Culture with Dorothy Burnham*, Thompson, J., Ed. Canadian Museum of Civilization: 17-66.
13. Thompson, J. (2001). The oldest Athabaskan Garment? In *Fascinating Challenges: Studying Material Culture with Dorothy Burnham*, Thompson, J., Ed. Canadian Museum of Civilization: 67-89.
14. Sherr Dubin, L. (1987). North America. In *The history of beads: from 30,000 B.C. to the present*, Thames and Hudson: 261-289.
15. Wentzel, W. F. (1889). Letter N° 5, February 28th, 1814 to the Hon. Roderic McKenzie. In *Les bourgeois de la Compagnie du Nord-Ouest: Récits de voyages, lettres et rapports inédits relatifs au Nord-Ouest canadien, Vol. 1*, Masson, L. R., Ed. 110.
16. Harmon, D. W. (1820). *A journal of voyages and travel in the interior of North America*. Andover, p 377-378.
17. Osgood, C. (1932). *The ethnography of the Great Bear Lake Indians*. National Museum of Canada Bulletin 70, Ottawa, p 31-97.
18. Wentzel, W. F. (1889). Letter N° 1, March 27th, 1807 to the Hon. Roderic McKenzie. In *Les bourgeois de la Compagnie du Nord-Ouest: Récits de voyages, lettres et rapports inédits relatifs au Nord-Ouest canadien, Vol. 1*, Masson, L. R., Ed. 80-87.
19. Forster, J. R. (1772). A Letter from Mr. John Reinhold Forster, F. R. S. to William Watson, M. D. Giving Some Account of the Roots Used by the Indians, in the Neighbourhood of Hudson's-Bay, to Dye Porcupine Quills. *Phil. Trans. R. Soc.*, **62**, 54-59.
20. Cardon, D. (2003). *Le monde des teintures naturelles*. Belin, Paris.
21. Whitehead, R. H. (1982). *Micmac quillwork: Micmac Indian techniques of porcupine quill decoration, 1600-1950*. Nova Scotia Museum.
22. Andrews, T. D. (2006). *Dè T'a Hoti Ts'eeda, We live securely by the land: An exhibition of Dene material selected from the collections from the National Museums Scotland*. Prince of Wales Northern Heritage Centre.
23. Knowles, C. (2007). Objects journeys: outreach work between National Museums Scotland and the Tlicho. In *Material Histories*, Marischal Museum, University of Aberdeen.
24. Wilson, G. (1855). What is Technology? An Inaugural Lecture. Delivered in the University of Edinburgh on November 7, 1855. 3.
25. Anderson, R. G. W. (1992). Presidential Address: 'What Is Technology?': Education through Museums in the Mid-Nineteenth Century. *Brit. J. Hist. Sci.*, **25**, 169-184.
26. Geoffrey, R., Anderson, W. (1978). *The Playfair Collection and the Teaching of Chemistry at the University of Edinburgh, 1713-1858*. Royal Scottish Museum Studies; illustrated edition.
27. Lindsay, D. (1993). *Science in the Subarctic: trappers, traders, and the Smithsonian Institution*. Smithsonian Institution Press, Washington.
28. Lindsay, D. (1987). The Hudson's Bay Company-Smithsonian Connection and Fur Trade Intellectual Life: Bernard Rogan Ross, A Case Study. In *Le Castor Fait Tout: Selected Papers of the*

*Fifth North America Fur Trade Conference*, Trigger, B. G., Ed. Montreal: Lake St Louis Historical Society: 587-617.

29. McFadyen Clark, A. (1974). The Athapaskans: Strangers of the North. In *The Athapaskans: Strangers of the North. An international travelling exhibition from the collection of the National Museum of Man, Canada, and the Royal Scottish Museum*, National Museum of Man: Ottawa, 102.
30. Travis, A. S. (1993). *The Rainbow Makers: The Origins of the Synthetic Dyestuffs Industry in Western Europe*. Lehigh University Press.
31. Hofenk de Graaf, J. H. (2005). *The Colourful Past*. Archetype Publications.
32. Valianou, L., Karapanagiotis, I., Chryssoulakis, Y. (2009). Comparison of extraction methods for the analysis of natural dyes in historical textiles by High-Performance Liquid Chromatography. *Anal. Bioanal. Chem.*, **395**, 2175-2189.
33. Degano, I., Lucejko, J. J., Colombini, M. P. (2011). The unprecedented identification of Safflower dyestuff in a 16th century tapestry through the application of a new reliable diagnostic procedure. *J. Cult. Herit.*, **12**, 295-299.
34. Li, S., Yuan, W., Deng, G., Wang, P., Yang, P., Aggarwal, B. B. (2011). Chemical Composition and Product Quality Control of Turmeric (*Curcuma longa* L.). *Pharmaceutical Crops*, **2**, 28-54.
35. Cheng, J., Weijun, K., Yun, L., Jiabo, W., Haitao, W., Qingmiao, L., Xiaohe, X. (2010). Development and validation of UPLC method for quality control of *Curcuma longa* Linn.: Fast simultaneous quantitation of three curcuminoids. *J. Pharm. Biomed. Anal.*, **53**, 43-49.
36. Wouters, J., Verhecken, A. (1989). The Coccid Insect Dyes: HPLC and Computerized Diode-Array Analysis of Dyed Yarns. *Studies in Cons.*, **34**, 189-200.
37. Ferreira, E. S. B., Quye, A., McNab, H., Hulme, A. N., Wouters, J., Boon, J. J. (1999). The analytical characterisation of flavonoid photodegradation products: a novel approach to identifying natural yellow dyes in ancient textiles. *Preprint of the ICOM Committee for Conservation, 12th Triennial Meeting*, **1**, 221-227.
38. Peggie, D. A. (2006). *The Development and Application of Analytical Methods for the Identification of Dyes on Historical Textiles*. The University of Edinburgh, PhD Thesis.
39. Wouters, J., Verhecken, A. (1989). The scale insect dyes (*Homoptera: Coccoidea*). Species recognition by HPLC diode array analysis of the dyestuffs. *Annl. Soc. ent. Fr. (N.S.)*, **25**, 393 - 410.
40. Peggie, D. A., Hulme, A. N., McNab, H., Quye, A. (2008). Towards the identification of characteristic minor components from textiles dyed with weld (*Reseda luteola* L.) and those dyed with Mexican cochineal (*Dactylopius coccus* Costa). *Microchim. Acta*, **162**, 371-380.
41. Deveoglu, O., Karadag, R., Yurdun, T. (2011). Qualitative HPLC determination of main anthraquinone and lake pigment contents from *Dactylopius coccus*; dye insect. *Chemistry of Natural Compounds*, **47**, 103-104.
42. de Keijzer, M., van Bommel, M. R., de Keijzer, R., Hofmann, Knaller, R., Oberhumer, E. (2012). Indigo carmine: Understanding a problematic blue dye *Studies in Conservation*, **57**, 87-95.

43. Kirby, J., Spring, M., Higgitt, C. (2005). The technology of eighteenth and nineteenth-century red lake pigments. *National Gallery Technical Bulletin*, **28**, 69-95.
44. Sirois P. J., S. G. (2001). Analysis of Museum objects for hazardous pesticide residues : a guide to techniques. *Collection Forum*, **17**, 49-66.
45. Marte, F., Péquino, A., Von Endt, D. W. (2006). Arsenic in taxidermy collections: history, detection and management. *Collection Forum*, **21**, 143–150.
46. Lee, R. L. (1951). American Cochineal in European Commerce, 1526-1625. *J. Mod.Hist.* , **23**, 205-224.
47. Ray, A. J. (1975). The Early Hudson's Bay company Account books as sources for historical research: an Analysis and Assessment. *Archivaria*, **I**.
48. Rickard, T. A. (1934). Use of Native Copper by the Indigenes of North-America. *JRAI (UK)*, **64**, 265-287.
49. Emmons, G. T. (1908). Copper-Neck-Rings of Southern Alaska. *Am. Anthropol.*, **10**, 644-649.
50. Harper, J. R. (1957). Two Seventeenth Century Micmac "Copper Kettle" Burials. *Anthropologica*, 11-36.
51. Martin, C. (1975). The Four Lives of a Micmac Copper Pot. *Ethnohist.*, **22**, 111-133.
52. Turgeon, L. (1997). The Tale of the Kettle: Odyssey of an Intercultural Object. *Ethnohist.*, **44**, 1-29.
53. Ford, B. L. (2011). Lighting guidelines and the lightfastness of Australian indigenous objects at the National Museums of Australia. *Preprint of the ICOM Committee for Conservation, 16th Triennial Meeting, Lisbon*.
54. del Hoyo-Meléndez, J. M., Mecklenburg, M. F. (2010). A survey on the light-fastness properties of organic-based Alaska Native artifacts. *J. Cult. Herit.*, **11**, 493-499.
55. del Hoyo-Meléndez, J. M., Mecklenburg, M. F. (2011). An Investigation of the Reciprocity Principle of Light Exposures Using Microfading Spectrometry. *Spectrosc Lett.*, **44**, 52-62.

# CHAPTER 6

<b>6</b>	<b>CONCLUSION .....</b>	<b>258</b>
6.1	ULTRA PERFORMANCE LIQUID CHROMATOGRAPHY (UPLC) .....	258
6.2	DYER'S GREENWEED MINOR COMPONENTS .....	259
6.3	EARLY ENGLISH «SHELDON» TAPESTRIES .....	259
6.4	SORPTION OF METALLIC IONS ON PORCUPINE QUILLS .....	260
6.5	MID NINETEENTH CENTURY NATIVE AMERICAN QUILL WORK .....	261
6.6	CONCLUSION .....	261

## 6 CONCLUSION

This chapter summarises briefly the key results in the thesis, and stresses the significance of the work in the field of heritage science.

### 6.1 ULTRA PERFORMANCE LIQUID CHROMATOGRAPHY (UPLC)

The thesis reports some of the first applications of Ultra Pressure Liquid Chromatography (UPLC) to the analysis of textile samples from the cultural heritage field. Using this technique has allowed objects which were previously considered to be ineligible for sampling (and thus accurate dyestuff analysis) to be studied due to the greatly reduced sample size, and new substrates (*e.g.* North American quill work) where the dyestuff is found in much reduced quantities to be analysed.

The use of Ultra Performance Liquid Chromatography (UPLC) for the analysis of natural product dyestuffs has been pioneered as part of this research, and the limit of detection and limit of quantification (LOD and LOQ) of a range of dyestuffs was determined. This research has demonstrated that up to 10-fold improvements in sensitivity may be achieved using Ultra Performance Liquid Chromatography (UPLC) as compared to the equivalent High Performance Liquid Chromatography (HPLC) separation, allowing far smaller samples sizes to be taken and/or samples of more fugitive (or more degraded) dyestuffs to be successfully analysed. In total, over 100 samples have been analysed by UPLC, and it is clear that the greatly reduced LOD and LOQ which this technique offers means that it will see widespread application in the field of heritage science.

Two UPLC methods were developed; the first method used a BEH C18 column (50 × 2.1 mm, length × i.d.) with a shorter run time, and provided excellent separation for a wide range of dyestuffs; it is anticipated that this method will enable the rapid analysis of multiple samples from objects. The second method used a PST BEH C18 column (150 × 2.1 mm, length × i.d.) and a longer run time; this method enabled the identification of very minor components and closely-eluting regio-isomers and was combined effectively with ESI-MS analysis.

These methods were validated through the analysis of some heavily degraded, late sixteenth century wool and silk samples from the outstanding collections held at the Burrell Collection (Glasgow, UK) and the Bodleian Library (Oxford, UK) generating exciting new information about the dyestuffs which have been employed in their preparation. It is anticipated that these methods will become the standard protocol in the heritage science field world-wide. Furthermore, the application of related UPLC-MS methods will allow future studies using isotope ratios to pinpoint the provenance of objects and will also allow rapid identification of the photo-degradation products of natural product dyestuffs.

## 6.2 DYER'S GREENWEED MINOR COMPONENTS

UPLC analysis of silk and wool reference yarns dyed with dyers' greenweed (*Genista tinctoria* L.) showed for the first time that both luteolin methyl-ethers chrysoeriol and diosmetin are present in low levels in the acid hydrolysed extracts. It also provided the identification of four previously unreported *Genista* related components, named Gt1, Gt2, Gt3 and Gt4 that were characterised by TOF-ESI-MS analysis combined with PDA-UPLC. This allowed the attribution of some possible structures to these minor components; with the minor component Gt2 corresponding to the isoflavone genistein with an additional OH substituent, while the minor component Gt3 corresponded to an *O*-methylated isoflavonoid related to genistein. Further analysis using MS-MS fragmentations will be carried out in order to offer definitive structures for these components. These findings will have an impact in a broad range of fields outside that of cultural heritage - from those with current interests in the use of natural product dyestuffs, to scientists working in species identification/phylogeny and traditional medicines.

## 6.3 EARLY ENGLISH «SHELDON» TAPESTRIES

Thirteen tapestries from the Burrell collection and three key tapestry maps from the Bodleian collection were sampled and as a result, more than five hundred samples were investigated by chromatographic analysis. Through pioneering the use of UPLC techniques for the analysis of natural product dyestuffs it was possible to characterise



traces of safflower dye (*Carthamus tinctorius* L.) on all the Sheldon tapestries from the Burrell collection. Safflower is a well-known fugitive dye and, thus far, its use in Europe prior the eighteenth century has been only rarely recorded. This research strongly suggests that this dye was actually already in use in Europe in the late sixteenth century. This finding is especially relevant to art historical researchers, with interests in trade and exchange, and will initiate further research (*e.g.* Port Books or accounts records from the Great Wardrobe) to find information on the type of dyestuffs that London merchants were importing, as well as the materials bought for tapestry manufacture and repair.

#### 6.4 SORPTION OF METALLIC IONS ON PORCUPINE QUILLS

A small study using Inductively Coupled Plasma (ICP) coupled to Optical Emission Spectrometry (OES) was initiated on the sorption properties of porcupine quills, with a particular focus on the sorption of copper(II) and tin(II). This showed that for the range of dyebath concentrations considered (100 to 15,000  $\mu\text{g mL}^{-1}$ ), the sorption of metal ions exhibited a reasonably linear correlation with the initial dyebath metal ion concentration, and that the uptake of tin(II) was systematically higher than that of copper(II). The quantities of metal ions adsorbed by the porcupine quills were found to be much smaller than published studies on wool and this suggested that the thickness of the cuticle adversely affected metal ion exchange with the dyebath.

A non-invasive method for mordant analysis was developed using Particle Induced X-Ray Emission (PIXE) analysis, and this allowed the quantification of the trace elements present in reference porcupine quills. These pioneering experiments permitted the quantification of copper and tin present in the outer cuticle layer (first 80  $\mu\text{m}$ ), and when combined with Rutherford Backscattering Spectrometry (RBS) allowed complementary quantification of the light elements present in the cuticle layer, such as carbon, oxygen, nitrogen and sulfur, providing new information on the distribution of copper and tin in the cuticle layer. It was found that the first microns of the cuticle (1 – 2  $\mu\text{m}$ ) were richer in sulfur and metallic mordant (tin or copper). This non-invasive approach using a combination of PIXE and RBS analysis was then successfully applied to the study of nineteenth century porcupine quill work from the collections in the National Museums Scotland.

## 6.5 MID NINETEENTH CENTURY NATIVE AMERICAN QUILL WORK

The second objective of the research was the investigation of non-European ethnographical materials, which have received little systematic study in comparison to historical textiles. A unique group of dyed porcupine quill samples and objects that was collected in 1862 from Sub-Arctic Athapaspan Dene people was investigated for the first time and an analytical approach using a combination of UPLC analysis and Ion Beam Analysis (PIXE-RBS) allowed the characterisation of both natural dye sources and metallic mordants. This showed the exclusive use of traded “European” dyes, such as American cochineal (*Dactylopius coccus* Costa) and turmeric (*Curcuma longa* L.) associated with chemical mordants, such copper and tin, to achieve darker or brighter hues. This has not been reported before and has initiated exciting discussions with curatorial colleagues at National Museums Scotland and at the Prince of Wales Conservation Centre in Canada, opening new avenues for future research on porcupine quill work collections. Finally, the thesis will also help in the design of appropriate conditions and regimes for display, which will minimise further light damage, as published research into the lightfastness of natural dyes has shown that if cochineal and indigo are often moderately stable, turmeric and indigo-carmines fade relatively quickly. Further dye testing on the dyed quills from the Athapaspan collection is intended using micro-fading to gain a more complete understanding of all of the objects.

## 6.6 CONCLUSION

The Science and Heritage Programme aims to "*fund research activities that will deepen understanding and widen participation in research in the field of heritage science*". The work described in this thesis clearly relates closely to these objectives, as it has allowed collaborations between the University of Edinburgh and several museum institutions including National Museums Scotland and the Burrell Collection (Glasgow Museums) to be strengthened and new collaborations with the Bodleian Library (Oxford) to be developed. These collaborations have enabled important historical questions regarding the provenance of tapestries attributed to the "Sheldon" workshop to be addressed from a scientific perspective for the first time.

Furthermore, the analysis conducted on an internationally ranked collection of North American quill underpinned a scientific investigation of the nature of both dyestuffs and mordants and proved to have a significant impact upon the current understanding of cultural changes happening in the late nineteenth century in North America.

# CHAPTER 7

<b>7</b>	<b>EXPERIMENTAL.....</b>	<b>266</b>
7.1	MATERIALS AND CHROMATOGRAPHIC METHODS.....	266
7.1.1	References materials and chemicals.....	266
7.1.2	Sample preparation.....	266
7.1.3	Solutions of standards.....	267
7.1.4	Chromatographic Methods.....	268
7.1.4.1	HPLC system.....	268
7.1.4.2	UPLC system.....	269
7.1.4.3	UPLC ESI MS system.....	271
7.1.5	METHOD DEVELOPMENT.....	272
7.1.5.1	Calibration curves.....	272
7.1.5.2	Limit of detection (LOD) and quantification (LOQ).....	274
7.1.5.3	Comparison of response: $H_x$ (AU) and $[x]$ (ng) for genistein.....	278
7.1.6	Evaluation of sample preparation.....	279
7.1.7	Investigation of reference yarns.....	281
7.1.7.1	Weld ( <i>Reseda luteola</i> L.).....	281
7.1.7.2	Dyer's greenweed ( <i>Genista tinctoria</i> L.).....	282
7.2	INVESTIGATION OF MID 16 <sup>TH</sup> CENTURY ENGLISH TAPESTRIES.....	284
7.2.1	Extraction protocols.....	284
7.2.1.1	Hydrochloric acid extraction.....	284
7.2.1.2	Dimethyl Sulfoxide extraction.....	284
7.2.2	Chromatographic methods.....	285
7.2.2.1	HPLC system.....	285
7.2.2.2	UPLC system.....	285
7.2.3	Dye analysis.....	285
7.2.3.1	Weld ( <i>Reseda luteola</i> L.).....	285
7.2.3.2	Dyer's greenweed ( <i>Genista tinctoria</i> L.).....	290
7.2.3.3	Young fustic ( <i>Cotinus coggygria</i> S.).....	292
7.2.3.4	Madder species.....	294
7.2.3.5	Cochineal dyes.....	296
7.2.3.6	Safflower ( <i>Carthamus tinctorius</i> L.).....	297
7.2.3.7	Summary.....	298
7.3	CHARACTERISATION OF METALLIC MORDANT ON PORCUPINE QUILL.....	314
7.3.1	Scanning Electron Microscopy (SEM).....	314
7.3.2	References of $Cu^{2+}$ and $Sn^{2+}$ preparation.....	314
7.3.3	ICP-OES.....	315
7.3.3.1	Calibration of the system.....	315
7.3.3.2	ICP-OES sample preparation.....	316
7.3.3.3	Evaluation of dyebath conditions.....	317
7.3.3.4	ICP-OES investigation of references quills.....	321
7.3.3.5	Linear regression.....	323
7.3.4	PIXE Experiment.....	324
7.3.4.1	Keratin target.....	324
7.3.4.2	Mass absorption coefficient $\mu$ .....	325
7.3.4.3	PIXE measurements.....	326
7.3.5	Rutherford Backscattering Spectrometry (RBS).....	334
7.3.5.1	Calibration of detector.....	334
7.3.5.2	SIMNRA simulation of RBS spectra.....	339
7.4	INVESTIGATION OF NORTH AMERICAN ATHAPASCAN PORCUPINE QUILL WORK FROM NATIONAL MUSEUMS SCOTLAND.....	341
7.4.1	Porcupine quills.....	341
7.4.2	Scouring process.....	341
7.4.3	Dyeing experiments with natural dyestuffs.....	343
7.4.4	UPLC analysis.....	345
7.4.4.1	Chemicals.....	345
7.4.4.2	Solutions of standards.....	346
7.4.4.3	Chromatographic method.....	346
7.4.4.4	Sample preparation.....	346
7.4.4.5	Calibration curves, limit of detection (LOD), limit of quantification (LOQ).....	347
7.4.5	Turmeric analysis.....	349
7.4.5.1	Turmeric extraction.....	349

---

7.4.5.2	Historical samples.....	350
7.4.6	<i>Cochineal analysis</i> .....	350
7.4.6.1	Porcupine quill reference .....	350
7.4.6.2	Historical quills.....	351
7.4.7	<i>Mordant analysis by PIXE, PIGE and RBS</i> .....	352
7.4.7.1	Beam dose $Q$ and parameter files.....	352
7.4.7.2	PIXE Results.....	355
7.4.7.3	RBS Spectra.....	359
7.4.7.4	ICP-OES analysis.....	362

## 7 EXPERIMENTAL

### 7.1 MATERIALS AND CHROMATOGRAPHIC METHODS

#### 7.1.1 References materials and chemicals

HPLC: methanol (HPLC grade) and ortho-phosphoric acid (reagent grade) were used without further purification; mobile phases were prepared with high-purity water obtained from a Milipore *Mili-Q* system with a resistivity of at least 18 M $\Omega$  (ELGA system). UPLC: methanol, acetonitrile and water were LC-MS grade and used without further purification.

Standards of luteolin (3',4',5,7-Tetrahydroxyflavone, TLC > 98 %), genistein (4',5,7-Trihydroxyisoflavone, HPLC assay  $\geq$  98 %), apigenin (4',5,7-Trihydroxyflavone, HPLC assay  $\geq$  95 %), alizarin (1,2-Dihydroxyanthraquinone, dye content 97 %), purpurin (1,2,4-Trihydroxyanthraquinone, dye content, 90%) and carminic acid (7- $\alpha$ -D-Glucopyranosyl-9,10-dihydro-3,5,6,8-tetrahydroxy-1-methyl-9,10-dioxoanthracenecarboxylic acid, HPLC assay  $\geq$  96 %) were purchased from Sigma-Aldrich UK. Standards of fisetin (3,3',4',7-Tetrahydroxyflavone, HPLC assay > 99 %), sulfuretin (3',4',6-Trihydroxyaurone, HPLC assay > 99 %), chrysoeriol (4',5,7-Trihydroxy-3'-methoxyflavone, HPLC assay > 99 %), and diosmetin (3',5,7-Trihydroxy-4'-methoxyflavone, HPLC assay > 99 %) were purchased from ExtraSynthese, France.

Silk and wool reference samples prepared with natural dyestuffs at NMS and during the Monitoring of Damage to Historic Tapestries (FP5, EC contract number EVK4-CT-2001-00048) were used to validate the method. These samples included threads dyed with weld (*Reseda luteola* L.), dyers' greenweed (*Genista tinctoria* L.), madder (*Rubia tinctoria* L.), cochineal (*Dactylopius. Coccus* C.) and young fustic (*Cotinus coggygria* L.).

#### 7.1.2 Sample preparation

For HPLC analysis, the hydrochloric acid extraction protocol, developed for the routine analysis of the dye components from reference and historical samples, was as follows:

the dyed yarn or solid reference material (typically 1 - 5 mg) was placed in a 2 mL glass test tube, to which was added a mixture of 37% hydrochloric acid: methanol: water [400  $\mu\text{L}$ , 2:1:1 (v/v/v)]. The tube was then placed in a water bath at 100 °C and heated for precisely 10 min. After rapid cooling under cold water, the extract was filtered using a Polyethylene filter (55  $\mu\text{m}$ , 5 mm) from Crawford Scientific™. The frit was rinsed with methanol (200  $\mu\text{L}$ ) and the combined filtrates dried by rotary vacuum evaporation over a water bath at 40 °C. The dry residue was then reconstituted with methanol: water [50  $\mu\text{L}$ , 1:1 (v/v)].

For UPLC analysis, the hydrochloric acid extraction protocol above was adapted as follows: the sample (typically 0.1 - 1 mg) was extracted in a 1 mL glass test tube, to which was added a mixture of 37% hydrochloric acid: methanol: water [200  $\mu\text{L}$ , 2:1:1 (v/v/v)]. The tube was then placed on a heated block at 100 °C and heated for precisely 10 min. After cooling down at room temperature, the extract was transferred into a 1 mL Eppendorf vial and the glass tube was rinsed with water: methanol [100  $\mu\text{L}$ , 1:1 (v/v)]. The combined extracts were centrifuged for 10 min at 10,000 rpm and then filtered directly into Waters UPLC vials using a PTFE Phenomenex syringe filter (0.2  $\mu\text{m}$ , 4 mm). The extract was then cooled with liquid Nitrogen and dried under vacuum using a freeze drier system. The dry residue was then reconstituted with water: methanol [40  $\mu\text{L}$ , 1:1 (v/v)].

### 7.1.3 Solutions of standards

The HPLC system was calibrated using a stock solution of standards containing carminic acid, luteolin, genistein, apigenin, alizarin and purpurin (1.00  $\pm$  0.01 mg of each standard) in water: methanol [25 mL, 1:1 (v/v); equivalent to 40  $\mu\text{g mL}^{-1}$ ]. Diluted solutions were then prepared with components at concentrations of 20, 10, 5, 4, 2 and 0.5  $\mu\text{g mL}^{-1}$ , by dilution with water: methanol [1:1 (v/v)] using calibrated micro-pipettes.

Both UPLC methods were calibrated using four stock solutions of standards: 1. a solution containing carminic acid, fisetin, sulfuretin, luteolin and genistein (1.00  $\pm$  0.01 mg of each standard) in water:methanol [25 mL, 1:1 (v/v); equivalent to 40  $\mu\text{g mL}^{-1}$ ]; 2. a solution containing apigenin, chrysoeriol, alizarin and purpurin (0.20  $\pm$  0.01 mg of



each standard) in water:methanol [10 mL, 1:1 (v/v); equivalent to 20  $\mu\text{g mL}^{-1}$ ]; 3. a solution of diosmetin ( $1.00 \pm 0.01$  mg) in water:methanol [25 mL, 1:1 (v/v); equivalent to 40  $\mu\text{g mL}^{-1}$ ]; and 4. a solution of carminic acid ( $3.00 \pm 0.01$  mg) in water:methanol [10 mL, 1:1 (v/v); equivalent to 300  $\mu\text{g mL}^{-1}$ ]. Diluted solutions were then prepared with components at concentrations of 20, 10, 5, 1, 0.5, 0.1, 0.05, 0.02 and 0.01  $\mu\text{g mL}^{-1}$ , by dilution with water:methanol [1:1 (v/v)] using calibrated micro-pipettes. Additional calibration points for carminic acid used dilutions of stock solution 4 at the concentrations of 150 and 100  $\mu\text{g mL}^{-1}$ .

The solutions of standards were kept in a fridge at 4 °C.

#### 7.1.4 Chromatographic Methods

##### 7.1.4.1 HPLC system

A Waters 600 gradient pump and a Waters 2996 PDA detector were controlled by Waters Empower software and the data collected was processed with Origin 8.5 (OriginLab, Nohampton, MA, USA). Solvents were sparged using an in-line vacuum degasser and chromatographed peaks were monitored at 254 nm. The column was enclosed in a heat-controlled chamber and maintained at  $25 \pm 1$  °C. Sample extracts were manually injected *via* a Rheodyne injector with a 20  $\mu\text{L}$  sample loop. The PDA detector recorded all spectral information between 250 and 750 nm; chromatographed peaks were monitored at 254 nm. The bandwidth (resolution) was 2.4 nm, and response time set to 1 s.

Method A: used a Phenomenex Spherclone ODS(2) reverse phase column, 5  $\mu\text{m}$  particle size,  $150 \times 4.6$  mm (length  $\times$  i.d.), with a guard column containing the same stationary phase. The column temperature was set to 25 °C which allowed a back pressure of 1600-1800 psi to be employed. The total run time was 35 min at a flow rate of 1200  $\mu\text{L min}^{-1}$ . A tertiary solvent system was used; A = 20% (v/v) MeOH (aq.), B = MeOH, C = 5 % (v/v) ortho-phosphoric acid (aq.). The elution programme was isocratic for 3 min (67A: 23B: 10C) then a linear gradient from 3 min to 29 min (0A: 90B: 10C) before recovery of the initial conditions over 1 min and equilibration over 5 min.

#### 7.1.4.2 UPLC system

Two chromatographic methods were developed using a Waters Acquity UPLC® system comprising the Waters Binary Gradient Manager with Waters Sample Manager incorporating a Waters Column Heater with sample detection using a Waters PDA detector. Data were collected by Waters Empower 2 software and processed with Origin 8.5 (OriginLab, Northampton, MA, USA).

Solvents were sparged using an in-line vacuum degasser and chromatographed peaks were monitored at 254 nm. The autosampler used a strong wash of acetonitrile (200 µL) and a weak wash of acetonitrile: water [600 µL, 10:90 (v/v)]. Waters UPLC vials with a residual volume of 9 µL were used for preparation of the historical samples. The dry residue was reconstituted with water: methanol [40 µL, 1:1 (v/v)] - allowing a single injection of 10 µL. Sample extracts were injected *via* a Rheodyne injector with a 10 µL sample loop using the mode “partial loop with needle overfilled”. Sample extracts were injected automatically *via* a Rheodyne injector with a 10 µL sample loop. The PDA detector recorded all spectral information between 250 and 500 nm; chromatographed peaks were monitored at 254 nm. The bandwidth (resolution) was 1.2 nm with a sampling rate of 5 points s<sup>-1</sup>.

For both methods the column temperature was set to 55 °C, to reduce solvent viscosity, which allowed a back pressure of 8500 - 9000 psi to be employed. A pH 3 aqueous phase was prepared using H<sub>2</sub>O (250 mL) with the addition of glacial acetic acid (50 µL) using a calibrated micropipette (equivalent to 0.02 %).

Method B: used a BEH C18 reverse phase column, 1.7 µm particle size, 50 × 2.1 mm (length × i.d.), with in-line filter. The total run time was 6 min at a flow rate of 500 µL min<sup>-1</sup>. A binary solvent system was used; A = 0.02 % aqueous formic acid, B = MeOH. The elution programme was isocratic for 0.25 min (75A: 25B) then a linear gradient from 0.25 min to 4 min (20A: 80B) before recovery of the initial conditions over 10 s and equilibration over 2 min.

Method C: used a PST BEH C18 reverse phase column, 1.7 µm particle size, 150 × 2.1 mm (length × i.d.), with in-line filter. The total run time was 37.33 min at a flow rate of

250  $\mu\text{L min}^{-1}$ . A binary solvent system was used; A = 0.02 % aqueous formic acid, B = MeOH. The elution programme was isocratic for 3.33 min (75A: 25B) then a linear gradient from 3.33 min to 29 min (10A: 90B) before recovery of the initial conditions over 1 min and equilibration over 5 min.

Details of the columns and the chromatographic programmes used can be found below in tables 7.1 and 7.2.

Column Name	SphereClone ODS (2) 150 × 4.6 mm, 5 $\mu\text{m}$	BEH C18 50 × 2.1 mm, 1.7 $\mu\text{m}$	BEH C18 150 × 2.1 mm, 1.7 $\mu\text{m}$
Manufacturer	Phenomenex	Waters	Waters
Part Number	00F-4135-E0	186002350	186003556
Column L × i.d. [mm]	150 × 4.6	50 × 2.1	150 × 2.1
Technology		Ethylene Bridged Hybrid (BEH)	Peptide Separation Technology (PST)
Particle Substrate		Hybride	Hybride
Stationary phase		Ethylene Bridged Hybrid	Ethylene Bridged Hybrid
Ligand Type	C <sub>18</sub>	Trifunctional C <sub>18</sub>	Trifunctional C <sub>18</sub>
Ligand Density $\mu\text{mol/m}^2$		3.1	3.1
Surface Area $\text{m}^2/\text{g}$		185	185
Mode	Reverse Phase	Reverse Phase	Reverse Phase
Carbon load [%]		18	18
Partical Shape	Spherical	Spherical	Spherical
Particle size [ $\mu\text{m}$ ]	5	1.7	1.7
Pore diameter [ $\text{\AA}$ ] / Volume mL/g		130 $\text{\AA}$ 0.7 mL/g	130 $\text{\AA}$ 0.7 mL/g
Endcapped		Yes	Yes
pH range		1 - 12	1 - 12
Maximum Rated Pressure		18,000 PSI or 1241 bar	18,000 PSI or 1241 bar
L / dp	30,000	29,500	88,300
Volume Column ( $\pi \times r^2 \times L$ ) Ml	2.49	0.17	0.52

**Table 7.1:** Columns information.

Method A, HPLC, ODS(2), 150 × 4.6 mm, 5 $\mu\text{m}$					
Solvent System	A 20/80 MeOH:H <sub>2</sub> O v/v	B MeOH	C 5/95 Phos. Ac:H <sub>2</sub> O v/v	Gradient (min)	Curve
Programme	67	23	10	0	Initial
	67	23	10	3	11
	0	90	10	29	6
	67	23	10	30	6
Equilibration Period	67	23	10	35	11
Flow rate [ $\mu\text{l}/\text{min}$ ]	1200				

Temperature [°C]	25
Injected Volume [μl], manual injection	20

<b>Method B, UPLC, BEH C18, 50 x 2.1 mm, 1.7 μm</b>				
Solvent System	A	B	Gradient (min )	Curve
	0.02% CH <sub>3</sub> COOH aq.	MeOH		
Programme	75	25	0	Initial
	75	25	0.25	6
	20	80	4	6
	75	25	4.1	6
Equilibration Period	75	25	6	6
Flow rate [μl/min]	500			
Temperature	55			
Injected Volume [μl], autosampler	2.5			
Strong Wash	CH <sub>3</sub> CN 10/90			
Weak Wash	CH <sub>3</sub> CN:H <sub>2</sub> O, v/v			

<b>Method C, UPLC, BEH C18, 150 x 2.1 mm, 1.7 μm</b>				
Solvent System	A	B	Gradient (min )	Curve
	0.02% CH <sub>3</sub> COOH aq.	MeOH		
Programme	77	23	0	Initial
	77	23	3.33	6
	10	90	29.33	6
	77	23	30.33	6
Equilibration Period	77	23	37.33	6
Flow rate [μl/min]	250			
Temperature	55			
Injected Volume [μl], autosampler	5			
Strong Wash	CH <sub>3</sub> CN 10/90			
Weak Wash	CH <sub>3</sub> CN:H <sub>2</sub> O, v/v			

**Tables 7.2:** Chromatographic programmes.

#### 7.1.4.3 UPLC ESI MS system

Analysis was performed using a Waters Acquity UPLC<sup>®</sup> system coupled with a QTOF2 Mass Spectrometer (MS) (Micromass Waters Corporation, Manchester, UK) equipped with an electrospray ionization source. Method C': used a PST BEH C18 reverse phase column, 1.7 μm particle size, 150 × 2.1 mm (length × i.d.), with in-line filter. The total run time was 49.33 min at a flow rate of 250 μL min<sup>-1</sup>. A binary solvent system was used; A = 0.02 % aqueous formic acid, B = MeOH. The elution programme was isocratic for 3.33 min (75A: 25B), then a linear gradient from 3.33 min to 41.33 min

(10A: 90B) before recovery of the initial conditions over 1 min and equilibration over 5 min. MS analysis was conducted in negative ionization mode. Source conditions included a capillary voltage of 2.71 kV, a sample cone voltage of 35 V, a desolvation temperature of 300°C and a source temperature of 120 °C. Data was collected using Masslynx 4.1 (Waters Corporation, Milford, MA, USA) and processed with Origin 8.5 (OriginLab, Northampton, MA, USA).

### 7.1.5 METHOD DEVELOPMENT

#### 7.1.5.1 Calibration curves

The calibration curves and linearity of each standard were calculated at 254, 350 and 430 nm. For the HPLC system (Method A), standards were investigated once and the calibration was made using 6 solutions ranging between 2 and 40  $\mu\text{g mL}^{-1}$ . Samples were injected manually via a Rheodyne injector with a 20  $\mu\text{L}$  sample loop. For the UPLC system (Method B), each standard was investigated in triplicate using an auto-sampler and the calibration was made using 7 solutions ranging between 0.5 and 80  $\mu\text{g mL}^{-1}$  (carminic acid used 6 solutions ranging between 5 and 160  $\mu\text{g mL}^{-1}$ ). For the UPLC system (Method C), each standard was investigated in triplicate using an auto-sampler and the calibration was made using 6 to 8 solutions ranging between 0.2 and 40  $\mu\text{g mL}^{-1}$  (carminic acid used 8 solutions ranging between 5 and 300  $\mu\text{g mL}^{-1}$ ).

Calibration curves and linearity range for HPLC method A and UPLC methods B and C are presented in table 7.3. Flavonoids standards were studied at 254 and 350 nm, while anthraquinones standards were studied at 254 and 430 m.

Method A : HPLC ODS(2), 150 × 4.6 mm, 5 $\mu\text{m}$ : each standard analysed once						
Compound [x]	254 nm		350 nm		430 nm	
	[x] ( $\mu\text{g/mL}$ ) vs. $A_x$ ( $R^2$ )	n [ $\mu\text{g/mL}$ ]	[x] ( $\mu\text{g/mL}$ ) vs. $A_x$ ( $R^2$ )	n [ $\mu\text{g/mL}$ ]	[x] ( $\mu\text{g/mL}$ ) vs. $A_x$ ( $R^2$ )	n [ $\mu\text{g/mL}$ ]
carminic acid	$y = 15853x - 34641$ (0.9928)	n = 6 [2 - 40]			$y = 5157.5x - 12809$ (0.9975)	n = 6 [2 - 40]
Luteolin	$y = 58444x - 102841$ (0.9933)	n = 6 [2 - 40]	$y = 74471x - 134955$ (0.9918)	n = 6 [2 - 40]		
Genistein	$y = 116528x - 130158$ (0.9905)	n = 6 [2 - 40]	$y = 9003.8x - 14107$ (0.9864)	n = 6 [2 - 40]		
Apigenin	$y = 41300x - 34861$ (0.9878)	n = 6 [2 - 40]	$y = 65765x - 109885$ (0.9912)	n = 6 [2 - 40]		

Alizarin	$y = 84887x - 85741$ (0.9964)	n = 6 [2 - 40]			$y = 17343x - 28269$ (0.9989)	n = 6 [2 - 40]
Purpurin	$y = 40942x - 63162$ (0.9927)	n = 6 [2 - 40]			$y = 5272x - 10741$ (0.9957)	n = 6 [2 - 40]
<b>Method B : UPLC, 50 × 2.1 mm, 1.7 μm : each standard analysed in triplicate</b>						
Compound [x]	254 nm		350 nm		430 nm	
	[x] (μg/mL) vs. A <sub>x</sub> (R <sup>2</sup> )	n [μg/mL]	[x] (μg/mL) vs. A <sub>x</sub> (R <sup>2</sup> )	n [μg/mL]	[x] (μg/mL) vs. A <sub>x</sub> (R <sup>2</sup> )	n [μg/mL]
carminic acid	$y = 7231.5x - 14520$ (0.9977)	n = 6 [5 - 160]			$y = 1331.8x + 591.71$ (0.9859)	n = 6 [5 - 160]
Fisetin	$y = 10609x + 5767.8$ (0.9944)	n = 7 [0.5 - 80]	$y = 15219x - 7260.6$ (0.9984)	n = 7 [0.5 - 80]		
Sulfuretin	$y = 8738.8x + 7148.7$ (0.9956)	n = 7 [0.5 - 80]	$y = 17443x - 3441.9$ (0.9992)	n = 7 [0.5 - 80]	$y = 12777x - 6585.9$ (0.9966)	n = 7 [0.5 - 80]
Luteolin	$y = 17582x - 1094.9$ (0.9956)	n = 7 [0.5 - 80]	$y = 18025x - 971.32$ (0.9995)	n = 7 [0.5 - 80]		
Genistein	$y = 30627x + 4886$ (0.994)	n = 7 [0.5 - 80]	$y = 2574.5x - 158.27$ (0.9983)	n = 7 [0.5 - 80]		
Apigenin	$y = 9040.3x + 10742$ (0.9925)	n = 7 [0.5 - 80]	$y = 15723x - 1620.8$ (0.9989)	n = 6 [0.5 - 40]		
Chrysoeriol	$y = 7098.5x + 12683$ (0.9926)	n = 7 [0.5 - 80]	$y = 10261x + 5015.9$ (0.9972)	n = 6 [0.5 - 40]		
Diosmetin	$y = 10607x - 6776.1$ (0.9983)	n = 7 [0.5 - 80]	$y = 12648x - 11226$ (0.9976)	n = 7 [0.5 - 80]		
Alizarin	$y = 26897x + 20034$ (0.9944)	n = 7 [0.5 - 80]			$y = 5070.7x + 2932.8$ (0.9947)	n = 7 [0.5 - 80]
Purpurin	$y = 11311x - 15902$ (0.9979)	n = 7 [0.5 - 80]			$y = 1404.5x - 2420.5$ (0.9977)	n = 5 [5 - 80]
<b>Method C : UPLC, 150 × 2.1 mm, 1.7 μm : each standard analysed in triplicate</b>						
Compound [x]	254 nm		350 nm		430 nm	
	[x] (μg/mL) vs. A <sub>x</sub> (R <sup>2</sup> )	n [μg/mL]	[x] (μg/mL) vs. A <sub>x</sub> (R <sup>2</sup> )	n [μg/mL]	[x] (μg/mL) vs. A <sub>x</sub> (R <sup>2</sup> )	n [μg/mL]
carminic acid	$y = 21531x - 38694$ (0.9985)	n = 8 [5 - 300]			$y = 6250.1x - 39771$ (0.9979)	n = 7 [5 - 300]
Fisetin	$y = 52077x - 13517$ (0.9986)	n = 8 [0.2 - 40]	$y = 67736x - 14165$ (0.9988)	n = 7 [0.1 - 40]		
Sulfuretin	$y = 36740x + 2992.4$ (0.999)	n = 8 [0.2 - 40]	$y = 66468x + 3515.9$ (0.9997)	n = 7 [0.1 - 40]	$y = 49583x - 5394.3$ (0.9996)	n = 8 [0.1 - 40]
Luteolin	$y = 74376x + 3791.5$ (0.9998)	n = 8 [0.2 - 40]	$y = 76802x - 8180.5$ (0.9991)	n = 7 [0.1 - 40]		
Genistein	$y = 123813x + 7069.6$ (0.9998)	n = 8 [0.2 - 40]	$y = 8742.4x + 1178.2$ (0.9996)	n = 7 [0.1 - 40]		
Apigenin	$y = 48781x - 842.08$ (0.9998)	n = 6 [0.5 - 20]	$y = 64572x + 57708$ (0.9927)	n = 6 [0.5 - 40]		
Chrysoeriol	$y = 78188x + 900.28$ (0.9999)	n = 6 [0.5 - 20]	$y = 86431x + 80267$ (0.9927)	n = 7 [0.1 - 40]		

Diosmetin	$y = 70449x + 15823$ (0.995)	n = 8 [0.2 - 40]	$y = 83526x + 26901$ (0.9931)	n = 6 [0.5 - 40]		
Alizarin	$y = 135297x - 50758$ (0.9991)	n = 6 [0.5 - 20]			$y = 22916x + 3071$ (0.9974)	n = 7 [0.1 - 40]
Purpurin	$y = 46382x - 71845$ (0.9922)	n = 7 [0.5 - 40]			$y = 5991x - 18676$ (0.9941)	n = 5 [1 - 40]

**Table 7.3:** Calibration curves and linearity range for the standards analysed with Method A, Method B and Methods C, at 254 nm (all standards), 350 nm (only flavonoids) and 430 nm (only anthraquinones).

### 7.1.5.2 Limit of detection (LOD) and quantification (LOQ)

For both the HPLC and UPLC systems, the limit of detection (LOD) and limit of quantification (LOQ) were calculated based on the slopes of the calibration curves (Concentration vs. Peak Height) and the noise ( $s$ ) of the baseline noise of sample blanks analysed and calculated at 254, 350 and 430 nm. For the HPLC system (Method A), the noise ( $s$ ) was calculated using the average modulus of the baseline noise  $H_{\text{noise}}$  of 4 sample blanks using all data points (ASCII files); while for the UPLC system (Methods B and C) the noise ( $s$ ) was calculated using the average modulus of the baseline noise  $H_{\text{noise}}$  of 6 sample blanks, also using all data points (ASCII files). The Concentration vs. Peak Height relationship was calculated using the ASCII files of each standard and the intercepts of the equations were set to zero and used to calculate the LOD and LOQ values as 3.3 and 10 times the  $s$  values of the baseline, respectively. For a few samples the noise drifted slightly below zero (e.g.  $-(5 \pm 1) \times 10^{-4}$ ) and as a result the  $|H_{\text{noise}}|$  was used for the calculation of the LOD and LOQ.

On HPLC system (Method A), some issues arise during these experiments, possibly due to a recent replacement of the flow cell, and it was found at 254 nm that the baseline was drifting below zero while the organic phase was increasing in the gradient. For this reason, because of the negative value of the noise, the best estimation at 254 nm of the LOD and LOQ was obtained as  $(2.3 \times s)/S$  and the LOQ as  $(9 \times s)/S$ , using the  $|H_{\text{noise}}|$  of 4 solvent blanks analysed.

Details calculation of LOD and LOQ values for HPLC method A and UPLC methods B and C can be found in the tables 7.4 to 7.6. Flavonoids standards were studied at 254 and 350 nm, while anthraquinones standards were studied at 254 and 430 m.

<b>Method A: HPLC, ODS(2), 150 × 4.6 mm, 5 μm at 254 nm (injection volume 20 μL)</b>					
<b>Compound [x]</b>	<b>[x] (μg mL<sup>-1</sup>) vs. H<sub>x</sub><sup>a</sup> (AU), with b<sup>b</sup> = 0 (R<sup>2</sup>)</b>	<b>[x] (μg mL<sup>-1</sup>) vs. H<sub>x</sub><sup>a</sup>(AU), (R<sup>2</sup>)</b>	<b>H<sub>noise</sub> (AU) (n = 4)</b>	<b>LOD ± s (μg mL<sup>-1</sup>)</b>	<b>LOQ ± s (μg mL<sup>-1</sup>)</b>
carminic acid	y = 0.0009x (0.9674)	y = 0.0010x - 0.0025 (0.9836)	(7 ± 3) × 10 <sup>-5</sup>	0.24 ± 0.10	0.73 ± 0.30
luteolin	y = 0.0051x (0.9069)	y = 0.0065x - 0.0365 (0.9948)	-(12.3 ± 1.4) × 10 <sup>-3</sup>	7.96 ± 0.89	24.12 ± 2.68
genistein	y = 0.0099x (0.9589)	y = 0.0114x - 0.0398 (0.9928)	-(12.3 ± 1.4) × 10 <sup>-3</sup>	4.10 ± 0.46	12.43 ± 1.38
apigenin		y = 0.0050x - 0.0418 (0.9759)	-(19 ± 0.6) × 10 <sup>-3</sup>	12.53 ± 0.40	37.98 ± 1.21
<b>Method B: UPLC, BEH C18 Column, 2.1 × 50 mm, 1.7 μm at 254 nm (injection volume 2.5 μL)</b>					
<b>Compound [x]</b>	<b>[x] (μg mL<sup>-1</sup>) vs. H<sub>x</sub><sup>a</sup> (AU), with b<sup>b</sup> = 0 (R<sup>2</sup>)</b>	<b>[x] (μg mL<sup>-1</sup>) vs. H<sub>x</sub><sup>a</sup>(AU), (R<sup>2</sup>)</b>	<b>H<sub>noise</sub> (AU) (n = 6)</b>	<b>LOD ± s (μg mL<sup>-1</sup>)</b>	<b>LOQ ± s (μg mL<sup>-1</sup>)</b>
carminic acid	y = 0.0009x (0.996)	y = 0.001x - 0.0022 (0.9991)	(7 ± 1) × 10 <sup>-5</sup>	0.25 ± 0.05	0.74 ± 0.17
fisetin	y = 0.0028x (0.9994)	y = 0.0028x - 0.0006 (0.9996)	-(5 ± 1) × 10 <sup>-4</sup>	0.57 ± 0.12	1.73 ± 0.37
sulfuretin	y = 0.0022x (0.9997)	y = 0.0022x - 0.0002 (0.9997)	-(5 ± 1) × 10 <sup>-4</sup>	0.72 ± 0.16	2.20 ± 0.47
luteolin	y = 0.0045x (0.9994)	y = 0.0046x - 0.0019 (0.9995)	-(5 ± 1) × 10 <sup>-4</sup>	0.35 ± 0.08	1.07 ± 0.23
genistein	y = 0.0076x (0.9998)	y = 0.0077x - 0.0018 (0.9999)	-(5 ± 1) × 10 <sup>-4</sup>	0.21 ± 0.05	0.64 ± 0.14
apigenin	y = 0.0023x (0.9991)	y = 0.0023x - 0.0011 (0.9997)	-(7.0 ± 0.4) × 10 <sup>-4</sup>	1.00 ± 0.06	3.05 ± 0.17
chrysoeriol	y = 0.0019x (0.9961)	y = 0.0018x + 0.0008 (0.9965)	-(7.0 ± 0.4) × 10 <sup>-4</sup>	1.22 ± 0.07	3.69 ± 0.21
diosmetin	y = 0.0025x (0.9955)	y = 0.0026x - 0.0043 (0.9977)	-(7.0 ± 0.4) × 10 <sup>-4</sup>	0.89 ± 0.05	2.69 ± 0.14
alizarin	y = 0.0059x (0.9984)	y = 0.006x - 0.0042 (0.9996)	-(7.0 ± 0.4) × 10 <sup>-4</sup>	0.39 ± 0.02	1.19 ± 0.07
purpurin	y = 0.0019x (0.9955)	y = 0.0019x - 0.0041 (0.9987)	-(7.0 ± 0.4) × 10 <sup>-4</sup>	1.22 ± 0.07	3.69 ± 0.21
<b>Method C: UPLC, PST BEH C18 Column, 2.1 × 50 mm, 1.7 μm at 254 nm (injection volume 5 μL)</b>					
<b>Compound [x]</b>	<b>[x] (μg mL<sup>-1</sup>) vs. H<sub>x</sub><sup>a</sup> (AU), with b<sup>b</sup> = 0 (R<sup>2</sup>)</b>	<b>[x] (μg mL<sup>-1</sup>) vs. H<sub>x</sub><sup>a</sup>(AU), (R<sup>2</sup>)</b>	<b>H<sub>noise</sub> (AU) (n = 6)</b>	<b>LOD ± s (μg mL<sup>-1</sup>)</b>	<b>LOQ ± s (μg mL<sup>-1</sup>)</b>
carminic acid	y = 0.0014x (0.9675)	y = 0.0016x - 0.0067 (0.999)	(1.6 ± 0.9) × 10 <sup>-4</sup>	0.39 ± 0.21	1.17 ± 0.65
fisetin	y = 0.0103x (0.9993)	y = 0.0104x - 0.0032 (0.9996)	(9 ± 1) × 10 <sup>-4</sup>	0.28 ± 0.05	0.85 ± 0.14
sulfuretin	y = 0.0078x (0.9999)	y = 0.0078x + 0.0005 (0.9999)	(9 ± 1) × 10 <sup>-4</sup>	0.37 ± 0.06	1.12 ± 0.19



luteolin	$y = 0.0165x$ (0.9999)	$y = 0.0165x + 0.0007$ (0.9999)	$(9 \pm 1) \times 10^{-4}$	$0.17 \pm 0.03$	$0.53 \pm 0.09$
genistein	$y = 0.0276x$ (0.9999)	$y = 0.0276x +$ $0.00009$ (0.9999)	$(9 \pm 1) \times 10^{-4}$	$0.10 \pm 0.02$	$0.32 \pm 0.05$
apigenin	$y = 0.0107x$ (0.9873)	$y = 0.0103x + 0.0107$ (0.9903)	$(12.1 \pm 0.6) \times 10^{-4}$	$0.37 \pm 0.02$	$1.13 \pm 0.05$
chrysoeriol	$y = 0.0176x$ (0.9871)	$y = 0.0169x + 0.0181$ (0.9903)	$(12.1 \pm 0.6) \times 10^{-4}$	$0.23 \pm 0.01$	$0.69 \pm 0.03$
diosmetin	$y = 0.0165x$ (0.9991)	$y = 0.0164x + 0.0035$ (0.9993)	$(12.1 \pm 0.6) \times 10^{-4}$	$0.24 \pm 0.01$	$0.74 \pm 0.03$
alizarin	$y = 0.0261x$ (0.9964)	$y = 0.0259x + 0.0039$ (0.9964)	$(12.1 \pm 0.6) \times 10^{-4}$	$0.15 \pm 0.01$	$0.47 \pm 0.02$
purpurin	$y = 0.0087x$ (0.9786)	$y = 0.0093x - 0.0184$ (0.9894)	$(12.1 \pm 0.6) \times 10^{-4}$	$1.01 \pm 0.54$	$3.06 \pm 1.63$

**Table 7.4:** Details of LOD and LOQ calculations at 254 nm for Methods A, B and C.

<b>Method A: HPLC, ODS(2), 150 × 4.6 mm, 5 μm at 350 nm (injection volume 20 μL)</b>					
<b>Compound [x]</b>	<b>[x] (μg mL<sup>-1</sup>) vs. H<sub>x</sub><sup>a</sup> (AU), with b<sup>b</sup> = 0 (R<sup>2</sup>)</b>	<b>[x] (μg mL<sup>-1</sup>) vs. H<sub>x</sub><sup>a</sup>(AU), (R<sup>2</sup>)</b>	<b>H<sub>noise</sub> (AU) (n = 4)</b>	<b>LOD ± s (μg mL<sup>-1</sup>)</b>	<b>LOQ ± s (μg mL<sup>-1</sup>)</b>
luteolin	$y = 0.0072x$ (0.9819)	$y = 0.0079x - 0.0181$ (0.9965)	$-(3 \pm 1) \times 10^{-4}$	$0.15 \pm 0.06$	$0.47 \pm 0.17$
genistein	$y = 0.0008x$ (0.9904)	$y = 0.0009x - 0.0015$ (0.9982)	$-(3 \pm 1) \times 10^{-4}$	$1.27 \pm 0.47$	$3.84 \pm 1.44$
apigenin	$y = 0.0072x$ (0.9619)	$y = 0.008x - 0.0199$ (0.9789)	$-(3 \pm 1) \times 10^{-4}$	$0.14 \pm 0.05$	$0.42 \pm 0.16$
<b>Method B: UPLC, BEH C18 Column, 2.1 × 50 mm, 1.7 μm at 350 nm (injection volume 2.5 μL)</b>					
<b>Compound [x]</b>	<b>[x] (μg mL<sup>-1</sup>) vs. H<sub>x</sub><sup>a</sup> (AU), with b<sup>b</sup> = 0 (R<sup>2</sup>)</b>	<b>[x] (μg mL<sup>-1</sup>) vs. H<sub>x</sub><sup>a</sup>(AU), (R<sup>2</sup>)</b>	<b>H<sub>noise</sub> (AU) (n = 6)</b>	<b>LOD ± s (μg mL<sup>-1</sup>)</b>	<b>LOQ ± s (μg mL<sup>-1</sup>)</b>
Fisetin	$y = 0.0036x$ (0.9997)	$y = 0.0036x - 0.0006$ (0.9998)	$-(3 \pm 0.5) 10^{-4}$	$0.27 \pm 0.04$	$0.83 \pm 0.13$
sulfuretin	$y = 0.0041x$ (0.9997)	$y = 0.0041x + 0.0004$ (0.9997)	$-(3 \pm 0.5) 10^{-4}$	$0.24 \pm 0.04$	$0.73 \pm 0.11$
luteolin	$y = 0.0041x$ (0.9995)	$y = 0.0041x + 0.0008$ (0.9996)	$-(3 \pm 0.5) 10^{-4}$	$0.24 \pm 0.04$	$0.73 \pm 0.11$
genistein	$y = 0.0006x$ (0.9996)	$y = 0.0006x - 0.0002$ (0.9997)	$-(3 \pm 0.5) 10^{-4}$	$1.64 \pm 0.25$	$4.98 \pm 0.77$
apigenin	$y = 0.0029x$ (0.9944)	$y = 0.0029x + 0.0055$ (0.9970)	$-(3 \pm 0.5) 10^{-4}$	$0.34 \pm 0.05$	$1.03 \pm 0.16$
chrysoeriol	$y = 0.002x$ (0.9897)	$y = 0.0019x + 0.0047$ (0.9939)	$-(3 \pm 0.5) 10^{-4}$	$0.49 \pm 0.08$	$1.49 \pm 0.23$

diosmetin	$y = 0.003x$ (0.9953)	$y = 0.0031x - 0.0067$ (0.9985)	$-(3 \pm 0.5) 10^{-4}$	$0.33 \pm 0.05$	$1.00 \pm 0.15$
<b>Method C: UPLC, PST BEH C18 Column, 2.1 × 50 mm, 1.7 μm at 350 nm (injection volume 5 μL)</b>					
Compound [x]	[x] (μg mL <sup>-1</sup> ) vs. H <sub>x</sub> <sup>a</sup> (AU), with b <sup>b</sup> = 0 (R <sup>2</sup> )	[x] (μg mL <sup>-1</sup> ) vs. H <sub>x</sub> <sup>a</sup> (AU), (R <sup>2</sup> )	H <sub>noise</sub> (AU) (n = 6)	LOD ± s (μg mL <sup>-1</sup> )	LOQ ± s (μg mL <sup>-1</sup> )
fisetin	$y = 0.0133x$ (0.9988)	$y = 0.0135x - 0.006$ (0.9993)	$(3.3 \pm 0.4) 10^{-4}$	$0.08 \pm 0.01$	$0.24 \pm 0.03$
sulfuretin	$y = 0.0141x$ (0.9999)	$y = 0.0141x - 0.0004$ (0.9999)	$(3.3 \pm 0.4) 10^{-4}$	$0.08 \pm 0.01$	$0.23 \pm 0.03$
luteolin	$y = 0.0165x$ (0.9991)	$y = 0.0167x - 0.0053$ (0.9994)	$(3.3 \pm 0.4) 10^{-4}$	$0.07 \pm 0.01$	$0.20 \pm 0.02$
genistein	$y = 0.0019x$ (0.9999)	$y = 0.0019x + 0.0002$ (0.9999)	$(3.3 \pm 0.4) 10^{-4}$	$0.57 \pm 0.07$	$1.74 \pm 0.22$
apigenin	$y = 0.0164x$ (0.9872)	$y = 0.0158x + 0.016$ (0.9901)	$(3.3 \pm 0.4) 10^{-4}$	$0.07 \pm 0.01$	$0.20 \pm 0.03$
chrysoeriol	$y = 0.0224x$ (0.9868)	$y = 0.0216x + 0.0231$ (0.9900)	$(3.3 \pm 0.4) 10^{-4}$	$0.05 \pm 0.01$	$0.15 \pm 0.02$
diosmetin	$y = 0.0202x$ (0.9997)	$y = 0.0204x - 0.0026$ (0.9999)	$(3.3 \pm 0.4) 10^{-4}$	$0.05 \pm 0.01$	$0.16 \pm 0.02$

**Table 7.5:** Details of LOD and LOQ calculations at 350 nm for Methods A, B and C.

<b>Method A: HPLC, ODS(2), 150 × 4.6 mm, 5 μm at 430 nm (injection volume 20 μL)</b>					
Compound [x]	[x] (μg mL <sup>-1</sup> ) vs. H <sub>x</sub> <sup>a</sup> (AU), with b <sup>b</sup> = 0 (R <sup>2</sup> )	[x] (μg mL <sup>-1</sup> ) vs. H <sub>x</sub> <sup>a</sup> (AU), (R <sup>2</sup> )	H <sub>noise</sub> (AU) (n = 4)	LOD ± s (μg mL <sup>-1</sup> )	LOQ ± s (μg mL <sup>-1</sup> )
carminic acid	$y = 0.0003x$ (0.9820)	$y = 0.0003x - 0.0008$ (0.9975)	$-(1.6 \pm 0.3) 10^{-4}$	$1.78 \pm 0.28$	$5.40 \pm 0.83$
alizarin	$y = 0.0018x$ (0.9635)	$y = 0.002x - 0.0062$ (0.9887)	$-(5.2 \pm 0.3) 10^{-4}$	$0.96 \pm 0.05$	$2.91 \pm 0.16$
purpurin	$y = 0.0005x$ (0.9671)	$y = 0.0005x - 0.0017$ (0.9959)	$-(5.2 \pm 0.3) 10^{-4}$	$4.09 \pm 0.31$	$12.40 \pm 0.94$
<b>Method B: UPLC, BEH C18 Column, 2.1 × 50 mm, 1.7 μm at 430 nm (injection volume 2.5 μL)</b>					
Compound [x]	[x] (μg mL <sup>-1</sup> ) vs. H <sub>x</sub> <sup>a</sup> (AU), with b <sup>b</sup> = 0 (R <sup>2</sup> )	[x] (μg mL <sup>-1</sup> ) vs. H <sub>x</sub> <sup>a</sup> (AU), (R <sup>2</sup> )	H <sub>noise</sub> (AU) (n = 6)	LOD ± s (μg mL <sup>-1</sup> )	LOQ ± s (μg mL <sup>-1</sup> )
carminic acid	$y = 0.0002x$ (0.9915)	$y = 0.0002x - 0.0005$ (0.9964)	$-(9 \pm 5) 10^{-5}$	$1.46 \pm 0.74$	$4.44 \pm 2.24$
alizarin	$y = 0.001x$ (0.9938)	$y = 0.001x + 0.0007$ (0.9943)	$-(9 \pm 5) 10^{-5}$	$0.27 \pm 0.13$	$0.81 \pm 0.41$
purpurin	$y = 0.0002x$ (0.9962)	$y = 0.0002x - 0.0005$ (0.9989)	$-(9 \pm 5) 10^{-5}$	$1.46 \pm 0.74$	$4.44 \pm 2.24$

Method C: UPLC, PST BEH C18 Column, 2.1 × 50 mm, 1.7 μm at 430 nm (injection volume 5 μL)					
Compound [x]	[x] (μg mL <sup>-1</sup> ) vs. H <sub>x</sub> <sup>a</sup> (AU), with b <sup>b</sup> = 0 (R <sup>2</sup> )	[x] (μg mL <sup>-1</sup> ) vs. H <sub>x</sub> <sup>a</sup> (AU), (R <sup>2</sup> )	H <sub>noise</sub> (AU) (n = 6)	LOD ± s (μg mL <sup>-1</sup> )	LOQ ± s (μg mL <sup>-1</sup> )
carminic acid	y = 0.0004x (0.9949)	y = 0.0004x - 0.0016 (0.9977)	(1.7 ± 0.3) × 10 <sup>-4</sup>	1.40 ± 0.28	4.25 ± 0.85
alizarin	y = 0.005x (0.9976)	y = 0.005x - 0.0003 (0.9976)	(1.7 ± 0.3) × 10 <sup>-4</sup>	0.11 ± 0.02	0.34 ± 0.07
purpurin	y = 0.0011x (0.9654)	y = 0.0012x - 0.003 (0.9838)	(1.7 ± 0.3) × 10 <sup>-4</sup>	0.51 ± 0.10	1.55 ± 0.31

**Table 7.6:** Details of LOD and LOQ calculations at 430 nm for Methods A, B and C.

### 7.1.5.3 Comparison of response: H<sub>x</sub> (AU) and [x] (ng) for genistein

C (ug mL <sup>-1</sup> )	Quantity (ng)	Peak Height (AU)
<b>genistein (11): Method A, HPLC 5 × 150</b>		
40	800	0.4286877
20	400	0.1642442
10	200	0.0670349
5	100	0.02095031
4	80	0.006455172
2	40	-0.002868667
<b>genistein (11): Method B, UPLC 2.1 × 50</b>		
80	200	0.6118224
40	100	0.302143
20	50	0.1555234
10	25	0.0739036
5	12.5	0.03399162
1	2.5	0.006227607
0.5	1.25	3.07E-03
<b>genistein (11): Method C UPLC 2.1 × 150</b>		
40	200	1.106591
20	100	0.5505305
10	50	0.2774273
5	25	0.1378356
1	5	0.0284015
0.5	2.5	0.01408753

**Table 7.7:** Comparing the relation between H<sub>x</sub> (AU) and [x] (ng) for genistein at 254 nm; Method A: y = 0.0006x - 0.0398 [R<sup>2</sup> = 0.9928]; Method B: y = 0.0031x - 0.0018 [R<sup>2</sup> = 0.9999]; Method C: y = 0.0055x + 9E-05 [R<sup>2</sup> = 1].

### 7.1.6 Evaluation of sample preparation

Filtration of the extract prior to analysis is an important step in sample preparation, especially when dealing with historical textile samples that may well be compromised by solid contaminants, despite the inevitable accompanying loss of analyte. Thus analyte recovery and the reproducibility associated with the sample preparation protocol used for UPLC analysis, were compared with that of the sample preparation protocol routinely used for HPLC analysis using mock extraction protocols as follows.

A solution containing carminic acid, fisetin, sulfuretin, luteolin, genistein, chrysoeriol diosmetin, alizarin and purpurin standards in water:methanol [200  $\mu$ L, 1:1 (v/v)] was treated with 37% hydrochloric acid (200  $\mu$ L). The solution was then heated at 100 °C for precisely 10 min. After cooling down to room temperature, the extract was transferred into a 1 mL Eppendorf vial and the glass tube was rinsed with water:methanol [100  $\mu$ L, 1:1 (v/v)]. The combined extracts were centrifuged for 10 min at 10,000 rpm and then filtered directly into Waters UPLC vials using a Polyethylene filter (55  $\mu$ m, 5 mm) from Crawford Scientific™ [HPLC protocol], PTFE Phenomenex syringe filter (0.2  $\mu$ m, 4 mm) UPLC protocol]; RC Phenex Phenomenex syringe filters (0.2  $\mu$ m, 4 mm) UPLC protocol] and Strata SPE C18 Phenomenex (1 mL, 55  $\mu$ m) [UPLC protocol]. The extract was then cooled with liquid nitrogen and dried under vacuum using a freeze drier. The dry residue was then reconstituted with water: methanol [200  $\mu$ L, 1:1 (v/v)] and 5  $\mu$ L was injected onto the UPLC system for analysis. Each mock extraction protocol was performed in triplicate in order to evaluate the reproducibility of the sample preparation and compare recoveries.

	Compound [x]									
	33	14	15	9	11	10	12	13	26	28
	Standard Mixture ( $\mu\text{g mL}^{-1}$ )									
Analysis 1	74	15	16	17	16	13	8	16	13	12
Analysis 2	79	16	16	17	17	13	8	17	13	12
Analysis 3	79	16	16	17	17	12	8	17	13	12
<b>Average</b>	<b>77</b>	<b>16</b>	<b>16</b>	<b>17</b>	<b>17</b>	<b>13</b>	<b>8</b>	<b>17</b>	<b>13</b>	<b>12</b>
<b>stdv</b>	<b>3.0</b>	<b>0.1</b>	<b>0.1</b>	<b>0.1</b>	<b>0.1</b>	<b>0.1</b>	<b>0.1</b>	<b>0.1</b>	<b>0.1</b>	<b>0.2</b>
	<b>HCl extraction and filtration with PTFE filter (0.2 <math>\mu\text{m}</math>, 4 mm)</b>									
Analysis 1	34	9	15	13	15	13	11	13	13	10
Analysis 2	42	12	15	14	15	14	12	14	13	10
Analysis 3	44	9	15	13	14	12	10	13	13	12
Average	40	10	15	14	15	13	11	13	13	11
stdv	5.1	1.3	0.3	0.6	0.4	0.6	0.6	0.6	0.0	1.2
<b>Recovery %</b>	<b>52</b>	<b>66</b>	<b>94</b>	<b>80</b>	<b>89</b>	<b>103</b>	<b>139</b>	<b>81</b>	<b>92</b>	<b>88</b>
	<b>HCl extraction and filtration with RC Phenex filters (0.2 <math>\mu\text{m}</math>, 4 mm)</b>									
Analysis 1	36	9	13	13	14	12	10	13	11	10
Analysis 2	37	9	12	11	13	11	9	11	11	10
Analysis 3	52	11	14	14	14	13	11	14	12	13
Average	42	10	13	13	14	12	10	13	11	11
stdv	8.6	0.9	0.9	1.1	0.9	1.0	0.8	1.1	0.8	1.5
<b>Recovery %</b>	<b>54</b>	<b>64</b>	<b>84</b>	<b>74</b>	<b>82</b>	<b>97</b>	<b>128</b>	<b>76</b>	<b>83</b>	<b>90</b>
	<b>HCl extraction and Polyethylene filter (55 <math>\mu\text{m}</math>, 5 mm)</b>									
Analysis 1	38	6	14	13	15	13	11	14	12	5
Analysis 2	58	13	14	15	15	14	12	15	13	13
Analysis 3	51	12	15	16	15	14	12	15	13	12
Average	49	10	15	15	15	14	12	15	13	10
stdv	10.3	3.4	0.3	1.4	0.2	0.6	0.7	0.9	0.3	4.4
<b>Recovery %</b>	<b>64</b>	<b>67</b>	<b>92</b>	<b>86</b>	<b>91</b>	<b>111</b>	<b>147</b>	<b>89</b>	<b>92</b>	<b>84</b>
	<b>HCl extraction and filtration Strata SPE C18 (1 mL, 55 <math>\mu\text{m}</math>)</b>									
Analysis 1	7	5	13	10	13	10	8	9	10	4
Analysis 2	36	10	15	14	15	13	11	13	12	7
Analysis 3	28	8	15	13	14	12	10	12	12	8
Average	24	7	14	12	14	11	9	12	11	6
stdv	15.1	2.3	1.0	2.3	1.2	1.8	1.5	2.0	0.9	2.0
<b>Recovery %</b>	<b>31</b>	<b>48</b>	<b>91</b>	<b>71</b>	<b>83</b>	<b>92</b>	<b>120</b>	<b>70</b>	<b>82</b>	<b>51</b>

**Table 7.8:** Comparing relative recovery after hydrochloric acid hydrolysis followed by filtration using PTFE 0.2  $\mu\text{m}$  filters, RC Phenex 0.2  $\mu\text{m}$  filters, Polyethylene 55  $\mu\text{m}$  filters and Strata SPE C18 55  $\mu\text{m}$ .

### 7.1.7 Investigation of reference yarns

#### 7.1.7.1 Weld (*Reseda luteola* L.)

The reference yarns YS1a and YW1 prepared during the MODHT project were extracted using hydrochloric acid protocol and analysed on the UPLC system. Each yarn was investigated in triplicate and the relative amount of each dye component extracted at 254 nm can be found in the table below.

Sample ID	UPLC Entry	luteolin (9)	apigenin (10)	chrysoeriol (12)	diosmetin (13)
YS1a	-	93.0	4.0	3.0	ND
YS1a	107	92.8	4.1	3.1	ND
YS1a	167	92.6	4.1	3.3	ND
YS1a	313	91.9	4.5	3.6	ND
<i>Average</i>		<b>92.8</b>	4.0	3.1	
<i>Stdv</i>		<b>0.2</b>	0.1	0.1	
YW1	119	93.0	4.1	3.0	ND
YW1	311	92.6	4.6	2.8	ND
YW1	312	93.3	4.1	2.6	ND
<i>Average</i>		<b>93.0</b>	<b>4.3</b>	<b>2.8</b>	
<i>Stdv</i>		<b>0.4</b>	<b>0.3</b>	<b>0.2</b>	

**Table 7.9:** Characterisation of the relative amount of the flavonoid dyes characterised in the acid hydrolysed extract of reference yarns dyed with weld, YW1 and YS1a, monitored at 254 nm.

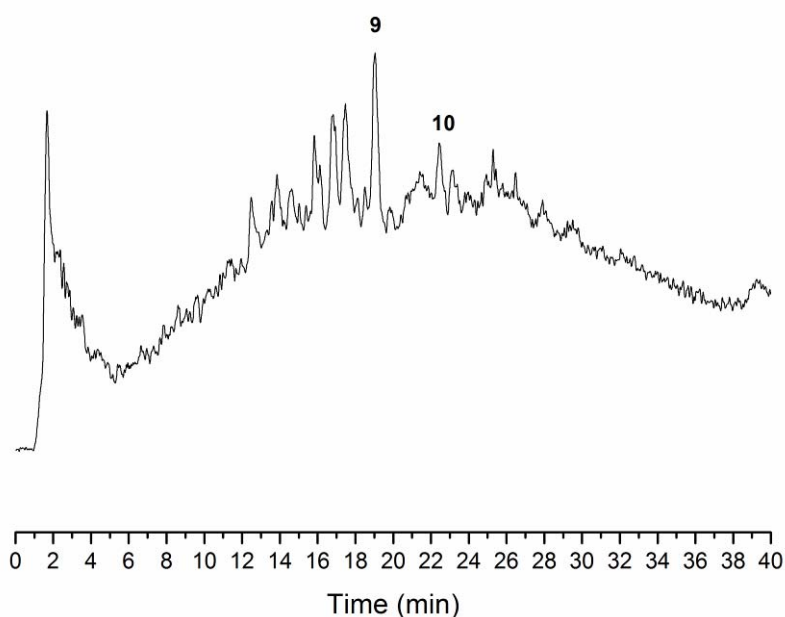


**Figure 7.1:** Total Ion Count (TIC) collected in negative ionization mode with UPLC Method C' of the acid hydrolysed reference MODHT YS1a (weld). Identified in the chromatogram are the  $[M-H]^-$  and significant cluster ions of the flavones luteolin (9) and apigenin (10).

### 7.1.7.2 Dyer's greenweed (*Genista tinctoria* L.)

The reference yarns YS3a, YS3b, YS3c, YS3d and YW2 prepared during the MODHT project were extracted using hydrochloric acid protocol and analysed on the UPLC system. Each yarn was investigated in triplicate and the relative amount of each dye component extracted at 254 nm can be found in the table below.

<i>Sample ID</i>	<i>UPLC Entry</i>	<i>Gt1</i>	<i>Gt2</i>	<i>Gt3</i>	luteolin (9)	genistein (11)	<i>Gt4</i>	apignin (10)	chrysoeriol (12)	diosmetin (13)
YW2	120	0.0	5.1	22.8	22.6	33.7	6.4	6.9	0.7	1.7
YW2	314	0.0	4.6	19.8	27.5	35.4	2.5	6.4	1.4	2.4
YW2	315	0.0	4.0	19.7	26.5	35.4	2.8	6.8	1.8	3.1
<i>average</i>		0.0	4.6	20.8	25.5	34.8	3.9	6.7	1.3	2.4
<i>stdv</i>		0.0	0.5	1.8	2.6	1.0	2.2	0.3	0.6	0.7
YS3a	-	1.8	3.7	15.9	33.9	33.6	2.0	5.5	1.2	2.4
YS3a	108	3.2	4.1	23.5	26.4	33.7	2.0	4.6	0.9	1.7
YS3a	316	0.8	1.4	19.9	30.1	36.8	1.9	5.4	1.3	2.3
YS3a	317	2.0	4.4	19.0	29.4	34.8	2.1	5.0	1.1	2.3
YS3a	318	2.3	4.6	17.7	31.0	32.5	2.4	5.5	1.4	2.6
<i>average</i>		<b>2.0</b>	<b>3.6</b>	<b>19.2</b>	<b>30.2</b>	<b>34.3</b>	<b>2.1</b>	<b>5.2</b>	<b>1.2</b>	<b>2.3</b>
<i>stdv</i>		<b>0.9</b>	<b>1.3</b>	<b>2.8</b>	<b>2.7</b>	<b>1.6</b>	<b>0.2</b>	<b>0.4</b>	<b>0.2</b>	<b>0.3</b>
YS3b	109	2.1	3.0	15.7	38.3	30.1	2.6	4.1	1.2	2.8
YS3b	319	0.0	0.3	13.6	39.9	35.0	1.5	4.7	1.5	3.5
YS3b	320	0.0	0.0	12.8	41.1	34.5	2.0	4.8	1.4	3.4
<i>average</i>		<b>0.7</b>	<b>1.1</b>	<b>14.0</b>	<b>39.8</b>	<b>33.2</b>	<b>2.0</b>	<b>4.6</b>	<b>1.4</b>	<b>3.2</b>
<i>stdv</i>		<b>1.2</b>	<b>1.6</b>	<b>1.5</b>	<b>1.4</b>	<b>2.7</b>	<b>0.6</b>	<b>0.4</b>	<b>0.1</b>	<b>0.3</b>
YS3c	110	0.0	2.5	12.6	42.8	27.6	3.4	5.2	1.7	4.3
YS3c	321	0.0	3.7	9.3	45.2	26.8	3.1	5.6	1.9	4.5
YS3c	322	0.0	4.5	12.3	40.7	31.2	2.9	4.3	1.2	3.1
<i>average</i>		<b>0.0</b>	<b>3.5</b>	<b>11.4</b>	<b>42.9</b>	<b>28.5</b>	<b>3.1</b>	<b>5.0</b>	<b>1.6</b>	<b>4.0</b>
<i>stdv</i>		<b>0.0</b>	<b>1.0</b>	<b>1.8</b>	<b>2.3</b>	<b>2.3</b>	<b>0.2</b>	<b>0.7</b>	<b>0.4</b>	<b>0.8</b>
YS3d	-	0.0	4.0	5.3	62.8	18.3	1.7	3.3	1.4	3.2
YS3d	111	2.8	5.2	10.2	53.7	20.4	1.6	2.7	1.1	2.5
YS3d	323	1.2	4.0	6.4	58.2	20.7	2.2	3.0	1.4	3.0
YS3d	324	2.0	6.3	6.2	58.2	18.8	2.0	2.6	1.2	2.6
<i>average</i>		<b>1.5</b>	<b>4.9</b>	<b>7.0</b>	<b>58.2</b>	<b>19.5</b>	<b>1.9</b>	<b>2.9</b>	<b>1.3</b>	<b>2.8</b>
<i>stdv</i>		<b>1.2</b>	<b>1.1</b>	<b>2.1</b>	<b>3.7</b>	<b>1.2</b>	<b>0.3</b>	<b>0.3</b>	<b>0.1</b>	<b>0.4</b>

**Table 7.10:** Characterisation of the relative amount of the flavonoid and isoflavonoid dyes characterised in the acid hydrolysed extract of reference yarns dyed with dyer's greenweed, YW2 and YS3a and others subjected to over dyeing (YS3b to d), monitored at 254 nm.

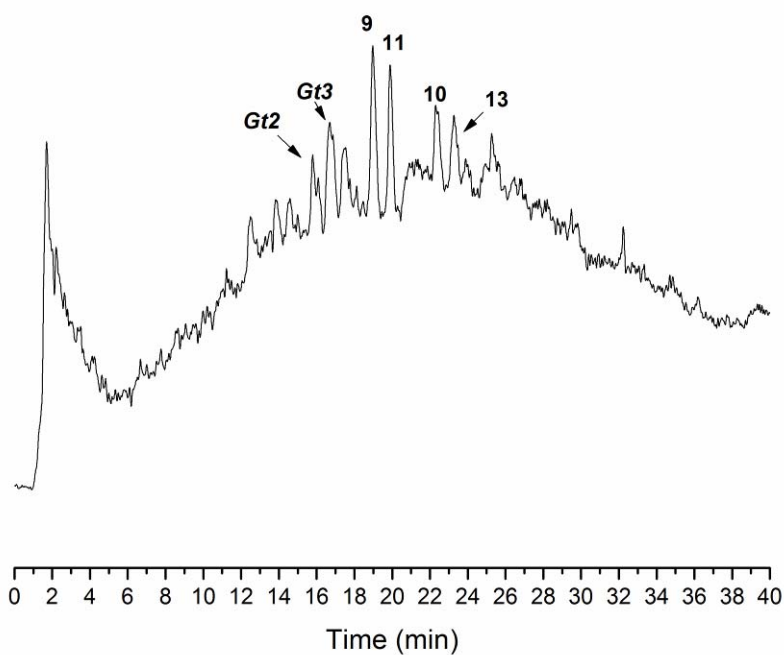


**Figure 7.2:** Total Ion Count (TIC) collected in negative ionization mode with UPLC Method C' of the acid hydrolysed reference MODHT YS3a (dyer's greenweed). Identified in the chromatogram are the  $[M-H]^-$  and significant cluster ions of unknown components **Gt2**, **Gt3**, the flavones luteolin (**9**) and apigenin (**10**), the isoflavone genistein (**11**), and a luteolin methyl-ether [identified by retention time in the UPLC chromatogram as diosmetin (**13**)].



## 7.2 INVESTIGATION OF MID 16<sup>TH</sup> CENTURY ENGLISH TAPESTRIES

### 7.2.1 *Extraction protocols*

#### 7.2.1.1 Hydrochloric acid extraction

For HPLC analysis, the dyed yarn (typically 1 - 5 mg) was placed in a 2 mL glass test tube, to which was added a mixture of 37% hydrochloric acid: methanol: water [400  $\mu$ L, 2:1:1 (v/v/v)]. The tube was then placed in a water bath at 100 °C and heated for precisely 10 min. After rapid cooling under cold water, the extract was filtered using a Polyethylene filter (55  $\mu$ m, 5 mm) from Crawford Scientific<sup>TM</sup>. The frit was rinsed with methanol (200  $\mu$ L) and the combined filtrates dried by rotary vacuum evaporation over a water bath at 40 °C. The dry residue was then reconstituted with methanol: water [50  $\mu$ L, 1:1 (v/v)] and 20  $\mu$ L was injected for analysis.

For UPLC analysis, the dyed yarn (typically 0.1 - 1 mg) was extracted in a 1 mL glass test tube, to which was added a mixture of 37% hydrochloric acid: methanol: water [200  $\mu$ L, 2:1:1 (v/v/v)]. The tube was then placed on a heated block at 100 °C and heated for precisely 10 min. After cooling down at room temperature, the extract was transferred into a 1 mL Eppendorf vial and the glass tube was rinsed with water: methanol [100  $\mu$ L, 1:1 (v/v)]. The combined extracts were centrifuged for 10 min at 10,000 rpm and then filtered directly into Waters UPLC vials using a PTFE Phenomenex syringe filter (0.2  $\mu$ m, 4 mm). The extract was then cooled with liquid Nitrogen and dried under vacuum using a freeze drier system. The dry residue was then reconstituted with water: methanol [40  $\mu$ L, 1:1 (v/v)] and 10  $\mu$ L was injected for analysis.

#### 7.2.1.2 Dimethyl Sulfoxide extraction

The dyed yarn (typically 0.1 - 1 mg) was placed in a 1 mL glass test tube, to which was added dimethyl sulfoxide [50  $\mu$ L]. The tube was then placed on a heated block at 100 °C and heated for precisely 60 min. After cooling down at room temperature, the extract was filtered directly into Waters UPLC vials using a PTFE Phenomenex syringe filter (0.2  $\mu$ m, 4 mm) and 10  $\mu$ L was injected for analysis.

## 7.2.2 Chromatographic methods

### 7.2.2.1 HPLC system

Method A: used a Phenomenex Spherclone ODS(2) reverse phase column, 5  $\mu\text{m}$  particle size, 150  $\times$  4.6 mm (length  $\times$  i.d.), with a guard column containing the same stationary phase. The column temperature was set to 25  $^{\circ}\text{C}$  which allowed a back pressure of 1600-1800 psi to be employed. The total run time was 35 min at a flow rate of 1200  $\mu\text{L min}^{-1}$ . A tertiary solvent system was used; A = 20% (v/v) MeOH (aq.), B = MeOH, C = 5 % (v/v) ortho-phosphoric acid (aq.). The elution programme was isocratic for 3 min (67A: 23B: 10C) then a linear gradient from 3 min to 29 min (0A: 90B: 10C) before recovery of the initial conditions over 1 min and equilibration over 5 min.

### 7.2.2.2 UPLC system

Method C: used a PST BEH C18 reverse phase column, 1.7  $\mu\text{m}$  particle size, 150  $\times$  2.1 mm (length  $\times$  i.d.), with in-line filter. The total run time was 37.33 min at a flow rate of 250  $\mu\text{L min}^{-1}$ . A binary solvent system was used; A = 0.02 % aqueous formic acid, B = MeOH. The elution programme was isocratic for 3.33 min (75A: 25B) then a linear gradient from 3.33 min to 29 min (10A: 90B) before recovery of the initial conditions over 1 min and equilibration over 5 min.

## 7.2.3 Dye analysis

### 7.2.3.1 Weld (*Reseda luteola* L.)

The great majority of the yellow historical yarns investigated were found to be dyed with weld (*Reseda luteola* L.). Weld was mixed with woad (*Isatis tinctoria* L.) in the green yarns, and madder species in the orange yarns. The majority of the samples were investigated on the HPLC system (method A), but a few samples were also analysed on the UPLC system (method C).

The characteristic components of weld were extracted at 254 nm and the relative amounts integrated by Empower software, expressed as peak area in  $\mu\text{V} \times \text{sec}$ . The acid hydrolysed extracts contained the flavonoid luteolin (**9**), the flavones apigenin (**10**) and the luteolin methyl ether chrysoeriol (**12**). The presence of the minor

component chrysoeriol (**12**) was systematically integrated at both 254 and 350 nm. The silk yarns were found to contain a higher level of flavonoid dyes and were therefore extracted at 254 nm, with only a few exceptions that presented a very low level of flavonoid dyes and were extracted at 350 nm (table 7.7). The wool yarns were found to present a much noisier baseline than the silk yarns and also contained less flavonoid dyes. It was therefore decided to integrate these samples at both 254 and 350 nm, where the signal to noise was better. The relative amounts were found to be very similar at both wavelengths and the results presented in table 7.8 correspond to the relative amounts obtained at 350 nm. When possible, a few samples were also investigated on the UPLC system which gave a much better signal to noise ratio at 254 nm. Finally for some samples, the quantity of chrysoeriol (**12**) was found to be close to the limit of detection and did not allowed a clear integration of the peak area. These samples are indicated in the table below by a star symbol (\*).

Tables 7.11 and 7.12 present the relative composition of the historical samples dyed with weld. The samples are identified by their entry on HPLC or UPLC systems and described with a sample code: tapestry number followed by the type of yarn: silk (S) or wool (W) and colours: yellow (Y), green (G) and orange (O), while the last number corresponds to the number of the sample, as several samples were collected from each tapestry.

Entry	Sample Name	$\lambda$ nm	Relative amount (Area %)		
			Luteolin (9)	Apigenin (10)	Chrysoeriol (12)
HPLC System			<i>Retention time (min)</i>		
<i>Yellow silk yarns</i>			<i>15.1</i>	<i>17.3</i>	<i>17.8</i>
1	47.6 YS8 - I (2)	254	87.7	6.8	5.5
2	47.6 YS15 - I (2)	254	92.0	5.1	2.9
3	47.6 YS15 - I (3)	254	88.1	7.2	4.7
4	47.6 YS18 - I (2)	254	89.4	5.8	4.8
5	47.6 YS25 - I (2)	254	87.4	7.2	5.4
6	47.6 YS3 - II (1)	350	81.7	11	7.3
7	47.7 YS4	254	78.7	13.4	7.9
8	47.7 YS9	254	79.8	13.1	7.1
9	47.8 YS1	254	86.2	8.6	5.2
10	47.8 YS8	254	80.1	14.3	5.6
11	47.9 YS2 - I (2)	254	87.7	6.2	6.1*
12	47.9 YS2 - I (3)	254	85.6	7.7	6.6

13	47.9 YS4 - I (2)	254	91.9	4.4	3.7
14	47.9 YS5 - II (1)	254	89.0	5.9	5.1
15	47.9 YS5 - II (2)	254	87.4	7.0	5.6
16	47.9 YS7 - I (2)	254	88.9	7.2	3.9
17	47.9 YS10 - I (2)	254	85.2	9.4	5.4
18	47.9 YS10 - I (3)	254	84.6	9.4	6
19	47.9 YS18 - I (2)	254	84.3	9.7	6
20	47.9 YS26 - I (2)	254	85.1	9.1	5.8
21	47.9 YS26 - I (3)	254	85.1	9.1	5.8*
22	47.10 YS4	254	83.1	9.7	7.1
23	47.10 YS6	254	86.3	7.6	6.1
24	47.11 YS4	254	88.0	7.1	4.9
25	47.11 YS8	254	86.2	8.3	5.6
26	47.12 YS2	254	88.0	6.6	5.4
27	47.12 YS6	254	86.1	8.7	5.2
28	47.12 YS6 (2)	254	87.9	7.1	5
29	47.12 YS10	254	86.8	7.5	5.7
30	47.13 YS5	254	88.5	7.2	4.3
31	47.13 YS9	254	84.8	9.6	5.6
32	47.13 YS11	254	87.9	7.1	5
33	47.14 YS2	254	84.7	8.7	6.6
34	47.14 YS7	254	89.0	6.5	4.5
35	47.17 YS1	254	88.5	7.8	3.7
36	47.17 YS9	254	86.2	8.8	4.9
37	47.19 YS1(2)	254	75.1	20.3	4.6
38	47.19 YS1b	254	76.2	19.4	4.4
39	47.19 YS2	254	86.2	9	4.8
40	47.19 YS11	254	83.7	11	5.3
41	47.23 YS1 (1)	254	88.5	10.3	1.2
42	47.23 YS1 (2)	350	88.3	9.6	2.1
43	47.23 YS2	254	91.0	5.3	3.7
44	47.23 YS3	254	89.0	6.1	4.9
45	47.23 YS18 (2)	254	87.8	7.9	4.3
46	MAP 1 YS3 (2)	254	87.2	7.6	5.2
47	MAP 1 YS11 (2)	254	87.8	7.5	4.7
48	MAP 3 YS7 (2)	350	88.6	8.9	4.5
<i>Green silk yarns</i>					
49	47.8 GS10	254	84.8	9.4	5.8*
50	47.9 GS6 - II (1)	254	90.0	6.2	3.8
51	47.9 GS6 - II (2)	254	87.3	7.8	4.8
52	47.9 GS28 - I (2)	254	88.0	7.4	4.6
53	47.10 GS5a	254	86.2	8.2	5.6
54	47.10 GS5b	254	87.8	7.5	4.7
55	47.11 GS7	254	82.6	10.3	7.1
56	47.13 GS12	254	87.7	7.7	4.6

57	47.17 GS8	254	88.0	6.9	5.1
58	47.19 GS10a	254	86.4	8.3	5.3
59	47.19 GS10b	254	86.5	8.4	5.1
60	47.23 GS4	254	88.9	6.4	4.7
UPLC system		Retention time (min)			
Entry	Sample ID	$\lambda$ nm	13.66	15.49	15.91
22	MAP 1 YS11	254	84.9	9.6	5.6
92	47.12 YS6	254	86.1	8.6	5.3
93	MAP 1 YS3	254	84.2	9.6	6.2
97	47.11 GS7	254	84.9	9.1	6.0
100	47.17 YS1	254	81.6	11.6	6.8

**Table 7.11:** Relative amounts of the flavonoid components characterised in the acid hydrolysed samples of silk yarns dyed with weld (*Reseda luteola* L.). Integrations were carried out at 254 or 350 nm. \* corresponds to Limit of detection (LOD) level.

Entry	Sample ID	$\lambda$ nm	Relative amount, Area (%)		
			Luteolin (9)	Apigenin (10)	Chrysoeriol (12)
HPLC system		Retention time (min)			
<i>Yellow wool yarns</i>			15.1	17.3	17.8
61	MAP 1 YW1 (2) -1	350	90.8	5.8	3.4
62	MAP 1 YW1 (2) -2	254	93.5	4.3*	2.2*
63	MAP 1 YS3 (2)	254	87.2	7.6	5.2
64	MAP 1 YW7 (2)	350	88.7	9.9	1.4
65	MAP 1 YW12 (2)	350	84.6	11.2	4.2
66	MAP 1 YW18 (2)	350	88.2	8.4	3.4
67	MAP 1 YW19 (2)	350	85.7	10.2	4.1
68	MAP 2 YW4 (2)	350	89.9	6.5	3.6
69	MAP 2 YW6 (2)	350	87.5	8.5	4.0
70	MAP 2 YW11 (2)	350	89.5	6.9	3.6
71	MAP 3 YW2 (2)	350	86.4	9.6	4.0
72	MAP 3 YW10 (2)	254	96.5	2.9*	0.6*
73	MAP 3 YW11 (2)	254	89.4	6.8	3.8
<i>Green wool yarns</i>					
74	47.6 GW16 - I (2)	350	86.4	9.2	4.4
75	47.7 GW10	350	85.8	8.6	5.6*
76	47.8 GW6	350	82.6	11.2	6.2*
77	47.9 GW14 - I (2)	350	89.5	5.9	4.6
78	47.9 GW17 - I (2)	350	90.5	5.6	3.9*
79	47.9 GW30 - I (2)	350	90.9	5.4	3.7
80	47.10 GW7	350	88.9	6.6	4.5
81	47.10 GW8	350	90.0	6.1	3.9

82	47.11 GW3	350	87.5	7.4	5.0
83	47.12 GW7	350	89.0	6.5	4.4
84	47.14 GW8	350	92.1	4.7	3.2
85	47.14 GW9	350	89.7	6.1	4.2
86	47.17 GW10	350	95.5	2.2	2.3
87	47.19 GW8	254	92.9	4.2	2.9
88	47.19 GW9a	254	92.7	3.7	3.6
89	47.19 GW9b	254	93.5	3.5	3.0
90	47.21 GW3 (3)	350	90.6	5.8	3.6
91	47.21 GW5	254	91.8	5.7	2.5
92	47.21 BW34 (3)	350	91.2	4.4	3.4*
93	47.21 GW35 (3)	350	90.6	6.3	3.1*
94	MAP 1 GW13 (2)	350	86.3	9.7	4.0
95	MAP 1 GW15 (2)	350	92.7	4.1	3.0
96	MAP 2 GW10 (2)	254	95.1	2.9*	2.0*
97	MAP 3 GW9 (2)	350	94.1	3.3	2.6
<i>Red wool yarns</i>					
98	47.6 RW22 - I (2)	350	75.2	17.8	7.0
99	47.6 RW22 - I (3)	254	86.5	8.5	5.0
100	47.8 OW4	350	82.4	13.8	3.8
101	47.9 OW20 - I (2)	350	96.8	2.0	1.2
102	47.21 OW7 (3)	350	94.2	3.6	2.2
103	47.21 GW8 (3)	350	88.2	7.6	4.2
104	47.21 OW14 (2)	350	93.3	4.5	2.2
105	47.21 GW23 (3)	254	94.7	3.2	2.1
106	47.21 OW26 (3)	254	93.9	4.2	1.9*
107	47.21 OW37 (3)	350	94.8	3.0*	2.2*
108	47.21 OW38 (3)	350	92.7	4.6*	2.7*
109	MAP 1 OW10 (2) -1	350	88.8	7.8*	3.4*
110	MAP 1 OW10 (2) -2	350	92.1	6.2*	1.7*
111	MAP 1 PW17 (2) -1	350	86.8	7.0	6.2
112	MAP 1 PW17 (2) -2	350	87.0	6.9	6.1
UPLC system					
			<i>Retention time (min)</i>		
<b>Entry</b>	<b>Sample ID</b>	<b><math>\lambda</math> nm</b>	<b>13.66</b>	<b>15.49</b>	<b>15.9</b>
91	MAP 2 YW4	254	76.7	15.3	8.0
95	MAP 1 YW1	254	87.6	7.6	4.8
98	MAP 1 YW2	254	90.0	8.0	2.0

**Table 7.12:** Relative amounts of the flavonoid components characterised in the acid hydrolysed samples of wool yarns dyed with weld (*Reseda luteola* L.). Integrations were carried out at 254 or 350 nm. \* corresponds to Limit of detection (LOD) level.

### 7.2.3.2 Dyer's greenweed (*Genista tinctoria* L.)

A small numbers of historical samples were dyed with dyer's greenweed (*Genista tinctoria* L.) for the yellow yarns or a mixture of dyer's greenweed and woad (*Isatis tinctoria* L.) for the green yarns. The majority of the samples were investigated on the HPLC system (method A). The characteristic components of dyer's greenweed were extracted at 254 nm and the relative amounts integrated by Empower software, expressed as peak area in  $\mu\text{V} \times \text{sec}$ . Due to the maxima absorbance of isoflavonoid compounds, the samples had to be integrated at 254 nm, but it was found difficult to clearly identify the minor components present in the acid hydrolysed extract. As a result, several samples were also analysed on the UPLC system (method C).

The acid hydrolysed extracts were found to contain the isoflavone genistein (**11**), the methylated isoflavonoid compound *Gt3*, the flavonoid luteolin (**9**), the flavones apigenin (**10**) and a luteolin methyl ether component. Table 7.13 presents the relative composition of the historical samples dyed with dyer's greenweed. The samples are identified by their entry on HPLC or UPLC systems and described with a sample code: tapestry number followed by the type of yarn: silk (S) or wool (W) and colours: yellow (Y) and green (G), while the last number corresponds to the number of the sample, as several samples were collected from each tapestry.

Four historical samples were re-analysed by reconstituting an acid hydrolysed extract of the sample with a solution of diosmetin ( $2 \mu\text{g mL}^{-1}$ ) in methanol:water (1/1 v/v). Comparison of the diosmetin peak area for these spiked extracts with that of the starting solution of diosmetin showed a very close correlation; this combined with the obvious appearance of a new peak in the chromatogram strongly suggests that for all the samples that chrysoeriol (**12**) was the only luteolin methyl-ether present in the acid hydrolysed extract (table 7.14).

			Relative amount, Area (%)					
			Gt3	luteolin (9)	genistein (11)	apigenin (10)	luteolin methyl ether	
HPLC System			Retention time (min)					
Entry	Sample ID	$\lambda$ (nm)	12.4	15.1	15.4	17.6	17.8	
1	47.6 GW1 - I (2)	254	12.7	49.7	29.2	8.2	0.1*	
2	47.6 GW17 - I (2)	254	17.9	43.7	30.1	8.2	0.1*	
3	47.7 GW2	254	21.3	29.9	33.9	10.0	4.9*	
4	47.8 GW7	254	26.7	31.1	30	9.5	3.7*	
5	47.9 GW16 - I (2)	254	7.2	51.9	28	10.7	2.2	
6	47.10 GW9	254	11.4	92	17.8	6.2	2.6	
7	47.11 GW2	254	10.6*	65.5	14.9	6.2*	2.8*	
8	47.11 YW11	254	47.1	25.5	21.1	6.2	ND	
9	47.12 GW3	254	7.9*	64.5	16.5	6.7*	2.9*	
10	47.12 YW9 (2)	254	25.4	33.1	36.4	5.1	ND	
11	47.13 GW2	254	4.9	71	14.8	6.7	2.7	
12	47.13 GW4	254	15	64	12.75	5.7	2.5	
13	47.14 GW3	254	16.1	52.4	19.8	6.1	3.9	
14	47.21 GW27	254	14	35.5	42.8	7.7	ND	
15	47.21 GW36 (3)	254	ND	63	29.1	7.1*	ND	
16	47.21 YS4 (2)	254	20.7	31.6	41.6	6.1	ND	
17	47.21 YS11 (3)	254	5.7	37.7	45.6	10.9	ND	
18	47.21 YS19 (3)	254	4.1	24.1	54.1	16.7	0.9*	
19	47.21 YS21- I	254	6.5	24.1	56.4	13	ND	
20	47.21 YS28 (3)	254	11.2	33.2	45.3	9.5	0.8	
			Gt3	luteolin (9)	genistein (11)	apigenin (10)	chrysoeriol (12)	diosmetin (13)
UPLC System			Retention time (min)					
Entry	Sample ID	$\lambda$ (nm)	12.30	13.66	14.20	15.49	15.91	16.03
87	47.21 YS21	254	ND	30.0	47.8	14.9	7.3	ND
89	47.21 YS 28	254	16.5	22.0	53.9	7.6	ND	ND
99	MAP 2 YS12	254	ND	14.5	80.2	3.0	1.5	1.0
100	47.17 YS1	254	ND	79.2	11.3	6.6	2.9	ND
101	47.7 GW2	254	18.7	35.4	28.8	12.5	4.6	ND
102	47.12 GW3	254	15.9	47.0	19.0	11.1	7.0	ND
103	47.10 GW9	254	23.6	42.4	19.4	9.0	5.5	ND
105	47.13 GW2	254	ND	62.4	22.6	9.8	5.3	ND
106	47.12 GW3	254	16.5	52.2	15.4	10.7	5.2	ND

**Table 7.13:** Relative amounts of the flavonoid and isoflavonoid components characterised in the acid hydrolysed samples of historical yarns dyed with dyer's greenweed (*Genista tinctoria* L.). Integrations were carried out at 254 nm. ND stands for not detected.



UPLC system		Identified compound [x] Area ( $\mu\text{V} \times \text{sec}$ ) and % recovery (n=1) at 350 nm					
Entry	Sample ID	luteolin (9)	genistein (11)	Apigenin (10)	chrysoeriol (12)	diosmetin (13)	Recovery %
136	47.14 GW3	1672111	32243	238364	67571	263523	89
137	47.21 YS21	736521	143314	542363	22984	293018	99
160	47.21 YSIII-1	2787069	107970	605737	29573	303657	103
165	47.11 GW-II-1	960518	178938	103816	34828	269887	91
		<b>Spiking solution, diosmetin [<math>2 \mu\text{g mL}^{-1}</math>] Area (<math>\mu\text{V} \times \text{sec}</math>) (n=3) at 350 nm</b>					
		diosmetin (13)					
	Spiking solution	296127 $\pm$ 4648					

**Table 7.14:** Peak areas of identified flavonoid and isoflavonoid dyes extracted at 350 nm in the acid hydrolysed extract of four historical samples reconstituted in a solution of diosmetin at  $2 \mu\text{g mL}^{-1}$ .

### 7.2.3.3 Young fustic (*Cotinus coggygia* S.)

A group of pale orange wool were found to contain a mixture of young fustic (*Cotinus coggygia* S.) mixed in some cases with weld (*Reseda luteola* L.) or dyer's greenweed (*Genista tinctoria* L.). The characteristic components were extracted at 254 nm and 350 nm and the relative amounts integrated by Empower software, expressed as peak area in  $\mu\text{V} \times \text{sec}$ . Due to the high level of degradation of the yarns, the samples were investigated on the UPLC system (method C). The integration of the acid hydrolysed extracts was done at 254 nm and 350 nm in order to allow the identification of both flavonoid and flavonol dyes but also several isoflavonoid dyes (table 7.15). For two samples the level of degradation was so high that it was only possible to integrate the dye components at 350 nm. Two unidentified components, related to fisetin were characterised in all the extracts; these compounds eluted shortly after fisetin and were named yf1 and yf2. In the sample containing dyer's greenweed, the isoflavone genistein was characterised associated to the methylated isoflavonoid compound Gt3.

The samples are identified by their entry on HPLC or UPLC systems and described with a sample code: tapestry number followed by the type of yarn: wool (W) and colours: yellow (Y) while the last number corresponds to the number of the sample, as several samples were collected from each tapestry.

		Relative amount, Area (%)									
		fis (14)	yf1	yf2	Gt3	sul (15)	lu (9)	gen (11)	ap (10)	chrys (12)	diosm (13)
UPLC system, 254 nm		Retention time (min)									
Sample ID	Entry	10.79	11.02	11.73	12.35	12.72	13.72	14.26	15.55	15.85	15.97
47.6 YW-I 21	37	ND	25.6	15.5	18.4	14.0	19.4	ND	7.1	ND	ND
47.7 YW3	36	10.8	29.3	19.3	ND	27.2	13.4	ND	ND	ND	ND
47.8 YW2	38	9.0	25.7	19.9	ND	26.9	18.5	ND	ND	ND	ND
47.9 YW2 II	83	ND	28.4	15.6	11.7	15.7	17.4	7.2	2.8	ND	1.2
47.9 YW13	32	6.5	17.2	14.8	14.8	13.7	10.5	15.7	6.9	ND	ND
47.10 YW3	35	7.6	10.9	10.9	18.5	17.5	11.9	17.6	3.3	0.5	1.4
47.11 YW9	34	8.6	9.5	10.8	18.0	19.4	12.1	16.5	3.9	ND	1.3
47.12 YW9	27	7.6	11.3	14.5	13.6	15.7	9.4	20.0	7.9	ND	ND
47.13 YW10	40	12.8	20.4	16.8	ND	15.3	28.7	ND	3.8	2.4	ND
47.14 YW10	39	10.3	11.3	17.0	ND	18.9	25.3	ND	7.8	ND	9.4
47.17 YW II - 3	44	ND	2.8	6.2	ND	10.2	67.9	ND	7.6	ND	5.2
47.19 YW3	33	11.4	11.2	9.6	ND	47.1	20.7	ND	ND	ND	ND
UPLC system, 350 nm											
47.6 YW7	82	ND	23.6	22.6	ND	25.9	18.5	ND	6.3	3.1	ND
47.6 YW25-A	84	ND	12.9	14.8	ND	24.3	29.2	ND	9.8	3.3	5.7
47.6 YW-I 21	37	2.4	17.0	17.8	ND	34.4	23.1	ND	3.5	ND	1.9
47.7 YW3	36	4.5	14.1	18.8	ND	47.4	10.1	ND	1.9	2.0	1.2
47.8 YW2	38	4.9	14.0	20.8	ND	38.1	15.62	ND	2.8	2.4	1.4
47.9 YW2 II	83	ND	9.4	14.6	ND	32.3	31.5	1.0	7.2	1.0	3.2
47.9 YW13	32	7.0	11.9	16.1	ND	39.0	13.1	2.7	6.7	1.7	1.8
47.10 YW3	35	7.3	8.9	12.8	43.2	1.8	15.8	2.8	5.6	0.8	1.1
47.11 YW9	34	5.6	8.9	12.1	46.5	0.4	15.6	2.5	6.2	0.9	1.3
47.12 YW9	27	7.1	10.1	13.4	37.6	5.5	13.7	4.3	6.1	1.0	1.2
47.13 YW10	40	1.7	5.3	13.2	ND	22.2	44.9	ND	8.1	0.3	4.2
47.14 YW10	39	4.1	6.0	12.5	ND	21.6	44.2	ND	7.6	ND	4.0
47.17 YW II - 3	44	0.9	1.7	4.0	ND	11.2	67.6	ND	8.6	0.1	5.8
47.19 YW3	33	10.9	7.3	10.9	ND	53.6	13.4	ND	2.6	ND	1.4

**Table 7.15:** Relative amounts of the flavonoid, flavonol and isoflavonoid components characterised in the acid hydrolysed samples of historical yarns dyed with a mixture of young fustic (*Cotinus coggygra* S.) with weld (*Reseda luteola* L.) or dyer's greenweed (*Genista tinctoria* L.). Integrations were carried out at 254 nm or 350 nm. ND stands for not detected.

### 7.2.3.4 Madder species

Madder species were identified in several wool yarns that exhibited a large range of colour. Madder was found to realise red hues, it was mixed with weld (*Reseda luteola* L.) in the orange hues, while it was mixed with woad (*Isatis tinctoria* L.) in purple hues. The interpretation of the madder source was limited due to the use of a strong hydrochloric acid extraction, as several anthraquinones dyes particularly sensitive to esterification or decarboxylation of carboxyphenols. Only alizarin and purpurin could be identified, but several unknown components were found associated in various level named rubia 1 - 5. The components named rubia 1, rubia 2, eluted before and after alizarin, while rubia 3, rubia 4 and rubia 5 eluted after purpurin. The characteristic components present in the madder-containing samples were extracted at 254 nm and the relative amounts integrated by Empower software, expressed as peak area in  $\mu\text{V} \times \text{sec}$ . The relative amount of purpurin and alizarin were found to be highly variable and table 7.16. Most of the samples were investigated on the HPLC system (method A), but a few samples were analysed on the UPLC system (method C).

The samples are identified by their entry on HPLC or UPLC systems and described with a sample code: tapestry number followed by the type of yarn: wool (W) and colours: red (R), orange (O) or purple (P), while the last number corresponds to the number of the sample, as several samples were collected from each tapestry.

		Relative amount, Area (%)						
		rubia 1	alizarin (26)	rubia 2	purpurin (28)	rubia 3	rubia 4	rubia 5
HPLC System, 254 nm		Retention time (min)						
Entry	Sample ID	18.78	20.35	21.31	24.67	25.23	27.15	30.92
124	47.6 RW4 - II (2)	4.4	26.1	ND	67.8	ND	ND	1.8
125	47.6 RW22 - I (2)	ND	39.6	ND	60.4	ND	ND	ND
126	47.7 RW6	15.7	24.9	ND	56.7	1.1	1.7	ND
127	47.7 RW7	3.7	14.3	0.9	74.8	1.5	1.3	3.5
128	47.7 PW8	14.5	13.9	ND	69.8	1.7	ND	ND
129	47.7 PW8	14.1	14.5	ND	69.2	ND	ND	2.2
130	47.8 PW11	ND	19.2	ND	79.7	ND	ND	1.0
131	47.8 OW4	ND	19.3	ND	78.9	ND	ND	1.8

132	47.8 RW3	5.3	13.1	0.8	73.7	1.6	0.9	4.6
133	47.9 OW20 - I (2)	2.8	19.7	ND	77.4	ND	ND	ND
134	47.10 RW10	4.0	29.1	ND	59.5	1.1	0.9	5.5
135	47.10 RW10	3.8	29.8	ND	60.5	0.5	ND	5.4
136	47.10 PW11	5.3	13	ND	77.9	1.4	ND	2.4
137	47.11 RW6	4.9	24.7	ND	61.0	1.2	0.9	7.3
138	47.12 RW5	6.0	25.8	ND	59.8	0.8	0.3	6.7
139	47.14 RW4	ND	56.9	ND	43.1	ND	ND	ND
140	47.19 PW6	7.5	20.6	ND	67.5	1.5	0.9	2.0
141	47.21 OW37 - I	ND	14.3	28.0	57.7	ND	ND	ND
142	47.21 OW26 - I	ND	48.9	29.9	21.3	ND	ND	ND
143	47.21 OW38 - I	ND	42.4	34.9	22.7	ND	ND	ND
144	47.21 OW7 - I	ND	34.8	45.5	20.0	ND	ND	ND
145	47.23 RW6	7.3	15.8	ND	74.6	1.1	3.7	ND
146	MAP 1 OW10 (2) -1	7.9	25.2	10.8	54.1	ND	ND	2.0
147	MAP 2 RW1 (2)	11.9	36.9	0.9	44.3	0.7	0.3	3.1
148	MAP 3 RW3 (2)	12.6	36.1	0.8	42.7	1.1	1.7	3.2
149	MAP 3 OW8 (2)	5.9	39.5	1.0	47.8	1.4	2.2	0.7
150	MAP 1 PW17 (2) -1	ND	20.4	ND	75.8	ND	ND	ND
151	MAP 1 OW10 (2) -2	6.2	22.4	9.6	43.7	17.0	ND	1.0
UPLC System (254 nm)		<i>Retention time (min)</i>						
<i>Entry</i>	<i>Sample ID</i>	<i>17.53</i>	<i>18.00</i>		<i>21.08</i>	<i>22.87</i>	<i>23.95</i>	<i>24.49</i>
23	MAP2 RW1	13.7	48.7		31.8	0.5	0.8	0.2
28	47.12 RW5	4.3	36.0		52.7	ND	0.3	3.4
31	47.8 RW4	16.2	24.8		57.5	0.0	0.0	0.5
52	47.12 PW-II 3	14.4	32.9		50.1	1.2	0.3	0.3
61	47.9 PW-III 3	5.3	32.9		58.3	1.2	0.8	0.7
77	47.13 RW3	ND	48.7		48.8	0.0	0.3	0.9
78	47.7 RW6	ND	45.6		51.9	0.3	0.4	0.7

**Table 7.16:** Relative amounts of the anthraquinones components characterised in the acid hydrolysed samples of historical yarns dyed with madder species. Integrations were carried out at 254 nm. ND stands for not detected.

### 7.2.3.5 Cochineal dyes

Cochineal dyes were detected in several samples and the relative amount of carminic acid (**33**) and the characteristic minor components Dc II (**32**), Dc IV, Dc VII, flavokermesic acid (**35**) and kermesic acid (**37**) were extracted at 275 nm and the relative amounts integrated by Empower software, expressed as peak area in  $\mu\text{V} \times \text{sec}$ . This allowed comparison of the samples with published results. In a few faded samples only traces carminic acid and indigotin (**52**) were detected in the acid hydrolysed extracts, and did not allow a species identification.

		Relative amount, Area (%)					
		Dc II ( <b>32</b> )	carminic acid ( <b>33</b> )	Dc IV	Dc VII	Fk ( <b>35</b> )	K ( <b>34</b> )
HPLC system, 275 nm		<i>Retention time (min)</i>					
Entry	Sample ID	5.16	5.73	12.15	13.80	17.51	18.34
154	MAP 1 - PW5-2	1.0	94.8	1.5	0.4	1.5	0.9
155	MAP 1 PW5-1	3.9	90.9	1.7	0.6	1.8	0.9
156	MAP 1 PW5-2	4.0	90.9	1.9	0.6	1.9	0.6
157	MAP 2 PW2-1	4.3	90.9	1.9	0.9	2.0	0.2
158	MAP 2 PW2-2	4.6	90.6	2.1	0.6	1.9	0.2
159	MAP 2 PW2-2	4.6	90.6	2.1	0.6	1.9	0.2
160	MAP 3 PW4-1	1.2	94.1	2.2	0.6	1.8	0.1
161	MAP 3 PS6-1	0.8	94.7	1.8	0.7	1.8	0.1
162	MAP 3 PS6-2	0.4	95.4	1.8	0.1	0.6	1.8
163	47.6 PW1-II	3.7	89.7	1.8	1.5	2.5	0.8
164	47.8 PW5	12.6	79.9	2.2	0.8	1.7	2.8
165	47.17 PW2	6.1	88.1	1.8	2.1	0.7	0.4
166	47.17 PS4	3.8	92.1	1.8	1.8	0.2	0.3
167	47.12 PW8	2.6	91.9	3.3	1.8	0.3	ND
168	47.19 PW7	4.1	87.6	4.1	2.7	0.9	0.6
169	47.23 PW7	9.6	81.6	3.4	2.0	1.4	1.0
170	MODHT RW5	4.5	87.7	3.2	2.9	0.6	0.2
171	MODHT RS3	2.0	91.9	1.9	2.5	0.4	0.3

**Table 7.17:** Relative amounts of the anthraquinones components characterised in the acid hydrolysed samples of historical yarns dyed with cochineal species. Integrations were carried out at 275 nm.

### 7.2.3.6 Safflower (*Carthamus tinctorius* L.)

Several pink to light orange silk yarns were investigated on the UPLC system (method C) and showed the presence of several flavonoid dyes present in trace quantities: the flavonoid luteolin (**9**), the flavones apigenin (**10**) and the luteolin methyl ether chrysoeriol (**12**) systematically associated to several colourless components named Ct1, Ct2, Ct3 and Ct4 recently characterised as the minor flavonoid components present in safflower (*Carthamus tinctorius* L.). The characteristic components present in these samples were extracted at 300 nm and the relative amounts integrated by Empower software, expressed as peak area in  $\mu\text{V} \times \text{sec}$ .

The main component of safflower is carthamin (**4**), a dye which is very sensitive to hydrochloric extraction, although it may be eluted from the thread using DMSO (UPLC entry 19b and 30b), and was integrated by Empower software at 500 nm.

		Relative amount, Area (%)							
		Ct1	Luteolin ( <b>9</b> )	Ct2'	Ct2	Ct3	Ct4	Apigenin ( <b>10</b> )	Chrysoeriol ( <b>12</b> )
UPLC system, 300 nm		Retention time (min)							
Entry	Sample ID	13.34	13.72	14.03	14.10	14.69	15.33	15.55	15.96
4	47.8 Pink Silk 9a	2.5	19.7	9.0	8.3	29.1	15.9	12.9	2.8
9	47.19 Pink S4	16.4	17.0	9.3	10.2	25.1	11.4	7.5	3.1
11	47.8 Pink S5	10.9	22.0	5.6	5.0	22.6	19.6	10.1	4.2
12	47.7 Pink Silk 5	13.1	7.5	17.2	17.7	28.1	5.3	11.2	ND
17	47.23 Pink S5	8.7	22.0	11.7	13.3	23.8	6.6	11.7	2.2
19	47.19 Pink S5	25.5	4.6	6.6	23.6	26.2	6.6	6.9	ND
30	47.12 Pink S4	11.7	13.1	13.6	16.6	27.9	6.9	8.5	1.8
UPLC system, DMSO extraction, 500 nm		Carthamin ( <b>4</b> )							
Entry	Sample ID	17.57							
19b	47.19 Pink S5	detected							
30b	47.23 Pink S5	detected							

**Table 7.18:** Relative amounts of the unknown Ct components and flavonoid dyes characterised in the acid hydrolysed samples of historical yarns dyed with safflower (*Carthamus tinctorius* L.) mixed with weld (*Reseda luteola* L.). Integrations were carried out at 300 nm.

## 7.2.3.7 Summary

<i>Entry</i>	<i>Identified Chromophores</i>	<i>Dye Source</i>
<b>47.6</b>		
47.6 GW1 - I (2)	Gt3, luteolin, diosmetin, apigenin, chrysoeriol, traces indigotin	Dyer's greenweed ( <i>Genista tinctoria L.</i> ) with indigo-type dyestuff ( <i>Isatis tinctoria L.</i> or <i>Indigofera tinctoria L.</i> )
47.6 YS2 (2)	luteolin, apigenin, chrysoeriol and unknowns peaks	Weld ( <i>Reseda luteola L.</i> )
47.6 YW7 - I (2)	yf1, yf2, fisetin, sulfuretin, luteolin, apigenin, chrysoeriol	Weld ( <i>Reseda luteola L.</i> ) with young fustic ( <i>Cotinus coggygia Scop.</i> )
47.6 YS8 - I (2)	luteolin, apigenin, chrysoeriol and unknowns peaks	Weld ( <i>Reseda luteola L.</i> )
47.6 GW14 - I (2)	luteolin, apigenin, chrysoeriol, traces indigotin and unknown peaks	Weld ( <i>Reseda luteola L.</i> ) with indigo-type dyestuff ( <i>Isatis tinctoria L.</i> or <i>Indigofera tinctoria L.</i> )
47.6 YS15 - I (2)	luteolin, apigenin, chrysoeriol and unknowns peaks	Weld ( <i>Reseda luteola L.</i> )
47.6 YS15 - I (3)	luteolin, apigenin, chrysoeriol and unknowns peaks	Weld ( <i>Reseda luteola L.</i> )
47.6 GW16 - I (2)	uteolin, apigenin, chrysoeriol, traces indigotin	Weld ( <i>Reseda luteola L.</i> ) with indigo-type dyestuff ( <i>Isatis tinctoria L.</i> or <i>Indigofera tinctoria L.</i> )
47.6 GW17 - I (2)	Gt3, luteolin, genistein, apigenin, chrysoeriol, traces indigotin	Dyer's greenweed ( <i>Genista tinctoria L.</i> ) with indigo-type dyestuff ( <i>Isatis tinctoria L.</i> or <i>Indigofera tinctoria L.</i> )
47.6 YS18 - I (2)	luteolin, apigenin, chrysoeriol and unknowns peaks	Weld ( <i>Reseda luteola L.</i> )
47.6 RW22 - I (2)	luteolin, apigenin, chrysoeriol, Nowick C and small amount of alizarin and purpurin	Weld ( <i>Reseda luteola L.</i> ) with small amount of Madder-type dyestuff and brazilwood
47.6 YS 25 - I (2)	luteolin, apigenin, chrysoeriol and unknowns peaks	Weld ( <i>Reseda luteola L.</i> )

47.6 PW1 - II (1)	carminic acid with traces indigotin	Coccid dyestuff (unknown origin) and indigo-type dyestuff ( <i>Isatis tinctoria L.</i> or <i>Indigofera tinctoria L.</i> )
47.6 PW1 - II (2)	carminic acid with traces indigotin and purpurin and unknown dye ( $\lambda_{\max} = 522$ nm, orcein?)	Coccid dyestuff (unknown origin) and indigo-type dyestuff ( <i>Isatis tinctoria L.</i> or <i>Indigofera tinctoria L.</i> ), traces madder-type dyestuff and lichens (orcein?)
47.6 YS3 - II (1)	luteolin, apigenin, chrysoeriol and unknowns peaks	Weld ( <i>Reseda luteola L.</i> )
47.6 RW4 - II (1)	carminic acid, dc II, traces flavokermesic acid, kermesic acid, alizarin, purpurin, luteolin, apigenin and chrysoeriol	American cochineal ( <i>Dactylopius coccus C.</i> ) with madder-type dyestuff and weld ( <i>Reseda luteola L.</i> )
47.6 RW4 - II (2)	alizarin, purpurin, traces indigotin	Madder-type dyestuff with indigo-type dyestuff ( <i>Isatis tinctoria L.</i> or <i>Indigofera tinctoria L.</i> )
47.6 YW7 - II	yf1, yf2, fisetin, sulfuretin, luteolin, apigenin	Weld ( <i>Reseda luteola L.</i> ) with young fustic ( <i>Cotinus coggygria Scop.</i> )
47.6 YW I - 21	yf1, yf2, sulfuretin, luteolin, apigenin, genistein, chrysoeriol	Dyer's greenweed ( <i>Genista tinctoria L.</i> ) with young fustic ( <i>Cotinus coggygria Scop.</i> )
<b>47.7</b>		
47.7 GW2	Gt3, luteolin, genistein, apigenin, chrysoeriol, traces indigotin	Dyer's greenweed ( <i>Genista tinctoria L.</i> ) with indigo-type dyestuff ( <i>Isatis tinctoria L.</i> or <i>Indigofera tinctoria L.</i> )
47.7 YW3	yf1, yf2, sulfuretin, luteolin, genistein, apigenin, chrysoeriol	Dyer's greenweed ( <i>Genista tinctoria L.</i> ) with young fustic ( <i>Cotinus coggygria Scop.</i> )
47.7 Pink Silk 5	Ct1, Ct2, Ct2', Ct4, luteolin, apigenin, chrysoeriol	Safflower ( <i>Carthamus tinctorius L.</i> ) and weld ( <i>Reseda luteola L.</i> )
47.7 YS4	luteolin, apigenin, chrysoeriol	Weld ( <i>Reseda luteola L.</i> )
47.7 RW6	alizarin, purpurin	Madder-type dyestuff
47.7 RW7	alizarin, purpurin	Madder-type dyestuff
47.7 PW8	alizarin, purpurin, traces indigotin	Madder-type dyestuff with indigo-type dyestuff ( <i>Isatis tinctoria L.</i> or <i>Indigofera tinctoria L.</i> )
47.7 YS9	luteolin, apigenin, chrysoeriol	Weld ( <i>Reseda luteola L.</i> )
47.7 GW10	luteolin, apigenin, chrysoeriol, traces indigotin and unknown peaks	Weld ( <i>Reseda luteola L.</i> ) with indigo-type dyestuff ( <i>Isatis tinctoria L.</i> or <i>Indigofera tinctoria L.</i> )



<b>47.8</b>		
47.8 YS1	luteolin, apigenin, chrysoeriol, traces indigotin ? (impure PDA)	Weld ( <i>Reseda luteola</i> L.) with indigo-type dyestuff ( <i>Isatis tinctoria</i> L. or <i>Indigofera tinctoria</i> L.)
47.8 YW2	yf1, yf2, fisetin, sulfuretin, luteolin, apigenin, chrysoeriol	Weld ( <i>Reseda luteola</i> L.) with young fustic ( <i>Cotinus coggygia</i> Scop.)
47.8 RW3	alizarin, purpurin	Madder-type dyestuff
47.8 OW4	alizarin, purpurin, Nowik C and traces Luteolin, apigenin, chrysoeriol	Madder-type dyestuff with small amount of brazilwood and probably weld ( <i>Reseda luteola</i> L.)
47.8 PW5	carminic acid, dc II, traces flavokermesic acid and kermesic acid and traces purpurin	American cochineal ( <i>Dactylopius coccus</i> C.), traces madder-type dyestuff
47.8 Pink Silk 5	Ct1, Ct2, Ct2', Ct4, luteolin, apigenin, chrysoeriol	Safflower ( <i>Carthamus tinctorius</i> L.) and weld ( <i>Reseda luteola</i> L.)
47.8 GW6	luteolin, apigenin, chrysoeriol, traces indigotin	Weld ( <i>Reseda luteola</i> L.) with indigo-type dyestuff ( <i>Isatis tinctoria</i> L. or <i>Indigofera tinctoria</i> L.)
47.8 GW7	Gt3, luteolin, genistein, apigenin, chrysoeriol, traces indigotin	Dyer's greenweed ( <i>Genista tinctoria</i> L.) with indigo-type dyestuff ( <i>Isatis tinctoria</i> L. or <i>Indigofera tinctoria</i> L.)
47.8 Pink Silk 9a	Ct1, Ct2, Ct2', Ct4, luteolin, apigenin, chrysoeriol	Safflower ( <i>Carthamus tinctorius</i> L.) and weld ( <i>Reseda luteola</i> L.)
47.8 YS8	luteolin, apigenin, chrysoeriol	Weld ( <i>Reseda luteola</i> L.)
47.8 GS10	luteolin, apigenin, chrysoeriol, traces indigotin	Weld ( <i>Reseda luteola</i> L.) with indigo-type dyestuff ( <i>Isatis tinctoria</i> L. or <i>Indigofera tinctoria</i> L.)
47.8 PW11	alizarin, purpurin, traces indigotin	Madder-type dyestuff with traces indigo-type dyestuff ( <i>Isatis tinctoria</i> L. or <i>Indigofera tinctoria</i> L.)
<b>47.9</b>		
47.9 GW1 - I (2)	three unidentified dyes : unknown 1 $\lambda_{\max}$ 394 nm; unknown 2 $\lambda_{\max}$ 622 nm unknown 3 $\lambda_{\max}$ 636 nm	Unidentified, possibly early synthetic dyes
47.9 YS2 - I (2)	luteolin, apigenin, chrysoeriol	Weld ( <i>Reseda luteola</i> L.)
47.9 YS2 - I (3)	luteolin, apigenin, chrysoeriol	Weld ( <i>Reseda luteola</i> L.)

47.9 YS4 - I (2)	luteolin, apigenin, chrysoeriol	Weld ( <i>Reseda luteola L.</i> )
47.9 YS7 - I (2)	luteolin, apigenin, chrysoeriol	Weld ( <i>Reseda luteola L.</i> )
47.9 YS10 - I (2)	luteolin, apigenin, chrysoeriol	Weld ( <i>Reseda luteola L.</i> )
47.9 YS10 - I (3)	luteolin, apigenin, chrysoeriol	Weld ( <i>Reseda luteola L.</i> )
47.9 YW13	yf1, yf2, Gt3, luteolin, genistein, apigenin, chrysoeriol	Dyer's greenweed ( <i>Genista tinctoria L.</i> ) with young fustic ( <i>Cotinus coggygia Scop.</i> )
47.9 GW14 - I (2)	luteolin, apigenin, chrysoeriol, traces indigotin	Weld ( <i>Reseda luteola L.</i> ) with indigo-type dyestuff ( <i>Isatis tinctoria L.</i> or <i>Indigofera tinctoria L.</i> )
47.9 GW16 - I (2)	Gt3, luteolin, genistein, apigenin, chrysoeriol, traces indigotin	Dyer's greenweed ( <i>Genista tinctoria L.</i> ) with indigo-type dyestuff ( <i>Isatis tinctoria L.</i> or <i>Indigofera tinctoria L.</i> )
47.9 GW17 - I (2)	luteolin, apigenin, chrysoeriol, traces indigotin	Weld ( <i>Reseda luteola L.</i> ) with indigo-type dyestuff ( <i>Isatis tinctoria L.</i> or <i>Indigofera tinctoria L.</i> )
47.9 YS18 - I (2)	luteolin, apigenin, chrysoeriol	Weld ( <i>Reseda luteola L.</i> )
47.9 OW20 - I (2)	luteolin, apigenin, chrysoeriol with purpurin, traces of alizarin and ellagic acid	Weld ( <i>Reseda luteola L.</i> ) with madder-type dyestuff and traces tannins
47.9 YS26 - I (2)	luteolin, apigenin, chrysoeriol with small amount of purpurin, alizarin and ellagic acid	Weld ( <i>Reseda luteola L.</i> ) with small amount of madder-type dyestuff and tannins
47.9 YS26 - I (3)	luteolin, apigenin, chrysoeriol with purpurin, traces of alizarin and ellagic acid	Weld ( <i>Reseda luteola L.</i> ) with small amount of madder-type dyestuff and tannins
47.9 YS26 - I (4)	luteolin, apigenin, chrysoeriol with purpurin, traces of alizarin and ellagic acid	Weld ( <i>Reseda luteola L.</i> ) with small amount of madder-type dyestuff and tannins
47.9 GW26 - I (2)	three unidentified dyes : unknown 1 $\lambda_{\max}$ 394 nm; unknown 2 $\lambda_{\max}$ 622 nm unknown 3 $\lambda_{\max}$ 636 nm	Unidentified, possibly early synthetic dyes

47.9 GS28 - I (2)	luteolin, apigenin, chrysoeriol, traces indigotin	Weld ( <i>Reseda luteola</i> L.) with indigo-type dyestuff ( <i>Isatis tinctoria</i> L. or <i>Indigofera tinctoria</i> L.)
47.9 GW29 - I (2)	three unidentified dyes: unknown 1 $\lambda_{\max}$ 406 nm, unknown 2 $\lambda_{\max}$ 649 nm unknown 3 $\lambda_{\max}$ 636 nm	Unidentified, possibly early synthetic dyes
47.9 GW30 - I (2)	luteolin, apigenin, chrysoeriol, traces indigotin	Weld ( <i>Reseda luteola</i> L.) with indigo-type dyestuff ( <i>Isatis tinctoria</i> L. or <i>Indigofera tinctoria</i> L.)
47.9 YW2 - II (1)	yf1, yf2, fisetin, sulfuretin, luteolin, genistein, apigenin, chrysoeriol	Dyer's greenweed ( <i>Genista tinctoria</i> L.) with young fustic ( <i>Cotinus coggygria</i> Scop.)
47.9 PW3 - II (1)	carminic acid with traces indigotin	Coccid dyestuff (unknown origin) and indigo-type dyestuff ( <i>Isatis tinctoria</i> L. or <i>Indigofera tinctoria</i> L.)
47.9 PW3 - II (2)	Orcein, small peak $\lambda_{\max}$ 514 nm	Lichen (orcein dye ?)
47.9 YS5 - II (1)	luteolin, apigenin, chrysoeriol	Weld ( <i>Reseda luteola</i> L.)
47.9 YS5 - II (2)	luteolin, apigenin, chrysoeriol	Weld ( <i>Reseda luteola</i> L.)
47.9 GS6 - II (1)	luteolin, apigenin, chrysoeriol, traces indigotin + unknown peaks	Weld ( <i>Reseda luteola</i> L.) with indigo-type dyestuff ( <i>Isatis tinctoria</i> L. or <i>Indigofera tinctoria</i> L.)
47.9 GS6 - II (2)	luteolin, apigenin, chrysoeriol, traces indigotin	Weld ( <i>Reseda luteola</i> L.) with indigo-type dyestuff ( <i>Isatis tinctoria</i> L. or <i>Indigofera tinctoria</i> L.)
<b>47.10</b>		
47.10 YW3	yf1, yf2, Gt3, luteolin, genistein, apigenin, chrysoeriol	Weld ( <i>Reseda luteola</i> L.) with young fustic ( <i>Cotinus coggygria</i> Scop)
47.10 YS4	luteolin, apigenin, chrysoeriol	Weld ( <i>Reseda luteola</i> L.)
47.10 GS5a	luteolin, apigenin, chrysoeriol, traces indigotin	Weld ( <i>Reseda luteola</i> L.) with indigo-type dyestuff ( <i>Isatis tinctoria</i> L. or <i>Indigofera tinctoria</i> L.)

47.10 GS5b	luteolin, apigenin, chrysoeriol, traces indigotin	Weld ( <i>Reseda luteola L.</i> ) with indigo-type dyestuff ( <i>Isatis tinctoria L.</i> or <i>Indigofera tinctoria L.</i> )
47.10 YS6	luteolin, apigenin, chrysoeriol	Weld ( <i>Reseda luteola L.</i> )
47.10 GW7	luteolin, apigenin, chrysoeriol, traces indigotin	Weld ( <i>Reseda luteola L.</i> ) with indigo-type dyestuff ( <i>Isatis tinctoria L.</i> or <i>Indigofera tinctoria L.</i> )
47.10 GW8	luteolin, apigenin, chrysoeriol, traces indigotin	Weld ( <i>Reseda luteola L.</i> ) with indigo-type dyestuff ( <i>Isatis tinctoria L.</i> or <i>Indigofera tinctoria L.</i> )
47.10 GW9	Gt3, luteolin, genistein, apigenin, chrysoeriol, traces indigotin	Dyer's greenweed ( <i>Genista tinctoria L.</i> ) with indigo-type dyestuff ( <i>Isatis tinctoria L.</i> or <i>Indigofera tinctoria L.</i> )
47.10 RW10	alizarin, purpurin, Nowik C, traces luteolin	Madder-type dyestuff with small amount of brazilwood and possibly weld ( <i>Reseda luteola L.</i> )
47.10 PW11	alizarin, purpurin, Nowik C, traces indigotin	Madder-type dyestuff with small amount of brazilwood and indigo-type dyestuff ( <i>Isatis tinctoria L.</i> or <i>Indigofera tinctoria L.</i> )
<b>47.11</b>		
47.11 GW2	Gt3, luteolin, genistein, apigenin, chrysoeriol, traces indigotin	Dyer's greenweed ( <i>Genista tinctoria L.</i> ) with indigo-type dyestuff ( <i>Isatis tinctoria L.</i> or <i>Indigofera tinctoria L.</i> )
47.11 GW3	luteolin, apigenin, chrysoeriol, traces indigotin	Weld ( <i>Reseda luteola L.</i> ) with indigo-type dyestuff ( <i>Isatis tinctoria L.</i> or <i>Indigofera tinctoria L.</i> )
47.11 YS4	luteolin, apigenin, chrysoeriol	Weld ( <i>Reseda luteola L.</i> )
47.11 RW6	alizarin, purpurin, Nowik C, traces luteolin and apigenin	Madder-type dyestuff with small amount of brazilwood and possibly weld ( <i>Reseda luteola L.</i> )
47.11 GS7	luteolin, apigenin, chrysoeriol, traces indigotin	Weld ( <i>Reseda luteola L.</i> ) with indigo-type dyestuff ( <i>Isatis tinctoria L.</i> or <i>Indigofera tinctoria L.</i> )

47.11 YS8	luteolin, apigenin, chrysoeriol	Weld ( <i>Reseda luteola</i> L.)
47.11 YW9	fisetin, yf1, yf2, Gt3, sulfuretin, luteolin, genistein, apigenin, chrysoeriol	Dyer's greenweed ( <i>Genista tinctoria</i> L.) with young fustic ( <i>Cotinus Coggrygia</i> Scop)
47.11 PW10	unidentified (no peaks)	Lichens (orcein ?)
47.11 YW11	Gt3, luteolin, genistein, aigenin, chrysoeriol	Dyer's greenweed ( <i>Genista tinctoria</i> L.)
<b>47.12</b>		
47.12 YS2	luteolin, apigenin, chrysoeriol	Weld ( <i>Reseda luteola</i> L.)
47.12 GW3	Gt3, luteolin, genistein, apigenin, chrysoeriol, traces indigotin	Dyer's greenweed ( <i>Genista tinctoria</i> L.) with indigo-type dyestuff ( <i>Isatis tinctoria</i> L. or <i>Indigofera tinctoria</i> L.)
47.12 Pink Silk 4	Ct1, Ct2, Ct2', Ct4, luteolin, apigenin, chrysoeriol	Safflower ( <i>Carthamus tinctorius</i> L.) and weld ( <i>Reseda luteola</i> L.)
47.12 RW5	alizarin, purpurin, Nowik C, traces luteolin	Madder-type dyestuff with small amount of brazilwood and possibly weld ( <i>Reseda luteola</i> L.)
47.12 YS6	luteolin, apigenin, chrysoeriol	Weld ( <i>Reseda luteola</i> L.)
47.12 GW7	luteolin, apigenin, chrysoeriol, traces indigotin	Weld ( <i>Reseda luteola</i> L.) with indigo-type dyestuff ( <i>Isatis tinctoria</i> L. or <i>Indigofera tinctoria</i> L.)
47.12 PW8	carminic acid, traces indigotin	Coccid dyestuff (unknown origin) and indigo-type dyestuff ( <i>Isatis tinctoria</i> L. or <i>Indigofera tinctoria</i> L.)
47.12 YW9 (2)	fisetin, yf1, yf2, Gt3, sulfuretin, luteolin, genistein, apigenin	Dyer's greenweed ( <i>Genista tinctoria</i> L.) with young fustic ( <i>Cotinus coggrygia</i> Scop.)
47.12 YS10	luteolin, apigenin, chrysoeriol	Weld ( <i>Reseda luteola</i> L.)
<b>47.13</b>		
47.13 PW1	indigotin and orcein? small peak $\lambda_{max}$ 522 nm	Indigo-type dyestuff ( <i>Isatis tinctoria</i> L. or <i>Indigofera tinctoria</i> L.) with lichens (orcein?)
47.13 GW2	Gt3, luteolin, genistein, apigenin, chrysoeriol, traces indigotin	Dyer's greenweed ( <i>Genista tinctoria</i> L.) with indigo-type dyestuff ( <i>Isatis tinctoria</i> L. or <i>Indigofera tinctoria</i> L.)
47.13 RW3	alizarin, purpurin, Nowik C, luteolin, apigenin, chrysoeriol	Madder-type dyestuff with small amount of brazilwood and weld ( <i>Reseda luteola</i> L.)

47.13 GW4	Gt3, luteolin, genistein, apigenin, chrysoeriol, traces indigotin	Dyer's greenweed ( <i>Genista tinctoria L.</i> ) with indigo-type dyestuff ( <i>Isatis tinctoria L.</i> or <i>Indigofera tinctoria L.</i> )
47.13 YS5	luteolin, apigenin, chrysoeriol	Weld ( <i>Reseda luteola L.</i> )
47.13 GW7	three unidentified dyes : unknown 1 $\lambda_{\max}$ 394 nm; unknown 2 $\lambda_{\max}$ 622 nm unknown 3 $\lambda_{\max}$ 636 nm	Un-identified, early synthetic dyes?
47.13 YS9	luteolin, apigenin, chrysoeriol, traces ellagic acid	Weld ( <i>Reseda luteola L.</i> ) with tannins
47.13 YW0	fisetin, yf1, yf2, luteolin, apigenin, chrysoeriol	Weld ( <i>Reseda luteola L.</i> ) and young fustic ( <i>Cotinus Coggryria Scop</i> )
47.13 YS11	luteolin, apigenin, chrysoeriol	Weld ( <i>Reseda luteola L.</i> )
47.13 GS12	luteolin, apigenin, chrysoeriol, traces indigotin	Weld ( <i>Reseda luteola L.</i> ) with indigo-type dyestuff ( <i>Isatis tinctoria L.</i> or <i>Indigofera tinctoria L.</i> )
<b>47.14</b>		
47.14 YS2	luteolin, apigenin, chrysoeriol	Weld ( <i>Reseda luteola L.</i> )
47.14 GW3	Gt3, luteolin, genistein, apigenin, chrysoeriol, traces indigotin	Dyer's greenweed ( <i>Genista tinctoria L.</i> ) with indigo-type dyestuff ( <i>Isatis tinctoria L.</i> or <i>Indigofera tinctoria L.</i> )
47.14 RW4	alizarin, purpurin, Nowick C, traces luteolin and apigenin	Madder-type dyestuff with small amount of brazilwood and possibly weld ( <i>Reseda luteola L.</i> )
47.14 PW6	traces indigotin and orcein? $\lambda_{\max}$ 522 nm	Indigo-type dyestuff ( <i>Isatis tinctoria L.</i> or <i>Indigofera tinctoria L.</i> ) with lichens (orcein?)
47.14 GS7	luteolin, apigenin, chrysoeriol, traces indigotin	Weld ( <i>Reseda luteola L.</i> ) with indigo-type dyestuff ( <i>Isatis tinctoria L.</i> or <i>Indigofera tinctoria L.</i> )
47.14 GW8	luteolin, apigenin, chrysoeriol, traces indigotin	Weld ( <i>Reseda luteola L.</i> ) with indigo-type dyestuff ( <i>Isatis tinctoria L.</i> or <i>Indigofera tinctoria L.</i> )
47.14 GW9	luteolin, apigenin, chrysoeriol, traces indigotin	Weld ( <i>Reseda luteola L.</i> ) with indigo-type dyestuff ( <i>Isatis tinctoria L.</i> or <i>Indigofera tinctoria L.</i> )
<b>47.17</b>		
47.17 YS1	luteolin, apigenin, chrysoeriol	Weld ( <i>Reseda luteola L.</i> )

47.17 PW2	carminic acid, dc II, traces flavokermesic acid and kermesic acid	American cochineal ( <i>Dactylopius coccus C.</i> )
47.17 RW3	alizarin, purpurin, Nowik C, traces luteolin	Madder-type dyestuff with small amount of brazilwood and probably weld ( <i>Reseda luteola L.</i> )
47.17 PS4	carminic acid, dc II, traces flavokermesic acid and kermesic acid, ellagic acid with traces of luteolin, apigenin and chrysoeriol	American cochineal ( <i>Dactylopius coccus C.</i> ) with tannins and traces weld ( <i>Reseda luteola L.</i> )
47.17 RW5	Un-identified dyes: unknown 1 $\lambda_{\max}$ 225, 310, 487 nm; unknown 2 $\lambda_{\max}$ 249, 339, 405, and 545 nm	Un- identified, synthetic dyes ?
47.17 Metal thread MT6	traces Nowick 3 and sulfuretin	Brazilwood and probably young fustic ( <i>Cotinus coggygria Scop.</i> ) Ag, traces Au, Cu
47.17 GS8	luteolin, apigenin, chrysoeriol, traces indigotin	Weld ( <i>Reseda luteola L.</i> ) with indigo-type dyestuff ( <i>Isatis tinctoria L.</i> or <i>Indigofera tinctoria L.</i> )
47.17 YS9	luteolin, apigenin, chrysoeriol	Weld ( <i>Reseda luteola L.</i> )
47.17 GW10	luteolin, apigenin, chrysoeriol, traces indigotin	Weld ( <i>Reseda luteola L.</i> ) with indigo-type dyestuff ( <i>Isatis tinctoria L.</i> or <i>Indigofera tinctoria L.</i> )
47.17 PW11	carminic acid, dc II, traces flavokermesic acid and kermesic acid	American cochineal ( <i>Dactylopius coccus C.</i> )
<b>47.19</b>		
47.19 YS1b	luteolin, apigenin, chrysoeriol	Weld ( <i>Reseda luteola L.</i> )
47.19 YS2	luteolin, apigenin, chrysoeriol	Weld ( <i>Reseda luteola L.</i> )
47.19 YW3	fisetin, yf1, yf2, sulfuretin, luteolin, apigenin, chrysoeriol	Weld ( <i>Reseda luteola L.</i> ) with young fustic ( <i>Cotinus coggygria Scop.</i> )
47.19 Pink Silk 4	Ct1, Ct2, Ct2', Ct4, luteolin, apigenin, chrysoeriol	Safflower ( <i>Carthamus tinctorius L.</i> ) and weld ( <i>Reseda luteola L.</i> )
47.19 Pink Silk 5	Ct1, Ct2, Ct2', Ct4, luteolin, apigenin, chrysoeriol	Safflower ( <i>Carthamus tinctorius L.</i> ) and weld ( <i>Reseda luteola L.</i> )
47.19 PW6	alizarin, purpurin	Madder-type dyestuff

47.19 PW7	carminic acid, dc II, traces flavokermesic acid and kermesic acid, Alizarin, purpurin	American cochineal ( <i>Dactylopius coccus C.</i> ) with madder-type dyestuff
47.19 GW8	luteolin, apigenin, chrysoeriol, traces indigotin	Weld ( <i>Reseda luteola L.</i> ) with indigo-type dyestuff ( <i>Isatis tinctoria L.</i> or <i>Indigofera tinctoria L.</i> )
47.19 GW9a	luteolin, apigenin, chrysoeriol, traces indigotin	Weld ( <i>Reseda luteola L.</i> ) with indigo-type dyestuff ( <i>Isatis tinctoria L.</i> or <i>Indigofera tinctoria L.</i> )
47.19 GW9b	luteolin, apigenin, chrysoeriol, traces indigotin	Weld ( <i>Reseda luteola L.</i> ) with indigo-type dyestuff ( <i>Isatis tinctoria L.</i> or <i>Indigofera tinctoria L.</i> )
47.19 GS10a	luteolin, apigenin, chrysoeriol, traces indigotin	Weld ( <i>Reseda luteola L.</i> ) with indigo-type dyestuff ( <i>Isatis tinctoria L.</i> or <i>Indigofera tinctoria L.</i> )
47.19 GS10b	luteolin, apigenin, chrysoeriol, traces indigotin	Weld ( <i>Reseda luteola L.</i> ) with indigo-type dyestuff ( <i>Isatis tinctoria L.</i> or <i>Indigofera tinctoria L.</i> )
47.19 YS11	luteolin, apigenin, chrysoeriol	Weld ( <i>Reseda luteola L.</i> )
<b>47.21</b>		
47.21 YS4 (2)	Gt3, luteolin, genistein, apigenin, diosmetin	Dyer's greenweed ( <i>Genista tinctoria L.</i> )
47.21 GW3 (3)	luteolin, apigenin, chrysoeriol, traces indigotin	Weld ( <i>Reseda luteola L.</i> ) with indigo-type dyestuff ( <i>Isatis tinctoria L.</i> or <i>Indigofera tinctoria L.</i> )
47.21 GW5	luteolin, apigenin, chrysoeriol, traces indigotin	Weld ( <i>Reseda luteola L.</i> ) with indigo-type dyestuff ( <i>Isatis tinctoria L.</i> or <i>Indigofera tinctoria L.</i> )
47.21 OW7 - I	luteolin, apigenin, chrysoeriol, traces alizarin, purpurin	Weld ( <i>Reseda luteola L.</i> ) with madder-type dyestuff
47.21 GW8 (3)	luteolin, apigenin, chrysoeriol, traces indigotin	Weld ( <i>Reseda luteola L.</i> ) with indigo-type dyestuff ( <i>Isatis tinctoria L.</i> or <i>Indigofera tinctoria L.</i> )
47.21 YS11 (2)	Gt3, luteolin, genistein, apigenin, chrysoeriol	Dyer's greenweed ( <i>Genista tinctoria L.</i> )



47.21 YS11 (3)	Gt3, luteolin, genistein, apigenin, chrysoeriol	Dyer's greenweed ( <i>Genista tinctoria L.</i> )
47.21 OW14 (2)	luteolin, apigenin, chrysoeriol, traces alizarin, purpurin	Weld ( <i>Reseda luteola L.</i> ) with Madder-type dyestuff
47.23 YS18 (2)	luteolin, apigenin, chrysoeriol	Weld ( <i>Reseda luteola L.</i> )
47.21 YS19 (3)	Gt3, luteolin, genistein, apigenin, chrysoeriol	Dyer's greenweed ( <i>Genista tinctoria L.</i> )
47.21 YS21 (2)	Gt3, luteolin, genistein, apigenin, chrysoeriol	Dyer's greenweed ( <i>Genista tinctoria L.</i> )
47.21 YS21 (3)	Gt3, luteolin, genistein, apigenin, chrysoeriol	Dyer's greenweed ( <i>Genista tinctoria L.</i> )
47.21 GW23 (3)	luteolin, apigenin, chrysoeriol, traces indigotin	Weld ( <i>Reseda luteola L.</i> ) with indigo-type dyestuff ( <i>Isatis tinctoria L.</i> or <i>Indigofera tinctoria L.</i> )
47.21 OW26 (3)	luteolin, apigenin, chrysoeriol, traces alizarin, purpurin	Weld ( <i>Reseda luteola L.</i> ) with madder-type dyestuff
47;21 GW27 (2)	luteolin, genistein, apigenin, diosmetin, traces indigotin	Dyer's greenweed ( <i>Genista tinctoria L.</i> ) with indigo-type dyestuff ( <i>Isatis tinctoria L.</i> or <i>Indigofera tinctoria L.</i> )
47.21 GW27 (3)	luteolin, genistein, apigenin, diosmetin, traces indigotin	Dyer's greenweed ( <i>Genista tinctoria L.</i> ) with indigo-type dyestuff ( <i>Isatis tinctoria L.</i> or <i>Indigofera tinctoria L.</i> )
47.21 YS28 (3)	luteolin, genistein, apigenin, diosmetin	Dyer's greenweed ( <i>Genista tinctoria L.</i> )
47.21 BW34 (3)	luteolin, apigenin, chrysoeriol, traces indigotin	Weld ( <i>Reseda luteola L.</i> ) with indigo-type dyestuff ( <i>Isatis tinctoria L.</i> or <i>Indigofera tinctoria L.</i> )

47.21 GW35 (3)	luteolin, apigenin, chrysoeriol, traces indigotin	Weld ( <i>Reseda luteola L.</i> ) with indigo-type dyestuff ( <i>Isatis tinctoria L.</i> or <i>Indigofera tinctoria L.</i> )
47.21 GW36 (3)	luteolin, genistein, apigenin, diosmetin, traces indigotin	Dyer's greenweed ( <i>Genista tinctoria L.</i> ) with indigo-type dyestuff ( <i>Isatis tinctoria L.</i> or <i>Indigofera tinctoria L.</i> )
47.21 OW37 (3)	luteolin, apigenin, chrysoeriol, traces alizarin, purpurin	Weld ( <i>Reseda luteola L.</i> ) with Madder-type dyestuff
47.21 OW38 (3)	luteolin, apigenin, chrysoeriol, traces alizarin, purpurin	Weld ( <i>Reseda luteola L.</i> ) with madder-type dyestuff
47.21 Metal Thread MT 41	ellagic acid with traces Nowick C and sulfuretin	Young fustic ( <i>Cotinus coggygia Scop.</i> ) with traces brazilwood and tannins Ag, traces Au, Cu
<b>47.23</b>		
47.23 YS1	ellagic acid with traces luteolin	Tannins with possibly small amount of weld ( <i>Reseda luteola L.</i> )
47.23 YS2	luteolin, apigenin, chrysoeriol	Weld ( <i>Reseda luteola L.</i> )
47.23 YS3	luteolin, apigenin, chrysoeriol	Weld ( <i>Reseda luteola L.</i> )
47.23 GS4	luteolin, apigenin, chrysoeriol, traces indigotin	Weld ( <i>Reseda luteola L.</i> ) with indigo-type dyestuff ( <i>Isatis tinctoria L.</i> or <i>Indigofera tinctoria L.</i> )
47.23 Pink Silk 5	Ct1, Ct2, Ct2', Ct4, luteolin, apigenin, chrysoeriol	Safflower ( <i>Carthamus tinctorius L.</i> ) and weld ( <i>Reseda luteola L.</i> )
47.23 RW6	alizarin, purpurin	Madder-type dyestuff
47.23 PW7	carminic acid, dc II, traces flavokermesic acid and kermesic acid, alizarin, purpurin	American cochineal ( <i>Dactylopius coccus C.</i> ) with madder-type dyestuff and brazilwood
<b>MAP 1</b>		
MAP 1 YW1 (2)	luteolin, apigenin, chrysoeriol	Weld ( <i>Reseda luteola L.</i> )

MAP 1 DW2 (2)	traces of Nowick C, luteolin, genistein, apigenin and indigotin	Dyer's greenweed ( <i>Genista tinctoria L.</i> ) with traces of brazilwood and indigo-type dyestuff ( <i>Isatis tinctoria L.</i> or <i>Indigofera tinctoria L.</i> )
MAP 1 YS3 (2)	luteolin, apigenin, chrysoeriol	Weld ( <i>Reseda luteola L.</i> )
MAP 1 PW5 (1) -1	carminic acid, dc II, traces flavokermesic acid and kermesic acid	American Cochineal ( <i>Dactylopius coccus C.</i> )
MAP 1 PW5 (1) -2	carminic acid, dc II, traces flavokermesic acid and kermesic acid	American Cochineal ( <i>Dactylopius coccus C.</i> )
MAP 1 PW5 (2) -1	carminic acid, dc II, traces flavokermesic acid and kermesic acid	American Cochineal ( <i>Dactylopius coccus C.</i> )
MAP 1 PW5 (2) -2	carminic acid, small amount of dc II, traces flavokermesic acid and kermesic acid	American Cochineal ( <i>Dactylopius coccus C.</i> )
MAP 1 YW7 (2)	luteolin, apigenin, chrysoeriol	Weld ( <i>Reseda luteola L.</i> )
MAP 1 OW10 (2) -1	Nowick C, alizarin, purpurin, small amount of luteolin, apigenin and chrysoeriol	Brazilwood with madder-type dyestuff with traces of weld ( <i>Reseda luteola L.</i> )
MAP 1 OW10 (2) -2	Nowick C, alizarin, purpurin, small amount of luteolin, apigenin and chrysoeriol	Brazilwood with madder-type dyestuff with traces of weld ( <i>Reseda luteola L.</i> )
MAP 1 YS11 (2)	luteolin, apigenin, chrysoeriol	Weld ( <i>Reseda luteola L.</i> )
MAP 1 YW12 (2)	luteolin, apigenin, chrysoeriol	Weld ( <i>Reseda luteola L.</i> )
MAP 1 GW13 (2)	luteolin, apigenin, chrysoeriol, traces indigotin	Weld ( <i>Reseda luteola L.</i> ) with indigo-type dyestuff ( <i>Isatis tinctoria L.</i> or <i>Indigofera tinctoria L.</i> )

MAP 1 GW15 (2)	luteolin, apigenin, chrysoeriol, traces indigotin	Weld ( <i>Reseda luteola L.</i> ) with indigo-type dyestuff ( <i>Isatis tinctoria L.</i> or <i>Indigofera tinctoria L.</i> )
MAP 1 PW17 (2) -1	carminic acid, dc II, traces flavokermesic acid and kermesic acid with small amount of luteolin, apigenin, chrysoeriol, alizarin and purpurin	American cochineal ( <i>Dactylopius coccus C.</i> ) with traces weld ( <i>Reseda luteola L.</i> ) and madder-type dyestuff
MAP 1 PW17 (2) -2	carminic acid, dc II, traces flavokermesic acid and kermesic acid with small amount of luteolin, apigenin, chrysoeriol, alizarin and purpurin	American cochineal ( <i>Dactylopius coccus C.</i> ) with traces weld ( <i>Reseda luteola L.</i> ) and madder-type dyestuff
MAP 1 YW18 (2)	luteolin, apigenin, chrysoeriol	Weld ( <i>Reseda luteola L.</i> )
MAP 1 YW19 (2)	luteolin, apigenin, chrysoeriol	Weld ( <i>Reseda luteola L.</i> )
MAP 1 Dark Wool 21 (2)	luteolin, traces indigotin and purpurin	Possibly Weld ( <i>Reseda luteola L.</i> ) with traces of madder-type dyestuff and indigo-type dyestuff ( <i>Isatis tinctoria L.</i> or <i>Indigofera tinctoria L.</i> )
<b>MAP 2</b>		
MAP 2 RW1 (2)	alizarin, purpurin and traces Nowick C	Madder-type dyestuff with small amount of brazilwood
MAP 2 PW2 (1) -1	carminic acid, dc II, traces flavokermesic acid and kermesic acid	American cochineal ( <i>Dactylopius coccus C.</i> )
MAP 2 PW2 (1) -2	carminic acid, dc II, traces flavokermesic acid and kermesic acid	American cochineal ( <i>Dactylopius coccus C.</i> )
MAP 2 PW2 (2) -1	carminic acid, dc II, traces flavokermesic acid and kermesic acid	American cochineal ( <i>Dactylopius coccus C.</i> )

MAP 2 OW3 (2)	alizarin, purpurin and traces Nowick C and luteolin	Madder-type dyestuff with small amount of brazilwood and possibly traces of weld ( <i>Reseda luteola L.</i> )
MAP 2 YW4 (2)	luteolin, apigenin, chrysoeriol	Weld ( <i>Reseda luteola L.</i> )
MAP 2 YW6 (2)	luteolin, apigenin, chrysoeriol	Weld ( <i>Reseda luteola L.</i> )
MAP 2 Brown Wool 7	traces carminic acid	Coccid dyestuff (unknown origin)
MAP 2 GW10 (2)	luteolin, apigenin, chrysoeriol, traces indigotin	Weld ( <i>Reseda luteola L.</i> ) with indigo-type dyestuff ( <i>Isatis tinctoria L.</i> or <i>Indigofera tinctoria L.</i> )
MAP 2 YW11 (2)	luteolin, apigenin, chrysoeriol	Weld ( <i>Reseda luteola L.</i> )
MAP 2 YS12 (2)	luteolin, genistein, apigenin, chrysoeriol	Dyer's greenweed ( <i>Genista tinctoria L.</i> )
<b>MAP 3</b>		
MAP 3 YW1 (2)	luteolin, apigenin, chrysoeriol	Weld ( <i>Reseda luteola L.</i> )
MAP 3 YW2 (2)	luteolin, apigenin, chrysoeriol, traces alizarin and purpurin	Weld ( <i>Reseda luteola L.</i> ) with traces madder- type dyestuff
MAP 3 RW3 (2)	alizarin, purpurin	Madder-type dyestuff
MAP 3 PW4 (1) -1	carminic acid, dc II, traces flavokermesic acid and kermesic acid	Cochineal with low dcII, it could be Armenian cochineal ( <i>Porphyrophora hamelii B.</i> ) or Mexican cochineal ( <i>Dactylopius coccus C.</i> )
MAP 3 PW4 (2) -1	carminic acid, dc II, traces flavokermesic acid and kermesic acid	Cochineal with low dcII, it could be Armenian cochineal ( <i>Porphyrophora hamelii B.</i> ) or Mexican cochineal ( <i>Dactylopius coccus C.</i> )
MAP 3 PW4 (2) -2	carminic acid, dc II, traces flavokermesic acid and kermesic acid	Cochineal with low dcII, it could be Armenian cochineal ( <i>Porphyrophora hamelii B.</i> ) or Mexican cochineal ( <i>Dactylopius coccus C.</i> )

MAP 3 PS6 (1) -1	Carminic acid and ellagic acid with traces of dc II, flavokermesic acid and kermesic acid	Cochineal with low dcII, it could be Armenian cochineal ( <i>Porphyrophora hamelii</i> B.) or Mexican cochineal ( <i>Dactylopius coccus</i> C.) with tannins
MAP 3 PS6 (1) -2	Carminic acid and ellagic acid with traces of dc II, flavokermesic acid and kermesic acid	Cochineal with low dcII, it could be Armenian cochineal ( <i>Porphyrophora hamelii</i> B.) or Mexican cochineal ( <i>Dactylopius coccus</i> C.) with tannins
MAP 3 YS7 (2)	luteolin, apigenin, chrysoeriol	Weld ( <i>Reseda luteola</i> L.)
MAP 3 OW8 (2)	alizarin, purpurin	Madder-type dyestuff
MAP 3 GW9 (2)	luteolin, apigenin, chrysoeriol, traces indigotin	Weld ( <i>Reseda luteola</i> L.) with indigo-type dyestuff ( <i>Isatis tinctoria</i> L. or <i>Indigofera tinctoria</i> L.)
MAP 3 YW10 (2)	luteolin, apigenin, chrysoeriol	Weld ( <i>Reseda luteola</i> L.)
MAP 3 YW11 (2)	luteolin, apigenin, chrysoeriol	Weld ( <i>Reseda luteola</i> L.)

**Table 7.19:** Dye components and species identification, of the acid hydrolysed samples from early mid sixteenth to late sixteenth century English tapestries. Tapestries 47 are from the Burrell Collection, Glasgow; while tapestries maps are from the Bodleian Library, Oxford (MAP 1 corresponds to the map of Worcestershire and MAP 2 to the map of Oxfordshire; MAP 3 corresponds to the map of Warwickshire).

## 7.3 CHARACTERISATION OF METALLIC MORDANT ON PORCUPINE QUILL WORK

### 7.3.1 Scanning Electron Microscopy (SEM)

Cuticle measurements and porcupine quills imaging were undertaken using a CamScan MX2500 Scanning Electron Microscope operated in controlled pressure mode (Envac, 30 Pa, aperture 50  $\mu\text{m}$ ) coupled to Energy Dispersive X-ray analysis (EDX) with Noran Vantage system and Vista software. Images were recorded at a working distance of 20 mm using Backscattered Electron detector (BSC) or Absorbed Current detector (AEI) at voltages of 15 or 20 kV and with spot size 5-6. X-Ray analyses were recorded at a working distance of 35 mm with EDX detector at 35 °, the deadtime was below 20 % and each analysis was 200 sec.

	Quill 1	Quill 2	Quill 3	Quill 4	Quill 5	Quill 6	Quill 7
<i>Cuticle (<math>\mu\text{m}</math>)</i>	61.0	44.7	62.0	46.9	104.3	47.0	34.6
	60.2	47.7	66.5	47.0	102.7	40.4	31.6
	62.1	43.4	62.8	56.1	103.5	50.4	35.1
	62.0	45.9	69.0	50.0	105.9	50.9	37.6
	67.1	46.5	67.4	55.3	100.7	52.6	32.8
	60.6	40.0	60.5	51.8	103.2	58.9	34.8
	69.3	39.5	60.0	48.7	93.6	49.9	39.0
	70.5	41.3	61.6	48.1	95.1	49.6	37.5
	73.4	38.1	67.3	47.5	99.1	52.9	37.0
<i>Mean</i>	<i>65.1</i>	<i>43.0</i>	<i>64.1</i>	<i>50.2</i>	<i>100.9</i>	<i>50.3</i>	<i>35.6</i>
<i>Standard deviation</i>	<i>5.0</i>	<i>3.4</i>	<i>3.4</i>	<i>3.5</i>	<i>4.2</i>	<i>4.9</i>	<i>2.4</i>
<i>s<sub>r</sub> (%)</i>	<i>7.7</i>	<i>8.0</i>	<i>5.3</i>	<i>7.0</i>	<i>4.2</i>	<i>9.8</i>	<i>6.8</i>

**Table 7.20:** Cuticles measurements undertaken on several section of porcupine quills using Scanning Electron Microscopy.

### 7.3.2 References of $\text{Cu}^{2+}$ and $\text{Sn}^{2+}$ preparation

The solutions aqueous solutions of copper and tin were prepared from anhydrous copper(II) sulphate (> 99 %) and tin(II) chloride (98 %), both from Sigma Aldrich. The mass of mordant (mg) was calculated in order to obtain concentrations ranging between 100  $\mu\text{g}\cdot\text{mL}^{-1}$  and 15,000  $\mu\text{g}\cdot\text{mL}^{-1}$ , based on the mass (mg) of copper(II) and tin(II) present in 50 mL deionised water (table 7.21).

$M_w \text{ CuSO}_4 \text{ (g.mol}^{-1}\text{)}$	$M_w \text{ Cu (g.mol}^{-1}\text{)}$	$[\text{Cu}^{2+}] \text{ (mg.L}^{-1}\text{)}$	$\text{Cu}^{2+} \text{ (mg)}$	$\text{CuSO}_4 \text{ (mg)}$	$\text{pH}$
159.6	63.6	15000	750	1884	3.80
159.6	63.6	10000	500	1256	3.91
159.6	63.6	5000	250	628	4.07
159.6	63.6	2500	125	314	4.22
159.6	63.6	1000	50	126	4.41
159.6	63.6	500	25	63	4.65
159.6	63.6	100	5	13	4.66
$M_w \text{ SnCl}_2 \text{ (g.mol}^{-1}\text{)}$	$M_w \text{ Sn (g.mol}^{-1}\text{)}$	$[\text{Sn}^{2+}] \text{ (mg.L}^{-1}\text{)}$	$\text{Sn}^{2+} \text{ (mg)}$	$\text{SnCl}_2 \text{ (mg)}$	$\text{pH}$
189.6	118.7	15000	750	1198	1.95
189.6	118.7	10000	500	799	2.05
189.6	118.7	5000	250	399	2.23
189.6	118.7	2500	125	200	2.40
189.6	118.7	1000	50	80	2.60
189.6	118.7	500	25	40	2.80
189.6	118.7	100	5	8	3.30

**Table 7.21:** mass of copper(II) sulphate and tin(II) chloride used to prepare the different dye bath concentrations, considering a volume of 50 mL of deionised water.

### 7.3.3 ICP-OES

The samples were analysed by ICP-OES using a Perkin Elmer Optima 5300 DV, employing an RF forward power of 1400 W, with argon gas flows of 15, 0.2 and 0.75 L min<sup>-1</sup> for plasma, auxiliary, and nebuliser flows, respectively. Using a peristaltic pump, sample solutions were taken up into a Gem Tip cross-Flow nebuliser and Scotts spray chamber at a rate of 1.50 mL min<sup>-1</sup>.

The selected wavelengths for each element and were analysed in fully quant mode (three points per unit wavelength). Three replicate runs per sample were employed.

#### 7.3.3.1 Calibration of the system

The calibration of the system was done by diluting a stock solution of tin and copper (1000 parts per million), both from Fisher Scientific, with a solution of 2:98 (v/v) 37% hydrochloric acid: deionised water to produce solutions at concentration of 0.02 µg mL<sup>-1</sup>, 0.2 µg mL<sup>-1</sup>, 2 µg mL<sup>-1</sup>, 20 µg mL<sup>-1</sup>, 40 µg mL<sup>-1</sup>, 100 µg mL<sup>-1</sup> and 200 µg mL<sup>-1</sup> that were used to produce calibration curves (tables 7.22 and 7.23).



Copper standards (monitored at 327.4 nm)		
0.02 to 200 $\mu\text{g mL}^{-1}$		
Standard	Found	
Blank	-819.51	Slope = 69468
0.02 $\mu\text{g mL}^{-1}$	973.251028	Y-intercept = - 85943
0.2 $\mu\text{g mL}^{-1}$	10612.0309	$R^2 = 0.9999$
2 $\mu\text{g mL}^{-1}$	106453.652	
20 $\mu\text{g mL}^{-1}$	1057843.45	
40 $\mu\text{g mL}^{-1}$	13831675.2	
200 $\mu\text{g mL}^{-1}$	973.251028	

**Table 7.22:** The instrument calibration details for copper standard

Tin standards (monitored at 284 nm)		
Range 0.02 to 200 $\mu\text{g mL}^{-1}$		
Standard	Found	
Blank	-6.32	Slope = 5681.3
0.02 $\mu\text{g mL}^{-1}$	97.8721604	Y-intercept = - 6109.9
0.2 $\mu\text{g mL}^{-1}$	924.721097	$R^2 = 0.9996$
2 $\mu\text{g mL}^{-1}$	9073.30548	
20 $\mu\text{g mL}^{-1}$	89995.6465	
40 $\mu\text{g mL}^{-1}$	1131857.52	
200 $\mu\text{g mL}^{-1}$	97.8721604	

**Table 7.23:** The instrument calibration details for tin standard high concentration

### 7.3.3.2 ICP-OES sample preparation

The samples were prepared following the hydrochloric acid extraction protocol developed for the routine analysis of the dye components from reference and historical samples (section 7.1.2).

The sample of porcupine quill ( $1.0 \pm 0.1$  mg) was placed in a 2 mL glass test tube, to which was added a mixture of 37% hydrochloric acid: methanol: water [200  $\mu\text{L}$ , 2:1:1 (v/v/v)]. The tube was then placed in a heated block set to 100 °C and heated for precisely 10 min. After rapid cooling under cold water, the extract was centrifuged

for 10 minutes at 10,000 rounds per minutes and filtered using a Polyethylene filter (55  $\mu\text{m}$ , 5 mm) from Crawford Scientific™. The frit was rinsed with methanol (200  $\mu\text{L}$ ). The combined filtrates were then gravimetrically prepared (*ca.* 5 ml) using a solution of 37% hydrochloric acid: water [2:98, (v/v)]. The diluted extracts of the selected samples were analysed in triplicate and the mean concentration of tin and copper in each solution (per mg of yarn) was calculated.

200  $\mu\text{L}$  of the dyebaths were collected at different times and analysed in triplicate. 50  $\mu\text{L}$  of the solution were filtered using a Polyethylene filter (55  $\mu\text{m}$ , 5 mm) from Crawford Scientific™. The frit was rinsed with methanol (200 or 400  $\mu\text{L}$ ) and the combined filtrates were then gravimetrically prepared (*ca.* 5 ml) using a solution of 37% hydrochloric acid: water [2:98, (v/v)]. The diluted solutions were analysed in triplicate and the mean concentration of tin and copper in each solution ( $\mu\text{g}\cdot\text{mL}^{-1}$ ) was calculated.

### 7.3.3.3 Evaluation of dyebath conditions

A small amount of porcupine quills (200 mg) were prepared in a 50 mL deionised water containing cochineal (2 g) and copper(II) or tin(II) prepared at 1000  $\mu\text{g mL}^{-1}$ . After stirring the solution, a fraction of the dyebath (200  $\mu\text{L}$ ) was removed corresponding to the measurement at  $t = 0$ .

The dyebath was then set-up with a condenser and gently heated up to 85 °C for half an hour. The temperature was controlled with a thermostat, when temperature was reached, the quills were added. A fraction of the dyebath (200  $\mu\text{L}$ ) and two porcupine quills were collected after 1 hour, 2 hours and 5 hours for ICP-OES analysis. The quills were rinsed with deionised water and left to dry at room temperature for several days and the fractions of dyebath kept in the fridge at 4 °C. The dyebath fractions and porcupine quill samples were then analysed by ICP-OES (protocol described in section 7.3.3.2).

Time (h)	Sample ID	ICP OES [Sn <sup>2+</sup> ] µg mL <sup>-1</sup>	Mass of filtered extract (g)	Mass of sample after dilution (g)	Bath Fraction [Sn <sup>2+</sup> ] µg mL <sup>-1</sup>
<b>0 h</b>	Fraction 1	9.612	0.4174	5.0082	963
	Fraction 2	10.084	0.4190	5.0008	1009
	Fraction 3	10.033	0.4195	5.0009	1003
				<i>Mean</i>	<b>992</b>
				<i>Standard Deviation</i>	<b>25</b>
				<i>Standard Error <math>\sigma/\sqrt{n}</math></i>	<b>43</b>
				<i>(100 × <math>\sigma</math>)/ Mean</i>	<b>2.5 %</b>
<b>1h</b>	Fraction 1	2.192	0.4237	5.0220	220
	Fraction 2	2.982	0.4267	5.0020	298
	Fraction 3	2.094	0.4190	5.0256	210
				<i>Mean</i>	<b>243</b>
				<i>Standard Deviation</i>	<b>48</b>
				<i>Standard Error <math>\sigma/\sqrt{n}</math></i>	<b>83</b>
				<i>(100 × <math>\sigma</math>)/ Mean</i>	<b>19.8 %</b>
<b>2h</b>	Fraction 1	2.169	0.4198	5.0091	217
	Fraction 2	2.208	0.4232	5.0074	221
	Fraction 3	2.228	0.4207	5.0112	223
				<i>Mean</i>	<b>221</b>
				<i>Standard Deviation</i>	<b>3</b>
				<i>Standard Error <math>\sigma/\sqrt{n}</math></i>	<b>5</b>
				<i>(100 × <math>\sigma</math>)/ Mean</i>	<b>1.4 %</b>
<b>5h</b>	Fraction 1	2.394	0.4258	5.0093	240
	Fraction 2	2.357	0.4252	5.0033	236
	Fraction 3	2.226	0.4228	5.0052	223
				<i>Mean</i>	<b>233</b>
				<i>Standard Deviation</i>	<b>9</b>
				<i>Standard Error <math>\sigma/\sqrt{n}</math></i>	<b>15</b>
				<i>(100 × <math>\sigma</math>)/ Mean</i>	<b>3.8 %</b>

**Table 7.24:** ICP-OES analysis of dyebath fractions containing tin(II) at 1000 µg mL<sup>-1</sup> and removed at t = 0h, 1h, 2h and 5h

Time (h)	Sample ID	ICP OES [Cu <sup>2+</sup> ] µg mL <sup>-1</sup>	Mass of filtered extract (g)	Mass of sample after dilution (g)	Bath Fraction [Cu <sup>2+</sup> ] µg mL <sup>-1</sup>
<b>0 h</b>	Fraction 1	8.383	0.0510	5.0055	839
	Fraction 2	8.344	0.0500	5.0088	836
	Fraction 3	8.237	0.0496	5.0062	825
				<i>Mean</i>	<b>833</b>
				<i>Standard Deviation</i>	<b>7</b>
				<i>Standard Error <math>\sigma/\sqrt{n}</math></i>	<b>13</b>
				<i>(100 × <math>\sigma</math>)/ Mean</i>	<b>0.9 %</b>
<b>1h</b>	Fraction 1	2.405	0.2188	5.0290	242
	Fraction 2	2.457	0.2133	5.0086	246
	Fraction 3	2.389	0.2199	5.0095	239
				<i>Mean</i>	<b>242</b>
				<i>Standard Deviation</i>	<b>3</b>
				<i>Standard Error <math>\sigma/\sqrt{n}</math></i>	<b>6</b>
				<i>(100 × <math>\sigma</math>)/ Mean</i>	<b>1.4 %</b>
<b>2h</b>	Fraction 1	2.623	0.2051	5.0031	262
	Fraction 2	2.362	0.2198	5.0290	237
	Fraction 3	2.364	0.2298	5.0095	237
				<i>Mean</i>	<b>246</b>
				<i>Standard Deviation</i>	<b>14</b>
				<i>Standard Error <math>\sigma/\sqrt{n}</math></i>	<b>25</b>
				<i>(100 × <math>\sigma</math>)/ Mean</i>	<b>5.9 %</b>
<b>5h</b>	Fraction 1	3.294	0.212	5.0096	330
	Fraction 2	2.455	0.2242	5.0051	246
	Fraction 3	3.222	0.2223	5.0016	322
				<i>Mean</i>	<b>299</b>
				<i>Standard Deviation</i>	<b>46</b>
				<i>Standard Error <math>\sigma/\sqrt{n}</math></i>	<b>81</b>
				<i>(100 × <math>\sigma</math>)/ Mean</i>	<b>15.6 %</b>

**Table 7.25:** ICP-OES analysis of dyebath fractions containing copper(II) at 1000 µg mL<sup>-1</sup> and removed at t = 0h, 1h, 2h and 5h

Time (h)	Sample ID	ICP OES [Sn <sup>2+</sup> ] $\mu\text{g mL}^{-1}$	Mass of filtered extract (g)	Mass of sample after dilution (g)	m quill (mg)	[Sn <sup>2+</sup> ] ( $\mu\text{g mg}^{-1}$ )	
<b>1h</b>	Quill 1	0.125	0.2953	5.0120	0.90	0.69	
	Quill 2	0.142	0.2769	5.0095	0.90	0.79	
	Quill 3	0.138	0.2821	5.0038	0.90	0.77	
						<i>Mean</i>	<b>0.74</b>
						<i>Standard Deviation</i>	<b>0.05</b>
						<i>Standard Error <math>\sigma/\sqrt{n}</math></i>	<b>1.8</b>
						<i>(100 <math>\times</math> <math>\sigma</math>)/ Mean</i>	<b>7 %</b>
<b>2h</b>	Quill 1	0.127	0.2991	5.0055	1.00	0.64	
	Quill 2	0.195	0.2847	5.0048	1.10	0.89	
	Quill 3	0.121	0.2979	5.0055	1.10	0.55	
						<i>Mean</i>	<b>0.69</b>
						<i>Standard Deviation</i>	<b>0.17</b>
						<i>Standard Error <math>\sigma/\sqrt{n}</math></i>	<b>1.9</b>
						<i>(100 <math>\times</math> <math>\sigma</math>)/ Mean</i>	<b>25 %</b>
<b>5h</b>	Quill 1	0.124	0.2956	5.0018	1.10	0.57	
	Quill 2	0.127	0.2855	5.0057	0.90	0.71	
	Quill 3	0.194	0.3006	5.0090	1.20	0.81	
						<i>Mean</i>	<b>0.69</b>
						<i>Standard Deviation</i>	<b>0.12</b>
						<i>Standard Error <math>\sigma/\sqrt{n}</math></i>	<b>1.8</b>
						<i>(100 <math>\times</math> <math>\sigma</math>)/ Mean</i>	<b>18 %</b>

**Table 7.26:** ICP-OES analysis of porcupine quill samples dyed in a tin(II) dye bath at  $1000 \mu\text{g mL}^{-1}$  and removed at  $t = 1\text{h}, 2\text{h}$  and  $5\text{h}$ .

Time (h)	Sample ID	ICP OES [Cu <sup>2+</sup> ] $\mu\text{g mL}^{-1}$	Mass of filtered extract (g)	Mass of sample after dilution (g)	quill (mg)	[Cu <sup>2+</sup> ] ( $\mu\text{g mg}^{-1}$ )	
<b>1h</b>	Quill 1	0.125	0.2683	5.0077	0.90	0.85	
	Quill 2	0.142	0.2521	5.0034	0.90	0.72	
	Quill 3	0.138	0.2740	5.0048	0.90	0.81	
						<b>Mean</b>	<b>0.81</b>
						<b>Standard Deviation</b>	<b>0.07</b>
						<b>Standard Error <math>\sigma/\sqrt{n}</math></b>	<b>1.80</b>
						<b>(100 <math>\times</math> <math>\sigma</math>)/ Mean</b>	<b>10 %</b>
<b>2h</b>	Quill 1	0.127	0.2686	5.0050	1.00	0.92	
	Quill 2	0.195	0.2664	5.0010	1.10	1.10	
	Quill 3	0.121	0.2807	5.0035	1.10	0.89	
						<b>Mean</b>	<b>0.89</b>
						<b>Standard Deviation</b>	<b>0.12</b>
						<b>Standard Error <math>\sigma/\sqrt{n}</math></b>	<b>1.85</b>
						<b>(100 <math>\times</math> <math>\sigma</math>)/ Mean</b>	<b>14 %</b>
<b>5h</b>	Quill 1	0.124	0.2720	5.0032	1.10	0.84	
	Quill 2	0.127	0.2791	5.0013	0.90	1.68	
	Quill 3	0.194	0.2784	5.0042	1.20	0.96	
						<b>Mean</b>	<b>1.16</b>
						<b>Standard Deviation</b>	<b>0.45</b>
						<b>Standard Error <math>\sigma/\sqrt{n}</math></b>	<b>2.18</b>
						<b>(100 <math>\times</math> <math>\sigma</math>)/ Mean</b>	<b>39 %</b>

**Table 7.27:** ICP-OES analysis of porcupine quill samples dyed in a copper(II) dye bath at  $1000 \mu\text{g mL}^{-1}$  and removed at  $t = 1\text{h}$ ,  $2\text{h}$  and  $5\text{h}$ .

#### 7.3.3.4 ICP-OES investigation of reference quills

A small amount of porcupine quills (200 mg) were prepared in 50 mL deionised water containing cochineal (2 g) and copper(II) or tin(II) in order to obtain concentrations ranging from  $100 \mu\text{g mL}^{-1}$  to  $15,000 \mu\text{g mL}^{-1}$  (see table 7.21). The dye bath was set-up with a condenser and gently heated up to  $85 \text{ }^\circ\text{C}$  for half an hour. The temperature was controlled with a thermostat, when temperature was reached, the quills were added. After one hour, the solution was left to cool down at room temperature and the quills were rinsed with deionised water and left to dry at room temperature for several days. The porcupine quill samples were then extracted following the procedure described in section 7.3.3.2 and analysed by ICP-OES.

Dyebath [Sn <sup>2+</sup> ] µg mL <sup>-1</sup>	Sample ID	ICP OES [Sn <sup>2+</sup> ] µg mL <sup>-1</sup>	Mass of filtered extract (g)	Mass of sample after dilution (g)	quill (mg)	[Sn <sup>2+</sup> ] (µg mg <sup>-1</sup> )	
<b>100</b>	Quill 1	0.2480	0.4839	5.0030	1.0	1.24	
	Quill 2	0.2009	0.4941	5.0026	1.0	1.00	
	Quill 3	0.2112	0.4829	5.0154	1.0	1.06	
						<i>Mean</i>	<b>1.10</b>
						<i>Standard Deviation</i>	<b>0.12</b>
						<i>Standard Error <math>\sigma/\sqrt{n}</math></i>	<b>0.2</b>
						<i>(100 × <math>\sigma</math>)/ Mean</i>	<b>11 %</b>
<b>500</b>	Quill 1	0.1963	0.4746	5.0009	1.0	0.98	
	Quill 2	0.8287	0.5026	5.0008	1.1	3.77	
	Quill 3	0.2214	0.5078	5.0009	1.0	1.11	
						<i>Mean</i>	<b>1.95</b>
						<i>Standard Deviation</i>	<b>1.57</b>
						<i>Standard Error <math>\sigma/\sqrt{n}</math></i>	<b>2.7</b>
						<i>(100 × <math>\sigma</math>)/ Mean</i>	<b>81 %</b>
<b>1000</b>	Quill 1	0.2549	0.4915	5.0009	1.0	1.27	
	Quill 2	0.2415	0.4623	5.0090	1.0	1.21	
	Quill 3	0.2477	0.5031	5.0057	1.0	1.24	
						<i>Mean</i>	<b>1.24</b>
						<i>Standard Deviation</i>	<b>0.03</b>
						<i>Standard Error <math>\sigma/\sqrt{n}</math></i>	<b>0.06</b>
						<i>(100 × <math>\sigma</math>)/ Mean</i>	<b>3 %</b>
<b>2500</b>	Quill 1	5.2621	0.4832	5.0005	1.1	23.92	
	Quill 2	3.0152	0.5146	5.0096	1.1	13.73	
	Quill 3	4.3942	0.5124	5.0036	1.0	21.99	
						<i>Mean</i>	<b>19.88</b>
						<i>Standard Deviation</i>	<b>5.41</b>
						<i>Standard Error <math>\sigma/\sqrt{n}</math></i>	<b>9.4</b>
						<i>(100 × <math>\sigma</math>)/ Mean</i>	<b>27 %</b>
<b>5000</b>	Quill 1	4.2997	0.5162	5.0043	1.0	21.52	
	Quill 2	5.3879	0.504	5.0048	1.1	24.51	
	Quill 3	3.7379	0.4913	5.0000	1.0	18.69	
						<i>Mean</i>	<b>21.6</b>
						<i>Standard Deviation</i>	<b>2.91</b>
						<i>Standard Error <math>\sigma/\sqrt{n}</math></i>	<b>5.0</b>
						<i>(100 × <math>\sigma</math>)/ Mean</i>	<b>14 %</b>
<b>10000</b>	Quill 1	15.0090	0.5151	5.0030	1.0	75.09	
	Quill 2	12.5474	0.5340	5.0073	1.0	62.83	
	Quill 3	13.4697	0.5038	5.0090	1.0	67.47	
						<i>Mean</i>	<b>68.46</b>
						<i>Standard Deviation</i>	<b>6.19</b>
						<i>Standard Error <math>\sigma/\sqrt{n}</math></i>	<b>10.7</b>
						<i>(100 × <math>\sigma</math>)/ Mean</i>	<b>9 %</b>
<b>15000</b>	Quill 1	22.9671	0.5714	5.0070	1.2	95.83	
	Quill 2	19.0399	0.4893	5.0050	1.0	95.29	
	Quill 3	17.3309	0.6642	5.0054	1.0	86.75	
						<i>Mean</i>	<b>92.62</b>
						<i>Standard Deviation</i>	<b>5.10</b>
						<i>Standard Error <math>\sigma/\sqrt{n}</math></i>	<b>8.8</b>
						<i>(100 × <math>\sigma</math>)/ Mean</i>	<b>5 %</b>

Table 7.28: ICP-OES analysis of porcupine quill references samples - tin(II) dyebaths

Dyebath [Cu <sup>2+</sup> ] µg mL <sup>-1</sup>	Sample ID	ICP OES [Cu <sup>2+</sup> ] µg mL <sup>-1</sup>	Mass of filtered extract (g)	Mass of sample after dilution (g)	quill (mg)	[Cu <sup>2+</sup> ] (µg mg <sup>-1</sup> )	
<b>100</b>	Quill 1	0.016	0.4465	5.0080	1.0	0.08	
	Quill 2	0.017	0.4827	5.0010	1.1	0.08	
	Quill 3	0.023	0.4495	5.0040	1.0	0.11	
						<i>Mean</i>	<b>0.09</b>
						<i>Standard Deviation</i>	<b>0.02</b>
						<i>Standard Error <math>\sigma/\sqrt{n}</math></i>	<b>0.03</b>
						<i>(100 × <math>\sigma</math>)/ Mean</i>	<b>23 %</b>
<b>500</b>	Quill 1	0.038	0.4781	5.0060	1.0	0.19	
	Quill 2	0.044	0.4533	5.0054	1.0	0.22	
	Quill 3	0.071	0.4669	5.0160	1.0	0.35	
						<i>Mean</i>	<b>0.26</b>
						<i>Standard Deviation</i>	<b>0.09</b>
						<i>Standard Error <math>\sigma/\sqrt{n}</math></i>	<b>0.2</b>
						<i>(100 × <math>\sigma</math>)/ Mean</i>	<b>34 %</b>
<b>1000</b>	Quill 1	0.096	0.4293	5.0035	1.0	0.48	
	Quill 2	0.076	0.4244	5.0043	1.0	0.38	
	Quill 3	0.077	0.4704	5.0020	1.0	0.38	
						<i>Mean</i>	<b>0.41</b>
						<i>Standard Deviation</i>	<b>0.06</b>
						<i>Standard Error <math>\sigma/\sqrt{n}</math></i>	<b>0.1</b>
						<i>(100 × <math>\sigma</math>)/ Mean</i>	<b>14 %</b>
<b>2500</b>	Quill 1	0.470	0.4527	5.0030	0.9	2.61	
	Quill 2	0.402	0.4717	5.0029	1.1	1.83	
	Quill 3	0.473	0.4533	5.0006	1.0	2.37	
						<i>Mean</i>	<b>2.27</b>
						<i>Standard Deviation</i>	<b>0.40</b>
						<i>Standard Error <math>\sigma/\sqrt{n}</math></i>	<b>0.7</b>
						<i>(100 × <math>\sigma</math>)/ Mean</i>	<b>18 %</b>
<b>10000</b>	Quill 1	1.877	0.4786	5.0008	1.2	7.82	
	Quill 2	1.518	0.4990	5.0035	1.1	6.91	
	Quill 3	1.542	0.5330	5.0046	1.1	7.02	
						<i>Mean</i>	<b>7.25</b>
						<i>Standard Deviation</i>	<b>0.50</b>
						<i>Standard Error <math>\sigma/\sqrt{n}</math></i>	<b>0.9</b>
						<i>(100 × <math>\sigma</math>)/ Mean</i>	<b>7 %</b>
<b>15000</b>	Quill 1	2.928	0.4400	5.0000	1.0	14.64	
	Quill 2	2.392	0.4405	5.0050	1.2	9.98	
	Quill 3	2.413	0.4563	5.0027	1.1	10.97	
						<i>Mean</i>	<b>11.86</b>
						<i>Standard Deviation</i>	<b>2.46</b>
						<i>Standard Error <math>\sigma/\sqrt{n}</math></i>	<b>4.3</b>
						<i>(100 × <math>\sigma</math>)/ Mean</i>	<b>21 %</b>

**Table 7.29:** ICP-OES analysis of porcupine quill references samples - copper(II) dyebaths

### 7.3.3.5 Linear regression

The linear correlation between the mass of mordant sorbed by the quill (µg per mg quill) and the mordant dyebath concentration (µg.mL<sup>-1</sup>) were calculated using the



averaged values determined by ICP-OES. The regression statistics were obtained with Origin software (table 7.30 and 7.31).

Regression Statistics	
Residual Sum of Squares	0.52504
Pearson's R	0.99775
Adjusted R Square	0.99438
Observations	6

**Table 7.30:** Regression statistics obtained with Origin software for a linear correlation between the averaged mass of copper sorbed per mg porcupine quill ( $\mu\text{g mg}^{-1}$ ) obtained by ICP-OES vs the dyebath concentration ( $\mu\text{g mL}^{-1}$ ).

Regression Statistics	
Residual Sum of Squares	155.95341
Pearson's R	0.99069
Adjusted R Square	0.97776
Observations	7

**Table 7.31:** Regression statistics obtained with Origin software for a linear correlation between the averaged mass of tin sorbed per mg porcupine quill ( $\mu\text{g mg}^{-1}$ ) obtained by ICP-OES vs the dyebath concentration ( $\mu\text{g mL}^{-1}$ ).

### 7.3.4 PIXE Experiment

#### 7.3.4.1 Keratin target

The closest representation of a porcupine quill target is expressed by converting the keratin average elemental weight composition into its atomic composition.

Keratin	wt.% or g	$M_w$ (g/mol)	mol	atom% or mol
C 0.51	0.51	12.011	0.0425	0.330
H 0.06	0.06	1.00794	0.0595	0.462
O 0.21	0.21	15.9994	0.0131	0.102
N 0.17	0.17	14.00674	0.0121	0.094
S 0.05	0.05	32.066	0.0016	0.012
Sum	1 g or 100%			1 mol or 100%

**Table 7.32:** Conversion of the keratin composition from relative weight (Wt%) into atomic composition (%).

In order to evaluate the homogeneity of the cuticle layer, a porcupine quill prepared in a dye bath of  $[\text{Sn}^{2+}]$  at  $10000 \mu\text{g mL}^{-1}$ , was prepared as a polished cross-section in a polyester resin and submitted to Scanning Electron microscopy analysis (SEM-BSC). The repartition of the elements sulphur, and tin was mapped and showed that most of the higher concentration of sulphur is found in the cuticle, where the tin is also mainly present. Several analysis of the cuticle were undertaken at  $\times 500$  magnification and show minor variation in the level of tin and chlorine (table 7.33).

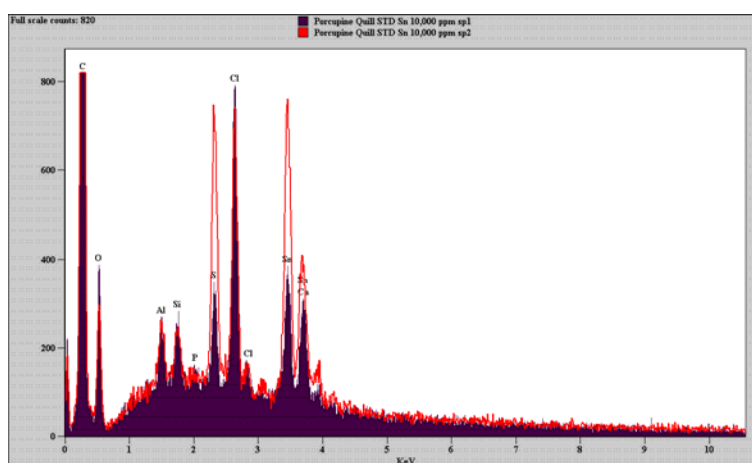


**Figure 7.3:** Energy Dispersive X-Ray analysis (EDX) showing the difference in composition of the cuticle (in red) and the inside of the porcupine quill (in black), at 20 kV,  $\times 500$  magnification.

	EDX analysis normalised to 100% Wt %		
	S -K	Cl-K	Sn-L
Sp1	14.5	14.8	70.7
Sp 2	14.5	18.3	67.2
Sp3	15.0	10.8	74.2
<i>average</i>	<i>14.7</i>	<i>14.6</i>	<i>70.7</i>
<i>standard deviation</i>	<i>0.3</i>	<i>3.8</i>	<i>3.5</i>

**Table 7.33:** EDX analysis of the cuticle of a porcupine quill dyed at  $10000 \mu\text{g.mL}^{-1}$  of tin(II), at  $\times 500$  magnification.

#### 7.3.4.2 Mass absorption coefficient $\mu$

The mass absorption coefficient  $\mu$  expressed in  $\text{cm}^2 \text{g}^{-1}$ , is calculated considering the total atomic absorption cross-section  $\sigma_a$  of the atoms constituting the material using the equation 6.1, where  $N_A$  corresponds to Avogadro number and  $A$  is the atomic weight.

$$\mu = \frac{N_A}{A} \times \sigma_A = \frac{N_A}{M_w} \sum_i x_i \sigma_{ai}$$

Equation 6.1

Keratin	wt.% or g	g/mol	mol	atom% or mol
C 0.51	0.51	12.011	0.0425	0.330
H 0.06	0.06	1.00794	0.0595	0.462
O 0.21	0.21	15.9994	0.0131	0.102
N 0.17	0.17	14.0067	0.0121	0.094
S 0.05	0.05	32.066	0.0016	0.012
Sum	1 g or 100%			1 mol or 100%

**Table 7.34:** conversion of the average weight composition of keratin (Wt %) in an atomic average composition (%).

	3.444 keV		25.271 keV		8.047 keV		Source
							X-RAY DATA BOOKLET
							Center for X-ray Optics and Advanced Light Source
							Lawrence Berkeley National Laboratory
	<b>Sn, L<sub>A</sub></b>		<b>Sn, K</b>		<b>Cu, K</b>		
C	59.56 (cm <sup>2</sup> g <sup>-1</sup> )		0.092394 (cm <sup>2</sup> g <sup>-1</sup> )		4.181 (cm <sup>2</sup> g <sup>-1</sup> )		mass absorption coefficient $\mu$ (cm <sup>2</sup> g <sup>-1</sup> )
H	0.1041 (cm <sup>2</sup> g <sup>-1</sup> )		0.00011079 (cm <sup>2</sup> g <sup>-1</sup> )		0.0057656 (cm <sup>2</sup> g <sup>-1</sup> )		mass absorption coefficient $\mu$ (cm <sup>2</sup> g <sup>-1</sup> )
O	147.4 (cm <sup>2</sup> g <sup>-1</sup> )		0.2762 (cm <sup>2</sup> g <sup>-1</sup> )		11.02 (cm <sup>2</sup> g <sup>-1</sup> )		mass absorption coefficient $\mu$ (cm <sup>2</sup> g <sup>-1</sup> )
N	94.91 (cm <sup>2</sup> g <sup>-1</sup> )		0.1646 (cm <sup>2</sup> g <sup>-1</sup> )		6.856 (cm <sup>2</sup> g <sup>-1</sup> )		mass absorption coefficient $\mu$ (cm <sup>2</sup> g <sup>-1</sup> )
S	941.7 (cm <sup>2</sup> g <sup>-1</sup> )		3.048 (cm <sup>2</sup> g <sup>-1</sup> )		89.79 (cm <sup>2</sup> g <sup>-1</sup> )		mass absorption coefficient $\mu$ (cm <sup>2</sup> g <sup>-1</sup> )
$\mu$	124.6 (cm <sup>2</sup> g <sup>-1</sup> )		0.3 (cm <sup>2</sup> g <sup>-1</sup> )		10.1 (cm <sup>2</sup> g <sup>-1</sup> )		mass absorption coefficient $\mu$ (cm <sup>2</sup> g <sup>-1</sup> )
$\rho$	<b>1.3 g cm<sup>-3</sup></b>						
$\mu$	162 l cm <sup>-1</sup>				13 l cm <sup>-1</sup>		linear absorption coefficient of keratin

**Table 7.35:** calcul of the mass absorption coefficient  $\mu$  (cm<sup>2</sup> g<sup>-1</sup>) Values obtained from [http://henke.lbl.gov/optical\\_constants/pert\\_form.html](http://henke.lbl.gov/optical_constants/pert_form.html)

### 7.3.4.3 PIXE measurements

In this study, all the measurements were undertaken at the AGLAE external micro-beam (Accelerator Grand Louvre d'Analyse Elementaire, LC2RMF-Paris). PIXE

measurements were carried out using a 3 MeV proton external set-up with two Si(Li) X-ray detectors: a Low Energy detector (LE), for the 1 - 15 keV range and a High Energy detector (HE), for the 1 - 40 keV range. These detectors recorded simultaneously the composition low-Z matrix elements and the high-Z trace elements present in the matrix and quantification was performed using the GUPIXWIN software package. The experiment was undertaken with an average current of 2 to 4 nA for an analysis time between 240 and 300 sec, corresponding to an integrated dose  $Q$  of 1  $\mu\text{C}$ . The high energy detector (HE) used a Beryllium filter (Be, 125  $\mu\text{m}$ ) and 28.5 mm air.

These measurements allowed to be calculated the exact beam charge ( $Q$ ) and the quantity ( $H$ ) values over the set of experiment, and provided an accurate quantification of the DR-N standard when summed up by GUPIXWIN to 100 percent. The values obtained for the different elements present in the DR-N standard were quantified for both low and high energy detectors and compared to their theoretical values.

Al <sub>2</sub> O <sub>3</sub>	CaO	FeO	Na <sub>2</sub> O	MgO	SiO <sub>2</sub>
0.19	0.07	0.12	0.03	0.05	0.54

**Table 7.36:** Oxide composition of the DR-N standard used for the calculation of the dose  $Q$ .

	Entry 1 to 57	Entry 60 to 89	Entry 90 to 107	Entry 108 to 118
Low Energy	Q <sub>1</sub> : 0.0065 $\mu\text{C}$ H: 1	Q <sub>2</sub> : 0.0075 $\mu\text{C}$ H: 1	Q <sub>3</sub> : 0.0105 $\mu\text{C}$ H: 1	Q <sub>2</sub> : 0.0075 $\mu\text{C}$ H: 1
High Energy (Be, 125 $\mu\text{m}$ and 28.5 mm air)	Q <sub>1</sub> : 0.0065 $\mu\text{C}$ H: 1	Q <sub>2</sub> : 0.0075 $\mu\text{C}$ H: 1	Q <sub>3</sub> : 0.0120 $\mu\text{C}$ H: 1	Q <sub>2</sub> : 0.0075 $\mu\text{C}$ H: 1

**Table 7.37:** Values of the beam dose ( $Q$ ) and the quantity ( $H$ ) for the different segments of the experiments.

Low Energy	Dose Q	Al <sub>2</sub> O <sub>3</sub> - K	SiO <sub>2</sub> - K	P <sub>2</sub> O <sub>5</sub> - K	K <sub>2</sub> O - K	CaO - K	TiO <sub>2</sub> - K	MnO - K	Fe <sub>2</sub> O <sub>3</sub> - K
15sep003	Q <sub>1</sub>	19.76	58.82	0.18	1.57	6.39	1.28	0.19	9.09
15sep004	Q <sub>1</sub>	20.50	61.52	0.23	1.62	6.62	1.09	0.21	9.43
15sep005	Q <sub>1</sub>	22.67	68.85	0.13	1.79	7.41	1.15	0.23	10.23
15sep023	Q <sub>1</sub>	19.84	54.98	0.18	1.68	6.39	0.99	0.21	9.20
15sep054	Q <sub>3</sub>	17.99	50.35	0.21	1.45	5.85	1.00	0.19	8.45
15sep119	Q <sub>3</sub>	22.07	64.40	0.28	1.96	7.67	1.32	0.26	10.85
<b>DR-N values</b>		<b>17.52</b>	<b>52.85</b>	<b>0.25</b>	<b>1.7</b>	<b>7.05</b>	<b>1.09</b>	<b>0.22</b>	<b>9.7</b>

**Table 7.38:** Quantification of the DR-N standards using low energy detector during the experiment, obtained values obtained are compared to theoretical values. Note that it was not possible to accurately quantify the elements Aluminium (Al, Z = 13) and Silicon (Si, Z = 14).

High Energy	Dose Q	K <sub>2</sub> O - K	CaO - K	TiO <sub>2</sub> - K	MnO - K	Fe <sub>2</sub> O <sub>3</sub> - K
15sep003	Q <sub>1</sub>	1.36	5.55	1.12	0.20	8.73
15sep004	Q <sub>1</sub>	1.41	5.80	0.94	0.21	9.24
15sep005	Q <sub>1</sub>	1.51	6.13	0.99	0.22	9.63
15sep023	Q <sub>1</sub>	1.45	5.60	0.94	0.20	8.87
15sep032	Q <sub>1</sub>	1.27	5.41	1.13	0.21	8.41
15sep054	Q <sub>3</sub>	1.18	4.86	0.86	0.18	7.91
15sep119	Q <sub>3</sub>	1.82	7.14	1.24	0.25	11.12
<b>DR-N values</b>		<b>1.7</b>	<b>7.05</b>	<b>1.09</b>	<b>0.22</b>	<b>9.7</b>

**Figure 7.39:** Quantification of the DR-N standards using high energy detector during the experiment, obtained values obtained are compared to theoretical values.

Entry	Sample ID	Dose /Sec.	t (sec)	Average. Current (nA)	Dose $\mu$ C
15sep001	Au / SiO <sub>2</sub>	654	327	3.058	1.00
15sep002	SiO <sub>2</sub>	554	344	2.907	1.00
15sep003	DR-N	548	365	2.740	1.00
15sep004	DR-N	506	388	2.577	1.00
15sep005	DR-N	762	304	3.289	1.00
15sep006	PQ Sn100 $\mu$ g mL <sup>-1</sup> - 1	296	684	1.466	1.00
15sep007	PQ Sn10000 $\mu$ g mL <sup>-1</sup> - 1	236	684	1.466	1.00
15sep008	PQ Sn10000 $\mu$ g mL <sup>-1</sup> - 2	282	677	1.481	1.00
15sep009	PQ Sn10000 $\mu$ g mL <sup>-1</sup> - 3	294	667	1.504	1.00
15sep010	PQ Sn10000 $\mu$ g mL <sup>-1</sup> - 4	284	663	1.513	1.00
15sep011	PQ Sn10000 $\mu$ g mL <sup>-1</sup> - 5	322	666	1.508	1.00
15sep012	PQ Sn 10000 $\mu$ g mL <sup>-1</sup> - 6	264	689	1.458	1.00
15sep013	PQ Sn 15000 $\mu$ g mL <sup>-1</sup> - 1	230	819	1.224	1.00
15sep014	PQ Sn 15000 $\mu$ g mL <sup>-1</sup> - 2	202	884	1.135	1.00
15sep015	PQ Sn 15000 $\mu$ g mL <sup>-1</sup> - 3	150	1159	0.865	1.00
15sep016	PQ Sn 15000 $\mu$ g mL <sup>-1</sup> - 4	160	1105	0.907	1.00
15sep017	PQ Sn 15000 $\mu$ g mL <sup>-1</sup> - 5	326	837	1.198	1.00
15sep018	PQ Sn 5000 $\mu$ g mL <sup>-1</sup> - 1	242	715	1.404	1.00
15sep019	PQ Sn 5000 $\mu$ g mL <sup>-1</sup> - 2	244	710	1.412	1.00

15sep020	PQ Sn 5000 $\mu\text{g mL}^{-1}$ - 3	7438	605	1.658	1.00
15sep021	PQ Sn 5000 $\mu\text{g mL}^{-1}$ - 4	5468	54	18.868	1.02
15sep022	PQ Sn 5000 $\mu\text{g mL}^{-1}$ - 4	664	318	3.175	1.01
15sep023	DR-N	720	286	3.876	1.11
15sep024	PQ Sn 5000 $\mu\text{g mL}^{-1}$ - 5	836	260	4.082	1.06
15sep025	PQ Sn 5000 $\mu\text{g mL}^{-1}$ - 6	804	248	4.219	1.05
15sep026	PQ Sn 2500 $\mu\text{g mL}^{-1}$ - 1	932	239	4.329	1.03
15sep027	PQ Sn 2500 $\mu\text{g mL}^{-1}$ - 2	782	233	4.386	1.02
15sep028	PQ Sn 2500 $\mu\text{g mL}^{-1}$ - 3	854	231	4.484	1.04
15sep029	PQ Sn 2500 $\mu\text{g mL}^{-1}$ - 4	982	226	4.608	1.04
15sep030	PQ Sn 2500 $\mu\text{g mL}^{-1}$ - 5	934	219	4.651	1.02
15sep031	PQ Sn 2500 $\mu\text{g mL}^{-1}$ - 6	960	216	4.630	1.00
15sep032	DR-N	842	211	4.739	1.00
15sep033	Au / SiO <sub>2</sub>	962	210	4.762	1.00
15sep036	PQ Sn 1000 $\mu\text{g mL}^{-1}$ - 1	962	213	4.695	1.00
15sep037	PQ Sn 1000 $\mu\text{g mL}^{-1}$ - 2	1016	210	4.762	1.00
15sep038	PQ Sn 1000 $\mu\text{g mL}^{-1}$ - 3	1010	205	4.878	1.00
15sep039	PQ Sn 1000 $\mu\text{g mL}^{-1}$ - 4	984	203	4.926	1.00
15sep040	PQ Sn 1000 $\mu\text{g mL}^{-1}$ - 5	1072	210	4.762	1.00
15sep041	PQ Sn 1000 $\mu\text{g mL}^{-1}$ - 6	1044	209	4.785	1.00
15sep042	PQ Sn 500 $\mu\text{g mL}^{-1}$ - 1	966	204	4.902	1.00
15sep043	PQ Sn 500 $\mu\text{g mL}^{-1}$ - 2	1076	197	5.076	1.00
15sep044	PQ Sn 500 $\mu\text{g mL}^{-1}$ - 3	1088	199	5.025	1.00
15sep045	PQ Sn 500 $\mu\text{g mL}^{-1}$ - 4	996	201	4.975	1.00
15sep046	PQ Sn 500 $\mu\text{g mL}^{-1}$ - 5	982	197	5.076	1.00
15sep047	PQ Sn 500 $\mu\text{g mL}^{-1}$ - 6	1012	193	5.181	1.00
15sep048	PQ Sn 100 $\mu\text{g mL}^{-1}$ - 2	1122	193	5.181	1.00
15sep049	PQ Sn 100 $\mu\text{g mL}^{-1}$ - 3	1124	197	5.076	1.00
15sep050	PQ Sn 100 $\mu\text{g mL}^{-1}$ - 4	1056	192	5.208	1.00
15sep051	PQ Sn 100 $\mu\text{g mL}^{-1}$ - 5	820	197	5.076	1.00
15sep052	PQ Sn 100 $\mu\text{g mL}^{-1}$ - 6	918	208	4.808	1.00
15sep053	PQ Sn 100 $\mu\text{g mL}^{-1}$ - 7	1020	213	4.695	1.00
15sep054	DR-N	952	200	5.000	1.00
15sep055	Au / SiO <sub>2</sub>	638	360	2.778	1.00
15sep057	Au / SiO <sub>2</sub>	758	327	3.058	1.00
15sep058	DR-N	428	511	1.957	1.00
15sep059	DR-N	430	514	1.946	1.00
15sep060	PQ Cu 15000 $\mu\text{g mL}^{-1}$ - 1	330	569	1.767	1.01
15sep061	PQ Cu 15000 $\mu\text{g mL}^{-1}$ - 2	476	382	2.646	1.01
15sep062	PQ Cu 15000 $\mu\text{g mL}^{-1}$ - 3	412	485	2.066	1.00
15sep063	PQ Cu 15000 $\mu\text{g mL}^{-1}$ - 4	466	452	2.222	1.00
15sep064	PQ Cu 15000 $\mu\text{g mL}^{-1}$ - 5	808	561	1.792	1.01
15sep065	PQ Cu 10000 $\mu\text{g mL}^{-1}$ - 1	814	261	3.876	1.01
15sep066	PQ Cu 10000 $\mu\text{g mL}^{-1}$ - 2	696	274	3.663	1.00
15sep067	PQ Cu 10000 $\mu\text{g mL}^{-1}$ - 3	710	298	3.39	1.01
15sep068	PQ Cu 10000 $\mu\text{g mL}^{-1}$ - 4	722	265	3.802	1.01
15sep069	PQ Cu 10000 $\mu\text{g mL}^{-1}$ - 5	716	262	3.846	1.01
15sep070	PQ Cu 10000 $\mu\text{g mL}^{-1}$ - 6	776	276	3.663	1.01
15sep071	PQ Cu 15000 $\mu\text{g mL}^{-1}$ - 6	454	380	2.646	1.01
15sep078	PQ Cu 2500 $\mu\text{g mL}^{-1}$ - 1	250	967	1.036	1.00
15sep079	PQ Cu 2500 $\mu\text{g mL}^{-1}$ - 2	484	822	1.22	1.00
15sep080	PQ Cu 2500 $\mu\text{g mL}^{-1}$ - 3	468	403	2.488	1.00
15sep081	PQ Cu 2500 $\mu\text{g mL}^{-1}$ - 4	468	427	2.353	1.00
15sep082	PQ Cu 2500 $\mu\text{g mL}^{-1}$ - 5	472	442	2.273	1.00
15sep083	PQ Cu 2500 $\mu\text{g mL}^{-1}$ - 6	498	405	2.488	1.01
15sep084	PQ Cu 1000 $\mu\text{g mL}^{-1}$ - 1	392	462	2.174	1.00
15sep085	PQ Cu 1000 $\mu\text{g mL}^{-1}$ - 2	490	450	2.237	1.01

15sep086	PQ Cu 1000 $\mu\text{g mL}^{-1}$ - 3	436	413	2.433	1.00
15sep087	PQ Cu 1000 $\mu\text{g mL}^{-1}$ - 4	492	391	2.577	1.01
15sep088	PQ Cu 1000 $\mu\text{g mL}^{-1}$ - 5	584	401	2.506	1.00
15sep089	PQ Cu 1000 $\mu\text{g mL}^{-1}$ - 6	344	514	1.949	1.00
15sep090	PQ Cu 500 $\mu\text{g mL}^{-1}$ - 1	1472	206	4.926	1.01
15sep091	PQ Cu 500 $\mu\text{g mL}^{-1}$ - 2	1560	143	7.092	1.01
15sep092	PQ Cu 500 $\mu\text{g mL}^{-1}$ - 3	1582	127	8	1.02
15sep093	PQ Cu 500 $\mu\text{g mL}^{-1}$ - 4	1738	124	8.264	1.02
15sep094	PQ Cu 500 $\mu\text{g mL}^{-1}$ - 5	1710	123	8.264	1.02
15sep095	PQ Cu 500 $\mu\text{g mL}^{-1}$ - 6	1498	127	8.065	1.02
15sep096	PQ Cu 100 $\mu\text{g mL}^{-1}$ - 1	1754	127	7.937	1.01
15sep097	PQ Cu 100 $\mu\text{g mL}^{-1}$ - 2	1676	124	8.197	1.02
15sep098	PQ Cu 100 $\mu\text{g mL}^{-1}$ - 3	1378	137	7.463	1.02
15sep099	PQ Cu 100 $\mu\text{g mL}^{-1}$ - 4	1670	129	7.874	1.02
15sep100	PQ Cu 100 $\mu\text{g mL}^{-1}$ - 5	1592	126	8.065	1.02
15sep101	PQ Cu 100 $\mu\text{g mL}^{-1}$ - 6	1718	124	8.197	1.02
15sep102	DR-N	1778	122	8.197	1.00
15sep103	DR-N	1626	118	8.475	1.00
15sep104	Au / SiO <sub>2</sub>	1702	117	8.547	1.00
15sep108	PQ Sn 1000 $\mu\text{g mL}^{-1}$ - 7	940	580	1.727	1.00
15sep109	A 848.15 Box 6 red orange quill - 1	378	491	2.049	1.01
15sep110	A 848.15 Box 6 red orange quill - 2	428	464	2.165	1.00
15sep111	A 848.15 Box 6 red orange quill - 3	448	474	2.123	1.01
15sep112	A 848.15 Box 6 dark red quill 2 - 1	438	484	2.079	1.01
15sep113	A 848.15 Box 6 dark red quill 2 - 2	550	433	2.32	1.00
15sep114	A 848.15 Box 6 dark red quill 2 - 3	476	429	2.336	1.00
15sep115	A 848.15 Box 17b green quill - 1	368	530	1.898	1.01
15sep116	A 848.15 Box 17b green blue - 1	252	512	1.965	1.01
15sep117	A 848.15 Box 8 orange quill - 1	346	552	1.825	1.01
15sep118	A 848.15 Box 8 orange quill - 2	408	521	1.931	1.01
15sep119	DR-N	336	494	2.024	1.00

**Figure 7.40:** Average current (nA) and irradiation time for each analysis point, integrated to an average value of 1  $\mu\text{C}$ .

Entry	Parameter File	50 Sn LA	29 Cu K	16 S K	17 Cl K	19 K K	20 Ca K	26 Fe K	30 Zn K
<b>PQ Sn 100 µg/mL</b>									
15sep 006	Pic_He_1_Mat.PAR	138	6	32130	244	4064	660	8	59
15sep 048	Pic_He_1_Mat.PAR	67	7	21139	193	3250	507	32	47
15sep 049	Pic_He_1_Mat.PAR	176	7	22837	324	3706	523	32	44
15sep 050	Pic_He_1_Mat.PAR	72	6	18974	134	3231	617	5	50
15sep 051	Pic_He_1_Mat.PAR	148	4	24492	147	3066	605	5	51
15sep 052	Pic_He_1_Mat.PAR	74	4	19125	134	3462	629	2	50
15sep 053	Pic_He_1_Mat.PAR	91	6	22083	165	3732	785	3	42
	<i>Average</i>	109	6	22969	192	3502	618	12	49
	<i>Standard deviation</i>	44	1	4493	70	351	92	14	6
<b>PQ Sn 500 µg/mL</b>									
15sep 042	Pic_He_1_Mat.PAR	289	6	18224	1267	859	6322	4	40
15sep 043	Pic_He_1_Mat.PAR	426	5	18640	1417	1311	4476	3	43
15sep 044	Pic_He_1_Mat.PAR	265	7	17567	1240	1165	4944	3	53
15sep 045	Pic_He_1_Mat.PAR	484	7	21328	1410	382	5610	6	41
15sep 046	Pic_He_1_Mat.PAR	363	5	20599	1512	330	6826	5	48
15sep 047	Pic_He_1_Mat.PAR	412	7	21813	1461	1021	5038	5	44
	<i>Average</i>	373	6	19695	1385	845	5536	4	45
	<i>Standard deviation</i>	84	1	1776	108	408	895	1	5
<b>PQ Sn 1000 µg/mL</b>									
15sep 036	Pic_He_1_Mat.PAR	799	8	22094	4323	3291	1062	6	38
15sep 037	Pic_He_1_Mat.PAR	690	8	20654	3991	2370	561	2	36
15sep 038	Pic_He_1_Mat.PAR	712	8	21516	4277	2414	760	3	36
15sep 039	Pic_He_1_Mat.PAR	723	8	27222	3848	1118	757	3	34
15sep 040	Pic_He_1_Mat.PAR	580	10	22868	3654	1399	938	2	32
15sep 041	Pic_He_1_Mat.PAR	778	6	22862	3957	2405	927	3	33
15sep 108	Pic_He_Z3_Mat.PAR	811	13	34227	4789	1972	1820	6	54
	<i>Average</i>	728	9	24492	4120	2138	975	4	38
	<i>Standard deviation</i>	80	2	4776	376	724	406	2	8
<b>PQ Sn 2500 µg/mL</b>									
15sep 026	Pic_He_1_Mat.PAR	26507	80	10851	6447	409	355	1	14
15sep 027	Pic_He_1_Mat.PAR	30464	64	16218	10503	293	74	5	7
15sep 028	Pic_He_1_Mat.PAR	28974	104	13522	9925	1095	267	16	31
15sep 029	Pic_He_1_Mat.PAR	6694	66	16789	10696	450	315	3	15
15sep 030	Pic_He_1_Mat.PAR	9230	87	14903	15115	771	1776	4	29
15sep 031	Pic_He_1_Mat.PAR	7674	124	7910	8072	642	1233	1	25
	<i>Average</i>	18257	88	13366	10126	610	670	5	20
	<i>Standard deviation</i>	11481	23	3416	2938	293	676	6	10



<b>PQ Sn 5000 µg/mL</b>									
15sep 018	Pic_He_1_Mat.PAR	52695	142	11541	9292	54	356	2	7
15sep 019	Pic_He_1_Mat.PAR	63171	156	14682	13121	56	405	2	10
15sep 022	Pic_He_1_Mat.PAR	43755	140	15332	17997	265	439	9	7
15sep 024	Pic_He_1_Mat.PAR	46417	112	19919	19470	140	110	1	5
15sep 025	Pic_He_1_Mat.PAR	39601	108	13294	15151	247	227	4	2
	<i>Average</i>	<b>49128</b>	<b>126</b>	<b>13158</b>	<b>14054</b>	<b>212</b>	<b>453</b>	<b>3</b>	<b>6</b>
	<i>Standard deviation</i>	<b>9178</b>	<b>21</b>	<b>3133</b>	<b>4034</b>	<b>101</b>	<b>137</b>	<b>3</b>	<b>3</b>
<b>PQ Sn 10000 µg/mL</b>									
15sep 007	Pic_He_1_Mat.PAR	127278	144	19551	35180	176	169	2	7
15sep 008	Pic_He_1_Mat.PAR	122088	148	18744	32986	221	30	5	9
15sep 009	Pic_He_1_Mat.PAR	13097	63	1943	3144	20	119	0	3
15sep 010	Pic_He_1_Mat.PAR	91328	90	17896	26197	68	0	0	0
15sep 011	Pic_He_1_Mat.PAR	132638	203	21703	29894	115	148	5	7
15sep 012	Pic_He_1_Mat.PAR	125800	217	20681	25903	47	50	2	4
	<i>Average</i>	<b>102038</b>	<b>144</b>	<b>16753</b>	<b>25551</b>	<b>108</b>	<b>86</b>	<b>2</b>	<b>5</b>
	<i>Standard deviation</i>	<b>45968</b>	<b>61</b>	<b>7381</b>	<b>11571</b>	<b>78</b>	<b>69</b>	<b>2</b>	<b>3</b>
<b>PQ Sn 15000 µg/mL</b>									
15sep 013	Pic_He_1_Mat.PAR	174579	206	23015	54951	266	270	6	19
15sep 014	Pic_He_1_Mat.PAR	198743	217	27354	65992	234	42	8	43
15sep 015	Pic_He_1_Mat.PAR	102387	148	13765	29545	175	660	5	7
15sep 016	Pic_He_1_Mat.PAR	123328	133	16510	34924	151	491	3	5
15sep 017	Pic_He_1_Mat.PAR	92096	103	12044	24747	128	472	0	3
	<i>Average</i>	<b>138227</b>	<b>161</b>	<b>18538</b>	<b>42032</b>	<b>191</b>	<b>387</b>	<b>4</b>	<b>15</b>
	<i>Standard deviation</i>	<b>46417</b>	<b>49</b>	<b>6458</b>	<b>17651</b>	<b>58</b>	<b>237</b>	<b>3</b>	<b>17</b>

**Table 7.41:** High Energy detector PIXE elemental composition in ppm ( $\mu\text{g g}^{-1}$ ) of the porcupine quills references – tin(II) dye bath. The values appearing in red are close to the Limit of Detection (LOD).

Entry	Parameter File	50 Sn La	29 Cu K	16 S K	17 Cl K	19 K K	20 Ca K	26 Fe K	30 Zn K
<b>PQ Cu 100 µg/mL</b>									
15sep 96	Pic_He_Cu_Mat.PAR	0	48	23281	90	1304	669	3	49
15sep 97	Pic_He_Cu_Mat.PAR	27	48	26709	69	1180	644	7	52
15sep 98	Pic_He_Cu_Mat.PAR	103	82	21915	86	2462	954	9	42
15sep 99	Pic_He_Cu_Mat.PAR	28	64	21146	86	2721	976	6	43
15sep 100	Pic_He_Cu_Mat.PAR	56	86	17935	109	2156	772	10	51
15sep 101	Pic_He_Cu_Mat.PAR	32	90	22547	94	2078	761	6	52
	<i>Average</i>	<b>41</b>	<b>70</b>	<b>22256</b>	<b>89</b>	<b>1984</b>	<b>796</b>	<b>7</b>	<b>48</b>
	<i>Standard deviation</i>	<b>35</b>	<b>19</b>	<b>2863</b>	<b>13</b>	<b>619</b>	<b>140</b>	<b>2</b>	<b>5</b>
<b>PQ Cu 500 µg/mL</b>									
15sep 90	Pic_He_Cu_Mat.PAR	19	319	26200	215	1162	830	5	43
15sep 91	Pic_He_Cu_Mat.PAR	27	329	24461	248	1544	947	4	36
15sep 92	Pic_He_Cu_Mat.PAR	0	396	22831	149	1056	950	5	46
15sep 93	Pic_He_Cu_Mat.PAR	60	383	21940	185	1167	900	4	46
15sep 94	Pic_He_Cu_Mat.PAR	66	381	20833	177	2406	967	6	47
15sep 95	Pic_He_Cu_Mat.PAR	54	395	22598	267	2712	1038	5	40
	<i>Average</i>	<b>38</b>	<b>367</b>	<b>23144</b>	<b>207</b>	<b>1675</b>	<b>939</b>	<b>5</b>	<b>43</b>
	<i>Standard deviation</i>	<b>26</b>	<b>34</b>	<b>1911</b>	<b>45</b>	<b>712</b>	<b>70</b>	<b>1</b>	<b>4</b>
<b>PQ Cu 1000 µg/mL</b>									
15sep 84	Pic_He_Cu_Mat.PAR	3	1168	43990	421	195	983	12	46
15sep 85	Pic_He_Cu_Mat.PAR	31	1290	47385	431	210	901	10	42
15sep 86	Pic_He_Cu_Mat.PAR	17	1367	62411	667	370	895	18	27
15sep 87	Pic_He_Cu_Mat.PAR	25	1170	51336	512	279	987	12	36
15sep 88	Pic_He_Cu_Mat.PAR	99	860	36630	112	1107	1477	8	34
15sep 89	Pic_He_Cu_Mat.PAR	59	814	41917	109	383	1103	8	37
	<i>Average</i>	<b>39</b>	<b>1112</b>	<b>47278</b>	<b>375</b>	<b>424</b>	<b>1058</b>	<b>11</b>	<b>37</b>
	<i>Standard deviation</i>	<b>35</b>	<b>226</b>	<b>8927</b>	<b>223</b>	<b>344</b>	<b>219</b>	<b>4</b>	<b>7</b>
<b>PQ Cu 2500 µg/mL</b>									
15sep 78	Pic_He_Z3_Mat.PAR	2	2964	49121	562	1121	1835	13	84
15sep 79	Pic_He_Z3_Mat.PAR	51	2590	58129	554	712	1464	8	64
15sep 80	Pic_He_Z3_Mat.PAR	77	4355	41000	465	830	1951	6	61
15sep 81	Pic_He_Z3_Mat.PAR	92	4372	39723	497	710	1636	9	45
15sep 82	Pic_He_Z3_Mat.PAR	10	4131	39038	536	863	1383	4	45
15sep 83	Pic_He_Z3_Mat.PAR	77	5004	38772	564	1206	1821	5	67
	<i>Average</i>	<b>52</b>	<b>3903</b>	<b>44297</b>	<b>530</b>	<b>907</b>	<b>1682</b>	<b>8</b>	<b>61</b>
	<i>Standard deviation</i>	<b>38</b>	<b>927</b>	<b>7805</b>	<b>40</b>	<b>210</b>	<b>225</b>	<b>3</b>	<b>15</b>
<b>PQ Cu 10000 µg/mL</b>									
15sep 65	Pic_He_Z3_Mat.PAR	75	19355	47175	688	1019	1461	14	57
15sep 66	Pic_He_Z3_Mat.PAR	42	15353	51375	690	994	1430	10	45
15sep 67	Pic_He_Z3_Mat.PAR	81	11982	50511	566	371	1069	13	43
15sep 68	Pic_He_Z3_Mat.PAR	5	10080	52576	624	319	1016	10	38
15sep 69	Pic_He_Z3_Mat.PAR	12	10046	47697	497	113	809	8	24
15sep 70	Pic_He_Z3_Mat.PAR	17	10501	48438	495	132	814	9	24
	<i>Average</i>	<b>39</b>	<b>12886</b>	<b>49629</b>	<b>593</b>	<b>491</b>	<b>1100</b>	<b>11</b>	<b>39</b>
	<i>Standard deviation</i>	<b>33</b>	<b>3752</b>	<b>2176</b>	<b>88</b>	<b>412</b>	<b>288</b>	<b>2</b>	<b>13</b>
<b>PQ Cu 15000 µg/mL</b>									
15sep 71	Pic_He_Z3_Mat.PAR	44	22680	44177	1101	405	748	16	17
15sep 60	Pic_He_Z3_Mat.PAR	5	23060	51943	1274	472	886	13	52
15sep 61	Pic_He_Z3_Mat.PAR	45	22467	57188	1300	414	809	12	53

15sep 62	Pic_He_Z3_Mat.PAR	36	19923	51450	1338	200	769	9	15
15sep 63	Pic_He_Z3_Mat.PAR	38	20162	47420	1223	147	779	11	31
15sep 64	Pic_He_Z3_Mat.PAR	47	27654	48370	1168	300	847	16	33
	<i>Average</i>	<b>36</b>	<b>22658</b>	<b>50091</b>	<b>1234</b>	<b>323</b>	<b>806</b>	<b>13</b>	<b>34</b>
	<i>Standard deviation</i>	<b>16</b>	<b>2788</b>	<b>4488</b>	<b>88</b>	<b>129</b>	<b>52</b>	<b>3</b>	<b>16</b>

**Table 7.42:** High Energy detector PIXE elemental composition in ppm ( $\mu\text{g g}^{-1}$ ) of the porcupine quills references – copper(II) dyebath. The values appearing in red are close to the Limit of Detection (LOD).

The linear correlation between the mass of mordant sorbed by the quill ( $\mu\text{g}$  per mg quill) and the mordant dyebath concentration ( $\mu\text{g.mL}^{-1}$ ) were calculated using the averaged values determined by ICP-EOS. The regression statistics were obtained with Origin software (table 7.43 and 7.44).

Regression Statistics	
Residual Sum of Squares	0.0342
Pearson's R	0.9959
Adjusted R Square	0.98977
Observations	6

**Table 7.43:** Regression statistics obtained with Origin software for a linear correlation between the average Wt % of copper obtained for 6 PIXE analysis vs the dyebath concentration ( $\mu\text{g.mL}^{-1}$ ).

Regression Statistics	
Residual Sum of Squares	10.41208
Pearson's R	0.97789
Adjusted R Square	0.94753
Observations	7

**Table 7.44:** Regression statistics obtained with Origin software for a linear correlation between the average Wt % of tin obtained by 6 PIXE analysis vs the dyebath concentration ( $\mu\text{g.mL}^{-1}$ ).

### 7.3.5 Rutherford Backscattering Spectrometry (RBS)

#### 7.3.5.1 Calibration of detector

The RBS measurements were recorded simultaneously to the PIXE experiments and the calibration of the spectra was obtained through the analysis of a standard of  $\text{SiO}_2$  coated with a thin layer of known thickness of gold (figure 7.4). And RBS spectra were simulated using the SIMNRA software by virtually overlapping the contribution of the different atoms present in the cuticle layer. As well as Rutherford cross-

sections, non-Rutherford cross-sections specific to the set-up used in AGLAE accelerator at  $150^\circ$  were used for the quantification of carbon, oxygen and nitrogen.

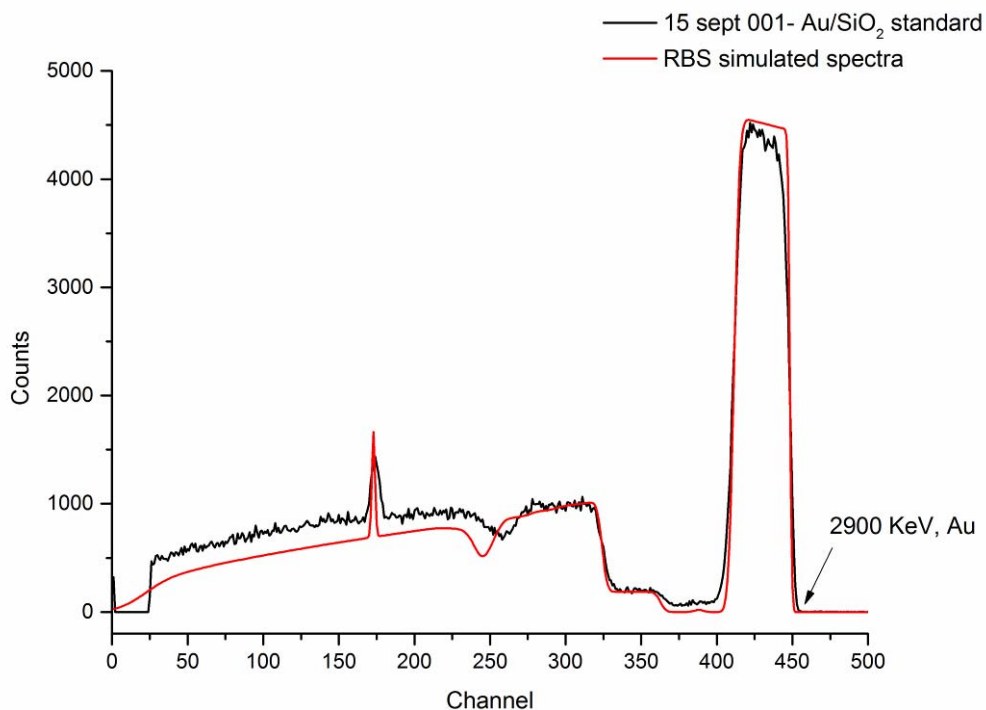


**Figure 7.4:** calibration of the RBS detector using a standard of  $\text{SiO}_2$  coated with gold.

Entry	Particles *sr	Layers			
		Layer 1 (1000.000)	Layer 2 (8900)	Layer 3 (80)	Layer 4 (10000000.000)
$\text{SiO}_2/\text{Au}$ standard	1.743E+10	He: 1	Au: 1	Cr: 1	Si: 0.333000 O: 0.667000

**Table 7.45:** Composition of the layers found in the  $\text{SiO}_2/\text{Au}$  standard used for the calibration of the RBS spectra

Reactions

Total number of elements in the target: 7

Prev Element Next Element

Scattering and reactions with H

RBS 2H (1H .1H )2H Rutherford cross section  
File: Internal  
from Emin (keV) 0.001 to Emax (keV) 2000.000

RBS 3H (1H .1H )3H Rutherford cross section  
File: Internal  
from Emin (keV) 0.001 to Emax (keV) 1000000.00

D(p,p)D Theta: 165.00  
File: HD165\_Langley.r33 Source: R.A. Langley (1976)  
from Emin (keV) 2002.900 to Emax (keV) 2799.400

Protons on H2; 1800 - 3000 keV; CM angle = 165; LAB angle = 151;  
File: PH\_LA76A.RTR Source: Langley, 197?  
from Emin (keV) 2005.000 to Emax (keV) 2785.000

Rutherford No Rutherford

OK Cancel Help

Reactions

Total number of elements in the target: 7

Prev Element Next Element

Scattering and reactions with He

RBS 3He(1H .1H )3He Rutherford cross section  
File: Internal  
from Emin (keV) 0.001 to Emax (keV) 1500.000

RBS 4He(1H .1H )4He Rutherford cross section  
File: Internal  
from Emin (keV) 0.001 to Emax (keV) 1600.000

Protons on He3; 2000 - 3000 keV; CM angle = 166; LAB angle = 159.2;  
File: PHELA76A.RTR Source: Langley, 197?  
from Emin (keV) 1520.000 to Emax (keV) 2863.000

Protons on He4; 1500 - 3700 keV; CM angle = 163; LAB angle = 161.4;  
File: PHELA76B.RTR Source: Langley, 197?  
from Emin (keV) 1690.000 to Emax (keV) 3494.000

Rutherford No Rutherford

OK Cancel Help

Reactions

Total number of elements in the target: 7

Prev Element Next Element

Scattering and reactions with C

RBS 11C (1H .1H )11C Rutherford cross section  
File: Internal  
from Emin (keV) 0.001 to Emax (keV) 1000000.00

RBS 12C (1H .1H )12C Rutherford cross section  
File: Internal  
from Emin (keV) 0.001 to Emax (keV) 990.000

RBS 13C (1H .1H )13C Rutherford cross section  
File: Internal  
from Emin (keV) 0.001 to Emax (keV) 1000000.00

RBS 14C (1H .1H )14C Rutherford cross section  
File: Internal  
from Emin (keV) 0.001 to Emax (keV) 1000000.00

Rutherford No Rutherford

OK Cancel Help

Reactions

Total number of elements in the target: 7

Prev Element Next Element

Scattering and reactions with C

12C(p,p)12C Theta: 170.00 Natural isotopic ratio  
File: 12cpcp\_2.r33 Source: R. Amirkas et al., Nucl. Instr. Meth. B77 (1993) 110  
from Emin (keV) 1000.000 to Emax (keV) 3500.000

12C(p,p)12C Theta: 150.0  
File: CP150.R33  
from Emin (keV) 1000.000 to Emax (keV) 3010.000

C(p,p)C Theta: 150.00  
File: H12C150\_Gurbich.r33 Source: A.F. Gurbich, Nucl. Instr. Meth. B136-138 (1998) 1  
from Emin (keV) 360.000 to Emax (keV) 3500.000

13C(p,p)13C Theta: 163.8  
File: H13C165\_Kashy.r33 Source: E. Kashy et al., Phys. Rev. 122(3) (1961) 884  
from Emin (keV) 2603.400 to Emax (keV) 4993.140

Rutherford No Rutherford

OK Cancel Help

Reactions

Total number of elements in the target: 7

Prev Element Next Element

Scattering and reactions with N

RBS 14N (1H .1H )14N Rutherford cross section  
File: Internal  
from Emin (keV) 0.001 to Emax (keV) 1850.000

RBS 15N (1H .1H )15N Rutherford cross section  
File: Internal  
from Emin (keV) 0.001 to Emax (keV) 1000000.00

15N(p,p)12C Theta: 140.00  
File: 15Np.p.R33 Source: F.B. Hagedorn and J.B. Marion, Phys. Rev., 108(1957), 101  
from Emin (keV) 912.000 to Emax (keV) 2857.000

N(p,p)N Theta: 140.00  
File: HN140\_Ramos.r33 Source: A.R. Ramos et al., Nucl. Instr. Meth. B190 (2002) 95  
from Emin (keV) 1498.000 to Emax (keV) 2500.000

Rutherford No Rutherford

OK Cancel Help

Reactions

Total number of elements in the target: 7

Prev Element Next Element

Scattering and reactions with N

Protons on N14; 650 - 1800 keV; CM angle = 154; LAB angle = 152;  
File: PN\_HA57E.RTR Source: Hagedorn et al., 1957  
from Emin (keV) 631.000 to Emax (keV) 1823.000

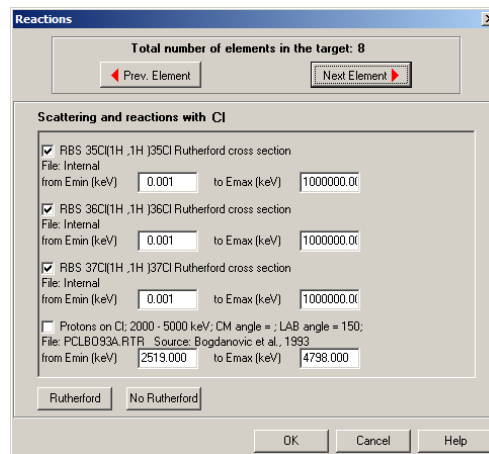
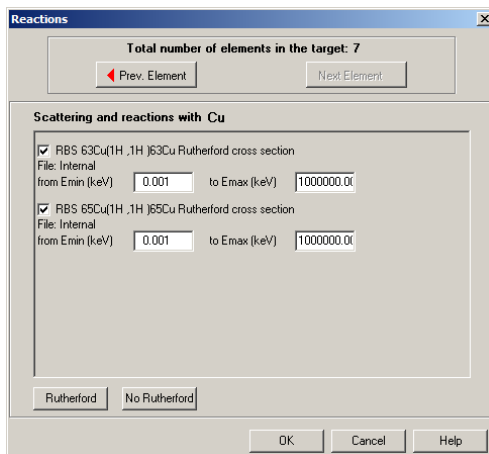
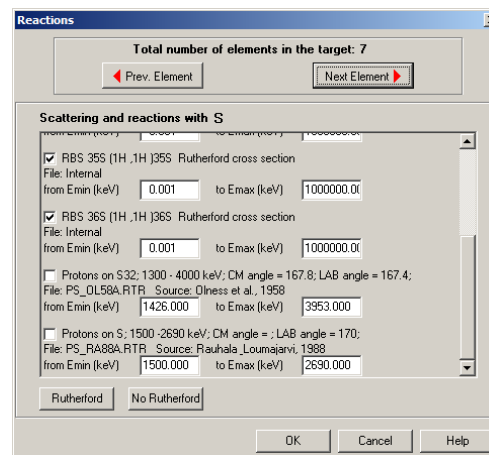
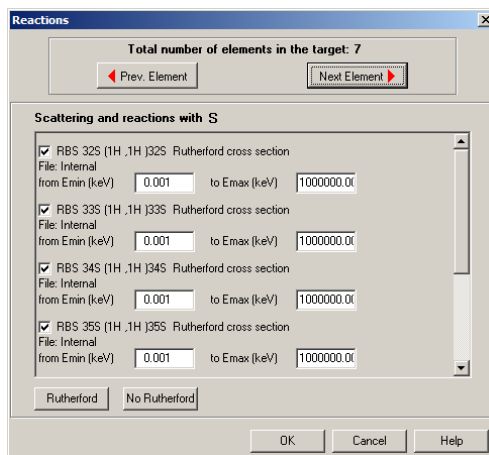
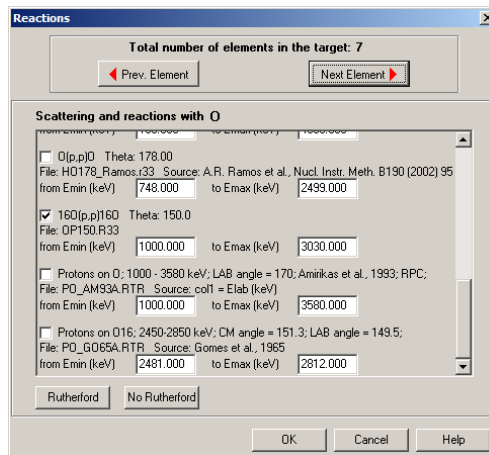
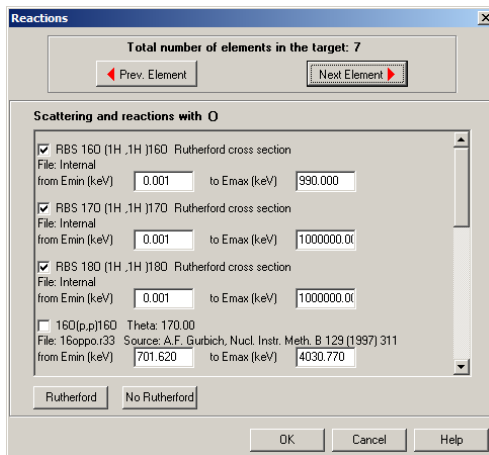
Protons on N14; 1850-3000 keV; CM angle = 156.9; LAB angle = 155.2;  
File: PN\_LA67A.RTR Source: Lambert\_Durand 1967  
from Emin (keV) 1855.000 to Emax (keV) 2999.000

Protons on N14; 1850-3000 keV; CM angle = 166.1; LAB angle = 165;  
File: PN\_LA67B.RTR Source: Lambert\_Durand 1967  
from Emin (keV) 1855.000 to Emax (keV) 2999.000

Protons on N14; 3600-4100 keV; CM angle = 168.1; LAB angle = 167.2;  
File: PN\_OL58A.RTR Source: D'Iness et al., 1958  
from Emin (keV) 3611.000 to Emax (keV) 4082.000

Rutherford No Rutherford

OK Cancel Help



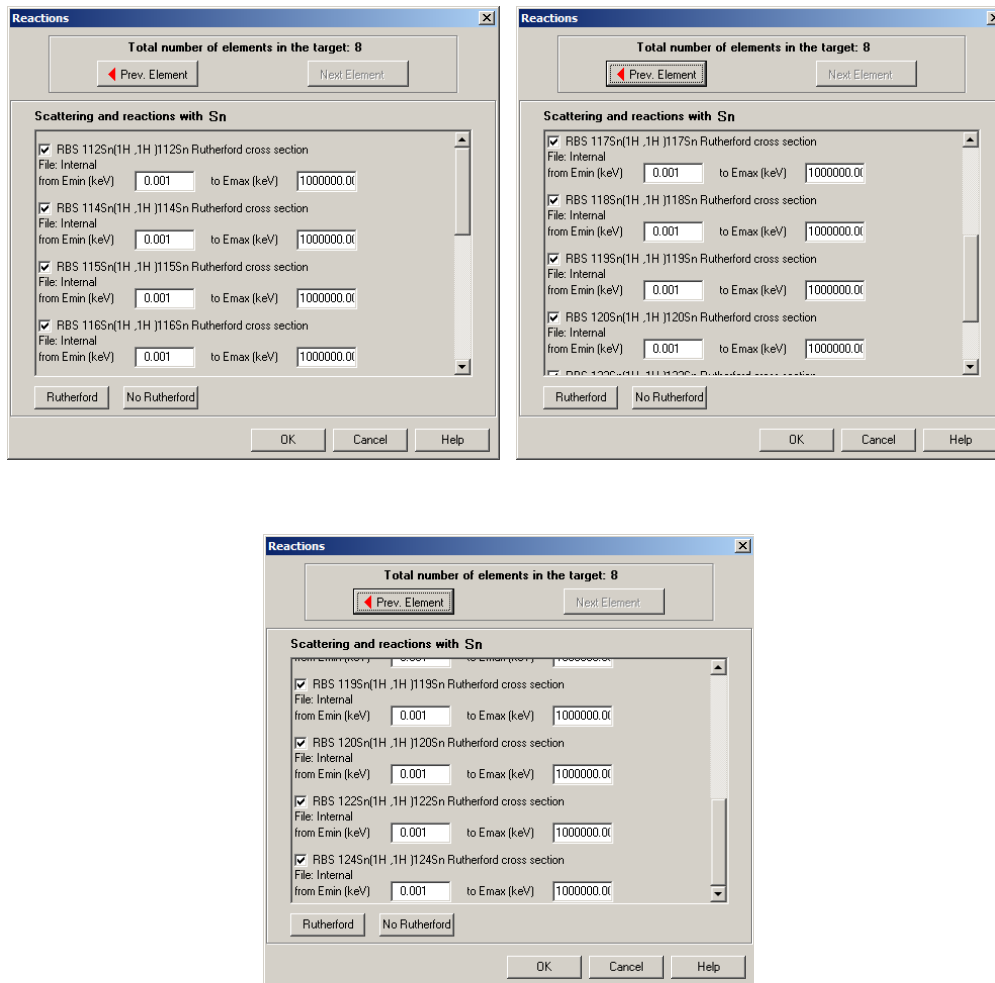


**Figure 7.5:** Rutherford cross-sections, non-Rutherford cross-sections specific to the set-up used in AGLAE accelerator at 150 ° used in the SIMNRA simulation software.

## 7.3.5.2 SIMNRA simulation of RBS spectra

<i>Entry</i>	<i>Particles *sr</i>	<i>Layer 1 (1000)</i>	<i>Layer 2 (10000000)</i>	<i>RBS Wt%</i>		<i>PIXE Wt%</i>	
				<i>S</i>	<i>Cu</i>	<i>S</i>	<i>Cu</i>
15sep062	3.01E+10	He : 1	C : 0.33 H : 0.4695 O : 0.1000 S : 0.008 N : 0.090 Cu : 0.0025	3.32	2.06	3.67	1.42
15sep067	3.37E+10	He : 1	C : 0.33 H : 0.4697 O : 0.1000 S : 0.009 N : 0.090 Cu : 0.0013	3.76	1.08	3.61	0.86
15sep080	3.06E+10	He : 1	C : 0.33 H : 0.4725 O : 0.1000 S : 0.007 N : 0.090 Cu : 0.0005	2.97	0.42	2.93	0.31
15sep087	3.41E+10	He : 1	C : 0.33 H : 0.4712 O : 0.1000 S : 0.0085 N : 0.090 Cu : 0.0003	3.59	0.25	3.67	0.08
15sep092	2.81E+10	He : 1	C : 0.33 H : 0.4722 O : 0.1000 S : 0.0075 N : 0.090 Cu : 0.0003	3.18	0.25	2.28	0.04

**Table 7.46:** Composition of the virtual layers simulated by SIMNRA software by virtually overlapping the contribution of the different atoms present in the cuticle layer, obtained for the porcupine quill reference containing tin.



Entry	Particles *sr	Layer 1 (1000)	Layer 2 (100000000)	RBS (Wt %)			PIXE corrected (Wt %)		
				S	Sn	Cl	S, K	Sn, La,	Cl, K
15 sept 015	2.22E+10	He : 1	C : 0.33 H : 0.452 O : 0.1000 S : 0.0800 N : 0.090 Sn : 0.012 Cl : 0.0800	2.77	15.42	3.06	2.00	14.96	4.45
15 sept 010	2.44E+10	He : 1	C : 0.33 H : 0.462 O : 0.1000 S : 0.005 N : 0.090 Sn : 0.009 Cl : 0.004	1.85	12.35	1.64	2.00	10.21	2.93
15 sept 025	1.76E+10	He : 1	C : 0.33 H : 0.4655 O : 0.1000 S : 0.008 N : 0.090 Sn : 0.0055 Cl : 0.001	3.11	7.93	0.43	2.00	5.96	2.28
15 sept 030	1.62E+10	He : 1	C : 0.33 H : 0.4722 O : 0.1000 S : 0.006 N : 0.090 Sn : 0.0015 Cl : 0.0003	2.50	2.32	0.14	2.00	1.94	2.04

**Table 7.47:** Composition of the virtual layers simulated by SIMNRA software by virtually overlapping the contribution of the different atoms present in the cuticle layer, obtained for the porcupine quill reference containing copper.

## 7.4 INVESTIGATION OF NORTH AMERICAN ATHAPASCAN PORCUPINE QUILL WORK FROM NATIONAL MUSEUMS SCOTLAND

### 7.4.1 Porcupine quills

Raw porcupine quills from *Erethizon* species were purchased from Sarah Tronti, a Native American artist still working today with porcupine quills.

<http://sevenwindsleather.com>, accessed 07/02/2013

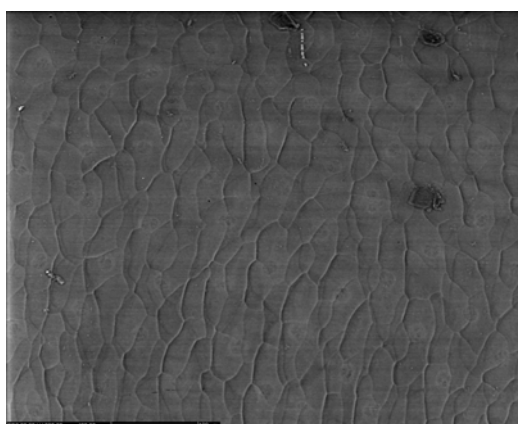
### 7.4.2 Scouring process

Several methods were tested in order to evaluate cleaning processes prior dyeing the porcupine quills. These treatments involved cleaning the quills in deionised water with several cleaning agents including soap (linseed oil, KOH), calcium oxide (CaO) and potassium bicarbonate (KHCO<sub>3</sub>). Each cleaning bath was undertaken at 85 °C for 1 hour. The surface of the quills was then observed under Scanning Electron Microscopy (SEM-BSC) to evaluate the different treatments by means of cleaning of the surface, lifting of the scales, as well as recording any damage of the surface resulting from the cleaning treatment. The most effective surface preparation was achieved by a combination of cleaning baths using calcium oxide and potassium bicarbonate (table 7.48).

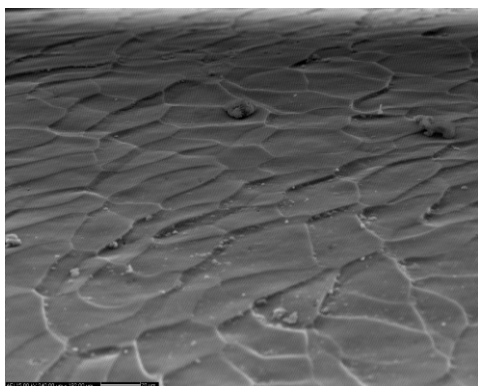
Cleaning Process	Fibre (g)	Cleaning agent	Volume (mL)	pH	SEM Observation	Efficiency	Colour
1	0.24	H <sub>2</sub> O	800	7.0	Scales closed, surface un-cleaned	--	Yellowish
2	0.26	2 mL Soap (KOH)	800	7.5	Some missing scales, but surface cleaned	-	Yellowish
3	0.24	0.15 g KHCO <sub>3</sub>	800	7.5	Scales slightly lifted, surface cleaned	+	Yellowish
4	0.26	0.05 g CaO	800	9.0	Scales lifted, surface cleaned, but some missing scales and quills turned yellow	+++ / - for the colour	Yellow
5	0.28	0.01 g CaO	800	8.5	Scales slightly lifted, surface cleaned	+	Yellowish
6	0.25	0.01 g CaO	800	8.5	Scales lifted, surface cleaned	++	White
		0.15 g KHCO <sub>3</sub>	800	7.5			
7a	3	2 mL soap (KOH)	800	7.5	Scales lifted, surface cleaned	+++	White
		0.05 g CaO	800	9.0			
		0.75 g KHCO <sub>3</sub>	800	7.5			
		H <sub>2</sub> O	800	7.0			

<b>7b*</b>	2.5	0.1 g CaO + 0.2 g KHCO <sub>3</sub>	800	8.0	Scales lifted, surface cleaned	+++	White
<b>8</b>	11	0.5 mL soap (KOH)	1000	7.5	Scales lifted, surface cleaned	+++	White
		0.125 g CaO	1000	9.0			
		1g KHCO <sub>3</sub>	1000	7.5			
		0.125 g CaO + 1g KHCO <sub>3</sub>	1000	9.0			
		H <sub>2</sub> O	1000	7.0			

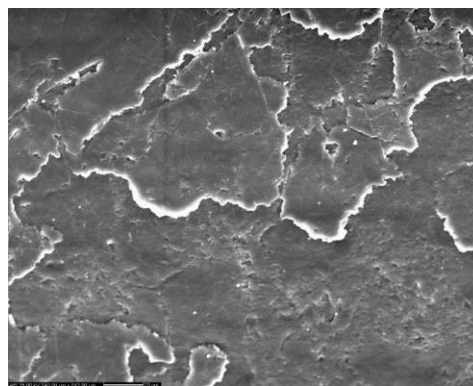
**Table 7.48:** description of the cleaning treatments tested for scouring porcupine quills (\*: 7b were prepared using some cleaned quills from process 7a).



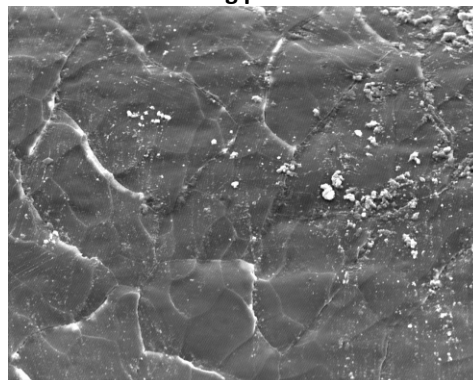
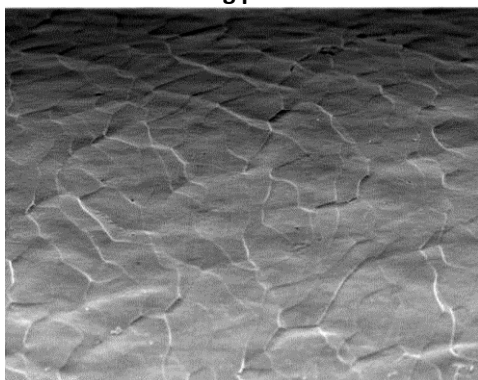
**Un-scoured quill (scale bar is 100 μm)**

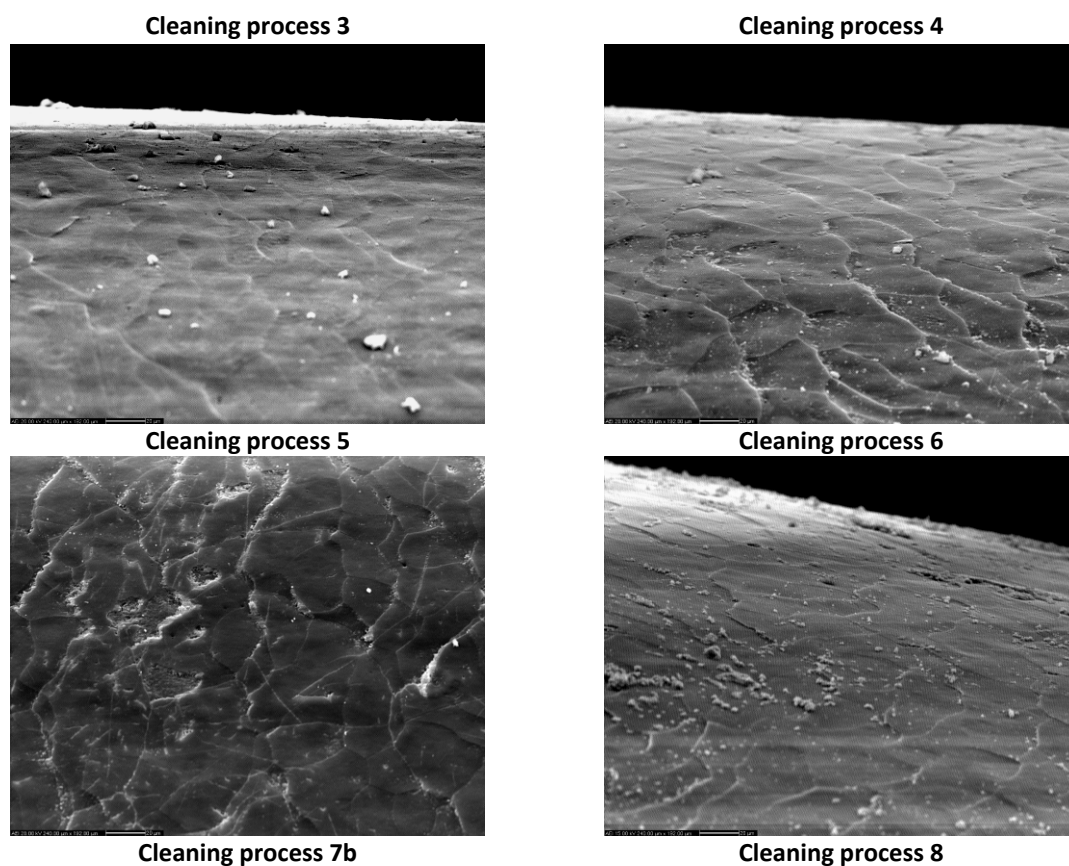


**Cleaning process 1**



**Cleaning process 2**





**Figures 7.6:** Scanning Electron Micrograph of the surface of the porcupine quills, recorded in controlled pressure Envac mode, using AEI detector at 15 kV voltage; Images were recorded at  $\times 500$  magnification with a working distance of 20 mm. For all images, scale is 20  $\mu\text{m}$ .

#### 7.4.3 Dyeing experiments with natural dyestuffs

Cochineal dye (*Dactylopius coccus* C.) was purchased from DBH Ltd Poole England, while turmeric (*Curcuma longa* L.) and madder (*Rubia tinctorum* L.) and a range of mordants, including copper(II) sulphate, tin(II) chloride, potassium dichromate(VI), alum, cream of tartar were purchased through George Veil Fibercrafts website. Several dyeing processes were tested by adjusting the concentration of dyestuffs and the temperature of the dyebath. Examples of the dyeing experiments are presented below.

The dyeing of porcupine quills was found to be a particularly complex process with several failed attempts to achieve proper dyeing of the quills. The best results were provided with quills that had been previously properly cleaned and with an excess of dyestuff in the dyebath typically 3:1 w/w of dry fibre and at a temperature of 85 to 90

°C. Below 85 °C little dyeing would occur even after several hours, while above 90 °C the quills would start to shrink and their cuticle to collapse. It was found difficult to obtain a good coloration when working with low dyestuff concentrations, and only pale hues were obtained. Finally, it was found to be crucial to soften the surface of the quills at 85 °C in deionised water prior transferring them in the dyebath.

PQ1 (yellow): the porcupine quills (0.34 g) were dyed in 100 mL deionised water containing turmeric (2:1 w/w, 0.72 g) and alum (1:1 w/w, 0.34 g). The dyebath was heated for two hour at 60 °C and the quills were then left in a ultra sound bath for two hours. The dyebath produced porcupine quills exhibiting a pale yellow colour.

PQ2 (orange): the porcupine quills (0.2 g) were dyed in 100 mL of madder solution (1g of madder extracted over night in 150 mL deionised water) and alum mordant (1:1 w/w, 0.2 g). The dyebath was heated for one hour at 85 °C. The The dyebath produced porcupine quills exhibiting a pale orange colour.

PQ4a (orange): the porcupine quills (0.3 g) were dyed in 100 mL of madder solution (2g of madder extracted over night in 100 mL deionised water) and alum mordant (0.25:1 w/w, 0.07 g). The dyebath was heated for one hour at 85 °C. The dyebath produced porcupine quills exhibiting a strong orange colour.

PQ4b (orange): the porcupine quills (0.3 g) were dyed in 100 mL of madder solution (2g of madder extracted over night in 100 mL deionised water) and alum mordant (0.25:1 w/w, 0.07 g). The dyebath was heated for one hour at 85 °C. After 1 hour, potassium dichromate (0.05:1 w/w, 0.015g) and cream of tartar (0.05:1 w/w dry fibre or 0.015g) were added and the solution was been left at 85 °C for another hour. The dyebath produced porcupine quills exhibiting a deep brown colour.

PQ5a (orange): the porcupine quills (0.38 g) were dyed in 100 mL of tumeric (1:1 w/w dry fibre or 0.38 g) with alum mordant (0.25:1 w/w of dry fibre, or 0.09 g) at 60 °C for one hour. After this, 50 mL of a solution containing American cochineal (0.5:1 w/w dry fibre, or 0.19 g in 50 mL, heated for one hour at 50 °C, then filtered) and tin(II) chloride (0.06:1 w/w, 0.02 g) was added. The dyebayh was heated at 60 °C for another hour. The dyebath produced porcupine quills exhibiting a not very intense but bright orange colour.

PQ5b (orange): a few porcupine quills prepared with the recipes 5a (0.2 g) were over-dyed in 50 mL solution containing American cochineal (3:1 w/w, 0.6 g) at 60 °C for one hour. The dyebath produced porcupine quills exhibiting a more intense orange colour.

PQ6 (yellow): the porcupine quills (0.44 g) were dyed in 100 mL of tumeric (2:1 w/w, 1 g) with alum mordant (0.5:1 w/w, 0.22 g) at 65 - 70 °C for three hours. The dyebath produced some yellow quills, exhibiting a bright yellow colour.

PQ7 (pink): the porcupine quills (0.38 g) were dyed in 100 mL of American cochineal (2:1 w/w, 0.72 g) with alum mordant (0.25:1 w/w, 0.09 g) and cream of tartar (0.06:1 w/w, 0.02 g). The dyebath was heated to 70 °C and tin(II) chloride was added (0.06:1 w/w, 0.02 g), the quills were dyed for two hours at 60 °C. The dyebath produced porcupine quills exhibiting a pink colour.

PQ8a (pink): the porcupine quills (0.30 g) were dyed in 100 mL of American cochineal (3:1 w/w, 1 g) with alum mordant (0.25:1 w/w, 0.075 g). The dyebath was heated to 85 °C for one hour. The dyebath produced porcupine quills exhibiting a strong pink colour.

PQ8b (red): the porcupine quills (0.30 g) were dyed in 100 mL of American cochineal (3:1 w/w, 1 g) with alum mordant (0.25:1 w/w, 0.075 g) and cream of tartar (0.06:1 w/w, 0.018 g). The dyebath was heated to 85 °C for one hour. The dyebath produced porcupine quills exhibiting a strong red colour.

PQ8c (scarlet): the porcupine quills (0.30 g) were dyed in 100 mL of American cochineal (3:1 w/w, 1 g) with alum mordant (0.25:1 w/w, 0.075 g), cream of tartar (0.06:1 w/w, 0.018 g) and tin(II) chloride (0.05:1 w/w, 0.015 g). The dyebath was heated to 85 °C for one hour. The dyebath produced porcupine quills exhibiting a strong scarlet colour.

#### 7.4.4 UPLC analysis

##### 7.4.4.1 Chemicals

Carminic acid (7- $\alpha$ -D-Glucopyranosyl-9,10-dihydro-3,5,6,8-tetrahydroxy-1-methyl-9,10-dioxoanthracenecarboxylic acid, HPLC assay  $\geq$  96 %) were purchased from

Sigma-Aldrich UK, standards of curcumin (Diferuloylmethane, HPLC assay  $\geq 97.5$  %) and juglone (5-Hydroxy-1,4-naphthoquinone, HPLC assay  $\geq 90$  %) were purchased from ExtraSynthese, France.

#### 7.4.4.2 Solutions of standards

UPLC system was calibrated using three stock solutions of standards: 1. a solution containing carminic acid ( $1.00 \pm 0.01$  mg) in water:methanol [25 mL, 1:1 (v/v); equivalent to  $40 \mu\text{g mL}^{-1}$ ]; 2. a solution containing juglone, curcumin ( $0.50 \pm 0.01$  mg of each standard) in water:methanol [25 mL, 1:1 (v/v); equivalent to  $20 \mu\text{g mL}^{-1}$ ]; and 3. a solution of carminic acid ( $3.00 \pm 0.01$  mg) in water:methanol [10 mL, 1:1 (v/v); equivalent to  $300 \mu\text{g mL}^{-1}$ ]. Diluted solutions were then prepared with components at concentrations of 20, 10, 5, 1, 0.5, 0.1, 0.05, 0.02 and  $0.01 \mu\text{g mL}^{-1}$ , by dilution with water:methanol [1:1 (v/v)] using calibrated micro-pipettes. Additional calibration points for carminic acid used dilutions of stock solution 3 at the concentrations of 150 and  $100 \mu\text{g mL}^{-1}$ .

#### 7.4.4.3 Chromatographic method

Method C: used a PST BEH C18 reverse phase column,  $1.7 \mu\text{m}$  particle size,  $150 \times 2.1$  mm (length  $\times$  i.d.), with in-line filter. The total run time was 37.33 min at a flow rate of  $250 \mu\text{L min}^{-1}$ . A binary solvent system was used; A = 0.02 % aqueous formic acid, B = MeOH. The elution programme was isocratic for 3.33 min (75A: 25B) then a linear gradient from 3.33 min to 29 min (10A: 90B) before recovery of the initial conditions over 1 min and equilibration over 5 min.

#### 7.4.4.4 Sample preparation

For turmeric extraction (TFA): the sample (typically 0.1 - 1 mg) was extracted in a 1 mL glass test tube, to which was added a 2 M trifluoroacetic acid: methanol: water [200  $\mu\text{L}$ , 2:1:1 (v/v/v)]. The tube was then placed on a heated block at  $100^\circ\text{C}$  and heated for precisely 60 min. After cooling down at room temperature, the extract was transferred into a 1 mL Eppendorf vial and the glass tube was rinsed with water: methanol [100  $\mu\text{L}$ , 1:1 (v/v)]. The combined extracts were centrifuged for 10 min at 10,000 rpm and then filtered directly into Waters UPLC vials using a PTFE Phenomenex syringe filter (0.2

$\mu\text{m}$ , 4 mm). The extract was then cooled with liquid Nitrogen and dried under vacuum using a freeze drier system. The dry residue was then reconstituted with water: methanol [40  $\mu\text{L}$ , 1:1 (v/v)] and 10  $\mu\text{L}$  were injected for analysis.

For turmeric extraction (DMSO): the sample (typically 0.1 - 1 mg) was extracted in a 1 mL glass test tube, to which was added dimethyl sulfoxide [50  $\mu\text{L}$ ]. The tube was then placed on a heated block at 100 °C and heated for precisely 60 min. After cooling down at room temperature, the extract was filtered directly into Waters UPLC vials using a PTFE Phenomenex syringe filter (0.2  $\mu\text{m}$ , 4 mm) and 10  $\mu\text{L}$  was injected for analysis.

For cochineal and madder extraction, the hydrochloric acid extraction protocol above was adapted as follows: the sample (typically 0.1 - 1 mg) was extracted in a 1 mL glass test tube, to which was added a mixture of 37% hydrochloric acid: methanol: water [200  $\mu\text{L}$ , 2:1:1 (v/v/v)]. The tube was then placed on a heated block at 100 °C and heated for precisely 10 min. After cooling down at room temperature, the extract was transferred into a 1 mL Eppendorf vial and the glass tube was rinsed with water: methanol [100  $\mu\text{L}$ , 1:1 (v/v)]. The combined extracts were centrifuged for 10 min at 10,000 rpm and then filtered directly into Waters UPLC vials using a PTFE Phenomenex syringe filter (0.2  $\mu\text{m}$ , 4 mm). The extract was then cooled with liquid Nitrogen and dried under vacuum using a freeze drier system. The dry residue was then reconstituted with water: methanol [40  $\mu\text{L}$ , 1:1 (v/v)] and 10  $\mu\text{L}$  was injected for analysis.

#### 7.4.4.5 Calibration curves, limit of detection (LOD), limit of quantification (LOQ)

The calibration curves and linearity of each standard were calculated at 254, 430 and 450 nm, each concentration standard were investigated in triplicate using an auto-sampler and the calibration was made for carminic acid using 8 solutions ranging between 5 and 300  $\mu\text{g mL}^{-1}$ , while the calibration of juglone was made using 7 solutions ranging between 0.1 and 40  $\mu\text{g mL}^{-1}$ . Finally curcumin could only be calibrated using 4 solutions ranging between 0.5 and 20  $\mu\text{g mL}^{-1}$ , above this concentration it was found that the linearity of Beer Lambert Law was not respected any more. Calibration curves and linearity ranges are presented in table 7.49.



Method C : UPLC, 150 x 2.1 mm, 1.7 $\mu\text{m}$ : each standard analysed in triplicate						
Compound [x]	254 nm		430 nm		450 nm	
	[x] ( $\mu\text{g/mL}$ ) vs. $A_x$ ( $R^2$ )	n [ $\mu\text{g/mL}$ ]	[x] ( $\mu\text{g/mL}$ ) vs. $A_x$ ( $R^2$ )	n [ $\mu\text{g/mL}$ ]	[x] ( $\mu\text{g/mL}$ ) vs. $A_x$ ( $R^2$ )	n [ $\mu\text{g/mL}$ ]
carminic acid	$y = 21531x - 38694$ (0.9985)	n = 8 [5 - 300]	$y = 6250.1x - 39771$ (0.9979)	n = 7 [5 - 300]		
juglone	$y = 70632x - 4482.7$ (0.999)	n = 8 [0.1 - 40]				
curcumin					$y = 22737x - 23237$ (0.9792)	n = 4 [0.5 - 20]

**Table 7.49:** Calibration curves and linearity range obtained for carminic acid, juglone and curcumin, at 254 nm (carminic acid and juglone), 430 nm (carminic acid) and 450 nm (curcumin).

The limit of detection (LOD) and limit of quantification (LOQ) were calculated based on the slopes of the calibration curves (Concentration vs. Peak Height) and the noise (s) of the baseline noise of sample blanks analysed and calculated at 254, 430 and 450 nm. The Concentration vs. Peak Height relationship was calculated using the ASCII files of each standard and the intercepts of the equations were set to zero and used to calculate the LOD and LOQ values as 3.3 and 10 times the s values of the baseline, respectively. Detailed calculations of LOD and LOQ values can be found in the table 7.50.

Method C: UPLC, PST BEH C18 Column, 2.1 x 50 mm, 1.7 $\mu\text{m}$					
Compound [x]	[x] ( $\mu\text{g mL}^{-1}$ ) vs. $H_x^a$ (AU), with $b^b = 0$ ( $R^2$ )	[x] ( $\mu\text{g mL}^{-1}$ ) vs. $H_x^a$ (AU), ( $R^2$ )	$ H_{\text{noise}} $ (AU) (n = 6)	LOD $\pm s_r$ $\mu\text{g mL}^{-1}$	LOQ $\pm s_r$ $\mu\text{g mL}^{-1}$
<b>At 254 nm (injection volume 5 <math>\mu\text{L}</math>)</b>					
carminic acid	$y = 0.0014x$ (0.9675)	$y = 0.0016x - 0.0067$ (0.999)	$0.000164 \pm 0.000091$	$0.39 \pm 0.21$	$1.17 \pm 0.65$
juglone	$y = 0.0104x$ (0.9975)	$y = 0.0103x + 0.0023$ (0.9977)	$0.00138 \pm 0.00006$	$0.44 \pm 0.02$	$1.33 \pm 0.05$
<b>At 430 nm (injection volume 5 <math>\mu\text{L}</math>)</b>					
carminic acid	$y = 0.0004x$ (0.9949)	$y = 0.0004x - 0.0016$ (0.9977)	$0.000170 \pm 0.000034$	$1.40 \pm 0.28$	$4.25 \pm 0.85$
<b>At 450 nm (injection volume 5 <math>\mu\text{L}</math>)</b>					
curcumin	$y = 0.0027x$ (0.9979)	$y = 0.0027x - 5E-06$ (0.9979)	$0.000652 \pm 0.000030$	$0.80 \pm 0.04$	$2.41 \pm 0.11$

**Table 7.50:** Calcul of limit of detection (LOD) and quantification (LOQ) for carminic acid, juglone and curcumin, at 254 nm (carminic acid and juglone), 430 nm (carminic acid) and 450 nm (curcumin).

### 7.4.5 Turmeric analysis

#### 7.4.5.1 Turmeric extraction

Two extraction methods were tested using a solution of 2 M trifluoroacetic acid (TFA): methanol: water [200  $\mu$ L, 2:1:1 (v/v/v)] and dimethyl sulfoxide (DMSO). It was found that the extraction method using the 2 M TFA solution was less effective (table 4.44) and also less reproducible. From 5 samples extracted with TFA solution, only one sample (entry 144) provided the characterisation of diarylheptanoids above limit of detection, while DMSO systematically allowed the characterisation of the turmeric dyes.

The extraction with DMSO was however found to be less reproducible than the concentrated hydrochloric acid method, and the extracts exhibited a higher standard deviation (table 7.51).

		bisdemethoxycurcumin (3)	demethoxycurcumin (2)	curcumin (1)
DMSO (uplc entry 335 b)	Retention Time	19.91	20.15	20.36
	Area	297370	130212	141765
	% Area	52.2	22.9	24.9
TFA (uplc entry 144)	Retention Time	20.53	20.71	20.87
	Area	167831	48258	48641
	% Area	63.4	18.2	18.4

**Table 7.51:** Comparing the extraction efficiency of turmeric from reference PQ6 using trifluoroacetic acid and dymethyl sulfoxide solutions, monitored at 450 nm.

UPLC entry	Relative Amount (%) at 450 nm		
	bisdemethoxycurcumin (3)	demethoxycurcumin (2)	curcumin (1)
PQ6 (219)	53.5	22.4	24.1
PQ6 (218)	68.9	17.3	13.8
PQ6 (218 b)	69.1	17.3	13.7
PQ6 (335 b)	52.2	22.9	24.9
PQ6 (336 b)	51.4	24.0	24.6
<i>Average (n = 5)</i>	<b>59.0</b>	<b>20.7</b>	<b>20.2</b>
<i>standard deviation</i>	<b>9.1</b>	<b>3.2</b>	<b>5.9</b>

**Table 7.52:** Relative amount of the diarylheptanoids extracted from 1 mg of porcupine quill (PQ6), using DMSO method, monitored at 450 nm.

### 7.4.5.2 Historical samples

Thirteen porcupine quills were selected for analysis and extracted using dimethyl sulfoxide. Curcumin (**1**), demethoxycurcumin (**2**) and bisdemethoxycurcumin (**3**) were characterised in all the extracts, with the exception of a dark blue quill which exhibited a high level of tannins (elagic acid). Turmeric was found to be associated to cochineal (carminic acid) in the orange samples, while it was mixed with an unidentified blue dye for the shades of green. Four samples exhibited an unknown component, eluting at 7.4 min and named unknown 1.

A.848.15	UPLC Entry	Relative amount (%) at 450nm			Detected		
		bisdemethoxy curcumin	demethoxy curcumin	curcumin	unknown 1	carminic acid	elagic acid
Box 4, yellow	145	52.3	22.6	25.1			
Box 3, light green	147	34.1	27.1	38.9			
Box 3, green	172	25.3	29.0	45.7			
Box 9a, spotted blue	177	-	-	-			x
Box 18, light green	269	30.6	27.3	42.1	x		
Box 18, dark green	271	46.1	23.1	30.8			
Box 3, dark blue	272	34.9	26.6	38.5			
Box 3, yellow green	273	43.2	24.3	32.5	x		
Box 3, light green	274	51.8	21.3	26.9	x		
Box 4, orange	275	44.6	25.5	29.9		x	
Box 4, yellow	276	53.9	22.3	23.8	x		
Box 4, yellow	277	58.5	20.7	20.8			
Box 8, orange	280	59.6	18.8	21.6		x	

**Table 7.53:** Relative amount of the diarylheptanoids extracted historical porcupine quills, using DMSO method, monitored at 450 nm.

### 7.4.6 Cochineal analysis

#### 7.4.6.1 Porcupine quill reference

Prior investigating historical porcupine quills, a reference quill dyed with American cochineal (*Dactylopius Coccus* Costa) was extracted using a strong hydrochloric acid solution in order to characterise its dye profile. In order to compare this with published data, the relative amount of the red components was extracted at 275 nm (table 7.54).

UPLC Entry	Relative Amount (%) at 275 nm					
	Dc II	carminic acid	Dc IV	Dc VII	Flavokermesic acid	Kermesic acid
PQ Sn 100 ppm (220)	8.9	86.0	3.2	nd	1.9	nd
PQ Sn100 ppm (220d)	5.1	89.8	3.2	nd	1.9	nd
PQ Sn 100 ppm (221d)	6.9	89.9	1.4	nd	1.8	nd
<i>average</i>	<i>7.0</i>	<i>88.5</i>	<i>2.6</i>	<i>nd</i>	<i>1.9</i>	<i>nd</i>
<i>standard deviation</i>	<i>1.9</i>	<i>2.2</i>	<i>1.0</i>	<i>-</i>	<i>0.1</i>	<i>-</i>

**Table 7.54:** Relative amount of the acid hydrolysed extract from 1 mg of porcupine quill (PQ Sn 100  $\mu\text{g mL}^{-1}$ ), monitored at 275 nm.

#### 7.4.6.2 Historical quills

Twenty three porcupine quills were selected from the sample box A.848.15, as well as five micro-samples removed during conservation (A.848.12; A.848.13; A.848.45 and A.848.49) and extracted using a strong hydrochloric acid solution. The relative amount of the dye components characterised in the acid hydrolysed extracts and monitored at 430 nm can be found in table 7.55.

A.848.15	UPLC Entry	Relative amount (%) at 430 nm					
		Dc II	carminic acid	Unkown 2	Dc IV	Dc VII ?	flavokermesic acid
Box 8, orange*	169	27.2	54.4	15.2	-	2.1	1.1
Box 8, orange	170	41.1	31.8	27.1	-	-	-
Box 6, red	175	5.2	91.9	-	1.9	-	1.1
Box 6, red	176	48.4	35.4	16.3	-	-	-
Box 14B, red	178	65.2	13.8	21.0	-	-	-
Box 14B, red	179	42.1	37.3	20.6	-	-	-
Box 4, red	173	2.7	97.3	-	-	-	-
Box 2 quill 1, red*	189	50.6	38.1	-	3.5	3.1	4.7
Box 2 quill 2, red*	190	28.7	55.2	7.8	3.2	-	5.0
Box 4, orange*	191	51.7	48.3	-	-	-	-
Box 5A, red*	192	49.1	26.8	16.6	1.3	2.9	3.3
Box 5B, red*	193	8.0	88.0	0.5	2.0	0.3	1.3
Box 5B, red*	194	9.5	85.9	1.1	2.0	0.3	0.4
Box 6 quill 1, red*	195	43.0	37.6	14.4	1.8	1.2	2.1
Box 6, quill 2, red*	196	16.4	79.0	1.6	2.2	-	0.9
Box 6, quill 3, red	197	9.4	86.9	-	2.0	0.3	1.4
Box 7, red*	198	29.2	54.7	7.9	1.9	-	6.3
Box 14A, red*	199	54.1	18.9	27.0	-	-	-
Box 14B, red*	200	58.7	9.8	31.5	-	-	-
Box 16B, red*	201	59.4	11.8	28.9	-	-	-
Box 16B, orange*	202	64.5	12.8	22.8	-	-	-
		Relative amount (%) at 430 nm					
Objects	UPLC Entry	Dc II	carminic acid	Unkown 2	Dc IV	Dc VII ?	flavokermesic acid
A.848.13 Red	203	41.3	43.0	15.7	-	-	-

A.848.12 Red	204	18.9	68.6	-	-	-	12.5	
A.848.45 Purple	205	42.2	57.8	-	-	-	-	
		<b>Relative amount (%) at 254 nm</b>						
		alizarin						Purpurin
A.848.45, orange	206	78.1						22.0
A.848.49, orange	207	96.0						4.0

**Table 7.55:** Relative amount of the red dyes characterised in the acid hydrolysed extract of historical porcupine quills, monitored at 430 nm.

### 7.4.7 Mordant analysis by PIXE, PIGE and RBS

#### 7.4.7.1 Beam dose $Q$ and parameter files

The measurements were undertaken at the AGLAE external micro-beam (Accelerator Grand Louvre d'Analyse Elementaire, LC2RMF-Paris). PIXE measurements were carried out using a 3 MeV proton external set-up with two Si(Li) X-ray detectors: a Low Energy detector (LE), for the 1 - 15 keV range and a High Energy detector (HE), for the 1 - 40 keV range. These detectors recorded simultaneously the composition low- $Z$  matrix elements and the high- $Z$  trace elements present in the matrix and quantification was performed using the GUPIXWIN software package. The experiment was undertaken with an average current of 2 to 4 nA for an analysis time between 240 and 300 sec, corresponding to an integrated dose  $Q$  of 1  $\mu\text{C}$ . The high energy detector (HE) used a Beryllium filter (Be, 125  $\mu\text{m}$ ) and 28.5 mm air.

These measurements allowed to be calculated the exact beam charge ( $Q$ ) and the quantity ( $H$ ) values over the set of experiment, and provided an accurate quantification of the DR-N standard when summed up by GUPIXWIN to 100 percent. The values obtained for the different elements present in the DR-N standard were quantified for both low and high energy detectors and compared to their theoretical values.

	Entry 61 to 93	Entry 94 to 113	Entry 114 to 157
Low Energy	Q <sub>1</sub> : 0.00238 $\mu\text{C}$ H: 0.063	Q <sub>2</sub> : 0.00270 $\mu\text{C}$ H: 0.063	Q <sub>3</sub> : 0.00230 $\mu\text{C}$ H: 0.063
High Energy (Be, 125 $\mu\text{m}$ , 28.5 mm air)	Q <sub>1</sub> : 0.00238 $\mu\text{C}$ H: 1	Q <sub>2</sub> : 0.00200 $\mu\text{C}$ H: 1	Q <sub>3</sub> : 0.00215 $\mu\text{C}$ H: 1

**Table 7.56:** values of the beam dose  $Q$  and the quantity  $H$  for the different segments of the experiments.

Low Energy	Dose Q	Na <sub>2</sub> O - K	MgO - K	Al <sub>2</sub> O <sub>3</sub> - K	SiO <sub>2</sub> - K	P <sub>2</sub> O <sub>5</sub> - K	K <sub>2</sub> O - K	CaO - K	TiO <sub>2</sub> - K	MnO - K	Fe <sub>2</sub> O <sub>3</sub> - K
01mar083	Q <sub>1</sub>	1.94	3.83	18.74	56.92	0.28	1.67	6.74	1.03	0.19	9.75
01mar097	Q <sub>2</sub>	2.47	4.02	19.13	55.96	0.15	1.64	6.77	1.19	0.22	9.52
01mar102	Q <sub>2</sub>	2.33	3.49	17.77	57.68	0.12	1.53	6.08	0.95	0.21	9.19
01mar135	Q <sub>3</sub>	2.15	3.72	18.64	56.12	0.32	1.54	6.55	1.06	0.24	9.42
01mar136	Q <sub>3</sub>	3.38	4.80	23.78	74.17	0.23	2.17	8.36	1.39	0.26	12.03
01mar158	Q <sub>3</sub>	1.84	3.38	18.58	55.83	0.20	1.73	6.67	1.05	0.23	9.22
<b>DR-N values</b>		<b>2.99</b>	<b>4.40</b>	<b>17.52</b>	<b>52.85</b>	<b>0.25</b>	<b>1.70</b>	<b>7.05</b>	<b>1.09</b>	<b>0.22</b>	<b>9.7</b>

**Table 7.57:** Quantification of the DR-N standards using low energy detector during the experiment, obtained values obtained are compared to theoretical values. Note that it was not possible to accurately quantify the elements Aluminium (Al, Z = 13) and Silicon (Si, Z = 14).

High Energy	Dose Q	K <sub>2</sub> O - K	CaO - K	TiO <sub>2</sub> - K	MnO - K	Fe <sub>2</sub> O <sub>3</sub> - K
01mar083	Q <sub>1</sub>	1.60	6.51	1.03	0.22	9.79
01mar097	Q <sub>2</sub>	1.75	6.84	1.22	0.23	9.93
01mar102	Q <sub>2</sub>	1.62	6.26	1.00	0.21	9.58
01mar135	Q <sub>3</sub>	1.65	6.79	1.12	0.22	9.93
01mar136	Q <sub>3</sub>	1.81	6.93	1.16	0.23	10.14
01mar158	Q <sub>3</sub>	1.72	6.76	1.06	0.22	9.62
<b>DR-N values</b>		<b>1.70</b>	<b>7.05</b>	<b>1.09</b>	<b>0.22</b>	<b>9.7</b>

**Table 7.58:** Quantification of the DR-N standards using high energy detector during the experiment, obtained values obtained are compared to theoretical values.

Entry	Sample ID	Dose /Sec.	Analysis Time (min)	Av. Current (nA) Mat	Dose $\mu$ C
01mar061	A.848.15 box 2 - red sp2	134	00:03:30	1.786	1.00
01mar062	A.848.15 box 2 - blue sp1	78	00:09:22	1.773	1.00
01mar063	A.848.15 box 2 - greenish sp1	98	00:09:28	1.89	1.00
01mar064	A.848.15 box 2 - white sp1	114	00:08:52	1.883	1.00
01mar065	A.848.15 box 2 - red 2 sp1	106	00:08:52	1.387	1.00
01mar066	A.848.15 box 1 - bright blue -sp1	30	00:12:03	0.923	1.00
01mar067	A.848.15 box 1 - greenish blue -sp1	22	00:18:08	0.561	1.00
01mar068	A.848.15 box 1 - greenish blue -sp2	94	00:29:46	2.016	1.00
01mar069	A.848.15 box 1 - green olive -sp1	20	00:08:20	2.049	1.00
01mar070	A.848.15 box 1 - green olive -sp2	124	00:08:11	2.288	1.00
01mar071	A.848.15 box 3 - yellow sp1	152	00:07:21	2.336	1.00
01mar072	A.848.15 box 3 - light green sp1	146	00:07:10	2.358	1.00
01mar073	A.848.15 box 3 -bright green sp1	126	00:07:08	2.874	1.00
01mar074	A.848.15 box 4 -light yellow sp1	130	00:05:52	3.021	1.00
01mar075	A.848.15 box 4 -light yellow sp2	140	00:05:34	2.809	1.00
01mar076	A.848.15 box 4 - yellow sp1	166	00:05:58	2.551	1.00
01mar077	A.848.15 box 4 - yellow sp2	142	00:06:35	2.398	1.00
01mar078	A.848.15 box 4 - orange sp1	100	00:07:01	2.506	1.00
01mar079	A.848.15 box 5a - red (1) sp1	152	00:06:43	2.5	1.00
01mar080	A.848.15 box 5a - red (2) sp1	122	00:06:43	2.294	1.00
01mar081	A.848.15 box 5b - red (1) sp1	148	00:07:18	2.703	1.00

01mar082	A.848.15 box 5b - red (2) sp1	140	00:06:12	2.747	1.00
01mar083	DR-N	116	00:06:08	2.732	1.00
01mar087	A.848.15 Box 7 Red quill sp1	2636	00:02:31	2.674	1.00
01mar088	A.848.15 Box 7 blue quill sp1	104	00:06:17	2.545	1.00
01mar089	A.848.15 Box 8 orange quill sp1	120	00:06:36	2.049	1.00
01mar090	A.848.15 Box 8 orange quill (2) sp1	124	00:08:12	2.451	1.00
01mar091	A.848.15 Box 9a faded green quill sp1	124	00:06:51	2.591	1.00
01mar092	A.848.15 Box 9a light blue quill sp1	140	00:06:31	2.513	1.00
01mar093	A.848.15 Box 9a bright blue quill sp1	128	00:06:42	2.571	1.00
01mar094	A.848.15 Box 9b yellowish quill sp1	96	00:06:33	5.618	1.00
01mar095	A.848.15 Box 9b light blue quill sp1	262	00:03:02	5.78	1.00
01mar096	A.848.15 Box 9b bright blue quill sp1	298	00:02:55	5.587	1.00
01mar097	DR-N	252	00:03:03	5.495	1.00
01mar098	A.848.15 Box 10 yellowish quill sp1	182	00:03:04	5.236	1.00
01mar099	A.848.15 Box 11a faded pink quill sp1	236	00:03:15	6.098	1.00
01mar100	A.848.15 Box 11a whitish quill sp1	316	00:02:49	6.452	1.00
01mar101	A.848.15 Box 11b whitish quill sp1	308	00:02:39	6.757	1.00
01mar102	DR-N	392	00:02:32	6.369	1.00
01mar105	A.848.15 Box 12a white quill sp1	282	00:02:47	6.173	1.00
01mar106	A.848.15 Box 12b white quill sp1	282	00:02:44	6.25	1.00
01mar107	A.848.15 Box 12b pinkish quill sp1	302	00:02:42	6.579	1.00
01mar108	A.848.15 Box 13a white quill sp1	366	00:02:36	6.211	1.00
01mar109	A.848.15 Box 13b white quill sp1	310	00:02:43	6.494	1.00
01mar110	A.848.15 Box 13b white blueish quill sp1	356	00:02:39	6.536	1.00
01mar111	A.848.15 Box 14a yellowish quill sp1	316	00:02:35	6.803	1.00
01mar112	A.848.15 Box 14a orange quill sp1	398	00:02:29	6.993	1.00
01mar113	A.848.15 Box 14b white quill sp1	394	00:02:26	2.545	1.00
01mar114	Blank 1	302	00:06:33	4.237	1.00
01mar115	Blank 2	158	00:03:58	3.802	1.00
01mar116	II 13	208	00:04:26	3.831	1.00
01mar117	II15	200	00:04:25	3.861	1.00
01mar118	II 17 (Cu)	142	00:04:22	3.861	1.00
01mar119	II 18a	172	00:04:21	3.289	1.00
01mar120	II 20	144	00:05:08	2.882	1.00
01mar121	II 16	136	00:05:49	2.89	1.00
01mar122	A.848.15 Box 14b orange quill sp1	162	00:05:50	3.106	1.00
01mar123	A.848.15 Box 15a yellow quill sp1	146	00:05:26	3.175	1.00
01mar124	A.848.15 Box 15a grey blue quill sp1	136	00:05:20	3.077	1.00
01mar125	A.848.15 Box 15a light blue quill sp1	160	00:05:28	3.049	1.00
01mar126	A.848.15 Box 15a bright blue quill sp1	154	00:05:31	3.135	1.00
01mar127	A.848.15 Box 15a light green quill sp1	134	00:05:24	2.994	1.00
01mar128	A.848.15 Box 15b yellow brown quill sp1	112	00:05:36	3.195	1.00
01mar129	A.848.15 Box 16a white quill sp1	126	00:05:15	3.268	1.00
01mar130	A.848.15 Box 16b light orange quill sp1	154	00:05:09	3.333	1.00
01mar131	A.848.15 Box 16b bright orange quill sp1	160	00:05:02	3.226	1.00
01mar132	A.848.15 Box 17a light blue quill sp1	160	00:05:13	3.521	1.00
01mar133	A.848.15 Box 17a light blue green quill sp1	160	00:04:47	3.663	1.00
01mar134	A.848.15 Box 17a green quill sp1	194	00:04:36	3.69	1.00
01mar135	DR-N	178	00:04:36	3.623	1.00
01mar136	DR-N	212	00:04:38	4.082	1.00
01mar137	A.848.15 Box 17b light blue quill sp1	188	00:04:07	3.846	1.00
01mar138	A.848.15 Box 17b light blue quill sp2	242	00:04:22	3.676	1.00
01mar139	A.848.15 Box 17b blue quill sp1	210	00:04:35	3.155	1.00
01mar140	A.848.15 Box 17b green quill sp1	154	00:05:19	3.436	1.00
01mar141	A.848.15 Box 18 faded yellow quill sp1	202	00:04:54	3.247	1.00
01mar142	A.848.15 Box 18 light green quill sp1	158	00:05:10	3.205	1.00
01mar143	A.848.15 Box 18 light green (2) quill sp1	136	00:05:13	3.521	1.00
01mar144	A.848.15 Box 18 lgreen quill sp1	184	00:04:47	3.717	1.00

01mar145	A.848.15 Box 18 Igreen quill sp2	214	00:04:31	3.759	1.00
01mar146	Ref I 8a (Al) sp 1	230	00:04:30	3.636	1.00
01mar147	Ref I 8b (Al, K) sp 1	192	00:04:37	3.472	1.00
01mar148	Ref I 5a (Al, K, Sn, Cl) sp 1	210	00:04:52	3.425	1.00
01mar149	Ref I 5b (Al, K, Sn, Cl) sp 1	176	00:04:55	2.933	1.00
01mar152	Ref II 12 (Al, K) sp 1	164	00:05:28	3.077	1.00
01mar153	Ref II 13 (Al, K, Sn) sp 1	148	00:04:53	3.096	1.00
01mar154	Ref II 15 (Al, K, Sn) sp 1	184	00:05:28	3.448	1.00
01mar155	Ref II 15 (Al, K, Sn) sp 2	246	00:04:01	4.115	1.00
01mar156	Ref I 8c (Al, K, Sn) sp 1	206	00:04:05	3.922	1.00
01mar157	Ref I 4b (Al, K, Cr) sp 1	174	00:04:18	4.219	1.00
01mar158	DR-N	206	00:04:01	3.236	1.00

**Table 7.59:** Average current (nA) and irradiation time for each analysis point, integrated to an average value of 1  $\mu$ C.

### 7.4.7.2 PIXE Results

Low Energy detector:

Entry	11 Na K	12 Mg K	13 Al K	14 Si K	15 P K	16 S K	17 Cl K	19 K K	20 Ca K	24 Cr K	26 Fe K
01mar061	0	426	142	0	225	37944	404	77	7	0	724
01mar062	0	627	931	375	0	52213	447	1507	274	0	40
01mar063	0	932	607	676	0	51643	197	2117	331	0	124
01mar064	0	511	342	246	0	33205	766	382	388	0	63
01mar065	617	702	87	468	322	35944	567	221	275	0	50
01mar066	0	1305	2009	479	0	67555	329	3958	1058	0	52
01mar067	0	2585	1392	524	0	61606	85	1098	220	0	74
01mar068	0	1371	1120	1298	0	72395	115	1492	204	0	38
01mar069	0	940	1436	1120	0	58537	53	1619	248	8	86
01mar070	0	1125	660	329	0	62070	42	1634	204	6	50
01mar071	0	851	1527	274	0	33440	226	396	243	0	103
01mar072	0	60	550	108	0	27508	335	440	186	0	68
01mar073	0	446	514	190	0	27895	294	888	271	14	59
01mar074	0	198	167	0	76	34578	153	408	122	8	0
01mar075	0	339	409	0	0	31716	188	403	130	0	16
01mar076	0	484	391	26	997	28651	444	2933	599	0	750
01mar077	0	396	430	192	573	31323	288	2325	480	0	756
01mar078	0	686	375	391	404	28248	240	267	432	0	132
01mar079	1252	616	545	1126	213	21507	327	414	266	0	96
01mar080	826	186	282	343	401	20994	559	500	570	0	95
01mar081	0	491	672	873	623	27064	893	339	285	0	113
01mar082	327	395	287	390	553	26303	921	230	346	0	48
01mar087	1866	3180	11937	0	172060	4598	1501	150	0	144	0
01mar088	860	30	0	538752	61	150	31	164	0	0	0
01mar089	17669	11166	61836	104587	0	423	143	3975	17539	0	37090
01mar090	482	0	387	870	320	42313	1313	202	362	0	86



01mar091	1522	<b>340</b>	1223	<b>328</b>	0	60978	1453	2466	366	0	<b>15</b>
01mar092	0	<b>495</b>	<b>392</b>	<b>370</b>	<b>78</b>	29245	428	435	<b>142</b>	0	<b>34</b>
01mar093	0	<b>403</b>	<b>81</b>	<b>234</b>	<b>52</b>	22337	326	<b>220</b>	<b>250</b>	<b>22</b>	<b>56</b>
01mar094	10539	<b>553</b>	<b>422</b>	<b>517</b>	0	78509	<b>359</b>	3646	581	0	165
01mar095	<b>517</b>	<b>412</b>	1714	587	0	39287	445	2915	492	0	<b>67</b>
01mar096	<b>169</b>	1219	3876	2143	0	39193	506	1551	616	<b>30</b>	211
01mar098	4156	<b>842</b>	3816	1850	0	49590	1095	1224	1273	0	498
01mar099	<b>438</b>	<b>290</b>	775	495	0	26220	675	695	499	<b>7</b>	<b>59</b>
01mar100	<b>422</b>	<b>169</b>	<b>300</b>	<b>154</b>	0	23482	508	242	<b>170</b>	0	<b>17</b>
01mar101	0	<b>47</b>	<b>70</b>	<b>178</b>	0	22840	498	902	287	0	0
01mar105	0	<b>197</b>	522	558	937	20886	655	<b>235</b>	<b>185</b>	<b>4</b>	280
01mar106	0	0	0	<b>27</b>	0	<b>138</b>	<b>10</b>	<b>19</b>	0	<b>1</b>	<b>5</b>
01mar107	1233	<b>251</b>	<b>69</b>	<b>185</b>	0	24652	<b>283</b>	358	163	0	<b>33</b>
01mar108	0	2450	9226	0	132898	3236	1322	<b>180</b>	<b>38</b>	<b>112</b>	<b>34</b>
01mar109	<b>48</b>	1907	9254	0	132936	3198	1303	<b>77</b>	0	<b>208</b>	0
01mar110	<b>569</b>	<b>474</b>	<b>447</b>	<b>243</b>	<b>30</b>	25093	504	349	356	0	<b>83</b>
01mar111	12634	<b>401</b>	1271	746	0	32395	522	764	801	0	<b>97</b>
01mar112	0	<b>269</b>	<b>243</b>	<b>276</b>	<b>353</b>	22428	573	<b>234</b>	340	<b>8</b>	276
01mar113	2418	0	<b>321</b>	<b>304</b>	<b>60</b>	23549	838	433	<b>107</b>	0	<b>81</b>
01mar114	0	<b>168</b>	0	<b>162</b>	0	31644	<b>51</b>	166	241	0	<b>10</b>
01mar115	0	<b>744</b>	0	<b>82</b>	0	42617	1301	0	402	<b>13</b>	<b>5</b>
01mar116	0	<b>513</b>	<b>18</b>	0	<b>199</b>	43436	335	251	0	0	0
01mar117	0	<b>446</b>	<b>15</b>	<b>70</b>	0	34829	<b>201</b>	2391	8789	<b>5</b>	<b>33</b>
01mar118	2856	0	<b>126</b>	<b>9</b>	<b>180</b>	42954	1140	829	<b>106</b>	0	0
01mar119	0	<b>490</b>	<b>275</b>	0	<b>270</b>	38569	1404	879	<b>58</b>	0	<b>67</b>
01mar120	<b>1259</b>	<b>676</b>	<b>234</b>	0	<b>552</b>	45262	673	1970	238	1888	0
01mar121	<b>13</b>	<b>566</b>	<b>345</b>	0	0	51380	2089	387	<b>81</b>	2732	<b>12</b>
01mar122	28408	<b>320</b>	<b>434</b>	<b>253</b>	<b>215</b>	16262	2748	2755	<b>511</b>	0	515
01mar123	2496	<b>120</b>	<b>519</b>	<b>210</b>	0	55345	<b>154</b>	717	319	0	<b>82</b>
01mar124	0	<b>514</b>	<b>743</b>	1154	0	56356	<b>285</b>	1159	249	<b>9</b>	105
01mar125	<b>339</b>	<b>947</b>	1978	779	<b>86</b>	48381	1188	2630	344	0	<b>66</b>
01mar126	0	<b>994</b>	3581	1388	0	40108	917	1661	220	0	<b>57</b>
01mar127	<b>55</b>	<b>1028</b>	<b>449</b>	<b>564</b>	0	59527	<b>273</b>	1266	<b>173</b>	<b>9</b>	<b>55</b>
01mar128	0	<b>787</b>	<b>914</b>	1129	0	74838	<b>158</b>	1276	390	0	88
01mar129	17345	<b>408</b>	1258	<b>378</b>	0	34110	1124	1008	1038	0	110
01mar130	0	<b>527</b>	<b>317</b>	<b>86</b>	0	27481	963	<b>253</b>	<b>92</b>	0	<b>39</b>
01mar131	0	<b>551</b>	943	608	<b>226</b>	23127	948	<b>178</b>	<b>70</b>	<b>8</b>	<b>78</b>
01mar132	0	<b>326</b>	865	<b>185</b>	0	25343	647	290	<b>151</b>	0	<b>131</b>
01mar133	0	<b>74</b>	<b>550</b>	<b>352</b>	<b>156</b>	24121	604	612	0	0	0
01mar134	<b>852</b>	<b>770</b>	2079	868	<b>28</b>	41884	<b>205</b>	7328	1433	<b>8</b>	282
01mar137	<b>712</b>	<b>105</b>	1121	<b>138</b>	0	32714	567	663	<b>135</b>	<b>23</b>	83
01mar138	<b>534</b>	0	<b>536</b>	<b>176</b>	0	31460	608	1126	<b>132</b>	<b>6</b>	114
01mar139	16663	<b>188</b>	3098	475	0	34381	1439	3098	<b>337</b>	<b>10</b>	130
01mar140	0	<b>635</b>	1531	<b>330</b>	0	45225	<b>283</b>	12234	1473	0	393
01mar141	0	<b>188</b>	<b>151</b>	<b>316</b>	0	31035	<b>219</b>	258	325	0	<b>10</b>
01mar142	0	0	<b>618</b>	<b>208</b>	0	38374	<b>199</b>	291	335	0	<b>50</b>

01mar143	193	228	442	186	41	27959	251	571	442	0	57
01mar144	673	215	2015	150	0	43562	0	3806	645	8	227
01mar145	1091	618	1798	323	0	38155	0	3185	389	0	106
01mar146	0	0	4	0	13	0	12	64	3	6	0
01mar147	458	422	348	19	212	37806	374	6751	1246	10	8
01mar148	101	337	226	53	0	36115	1502	10181	522	0	0
01mar149	0	260	222	52	111	38764	1070	5348	881	0	0
01mar150	0	276	784	156	0	29843	987	5766	963	0	0
01mar151	0	50	940	84	80	29211	83	796	553	0	10
01mar152	0	150	270	71	0	36140	0	829	26	0	9
01mar153	0	542	379	0	107	32712	783	3010	64	0	10
01mar154	0	401	0	146	0	40271	538	3162	118	9	19
01mar155	0	545	471	360	115	34937	454	3865	759	0	10
01mar156	0	525	158	66	0	39504	946	2696	688	9	0
01mar157	0	505	143	0	0	40191	0	7188	700	1229	0

**Table 7.60:** Low Energy detector PIXE elemental composition in ppm ( $\mu\text{g g}^{-1}$ ) of the porcupine quills samples analysed. The values appearing in red are close to the Limit of Detection (LOD) and in blue are below the Limit of Detection.

Entry	16 S K	17 Cl K	19 K K	20 Ca K	24 Cr K	25 Mn K	26 Fe K	29 Cu K	30 Zn K	50 Sn K	50 Sn LA	80 Hg LA
01mar061	16365	214	69	125	3	0	688	890	16	5333	7133	11
01mar062	23164	166	1019	162	0	0	40	369	18	857	547	89
01mar063	32711	40	1780	274	6	0	137	2019	48	2055	2458	11
01mar064	15252	270	312	305	2	6	65	11	76	0	72	0
01mar065	14296	208	160	222	0	2	70	200	45	11906	14898	12
01mar066	18408	69	1353	458	0	5	39	859	25	513	592	17
01mar067	33370	0	1057	174	4	0	44	411	9	488	341	142
01mar068	33760	0	1138	140	1	5	66	404	3	0	580	122
01mar069	26016	0	1084	217	2	10	83	753	23	888	924	34
01mar070	26527	0	1032	167	1	8	52	695	22	152	657	68
01mar071	17654	61	350	229	1	4	115	252	31	1526	1791	14
01mar072	12882	66	269	97	1	0	40	185	9	1955	1457	81
01mar073	15847	94	693	190	0	5	60	220	17	1536	1866	13
01mar074	16478	13	307	87	1	0	18	531	28	0	130	35
01mar075	16560	52	337	124	0	0	18	504	32	0	200	34
01mar076	13611	93	2039	479	1	10	815	1725	37	323	826	3
01mar077	14102	107	1503	381	0	14	775	1761	30	407	528	30
01mar078	14183	105	196	366	2	18	158	1449	24	6203	5733	8
01mar079	11441	173	324	321	0	2	66	5	26	4396	7744	0
01mar080	10749	209	449	422	1	10	93	15	39	4234	5282	9
01mar081	12456	449	278	293	0	6	100	1006	50	3549	3555	0
01mar082	13062	455	236	230	1	0	59	544	26	1275	2247	6
01mar087	17364	514	96	335	0	23	92	1196	46	4765	6228	22

01mar088	18245	389	1328	219	0	6	32	2689	26	0	0	39
01mar089	16281	226	365	137	0	0	59	250	52	2760	4315	54
01mar090	13098	175	230	224	0	2	69	239	40	8522	7965	71
01mar091	41149	218	2703	456	1	1	177	1631	57	1285	1391	33
01mar092	23921	167	2396	440	1	4	98	268	19	169	786	12
01mar093	22540	293	1388	508	0	3	222	323	16	460	1012	8
01mar094	16489	288	701	914	3	10	658	283	45	3666	2716	14
01mar095	18196	494	770	603	0	0	92	477	40	1125	1542	13
01mar096	18161	332	263	222	0	4	24	376	8	1249	1806	0
01mar098	16999	366	766	287	4	0	19	3	73	0	0	0
01mar099	19006	823	309	144	3	3	342	918	23	1950	4774	18
01mar100	19916	292	772	261	0	3	62	958	32	0	537	7
01mar101	16285	128	346	182	4	0	32	3	64	0	44	4
01mar105	19098	350	419	372	5	1	90	432	61	378	990	30
01mar106	21164	266	777	815	0	0	155	1134	62	933	1038	22
01mar107	18289	616	184	381	3	15	308	776	51	2657	4143	7
01mar108	18809	682	438	150	5	0	59	165	45	161	180	7
01mar109	18397	528	280	262	0	6	114	552	29	698	1294	11
01mar110	19828	581	302	221	0	1	125	118	37	204	548	3
01mar111	19685	675	2386	396	8	4	912	432	20	333	626	23
01mar112	14796	531	369	266	2	1	97	324	50	8458	9371	33
01mar113	20822	1143	923	801	3	2	116	544	56	235	506	33
01mar114	20651	52	118	274	0	3	4	3	54	0	0	0
01mar115	27666	899	5	377	2	1	11	6	73	0	28	0
01mar116	27378	98	230	58	1	0	13	3	45	226	338	5
01mar117	22954	204	1697	7711	0	108	22	2	49	0	0	0
01mar118	23950	897	715	108	0	2	7	232	40	0	77	0
01mar119	21799	907	600	65	0	0	60	1	8	0	0	3
01mar120	22901	556	1376	234	2158	14	13	5	48	0	0	0
01mar121	25022	894	267	77	2927	18	13	8	9	0	72	6
01mar122	11663	2086	2793	549	3	5	626	743	30	10480	12064	3
01mar123	39045	0	719	317	0	3	64	122	13	0	197	15
01mar124	34615	32	1095	236	9	1	138	2005	81	1137	1341	0
01mar125	20678	450	2078	345	3	5	80	2735	57	0	85	22
01mar126	23532	507	1663	235	0	4	85	2088	23	0	77	27
01mar127	32218	46	1056	161	0	4	74	1756	55	1053	1240	28
01mar128	29660	0	1132	315	8	2	94	1038	77	892	887	12
01mar129	21012	751	897	968	0	6	143	906	69	1161	1045	27
01mar130	17535	622	208	95	0	1	46	714	24	3970	4102	10
01mar131	13082	564	123	274	0	5	90	407	16	8018	8141	16
01mar132	16290	352	319	182	0	4	171	187	26	834	1139	18
01mar133	16331	240	498	194	0	3	99	468	11	4904	3903	13
01mar134	30521	175	7287	1512	4	11	385	1668	108	0	605	84
01mar137	17763	294	645	120	3	3	82	335	17	1719	2018	24
01mar138	18764	293	855	149	0	1	65	308	20	1312	1809	9
01mar139	17466	665	2372	245	5	0	134	448	30	3463	3974	14

01mar140	23195	122	8642	1012	0	22	478	6212	161	16186	15594	183
01mar141	18777	60	278	369	0	9	21	4	78	0	11	0
01mar142	21191	0	313	205	0	10	47	318	48	633	940	35
01mar143	18562	185	628	374	0	11	93	102	27	360	287	0
01mar144	24447	0	3297	652	1	15	214	536	74	856	1577	131
01mar145	25037	0	2823	359	4	8	111	389	29	739	1384	99
01mar146	22418	10	2213	297	0	1	2	9	52	0	0	0
01mar147	22780	279	5680	1078	0	5	0	4	47	0	52	0
01mar148	23082	1054	7573	388	4	0	0	15	56	0	121	0
01mar149	24173	859	4486	755	2	1	8	8	59	295	518	0
01mar150	21348	927	5142	863	0	1	1	7	47	0	246	5
01mar151	18251	38	809	559	2	8	13	1	21	0	0	0
01mar152	23507	40	682	9	4	4	5	4	16	0	0	0
01mar153	22517	558	2679	45	3	1	8	2	5	0	314	0
01mar154	21353	319	1815	79	0	0	3	0	6	0	0	0
01mar155	20177	290	2620	602	4	7	41	0	25	148	185	0
01mar156	21095	647	1992	562	0	0	5	2	45	215	315	0
01mar157	17648	52	4240	408	1378	3	9	5	94	0	0	0

**Table 7.61:** High Energy detector PIXE elemental composition in ppm ( $\mu\text{g g}^{-1}$ ) of the porcupine quills samples analysed. The values appearing in red are close to the Limit of Detection (LOD) and in blue are below the Limit of Detection.

#### 7.4.7.3 RBS Spectra

The RBS measurements were recorded simultaneously to the PIXE experiments and the calibration of the spectra was obtained through the analysis of a standard of  $\text{SiO}_2$  coated with a thin layer of known thickness of gold (figure 7.7). And RBS spectra were simulated using the SIMNRA software by virtually overlapping the contribution of the different atoms present in the cuticle layer. As well as Rutherford cross-sections, non-Rutherford cross-sections specific to the set-up used in AGLAE accelerator at  $150^\circ$  were used for the quantification of carbon, oxygen and nitrogen (see section 7.3.5.1).

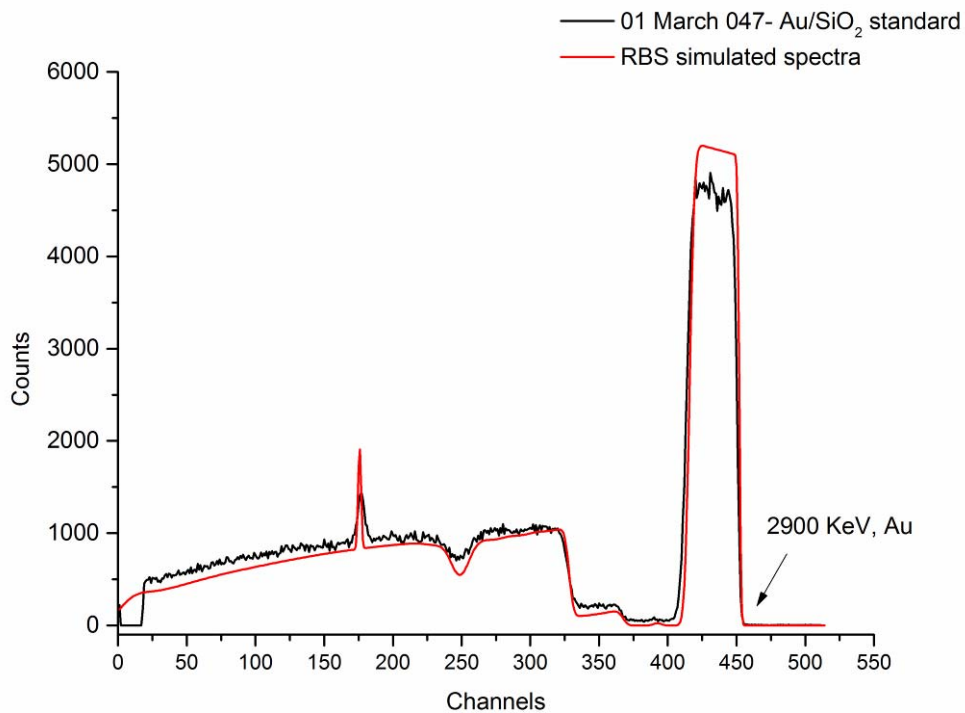


**Figure 7.7:** calibration of the RBS detector using a standard of SiO<sub>2</sub> coated with gold.

Entry	Particles *sr	Layers			
		Layer 1 (1000.000)	Layer 2 (8700)	Layer 3 (80)	Layer 4 (10000000.000)
SiO <sub>2</sub> / Au standard	2.000E+10	He: 1	Au: 1	Cr: 1	Si: 0.333000 O: 0.667000

**Table 7.62:** Composition of the layers found in the SiO<sub>2</sub>/Au standard used for the calibration of the RBS spectra.

Entry	dose $\mu\text{C}$	particles *sr	Layer 1 (1000)	Layer 2 (1000000)	RBS (Wt %)			PIXE (Wt %)		
					S	Sn	Cu	S	Sn	Cu
01 March 122	0.0023	$1.78 \times 10^{10}$	He: 1	H : 0.4706 O : 0.1000 S : 0.008 N : 0.090 Sn : 0.0014 Cu : 0.00	3.32	2.15	ND	1.17	1.21	0.07
01 March 107	0.002	$2.00 \times 10^{10}$	He: 1	C : 0.33 H : 0.4915 O : 0.1000 S : 0.008 N : 0.07 Sn : 0.0005 Cu : 0.00	3.48	0.81	ND	1.83	0.41	0.08
01 March 099	0.002	$2.00 \times 10^{10}$	He: 1	C : 0.33 H : 0.4823 O : 0.1000 S : 0.007 N : 0.08 Sn : 0.0005 Cu: 0.0002	3.00	0.80	0.17	1.9	0.48	0.09
01 March 134	0.0023	$1.92 \times 10^{10}$	He: 1	C : 0.33 H : 0.4906 O : 0.1000 S : 0.008 N : 0.07 Sn : 0.0001 Cu: 0.0003	3.50	0.16	0.26	3.01	0.06	0.17

**Table 7.63:** Composition of the virtual layers simulated by SIMNRA software by virtually overlapping the contribution of the different atoms present in the cuticle layer, obtained for historical porcupine quill samples.

## 7.4.7.4 ICP-OES analysis

The system calibration and sample preparation are described in section 7.3.3.

Sample ID	Mass of quill extract (g)	Mass of filtered extract (g)	Mass of sample after dilution (g)	ICP-OES ( $\mu\text{g mL}^{-1}$ )		Quills ( $\mu\text{g g}^{-1}$ )	
				283.998 nm Sn	327.393 nm Cu	[Sn <sup>2+</sup> ]	[Cu <sup>2+</sup> ]
<b>A.848.15</b>							
B2 red quill 1	0.6	0.4914	5.0006	3.487	0.236	29	2
B2 red quill 2	0.6	0.4719	5.0035	1.995	0.206	17	2
B4 orange	0.5	0.4836	5.0035	2.003	0.223	20	2
B4 yellow	0.6	0.4776	5.008	1.629	0.211	14	2
B5A bright Red	0.4	0.4889	5.0018	1.450	0.083	18	1
B5B quill 1Red	0.5	0.4704	5.0008	1.991	0.231	20	2
B5B quill 2 bright Red	0.5	0.491	5.0018	1.226	0.126	12	1
B6 bright red quill 1	0.5	0.4825	5.0016	1.044	0.071	10	1
B6 red quill 2	0.8	0.4709	5.0045	1.410	0.358	9	2
B6 red quill 3*	0.9	0.489	5.009	1.056	0.124	6	1
B7 red	0.8	0.4936	5.0095	1.076	1.854	7	12
B7 blue	0.6	0.4936	5.0095	1.091	0.144	9	1
B8 orange	0.5	0.4842	5.0093	1.359	0.253	14	3
B8 orange*	0.6	0.4631	5.0085	1.269	0.075	11	1
B14A red	0.5	0.4927	5.0017	1.183	0.199	12	2
B14A orange	0.6	0.4222	5.0067	1.165	0.075	10	1
B14B red	0.6	0.48	5.0084	1.336	0.731	11	6
B16B orange	0.7	0.4993	5.009	1.198	0.103	9	1
B16B faded orange	0.7	0.4636	5.0008	0.873	0.092	6	1
B9A bright blue	1	0.4708	5.0052	0.483	0.110	2	1
B9A spotted blue	0.6	0.4781	5.009	1.099	0.088	9	1
B9A pale blue	0.7	0.5033	5.0078	0.635	0.080	5	1
B17A green	0.7	0.4805	5.006	0.742	0.136	5	1
B17B green	0.8	0.4838	5.0014	2.020	0.715	13	4
B18 yellow	0.8	0.4285	5.007	0.538	0.057	3	0
<b>Objects</b>							
A.848.13 B18 pink	0.1	0.4746	5.0077	0.611	0.092	31	5
A.848.13 green	0.1	0.4812	5.0005	1.159	0.290	58	14
A.848.13 blue	0.1	0.5056	5.0056	0.572	0.080	29	4
A.848.13 colorless	0.2	0.4787	5.0019	0.446	0.090	11	2
A.849.7 green	0.1	0.4989	5.0039	0.388	0.097	19	5
A.849.7 blue	0.2	0.4878	5.009	0.514	0.205	13	5

**Table 7.64:** ICP-OES analysis of historical porcupine quills.